AD NUMBER
AD046640
CLASSIFICATION CHANGES
TO: **unclassified**
FROM: **confidential**
LIMITATION CHANGES
TO: **Approved for public release; distribution is unlimited.**
FROM: **Distribution authorized to DoD only; Administrative/Operational Use; AUG 1954. Other requests shall be referred to David Taylor Model Basin, Washington, DC. Pre-dates formal DoD distribution statements. Treat as DoD only.**
AUTHORITY
NASC ltr dtd 6 May 1966; NASC ltr dtd 6 May 1966

AD 46640

CONFIDENTIAL

89077

AERO REPORT 864

NAVY DEPARTMENT

THE DAVID W. TAYLOR MODEL BASIN

AERODYNAMICS LABORATORY

WASHINGTON 7, D.C.

WIND-TUNNEL TESTS OF THE AIRPLANE INTERFERENCE ON A 0.17-SCALE MODEL OF THE XAAM-N-4 ORIOLE MISSILE AND COMPARISON WITH THE AIRPLANE INTERFERENCE ON A 0.17-SCALE MODEL OF THE XAAM-N-2 SPARROW I MISSILE

PART II - MISSILES IN THE PROXIMITY OF A 0.179-SCALE MODEL OF THE F4D-1 AIRPLANE

by

E. M. Brower

TED No. TMB AD-3158
(Formerly DE-3158)

5

August 1954

NOTATION

Positive directions of axes, forces, moments, and angular displacements are shown by arrows.

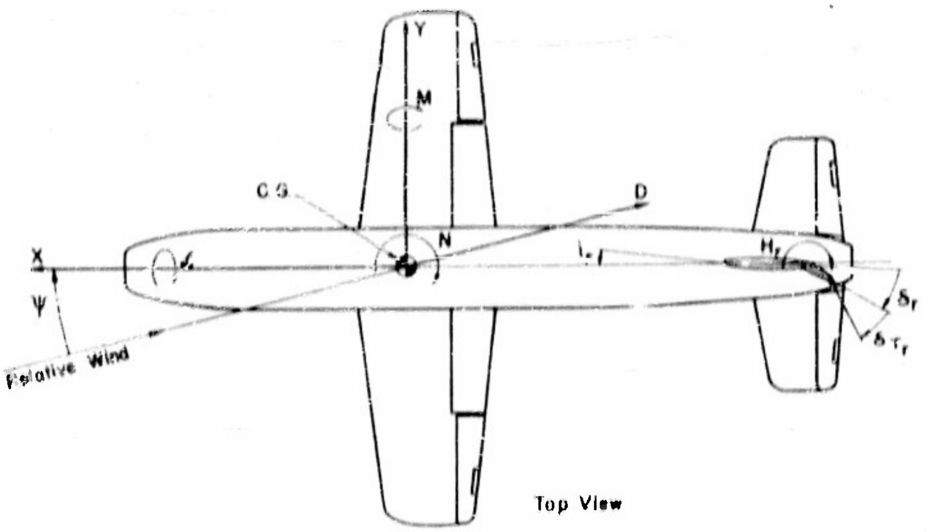

Top View

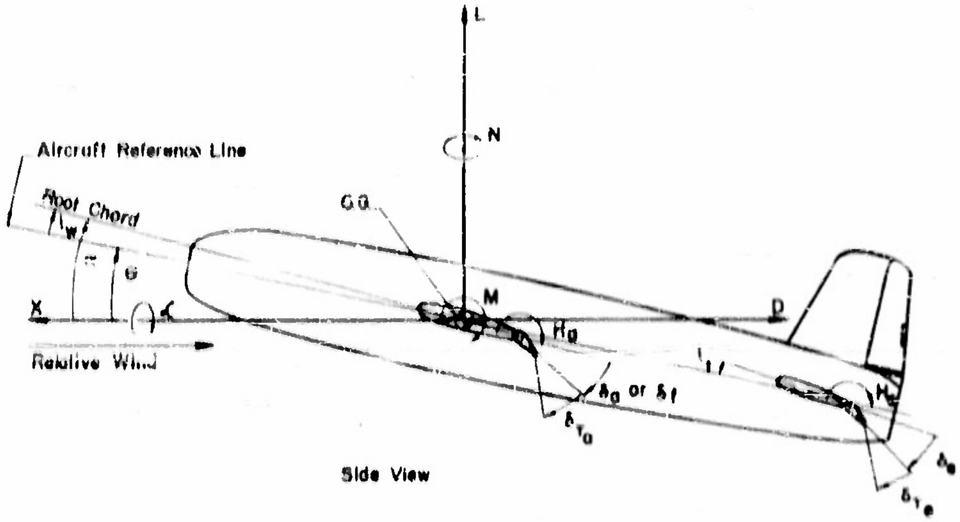

Side View

Axis	Force in pounds	Force Coefficient	Moment in pound-feet	Moment Coefficient
X	X	$C_X = X/qS$	$\mathcal{L}$ (rolling)	$C_l = \mathcal{L}/qSb$
D	D	$C_D = D/qS$	———	———
Y	Y	$C_Y = Y/qS$	M (pitching)	$C_m = M/qSc$
L	L	$C_L = L/qS$	N (yawing)	$C_n = N/qSb$
Hinge	—	———	H (hinge)	$C_h = H/qb\bar{c}^2$

General Symbols

S	area in square feet
c	mean aerodynamic chord in feet
b	span in feet
ℓ	characteristic length in feet
d	diameter in feet
$\bar{c}$	root-mean-square chord in feet
q	dynamic pressure $(\rho V^2/2)$ in pounds per square foot
V	airspeed in feet per second
R	Reynolds number $(\rho Vc/\mu$, $\rho V\ell/\mu$, or $\rho Vd/\mu)$
ρ	mass density of air in slugs per cubic foot
μ	absolute coefficient of viscosity of air in pound-second per square foot

Angular Settings

α	angle of attack in degrees (angle between root-chord of wing and the projection of the relative wind vector on the plane of symmetry of the aircraft)
α'	angle of attack in degrees (angle between root-chord of wing and the longitudinal axis of the tunnel)
θ	angle of pitch in degrees (angle between the aircraft reference line and the projection of the relative wind vector on the plane of symmetry of the aircraft)
θ'	angle of pitch in degrees (angle between the aircraft reference line and the longitudinal axis of the tunnel)
ψ	angle of yaw in degrees (angle between relative wind vector and plane of symmetry of the aircraft)
i_w	wing incidence in degrees (angle between the aircraft reference line and the root-chord of the wing)
i_t	angle of stabilizer in degrees (angle between the aircraft reference line and a reference line in the stabilizer)
i_F	angle of fin in degrees (angle between the plane of symmetry of the aircraft and the fin reference line)
δ	angle of control surface deflection in degrees, measured in a plane perpendicular to the hinge line

Subscripts

e	elevator	a	aileron	T	tab	L	left
r	rudder	f	flap	t	tail	R	right

NOTATION FOR MISSILE

Positive directions of axes, forces, moments, and angular displacements are shown by arrows

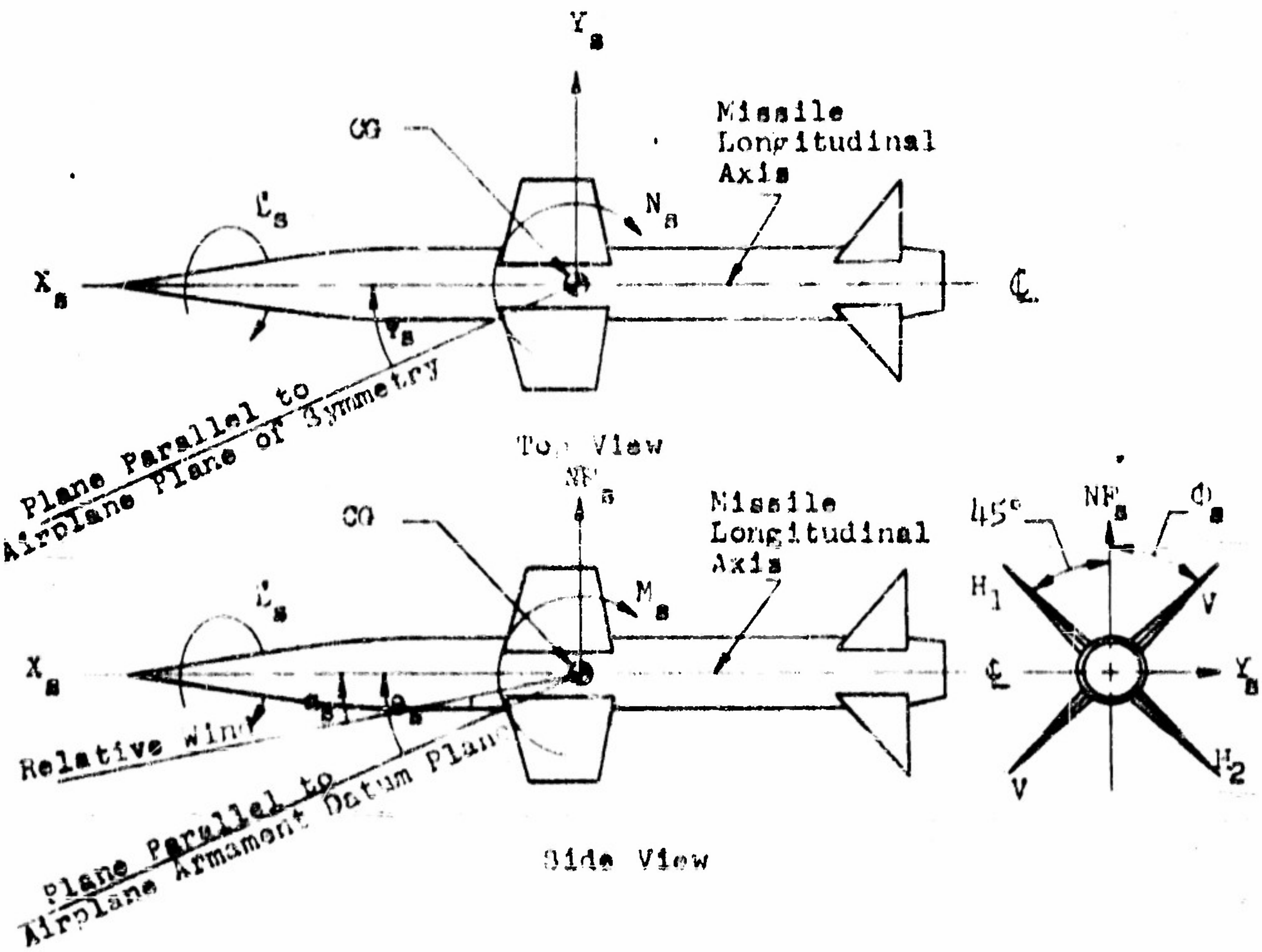

Top View

Side View

Axis	Force in Pounds	Force Coefficient	Moment in pound-feet	Moment Coefficient
Y_s	Y_s	$C_{Y_s} = \frac{Y_s}{qS_s}$	M_s (pitching)	$C_{m_s} = \frac{M_s}{qS_s c_s}$
NF_s	NF_s	$C_{N_s} = \frac{NF_s}{qS_s}$	N_s (yawing)	$C_{n_s} = \frac{N_s}{qS_s b_s}$
X_s	---	---	$\mathcal{L}_s$ (rolling)	$C_{l_s} = \frac{\mathcal{L}_s}{qS_s b_s}$

Additional Symbols

c_s mean aerodynamic chord of missile wing in feet

b_s wing span of missile in feet

S_s exposed area of horizontal or vertical wing of missile in square feet

x distance of missile forward of initial carry position in inches (distance along the armament datum plane)

z distance of missile below initial carry position in inches (distance perpendicular to the armament datum plane)

Δ used with the missile coefficient symbols as the interference of airplane on missile of the particular component noted

WL distance above airplane horizontal reference plane in inches

BL distance from airplane plane of symmetry in inches

FS distance aft of airplane transverse reference plane in inches

Angular Settings

θ_s missile angle of pitch in degrees (angle between longitudinal axis of missile and a plane parallel to the armament datum plane; positive, nose up)

ψ_s missile angle of yaw in degrees (angle between longitudinal axis of missile and airplane plane of symmetry; positive, nose right)

α_s missile angle of attack in degrees (angle between longitudinal axis of missile and the projection of the relative wind vector on a vertical plane through the missile longitudinal axis; positive, nose up)

Φ_s missile angle of roll in degrees (angle between normal-force axis and the plane of the vertical wing; positive, clockwise)

Angular Settings (Concluded)

$i_{w_{subs}}$	wing incidence of missile in degrees (angle between missile reference line and root chord of the missile wing, positive when leading edge is rotated toward airplane wing) (Used with subscripts, $\bar{H}_1$, $\bar{H}_2$, $\bar{V}$)

Subscripts

s	missile
H_1, H_2	horizontal wing panels of missile with missile rolled -45° from carry position
V	vertical wing of missile with missile rolled -45° from carry position

TABLE OF CONTENTS

TABLE OF CONTENTS (Continued)

TABLE OF CONTENTS (Concluded)

AERODYNAMICS LABORATORY
DAVID TAYLOR MODEL BASIN
UNITED STATES NAVY
WASHINGTON, D.C.

WIND-TUNNEL TESTS OF THE AIRPLANE INTERFERENCE ON A 0.17-SCALE MODEL OF THE XAAM-N-4 ORIOLE MISSILE AND COMPARISON WITH THE AIRPLANE INTERFERENCE ON A 0.17-SCALE MODEL OF THE XAAM-N-2 SPARROW I MISSILE

PART II - MISSILES IN THE PROXIMITY OF A 0.179-SCALE MODEL OF THE F4D-1 AIRPLANE

by

E. M. Brower

SUMMARY

An investigation was made in the Taylor Model Basin 8- by 10-foot wind tunnel on a 0.17-scale model of the XAAM-N-4 Oriole missile in the proximity of a 0.179-scale model of the F4D-1 airplane. A comparison is presented with a similar test on a model of the XAAM-N-2 Sparrow I missile to determine the applicability of interference data from one missile to another.

In the launch condition, the longitudinal instability of the Oriole missile increased over that of the missile alone. The instability of the missile at the outboard station is not as great as at the inboard station,

reaching a missile-alone value of stability in approximately one-half the distance forward that it took at the inboard station. A differential missile-wing incidence of 4° increased the rolling-moment coefficient by 0.04 at the carry position at both the inboard and the outboard stations; however, forward of the carry position the increase was 0.02 inboard and 0.03 outboard. Owing to the proximity of the two mounting stations, there was a considerable effect on the lateral-force, yawing-moment, and rolling-moment coefficients of the missile when another missile was at the adjacent station. The airplane minimum drag was increased 0.004 by the addition of four missiles.

A comparison of the interference on the Oriole and Sparrow shows good correlation of normal-force and pitching-moment coefficients. The lateral-force and yawing-moment coefficients are a rather poor comparison; however, in all cases the agreement improves as the distance from the wing increases. The rolling-moment coefficient provides the best correlation.

INTRODUCTION

In flight tests, trouble has been experienced in the firing of air-to-air guided missiles. It, therefore, became advisable to conduct a series of wind-tunnel tests to determine the cause of the trouble and a means of correction. Tests were made on a model of the XAAM-N-2 Sparrow I missile

to determine the missile characteristics in the proximity of several airplanes (References 1, 2, and 3). In order to determine whether a correlation could be made of the effects of a specific airplane on similar missiles, the Bureau of Aeronautics requested tests (Reference 4) of the XAAM-N-4 Oriole missile in the proximity of these same airplanes. The results of tests of a model of the Oriole in the proximity of a model of the F3H-1 airplane and a comparison of the airplane interference effects on the two missiles are presented in Reference 5. This report covers the characteristics of the XAAM-N-4 Oriole missile in the proximity of an F4D-1 airplane and a comparison of the airplane interference effects of the F4D-1 on the Sparrow I and Oriole missiles. The basic data of the Sparrow I in the proximity of the F4D-1 are given in Reference 2.

The tests were conducted during November and December 1953. Advance copies of these data were sent to the Bureau of Aeronautics, National Advisory Committee for Aeronautics, Sperry Gyroscope Corporation, Douglas Aircraft Company, Glenn L. Martin Company, and the Naval Air Missile Test Center shortly after completion of the tests.

MODEL

A 0.179-scale model of the F4D-1 airplane, designed and constructed by the Douglas Aircraft Company was used for these tests. Principal dimensions are shown in Figure 1.

A 0.17-scale model of the Oriole missile was designed and built by the TMB and is fully described in Part I of this report. A two-view drawing of the missile is shown in Figure 2 and a close-up photograph in Figure 3; other pertinent information is given in Table 1. The missile model was mounted under the left wing panel of the airplane on a five-component strain-gage-type balance, which measured all missile forces and moments except axial force. For most of the tests the balance and missile were supported from a sting mounting rig attached to the aft end of the fuselage (Figure 4). This permitted positioning the missile in several locations forward and below the airplane wing from the initial or carry position to obtain the effect of the airplane on the missile through the launch area. All movement was with respect to the carry position and parallel and perpendicular to the armament datum plane. The armament datum plane was at an angle of -4° to the plane of the wing chord. Figures 5 and 6 show this type of mounting at both the inboard and outboard stations and the coordinates of the carry position are given in Table 2. Angular control was possible in only one plane while pitching or yawing the missile. It was necessary for the angle in the other plane to be zero.

A few tests were made with the balance mounted directly on the wing by means of a steel bracket enclosed

in a pylon. The purpose of these tests was to determine an optimum carry position by testing an envelope of positions. At both the inboard and outboard stations the envelope formed a trapezoidal area as outlined by the center-of-gravity locations in Figure 7. The fifth center-of-gravity location tested at each station (1 and 6) was an arbitrary point within the envelope which corresponded roughly to the carry position used for the sting-mounted or launching tests. Figure 8 shows a typical installation of this type. The various missile center-of-gravity locations in terms of airplane FS, WL, and BL are given in Figure 1 and Table 2.

Three non-instrumented dummy missile models were used to obtain interference effects due to the proximity of the missiles and the effect of four missiles on the airplane. These models were made of laminated mahogany with fiberglass wings and tail fins. They were used only when two or four missiles were mounted to the pylons.

TESTS

The tests were conducted in the TMB 8- by 10-foot, closed throat, atmospheric Wind Tunnel 1 at a dynamic pressure of 50.0 pounds per square foot. This corresponds to an airspeed of 123 knots and a Reynolds number of 4,170,000 for the airplane based on a wing mean aerodynamic chord of 3.269 feet. The missile Reynolds number was 211,000 based on a missile wing mean aerodynamic chord of 0.165 foot.

A missile angle-of-attack range of -4° to 12° was used for the tests of the Oriole alone. All other tests were made with an airplane angle of attack of -2° to 12°. The range of missile pitch and yaw, θ_s and Ψ_s, was -6° through 6°. Each missile wing was independently variable from -12° to 12°. The missile was always rolled 45°. Some runs were made with the airplane yawed 3° and -3°.

The control surfaces of the airplane were locked in the neutral position for all tests.

RESULTS

The results are presented in the form of non-dimensional aerodynamic coefficients of the missile and airplane. Figure 9 is included from some later tests of the missile alone. Five-component missile characteristics are presented in Figures 10 through 21 and the airplane longitudinal characteristics in Figure 22. The data are referred to the system of axes shown in the notation with the center of gravity of the missile and airplane as shown in Figures 1 and 2. The missile coefficients are based on the exposed area, mean aerodynamic chord, and span of the missile wing. Airplane coefficients were based on area, span, and mean aerodynamic chord of the F4D-1 wing. The missile wing incidence was zero for all tests except those of Figures 13 and 18. The tests made with the sting mounting were made with a pylon on; Pylon 1 at the inboard station, and Pylon 6 at

the outboard station, unless otherwise noted. A comparison of the airplane interference effects on the Oriole and Sparrow I missiles is presented in Figures 24 through 33. Tables 3, 4, and 5 present a test schedule of the results showing where the various conditions may be found in the curves.

No jet-boundary corrections were applied to the missile coefficients. The airplane data were corrected for tare and interference of the supports and by the following jet-boundary corrections:

$$\Delta\alpha = 1.548\ C_L$$
$$\Delta C_D = 0.0270\ C_L^2$$
$$\Delta C_m = 0$$

The drag coefficient was also corrected for the static pressure gradient by the addition of an increment of 0.0007. The dynamic pressure was corrected during the test for model blockage.

DISCUSSION

The aerodynamic characteristics of the XAAM-N-4 Oriole missile model alone are shown in Figure 9. For this test, the missile sting-mounting system was similar to that used for mounting on the airplane. The Oriole is of symmetrical design; therefore, the displacements in pitching-moment and yawing-moment coefficients at $\alpha_s = 0°$ are assumed to be due to the mounting rig.

ORIOLE ON F4D-1 -- A composite plot of the missile characteristics at the inboard station for various distances forward and below the wing with $\theta_s = \Psi_s = 0°$ is presented in Figure 10. The Oriole is unstable in the launch condition for all positions tested; however, it becomes more stable as the distance forward and below the wing increases. At 18.36 inches forward of the carry position, $\partial C_{m_s}/\partial \alpha$ is approximately the same for all positions below the wing and for the missile alone. Generally $\partial C_{N_s}/\partial \alpha$ increases with increasing distance from the wing. The yawing-moment coefficient approaches zero as the missile moves away from the wing. The rolling moment coefficient is quite high while in the influence of the pylon and decreases to approximately zero at x = 18.36 inches.

At the inboard station, $\partial C_{N_s}/\partial \alpha$ increases from 0.11 at x = 6.12 to 0.18 at x = 15.36 with z = 0. The pitching-moment coefficient over the same distance shows small change per degree of θ_t (Figure 11). The normal-force-coefficient slope increases even more as the distance below the wing increases.

The tests with the missile yawed (Figure 12) show that the tail fins have an effect especially in close proximity to the fuselage. The $\partial C_{Y_s}/\partial \Psi_s$ is always larger through the negative yaw range except at the carry position. The yawing-moment coefficient becomes more negative with increasing distance forward of the carry position to x = 13.26

inches at $\alpha = 0°$. At x = 18.36 inches forward, C_{n_s} reverses and becomes slightly more positive at all yaw angles. The $\partial C_{n_s}/\partial \alpha$ increases from a negative to a positive value as the x-distance increases.

Figure 13 presents the variation due to missile wing incidence at various stations forward of the carry position and two angles of missile pitch. A differential wing setting of ±4° has the maximum effect on the rolling-moment coefficient at the carry position, approximately 0.04 C_l, which decreases rapidly to 0.02 as the distance forward increases. In all cases the increment is independent of the airplane angle of attack. A wing incidence setting equal on all four wings produces a $\partial C_{N_s}/\partial i_{w_s}$ of about 0.055 at the carry position. As the distance forward increases, $\partial C_{N_s}/\partial i_{w_s}$ becomes less linear especially through the positive incidence range (Figure 13g). At $\theta_s = 6°$, $\partial C_{N_s}/\partial i_{w_s}$ becomes non-linear closer to the carry position. The increment of pitching-moment coefficient due to i_{w_s} is about equal through the wing-incidence range, 12° to -12°, and at all missile locations.

The effects on the sting-mounted missile of airplane yaw and a pylon are shown in Figure 14 for the inboard station. At the carry position and $\Psi = 0°$, the presence of the pylon increases $\partial C_{l_s}/\partial \alpha$ from 0.0008 to 0.0145 and decreases $\partial C_{n_s}/\partial \alpha$ from -0.0362 to -0.0506. The increment of

C_{n_s} per degree of yaw is larger through the positive than through the negative range both with and without the pylon. This same characteristic is present with the missile as far from the airplane wing as z = 4.08 inches, x = 0 inch and z = 2.04 inches, x = 18.36 inches. Lateral force showed small variation due to airplane yaw at the three missile positions tested.

The tests at the outboard station were similar to those for the inboard station. Figure 15 presents the comparative results at various distances forward and below the carry position for $\theta_s = \Psi_s = 0°$. The interference of the F4D-1 on the Oriole missile at the carry position and the outboard station increases the longitudinal instability of the missile. The longitudinal stability becomes approximately equal to that of the missile alone at x = 9.18 inches. As would be expected the rolling-moment coefficient is greater outboard than inboard. The trends and changes due to increasing z distance are essentially the same as at the inboard station. Longitudinal instability decreases with increasing distance below the wing.

The results of the missile tests due to missile pitch, yaw, and wing incidence at the outboard station are presented in Figures 16, 17, and 18. Missile pitch causes results similar to those at the inboard station; however, $\partial C_{m_s}/\partial \theta_s$ shows less variation with distance forward at the

outboard station. At distances of 13.26 and 18.36 inches forward of the carry position, $\partial C_{m_s}/\partial \theta_s$ increases with increasing θ_s. Forward of the carry position the forces on the missile at the outboard station are very similar to those on it at the inboard station. A differential missile-wing incidence of ±4° at the carry position gives approximately the same amount of rolling-moment increment as at the inboard station. This decreases to 0.030 at 18.36 inches forward, which is only half as much a decrease as at the inboard station. The rolling-moment coefficient is larger outboard than inboard. The results of equal wing incidence on the normal-force coefficient are approximately the same as at the inboard station.

The effect of a pylon (Figure 19) on the rolling-moment coefficient at the outboard station is slightly greater than at the inboard station. Without the pylon, $\partial C_{l_s}/\partial \alpha$ is -0.0008 in comparison to 0.0008 at the inboard station. The $\partial C_{l_s}/\partial \alpha$ with the pylon on is the same at both stations. The rolling-moment coefficient is more positive outboard. Again the effect of airplane yaw varies little in general trend from the inboard station.

For use in determining the carry position for the missile, four locations were tested inboard and outboard as described under "Model." These results are presented in Figure 20.

Figure 21 presents the results of tests to determine the interference of a second missile at the adjacent station. In both cases there was an effect on the lateral-force, yawing-moment, and rolling-moment coefficients. The second missile decreased the lateral force and caused an effective deflection of the air flow in the area between the missiles increasing C_{n_s} at the inboard station and decreasing it at the outboard station. The rolling-moment coefficient of the inboard missile was reduced with a missile outboard. The rolling-moment coefficient of the missile showed a reduction in slope with airplane angle of attack due to the second missile. As can be seen in Figure 1, the two missiles are in close proximity spanwise and at the same chord-wise position rather than at a constant percent of the wing chord; therefore a rather large interference should be expected.

The drag increase of the airplane caused by four missiles is shown in Figure 22 for both the inverted and erect model conditions. The support system necessitated having the tail off when the model was inverted; however, with the tail on and the model erect, $C_{D_{min}}$ was increased only 0.002 over the tail-off configuration. The addition of the four missiles gave a drag increment of 0.004. The increase in C_L and decrease in longitudinal stability are small.

COMPARISON OF ORIOLE AND SPARROW I MISSILES -- A comparative sketch of the Oriole missile and the Sparrow I missile is given as Figure 23. The Oriole has a shorter body length, larger body diameter, smaller exposed wing area, and larger tail-fin area than the Sparrow I. A comparison of the F4D-1 airplane interference effects on the two missiles was made to determine whether or not the interference effects on a missile are dependent on missile design and what correlation can be made for various designs. The comparative data are presented in Figures 24 through 33 for the various components as functions of distance forward of the carry position and missile angle of attack. Because of the lack of data from the Sparrow I tests the comparison is omitted at z = 1.02 inches inboard station. Interference is calculated as the value of the coefficient in the presence of the airplane minus the value of the missile-alone coefficient. It should be noted here that the interference presented includes the effect of the airplane on the mounting rig. The magnitude and variability of this effect with pitch angle are not known; however, they are assumed to be small. For all components the correlation improves as the distance from the wing increases both forward and down.

Figure 24 presents the interference of the airplane on the normal-force coefficient of the missiles plotted against distance forward of the carry position for high

and low airplane angle of attack at $\theta_s = 0°$. The agreement between the Oriole and the Sparrow at the outboard station is very good at the low airplane angle of attack; even so, improvement can be noted with increasing distance below the wing. At the high airplane angle of attack the agreement at the outboard station is not good. For the inboard station there is considerably less difference in the degree of correlation at high and low airplane angles of attack. When compared on the basis of missile angle of attack (Figure 25), the best correlation inboard and outboard is at α_s less than 0°. The agreement is poorest from $\alpha_s = 2°$ through 8° in close proximity to the wing.

Airplane interference on the missile pitching-moment coefficient is presented in Figures 26 and 27. As was the case with the normal-force coefficients the outboard station provides the best correlation at the low airplane angle of attack. At high airplane angles of attack and in close proximity to the wing the missile pitching-moment coefficients correlate better at the inboard station; at z = 2.04 the correlation at the outboard station is again better. The comparison versus missile angle of attack is very good especially at 18.36 inches forward of the carry position. Again the interference at the outboard station is more nearly equal for the two missiles than at the inboard station.

The airplane interference on the lateral-force coefficient (Figures 28 and 29) is rather high for both missiles; however, the ΔC_{Y_s} on the Sparrow is always less than on the Oriole. At high angles of attack the correlation between the missiles is very poor. From Figure 29 it is apparent that the degree of the correlation does not appreciably very with missile angle of attack.

The interference on the yawing-moment coefficient (Figure 30) indicates the same trends for both missiles. In most cases there is an almost constant difference in interference between the Oriole and Sparrow over the 18 inches of forward travel tested. At the low angle of attack the numerical correlation is poor and the interference of the inboard and outboard stations of one missile are in closer agreement. A large difference between the interference of the two missiles at the high airplane angle of attack is shown in Figure 31.

The interference of the F4D-1 on the rolling-moment coefficients (Figure 32) of the two missiles is high at the carry position and decreases with increasing distance forward until it approaches zero at about x = 15 inches for the low airplane-angle-of-attack condition. At the high airplane angle of attack, ΔC_{l_s} is very high at x = 0 inch, especially for the Oriole outboard, and approaches zero at 17 inches forward of the carry position. At z = 2.04 inches

for both high and low angle of attack, ΔC_{l_s} is less than 0.01 and shows little change with increasing distance forward. In most cases there is very small variation with missile angle of attack at $\alpha = 0°$ and $6°$ (Figure 33).

CONCLUSIONS

1. The interference of the F4D-1 increased the longitudinal instability of the Oriole missile at the carry position. Missile-alone stability was approached at 18.36 inches forward for the inboard station and 9.18 inches forward for the outboard station.

2. A differential missile-wing incidence of 4° increased C_{l_s} from 0.02 to 0.04 depending on distance forward at the inboard station and from 0.03 to 0.04 at the outboard station.

3. The presence of the pylon increased the rolling-moment coefficient greatly at the carry position. The increase was greater at the outboard station owing to spanwise flow.

4. A missile at the adjacent station produced a large effect on lateral-force, yawing-moment, and rolling-moment coefficients because of the proximity of the two missiles.

5. There was an increase of 0.004 in $C_{D_{min}}$ of the airplane with the addition of four missiles.

6. The interference correlation of the F4D-1 airplane on the normal-force and pitching-moment coefficients

of the Oriole and Sparrow missiles was generally good.

7. The agreement of the interference on the lateral-force and yawing-moment coefficients was rather poor. Some difficulty might be experienced in predicting this interference on other missiles.

8. The interference on the missile rolling-moment coefficients showed the best correlation. The effects of the pylon at the carry position were slightly unpredictable.

Aerodynamics Laboratory
David Taylor Model Basin
Washington, D. C.
August 1954

REFERENCES

1. Kuldell, P. D. and Barnard, G. A.; Wind-Tunnel Tests of a 0.17-Scale Model XAAM-N-2 Sparrow I Missile in the Proximity of a 0.17-Scale F2H-3 Airplane Model. (U. S.) TMB Aero Report 856, March 1954. 9 l. illus. CONFIDENTIAL

2. Kuldell, P. D. and Wright, John; Wind-Tunnel Tests of a 0.17-Scale Model XAAM-N-2 Sparrow I Missile in the Proximity of a 0.179-Scale F4D-1 Airplane Model. (U. S.) TMB Aero Report 865, May 1954. 71 l. incl. illus. CONFIDENTIAL

3. Wright, John; Wind-Tunnel Tests of a 0.17-Scale Model XAAM-N-2 Sparrow I Missile in the Proximity of a 0.15-Scale F3H-1 Airplane Model. (U. S.) TMB Aero Report (in preparation) CONFIDENTIAL

4. BuAer CONF ltr Aer-DE-31 Serial 07850 on TED No. TMB DE-3158 dated 11 May 1953.

5. Brower, E. M.; Wind-Tunnel Tests of the Airplane Interference on a 0.17-Scale Model of the XAAM-N-4 Oriole Missile and Comparison With the Airplane Interference on a 0.17-Scale Model of the XAAM-N-2 Sparrow I Missile. Part I - Missiles in the Proximity of a 0.15-Scale Model of the F3H-1 Airplane. (U. S.) TMB Aero Report 864 Part I, June 1954. 152 l. incl. illus. CONFIDENTIAL

TABLE 1

Principal Dimensions and Data for the XAAM-N-4 Oriole Missile

Component	Item	0.17-Scale	Full-Scale
Body	Length in inches	23.46	138.00
	Diameter in inches	1.87	11.00
Wing	Exposed area (horizontal or vertical) in square feet	0.0574	2.00
	Span in feet	0.549	3.23
	MAC in feet	0.165	0.97
	Airfoil section	4% double wedge	4% double wedge
	Aspect ratio	2.65	2.65
	Incidence range (horizontal) in degrees	±12	±16
	Incidence range (vertical) in degrees	±12	±20
Tail	Exposed area (horizontal or vertical) in square feet	0.065	2.25
	Airfoil section	2.8% double wedge	2.8% double wedge
	Aspect ratio	0.90	0.90
Center-of-gravity location		FS 14.67	FS 86.30

TABLE 2

Center-of-Gravity Locations of Missile Model for Various Mounting Positions in Terms of F4D-1 Model Stations

Mounting	Inboard Station		
	FS	WL	BL
Sting	51.57	-5.31	16.26
Pylon 1	51.43	-5.27	16.31
Pylon 2	48.49	-4.34	16.24
Pylon 3	48.63	-6.34	16.28
Pylon 4	51.46	-6.27	16.29
Pylon 5	51.47	-4.34	16.30
Mounting	**Outboard Station**		
	FS	WL	BL
Sting	51.49	-4.90	22.81
Pylon 6	51.58	-4.83	22.97
Pylon 7	50.70	-4.22	22.90
Pylon 8	50.58	-5.50	22.96
Pylon 9	54.63	-5.64	22.88
Pylon 10	54.63	-4.41	22.92

TABLE 3

Outline of Tests and Index of Test Results

Variation of Missile Characteristics With Missile Angle of Attack

Test	Figure
Missile alone	9

Variation of Missile Characteristics With Airplane Angle of Attack (Missile in Proximity of Airplane)

Test		Figure
Missile positions ahead of carry position; $\psi=0°$, $\psi_s=0°$, $\theta_s=0°$, $z=0"$	inboard station	10
$x=0"$, 3.06", 6.12", 13.26", 18.36"	outboard station	15

Effect of missile pitch; $\psi = 0°$, $\psi_s = 0°$

θ_s in degrees	x in inches	z in inches	Station*	
6,3,0	6.12	0	In.	11a
6,3,0	6.12	0	Out.	16a
6,3,0	9.18	0	In.	11b
6,3,0	9.18	0	Out.	16b
6,3,0	13.26	0	In.	11c
6,3,0	13.26	0	Out.	16c
6,3,0,-3,-5	18.36	0	In.	11d
6,3,0,-3,-5	18.36	0	Out.	16d
6,3,0,-3	6.12	1.02	In.	11e
6,3,0,-3	6.12	1.02	Out.	16e
3,0,-3	9.18	1.02	In.	11f
0,-3,-6	13.26	1.02	In.	11g
0,-3,-6	13.26	1.02	Out.	16f
6,3,0,-3,-6	18.36	1.02	In.	11h
6,3,0,-3,-6	18.36	1.02	Out.	16g
6,3,0,-3,-6	0	2.04	In.	11i
6,3,0,-3,-6	0	2.04	Out.	16h
6,3,0,-3,-6	6.12	2.04	In.	11j
6,3,0,-3,-6	6.12	2.04	Out.	16i

* In. refers to the inboard station, BL = 16.26
Out. refers to the outboard station, BL = 22.87

TABLE 3 (Continued)

Test					Figure
Effect of missile pitch; $\Psi = 0°, \Psi_s = 0°$ (Continued)					
θ_s in degrees	x in inches	z in inches	Station*		
0,-3,-6	13.26	2.04	In.		11k
0,-3,-6	18.36	2.04	In.		11ℓ
0,-3,-6	18.36	2.04	Out.		16j
6,0,-6	0	4.08	In.		11m
6,0,-6	0	4.08	Out.		16k
Effect of missile yaw; $\Psi = 0°, \theta_s = 0°, z = 0"$					
Ψ_s in degrees	x in inches	Station*	Pylon		
2,0,-2	0	In.	On		12a
2,0,-2	0	Out.	On		17a
3,0,-3	6.12	In.	On		12b
3,0,-3	13.26	In.	On		12c
3,0,-3	13.26	In.	Off		12d
3,0,-3	13.26	Out.	On		17b
3,0,-3	13.26	Out.	Off		17c
6,3,0,-3,-6	18.36	In.	On		12e
6,3,0,-3,-6	18.36	Out.	On		17d
Effect of missile wing-incidence settings; $\Psi = 0°, \Psi_s = 0°, z = 0"$					
θ_s in degrees	i_{w_H} in degrees	i_{w_V} in degrees	x in inches	Station†	
0	0,±4,4,-8	0,4,-8	0	In.	13a
0	0,±4,4,-8, -12	0,4,-8,-12	0	Out.	18a
0	0,±4,4,-8	0,4,-8	6.12	In.	13b
6	0,±4,4,-8	0,4,-8	6.12	In.	13c
0	0,±4,12,8, 4,-4,-8,-12	0,12,8, 4,-4,-8,-12	13.26	In.	13d
6	0,±4,12,8, 4,-4,-8,-12	0,12,8,4, -4,-8,-12	13.26	In.	13e

TABLE 3 (Concluded)

Test					Figure
Effect of missile wing-incidence settings; $\psi = 0°$, $\psi_s = 0°$, $z = 0"$					
θ_s in degrees	i_{w_H} in degrees	i_{w_V} in degrees	x in inches	Station*	
0	0,±4,12,8, 4,-4,-8,-12	0,12,8,4, -4,-8,-12	13.26	Out.	18b
6	0,±4,12,4, -4,-12	0,12,4,-4, -12	13.26	Out.	18c
0	0,±4,12,8, 4,-4,-8,-12	0,12,8,4, -4,-8,-12	18.36	In.	13f
6	0,±4,12,8, 4,-4,-8,-12	0,12,8,4, -4,-8,-12	18.36	In.	13g
0	0,±4,12,8, 4,-4,-8,-12	0,12,8,4, -4,-8,-12	18.36	Out.	18d
6	0,±4,12,4, -4,-12	0,12,4, -4,-12	18.36	Out.	18e

Effect of airplane yaw; $\psi_s = 0°$						
θ_s in deg.	ψ in deg.	x in in.	z in in.	Pylons	Station*	Figure
0	3,0,-3	0	0	1 on, off	In.	14a
0	3,0,-3	0	0	6 on, off	Out.	19a
0	3,0,-3	18.36	2.04	1	In.	14b
0	3,0,-3	18.36	2.04	6	Out.	19b
0	3,0,-3	0	4.08	1	In.	14c
0	3,0,-3	0	4.08	6	Out.	19c

Effect of pylons; $\psi_s = 0°$, $\theta_s = 0°$, $\psi = 0°$		
Pylons	Station*	Figure
1,2,3,4,5,	In.	20a
6,7,8,9,10	Out.	20b

Effect of dummy missile and of airplane yaw; $\theta_s = 0°$, $\psi_s = 0°$, $x = 0"$, $z = 0"$			
ψ in degrees	Dummy	Station*	Figure
3,0,-3	on and off	In.	21a
3,0,-3	on and off	Out.	21b

Airplane longitudinal characteristics	Figure
Model inverted, tail off	22a
Model erect, tail on	22b

TABLE 4

Index of Figures Showing Variation of Airplane Interference With Distance Forward of the Carry Position

Interference Coefficient	θ_s in degrees	α_s in degrees	α in degrees	Figure
ΔC_{N_s}	0	0	4	24a
	0	6	10	24b
ΔC_{m_s}	0	0	4	26a
	0	6	10	26b
ΔC_{Y_s}	0	0	4	28a
	0	6	10	28b
ΔC_{n_s}	0	0	4	30a
	0	6	10	30b
ΔC_{l_s}	0	0	4	32a
	0	6	10	32b

In each figure interference is shown for both the inboard and outboard stations and at the three positions, $z = 0$ inch, 1.02 inches, and 2.04 inches.

TABLE 5

Index of Figures Showing Variation of Airplane
Interference With Missile Angle of Attack

Interference Coefficient	z in inches	x in inches	Station*	Figure
	0	18.36	In.	25a
	0	9.18,18.36	Out.	25b
	1.02	6.12,13.26,18.36	Out.	25c
ΔC_{N_s}	2.04	0,6.12,13.26	In.	25d
	2.04	0,6.12,18.36	Out.	25e
	4.08	0	In.	25f
	4.08	0	Out.	25g
	0	18.36	In.	27a
	0	9.18,18.36	Out.	27b
	1.02	6.12,13.26,18.36	Out.	27c
ΔC_{m_s}	2.04	0,6.12,13.26	In.	27d
	2.04	0,6.12,18.36	Out.	27e
	4.08	0	In.	27f
	4.08	0	Out.	27g
	0	18.36	In.	29a
	0	9.18,18.36	Out.	29b
	1.02	6.12,13.26,18.36	Out.	29c
ΔC_{Y_s}	2.04	0,6.12,13.26	In.	29d
	2.04	0.6.12,18.36	Out.	29e
	4.08	0	In.	29f
	4.08	0	Out.	29g

TABLE 5 (Concluded)

Interference Coefficient	z in inches	x in inches	Station*	Figure
	0	18.36	In.	31a
	0	9.18,18.36	Out.	31b
	1.02	6.12,13.26,18.36	Out.	31c
ΔC_{n_s}	2.04	0,6.12,13.26	In.	31d
	2.04	0,6.12,18.36	Out.	31e
	4.08	0	In.	31f
	4.08	0	Out.	31g
	0	18.36	In.	33a
	0	9.18,18.36	Out.	33b
	1.02	6.12,13.26,18.36	Out.	33c
ΔC_{l_s}	2.04	0,6.12,13.26	In.	33d
	2.04	0, 6.12,18.36	Out.	33e
	4.08	0	In.	33f
	4.08	0	Out.	33g

In each figure the interference is shown at both $\alpha = 0°$ and 6°.

* In. refers to the inboard station, BL = 16.26

Out. referes to the outboard station, BL = 22.87

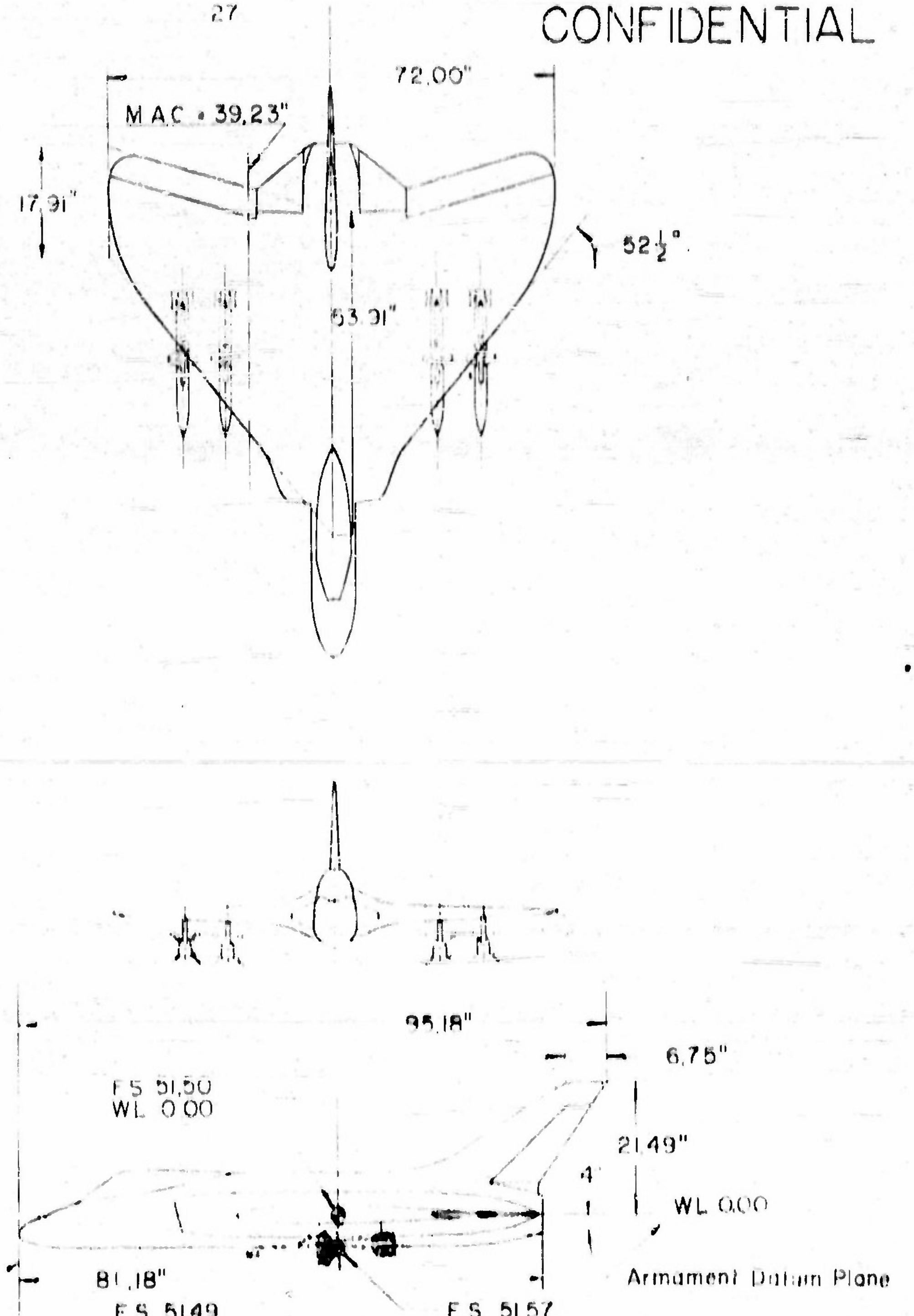

Figure 1 Principal Dimensions of a 0.179-Scale Model of the F4D-1 Airplane With Oriole Missiles

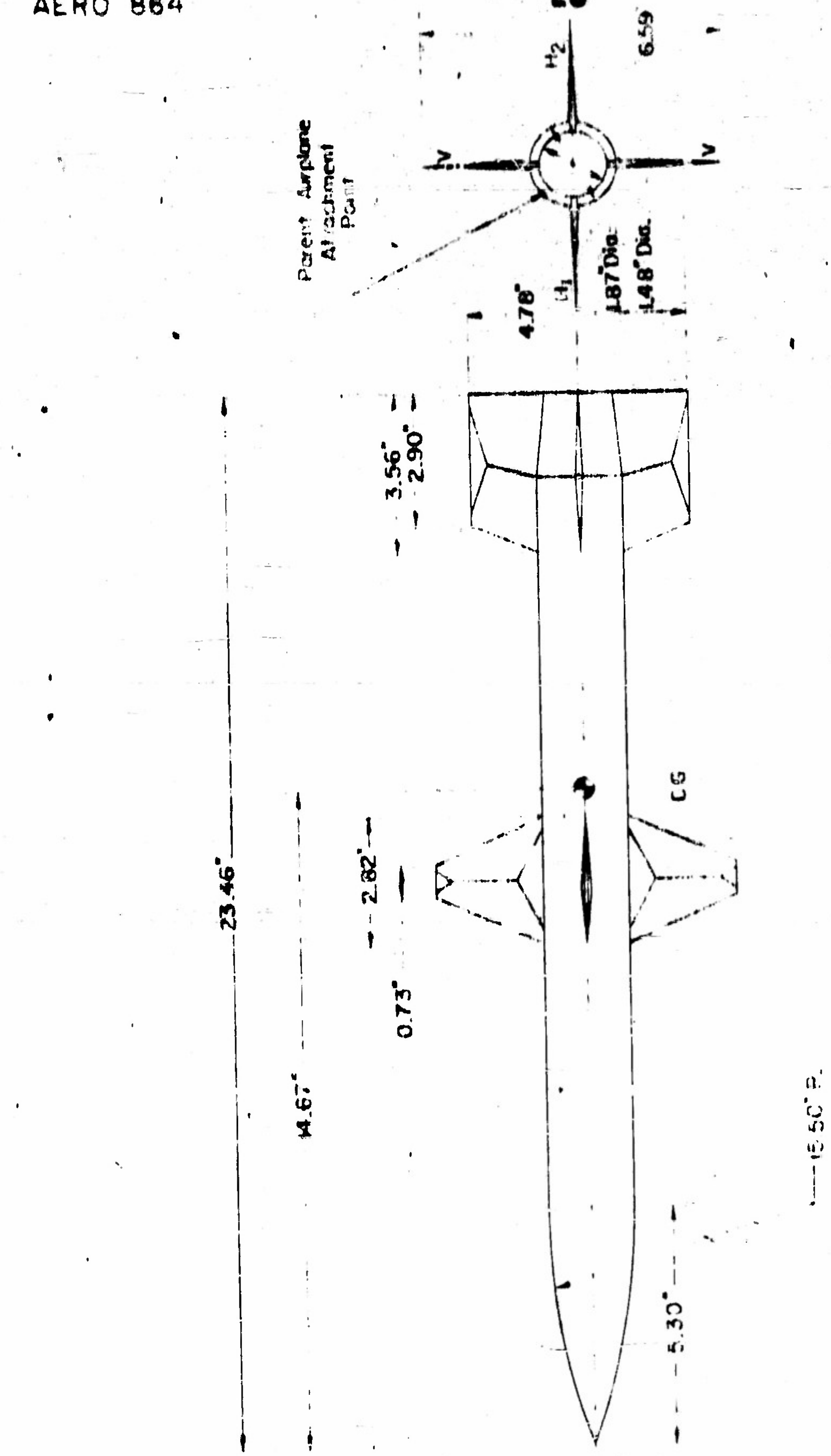

Figure 2-Principal Dimensions of a 0.17-Scale Model XAAM-N-4 Oriole Missile

Figure 3 - Close-Up of a 0.17-Scale Model XAAM-N-4 Oriole Missile in the Proximity of a Model F4D-1 Airplane

NP21-55304 2 Dec 1953

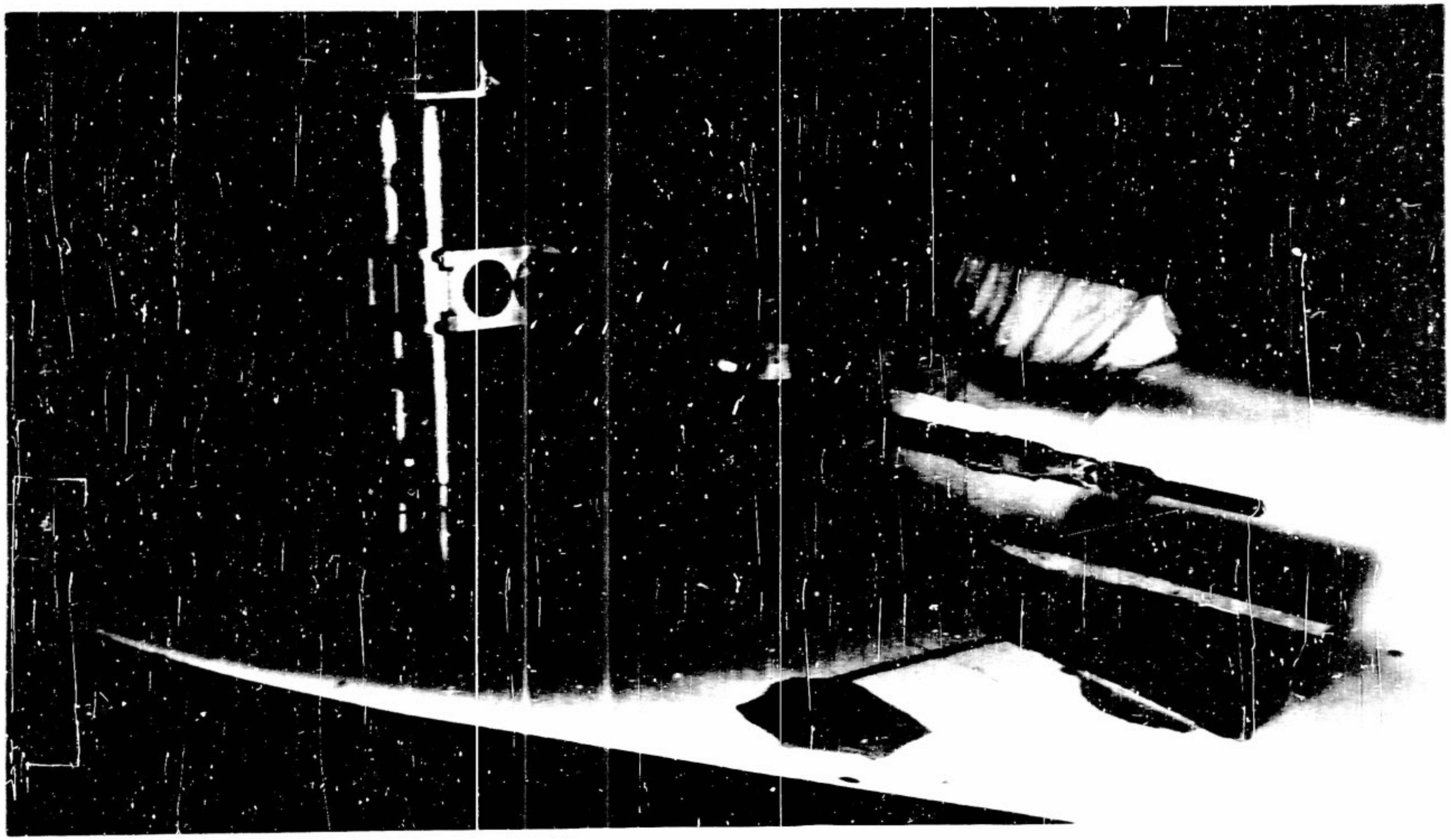

Figure 4 - Close-Up View Showing Strain-Gage Balance and Sting-Mounting System on a 0.179-Scale Model F4D-1 Airplane Installed Inverted in the Wind Tunnel

NP21-55303 2 Dec 1953

CONFIDENTIAL

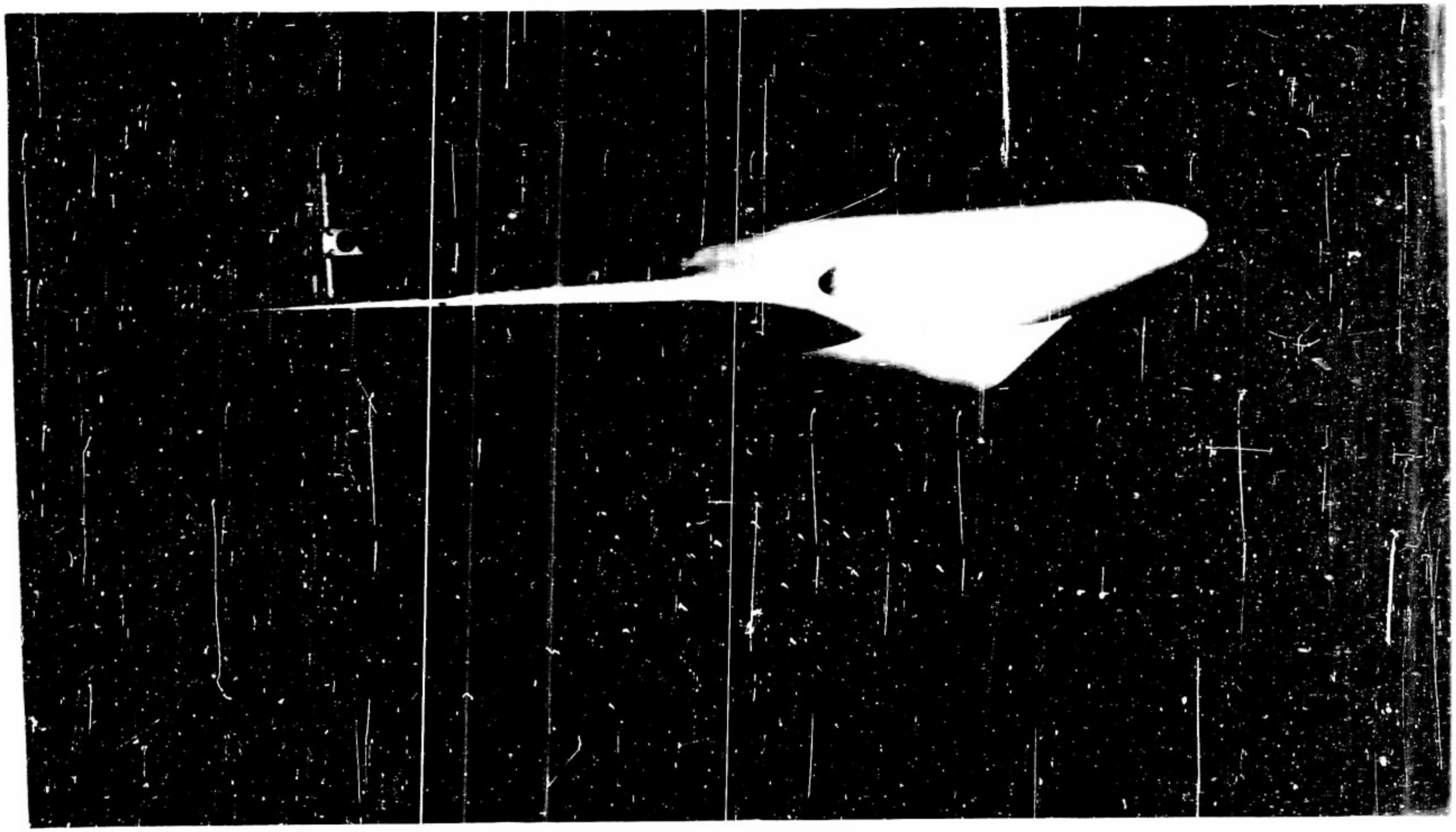

Figure 5 - View of a 0.17-Scale Model XAAM-N-4 Oriole Missile Sting Mounted at the Inboard Station (BL 16.26) on a 0.179-Scale Model F4D-1 Airplane Installed Inverted in the Wind Tunnel, x = 13.26", z = 0"

NP21-55299

2 Dec 1953

CONFIDENTIAL

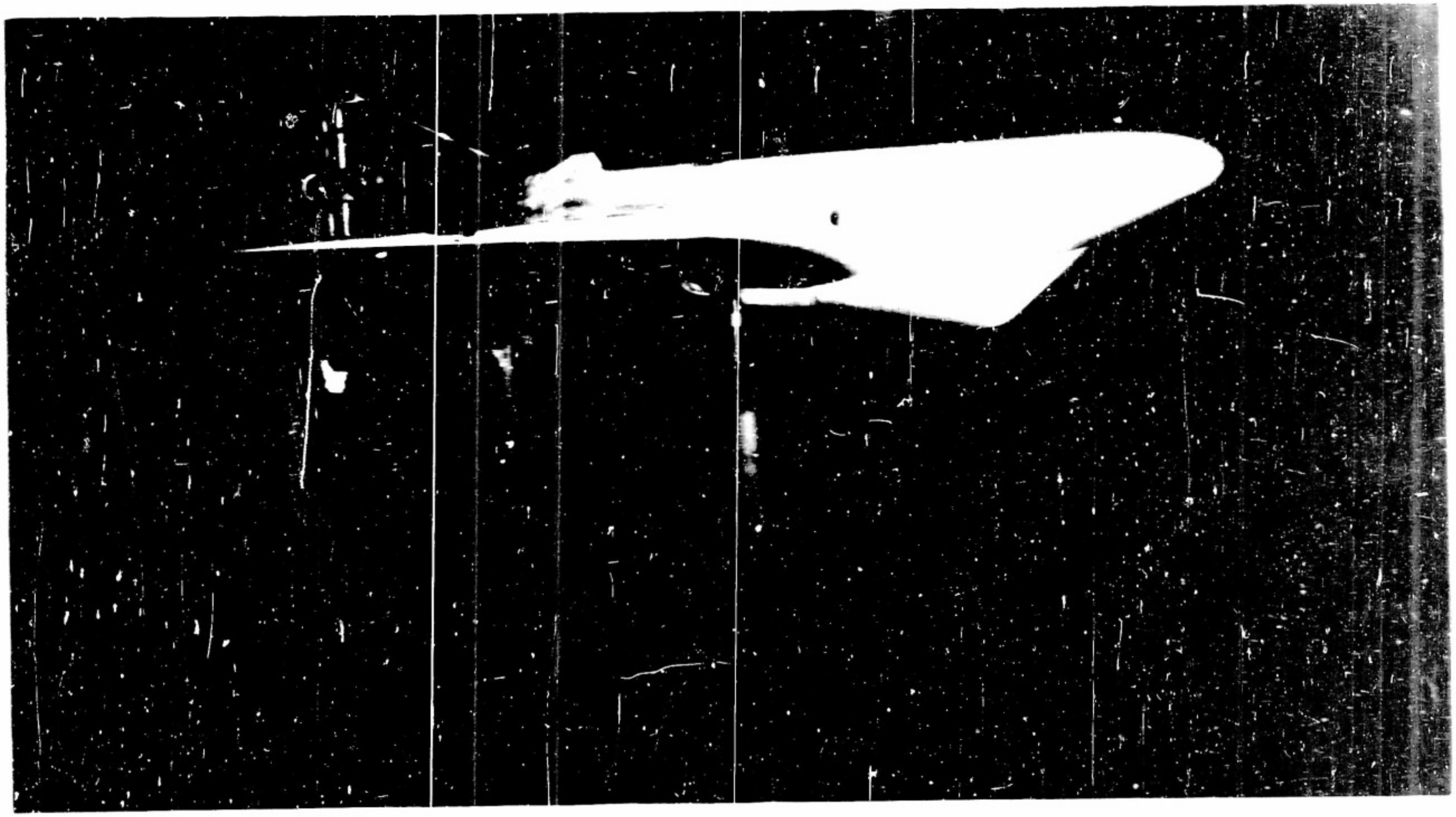

Figure 6 - View of a 0.17-Scale Model XAAM-N-4 Oriole Missile Sting Mounted at the Outboard Station (BL 22.81) on a 0.179-Scale Model F4D-1 Airplane Installed Inverted in the Wind Tunnel, x = 0", z = 0"

NP21-55302

2 Dec 1953

CONFIDENTIAL

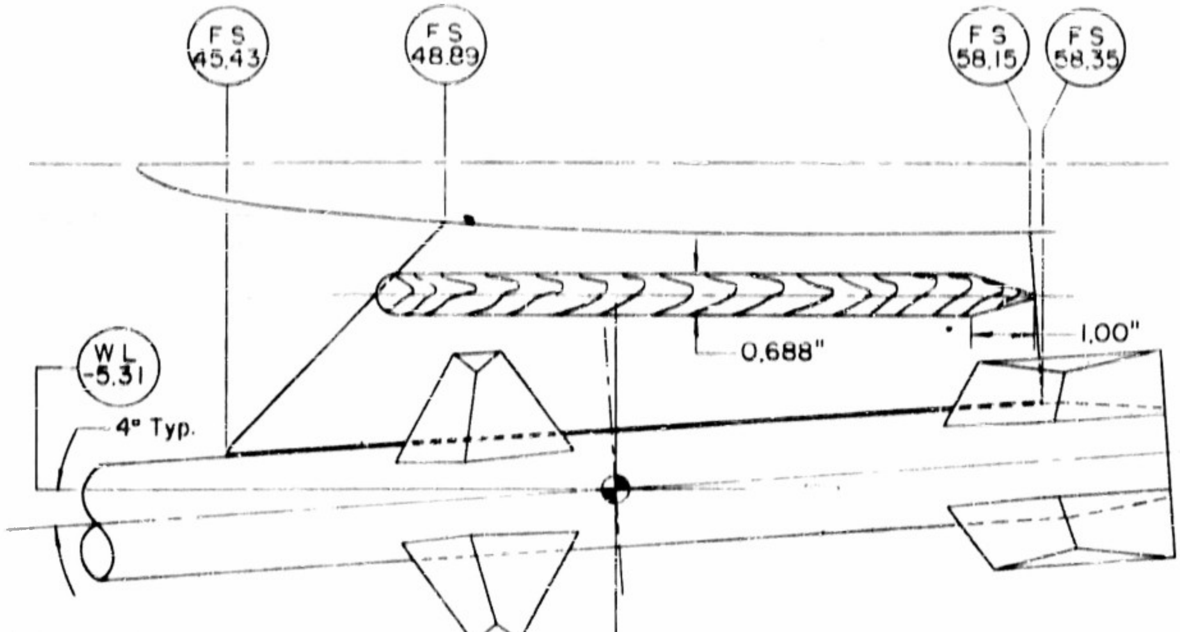

C-G Location

Pylon / Sta	1	2	3	4	5
F S In.	51.43	48.49	48.63	51.46	51.47
W L In.	-5.27	-4.34	-6.34	-6.27	-4.34

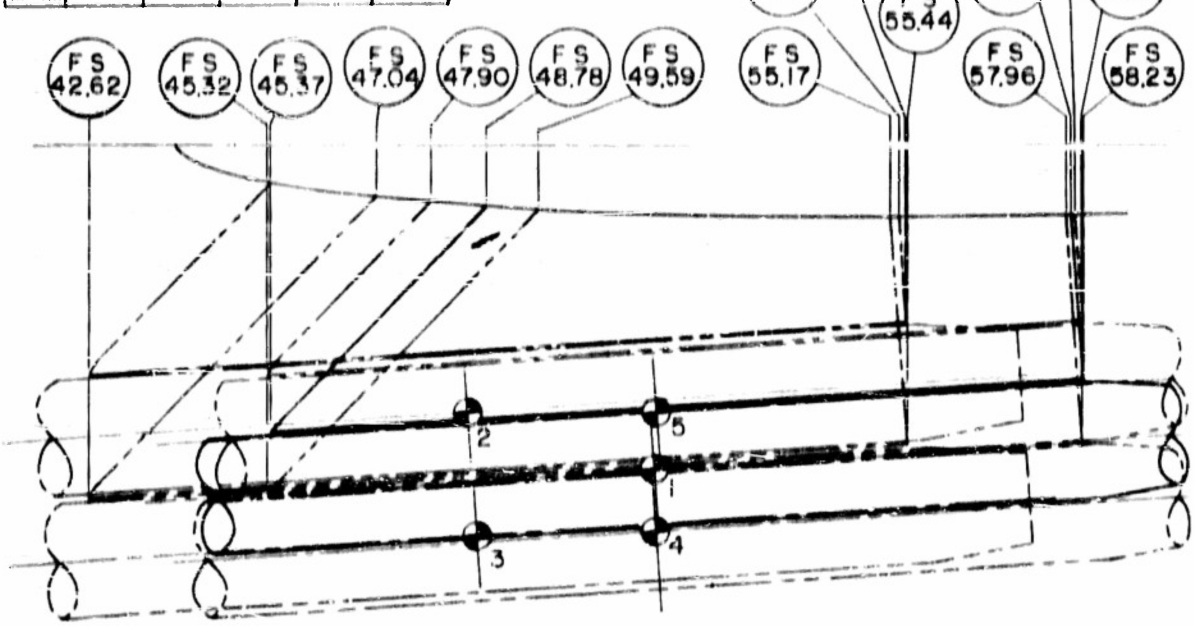

Figure 7 Pylon Design and Missile Center-of-Gravity Locations for Attachment of a 0.17-Scale Model XAAM-N-4 Oriole Missile on a 0.179-Scale Model F4D-1 Airplane
(a) Inboard Station (B L 16.26)

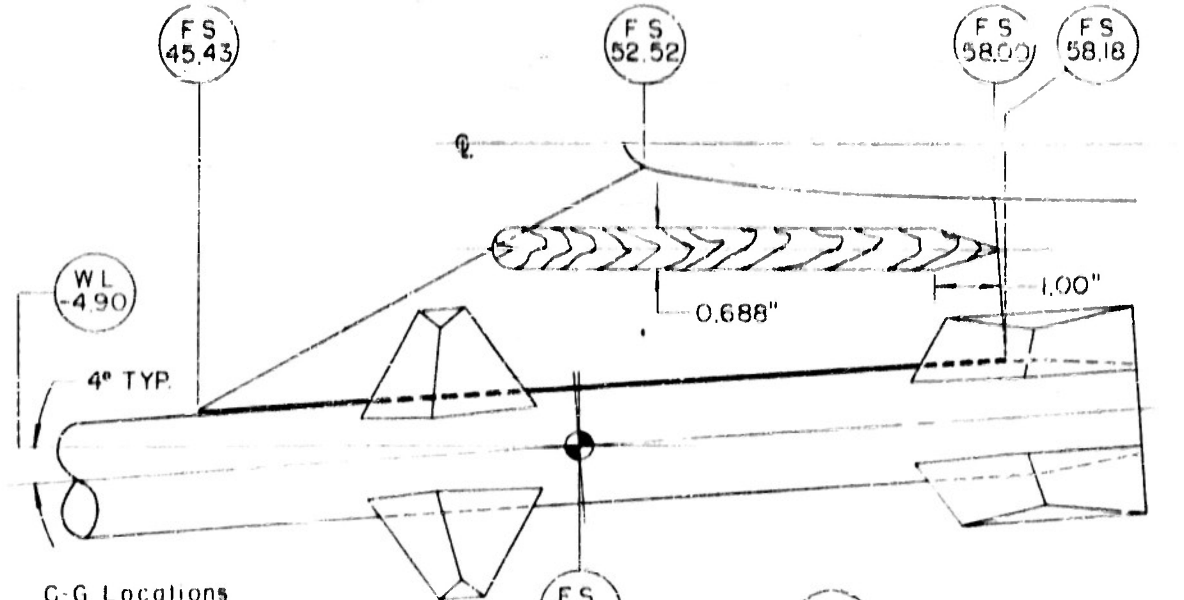

C-G Locations

Pyl n / Sta	6	7	8	9	10
F S in.	51.58	50.70	50.58	54.63	54.63
W L in.	-4.83	-4.22	-5.50	-5.64	-4.41

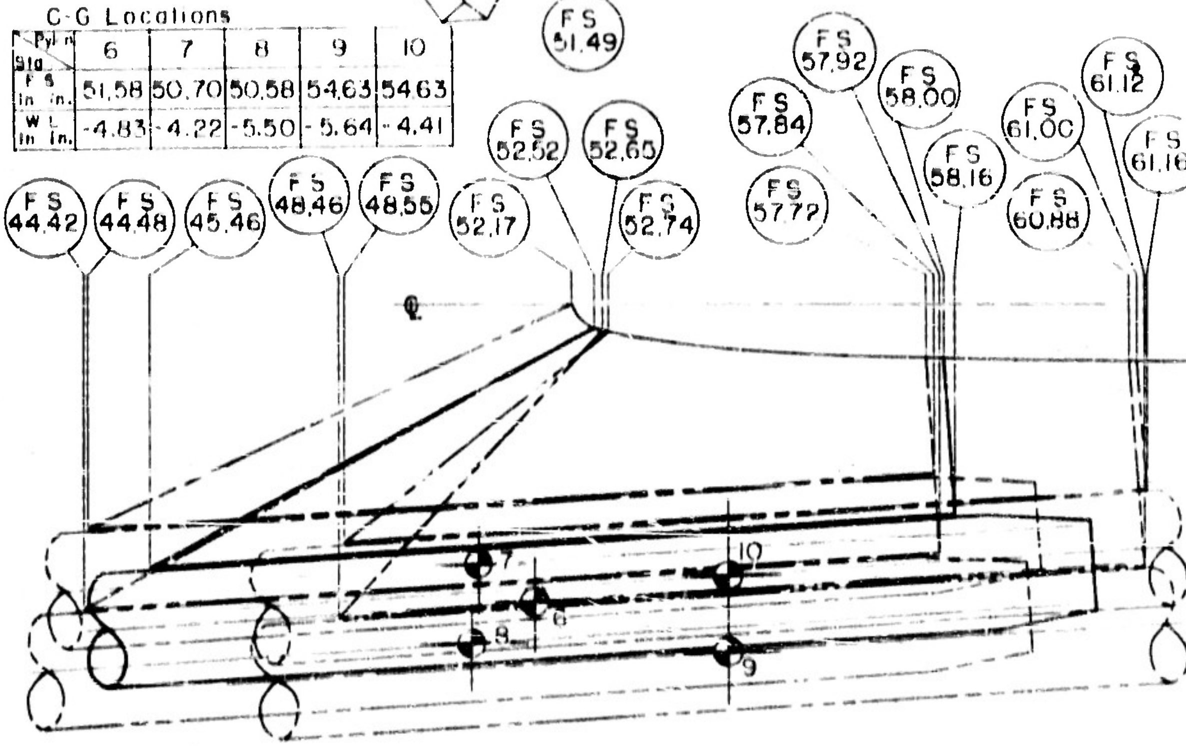

Figure 7 (Concluded)
(b) Outboard Station
(BL 22.87)

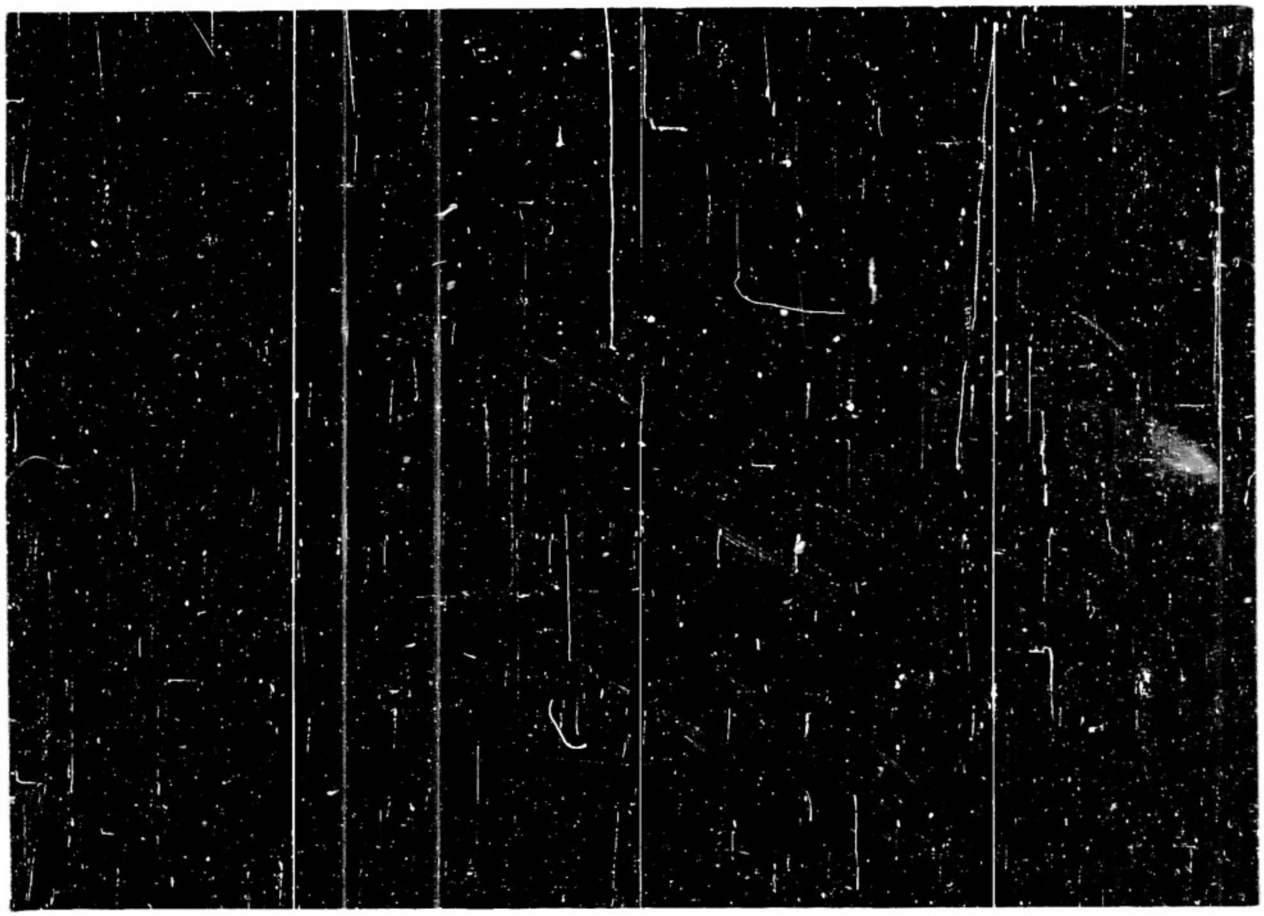

Figure 8 - View of a 0.17-Scale Model XAAM-N-4 Oriole Missile Mounted Directly to the Pylon at the Inboard Station (BL 16.26) on a 0.179-Scale Model F4D-1 Airplane Installed Inverted in the Wind Tunnel

NP21-55353 14 Dec 1953

CONFIDENTIAL

CONFIDENTIAL

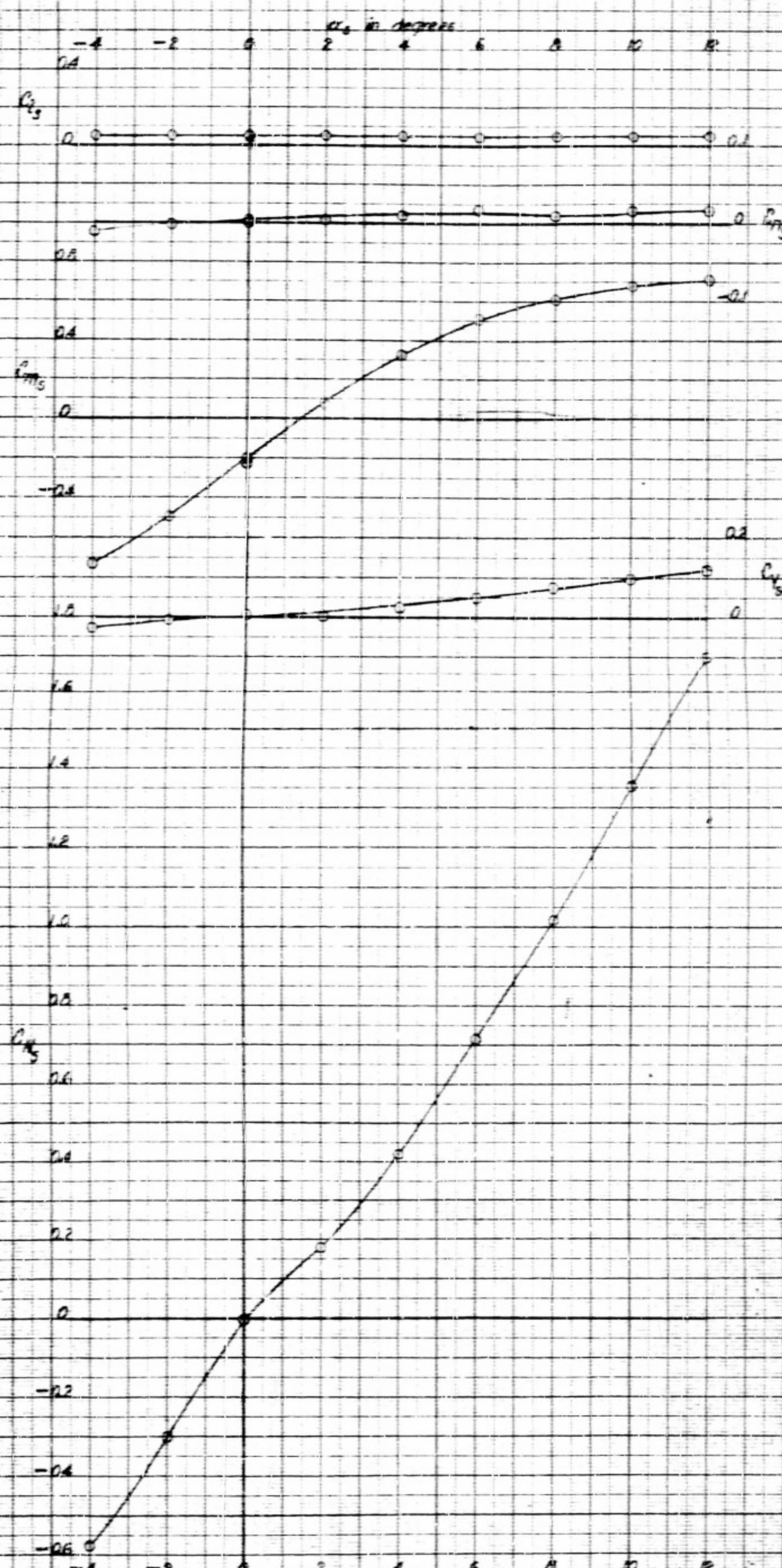

Figure 9—Aerodynamic Characteristics of a 0.17-Scale Model of the XAAM-N-4 Oriole Missile Sting Mounted Alone in the Wind Tunnel.
Sting Mounted in Pitch Plane

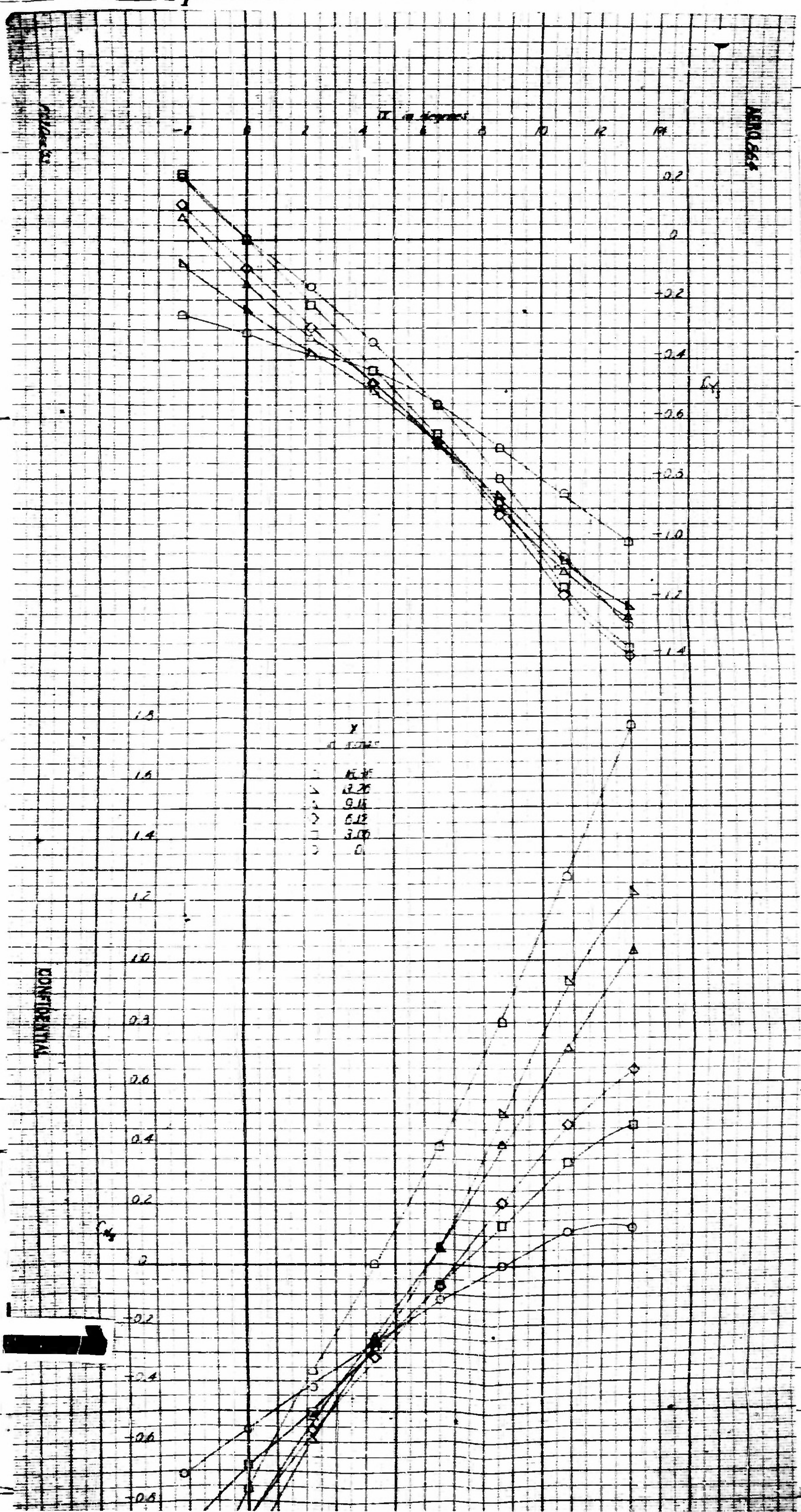
AERO 864
CONFIDENTIAL
-2
0
2
4
6
8
10
12
14
0.2
0
-0.2
-0.4
-0.6
-0.8
-1.0
-1.2
-1.4
1.8
1.6
1.4
1.2
1.0
0.8
0.6
0.4
0.2
0
-0.2
-0.4
-0.6
-0.8
γ
6.12
3.06
0

[redacted]

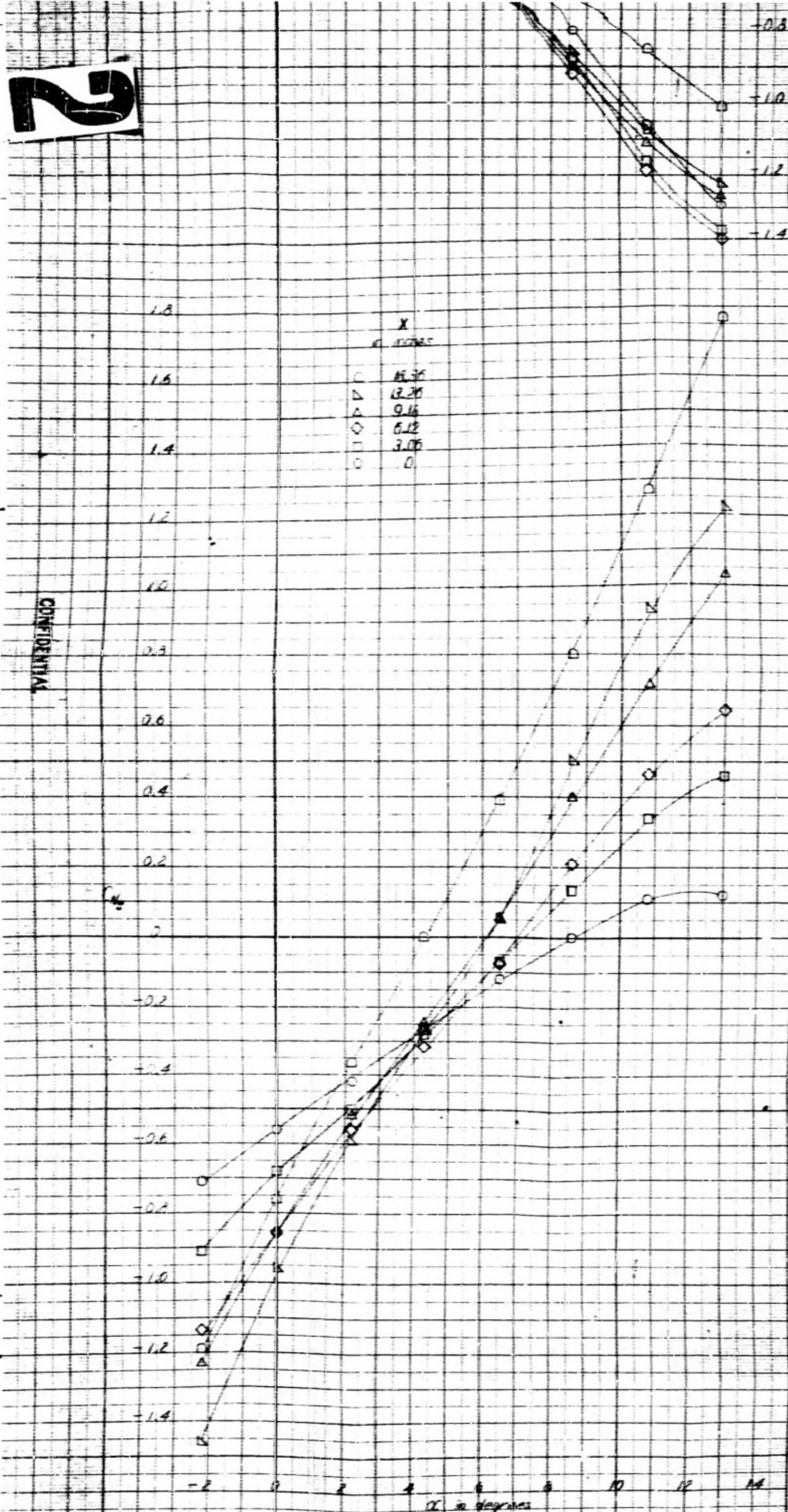

Figure 10 - Aerodynamic Characteristics of a 0.17-Scale Model XAAM-N-4 Oriole Missile for Various Distances Forward of the Carry Position in the Proximity of a 0.179-Scale Model F4D-1 Airplane at the Inboard Station

(a) $z = 0$ Inch, $\theta_c = 0°$, $\psi_c = 0°$, $\phi = 0°$, Pylon On

CONFIDENTIAL

FIGURE 10a

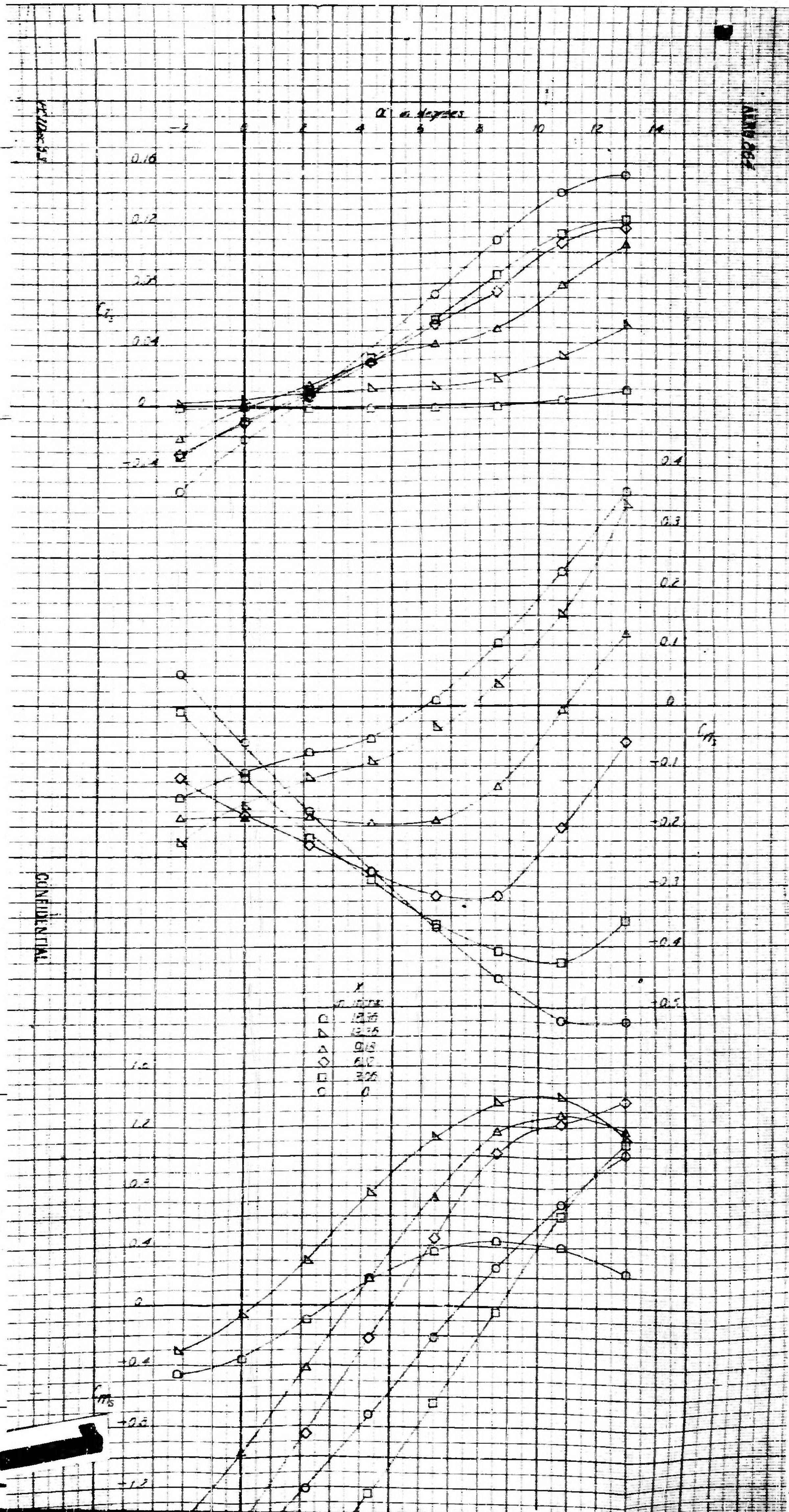
α in degrees
CONFIDENTIAL

CONFIDENTIAL

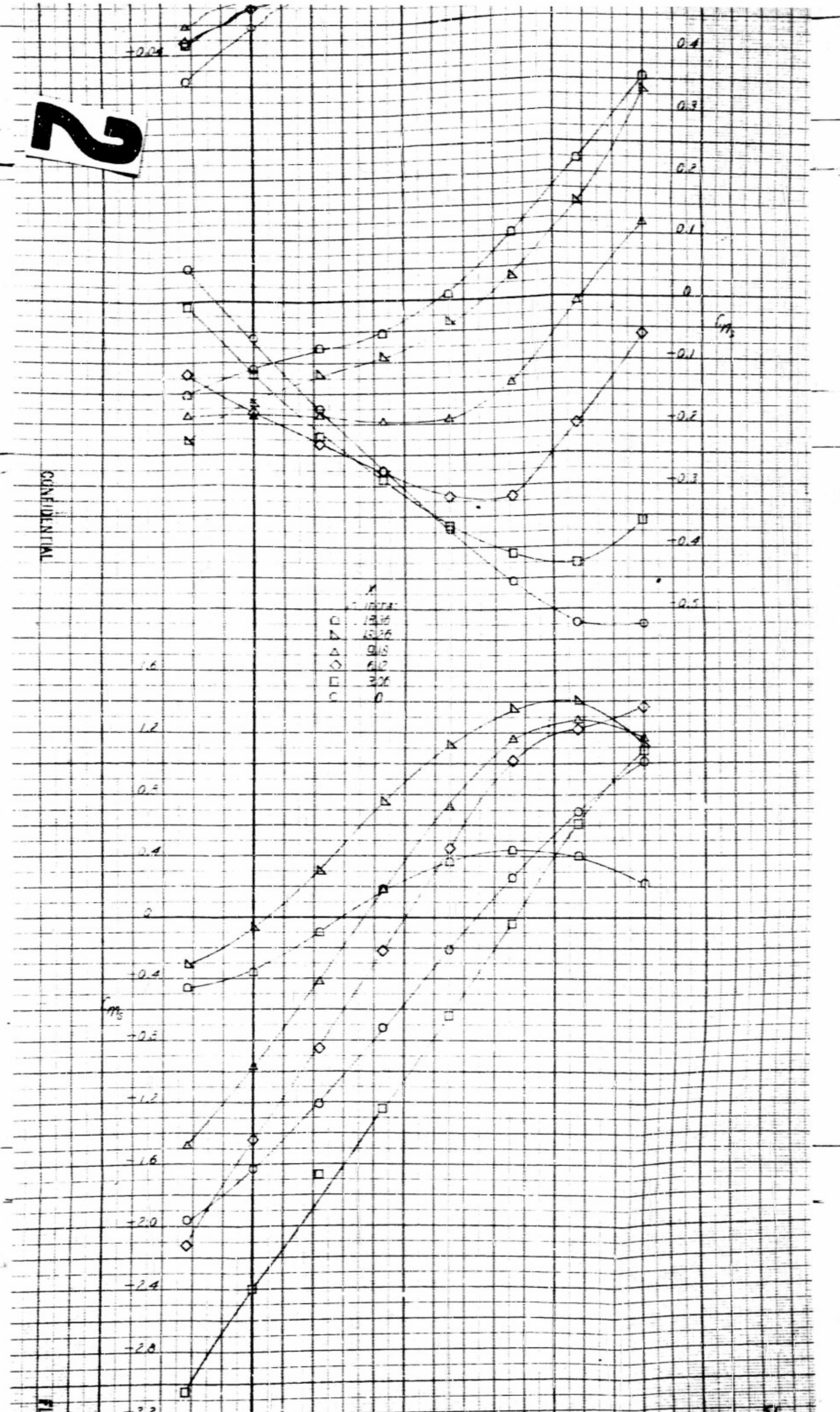

Figure 10 (Continued)

(b) Concluded

CONFIDENTIAL

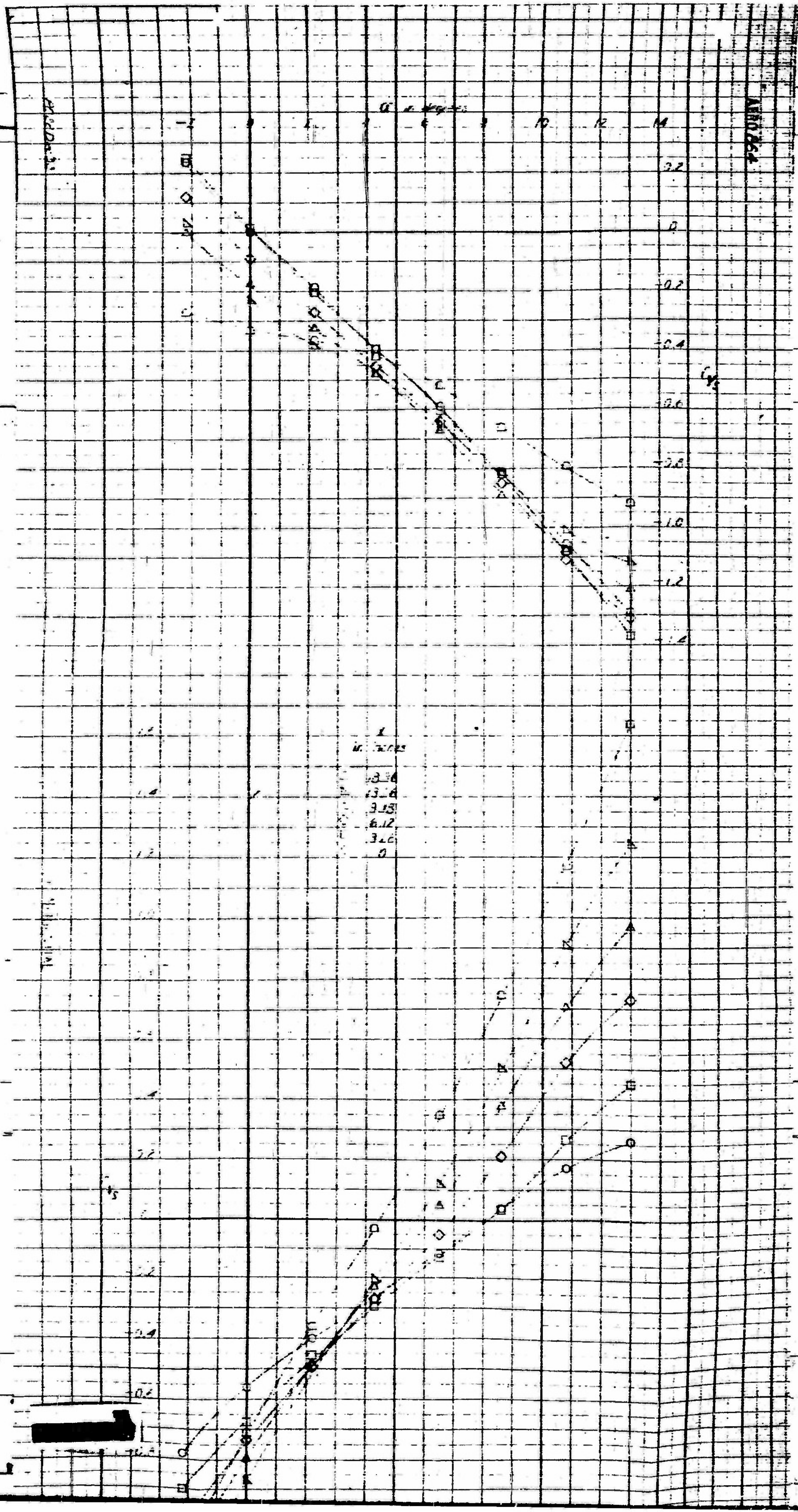
AERO 864

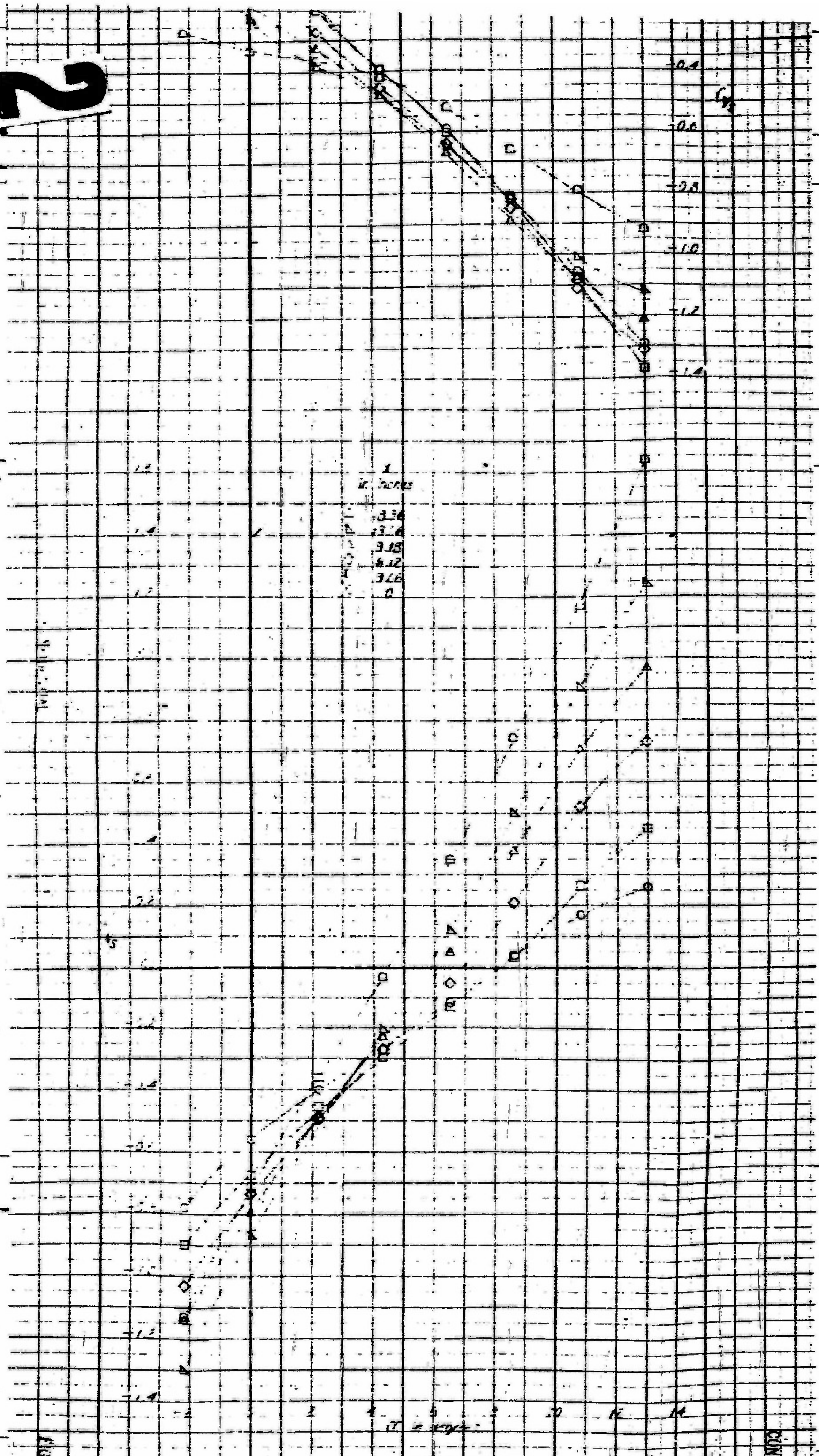

Figure 10 (Continued)

(j) z = 1.02 Inches. $\theta_c = 0°$, $\delta_s = 0°$, $\phi = 0°$, Fin on

CONFIDENTIAL

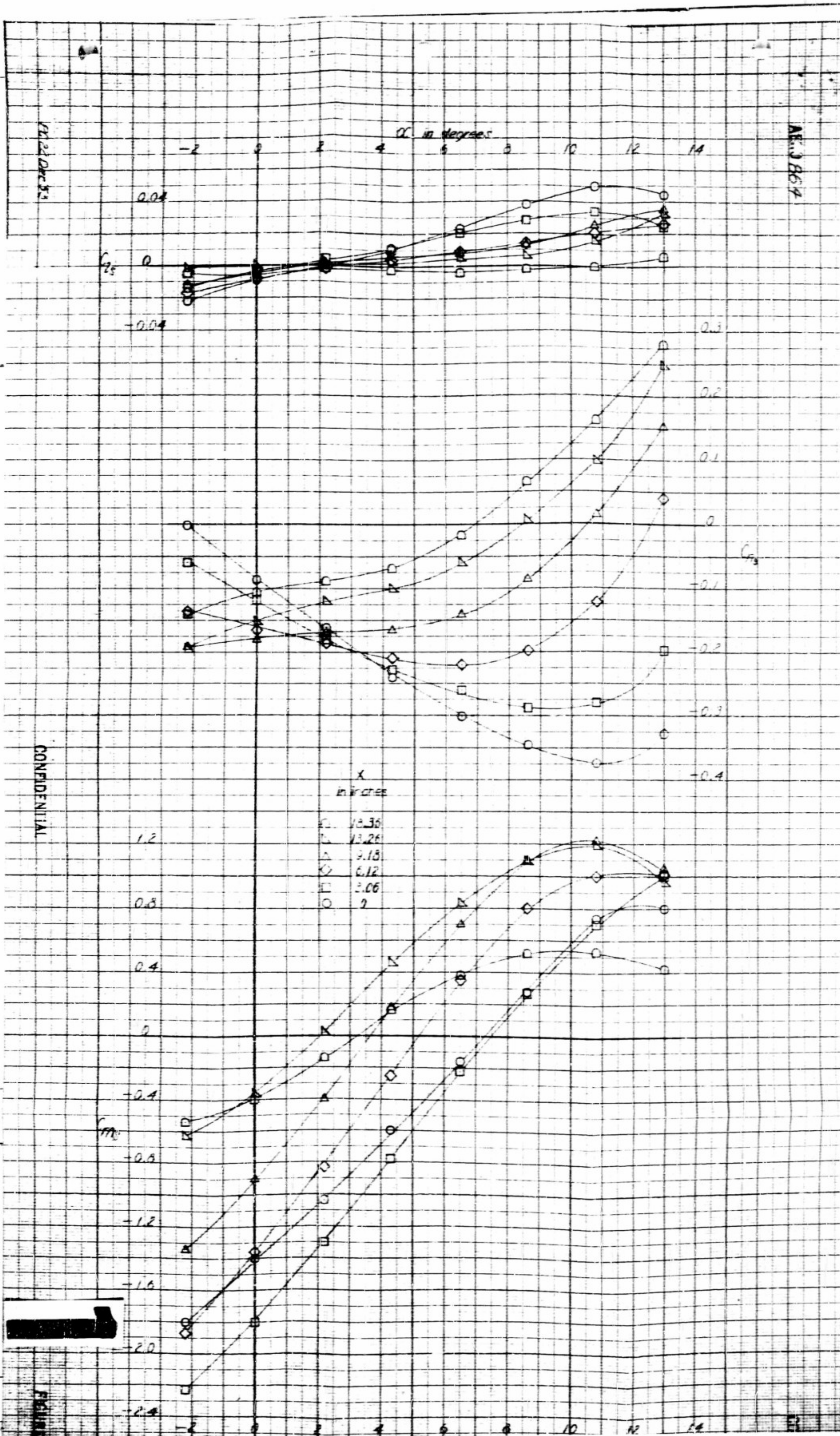

α in degrees
C_{l_S}
C_{n_S}
C_{m_S}
x in inches
18.36
15.26
9.18
6.12
3.06
0
CONFIDENTIAL
AE.3864

[redacted]

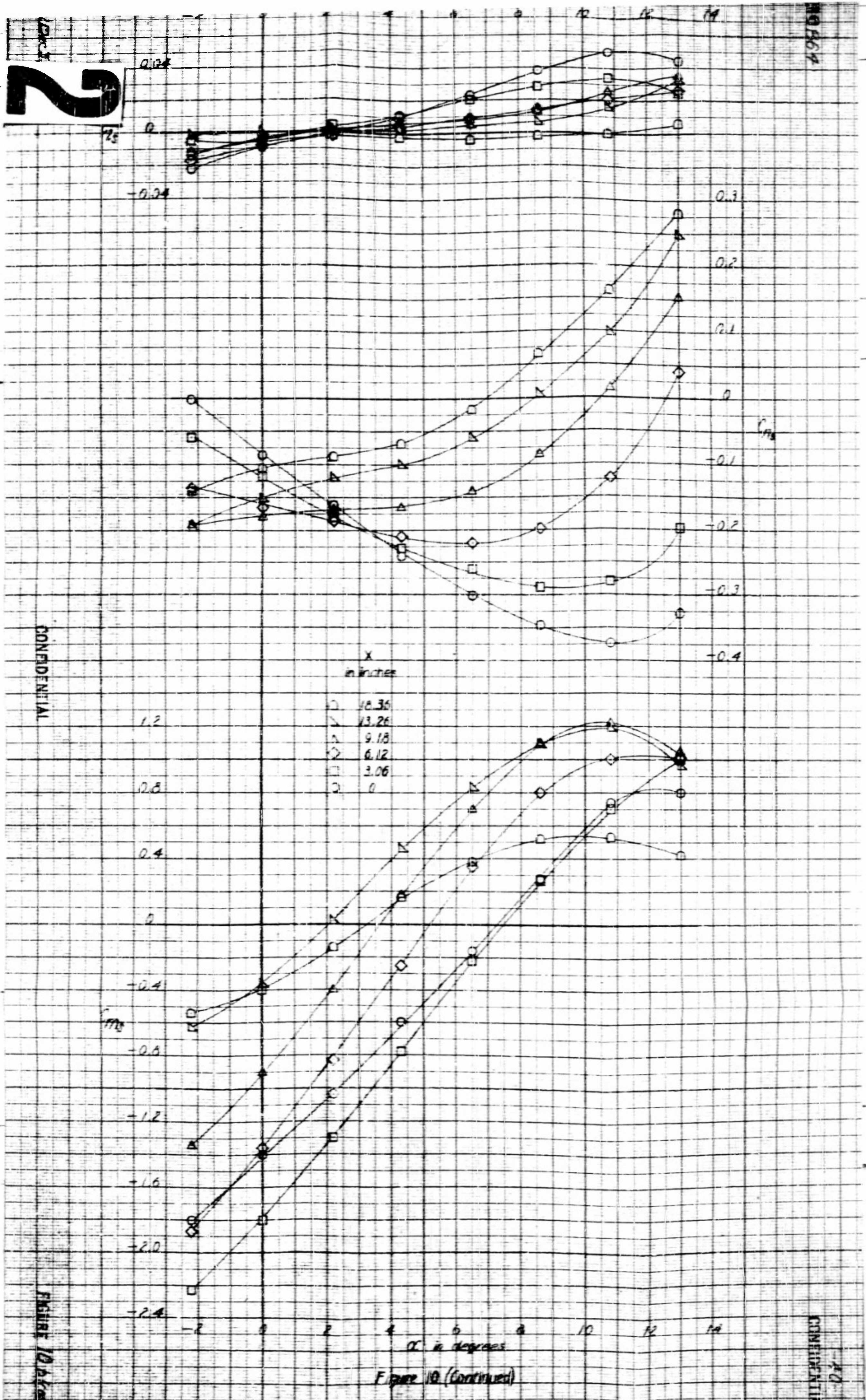

Figure 10 (Continued)

(b) Concluded

CONFIDENTIAL

FIGURE 10 (b) Concl'd

CONFIDENTIAL

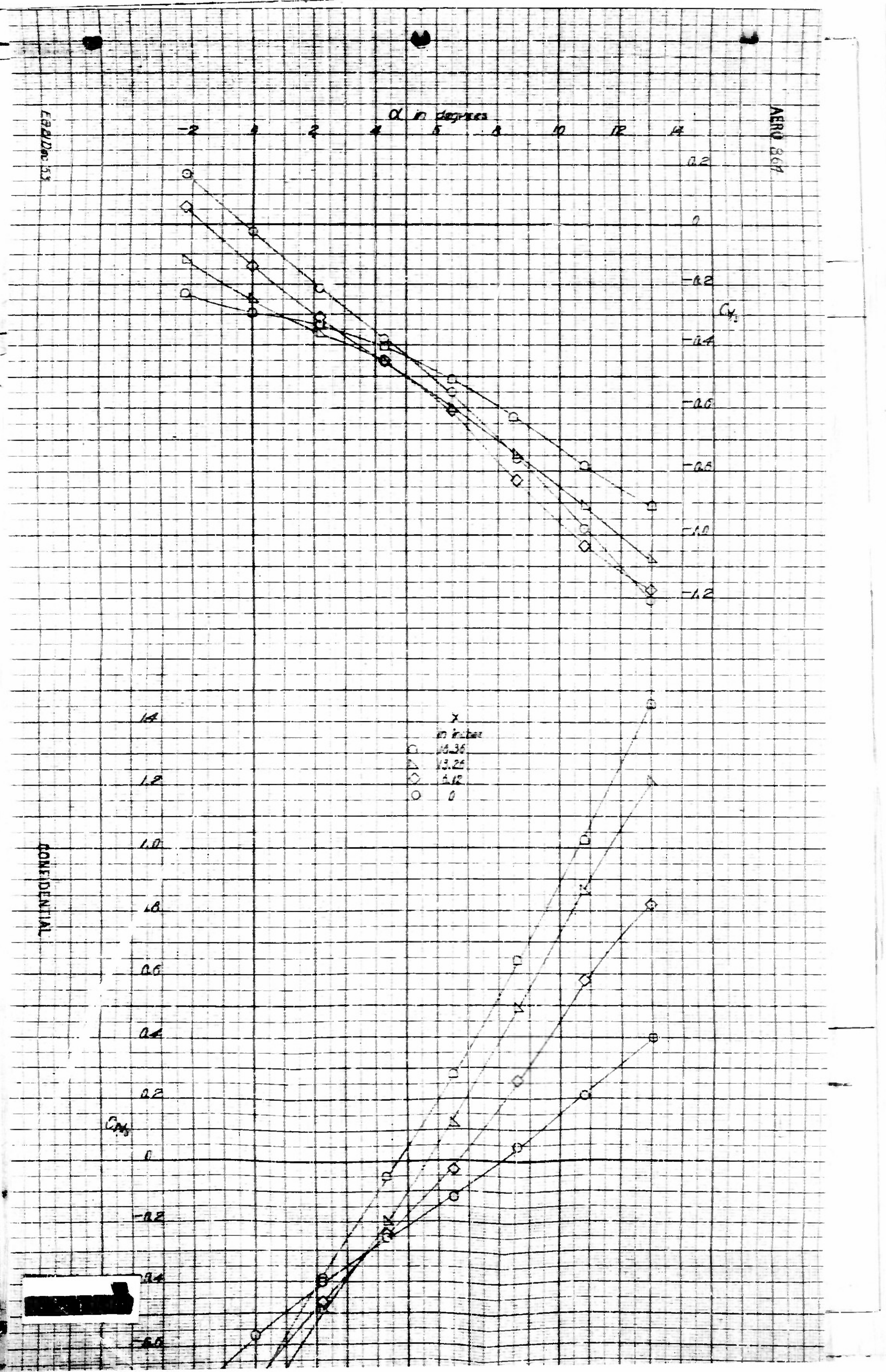

ERA/Doc 53

AERO 867

CONFIDENTIAL

[redacted]

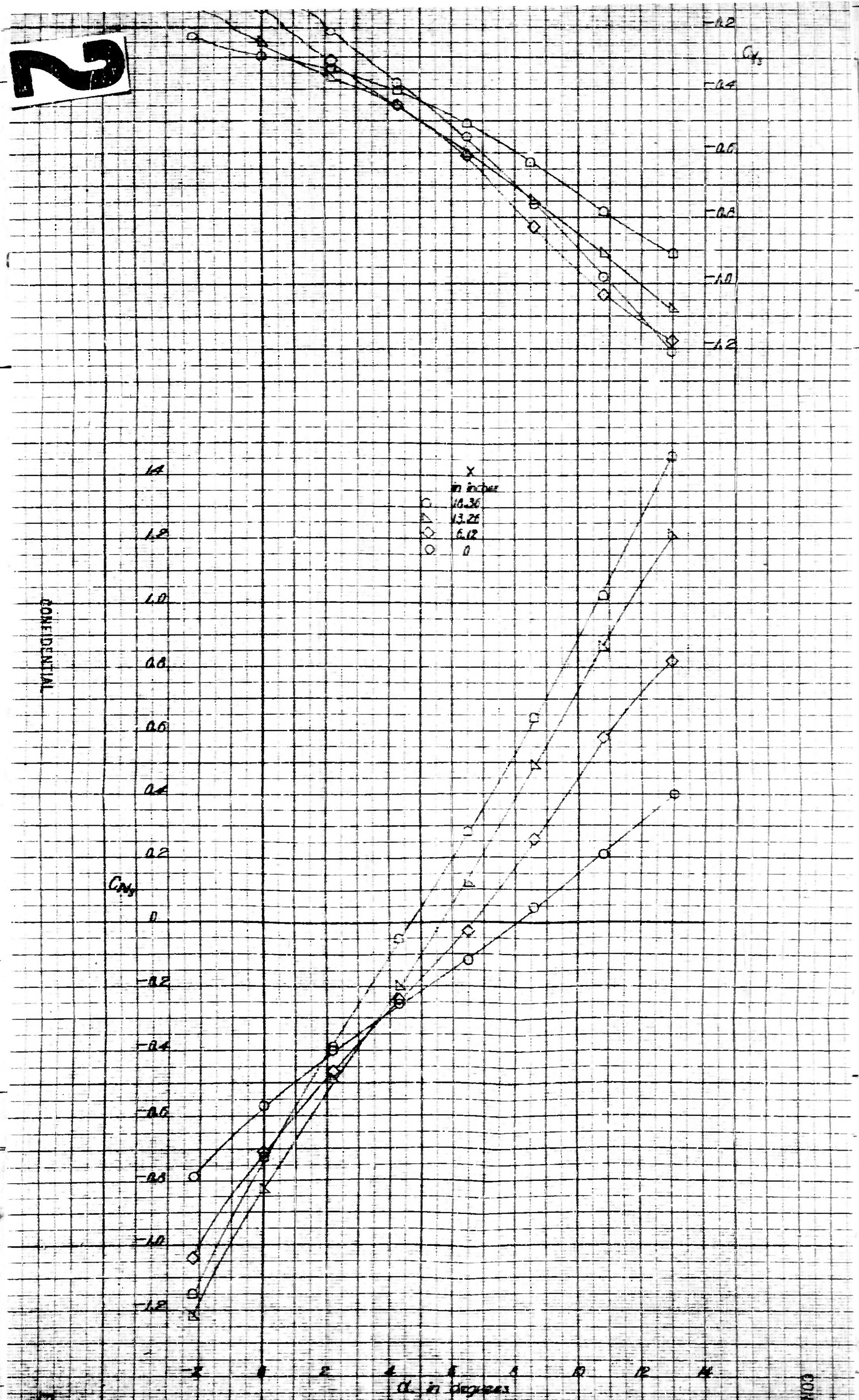

CONFIDENTIAL

AERO 864

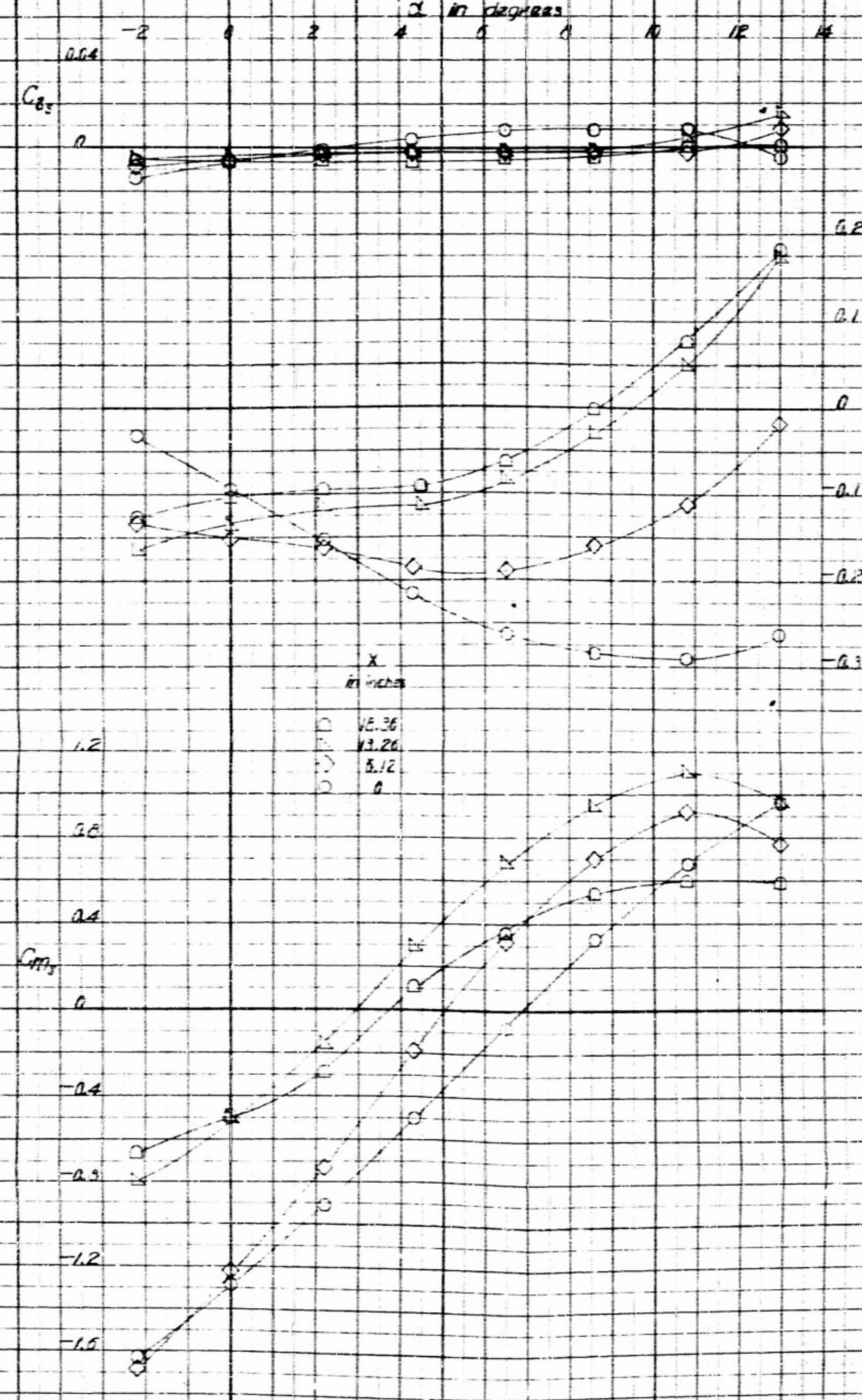

Figure 10 (Concluded)

(c) Concluded

CONFIDENTIAL

CONFIDENTIAL

AERO 864

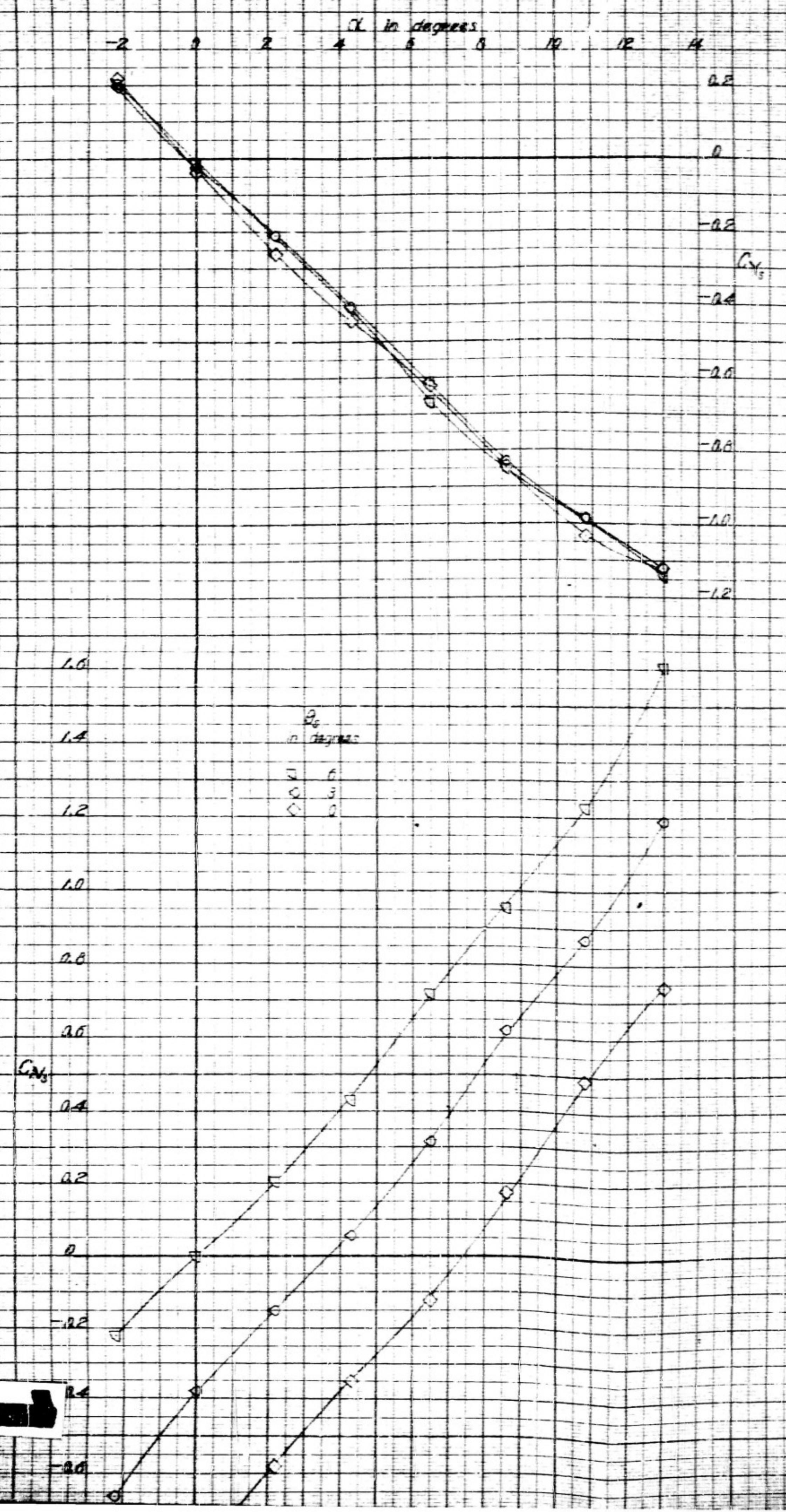

CONFIDENTIAL

[redacted]

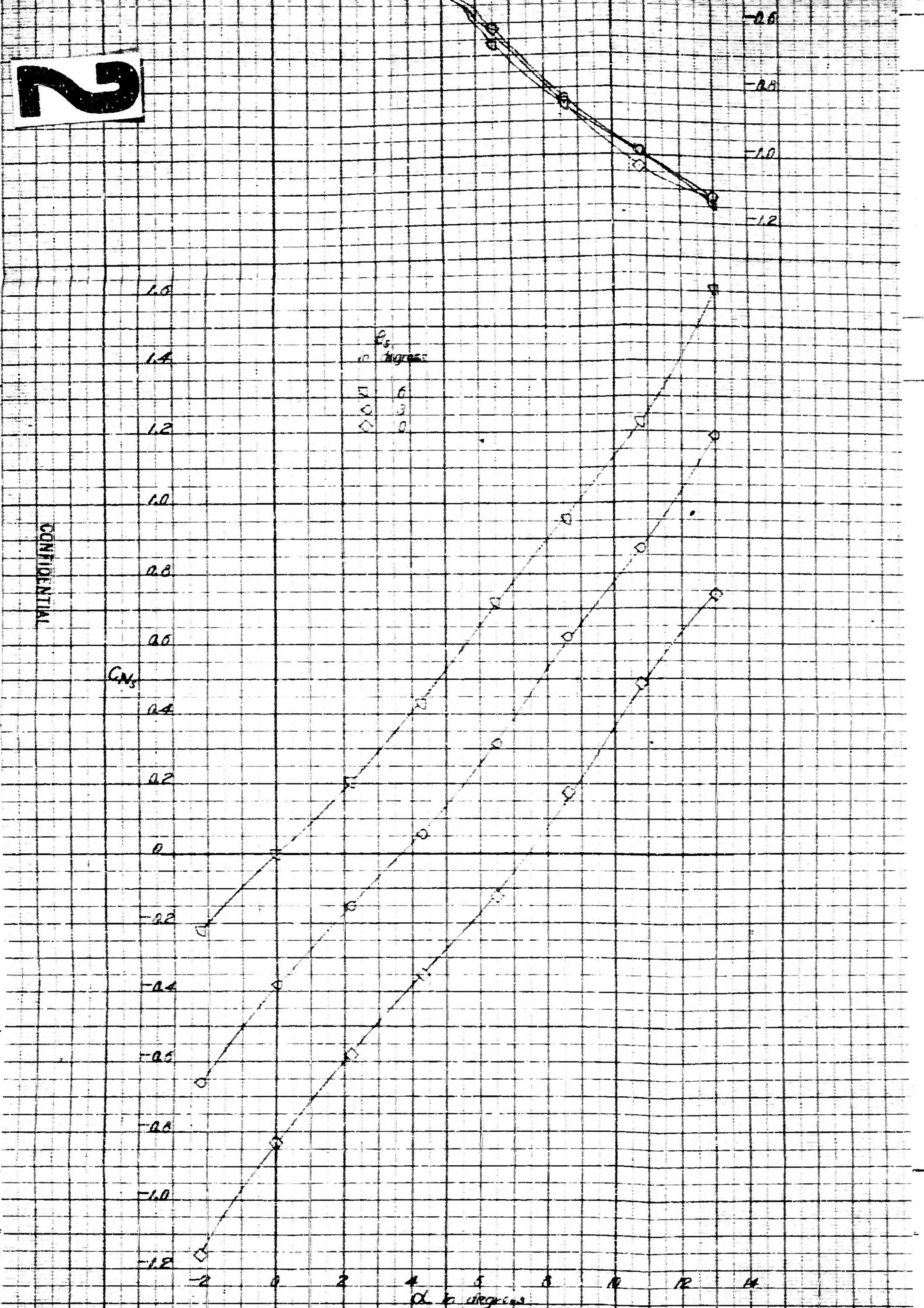

Figure 11. Aerodynamic Characteristics of a 0.17-Scale Model XAAM-N-4 Chale Missile Due to Missile Pitch in the Proximity of a 0.079-Scale Model F4D-1 Airplane at the Inboard Station

(a) $z = 0$ Inch, $x = 6.12$ Inches, $\psi_s = 0°$, $\psi = 0°$, Pylon Off

FIGURE 11a2

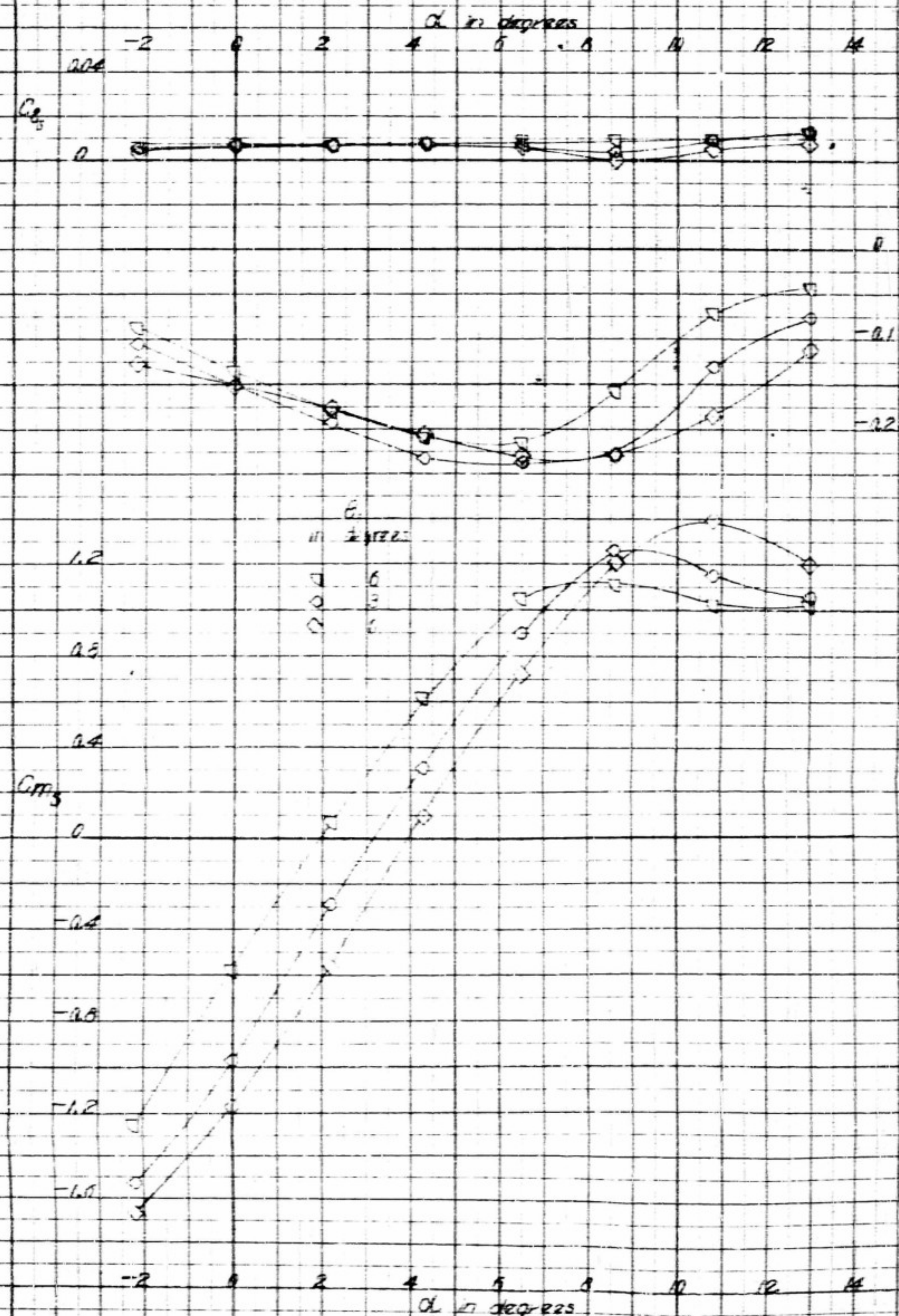

Figure 11 (Continued)

(a) Concluded

CONFIDENTIAL

FIGURE 11a (Cont'd)

CONFIDENTIAL

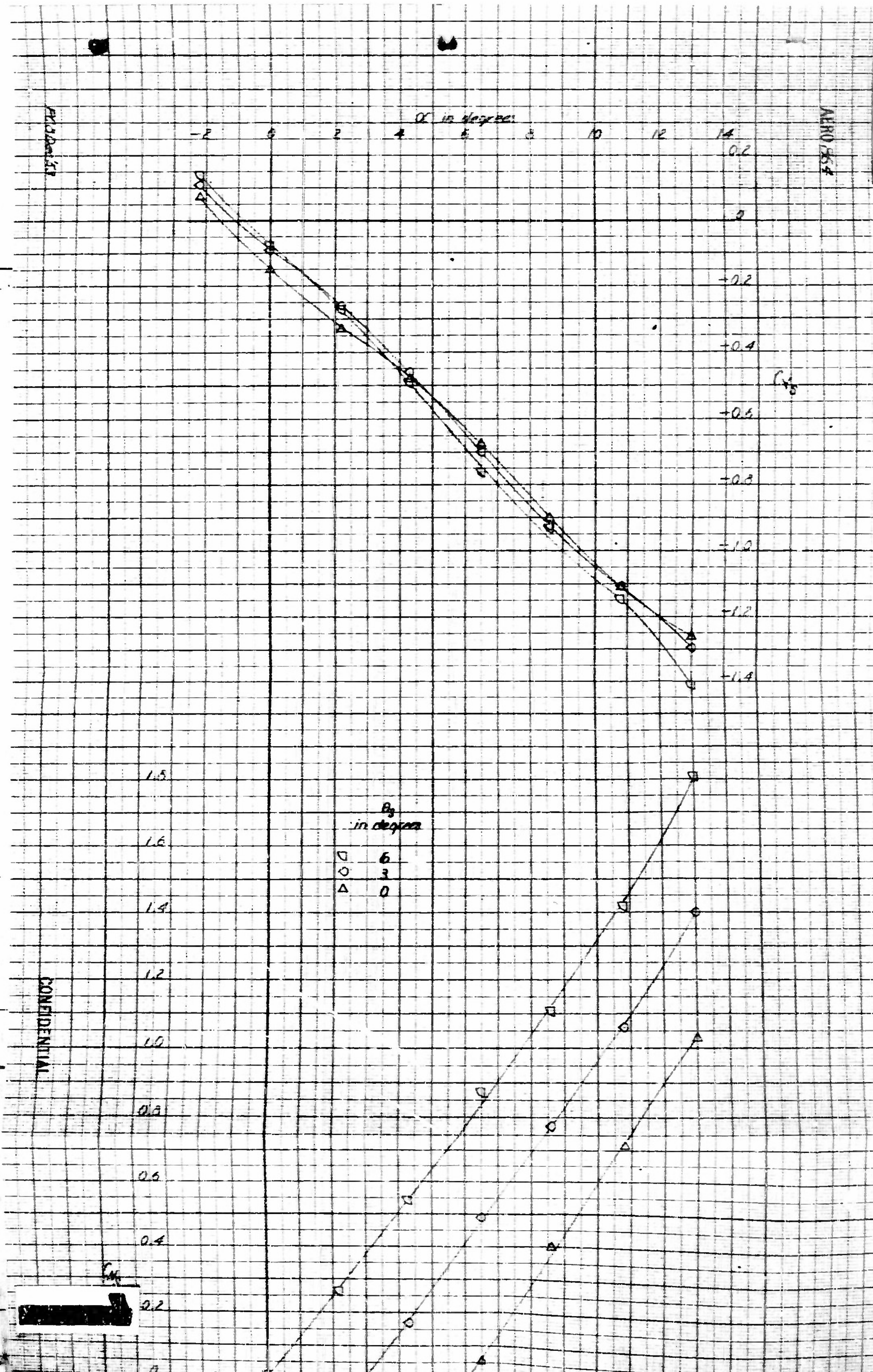

FIGURE 37

AERO 864

CONFIDENTIAL

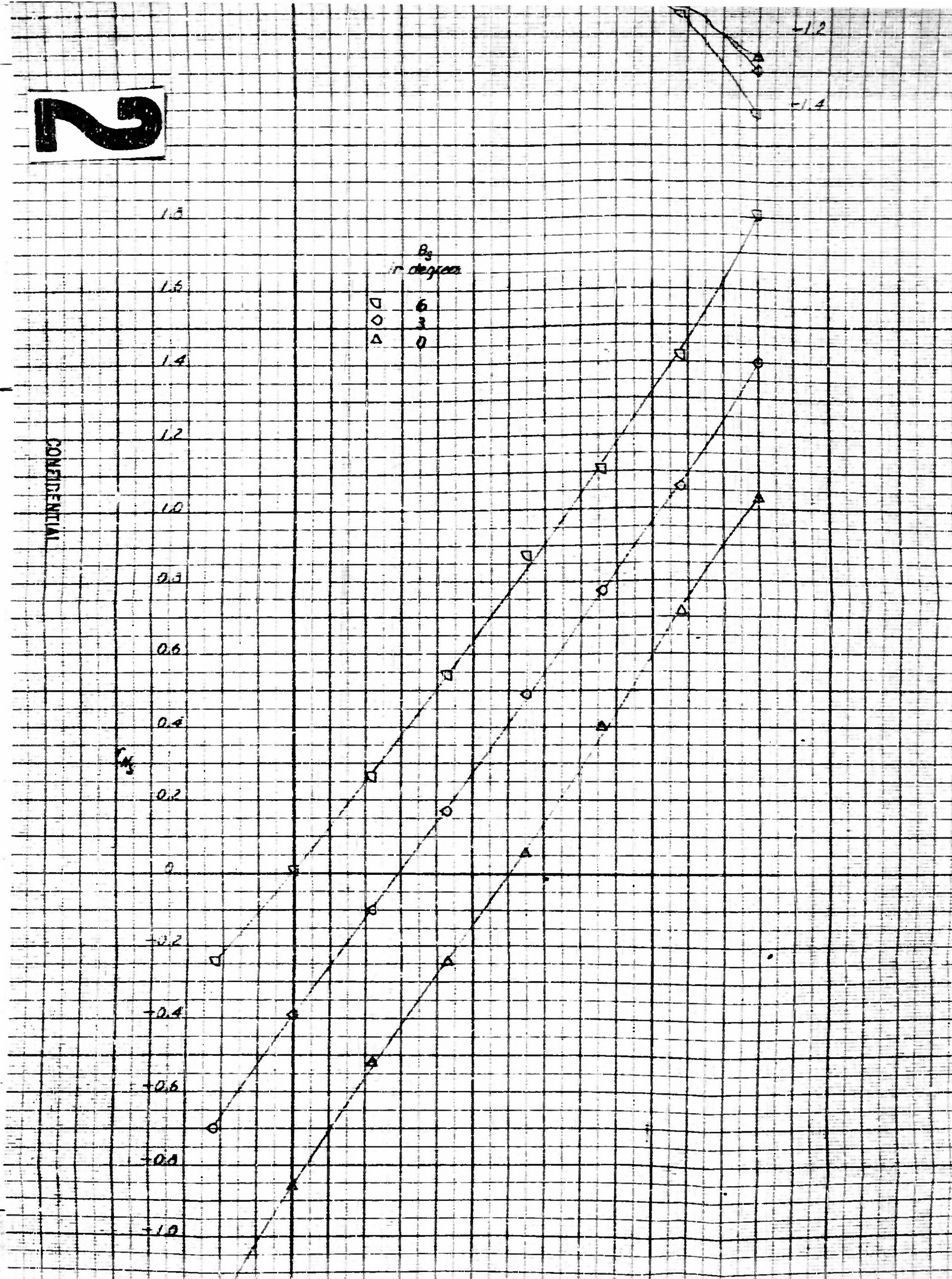

Figure 11 (Continued)

(b) z = 0 Inch, x = 9.18 Inches, M_s = 0, ψ = 0°, Pylon On

FIGURE 11 b

CONFIDENTIAL

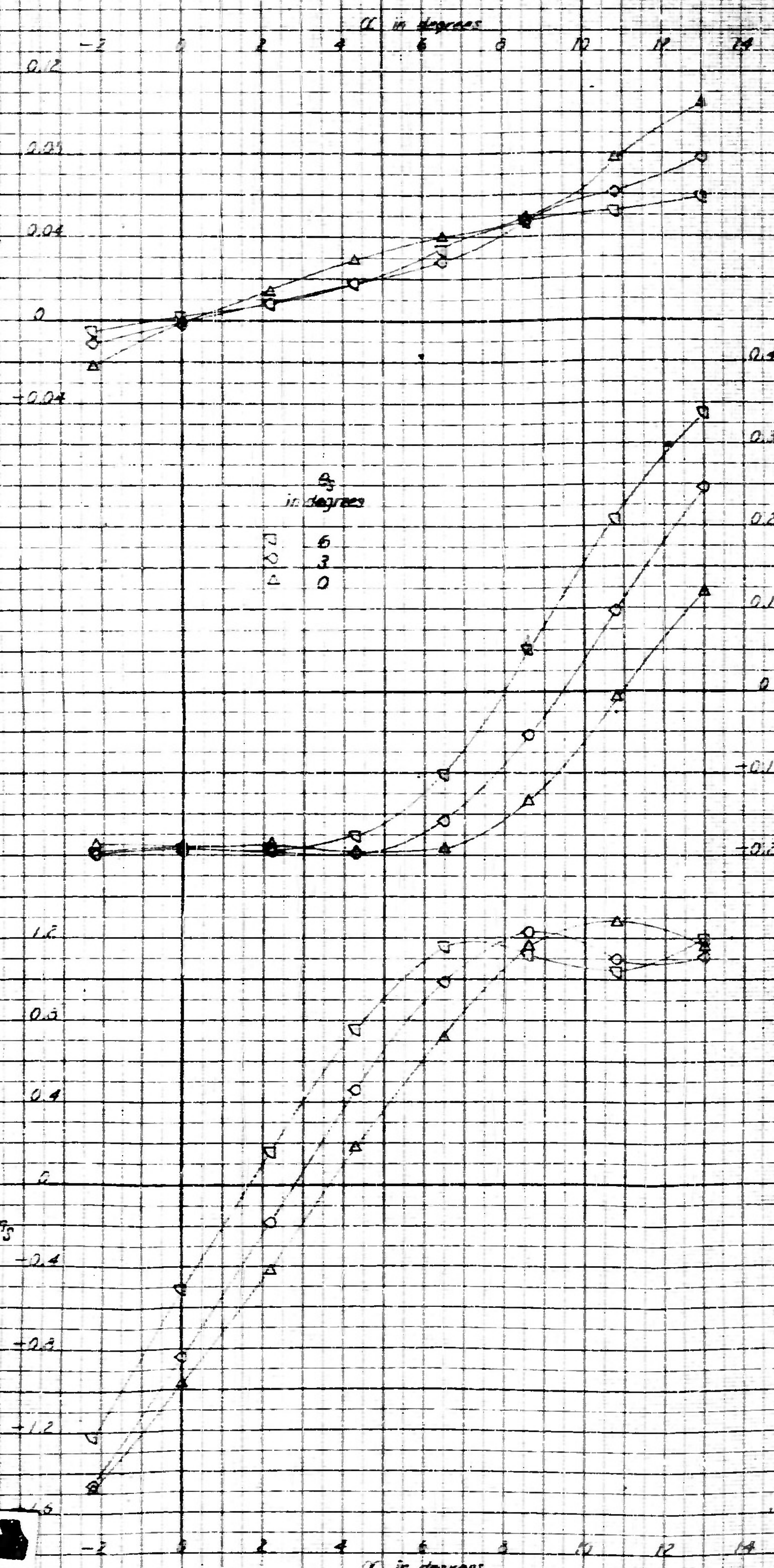

Figure 11 (Continued)

(b) Concluded

CONFIDENTIAL

[redacted]

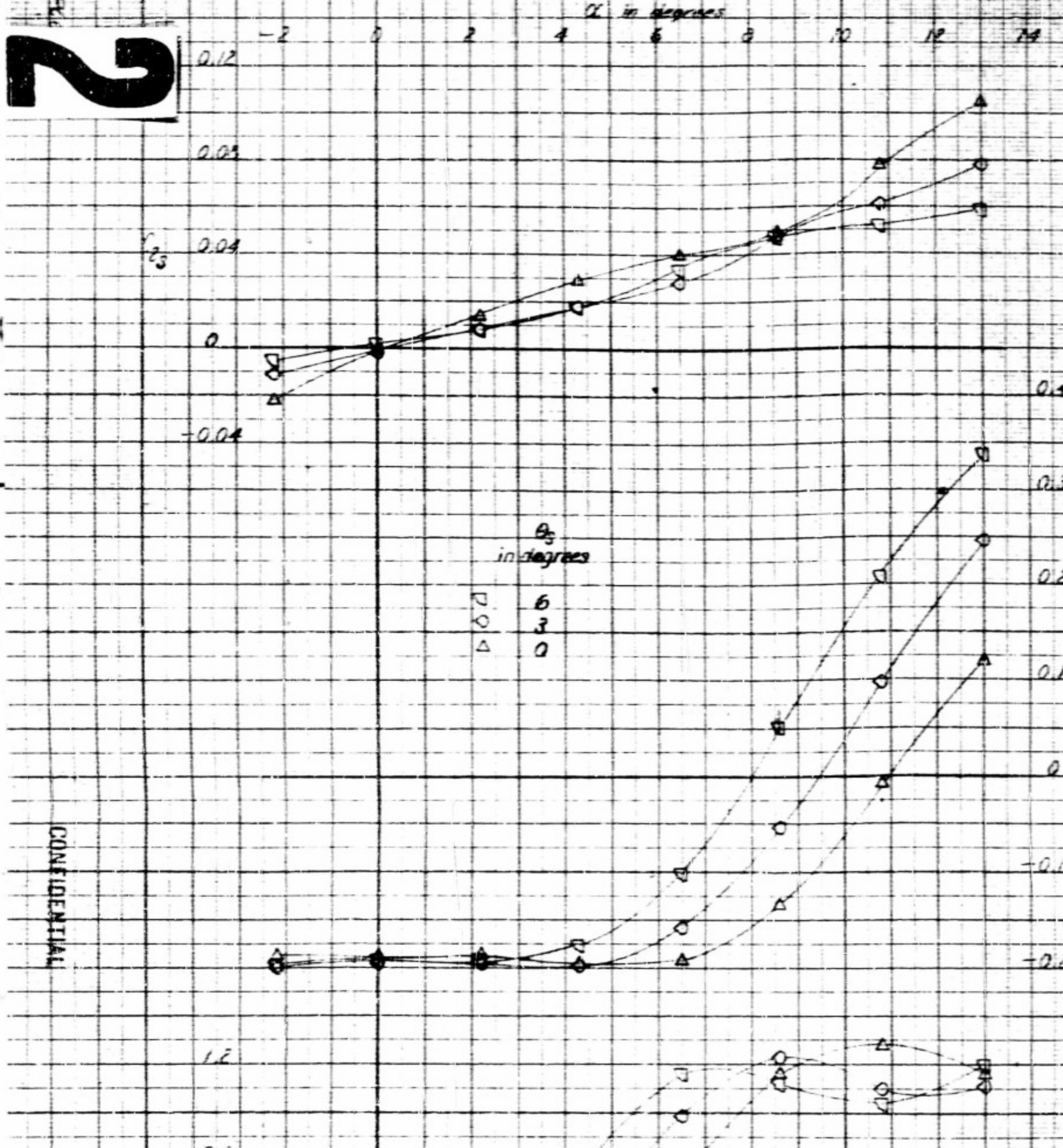

Figure 11 (Continued)

(b) Concluded

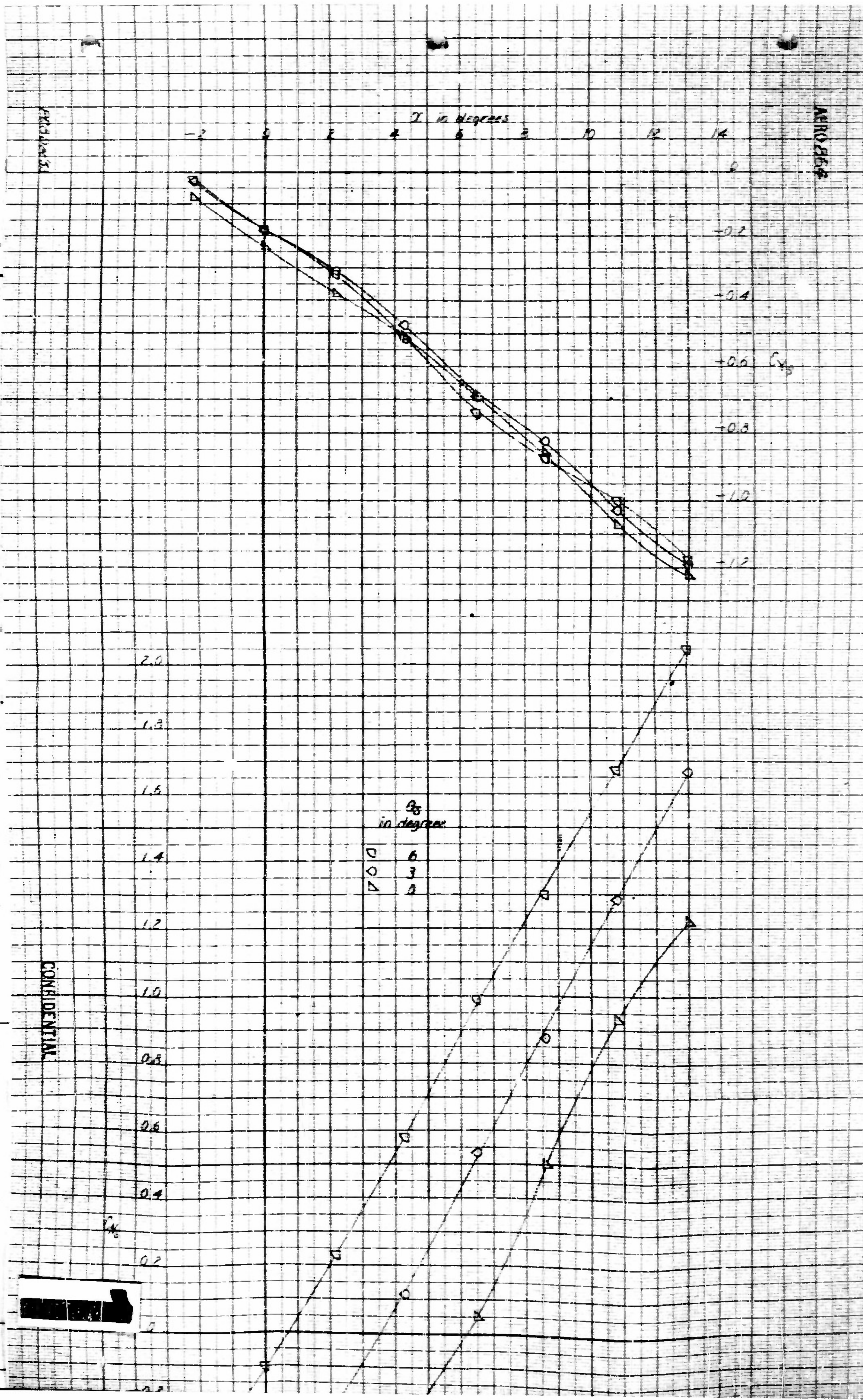

CONFIDENTIAL

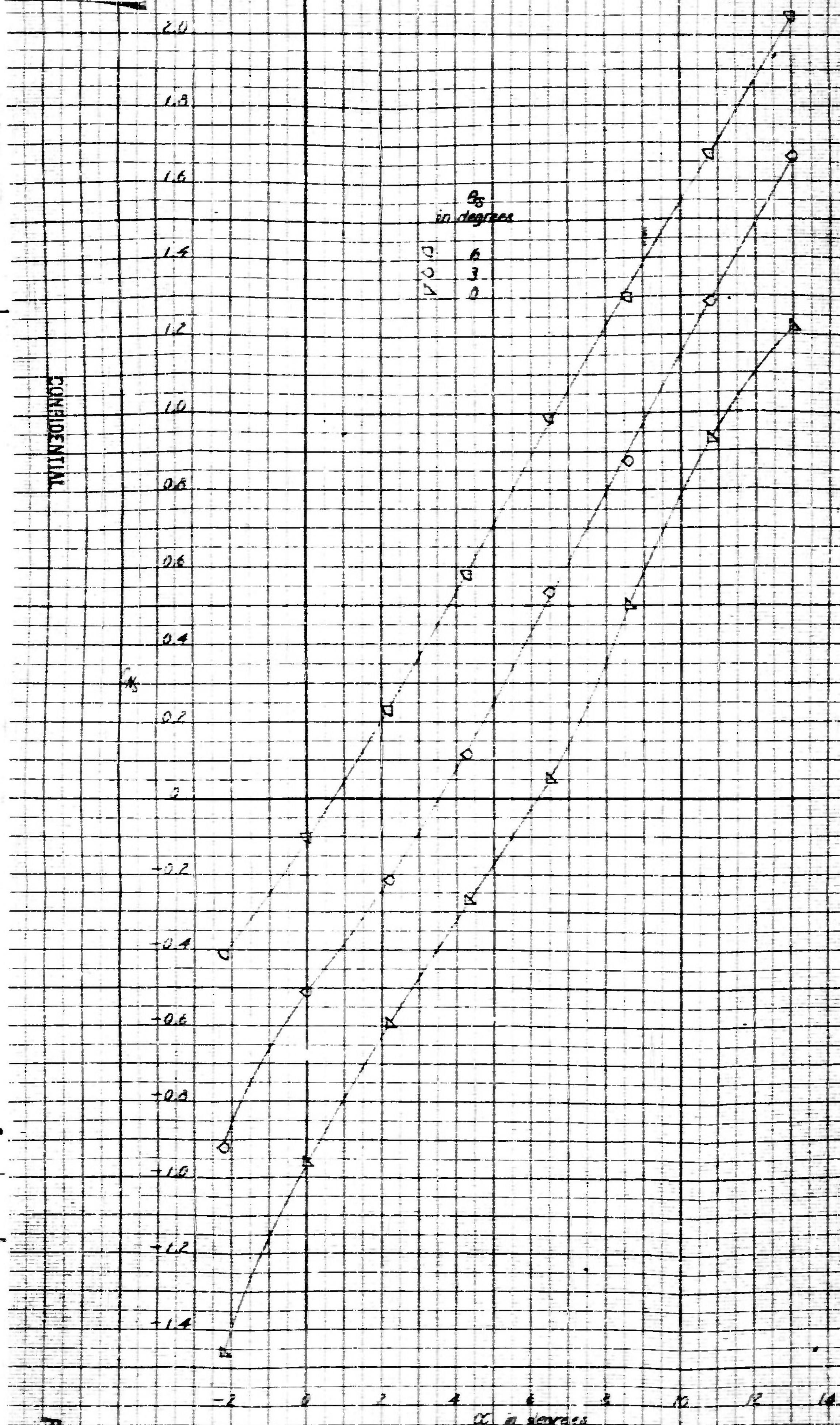

Figure 11 (Continued)

(c) τ = 0 Inch, x = 13.26 Inches, ψ_s = 0°, β = 0°, Pylon On

FIGURE 11 C

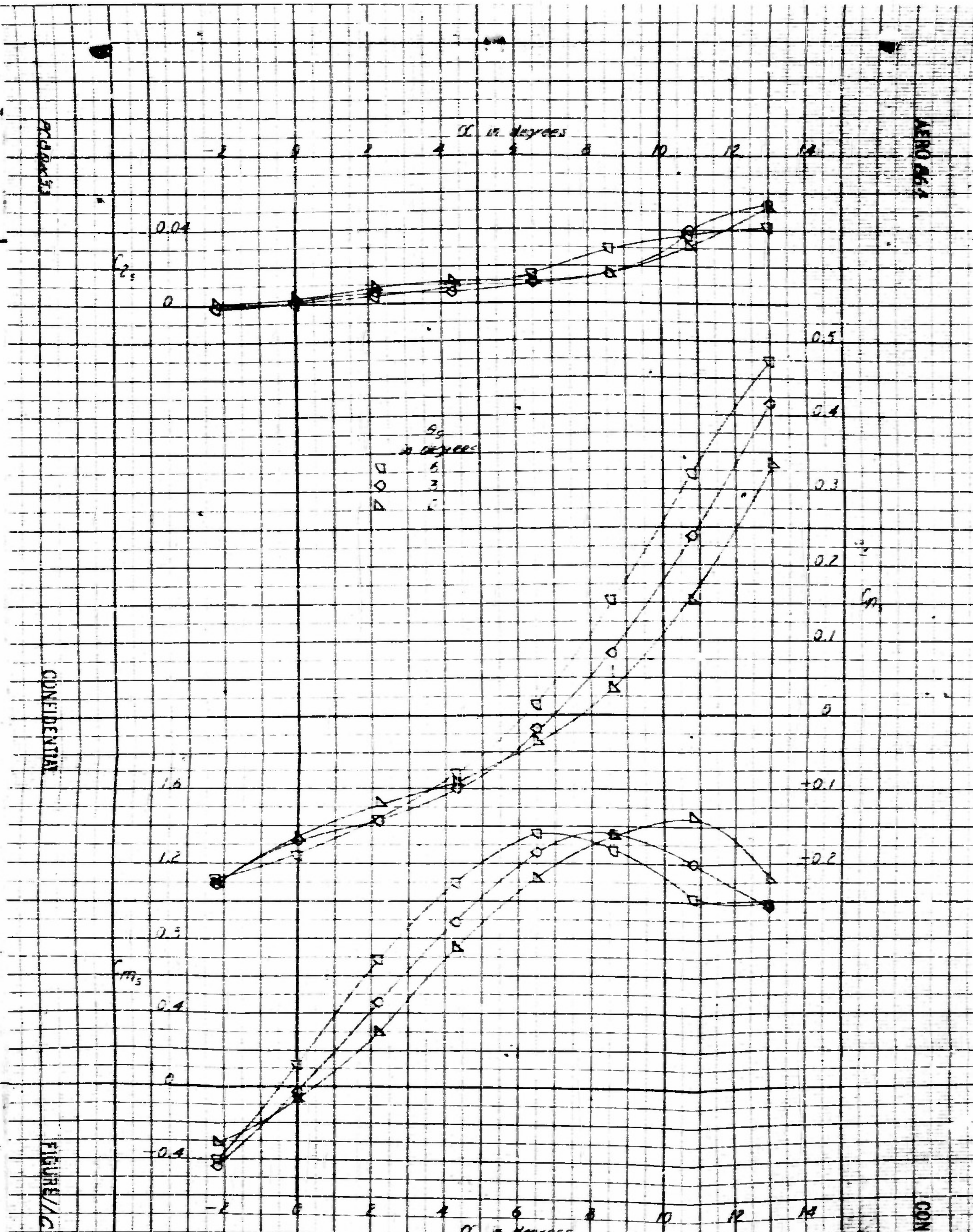

Figure 11 (Continued)

(c) Concluded

CONFIDENTIAL

FIGURE 11C (Concl.)

CONFIDENTIAL

RC9Dec33

AERO 864

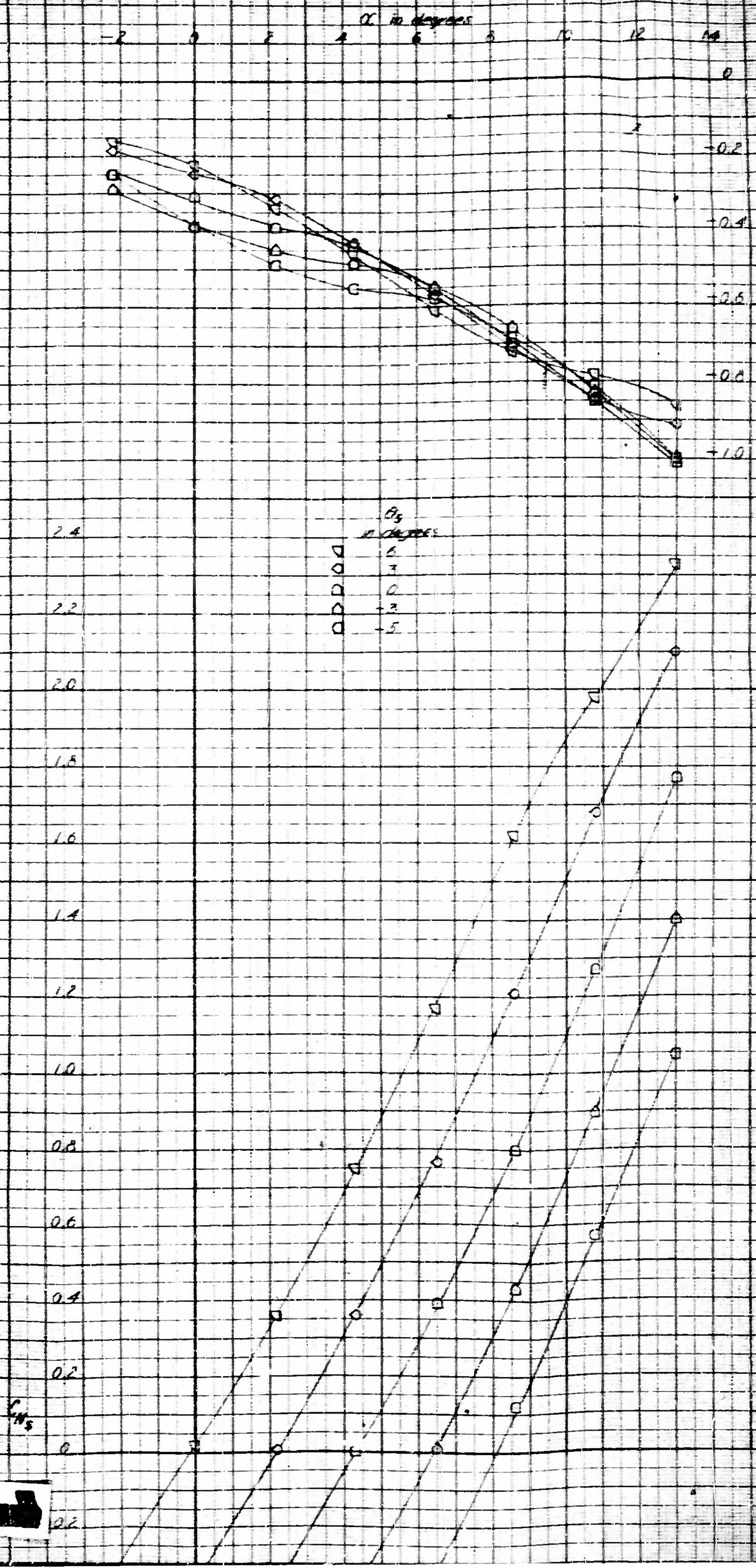

CONFIDENTIAL

[redacted]

CONFIDENTIAL

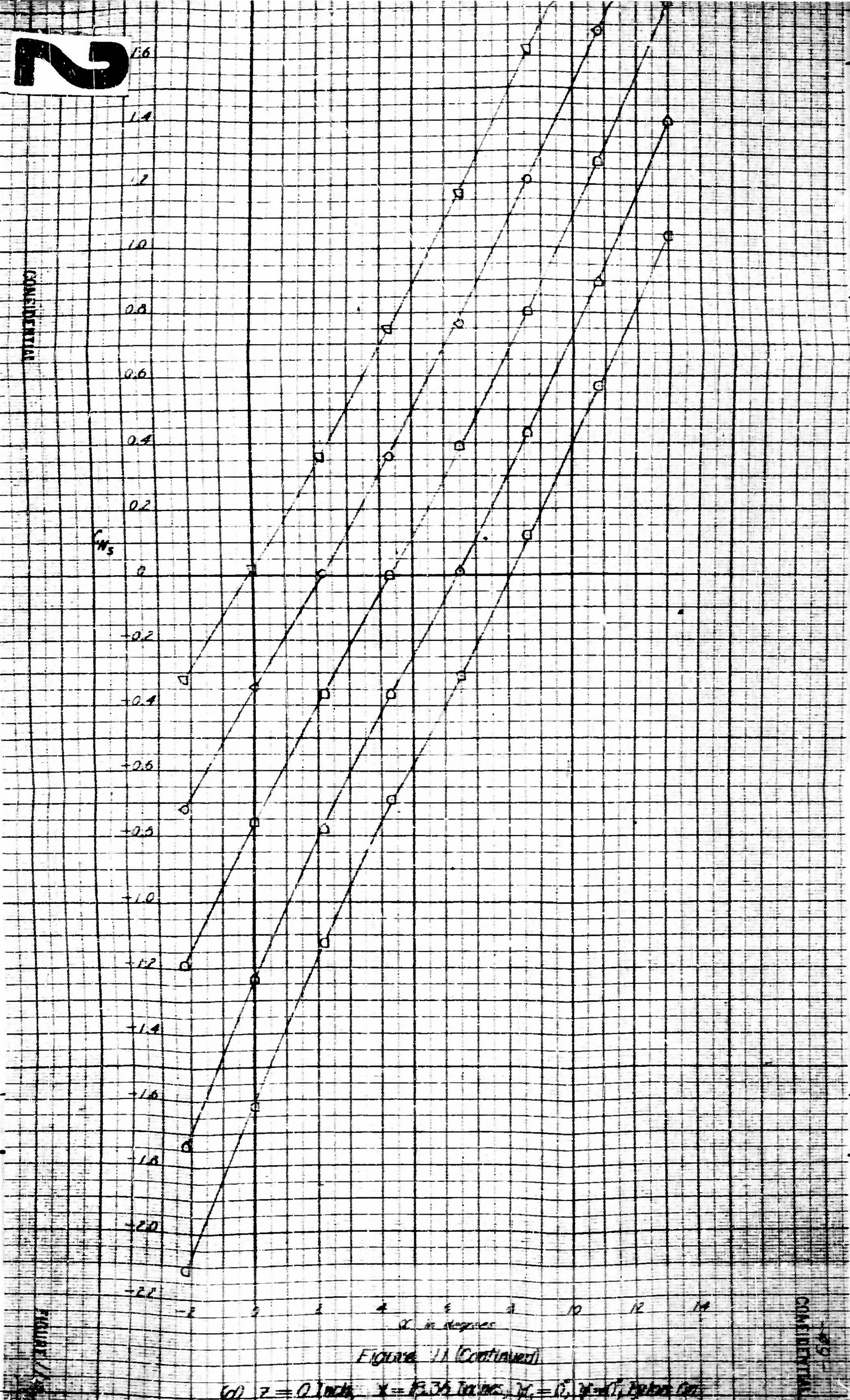

Figure 11 (Continued)

(d) z = 0 Inch, x = 13.36 Inches, ψ_s = [illegible], ψ = [illegible], Rotor On

FIGURE 11 [illegible]

CONFIDENTIAL

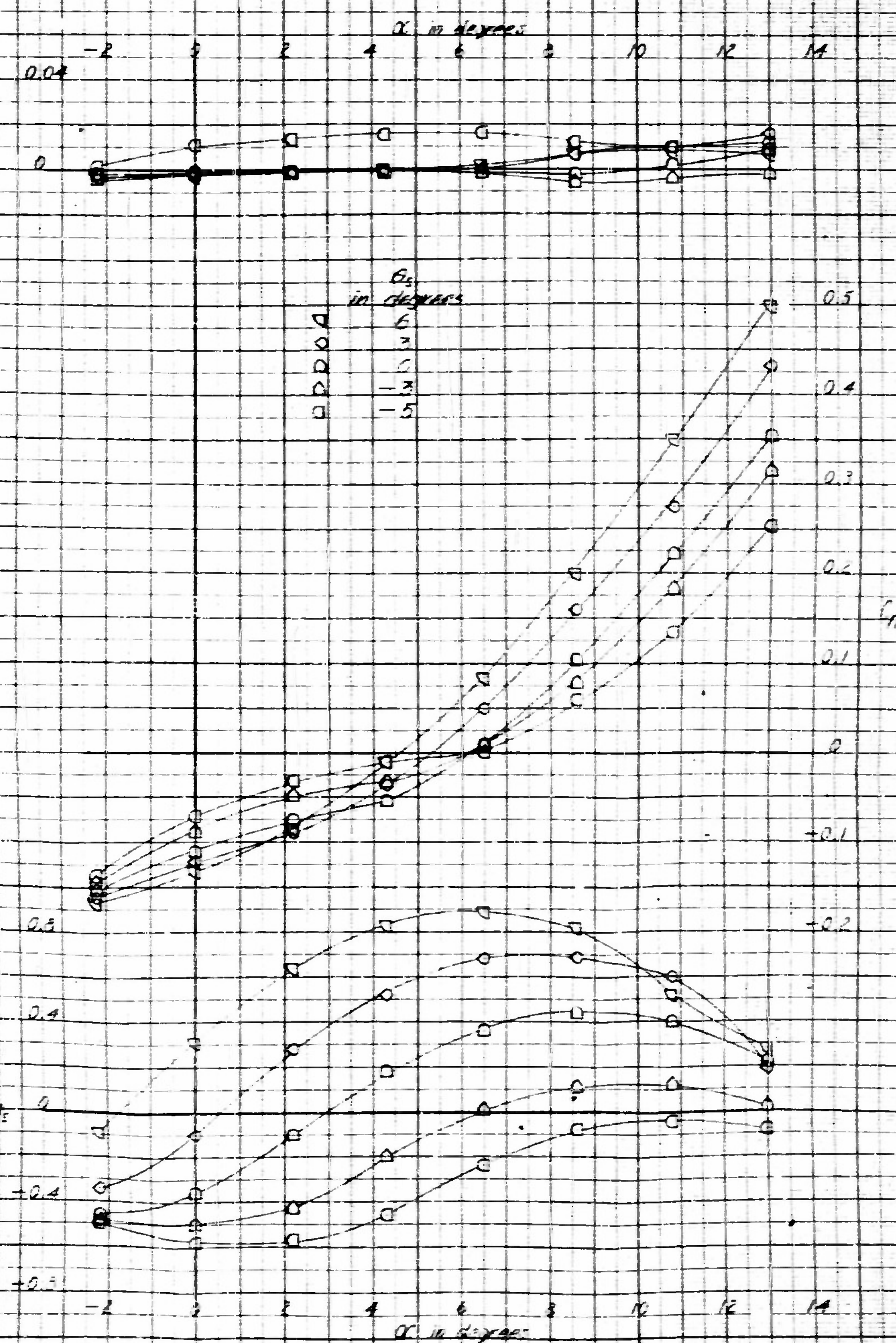

Figure 11 (Continued)

(d) Concluded

FIGURE 11 (cont'd)

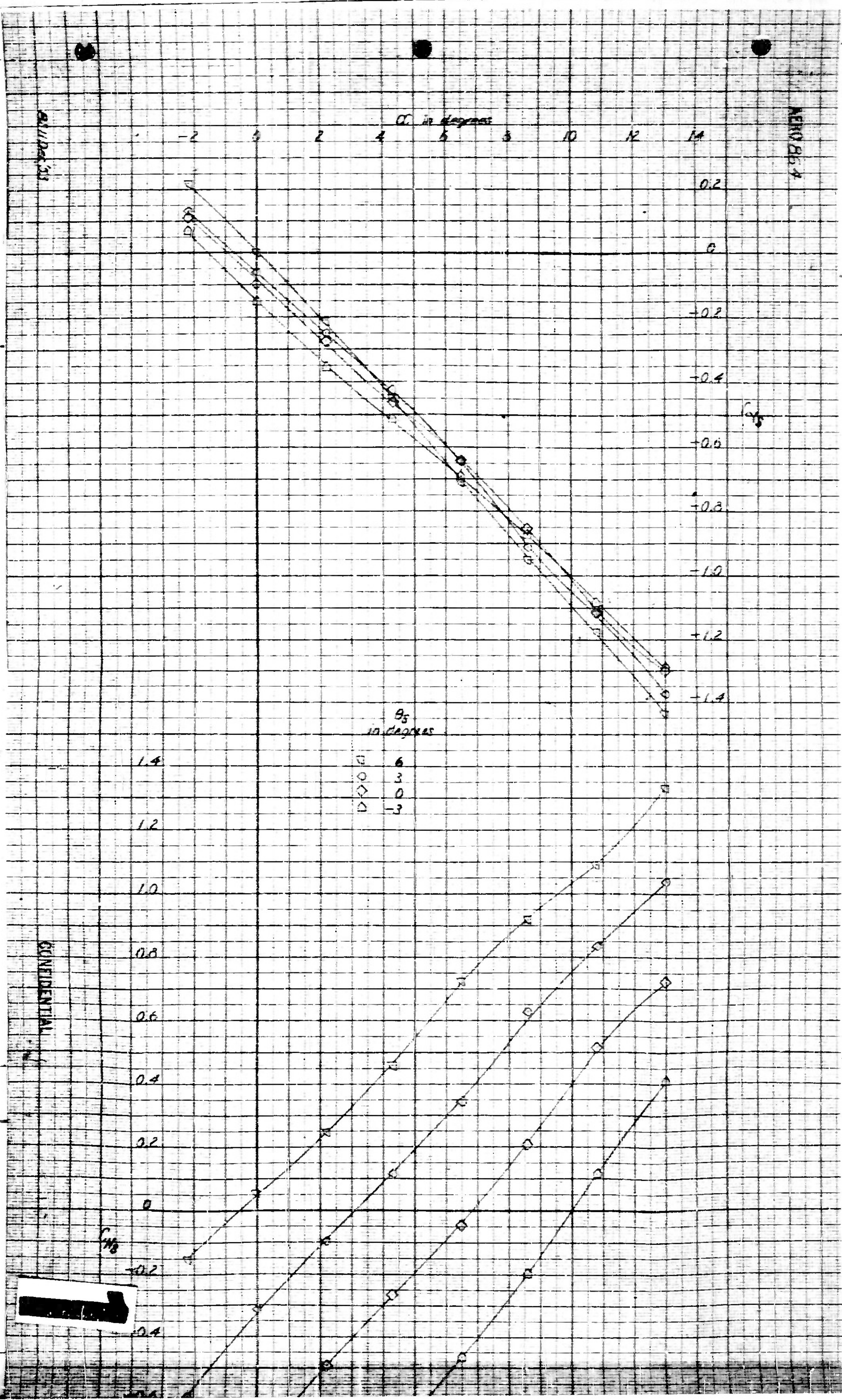
α in degrees
-2
0
2
4
6
8
10
12
14
0.2
0
-0.2
-0.4
-0.6
-0.8
-1.0
-1.2
-1.4
C_{A_S}
θ_S in degrees
6
3
0
-3
1.4
1.2
1.0
0.8
0.6
0.4
0.2
0
-0.2
-0.4
C_{N_S}
CONFIDENTIAL
AERO 864
[redacted]

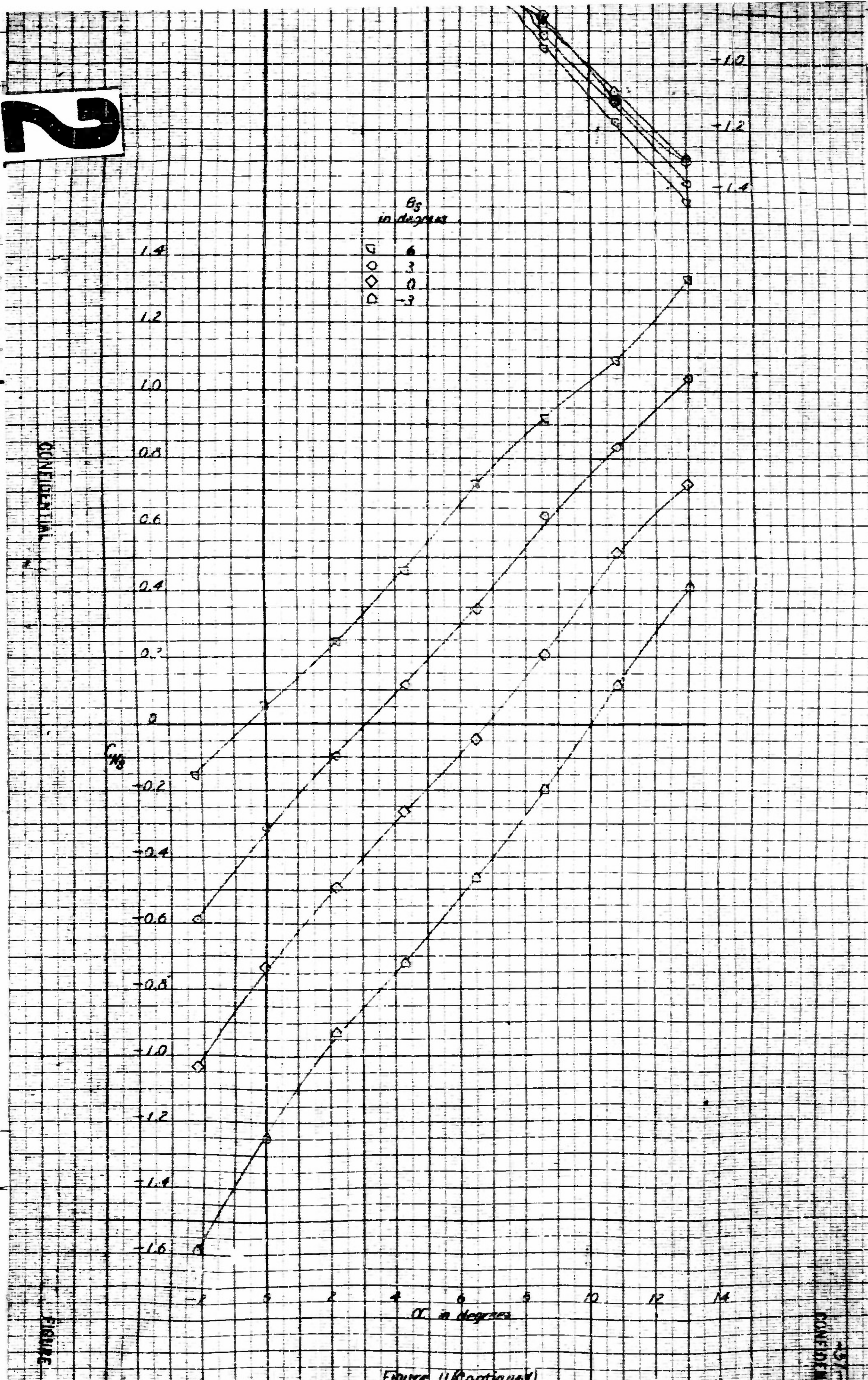

Figure 11 (Continued)

(e) Z = 1.02 Inches, X = 6.12 Inches, $\psi_0 = 0°$, $\phi = 0°$, Pylon On

CONFIDENTIAL

FIGURE 11

CONFIDENTIAL

CONFIDENTIAL

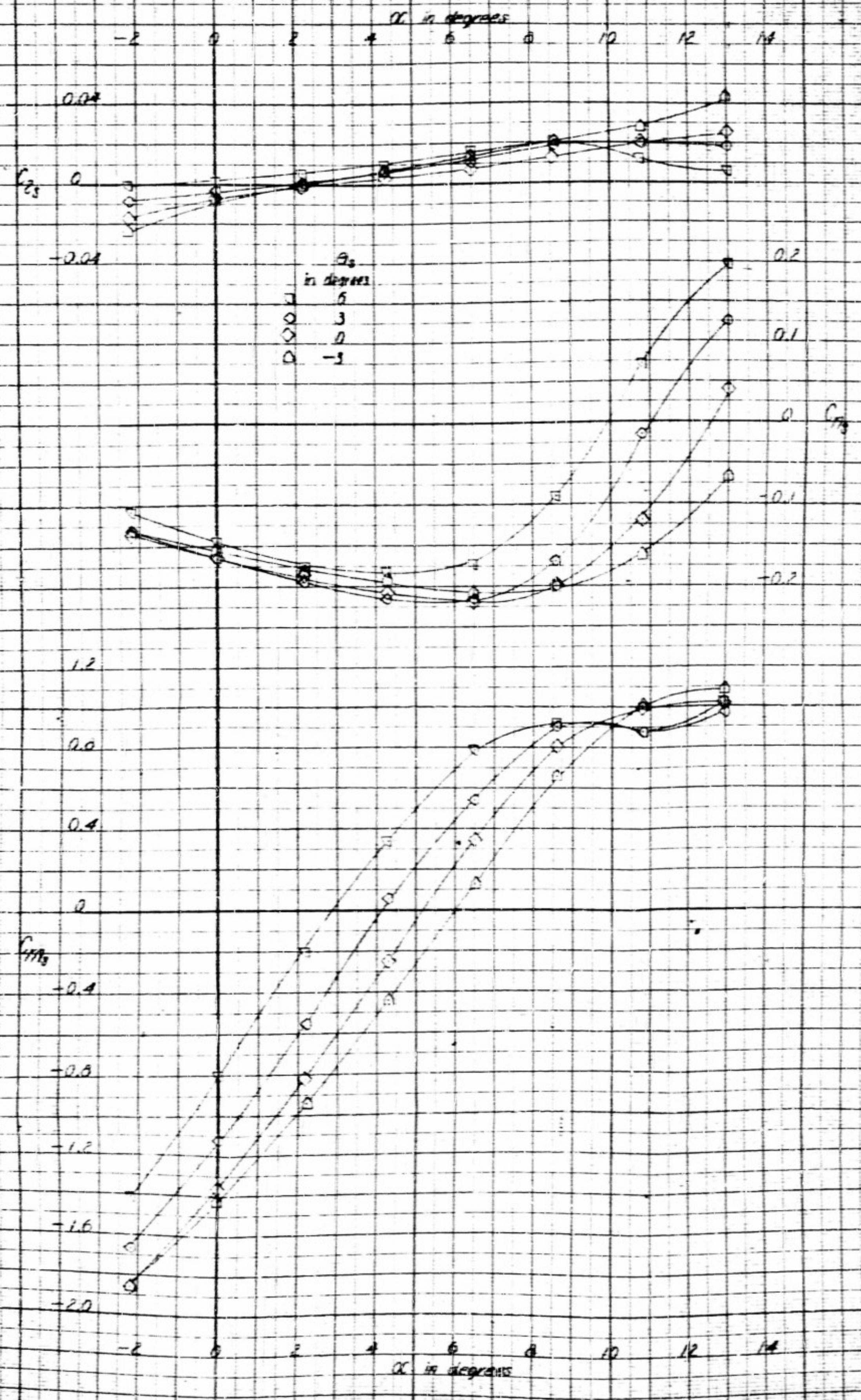

Figure 11 (Continued)

(e) Concluded

CONFIDENTIAL

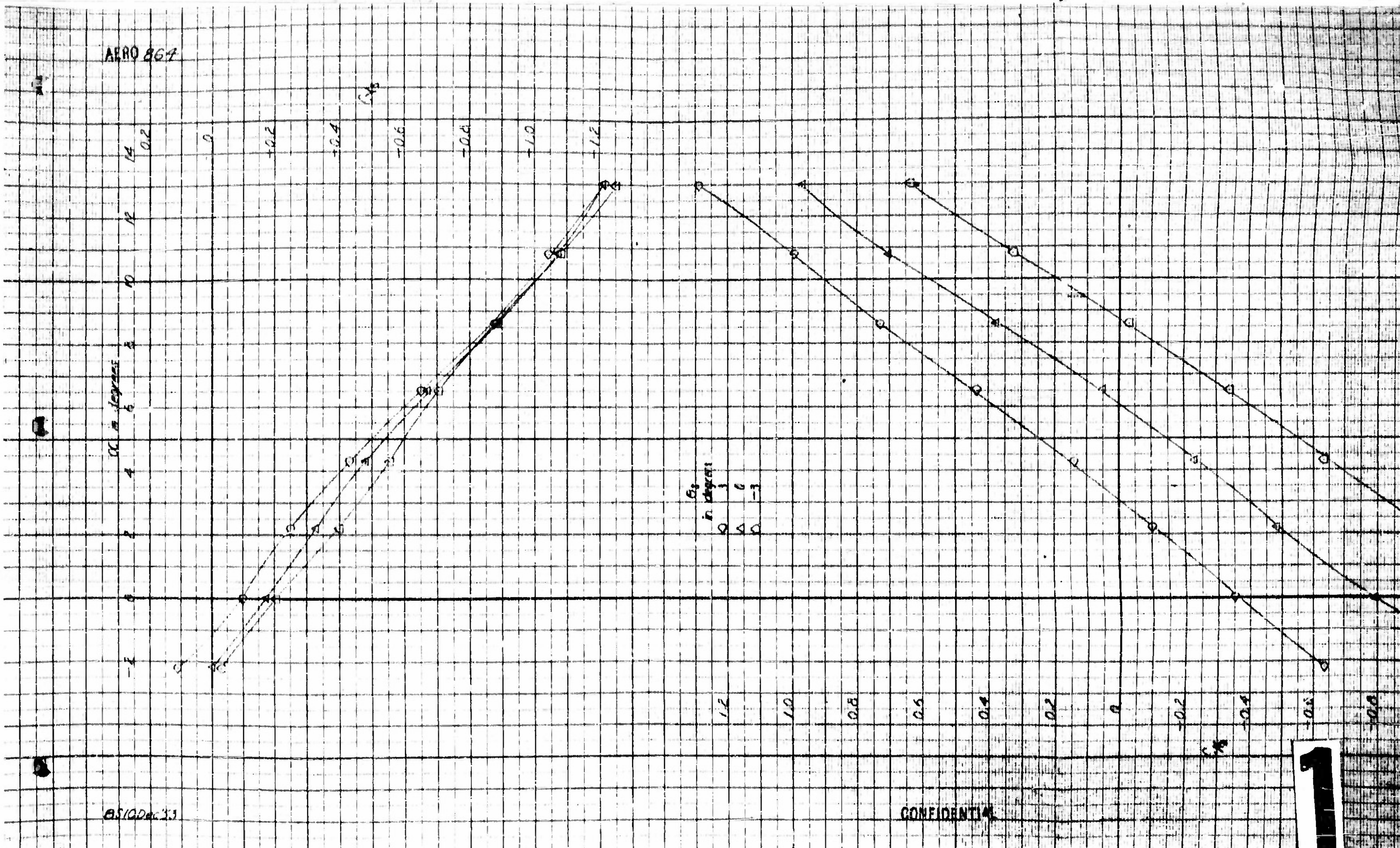
AERO 864
α in degrees
-2
0
2
4
6
8
10
12
14
C_{Y_S}
0.2
0
-0.2
-0.4
-0.6
-0.8
-1.0
-1.2
θ_s in degrees
3
0
-3
C_{N_S}
1.2
1.0
0.8
0.6
0.4
0.2
0
-0.2
-0.4
-0.6
-0.8
BS10Dec33
CONFIDENTIAL
1

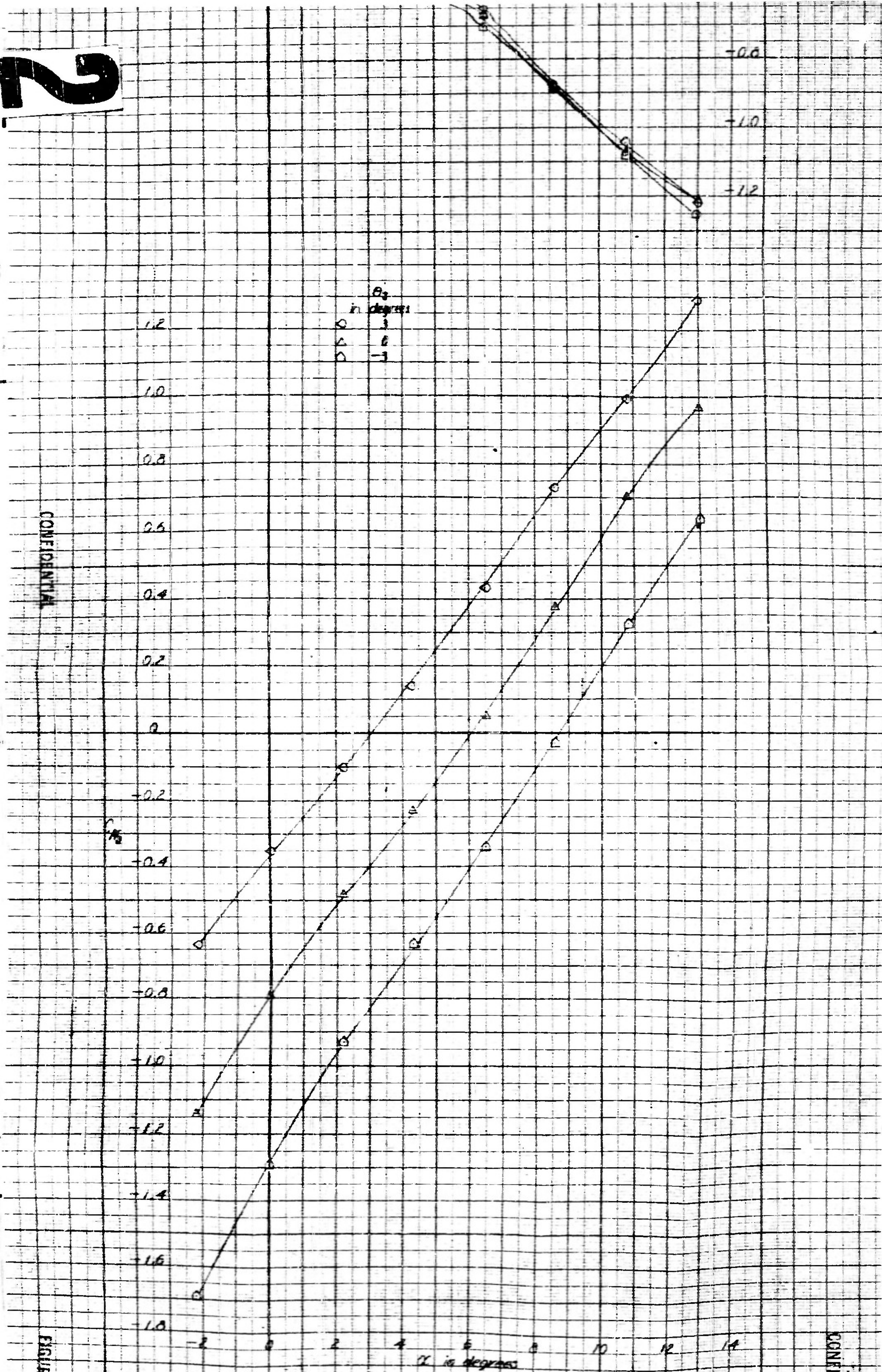

Figure 11 (Continued)

(f) $z = 1.02$ Inches, $x = 9.18$ Inches; $\psi_s = 0°$, $\psi = 0°$, Pylon On

FIGURE 11 f

RS 10 Dec 53

CONFIDENTIAL

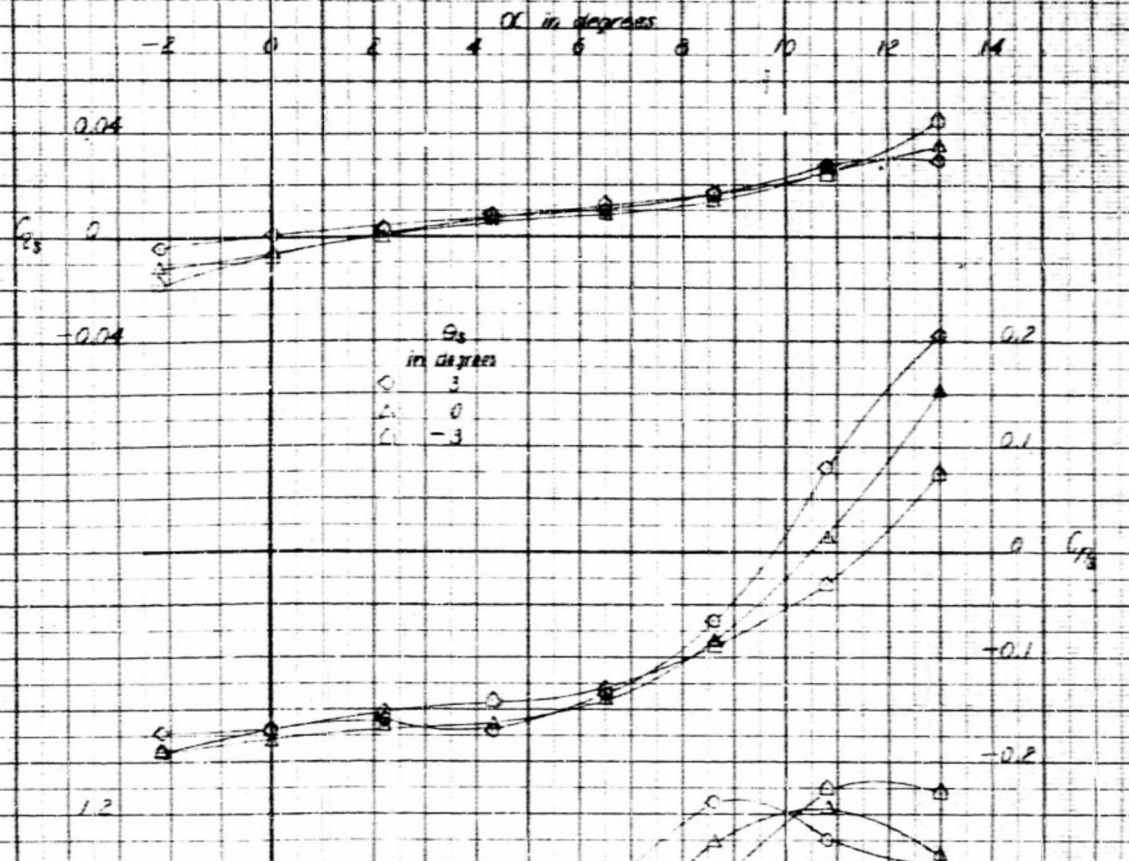

Figure 11 (Continued)

(f) Concluded

FIGURE 11 Contd

CONFIDENTIAL

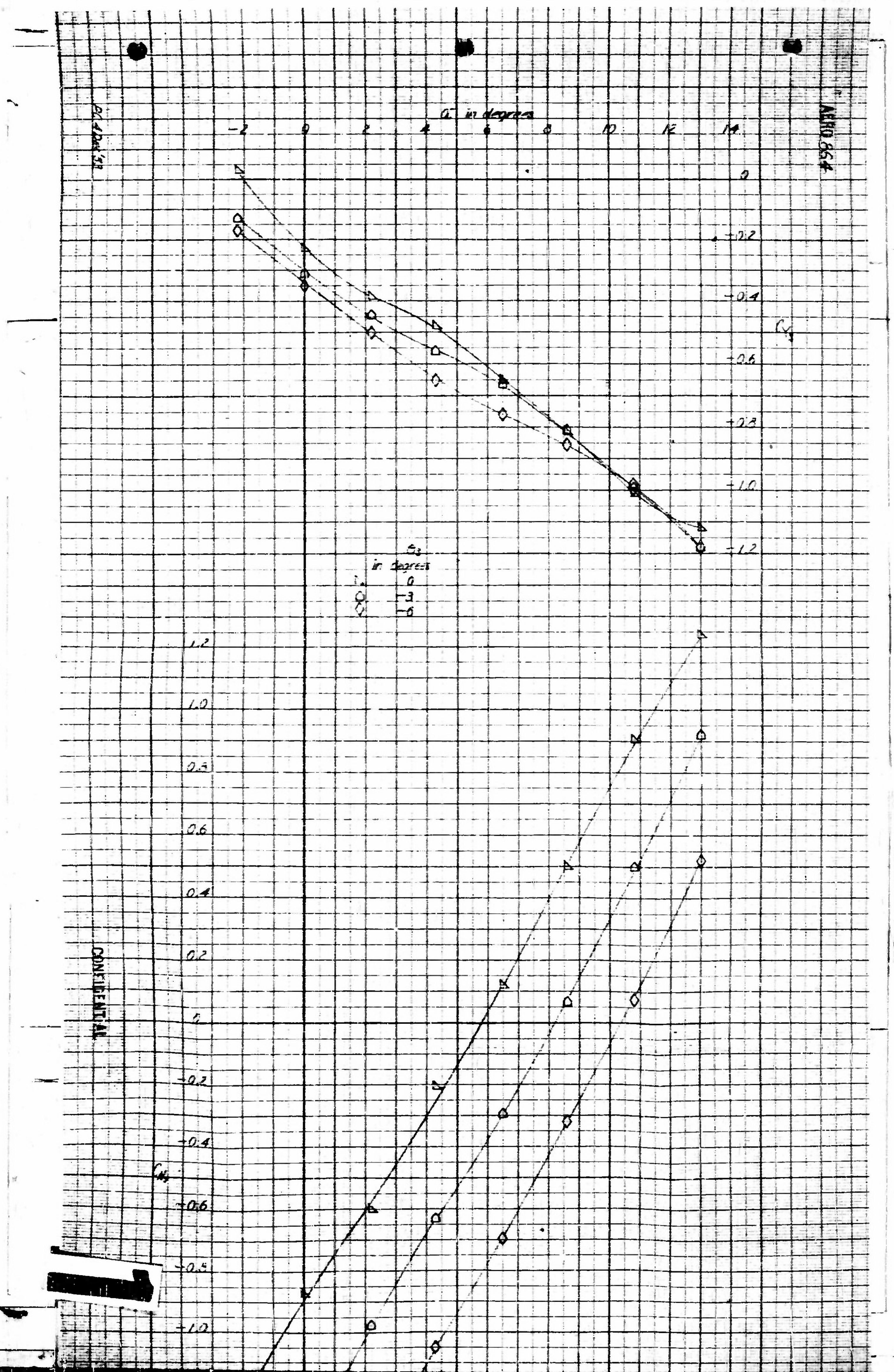

AERO 864
CONFIDENTIAL
α in degrees
-2
0
2
4
6
8
10
12
14
0
-0.2
-0.4
-0.6
-0.8
-1.0
-1.2
C_Y
δ_3 in degrees
0
-3
-6
1.2
1.0
0.8
0.6
0.4
0.2
0
-0.2
-0.4
-0.6
-0.8
-1.0
C_{n_3}
[redacted]

CONFIDENTIAL

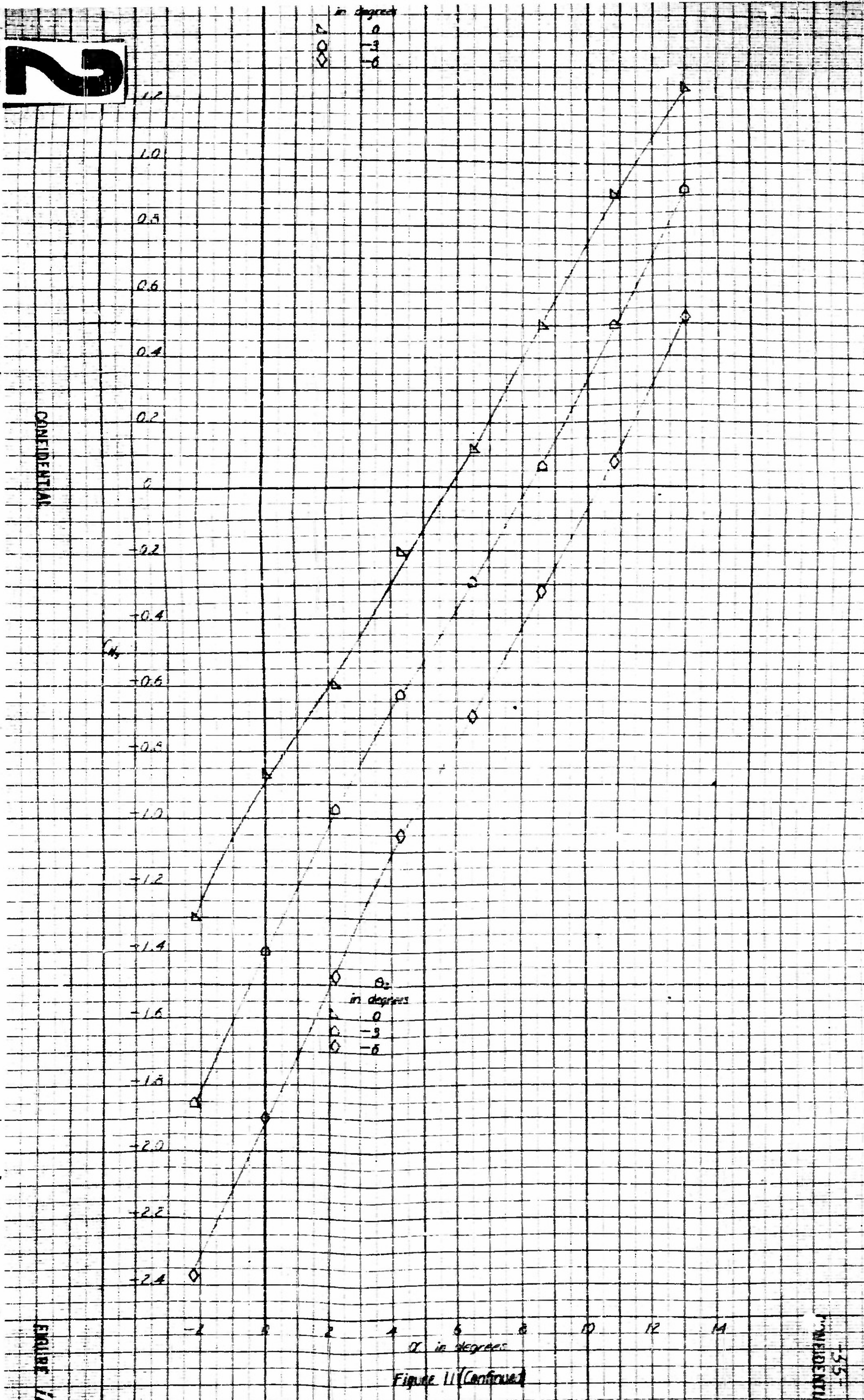

Figure 11 (Continued)

(g) z=1.02 Inches, x=13.25 Inches, $\psi_s=0°$, $\psi=0°$, Pylon On

FIGURE 11g

CONFIDENTIAL

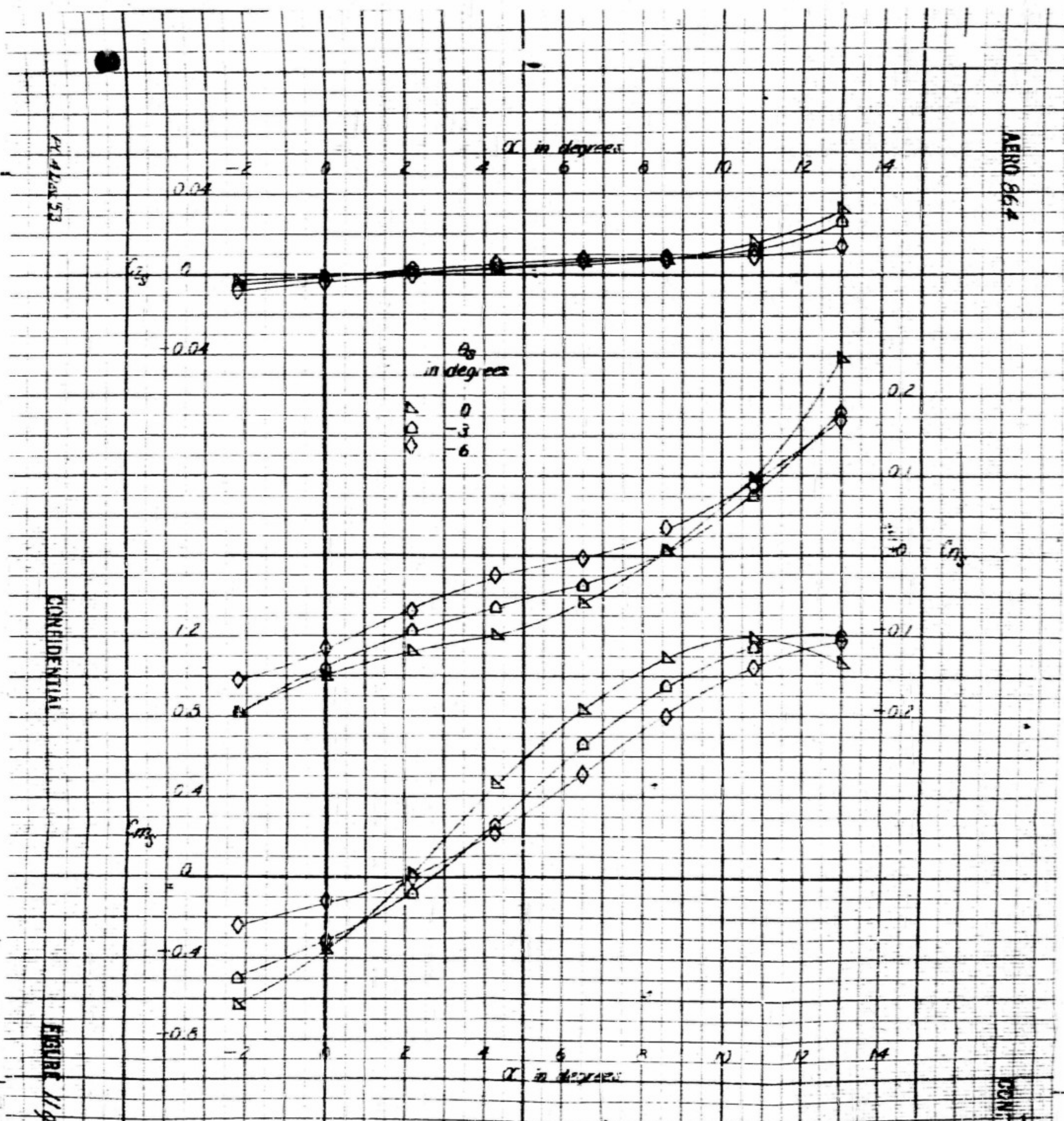

Figure 11 (Continued)
(g) Concluded

CONFIDENTIAL

FIGURE 11 g (concl)

CONFIDENTIAL

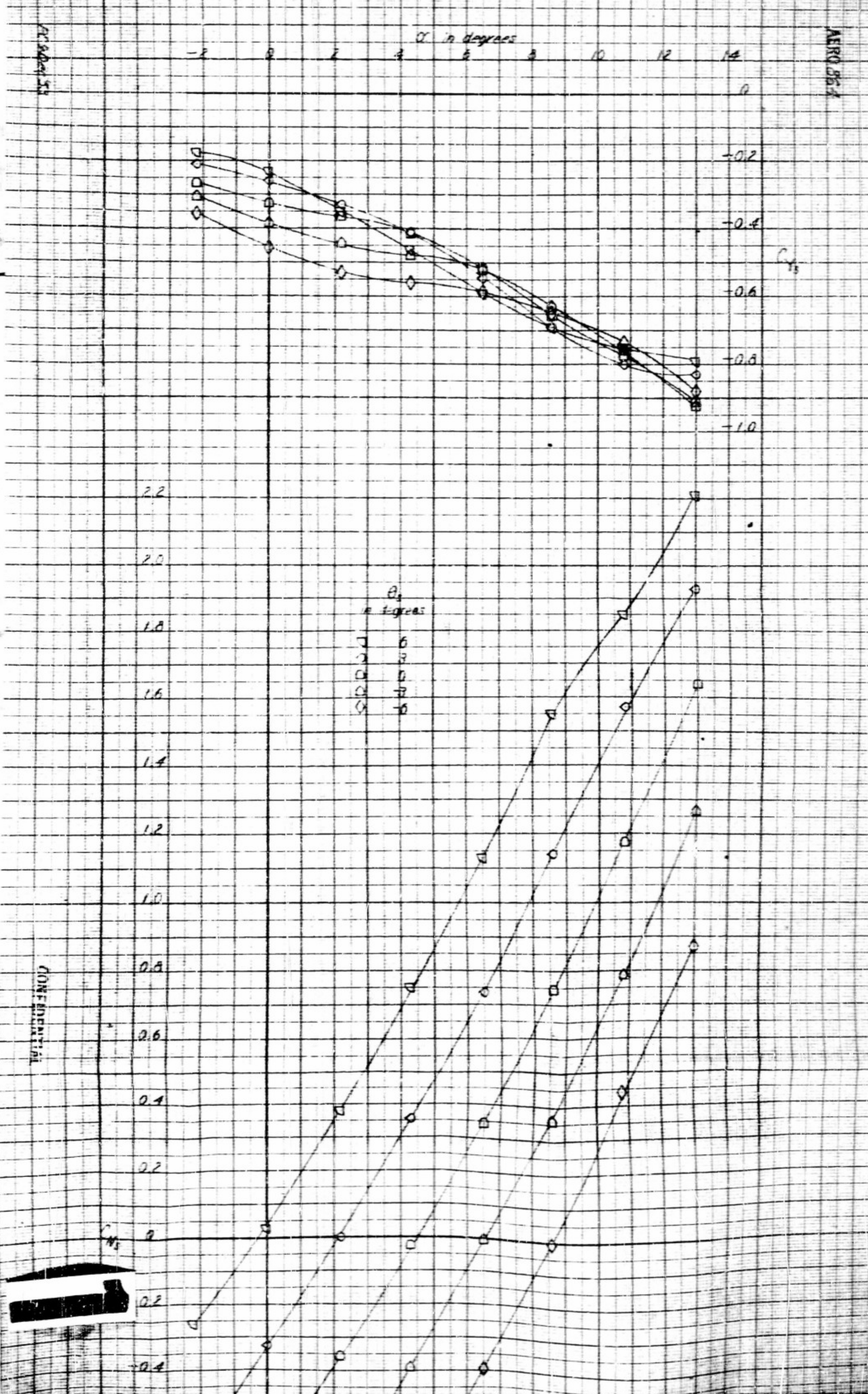

AERO 864

CONFIDENTIAL

[redacted]

CONFIDENTIAL

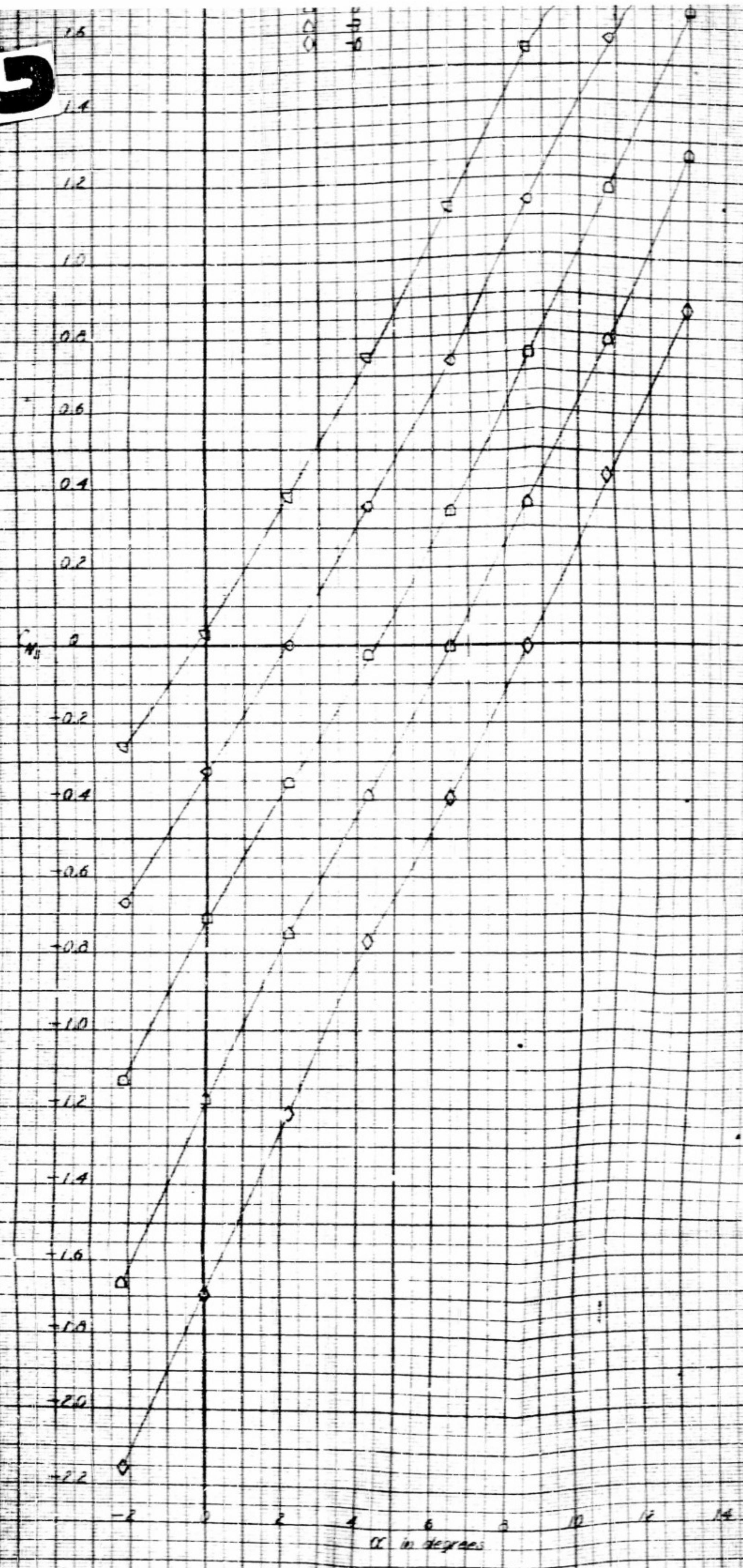

Figure 11 (Continued)

(h) z = [illegible] inches, x = 18.36 inches, $\delta_s = 0°$, $\psi = 0°$, Pylon On

FIGURE 11(h)

CONFIDENTIAL

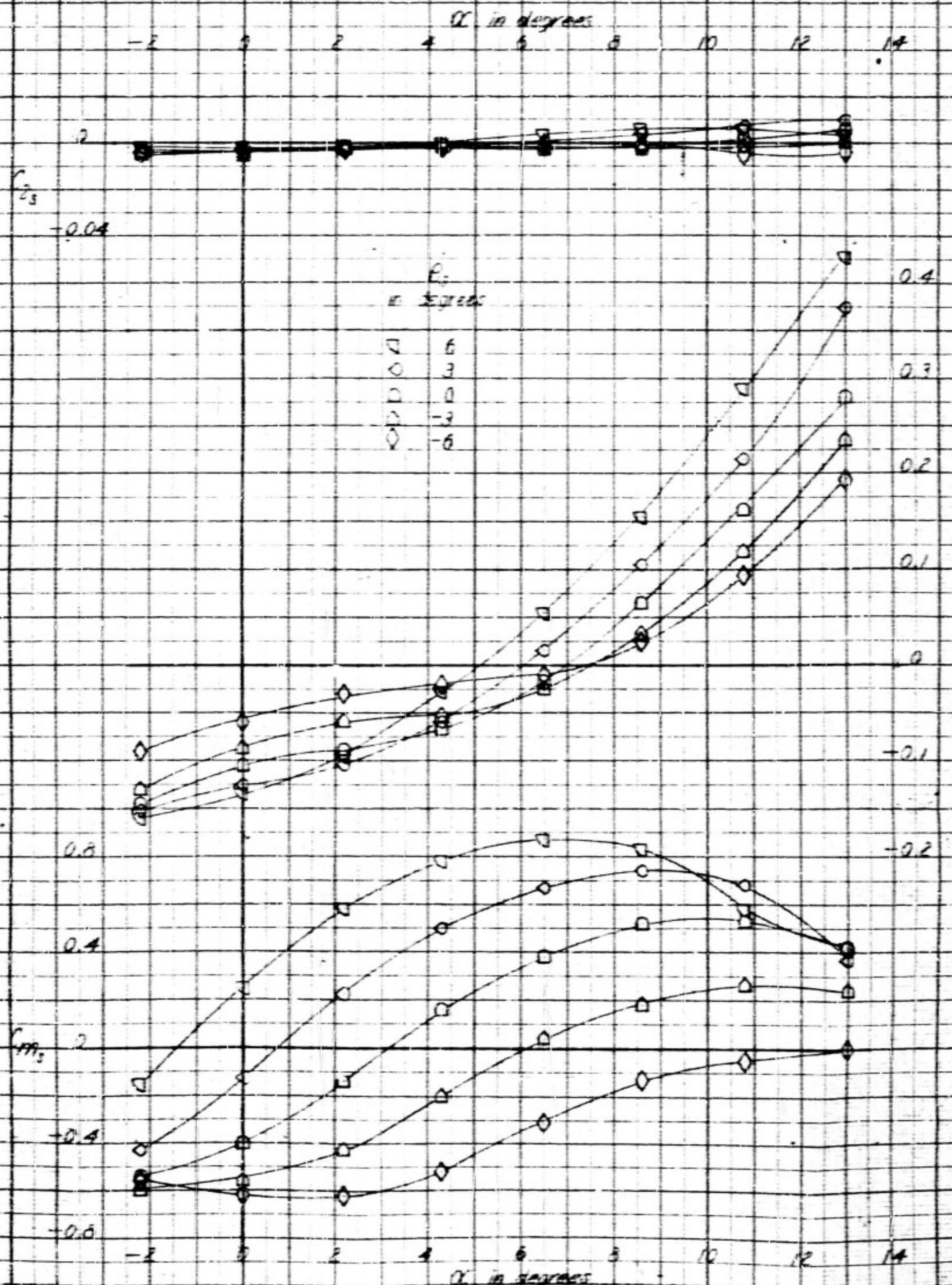

Figure 11 (Continued)

(h) Concluded

CONFIDENTIAL

FIGURE 11(h) (cont'd)

CONFIDENTIAL

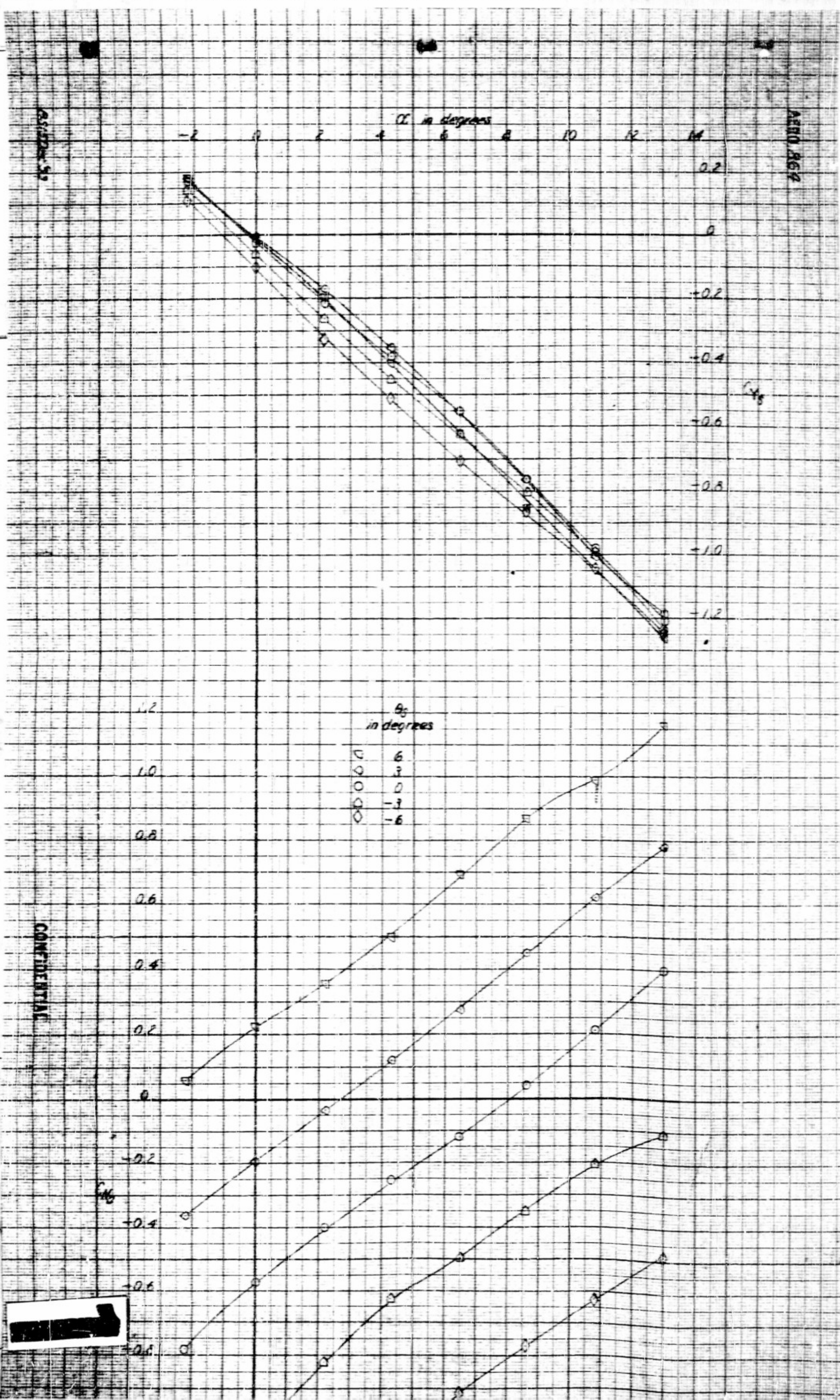

CONFIDENTIAL

AERO 869

[redacted]

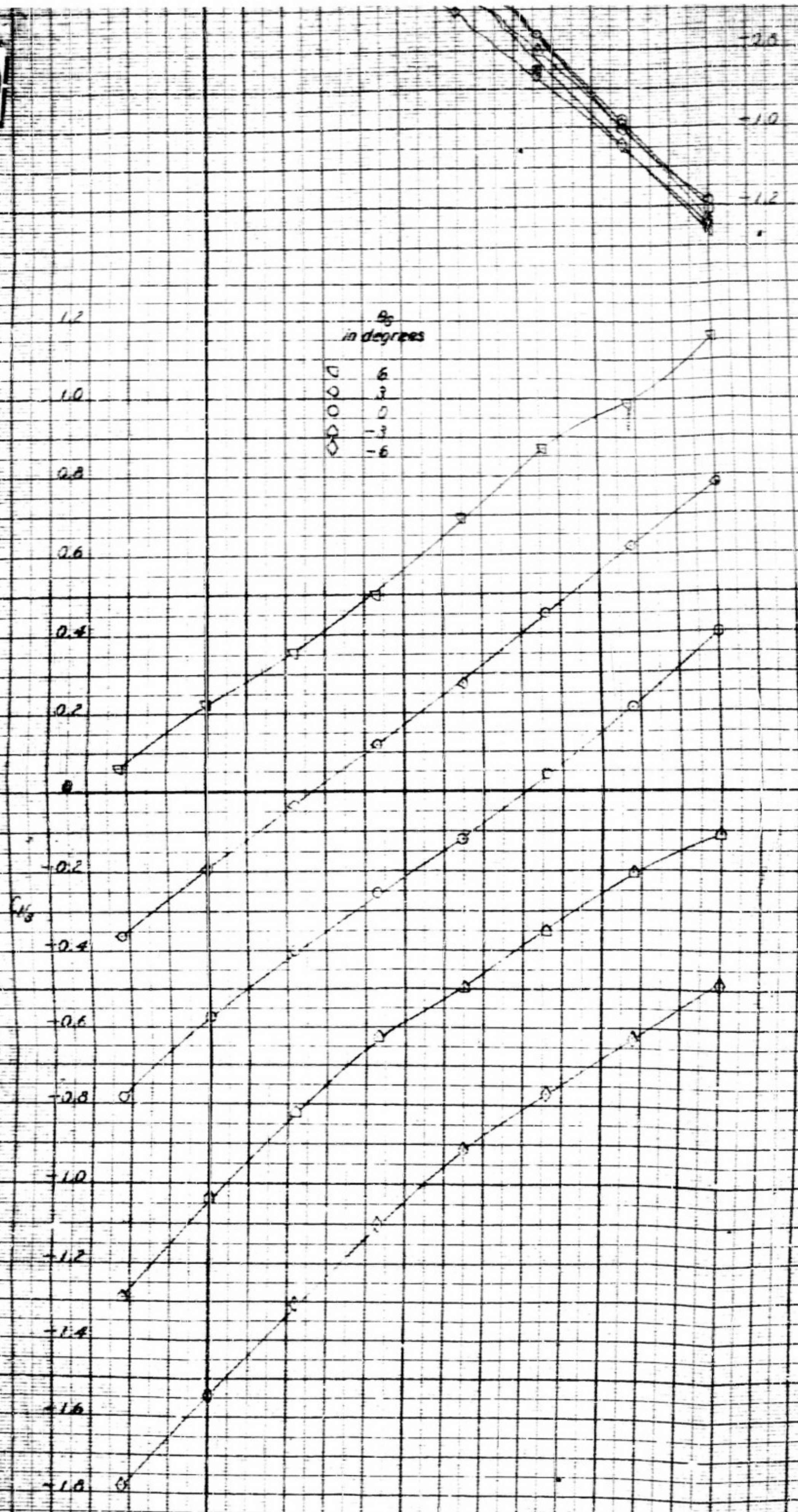

Figure 11 (Continued)

(i) z = 2.04 inches; x = 0 inch, $\phi_S = 0°$, M = 0, Pylon On

CONFIDENTIAL

FIGURE 11 Z.

CONFIDENTIAL

CONFIDENTIAL

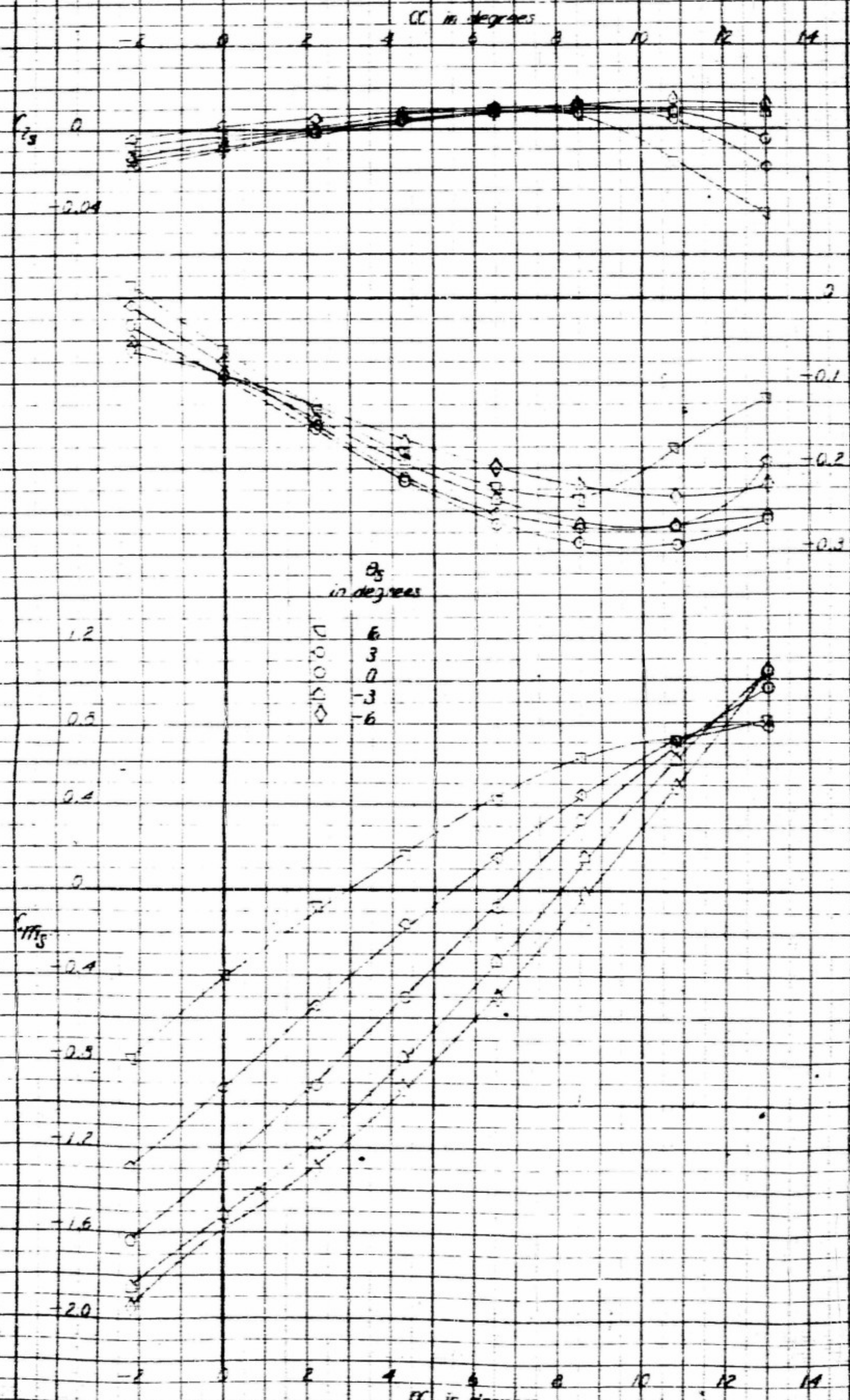

Figure 11 (Continued)
(i) Concluded

FIGURE 11 (concl.)

FIG. 37

AERO 864

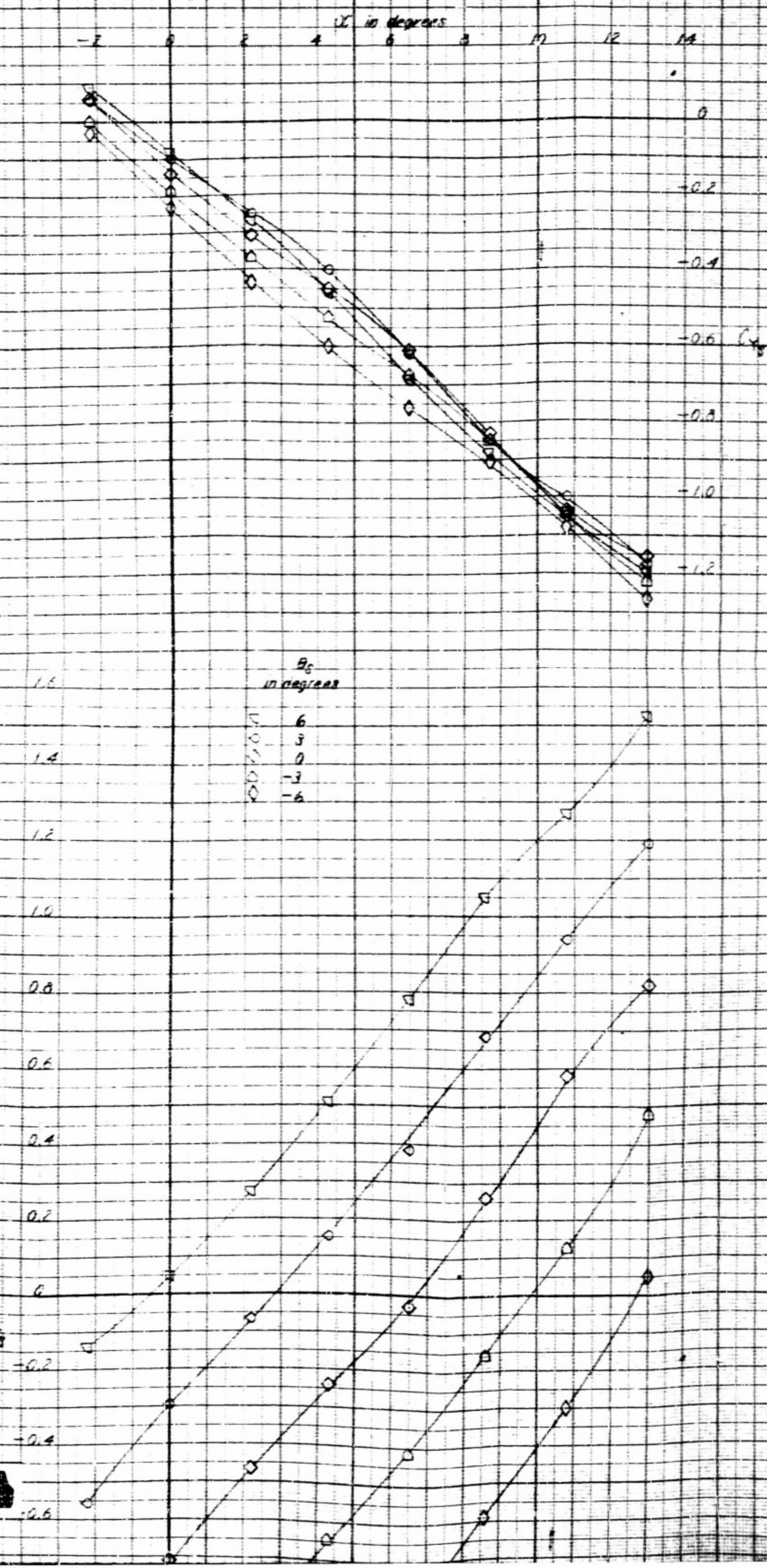

CONFIDENTIAL

[redacted]

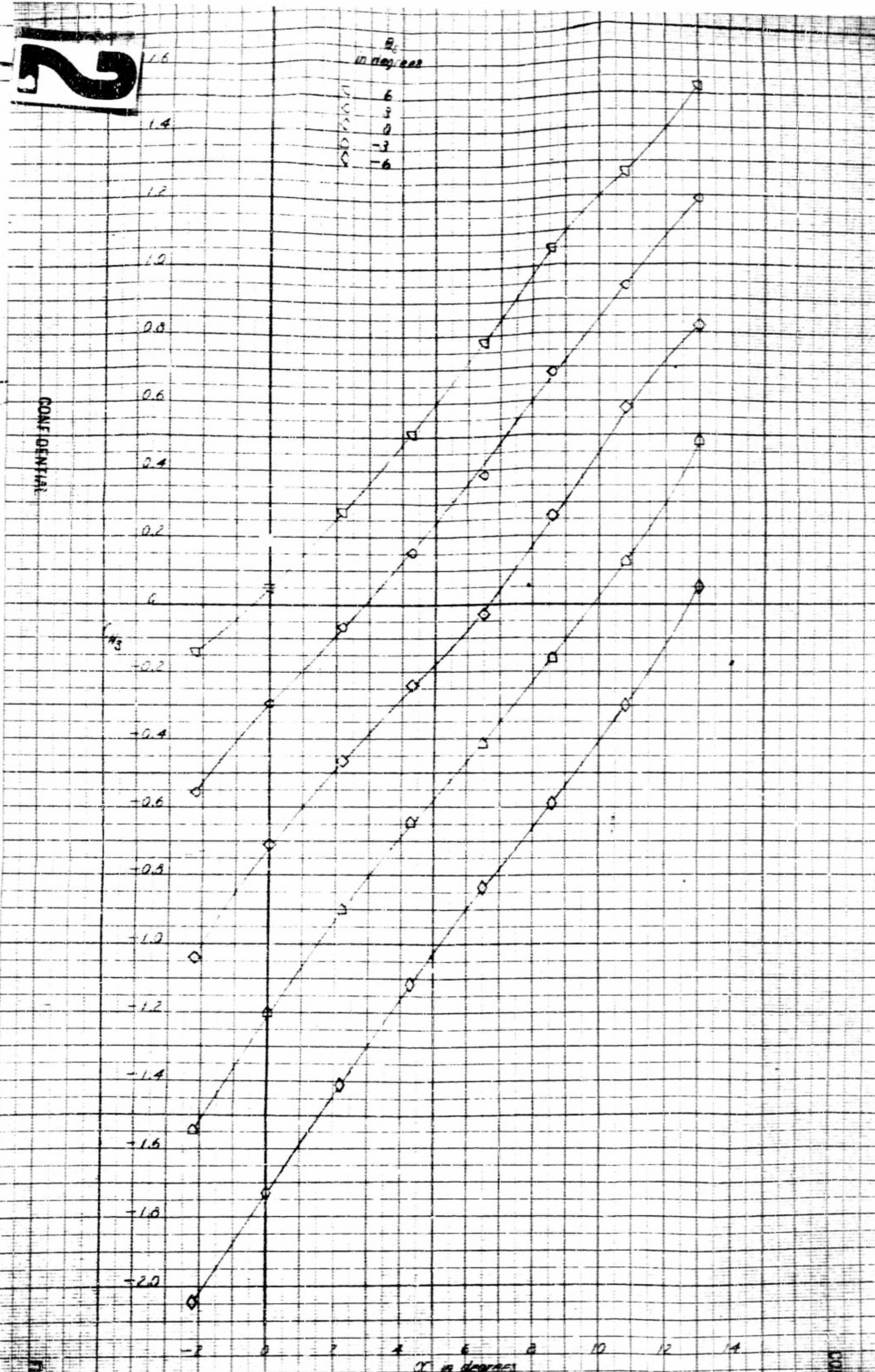

Figure 11 (Continued)

(j) z = 2.04 Inches, x = 6.12 Inches, $\psi_s = 0$, $\psi = 0°$, Pylon On

FIGURE 11 j

CONFIDENTIAL

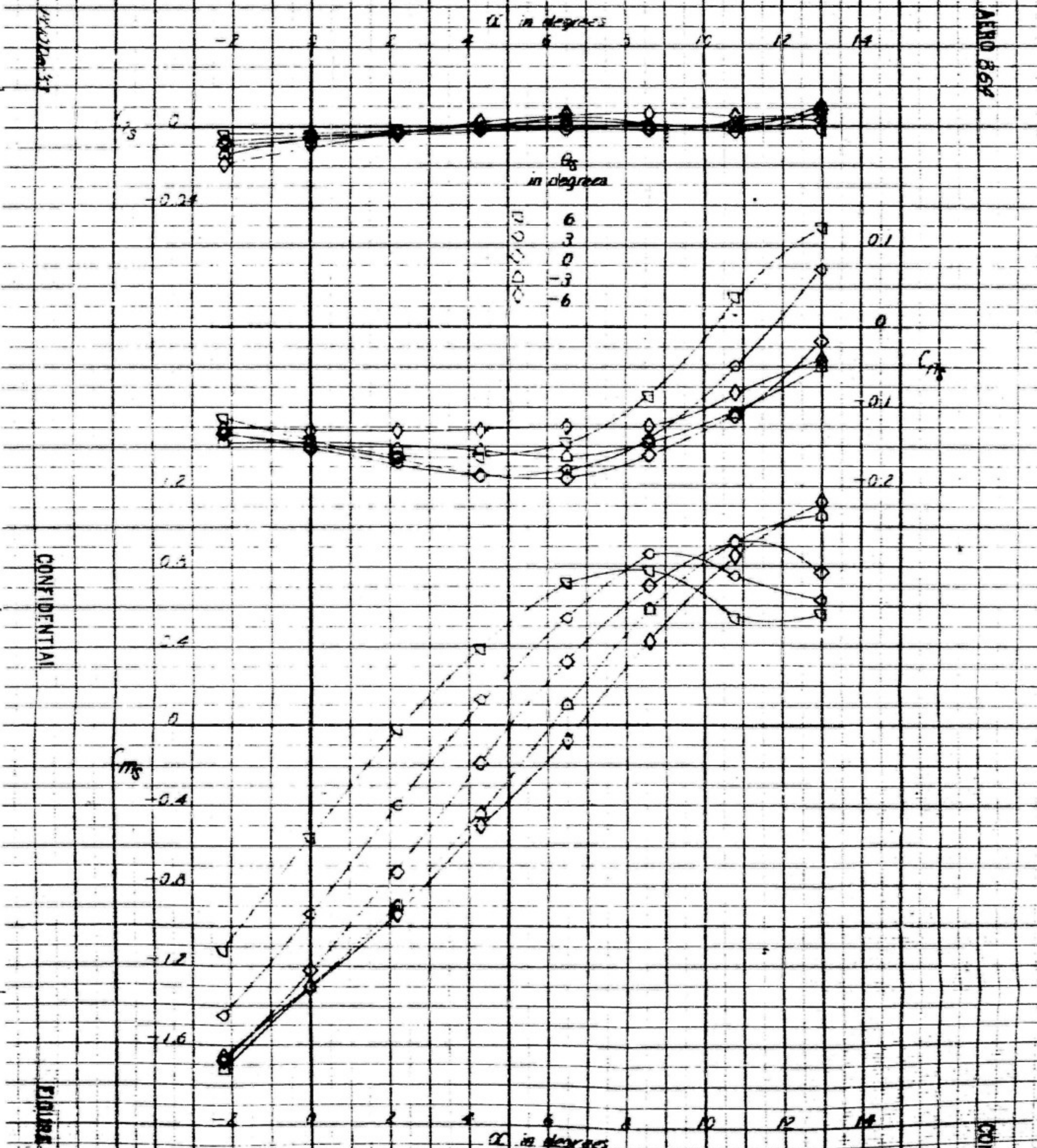

Figure 11 (Continued)

(j) Concluded

FIGURE 11(j) Concl.

CONFIDENTIAL

FIGURE 37

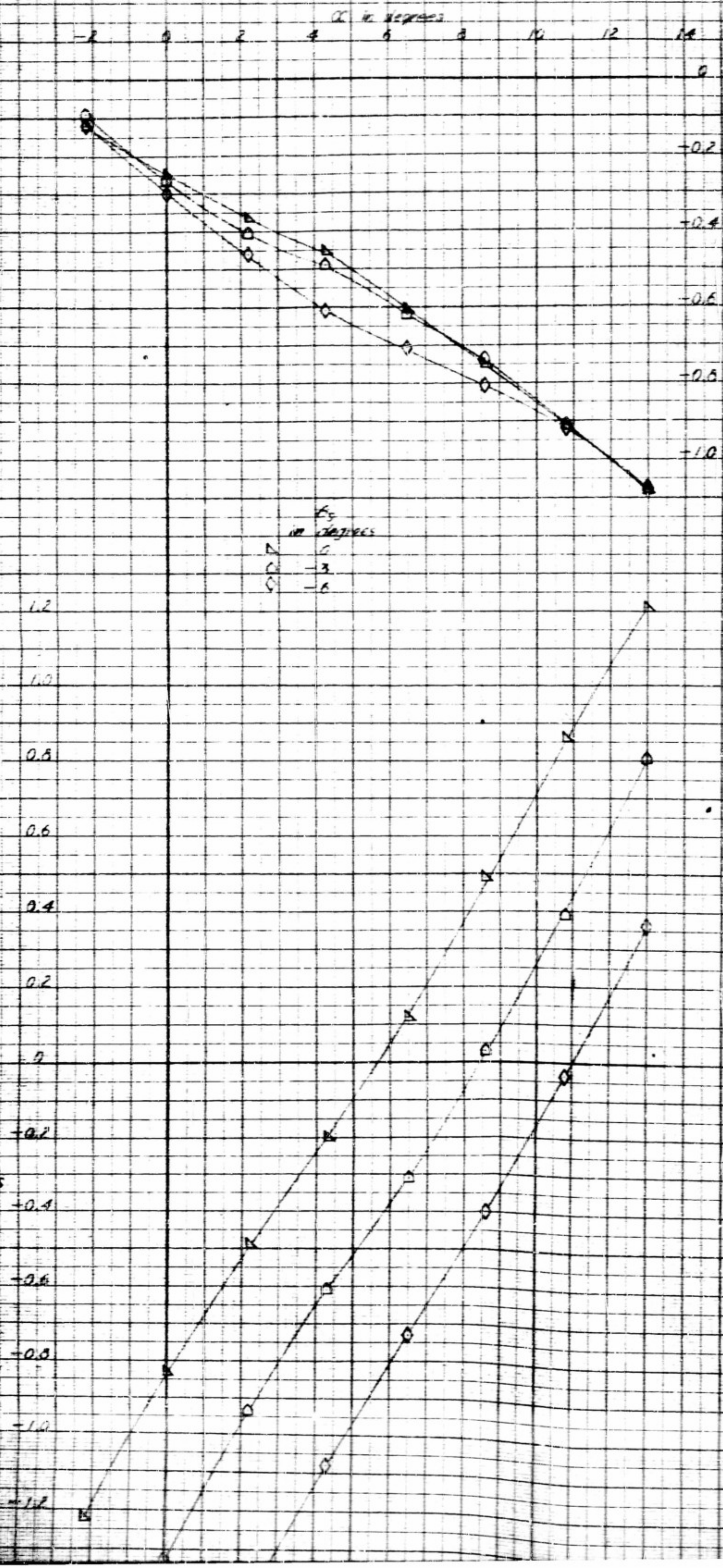

CONFIDENTIAL

AERO 864

[redacted]

CONFIDENTIAL

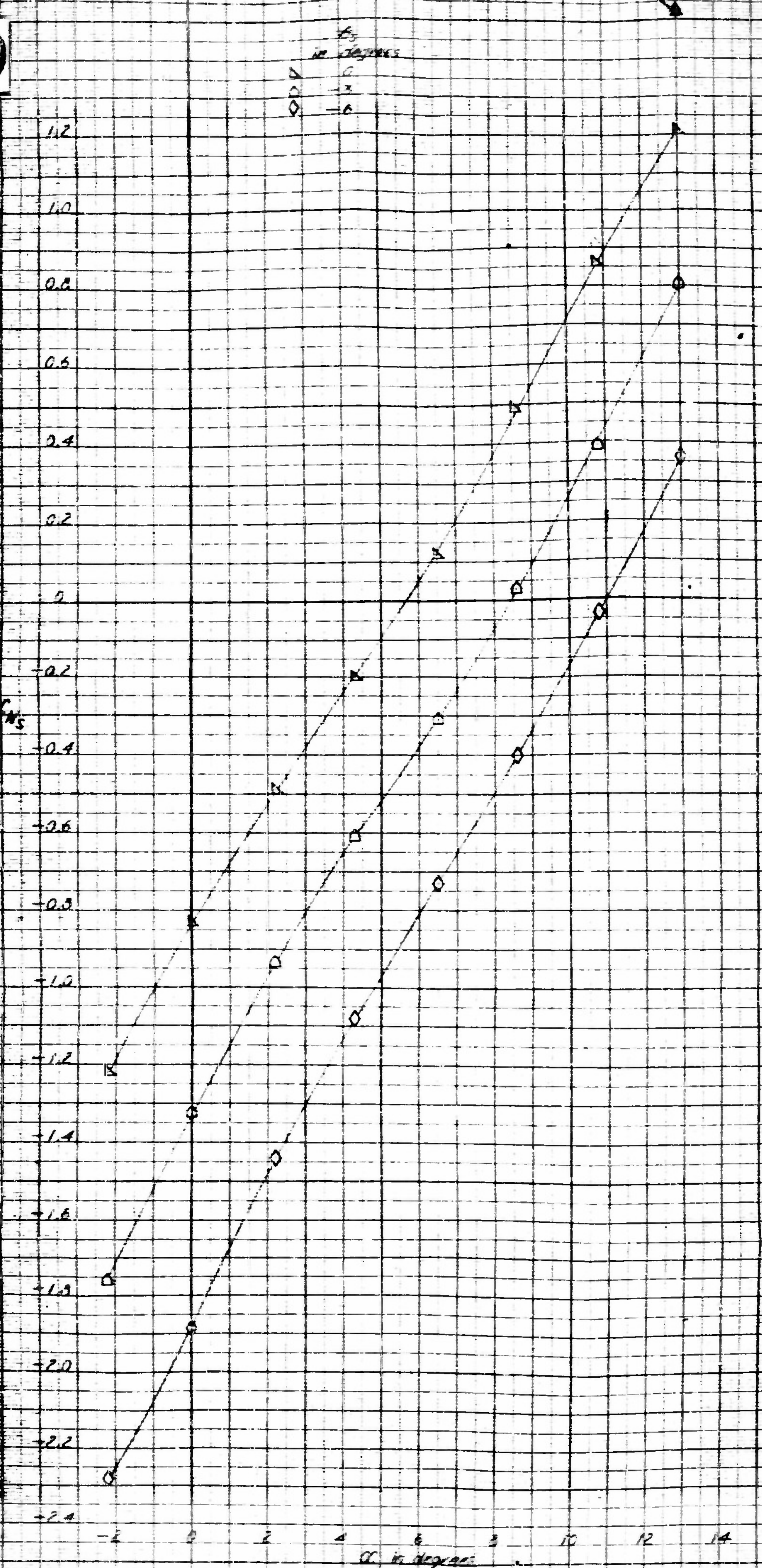

Figure 11 (Continued)

(x) z = 2.04 Inches, x = 13.26 Inches, ψ_s = 0, ψ = 0°, Pylon On

FIGURE 11 X

CONFIDENTIAL

CONFIDENTIAL

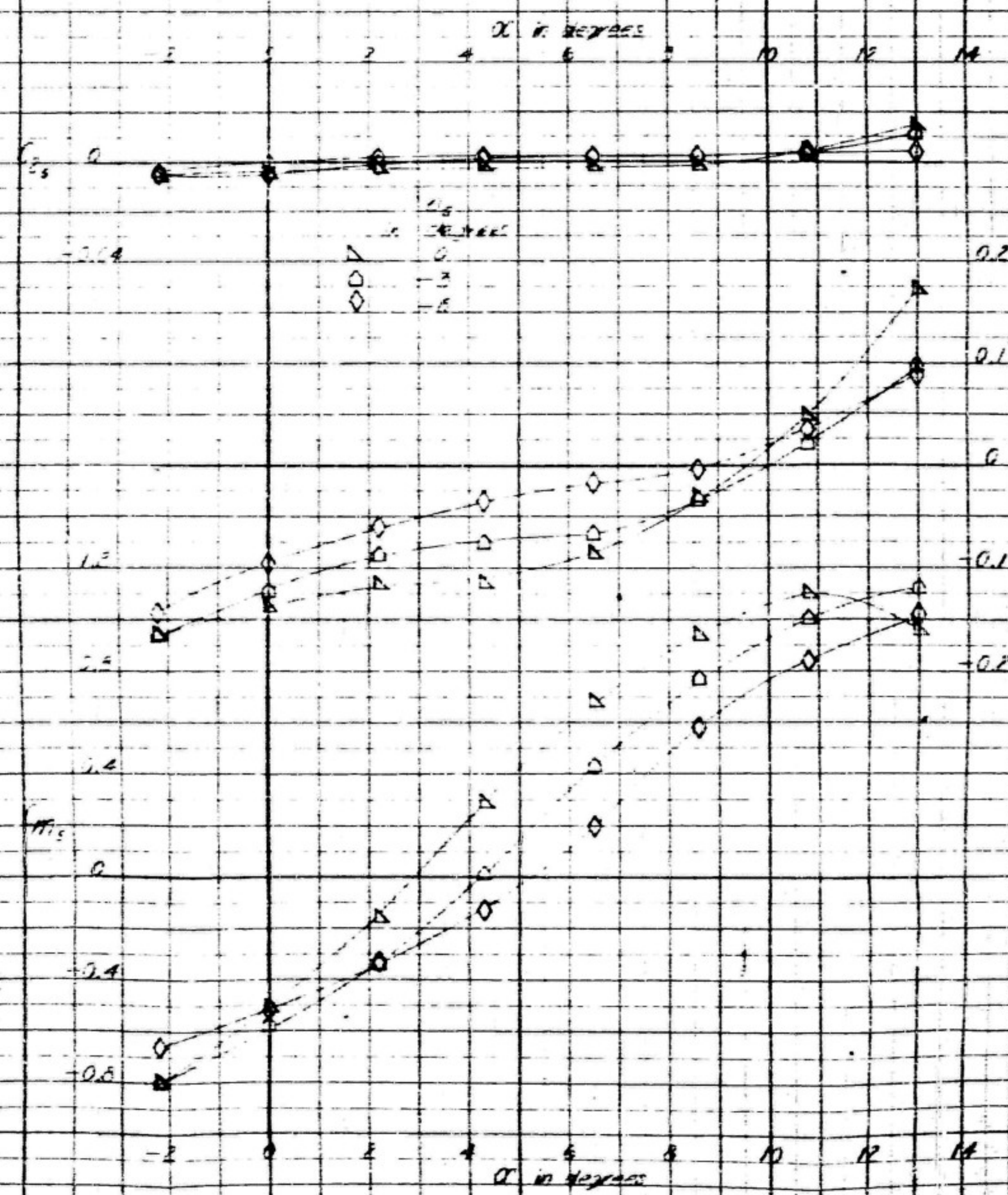

Figure 11 (Continued)

(k) Concluded

FIGURE 11 K (Concl.)

CONFIDENTIAL

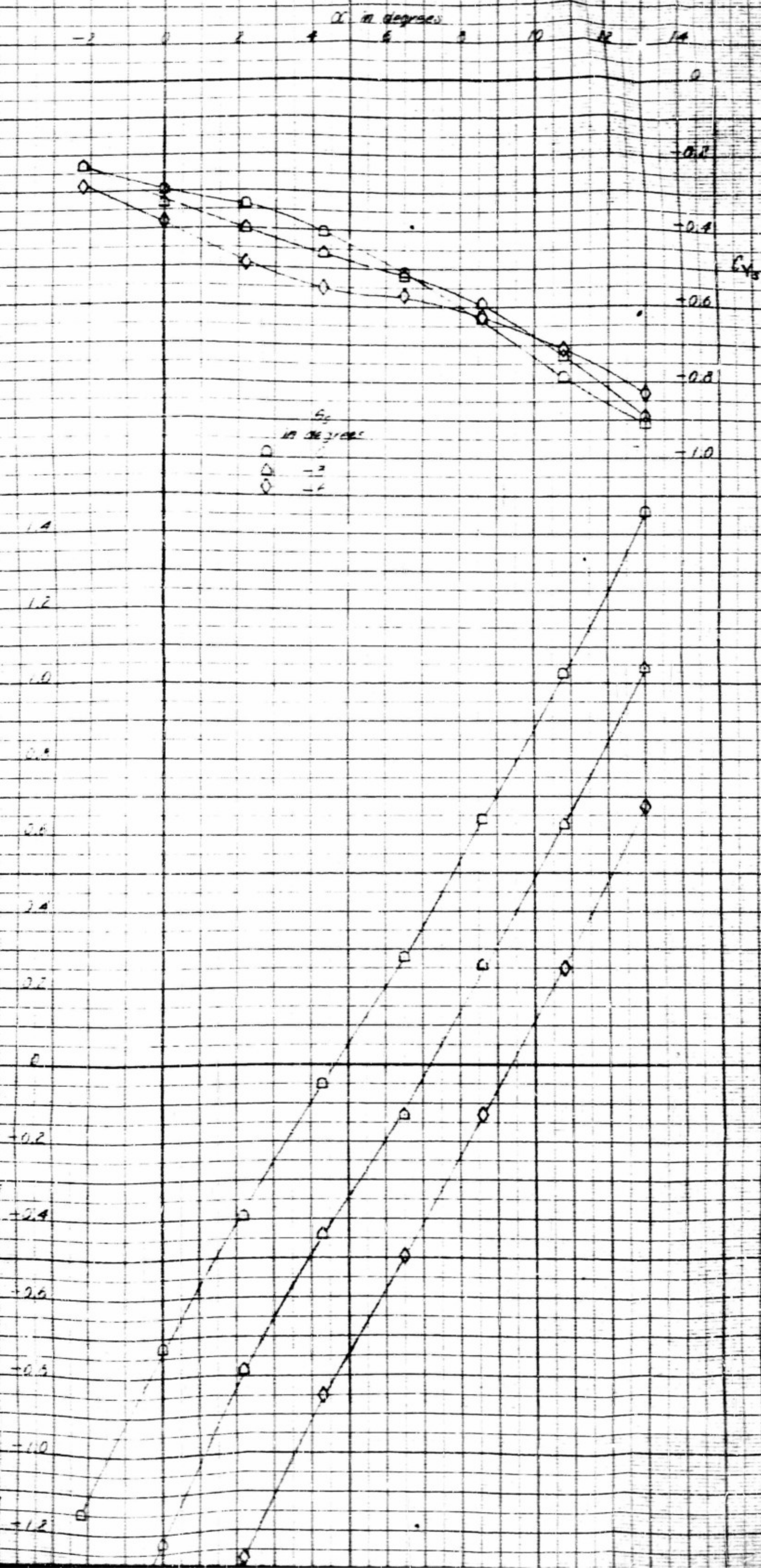

AERO 869

R.1/12a 35

CONFIDENTIAL

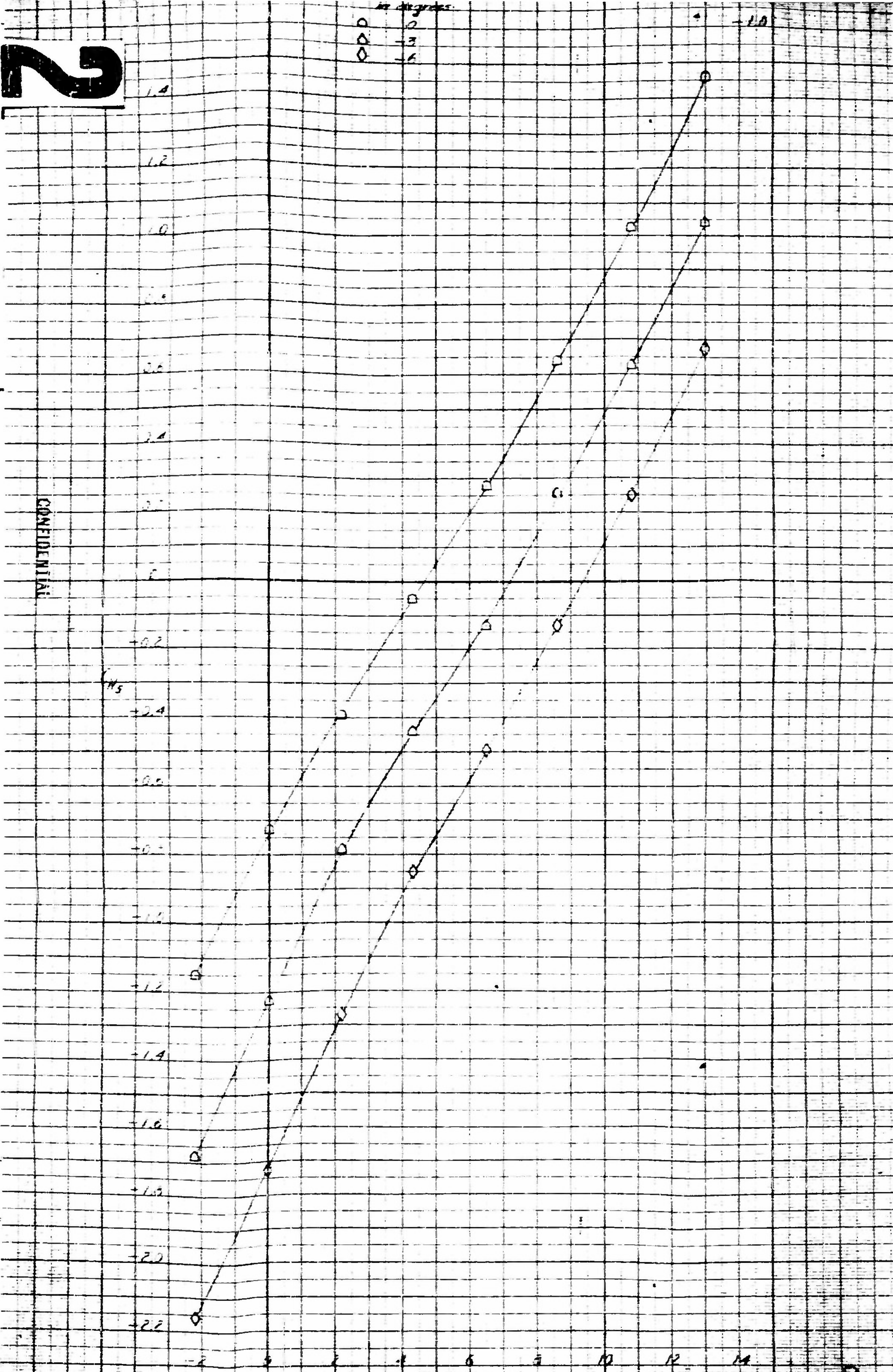

Figure 11 (Continued)

Lel. z = 2.04 Inches, x = 18.36 Inches, ψ = 6°, γ = 0. Pylon On

FIGURE 11 C

CONFIDENTIAL

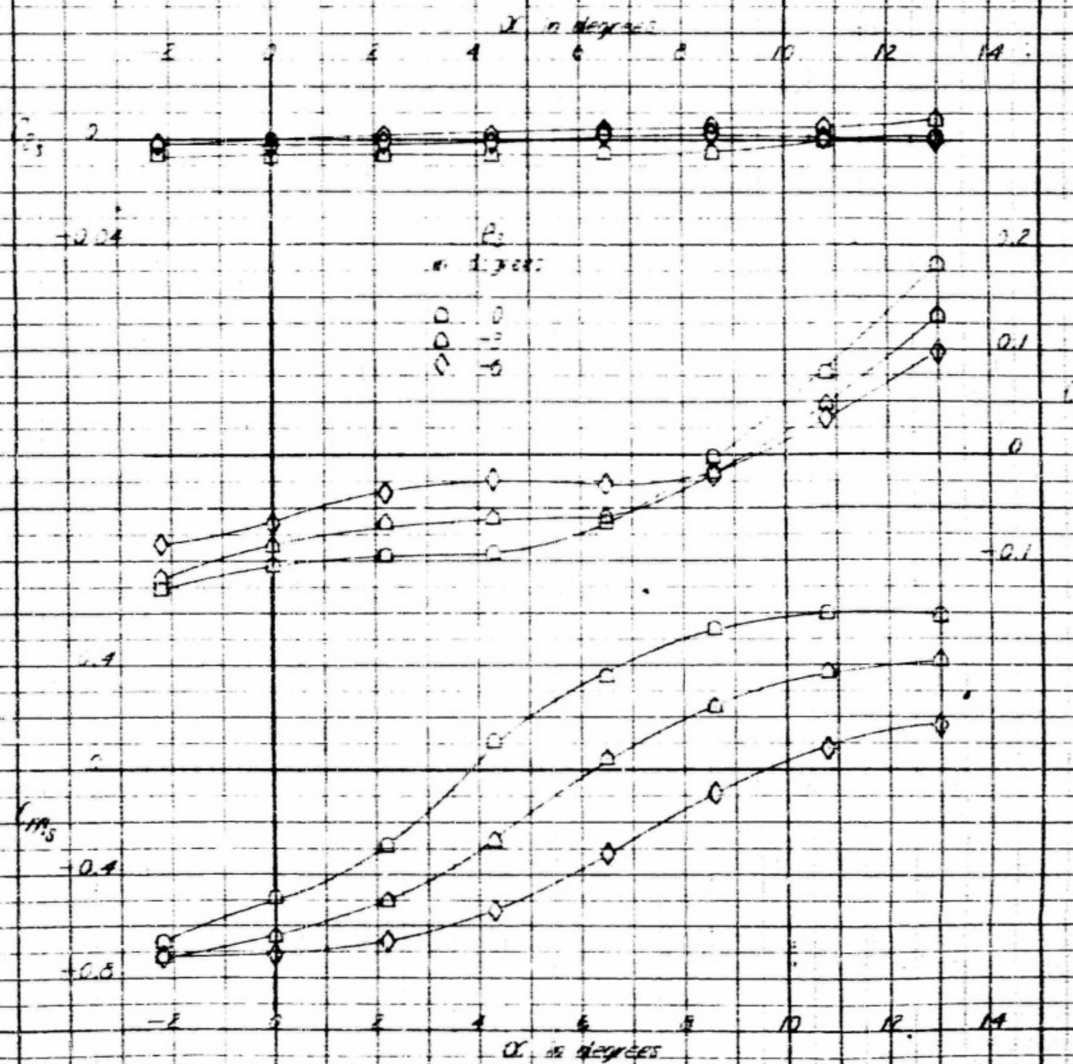

Figure 11 (Continued)

(b) Concluded

AERO 864

CONFIDENTIAL

FIGURE 11 (Concl)

CONFIDENTIAL

AERO 664

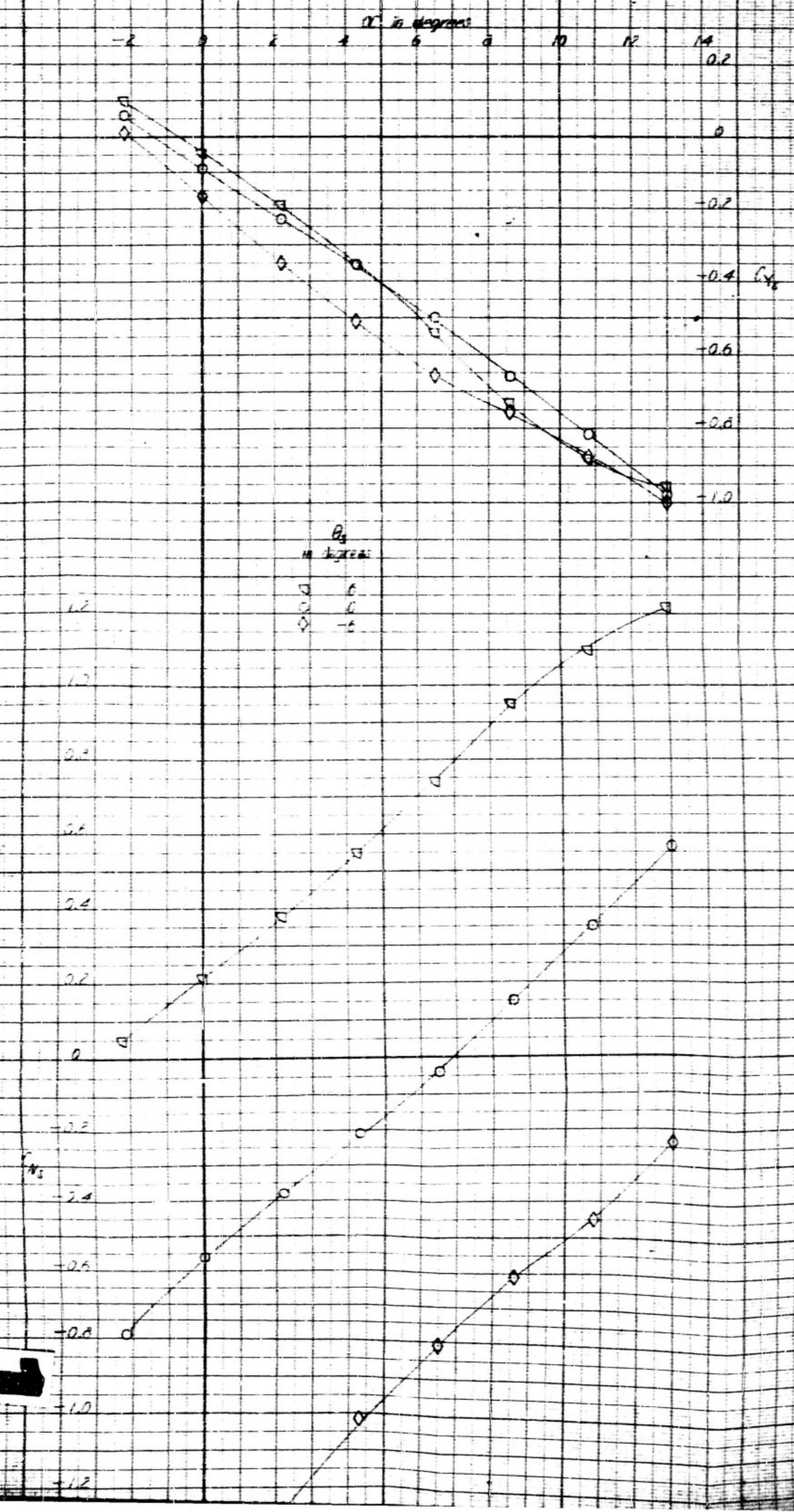

CONFIDENTIAL

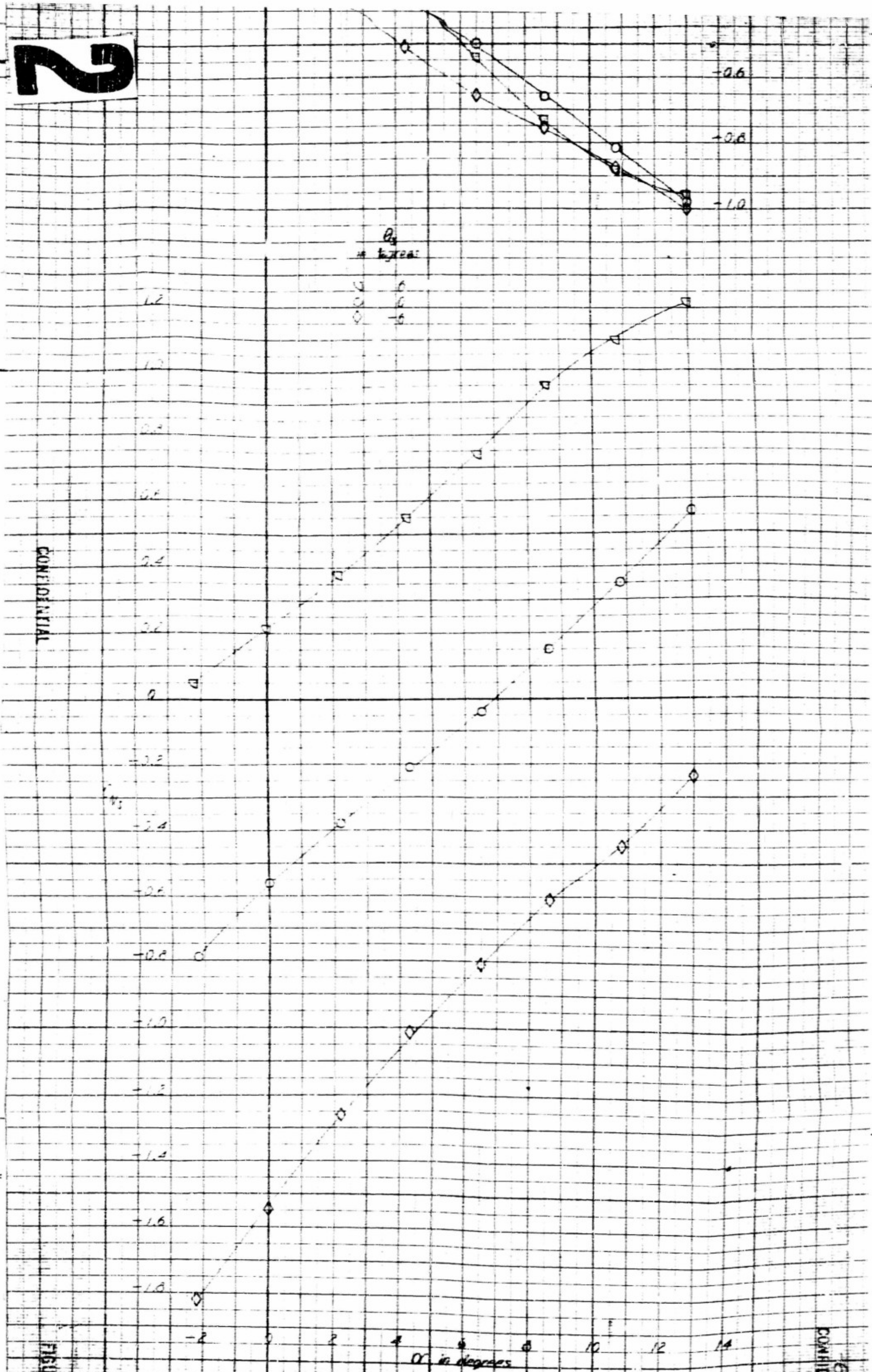

Figure 11 (Continued)

(m) z = 4.38 Inches; x = 0 Inch; $\psi_s = 0°$; $\phi = 0°$; Pylon On

FIGURE 11m

CONFIDENTIAL

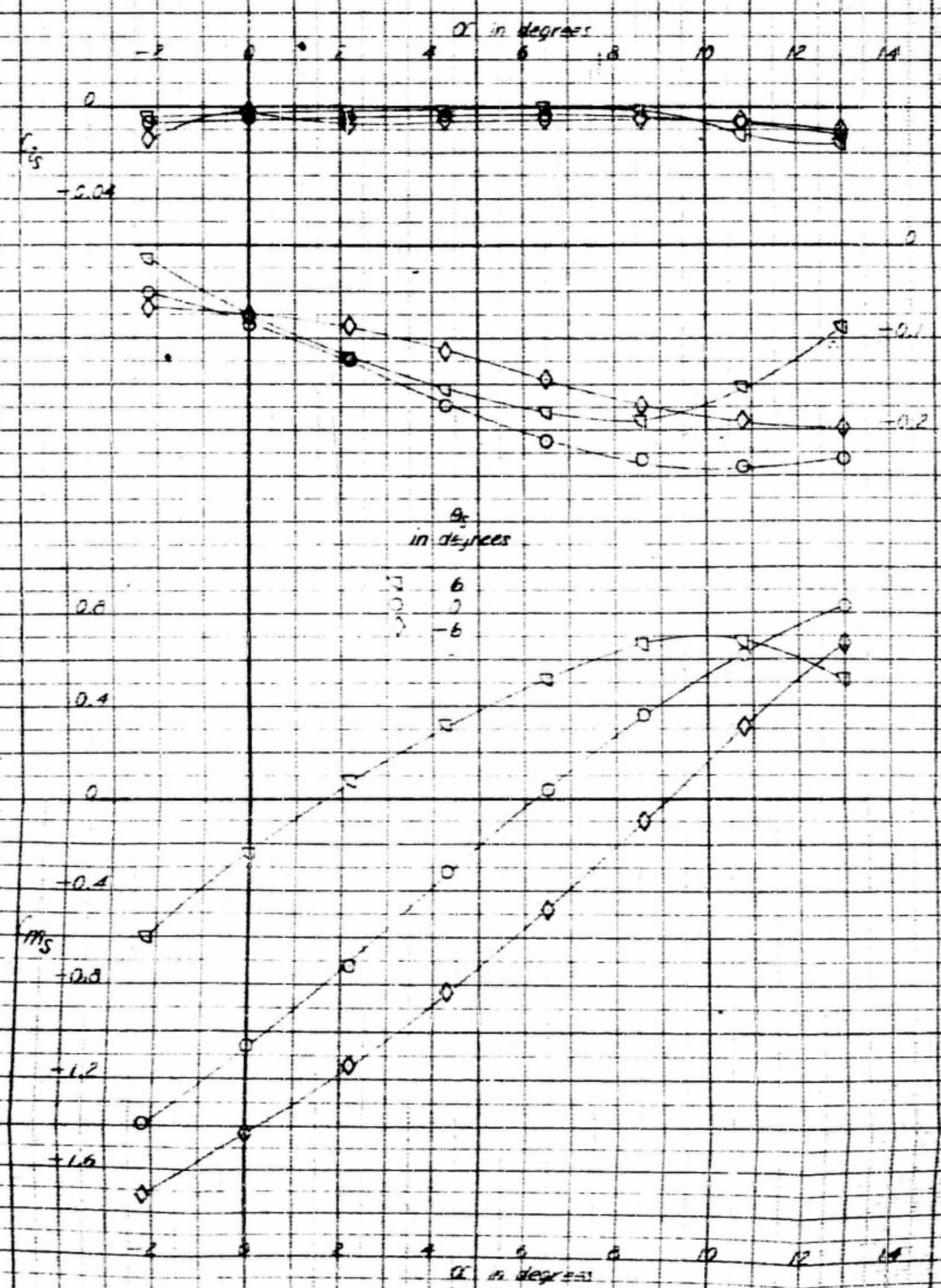

Figure 11 (Concluded)

(a) Concluded

FIGURE 11a (cont)

CONFIDENTIAL

AERO 864

CONFIDENTIAL

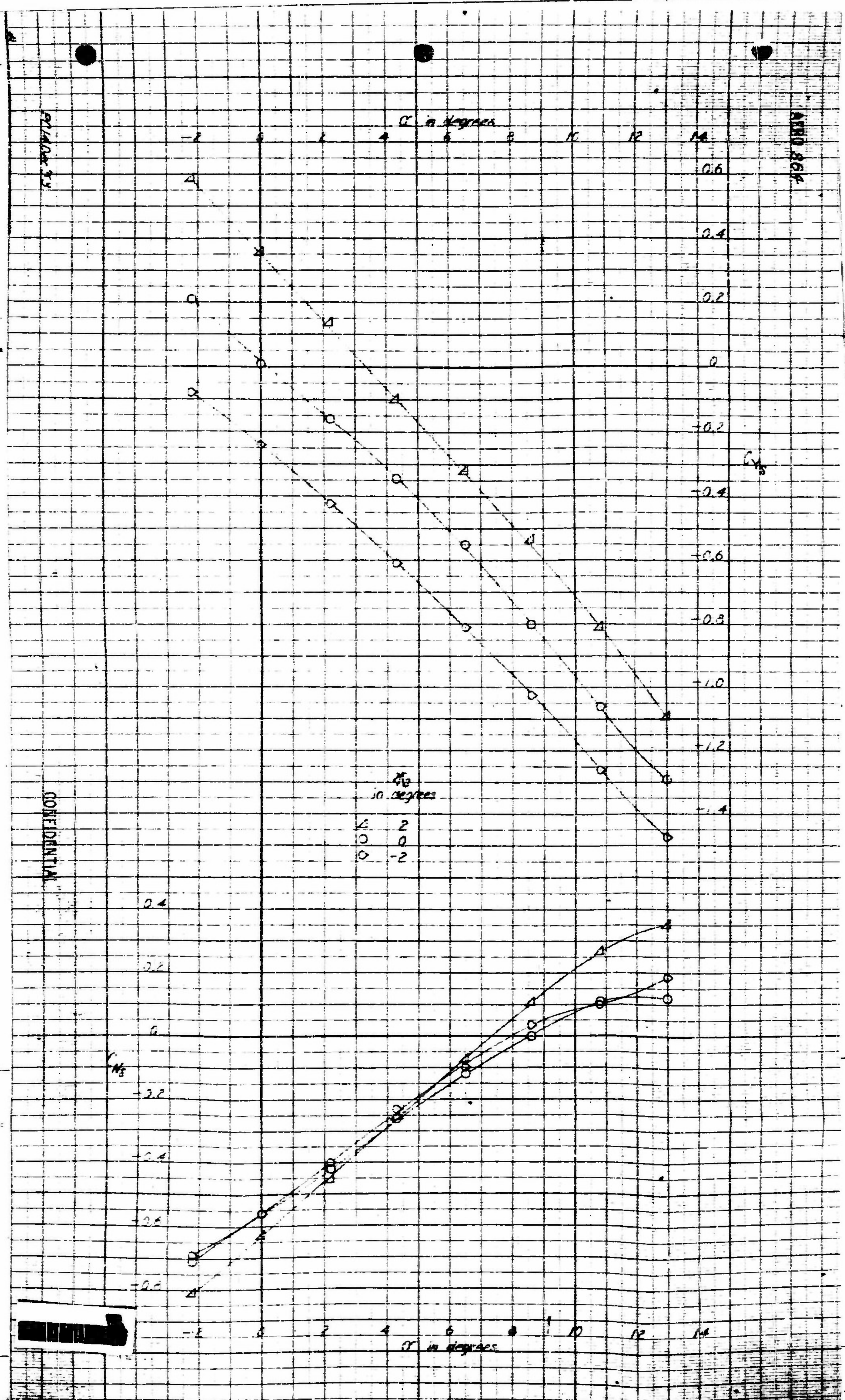

[redacted]

Figure 12 - Aerodynamic Characteristics of a ...

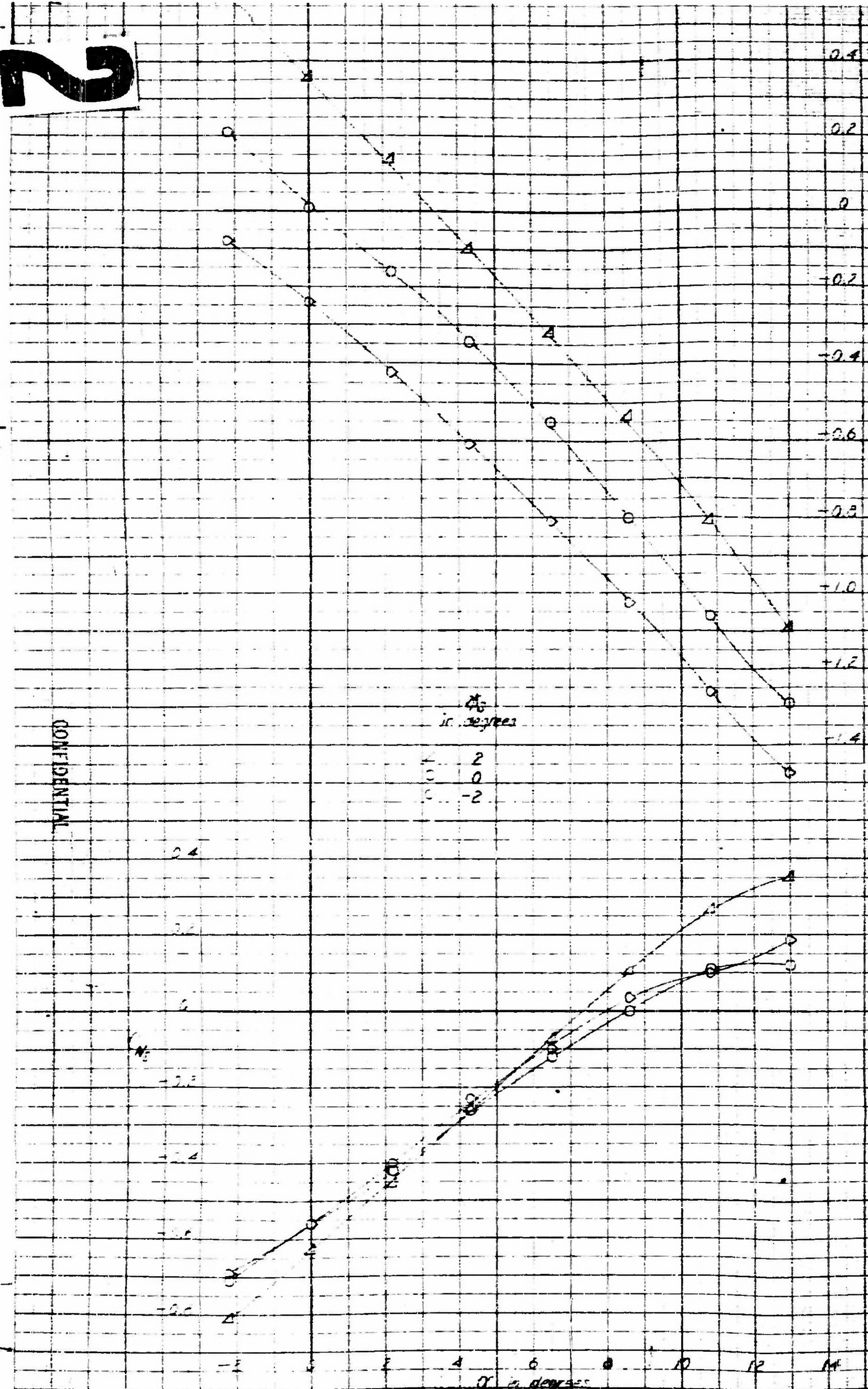

Figure 12 - Aerodynamic Characteristics of a 0.17-Scale Model XAAM-N-4 Oriole Missile Due to Missile Yaw in the Proximity of a 0.179-Scale Model F4D-1 Airplane at the Inboard Station

(a) z = 0 Inch, x = 0 Inch, $\theta_S = 0°$, $\psi = 0°$, Pylon On

FIGURE 12a

CONFIDENTIAL

CONFIDENTIAL

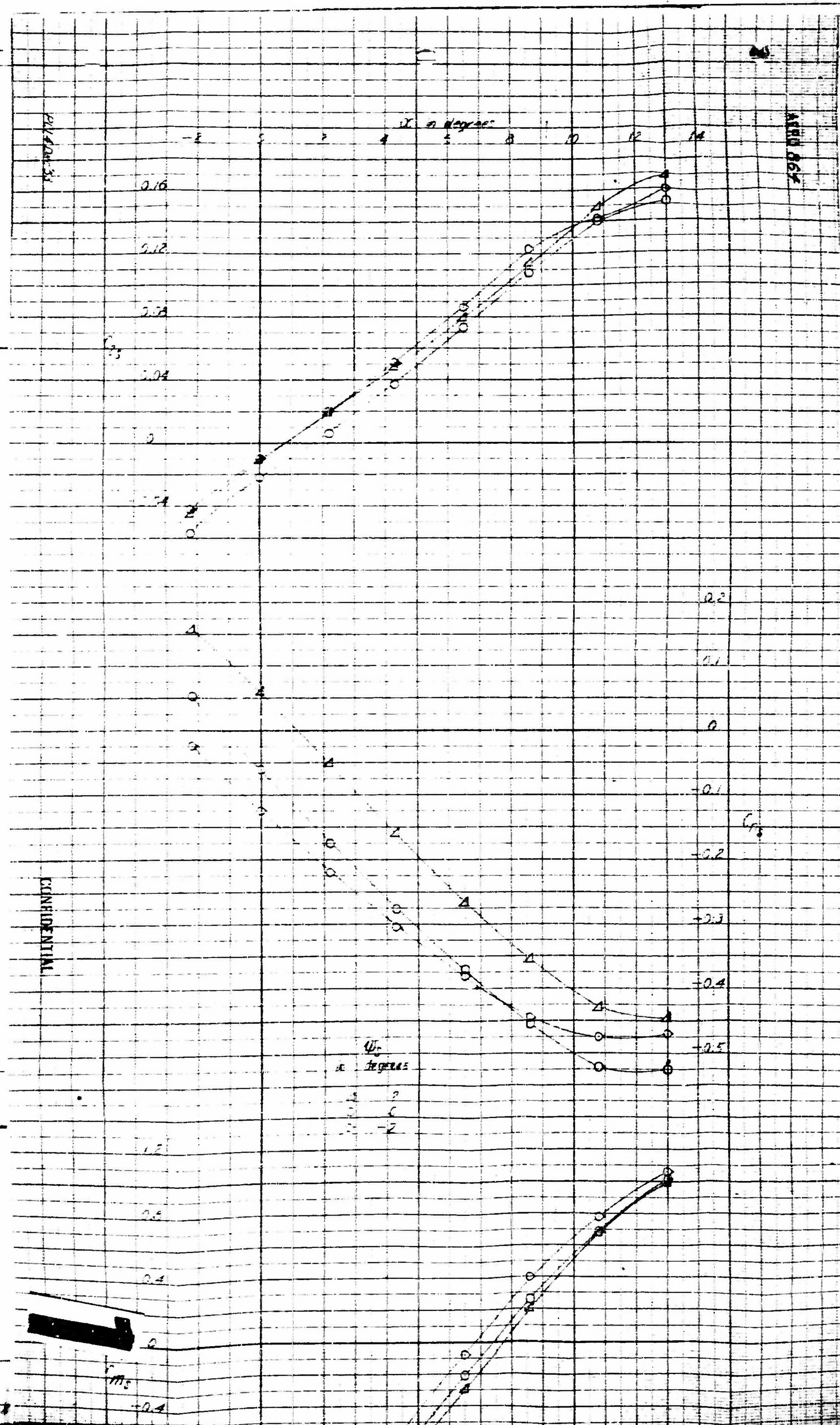
α in degrees
-2
0
2
4
6
8
10
12
14
0.16
0.12
0.08
0.04
0
-0.04
0.2
0.1
0
-0.1
-0.2
-0.3
-0.4
-0.5
ψ
in degrees
2
0
-2
0.4
0
-0.4
CONFIDENTIAL

CONFIDENTIAL

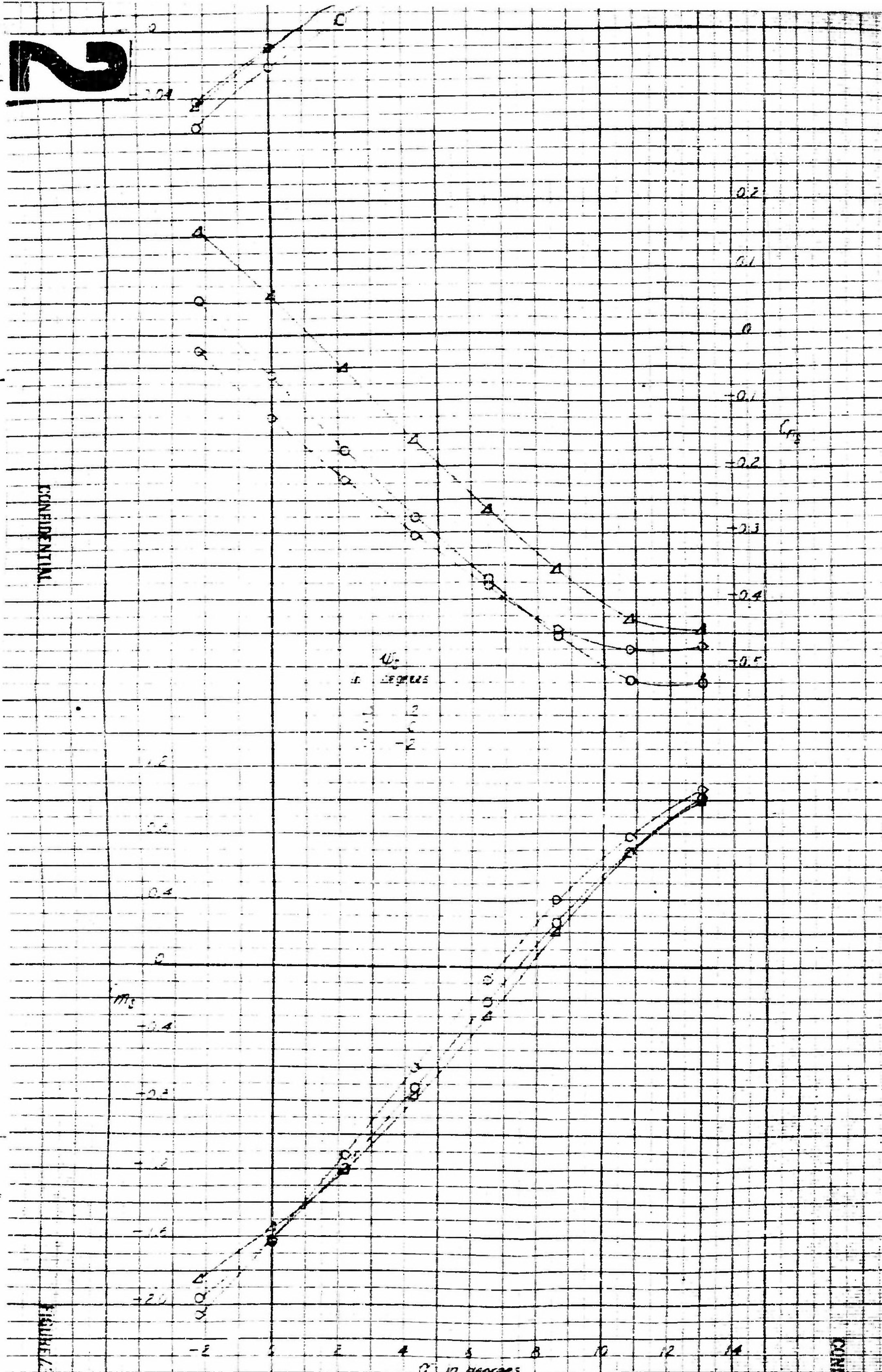

Figure 12 Continued

(a) Concluded

FIGURE 12(a) (Cont'd)

CONFIDENTIAL

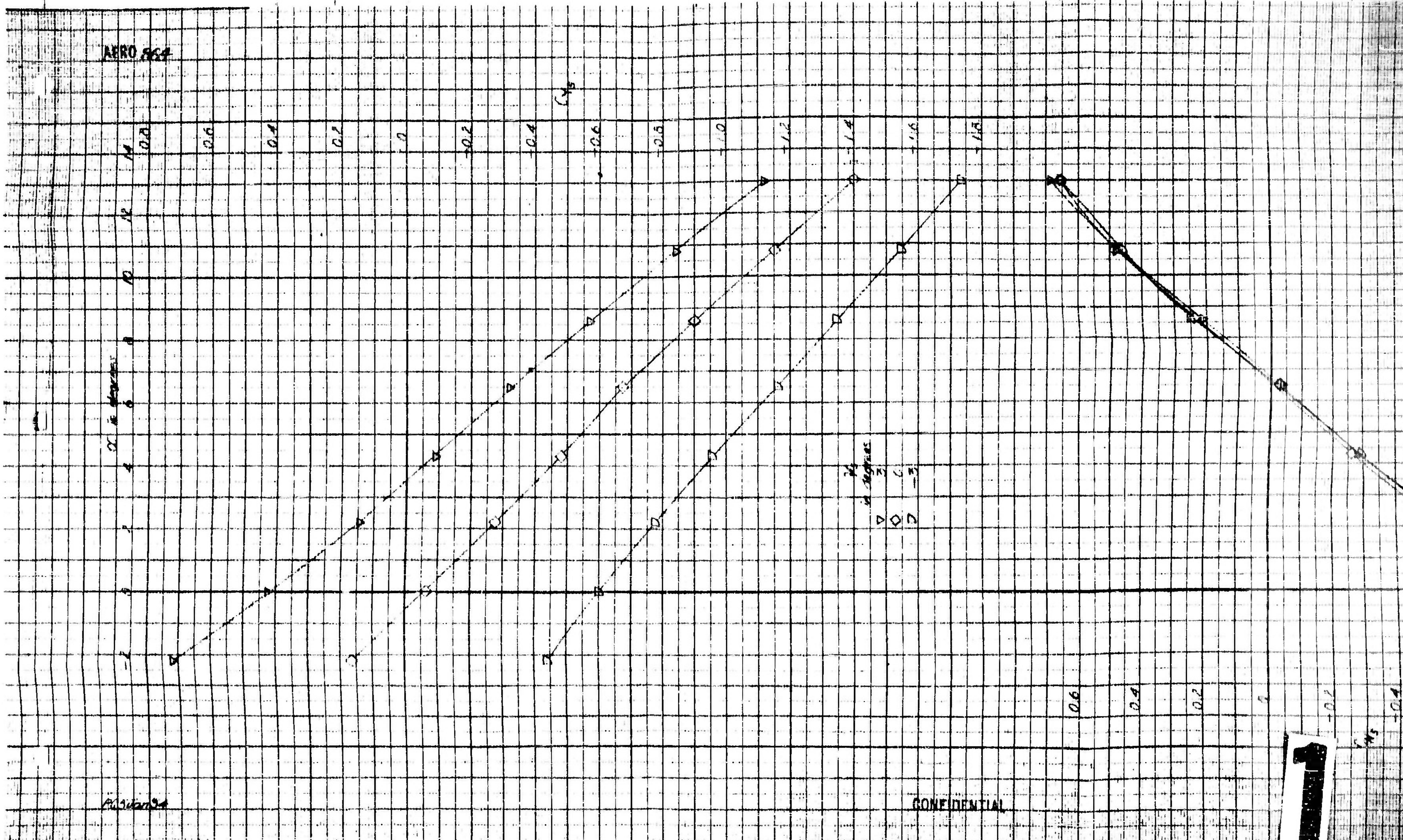
AERO 864
α in degrees
C_{Y_S}
ψ_S in degrees
3
0
-3
C_{N_S}
CONFIDENTIAL

CONFIDENTIAL

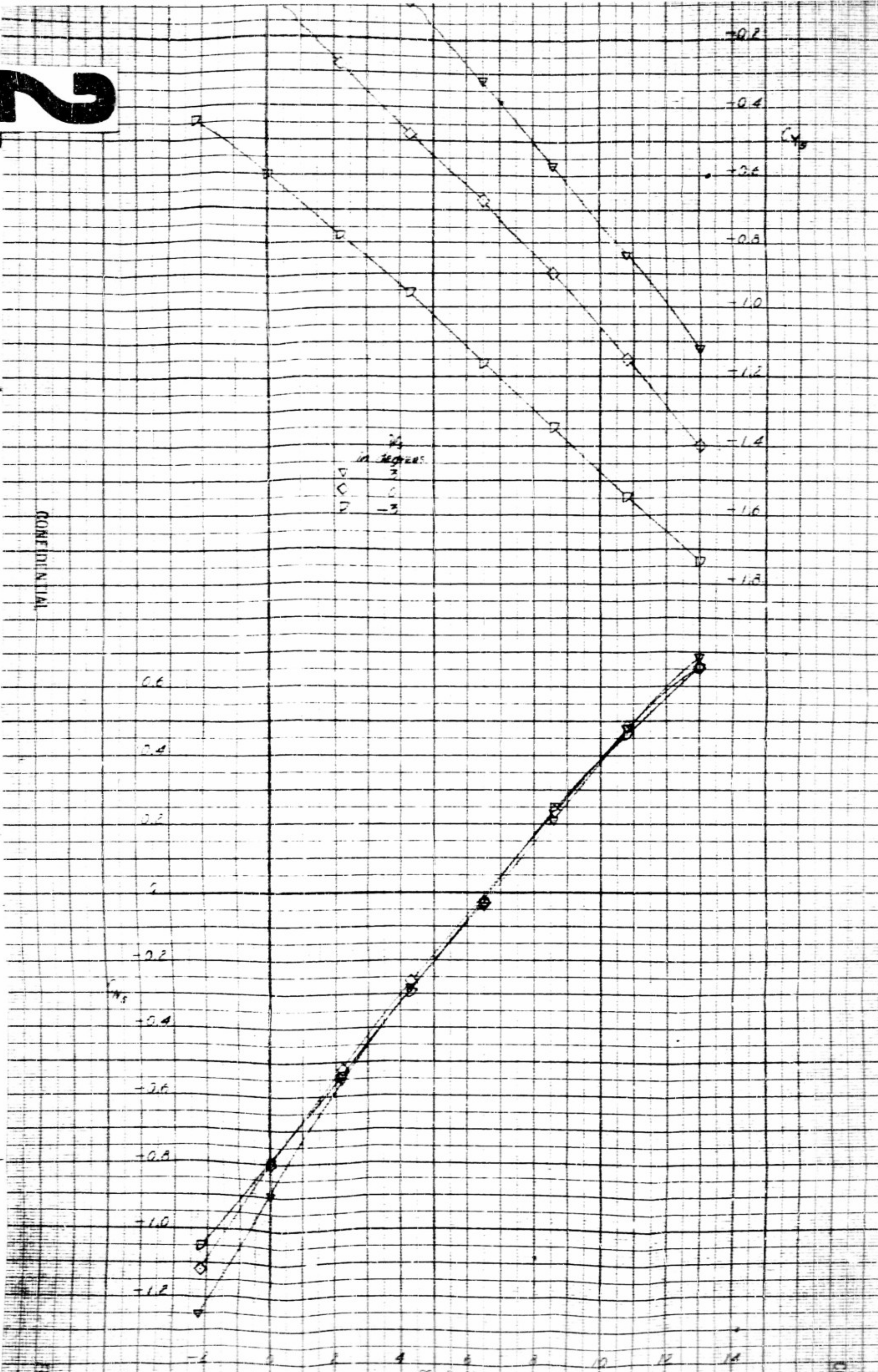

Figure 12 (Continued)

(c) $z = 0$ Inches, $X = 6.12$ Inches, $\delta_s = 0°$, $\beta = 0°$, Pylon On

FIGURE 12

CONFIDENTIAL

CONFIDENTIAL

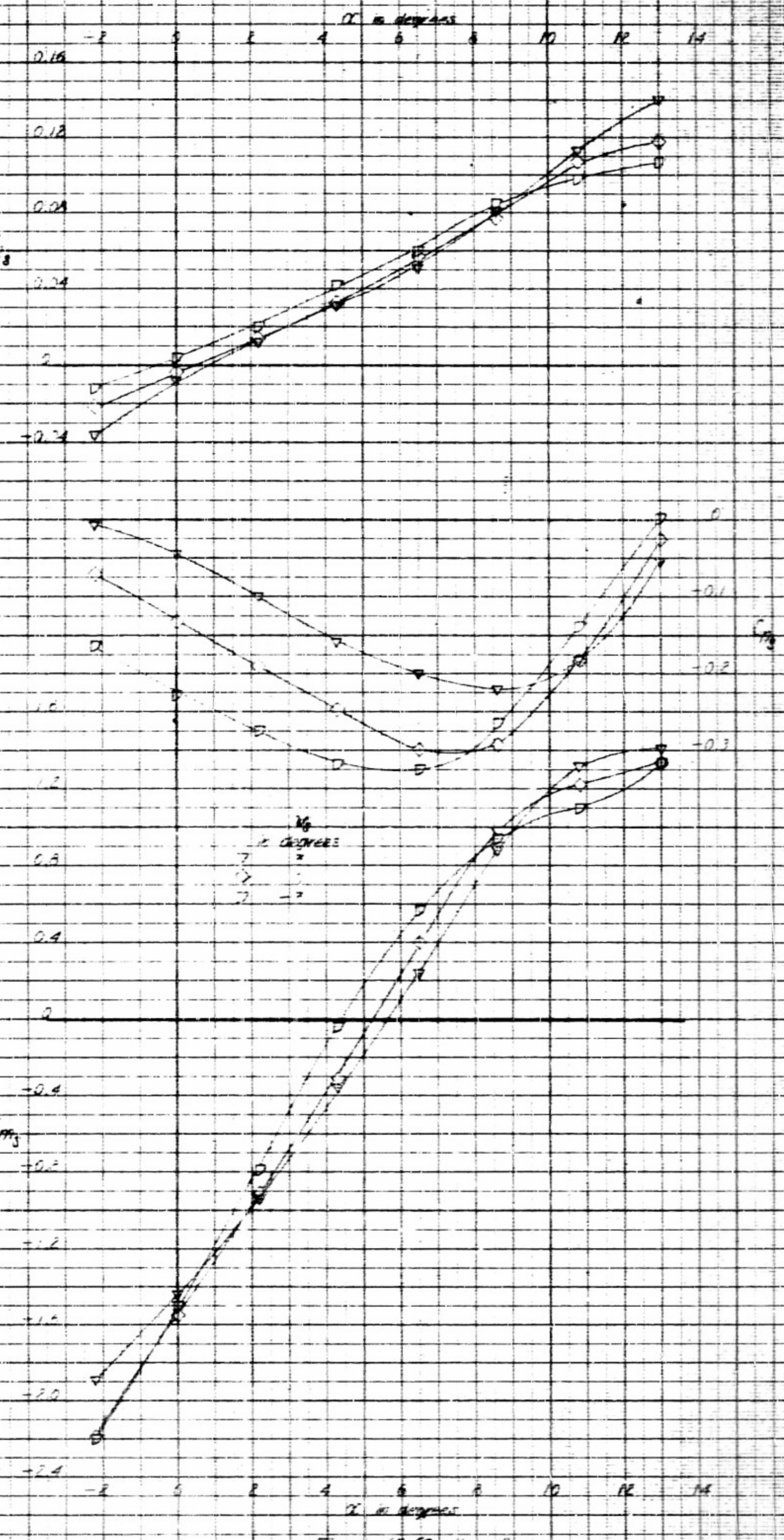

Figure 12 (Continued)

(b) Concluded

FIGURE 12 b (Concl.)

CONFIDENTIAL

AERO 864

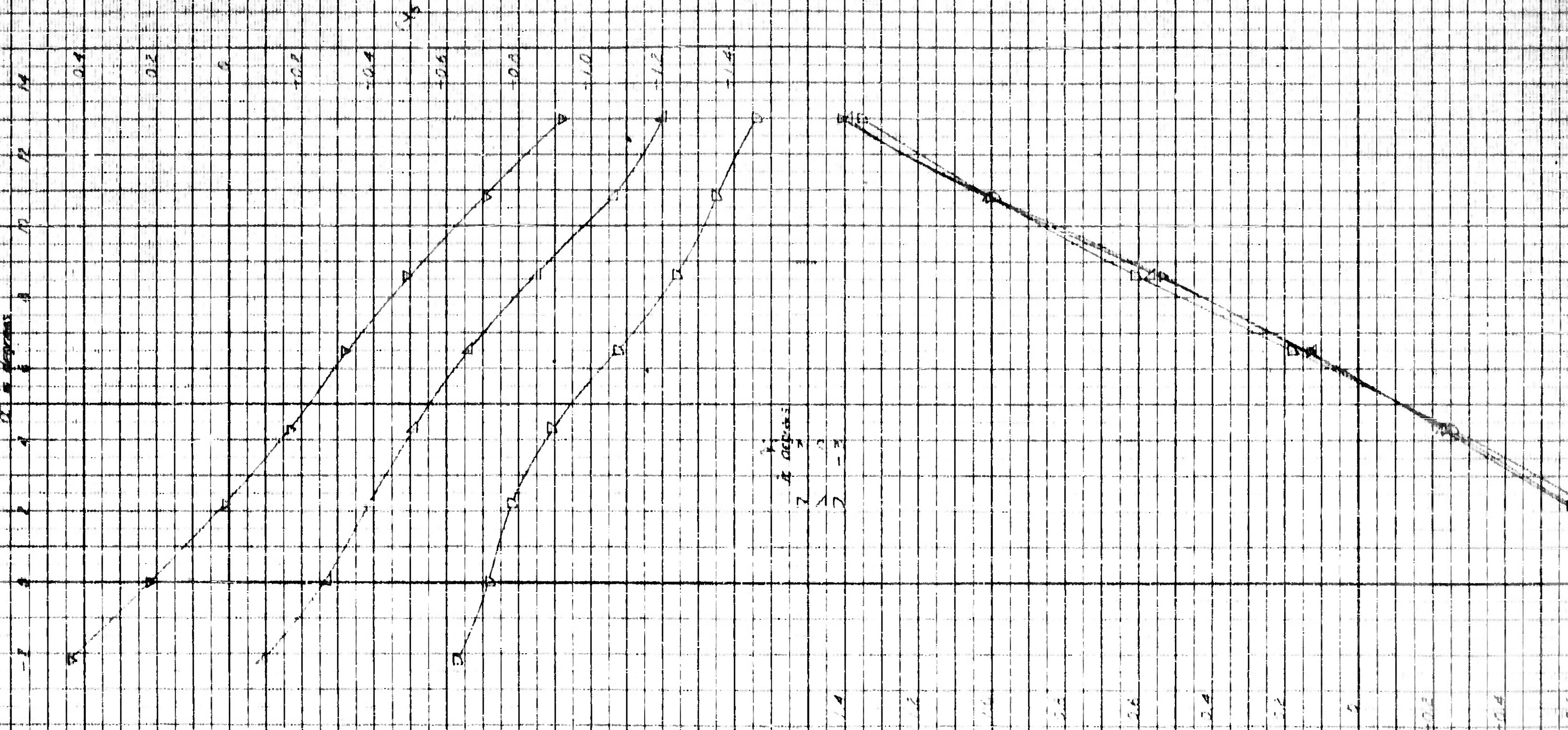

CONFIDENTIAL

CONFIDENTIAL

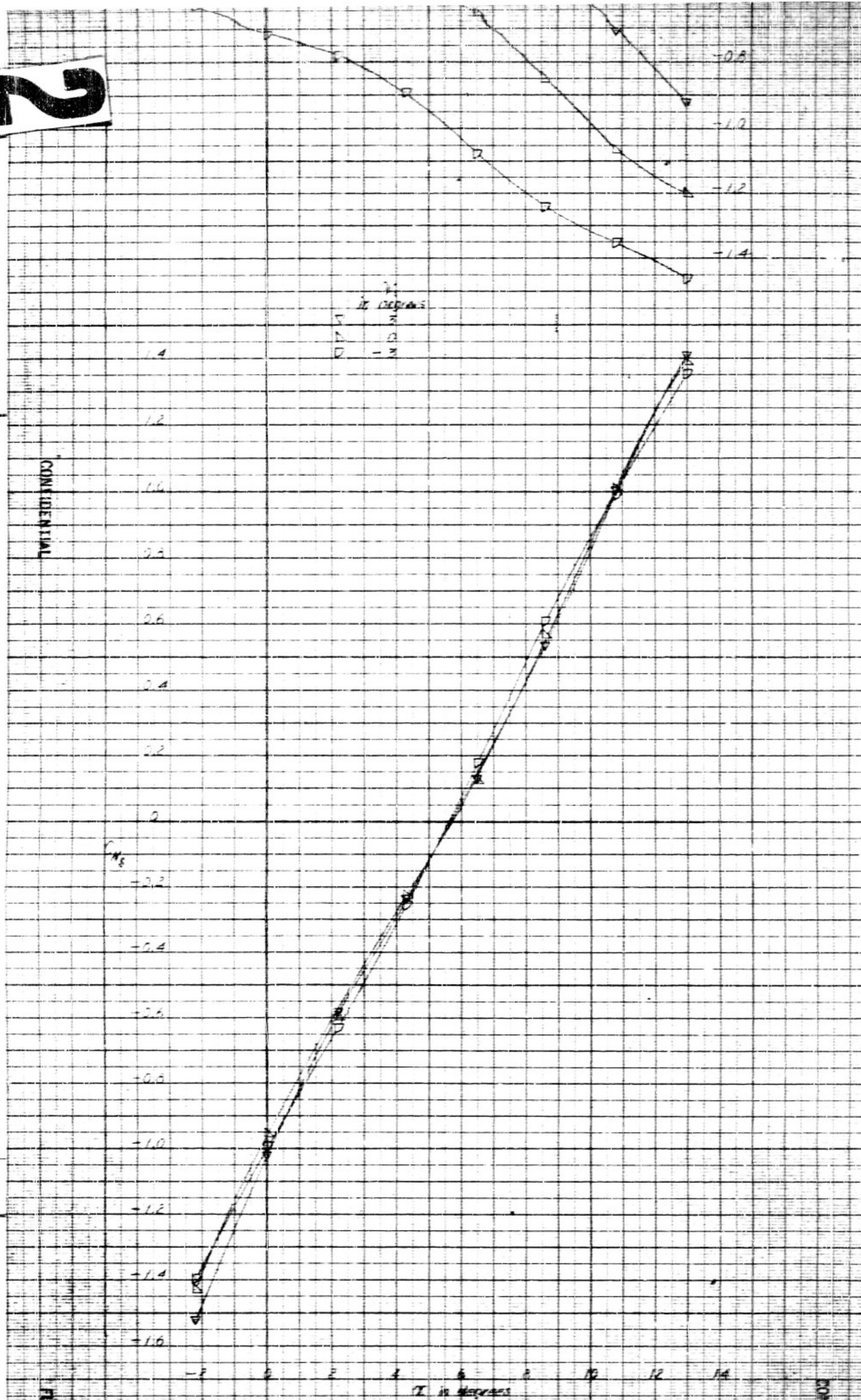

Figure 12 (Continued)

(c) $z = -0.1 \times h$, 13.26 Inches, $\theta = 0°$, $\psi = 0°$, Pylon On

FIGURE 12c

CONFIDENTIAL

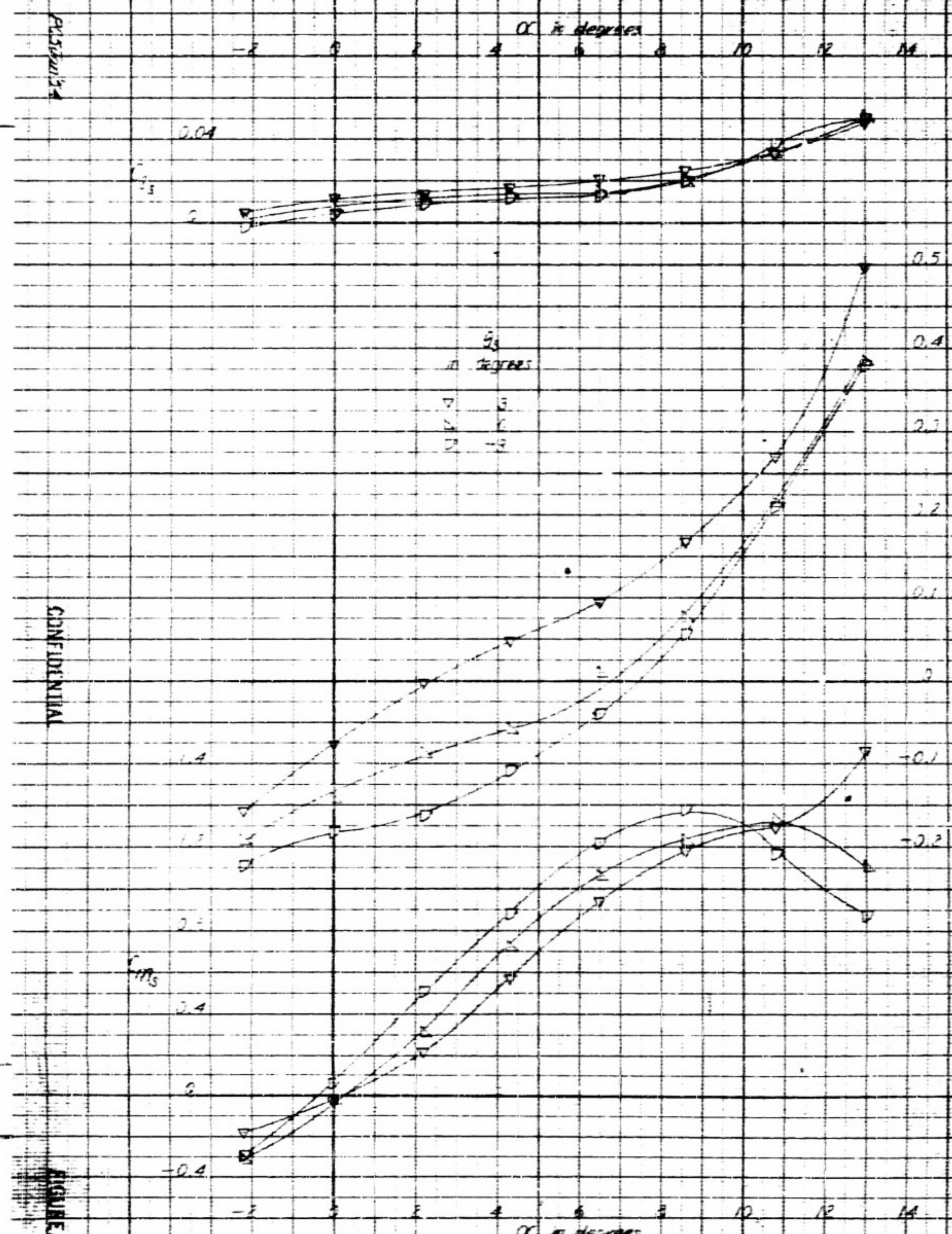

Figure 12 (Continued)

(c) Concluded


AERO 864
α in degrees
-2
0
2
4
6
8
10
12
14
C_{Y_f}
1.0
0.8
0.6
0.4
0.2
0
-0.2
-0.4
-0.6
-0.8
-1.0
-1.2
-1.4
-1.6
-1.8
1.6
1.4
1.2
1.0
0.8
0.6
ψ_f
in degrees
JE 17 Dec 53
CONFIDENTIAL

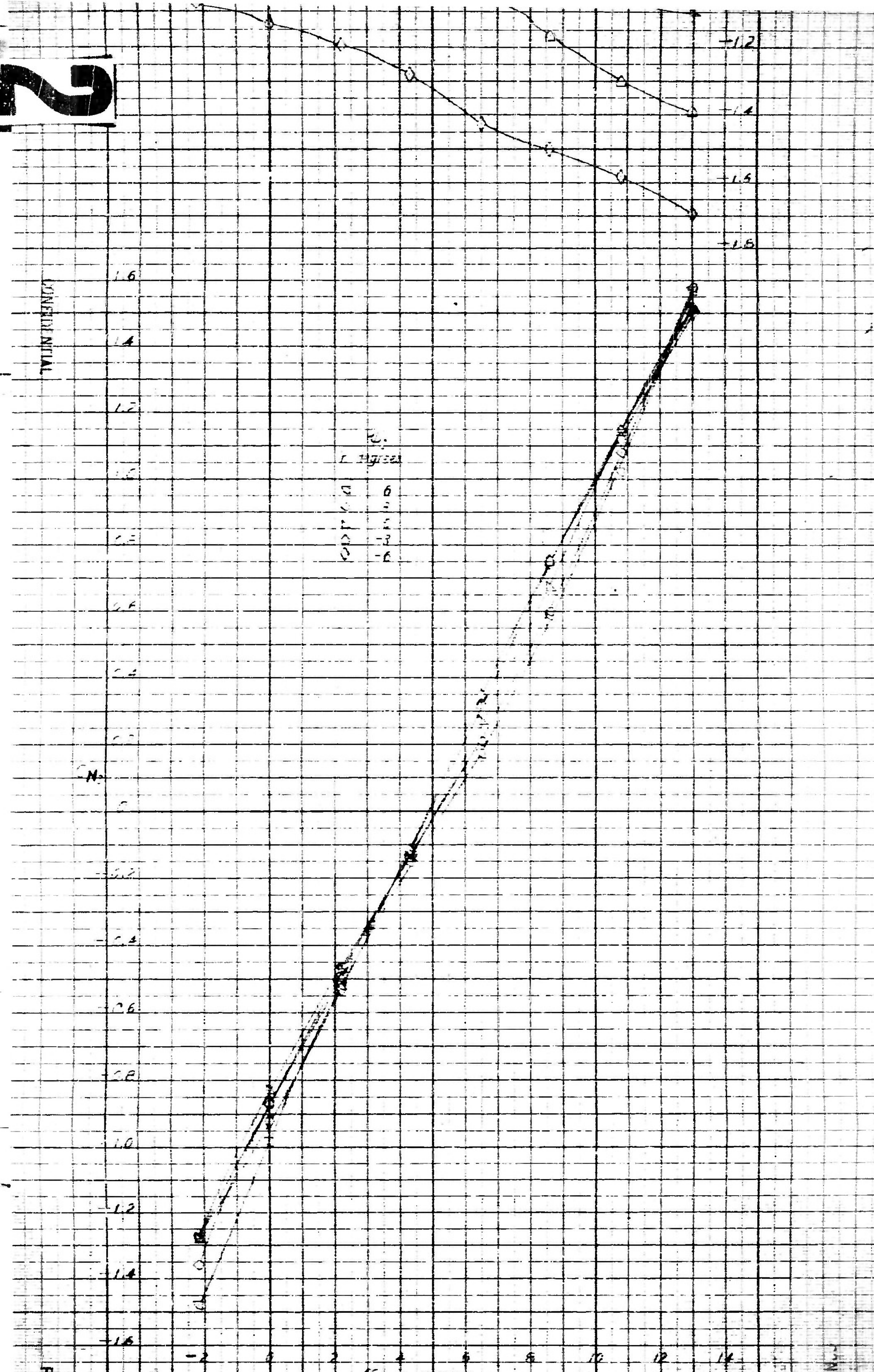

Figure 12 (Continued)

(d) $z = 0$ Inch, $y = 13.36$ Inches, $\theta_3 = 0°$, $\Phi = 0°$, Pylon Off

FIGURE 12d

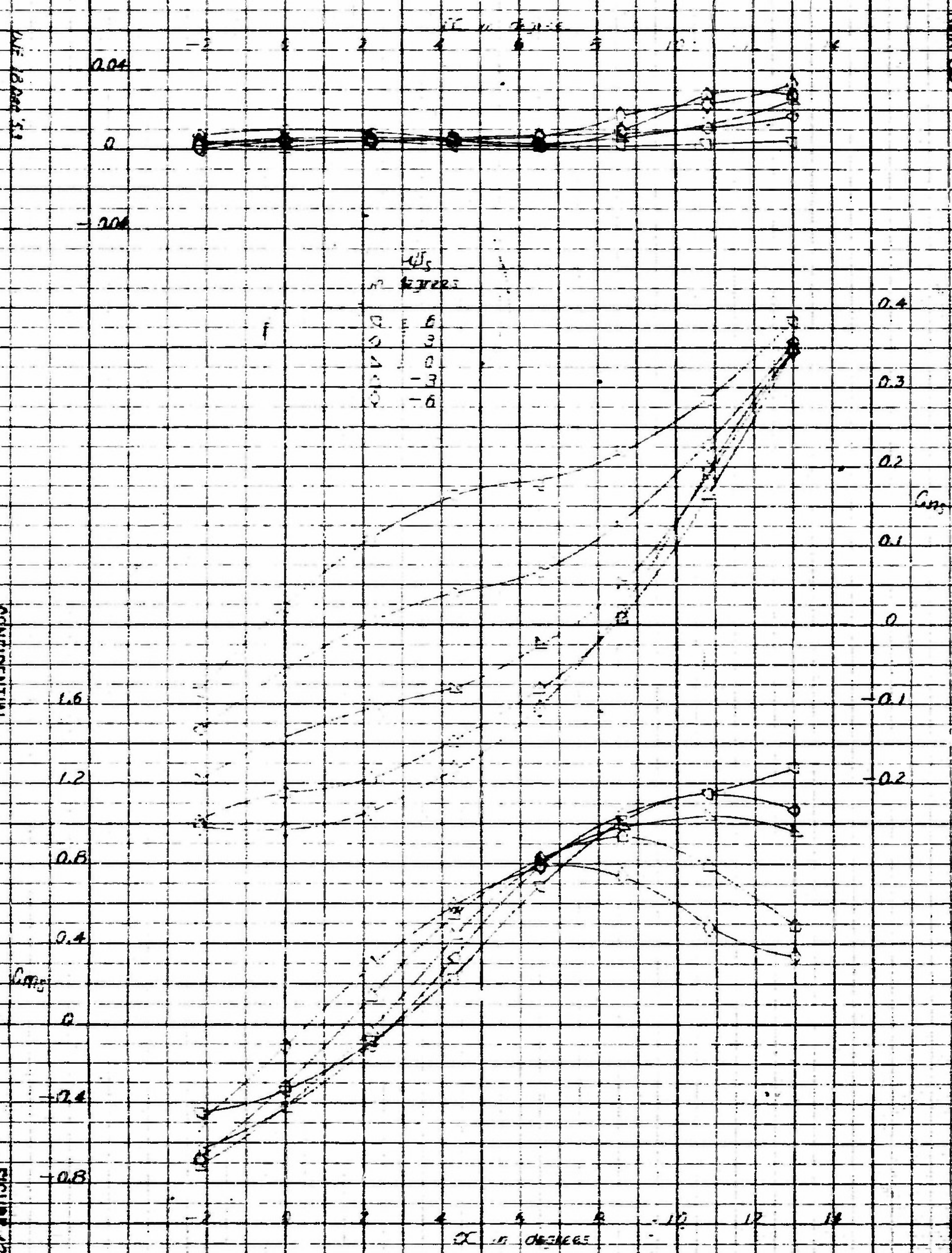

Figure 12 (Continued)
(d) Concluded

CONFIDENTIAL

FIGURE 12d (Concl)

CONFIDENTIAL

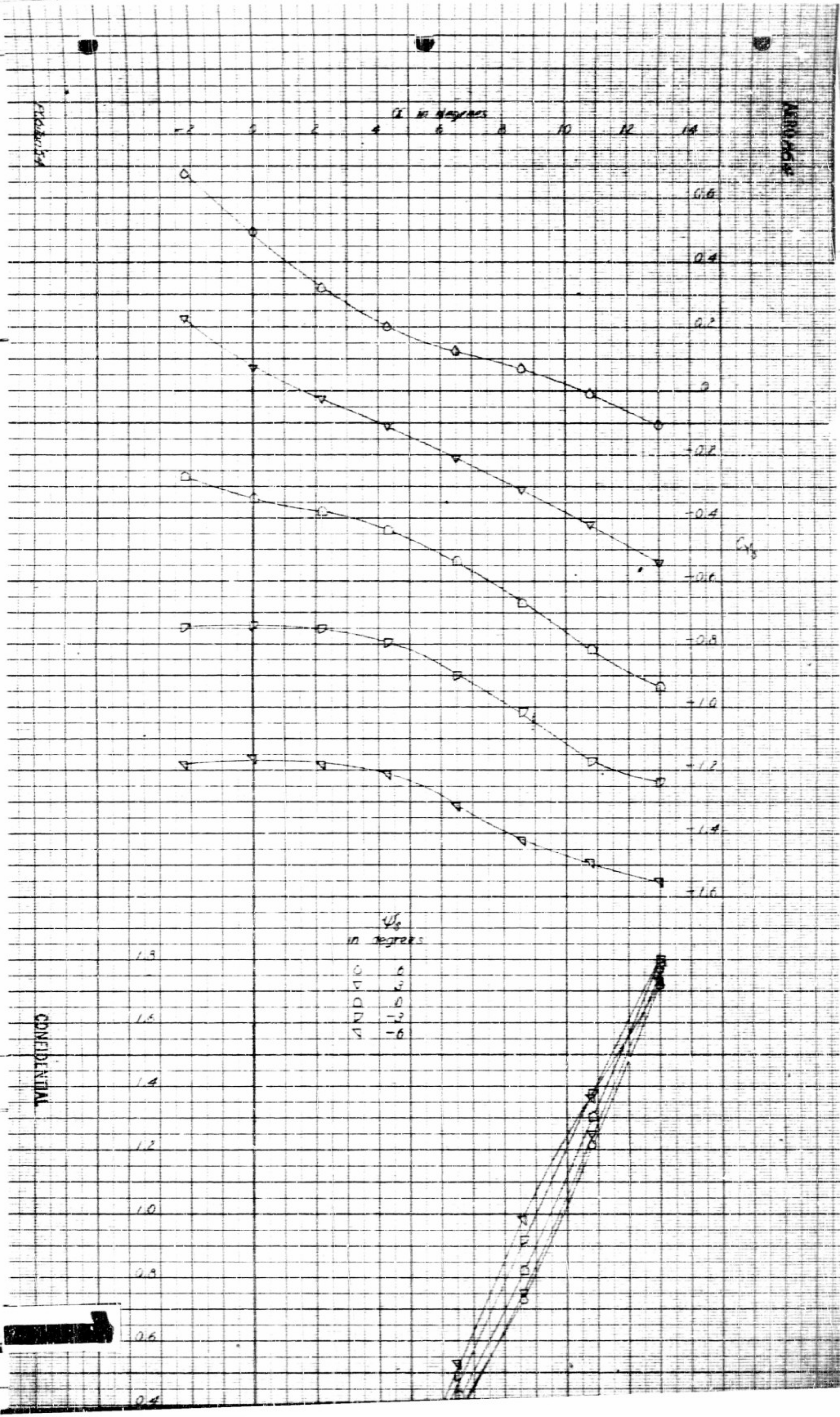
α in degrees
-2
0
2
4
6
8
10
12
14
0.6
0.4
0.2
0
-0.2
-0.4
-0.6
-0.8
-1.0
-1.2
-1.4
-1.6
1.8
1.6
1.4
1.2
1.0
0.8
0.6
0.4
ψ in degrees
6
3
0
-3
-6
CONFIDENTIAL
[redacted]

CONFIDENTIAL

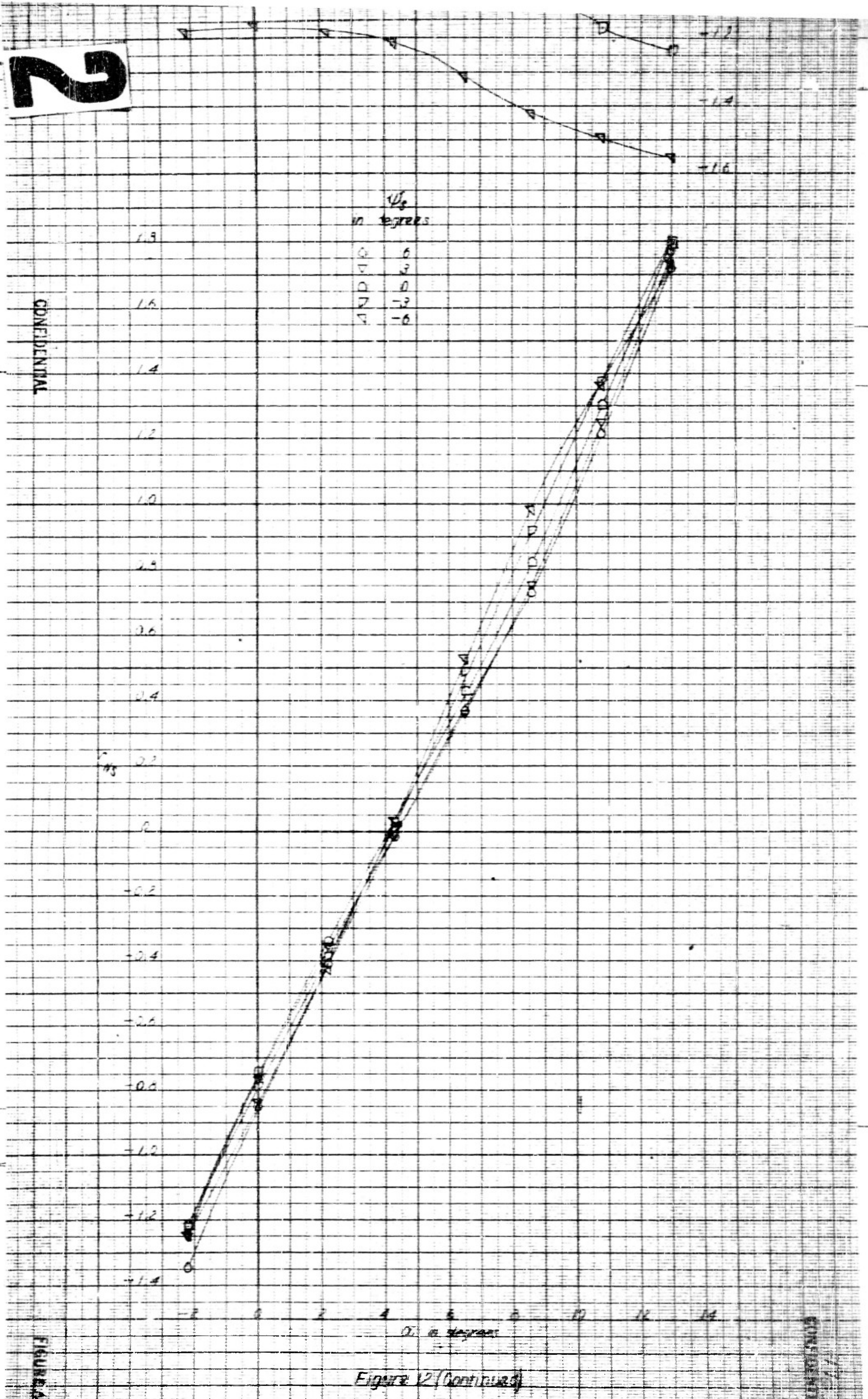

Figure 12 (Continued)

(e) z = 0 Inch, x = 18.36 Inches, $\delta_s = 0°$, $\psi = 0$; Pylon On

FIGURE 12e

CONFIDENTIAL

CONFIDENTIAL

FIGURE 12 (Concl.)

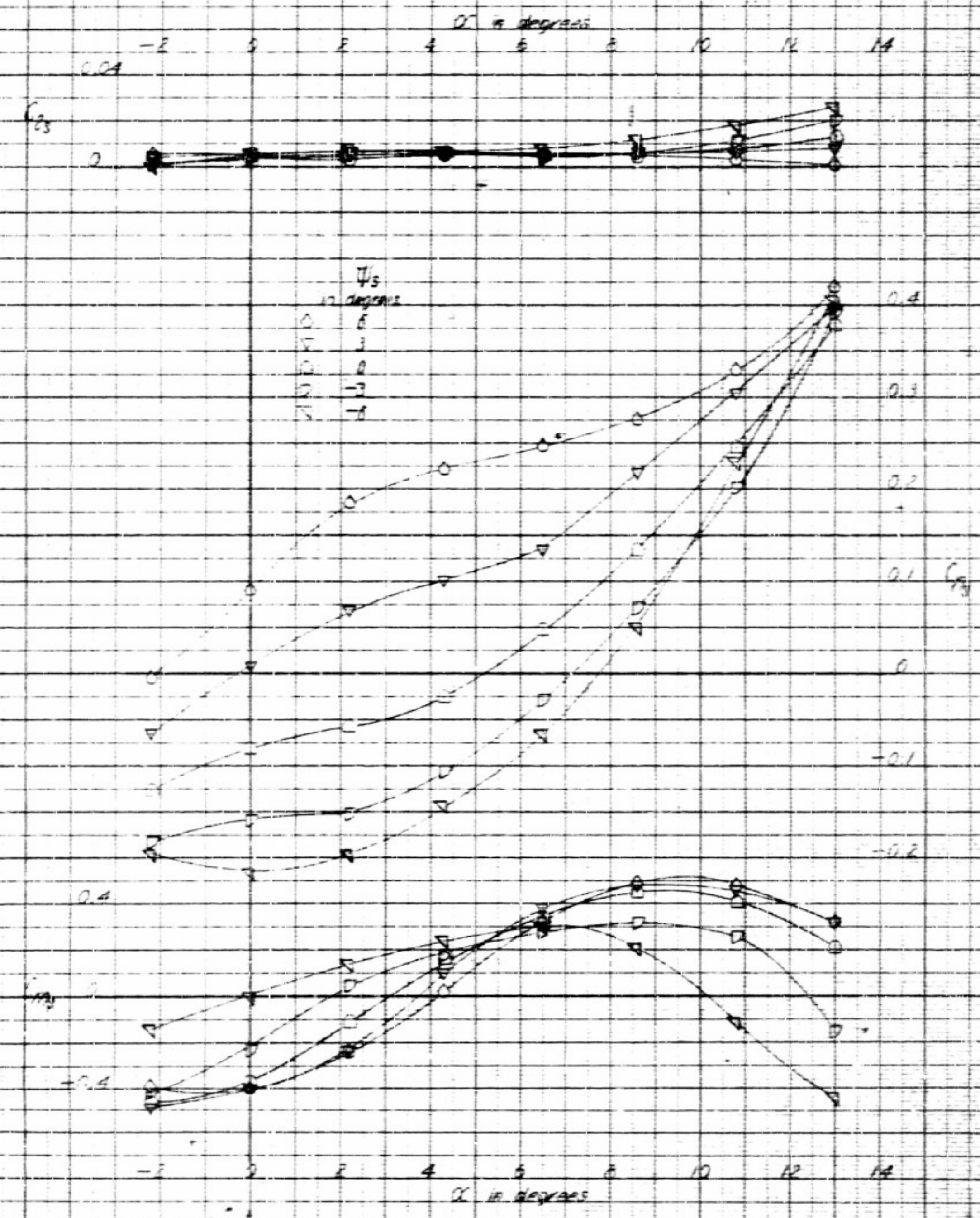

Figure 12 (Concluded)

(b) Concluded

CONFIDENTIAL

Figure 13 – Aerodynamic Characteristics of a 0.17-Scale Model XAAM-N-4

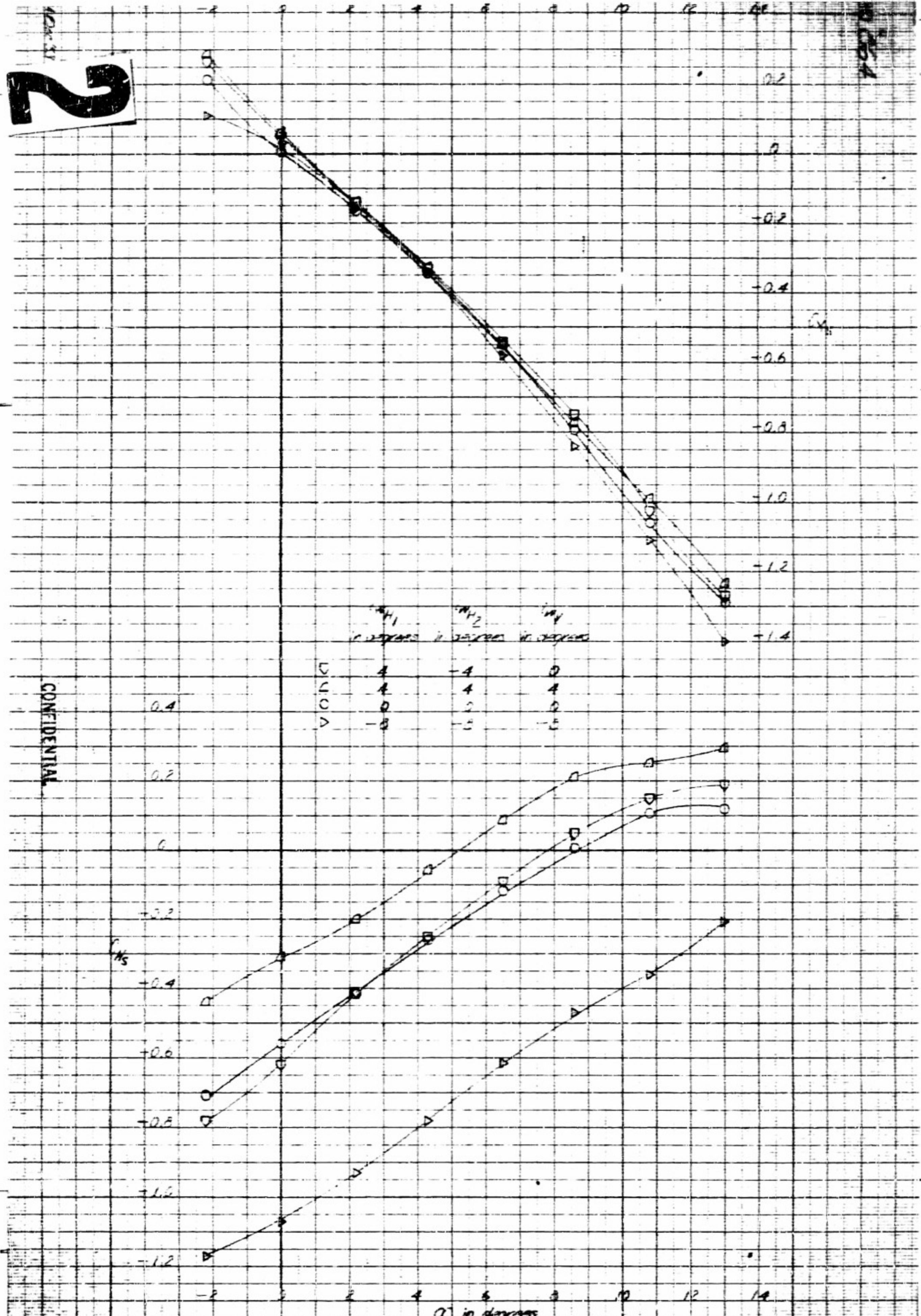

Figure 13 – Aerodynamic Characteristics of a 0.10-Scale Model XAAM-N-4 Oriole Missile Due to Missile Wing Incidence in the Proximity of a 0.10-Scale Model F4D-1 Airplane at the Inboard Station

(a) Z = 0 inch, Y = 0 inch, θ_s = 0°, ψ_s = 0°, ψ = 0°, Pylon On

CONFIDENTIAL

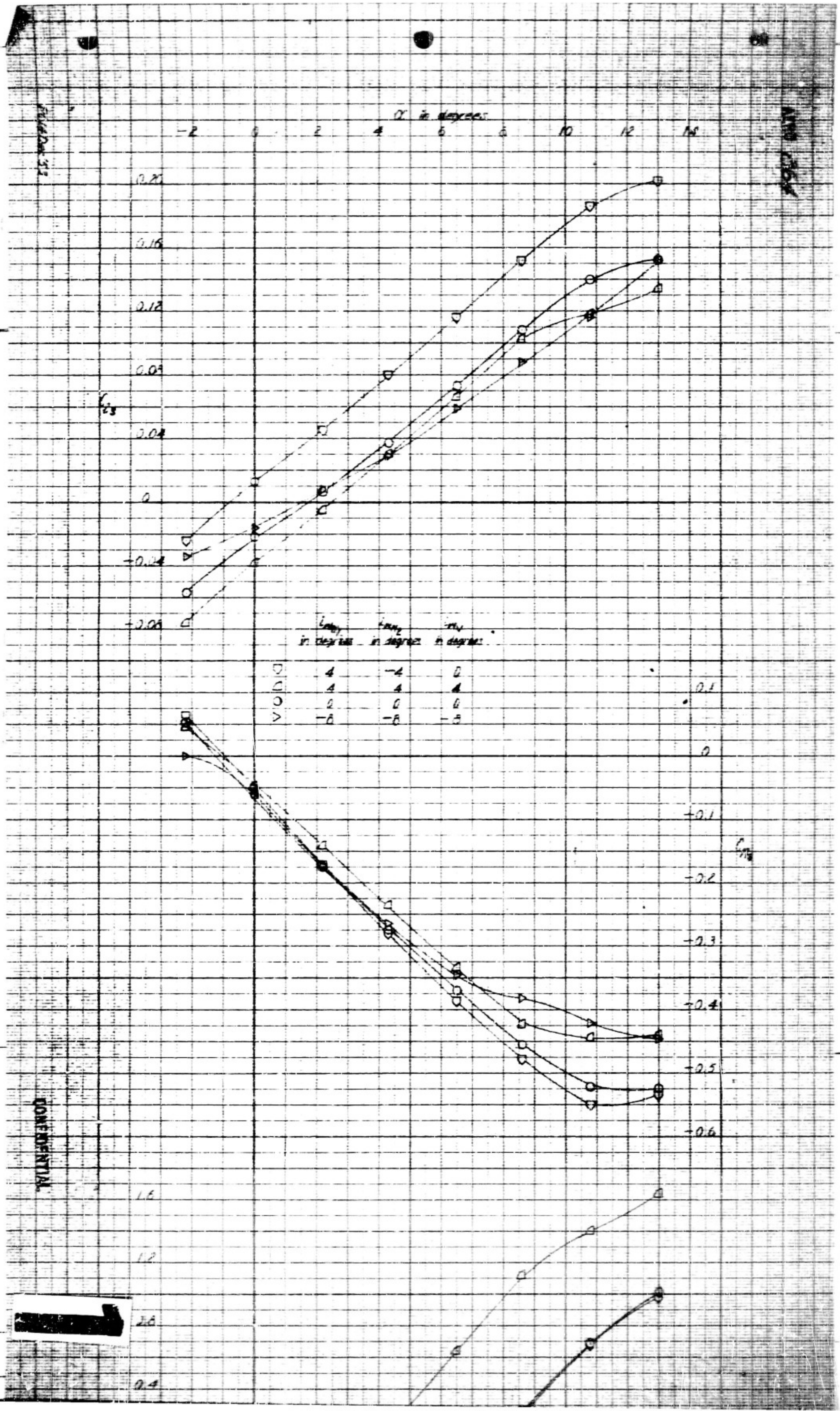
α in degrees
-2 0 2 4 6 8 10 12 14
0.20
0.16
0.12
0.08
0.04
0
-0.04
-0.08
i_{m_1} in degrees
i_{m_2} in degrees
i_v in degrees
4 -4 0
4 4 4
0 0 0
-8 -8 -8
0.1
0
-0.1
-0.2
-0.3
-0.4
-0.5
-0.6
1.6
1.2
0.8
0.4
CONFIDENTIAL
[redacted]

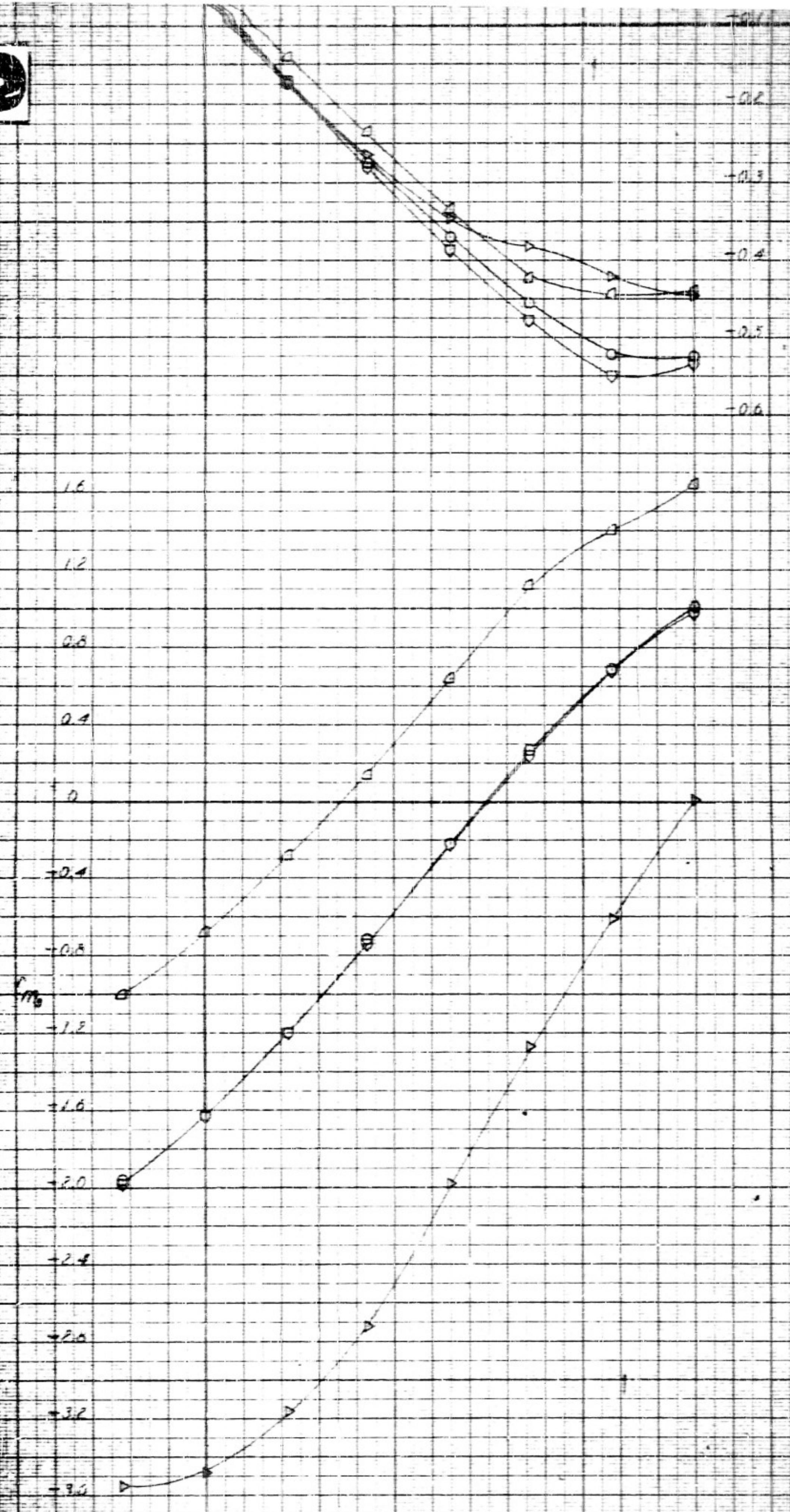

Figure 13 (Continued).

(a) Concluded.

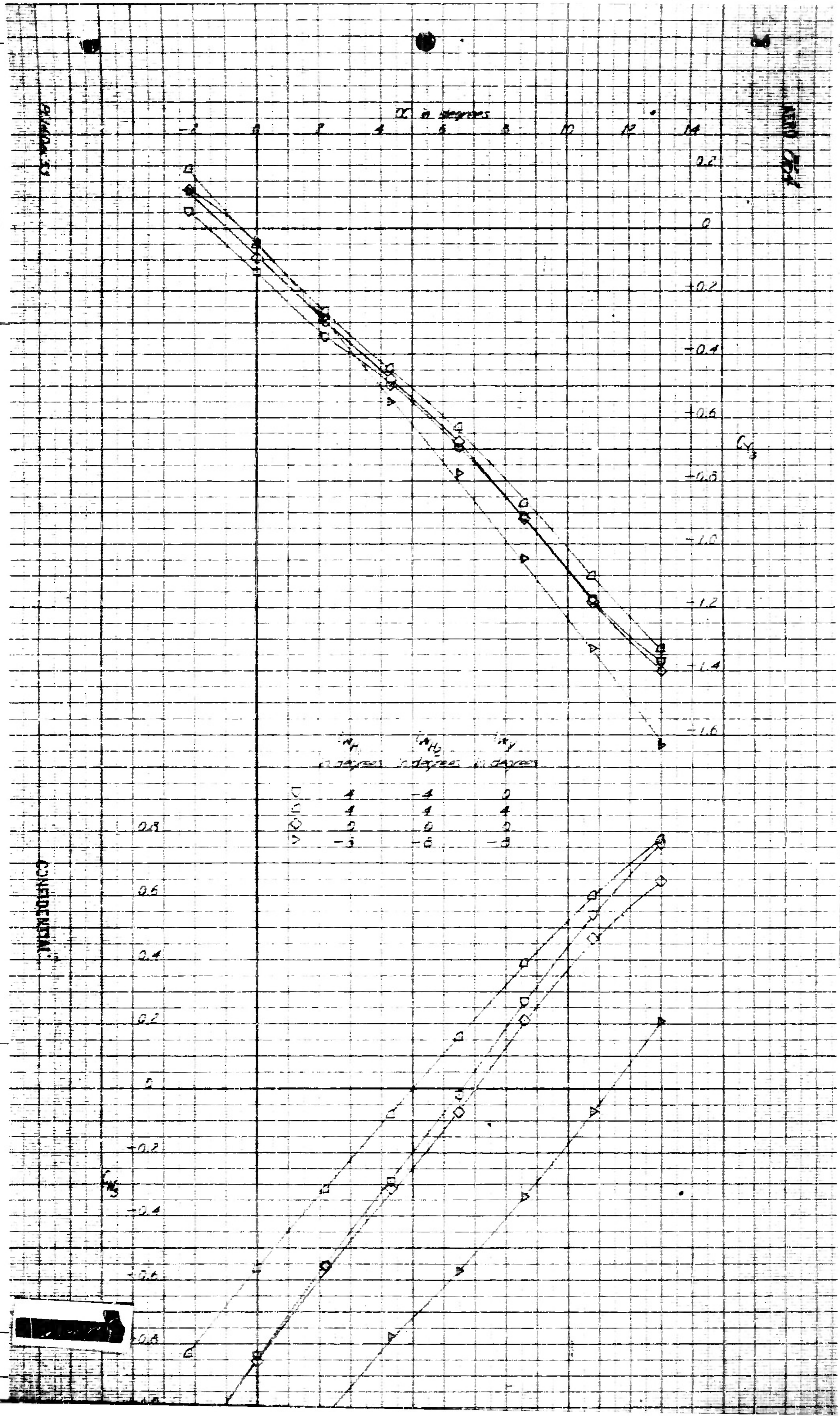

α in degrees
-2 0 2 4 6 8 10 12 14
0.2 0 -0.2 -0.4 -0.6 -0.8 -1.0 -1.2 -1.4 -1.6
C_{Y_3}
i_{H_1} in degrees
i_{H_2} in degrees
i_V in degrees
4 -4 0
4 4 4
0 0 0
-8 -8 -8
0.8 0.6 0.4 0.2 0 -0.2 -0.4 -0.6 -0.8
C_{n_3}
CONFIDENTIAL

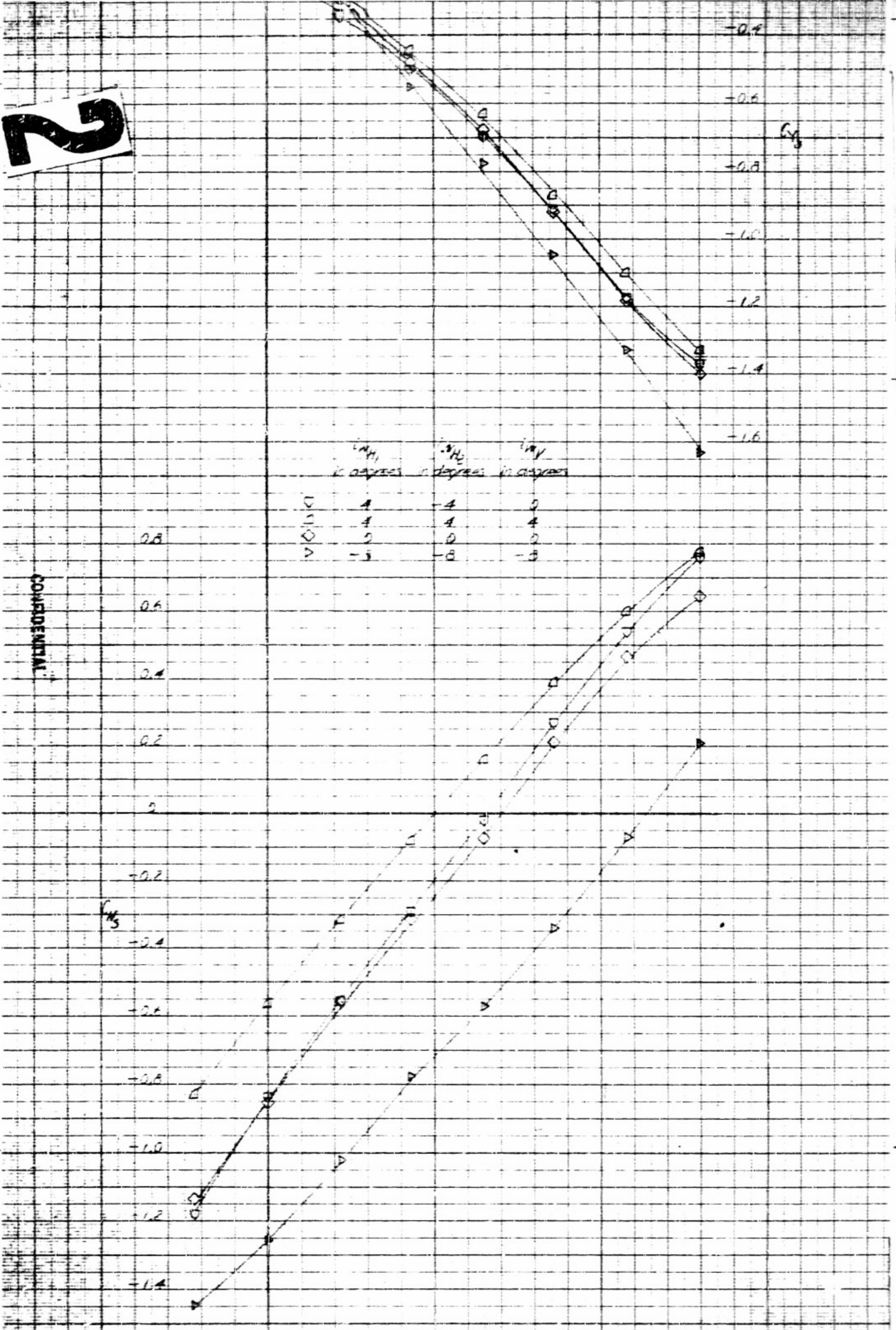

Figure 13 (Continued)

(b) Z = 0 inch, X = 5.12 inches, $\theta_j = 0°$, $\psi_S = 0°$, $\phi = 0°$; Pylon On

Figure 31

AERO 864

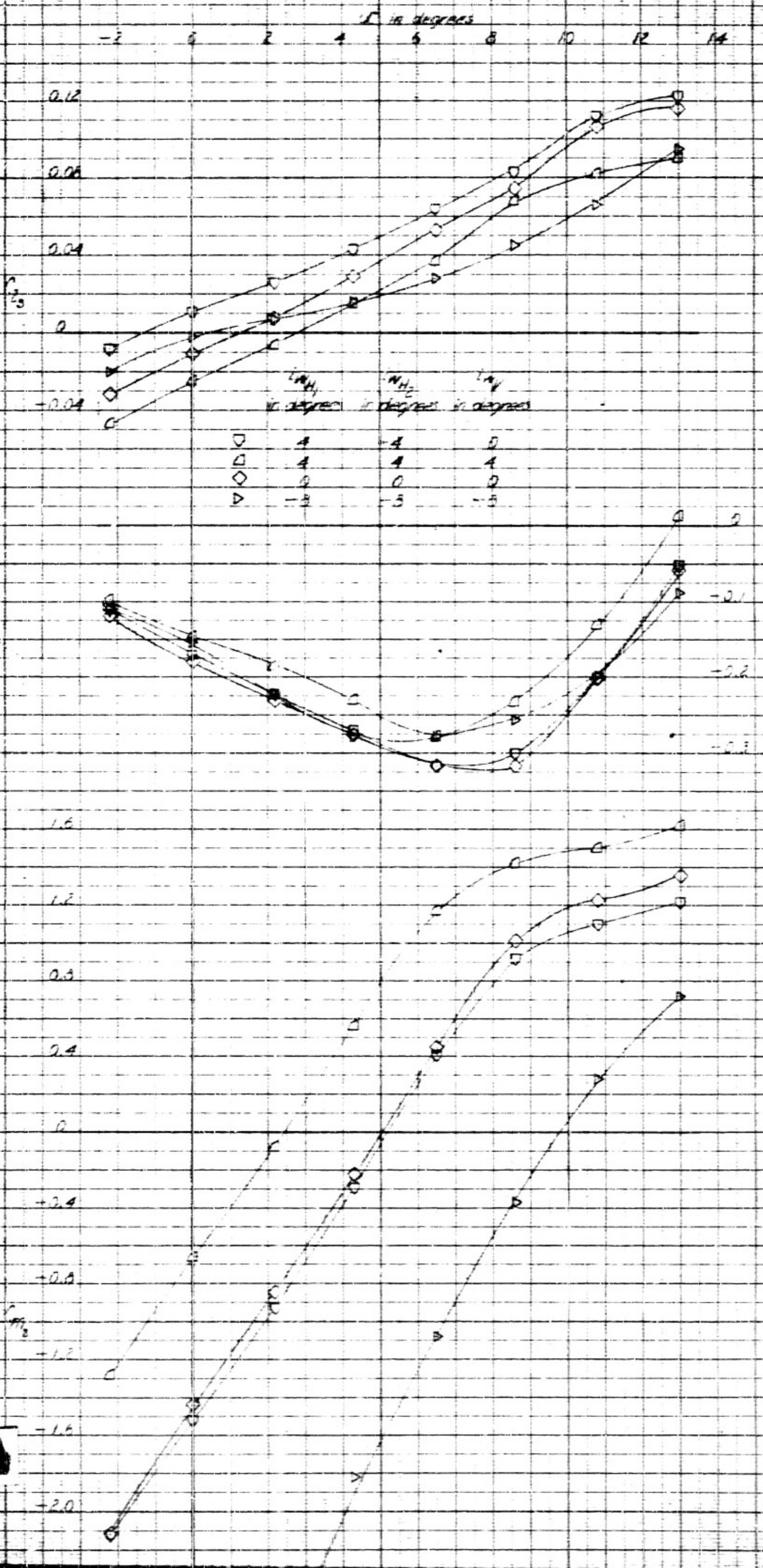

CONFIDENTIAL

[redacted]

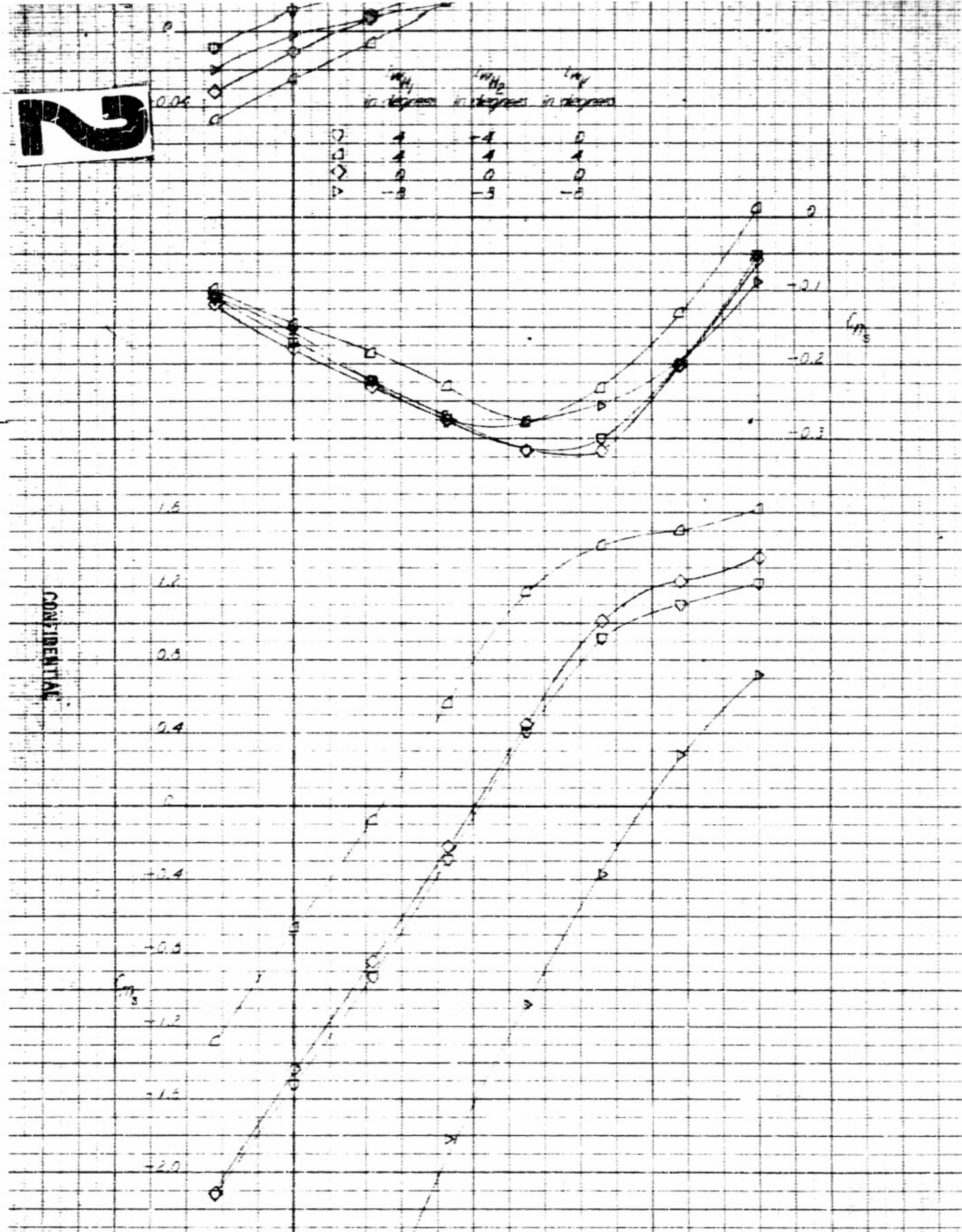

Figure 13 (Continued)

(a) Concluded.

CONFIDENTIAL

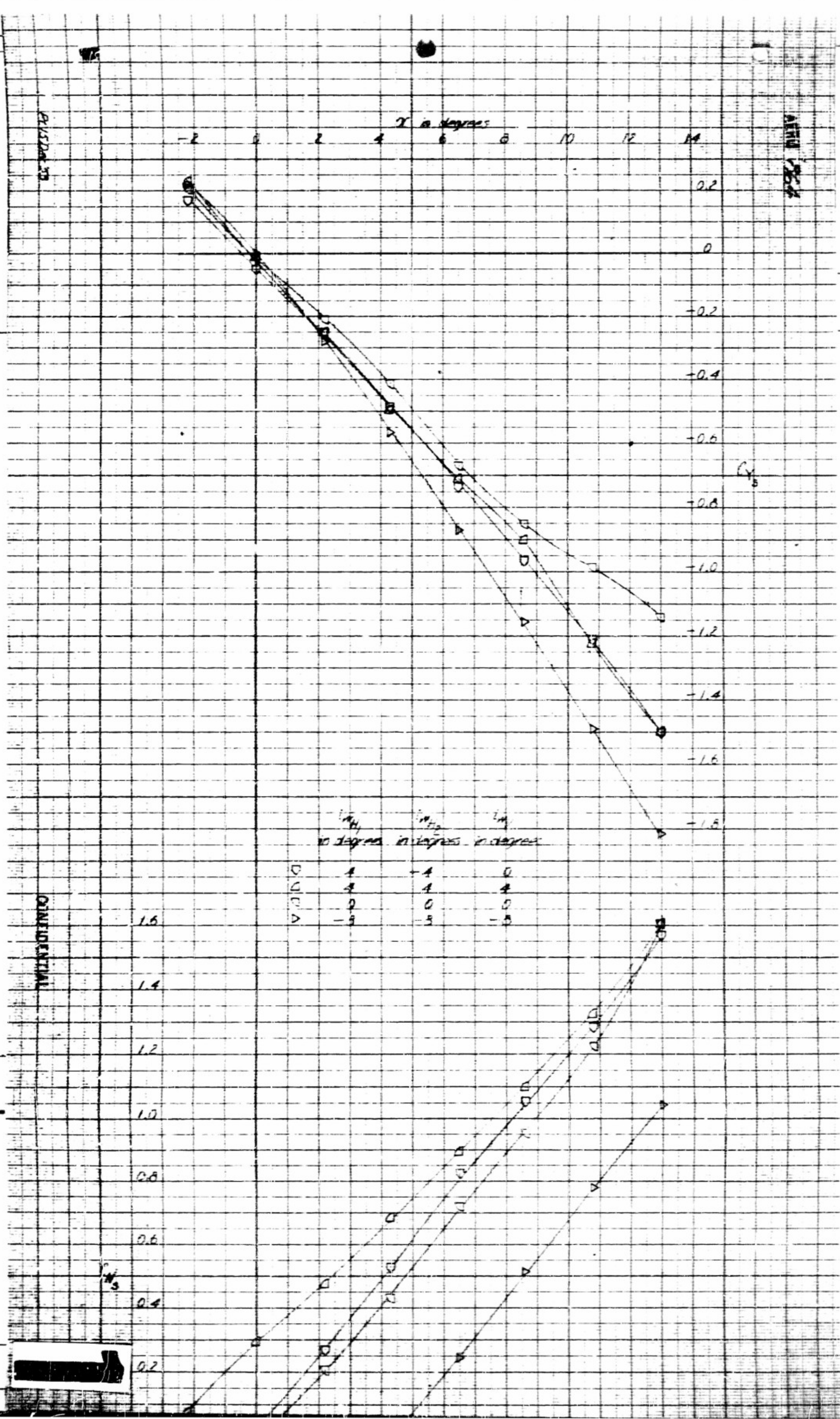

α in degrees
-2
0
2
4
6
8
10
12
14
0.2
0
-0.2
-0.4
-0.6
-0.8
-1.0
-1.2
-1.4
-1.6
-1.8
C_{Y_S}
$i_{w_{H_1}}$ in degrees
$i_{w_{H_2}}$ in degrees
i_w in degrees
4 -4 0
4 4 4
0 0 0
-5 -5 -5
1.6
1.4
1.2
1.0
0.8
0.6
0.4
0.2
i_{w_S}
CONFIDENTIAL
AERO 764

CONFIDENTIAL

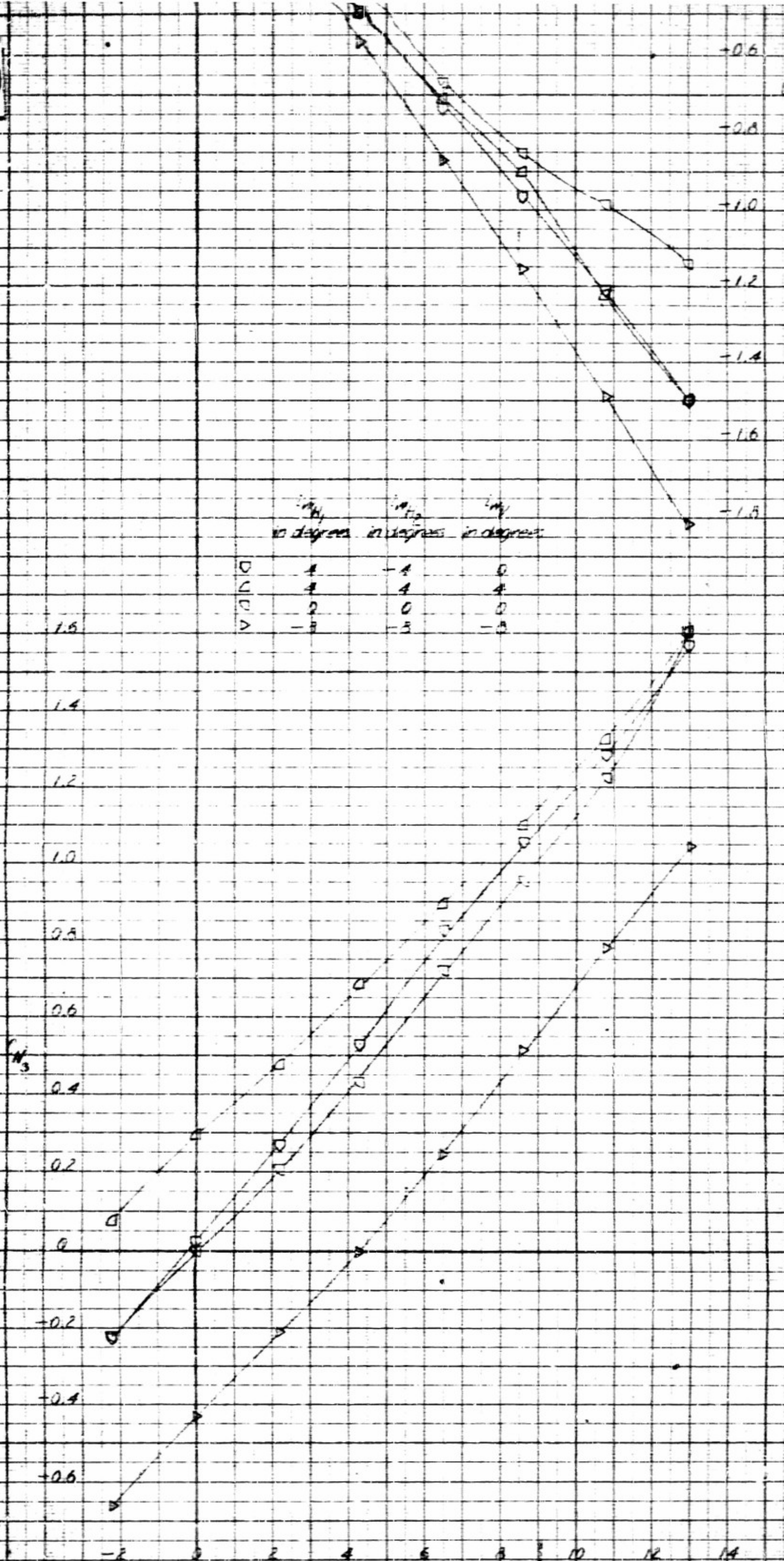

Figure 13 (Continued)

(c) $Z = 0$ inch, $X = 6.12$ inches, $\theta_j = 6°$, $\psi_s = 0°$, $\psi = 0°$, Pylon On

FIGURE 13

CONFIDENTIAL

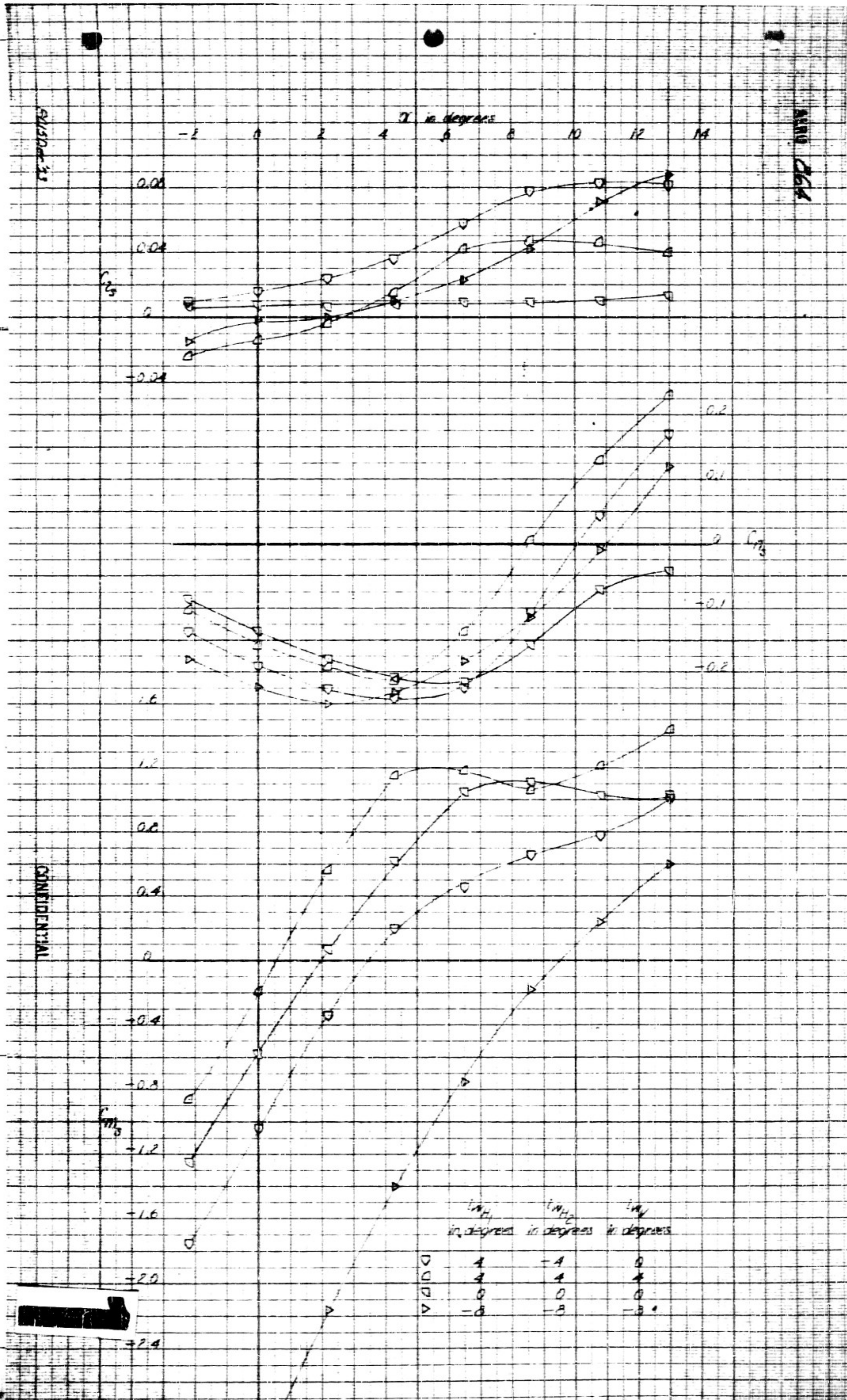
α in degrees
-2
0
2
4
6
8
10
12
14
C_{l_s}
0.08
0.04
0
-0.04
C_{n_s}
0.2
0.1
0
-0.1
-0.2
C_{m_s}
1.6
1.2
0.8
0.4
0
-0.4
-0.8
-1.2
-1.6
-2.0
-2.4
$i_{w_{H_1}}$ in degrees
$i_{w_{H_2}}$ in degrees
i_{w_V} in degrees
4 -4 0
4 4 4
0 0 0
-8 -8 -8
CONFIDENTIAL

[redacted]

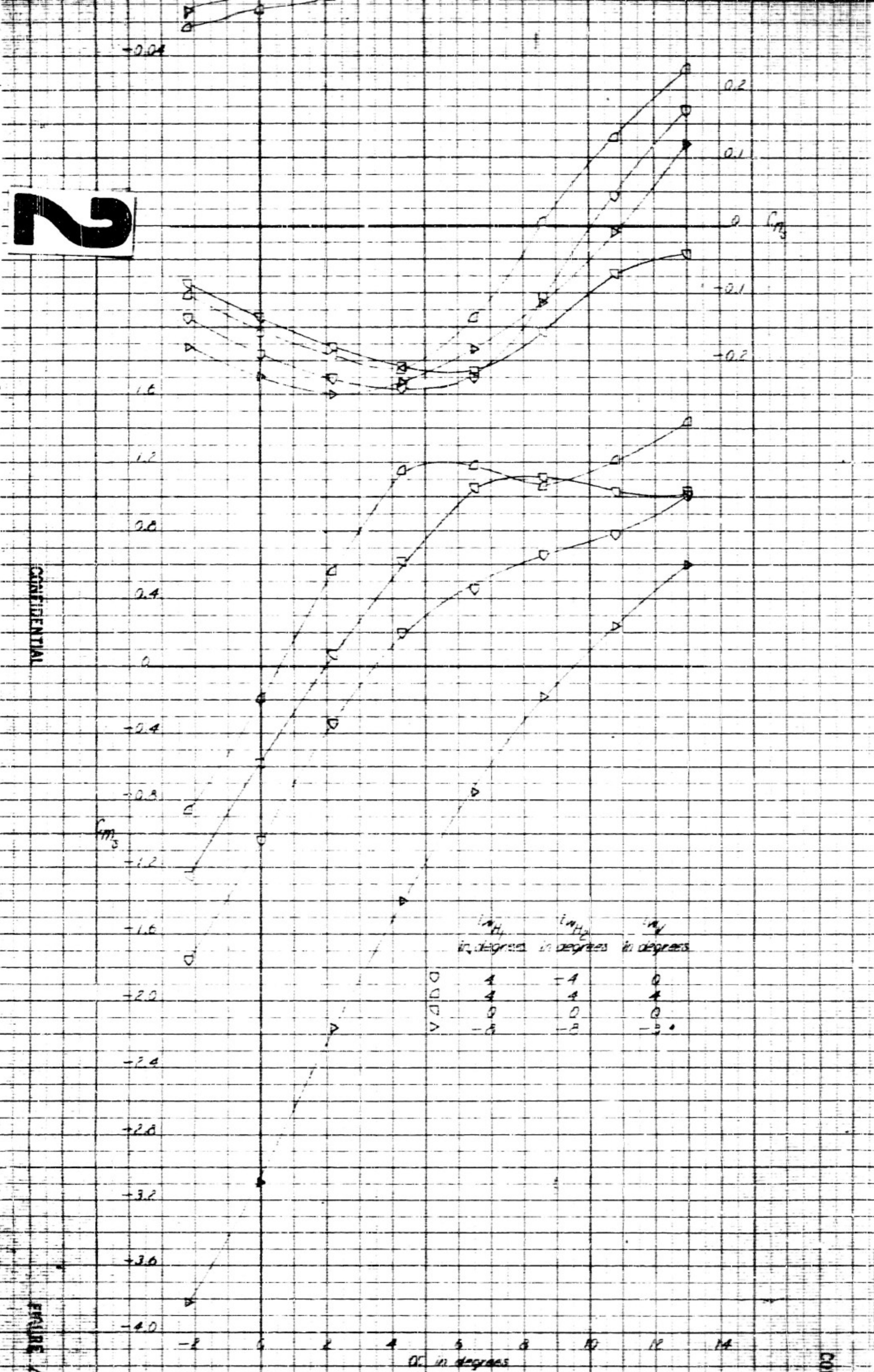

CONFIDENTIAL

Figure 13 (Continued)

(c) Concluded

FIGURE 13 (Contd.)

CONFIDENTIAL

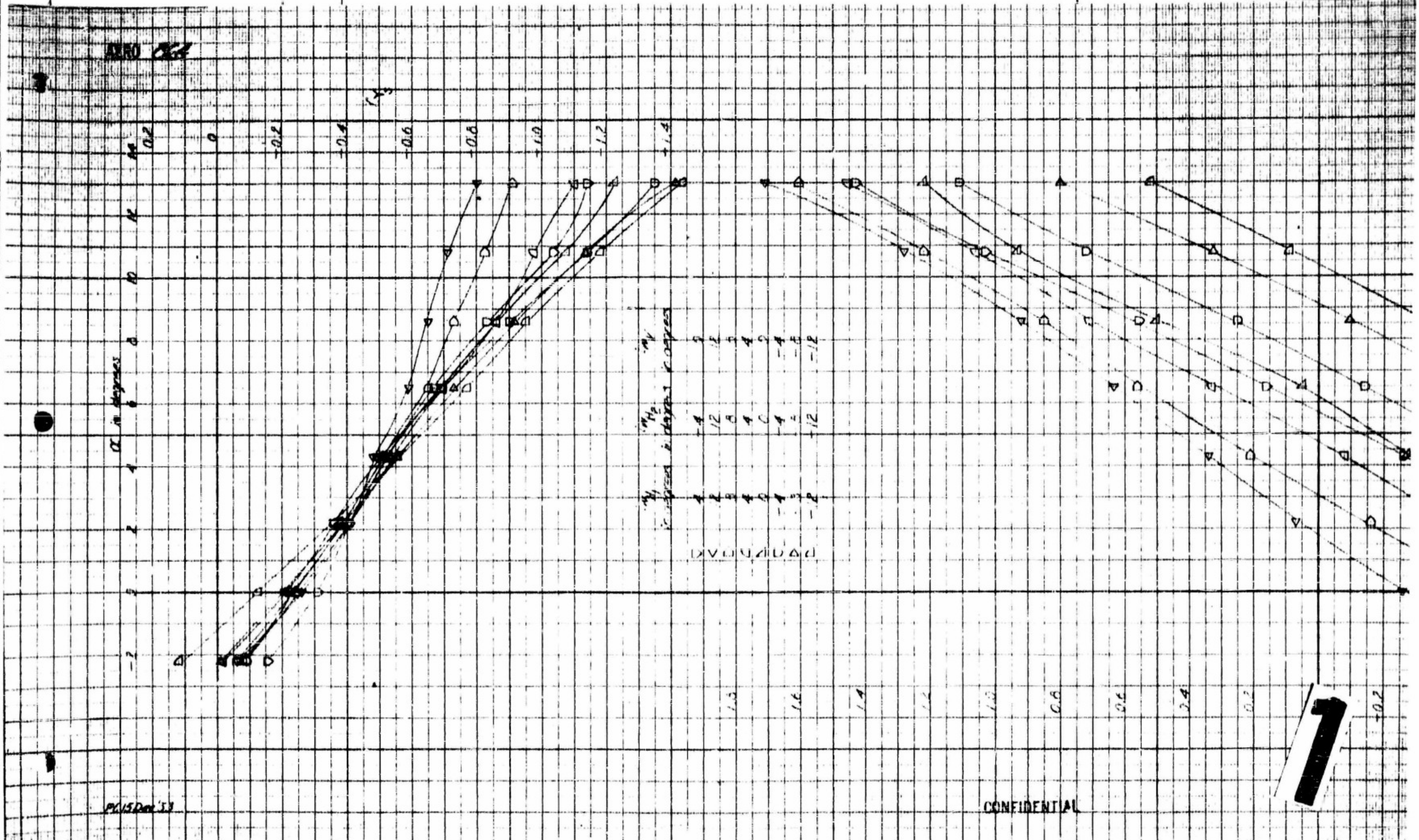

CONFIDENTIAL

CONFIDENTIAL

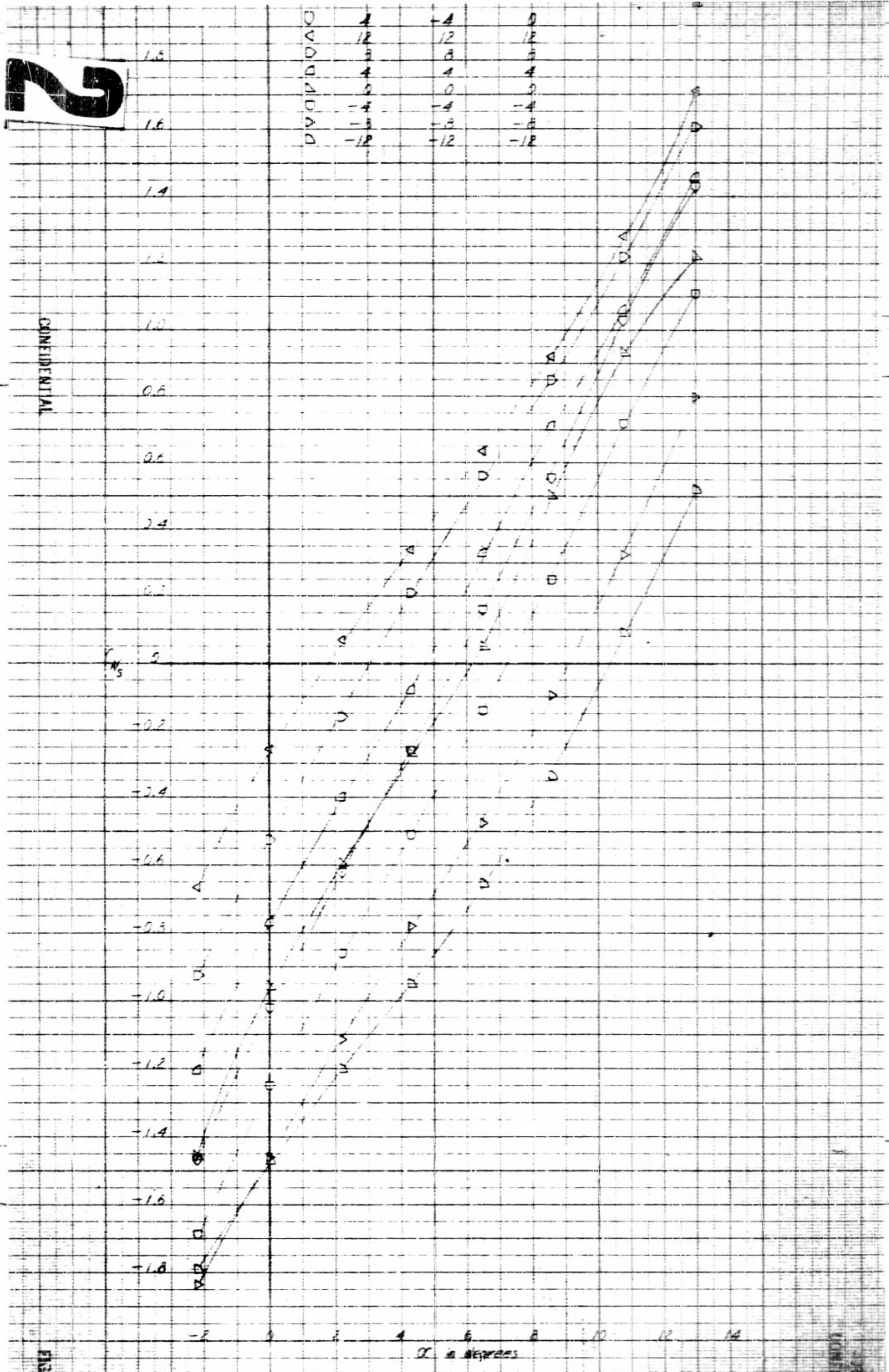

Figure 13 (Continued)

(a) Z = 0 inch, X = 13.26 inches, $\theta_s = 0°$, $\psi_s = 0°$, $\phi = 0°$, Pylon On

FIGURE 1/2

CONFIDENTIAL

[redacted]

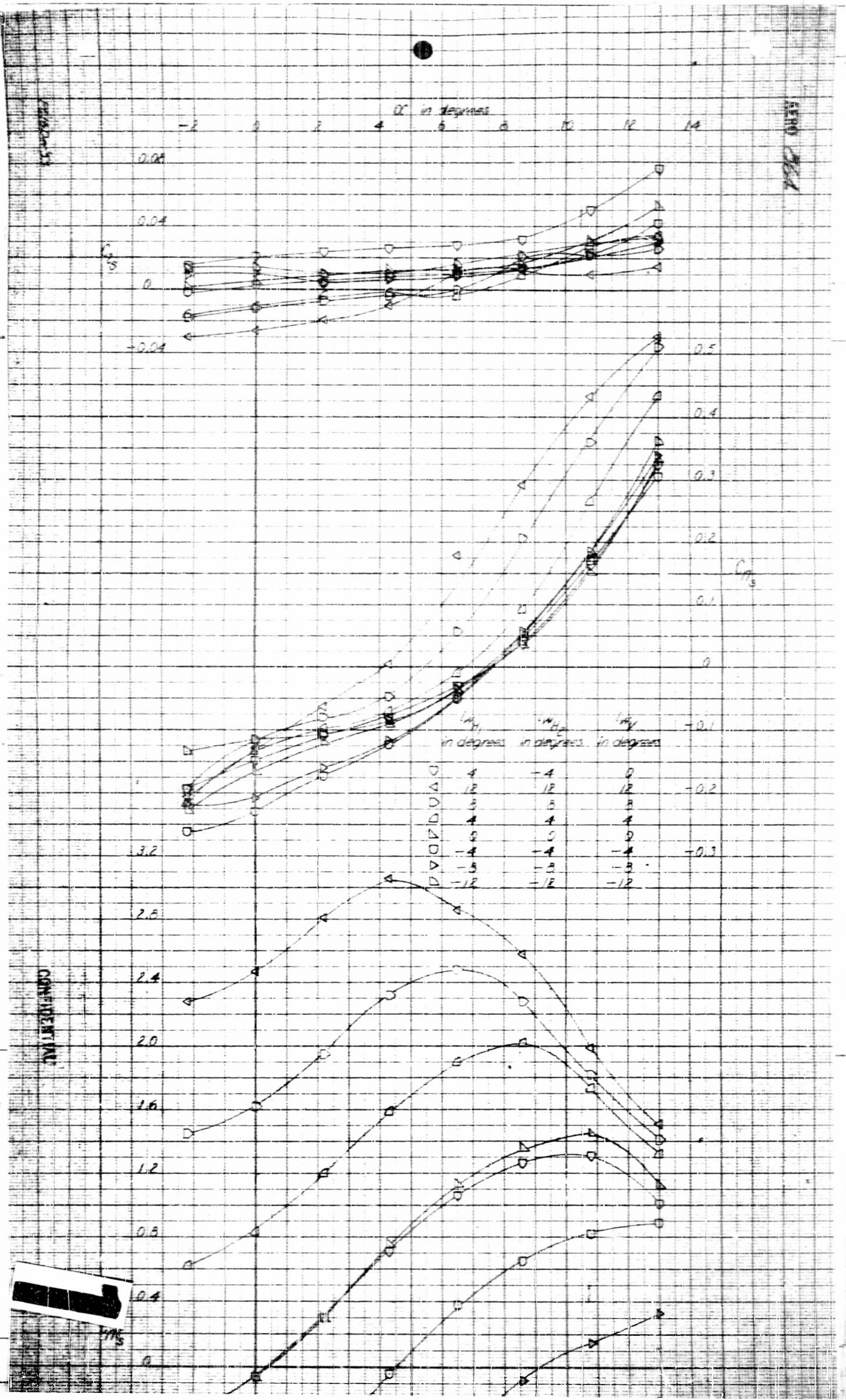

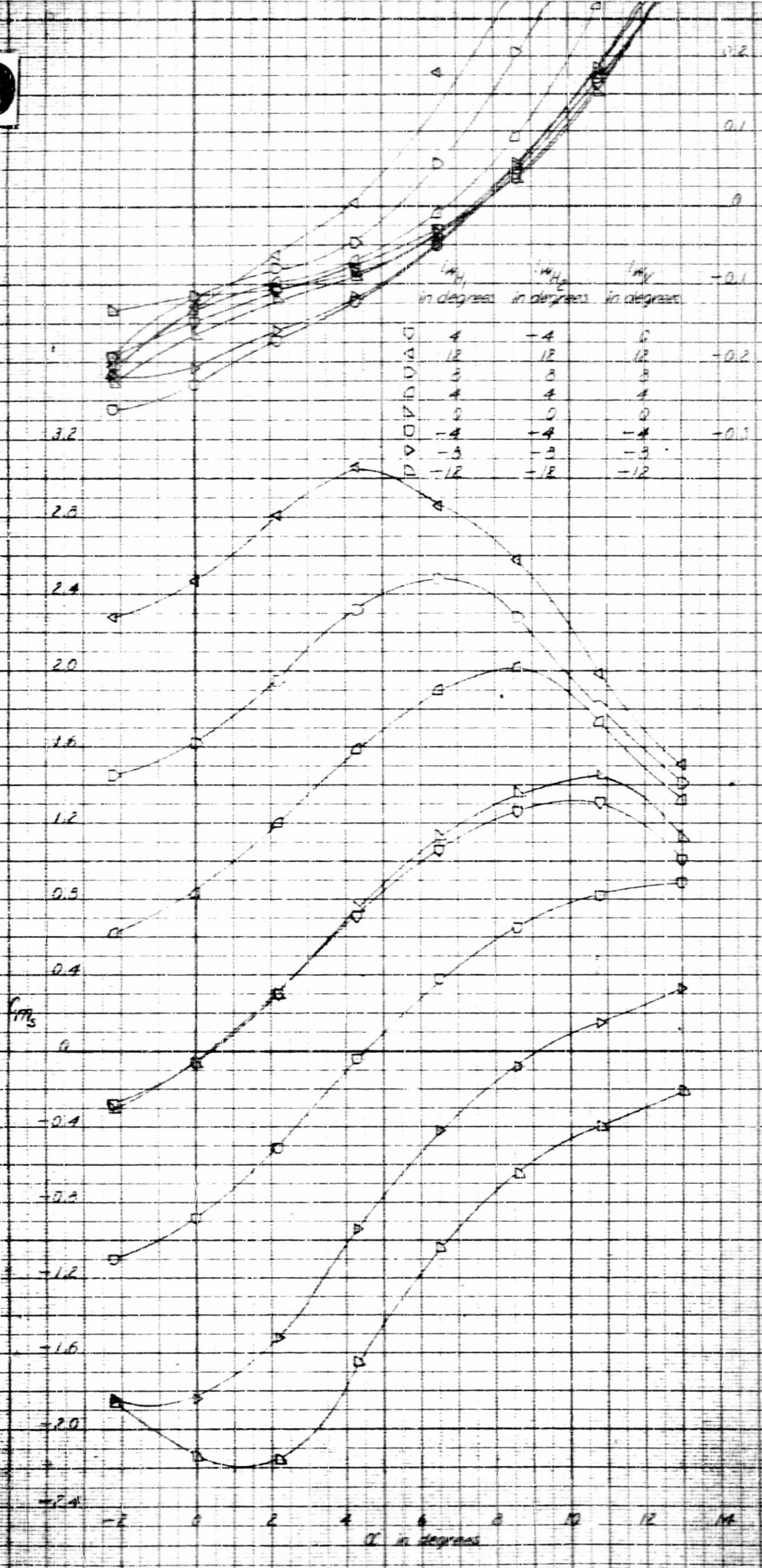

Figure 13 (Continued)

(d) Concluded

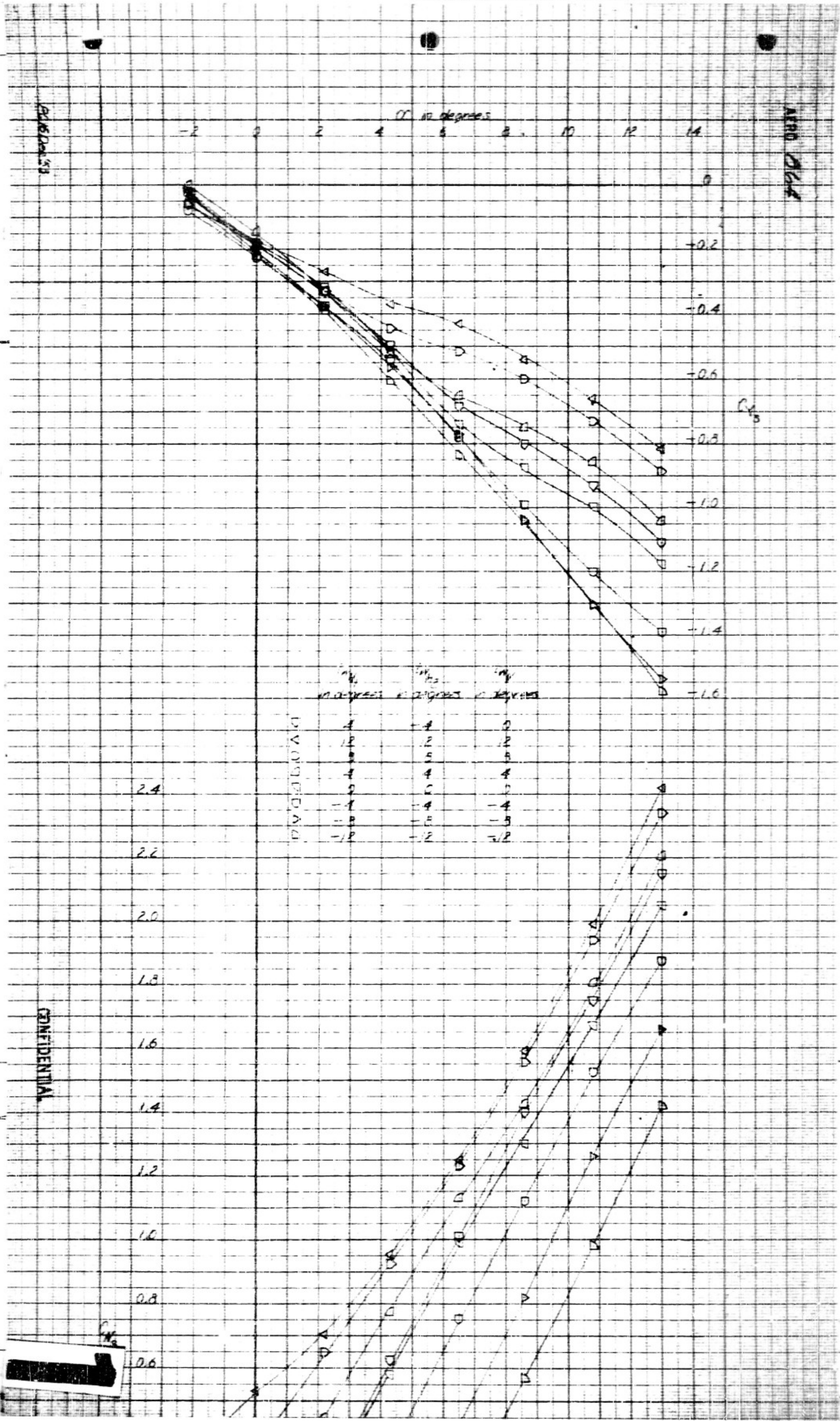
AERO 1064
CONFIDENTIAL
α in degrees
-2
0
2
4
6
8
10
12
14
0
-0.2
-0.4
-0.6
-0.8
-1.0
-1.2
-1.4
-1.6
C_{l_β}
2.4
2.2
2.0
1.8
1.6
1.4
1.2
1.0
0.8
0.6
C_{n_β}
δ_{h_1} in degrees
δ_{h_2} in degrees
δ_v in degrees
4 -4 0
12 12 12
8 8 8
4 4 4
0 0 0
-4 -4 -4
-8 -8 -8
-12 -12 -12
[redacted]

CONFIDENTIAL

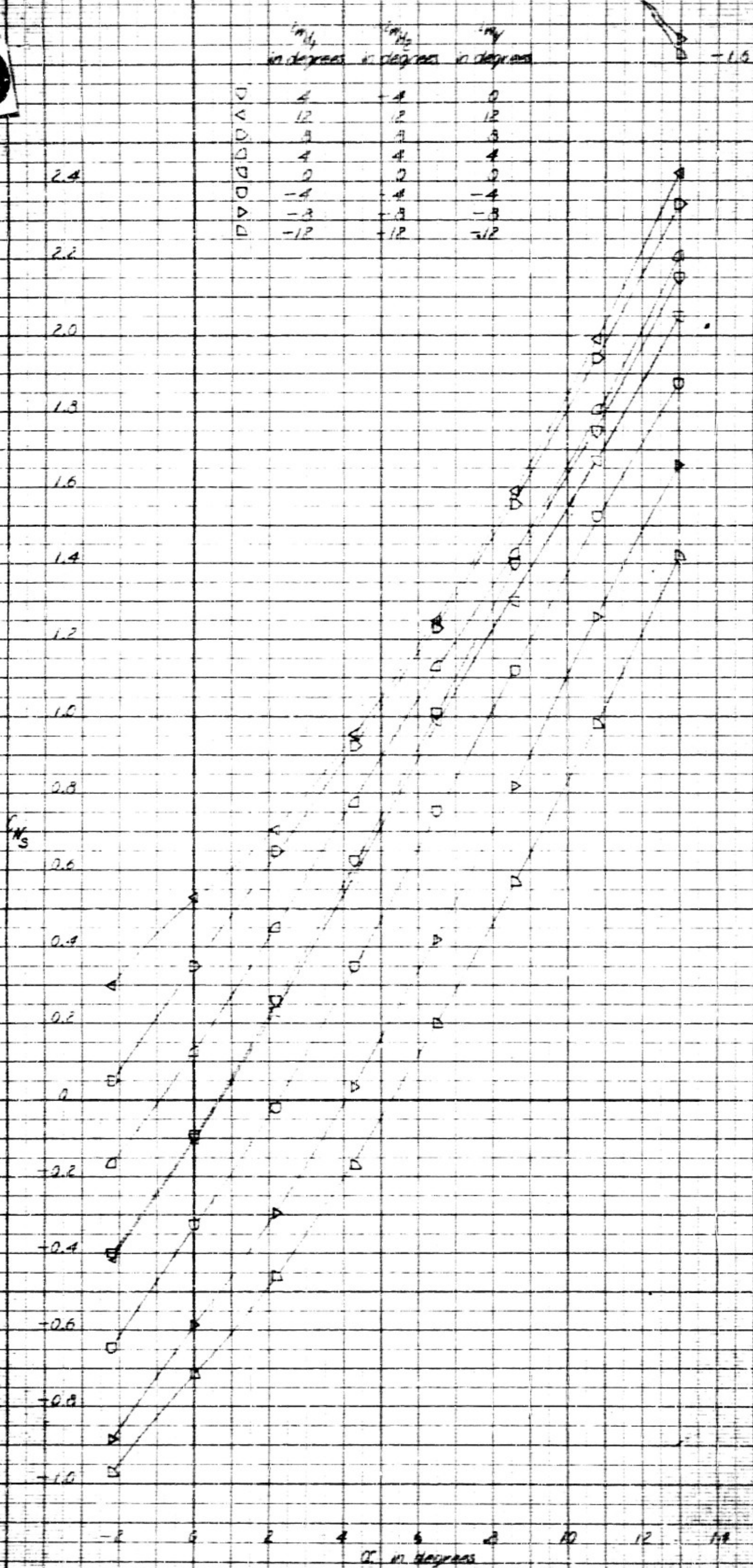

Figure 13 (Continued)

(e) $Z = 0$ inch, $\bar{x} = 13.26$ inches, $\theta_s = -6°$, $\psi_s = 0°$, $\psi = 0°$, Pylon On

CONFIDENTIAL

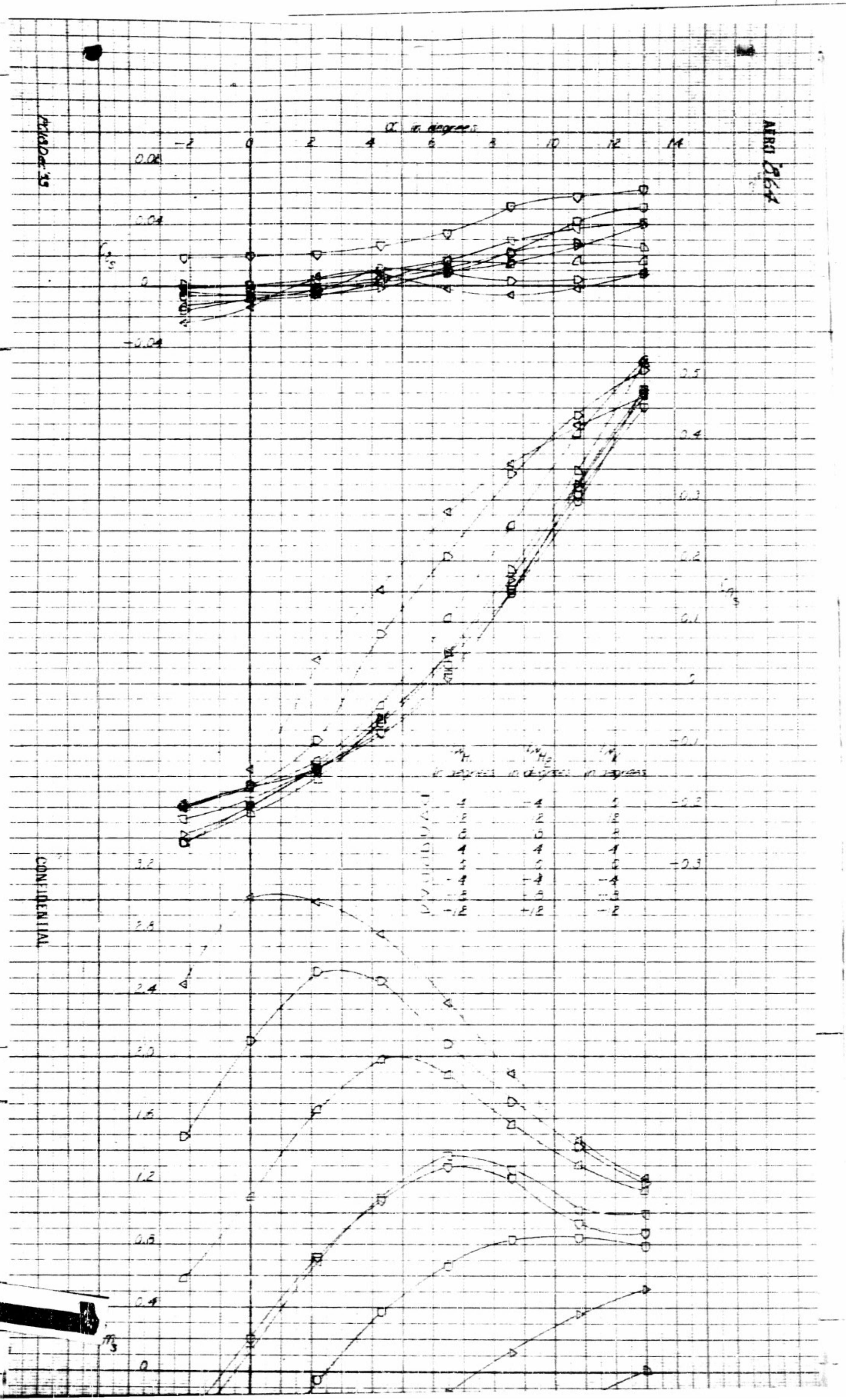

AERO 864
CONFIDENTIAL
α in degrees
-2
0
2
4
6
8
10
12
14
0.08
0.04
0
-0.04
0.5
0.4
0.3
0.2
0.1
0
-0.1
-0.2
-0.3
3.2
2.8
2.4
2.0
1.6
1.2
0.8
0.4
0

CONFIDENTIAL

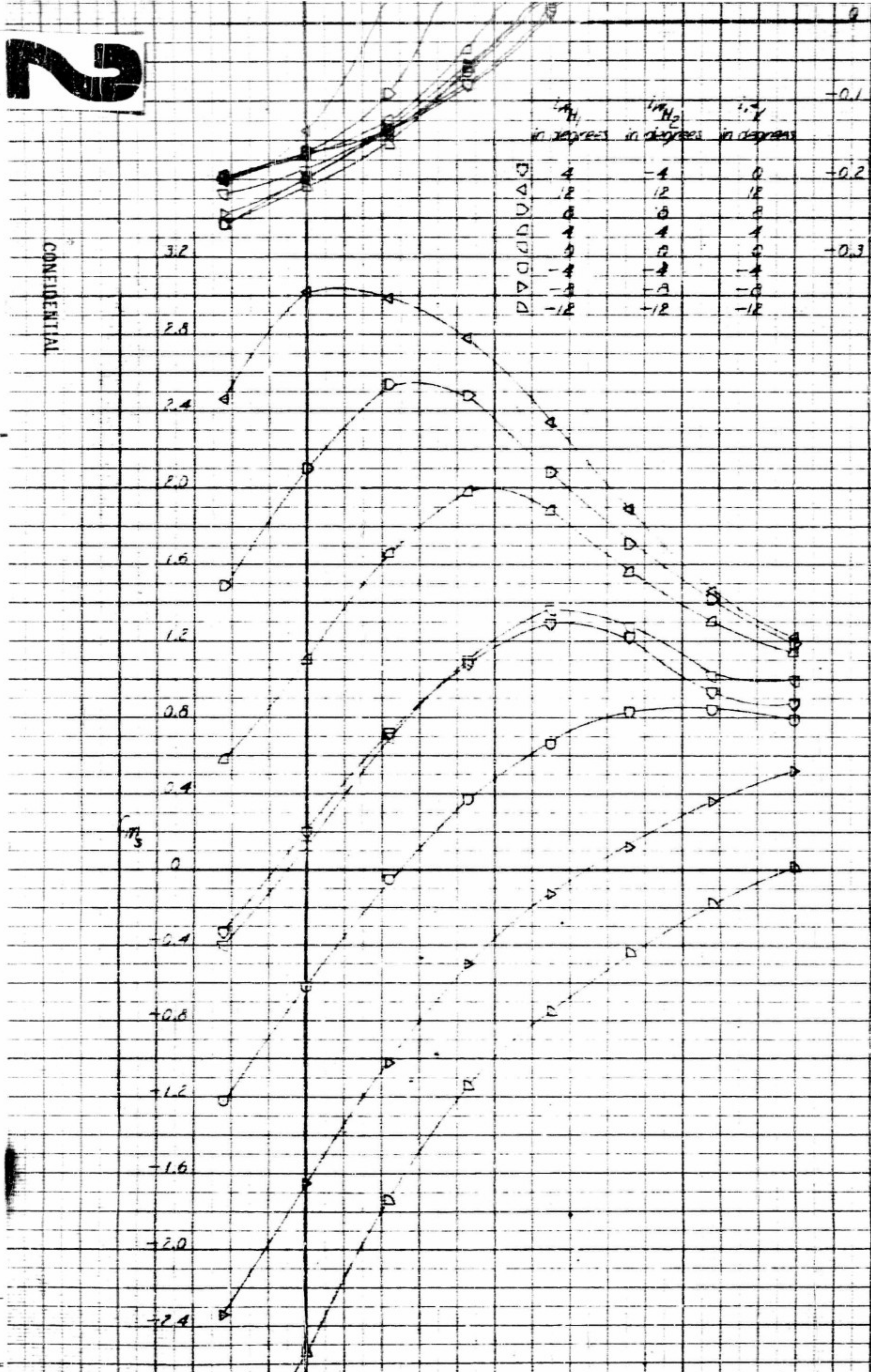

Figure 13 (Continued)

(e) Concluded

CONFIDENTIAL

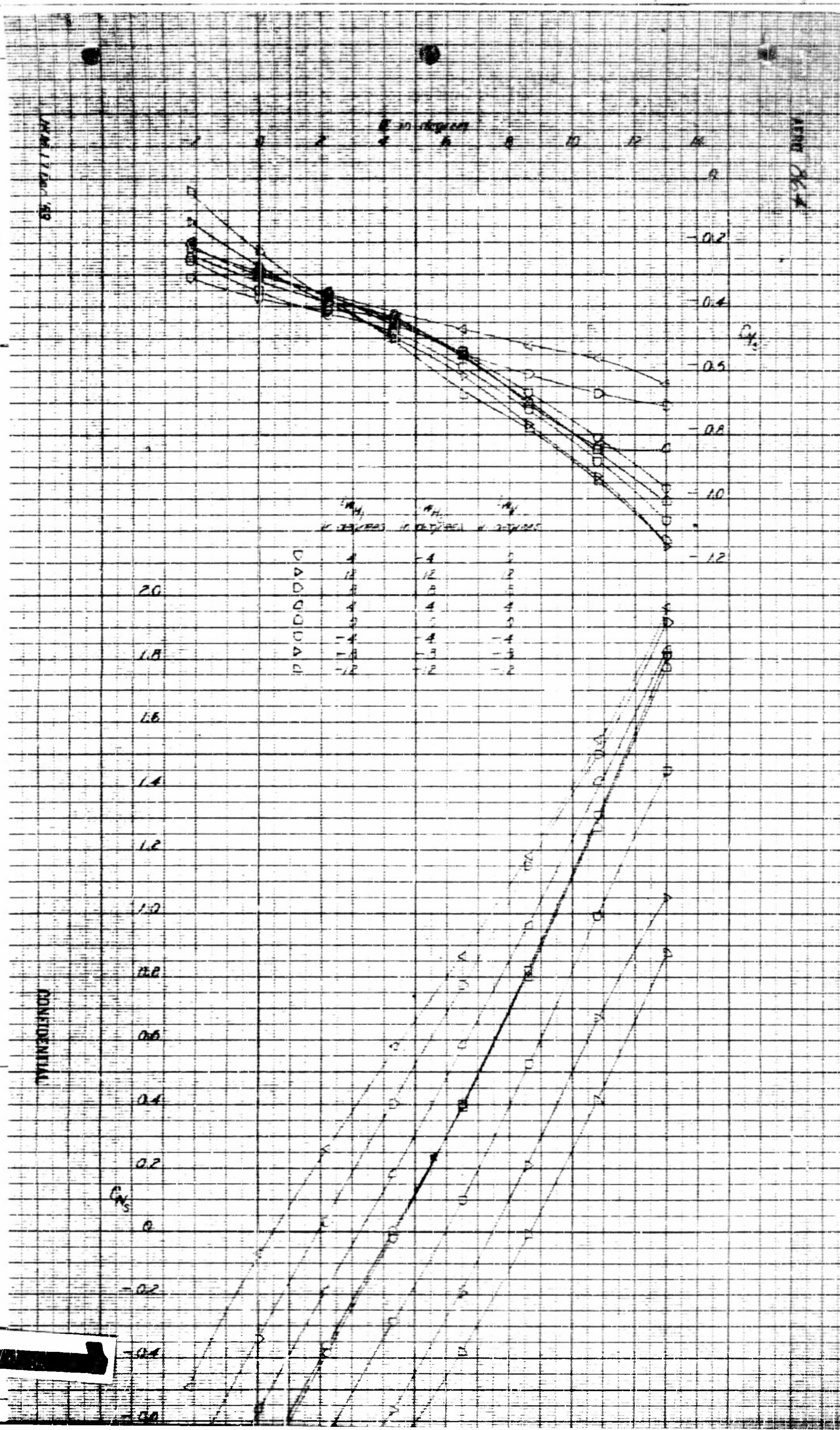

CONFIDENTIAL

[redacted]

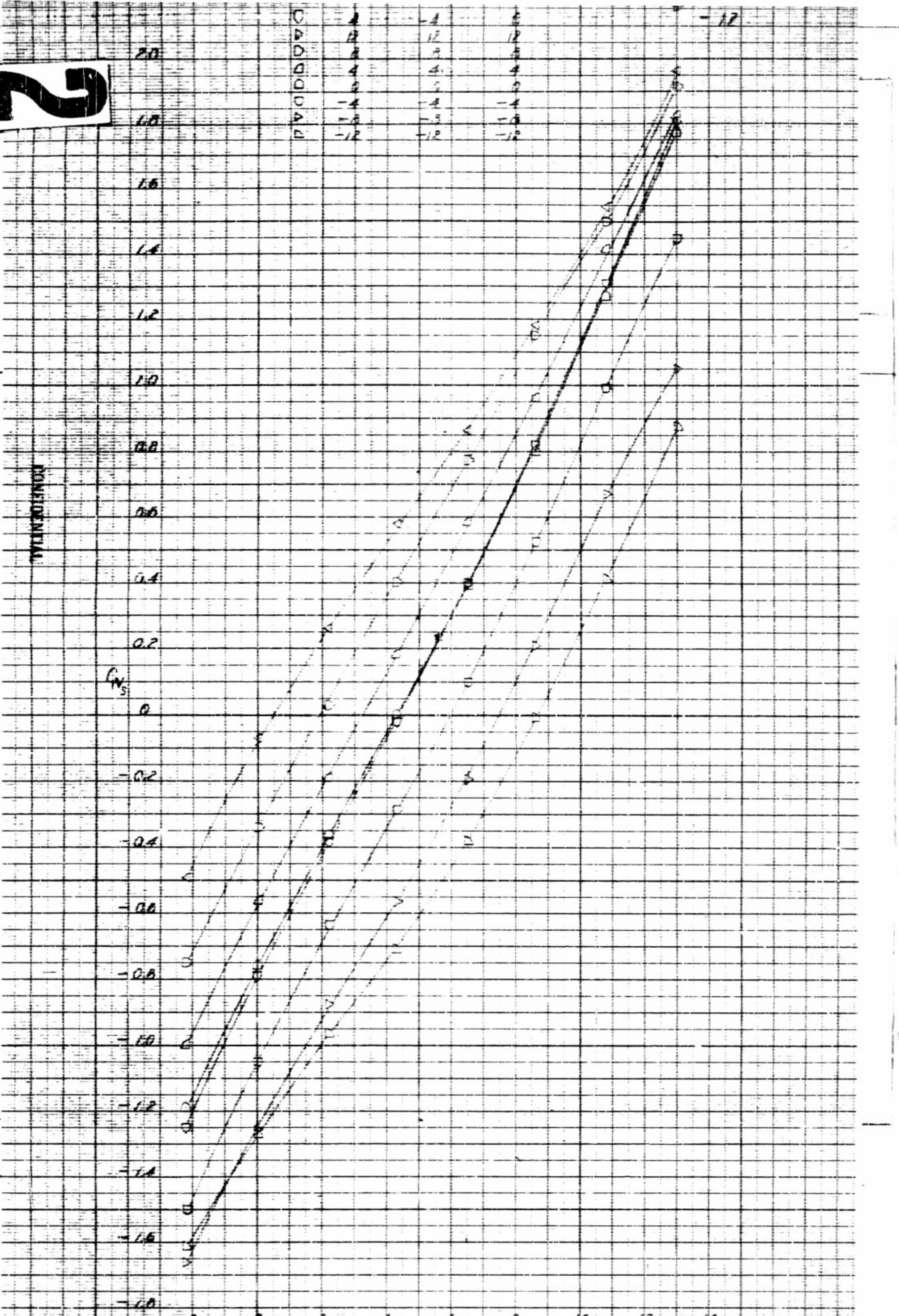

Figure 13 (continued)

(f) $Z = 0$ inch, $X = 18.36$ inches, $\theta_s = 0°$, $\psi_s = 0°$, $\psi = 0°$, Pylon On

FIGURE 13

TKM 18 Dec 38

AERO 664

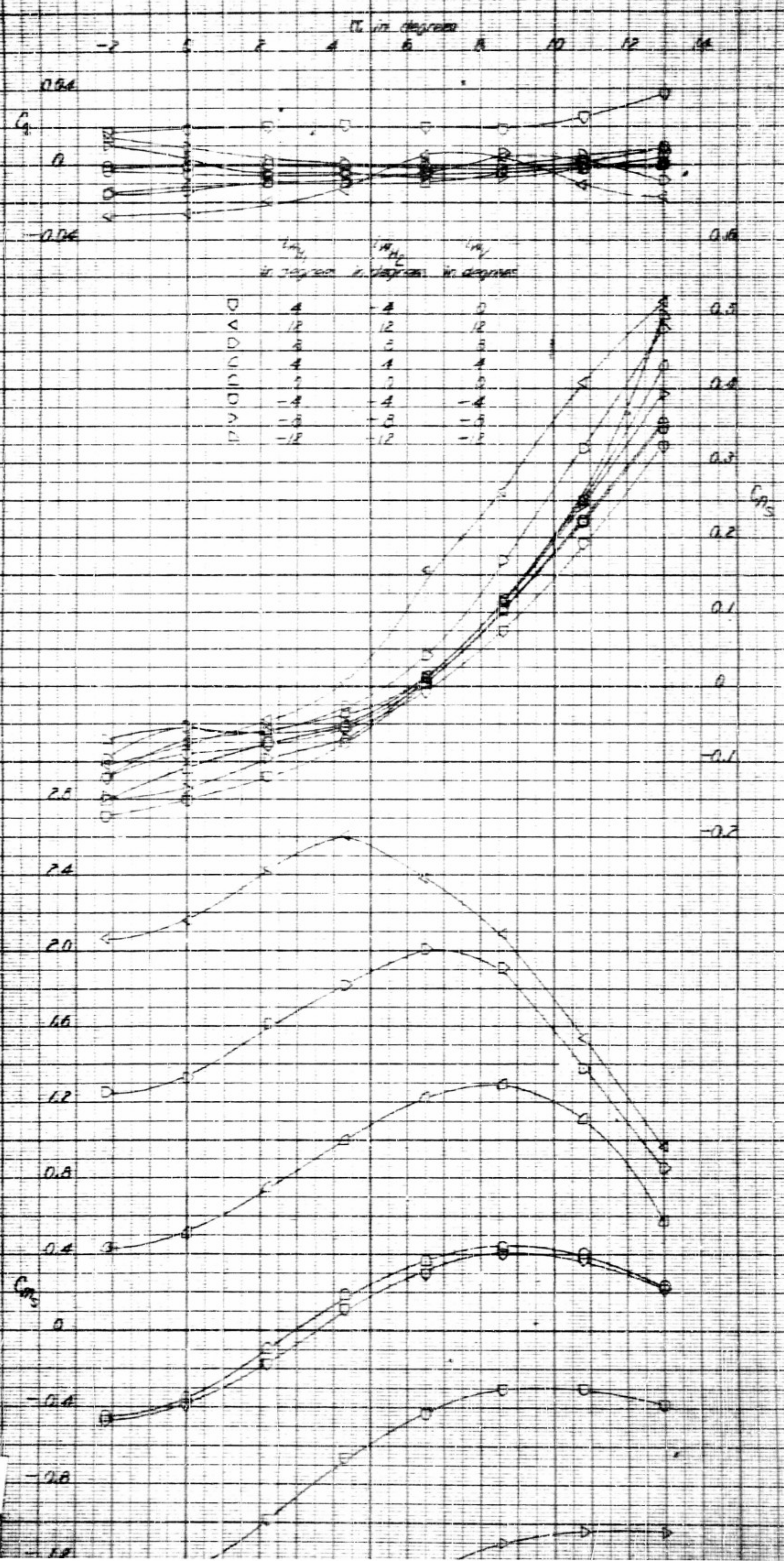

CONFIDENTIAL

[redacted]

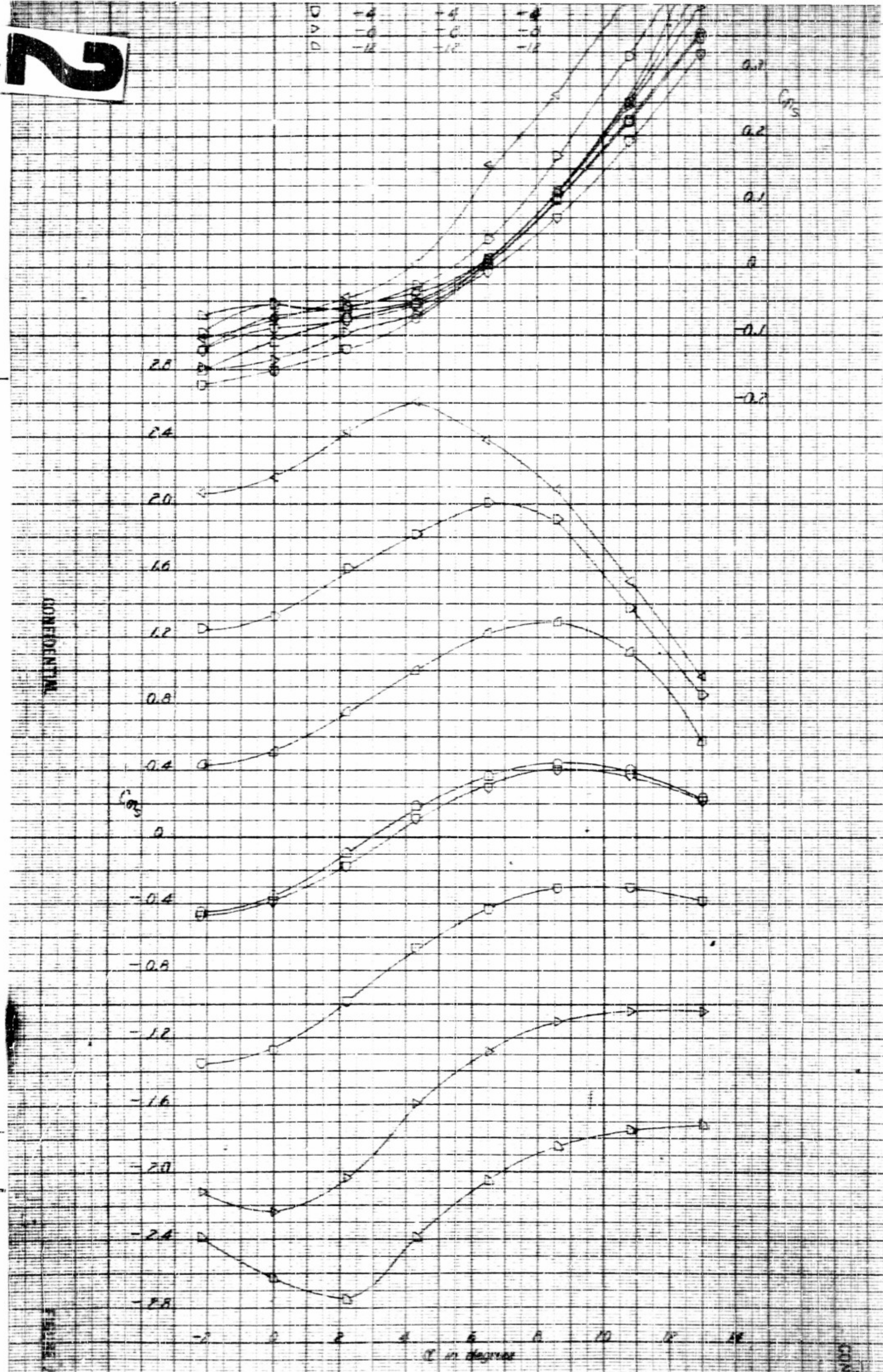

Figure 13 (Continued)

(f) Concluded

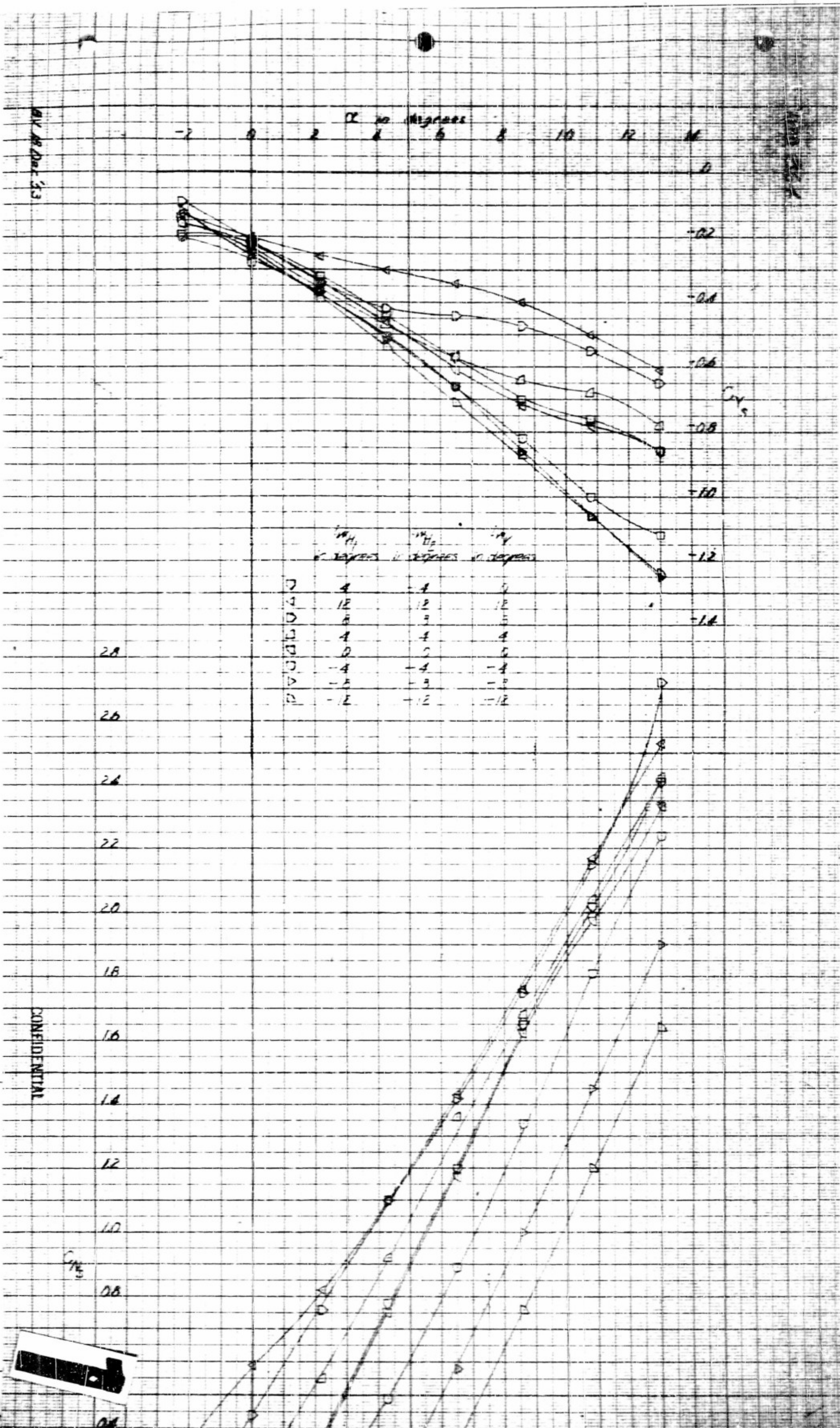
α in degrees
-2
0
2
4
6
8
10
12
14
0
-0.2
-0.4
-0.6
-0.8
-1.0
-1.2
-1.4
2.8
2.6
2.4
2.2
2.0
1.8
1.6
1.4
1.2
1.0
0.8
0.4
in degrees
in degrees
in degrees
CONFIDENTIAL

CONFIDENTIAL

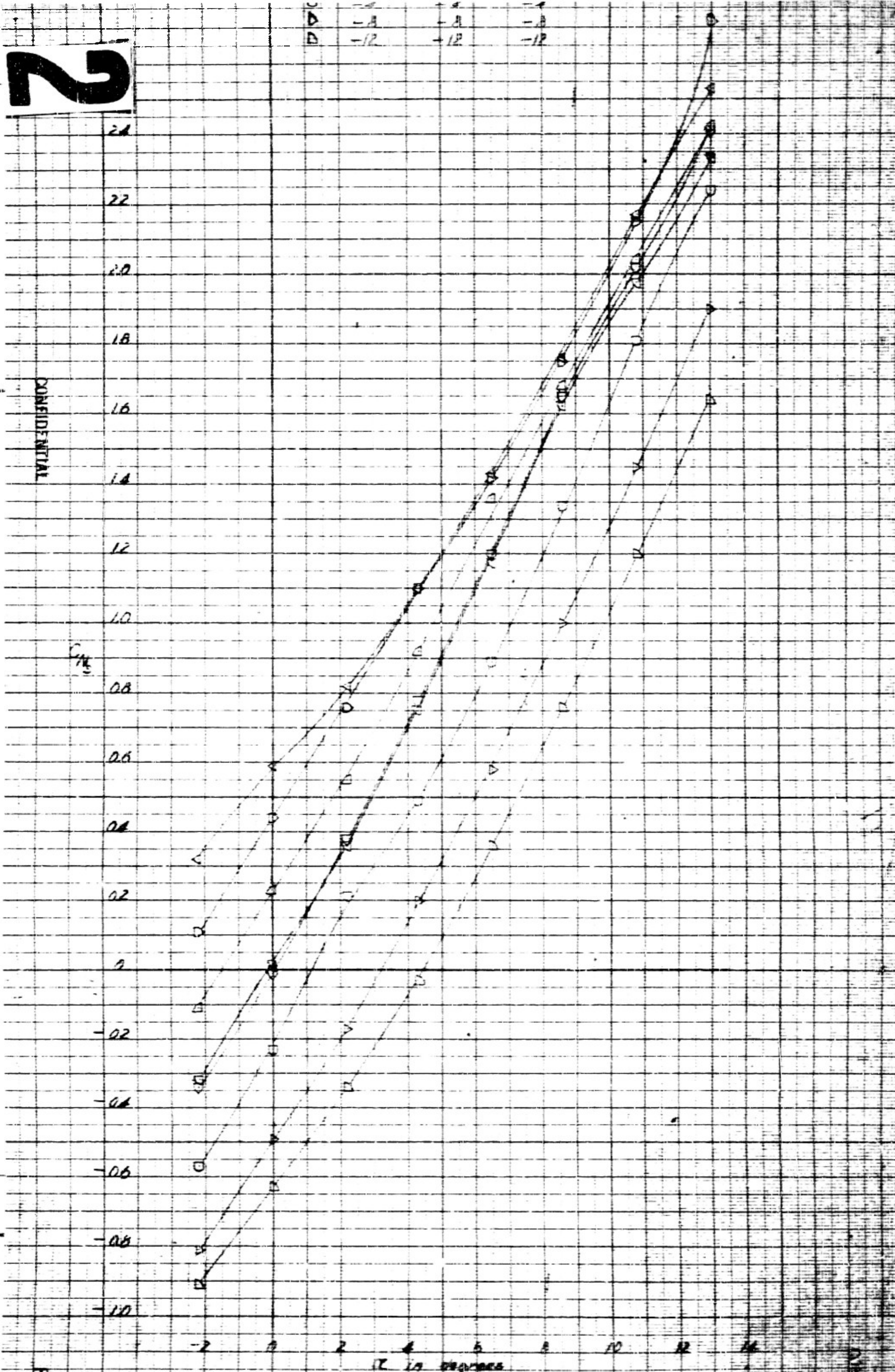

Figure 13 (Continued)

(g) Z = 0 inch, X = 15.36 inches, $\theta_s = -6°$, $\delta_s = 0°$, $\psi = 0°$, Pylon On

FIGURE 13

CONFIDENTIAL

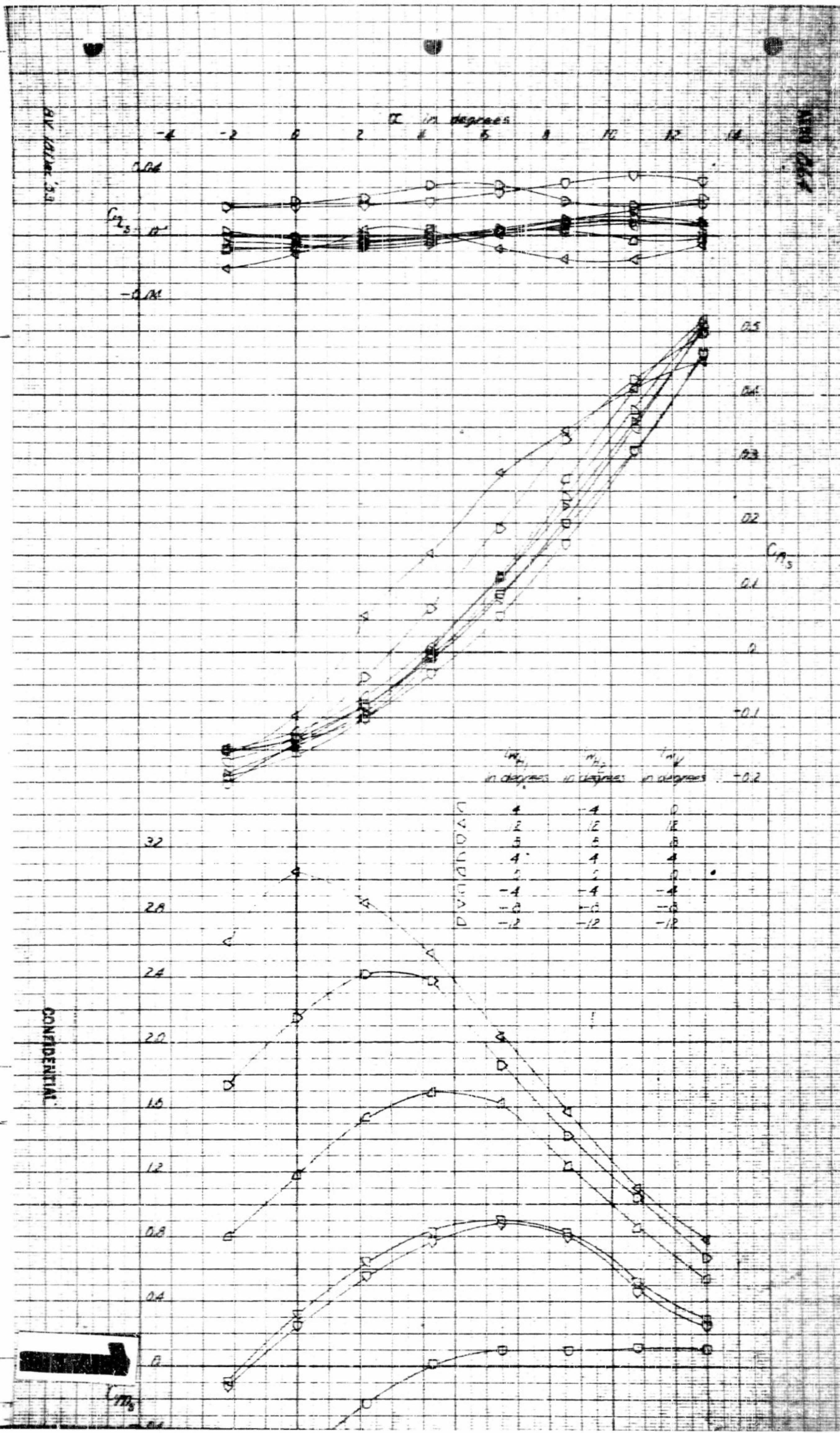

CONFIDENTIAL

[redacted]

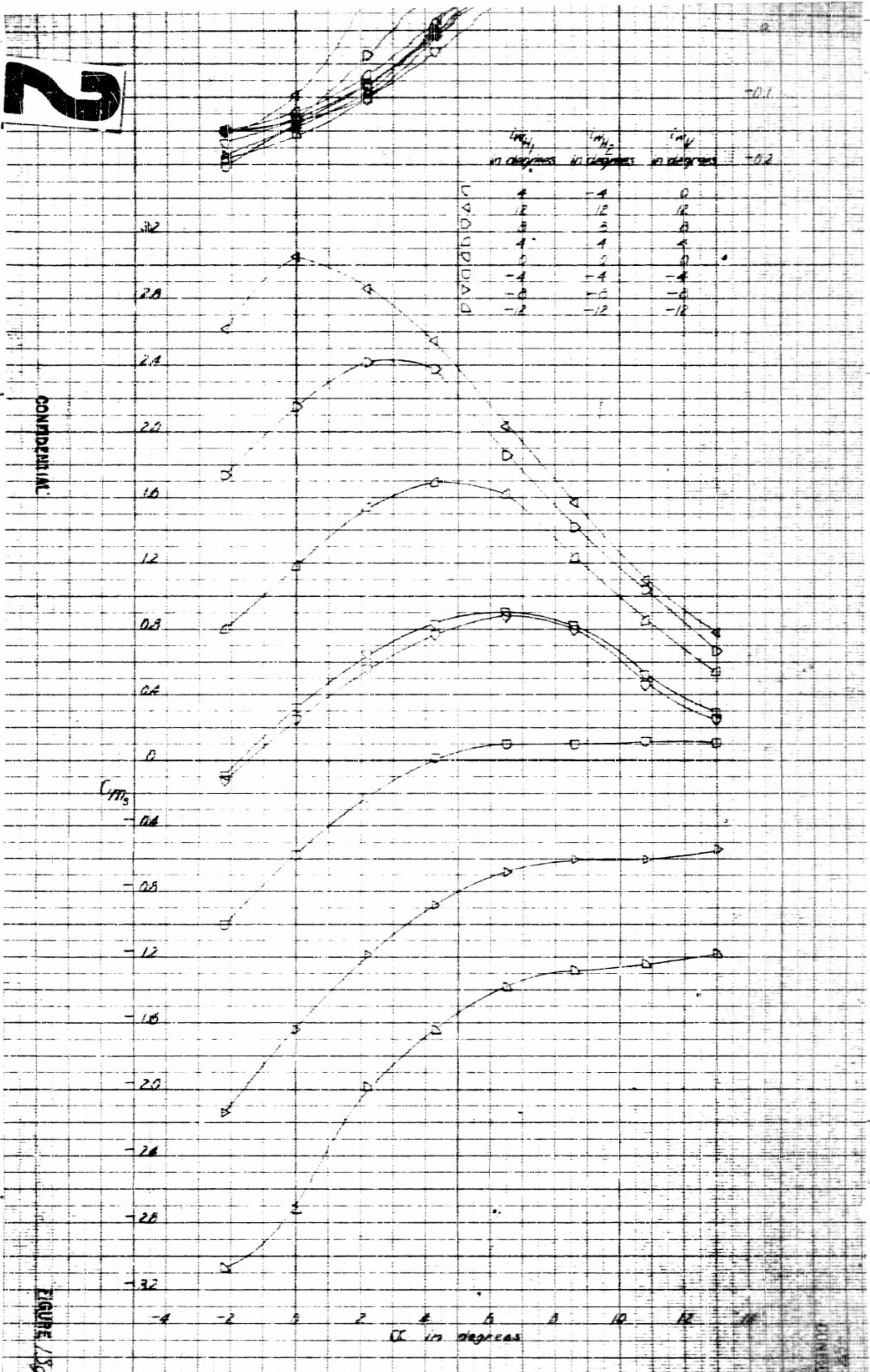

CONFIDENTIAL

Figure 13 (Concluded)

(b) Concluded

FIGURE 13 (concluded)

AERO 564

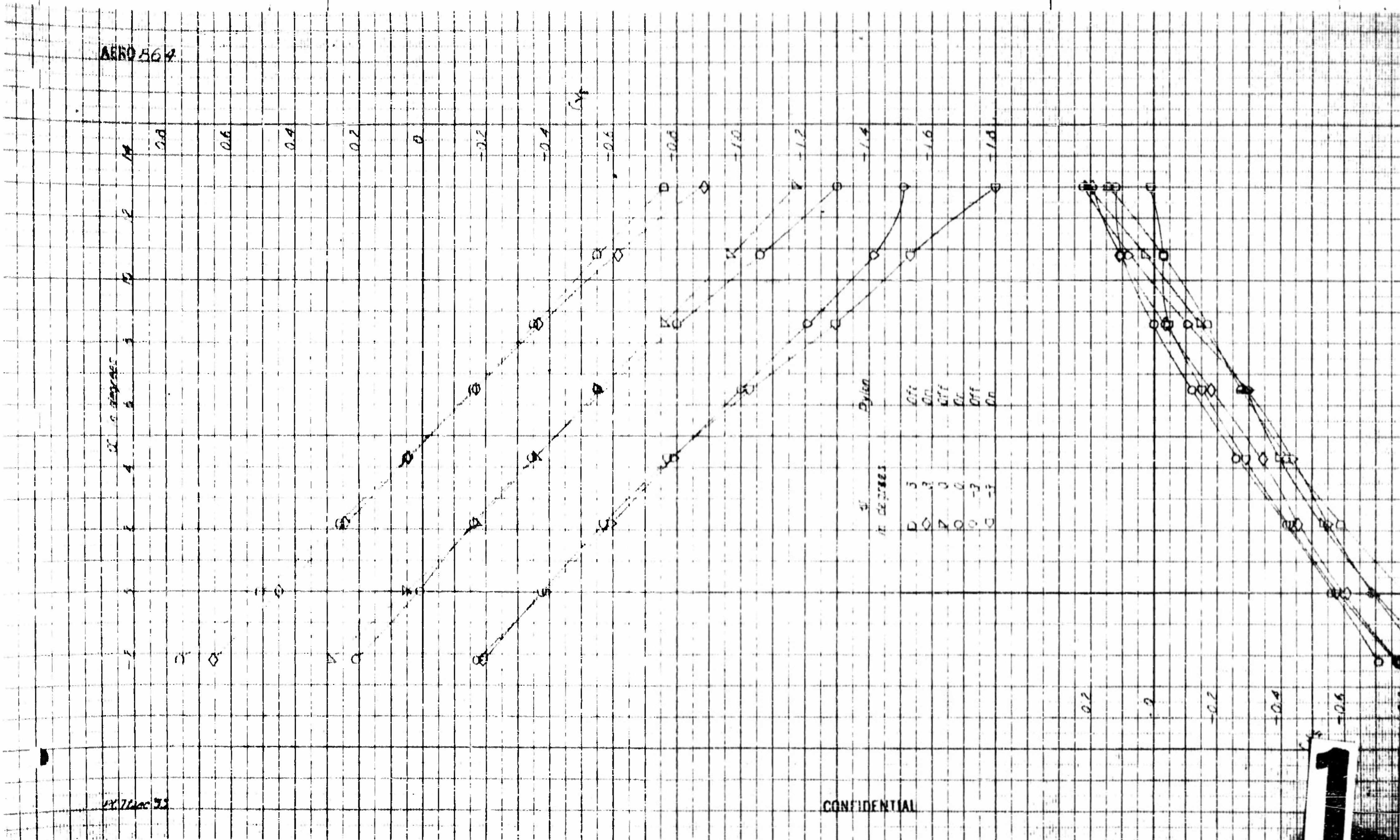

CONFIDENTIAL

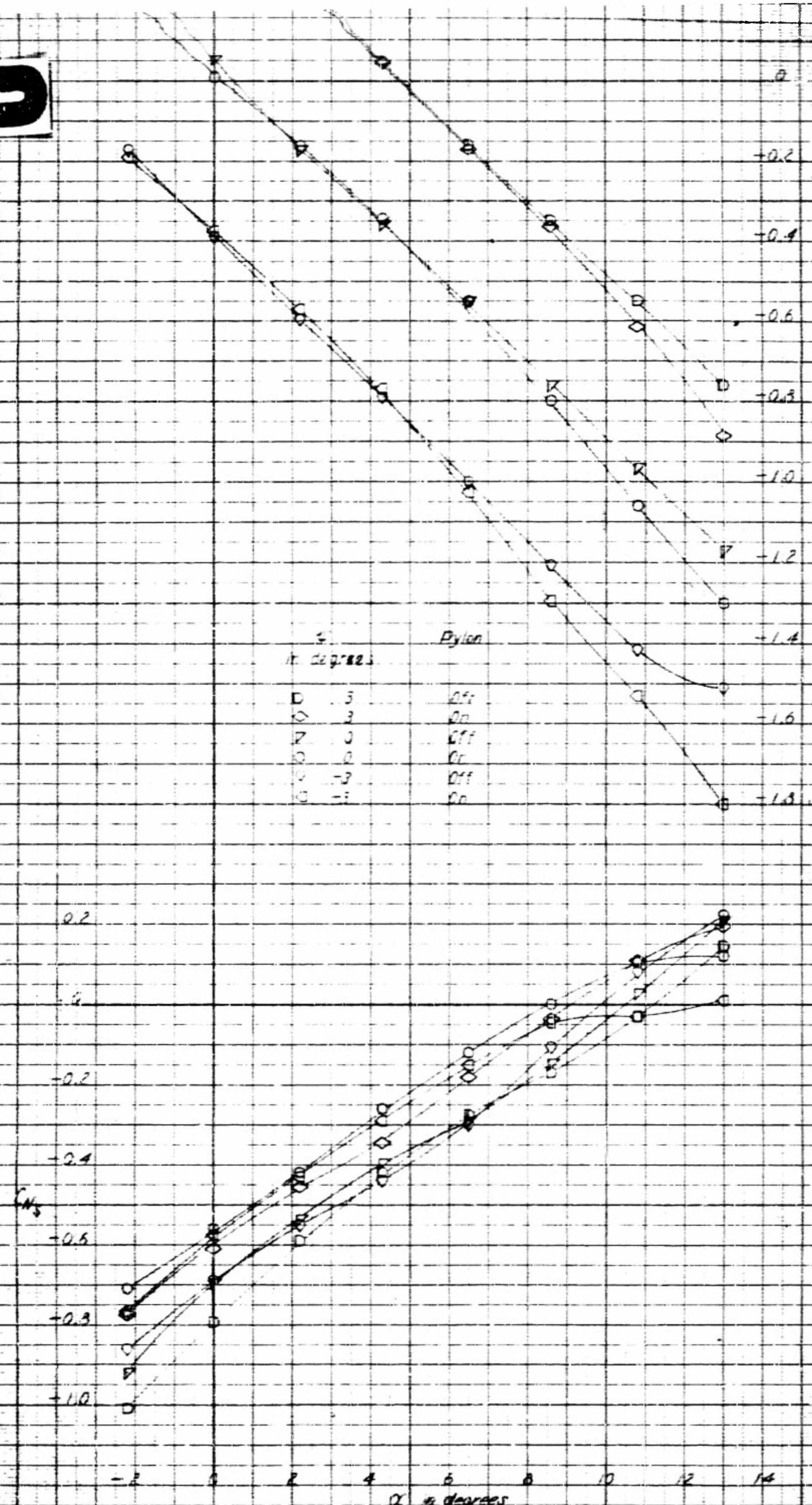

Figure 14—Effect of the Pylon and Airplane Yaw Upon the Aerodynamic Characteristics of a 0.17-Scale Model XAAM-N-4 Oriole Missile in the Proximity of a 0.179-Scale Model F4D-1 Airplane at the Inboard Station

(a) z=0 Inch, x=0 Inch, $\theta_s=0°$, $\psi_s=0°$

CONFIDENTIAL

FIGURE 14a

CONFIDENTIAL

AERO 864

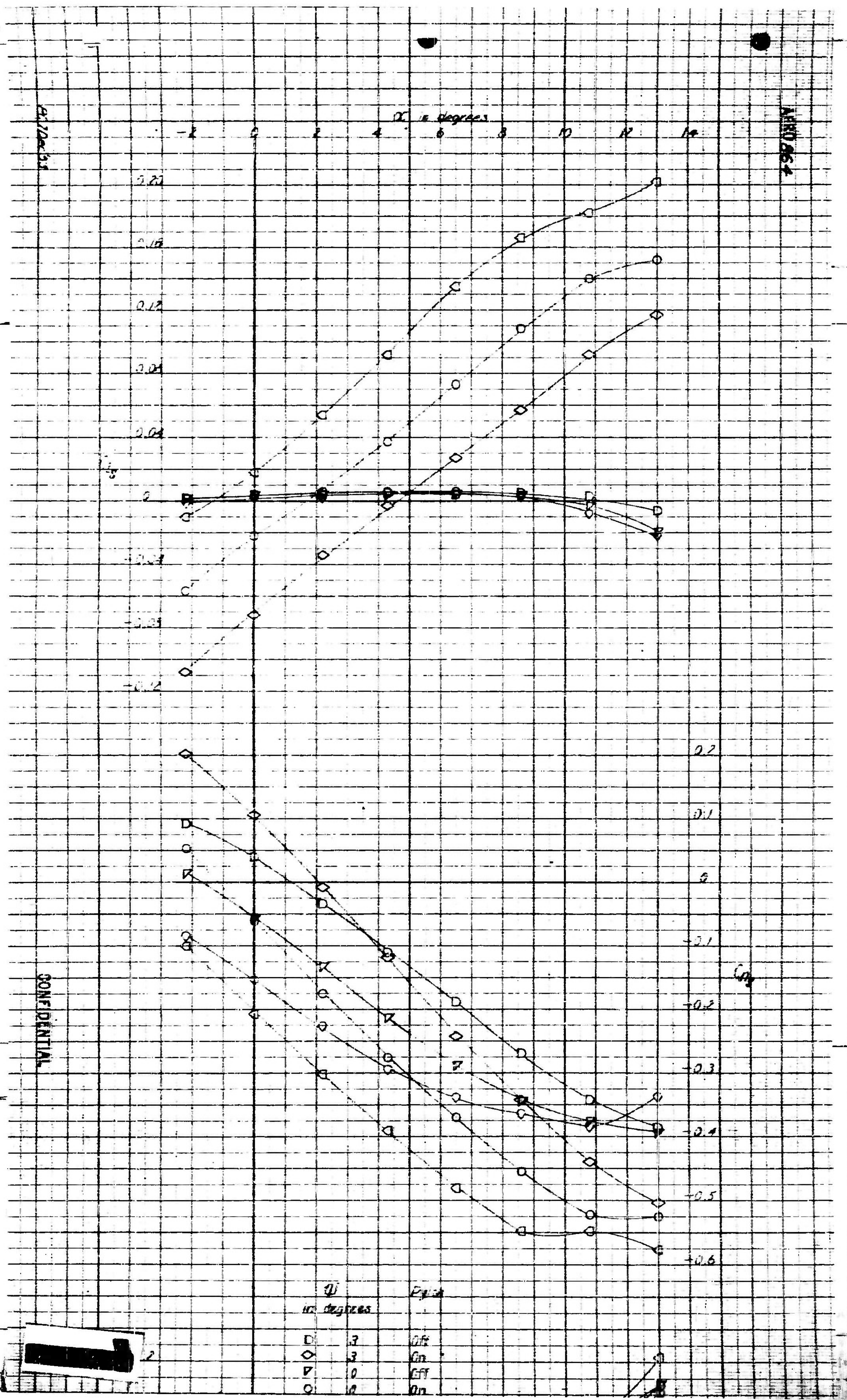

CONFIDENTIAL

[redacted]

CONFIDENTIAL

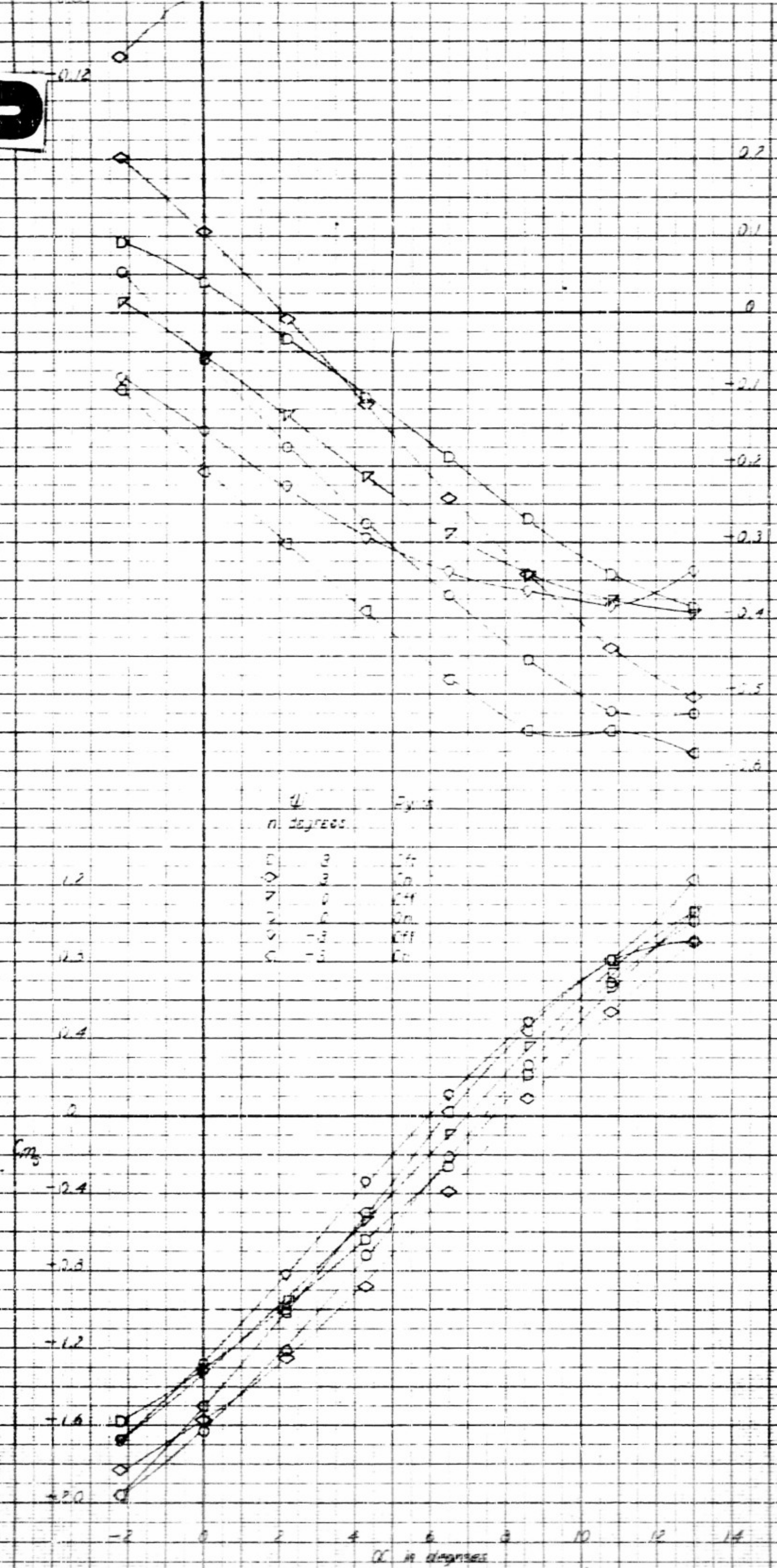

Figure 14 (Continued)

(n) Concluded

Figure 14a (cont'd)

CONFIDENTIAL

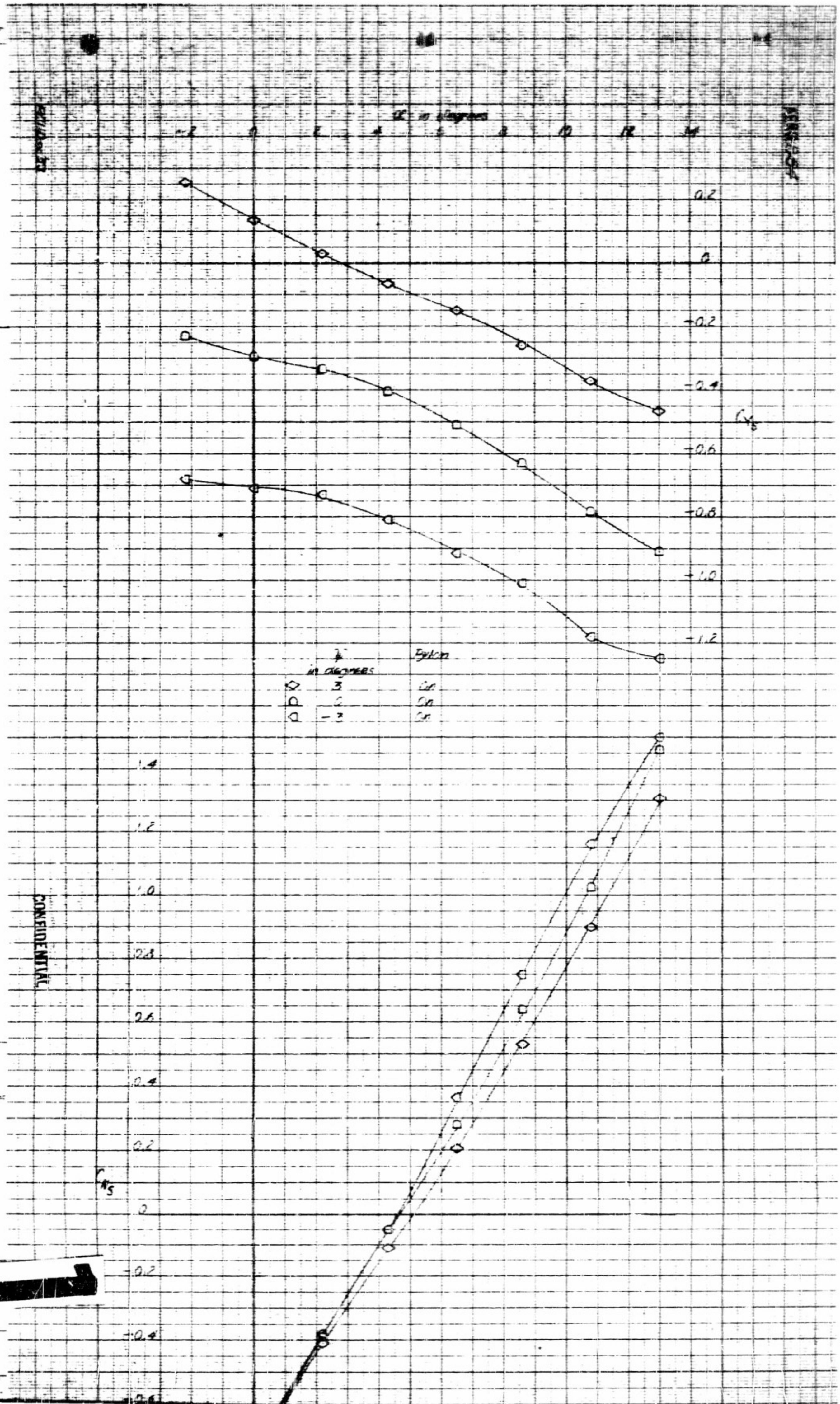

CONFIDENTIAL

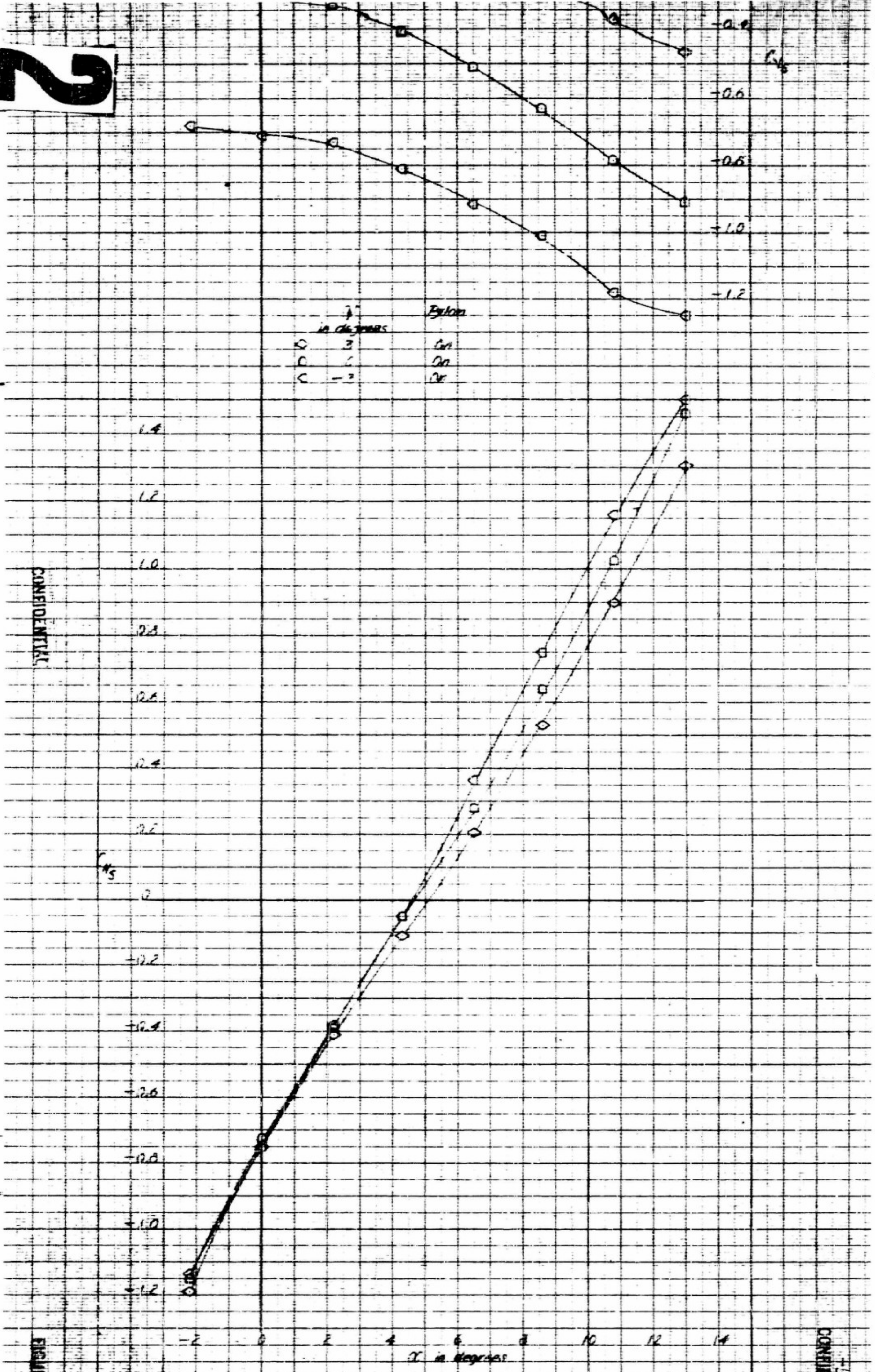

Figure 14 (Continued)

(h) $z' = 2.04$ Inches, $x = 18.36$ Inches, $\theta_S = 0°$, $\phi_S = 0°$

FIGURE 14h

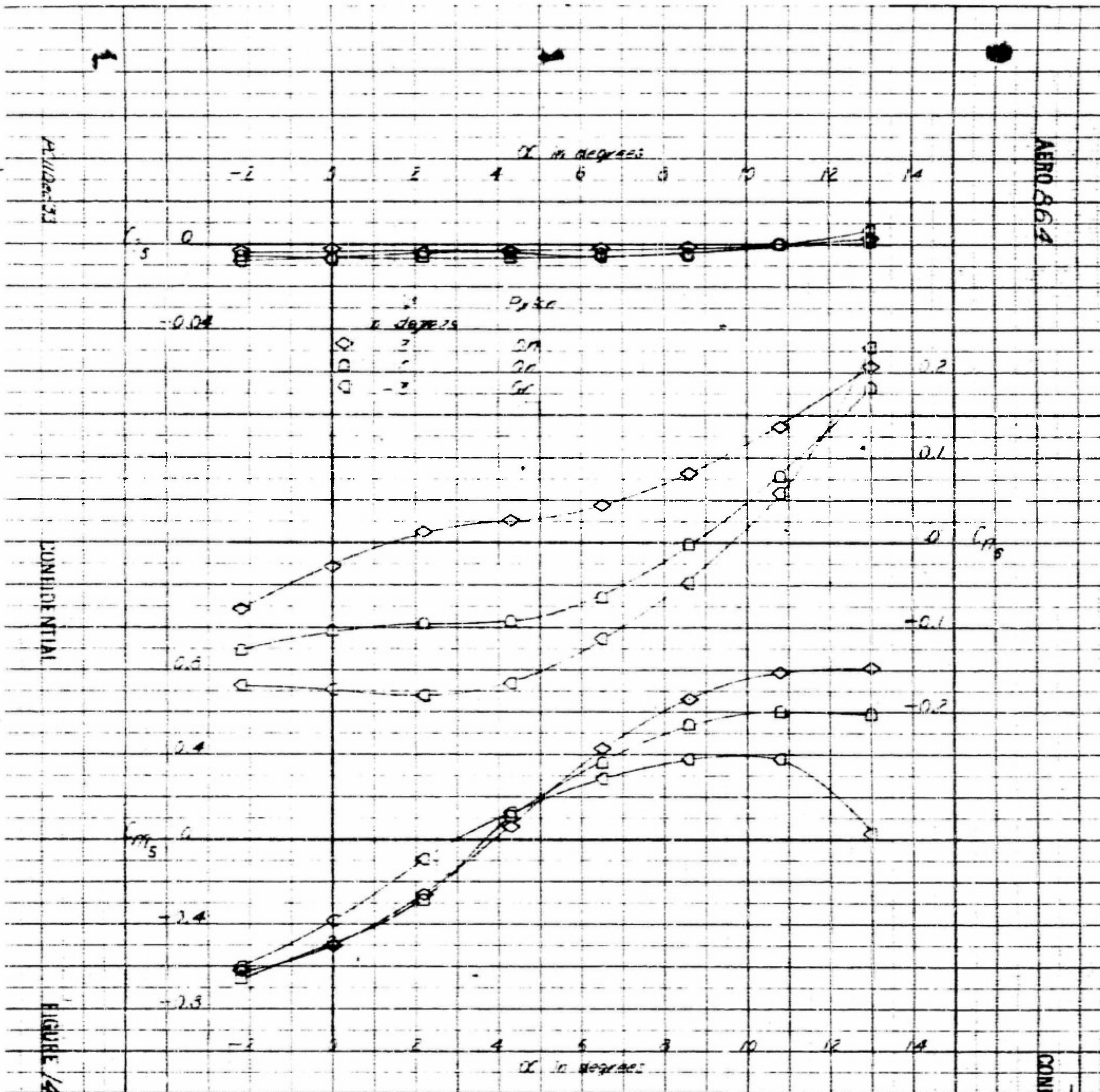

Figure 14 (Continued)

(b) Concluded

AERO 864

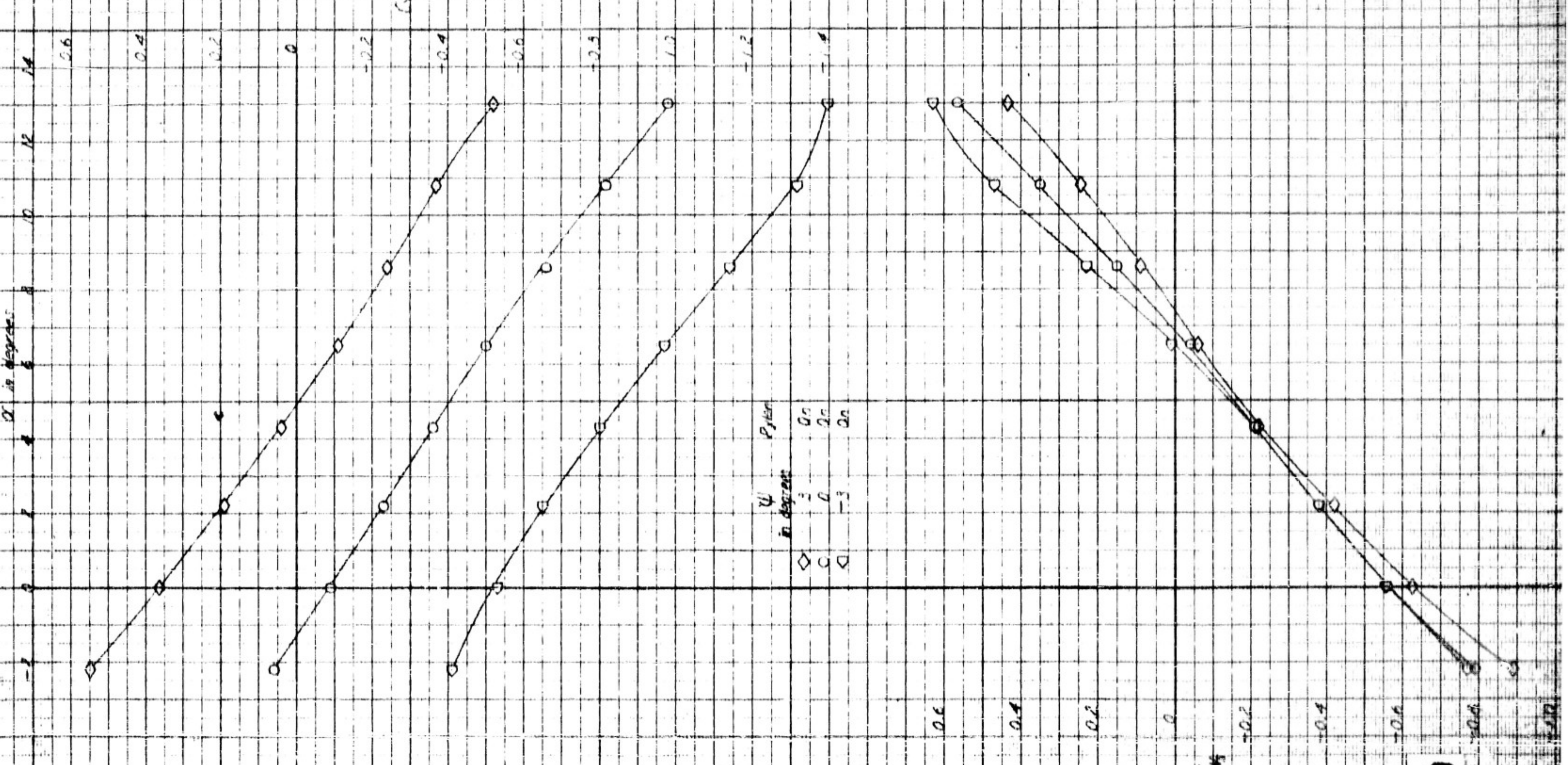

PC 11Dec'53

CONFIDENTIAL

CONFIDENTIAL

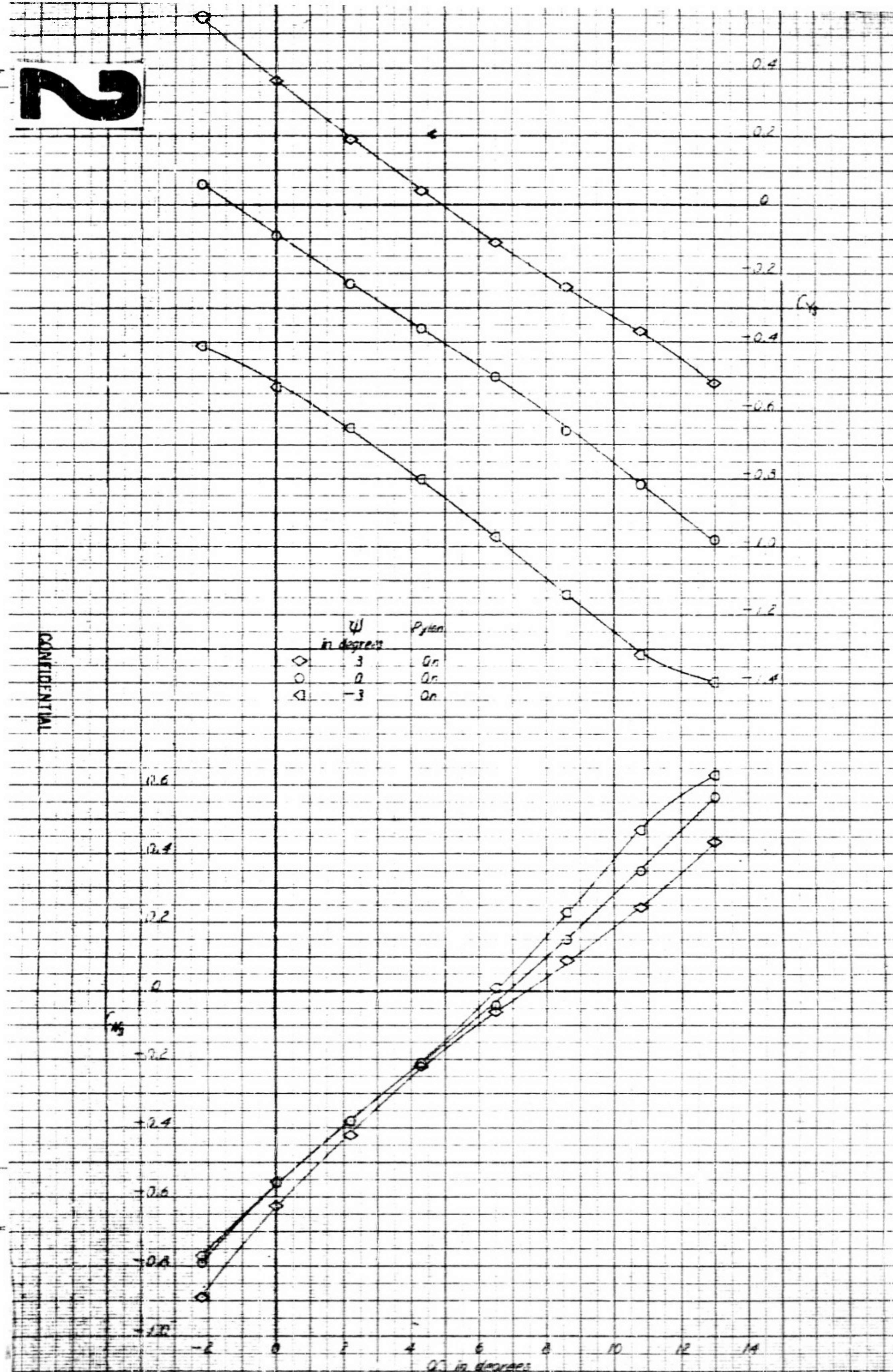

Figure 14 (Continued)

CONFIDENTIAL

CONFIDENTIAL

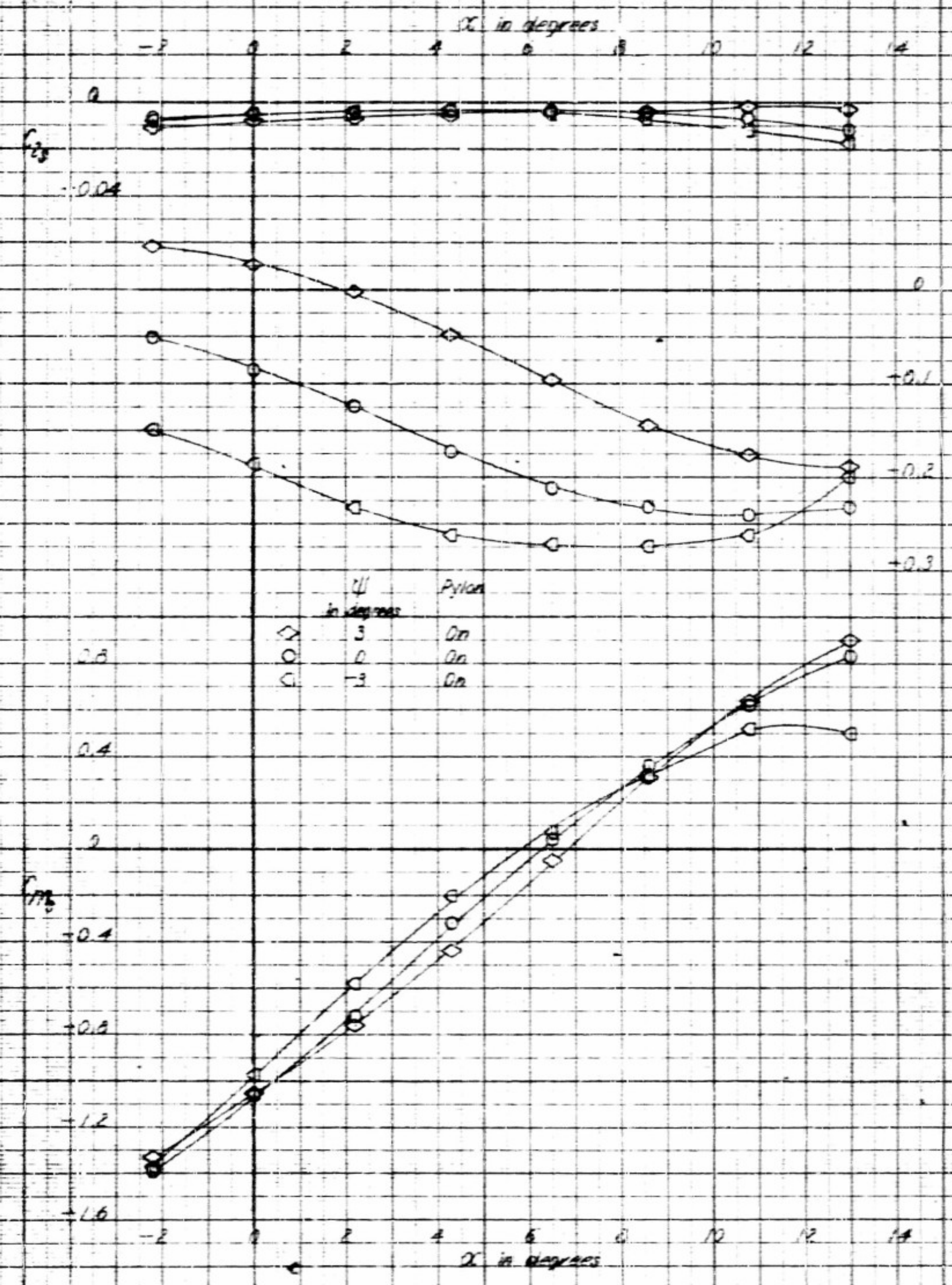

Figure 14 (Concluded)

(c) Concluded

FIGURE 14 c(concl.)

CONFIDENTIAL

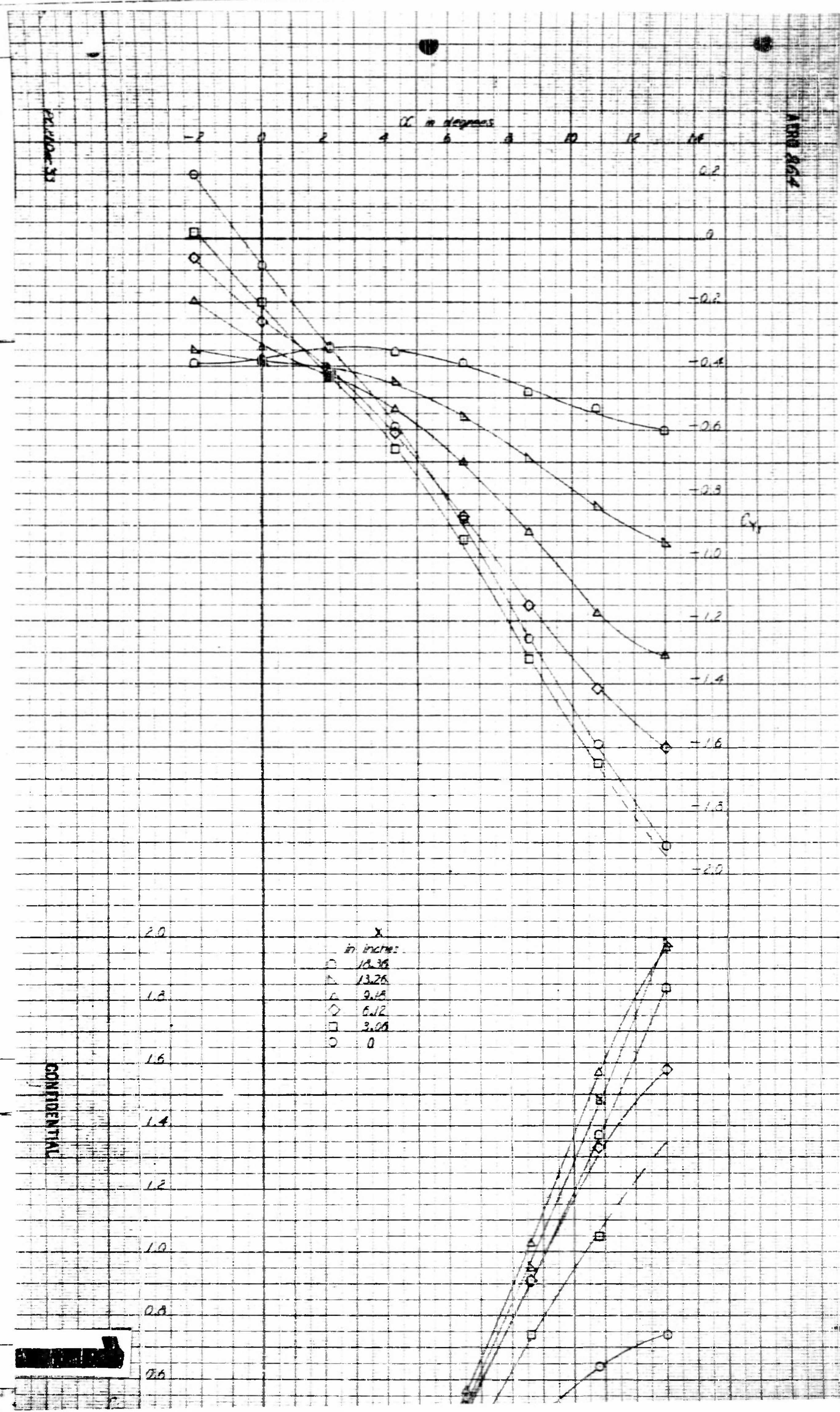
AERO 864
α in degrees
-2
0
2
4
6
8
10
12
14
0.2
0
-0.2
-0.4
-0.6
-0.8
-1.0
-1.2
-1.4
-1.6
-1.8
-2.0
C_{Y_T}
2.0
1.8
1.6
1.4
1.2
1.0
0.8
0.6
x
in inches
18.36
13.26
9.18
6.12
3.06
0
CONFIDENTIAL

[redacted]

CONFIDENTIAL

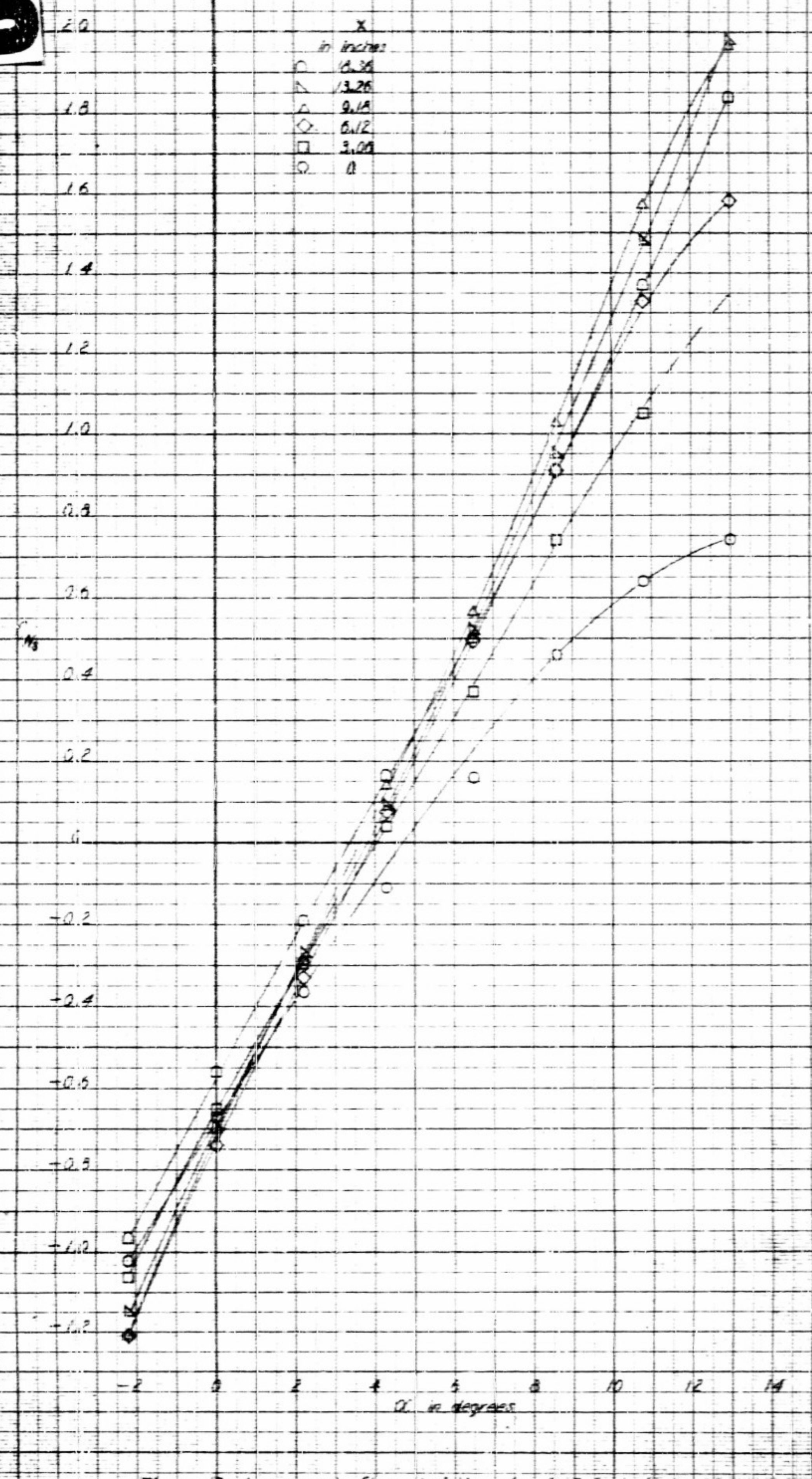

Figure 15 - Aerodynamic Characteristics of a 0.17-Scale Model XAAM-N-4 Orion Missile for Various Distances Forward of the Carry Position in the Proximity of a 0.179-Scale Model F4D-1 Airplane at the Outboard Station

(a) z = 0 Inch, $\psi = 0°$; $\phi_S = 0°$; $\delta = 0°$; Pylon On

FIGURE 15(a)

CONFIDENTIAL

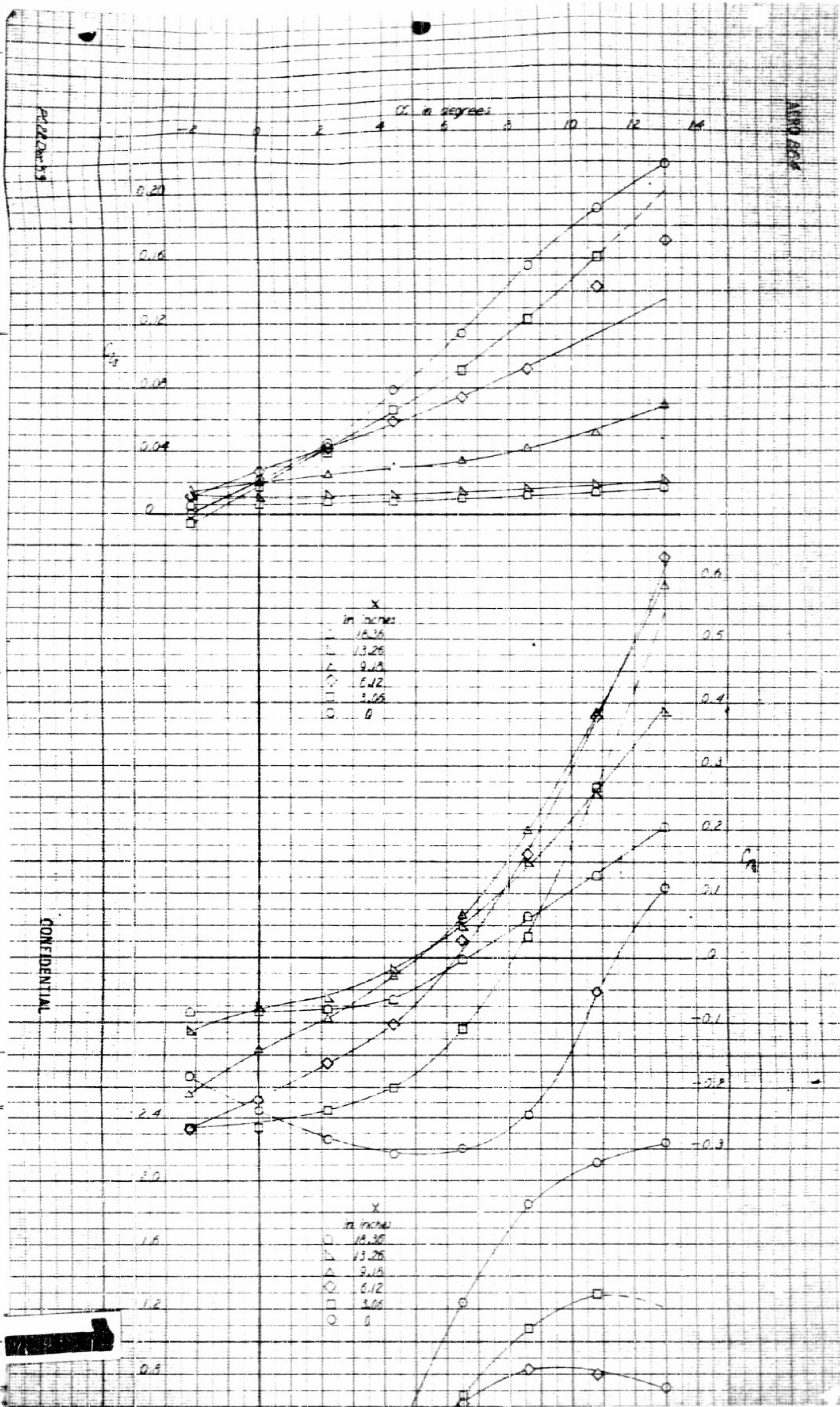
AERO 864
CONFIDENTIAL
α in degrees
X
in inches
15.36
13.26
9.18
6.12
3.06
0
[redacted]

CONFIDENTIAL

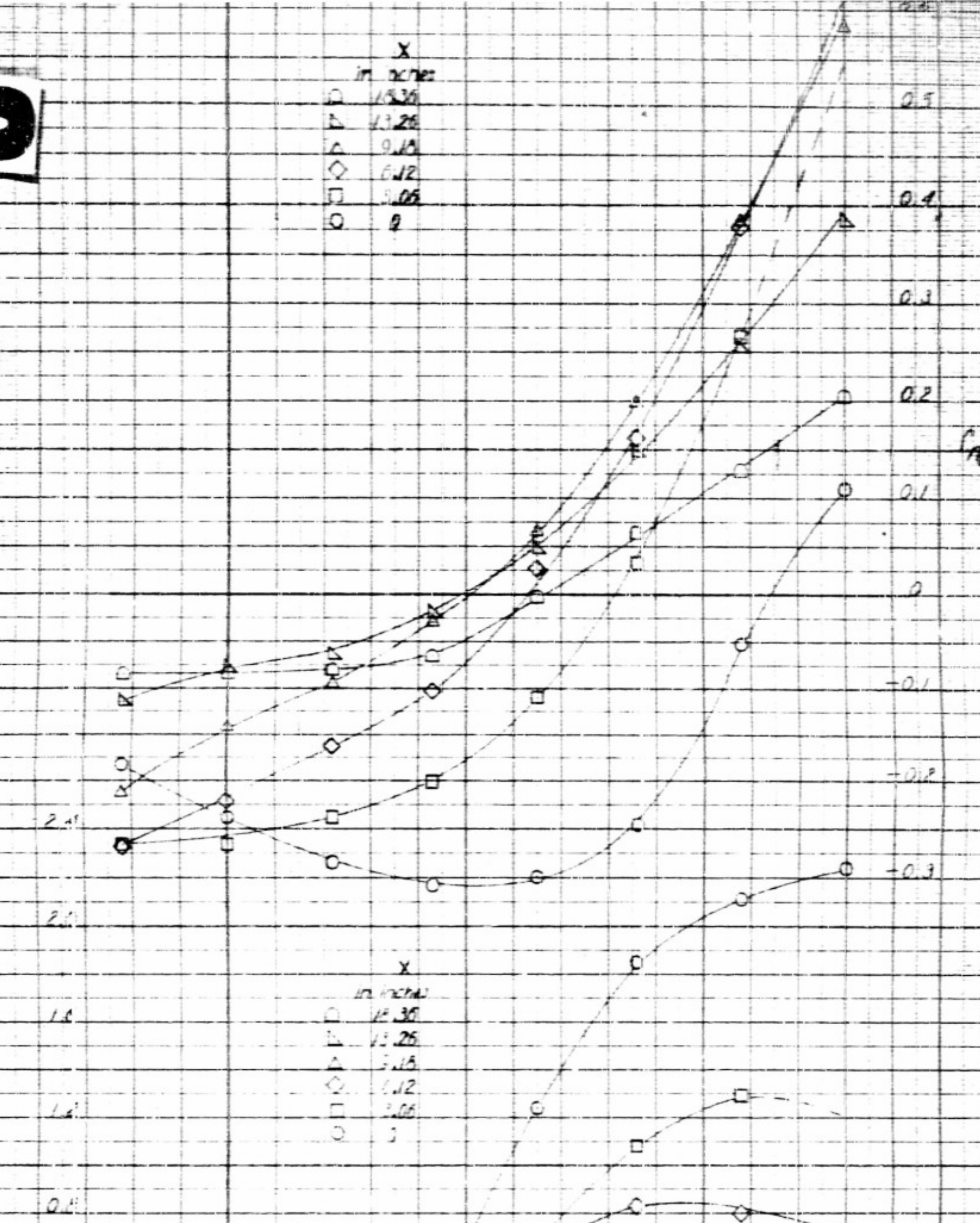

Figure 15 (Continued)

(a) Concluded

FIGURE 15 a(conc)

CONFIDENTIAL

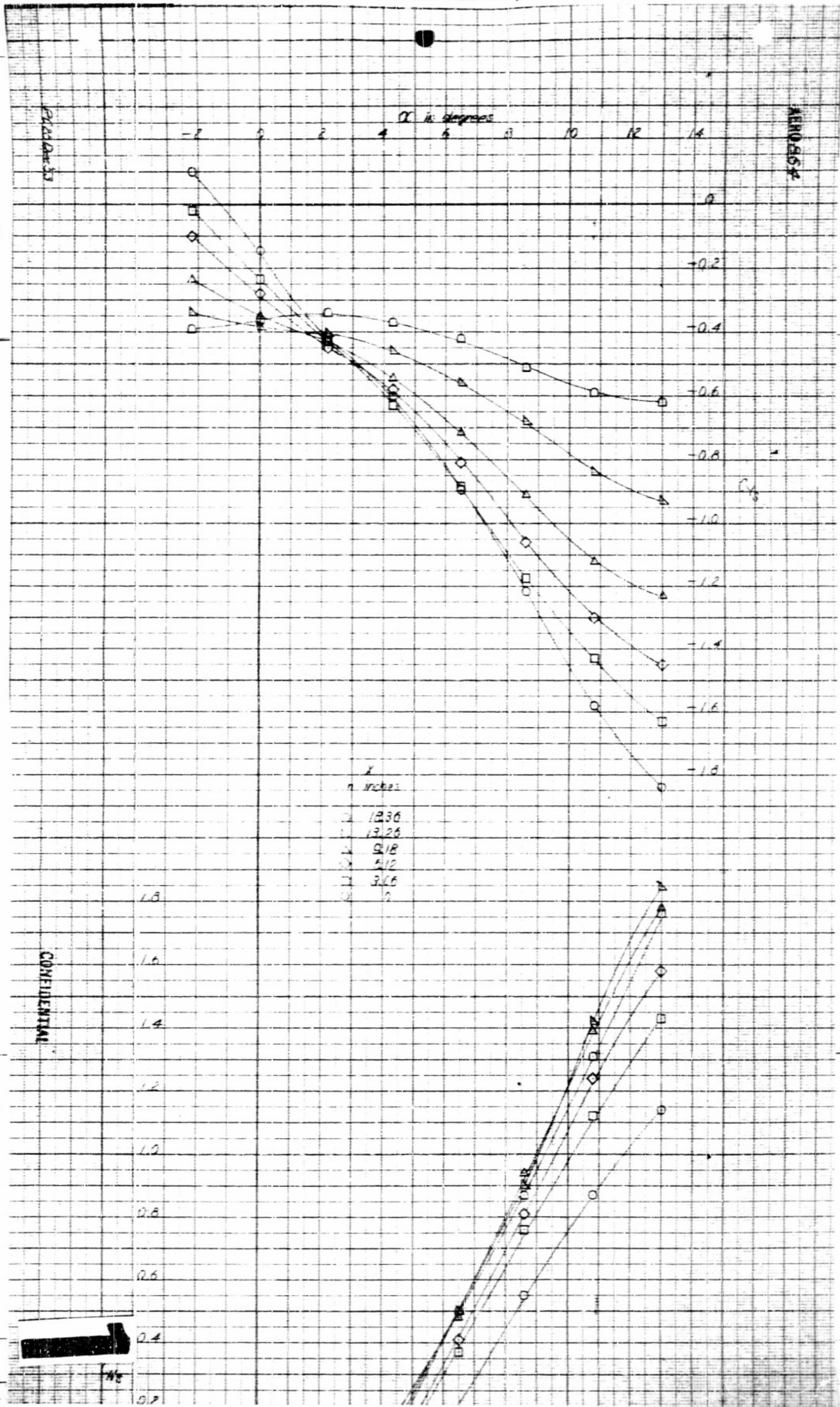
AERO 564
CONFIDENTIAL
α in degrees
-2
0
2
4
6
8
10
12
14
0
-0.2
-0.4
-0.6
-0.8
-1.0
-1.2
-1.4
-1.6
-1.8
x
in inches
18.36
13.26
9.18
5.12
3.06
0
1.8
1.6
1.4
1.2
1.0
0.8
0.6
0.4

CONFIDENTIAL

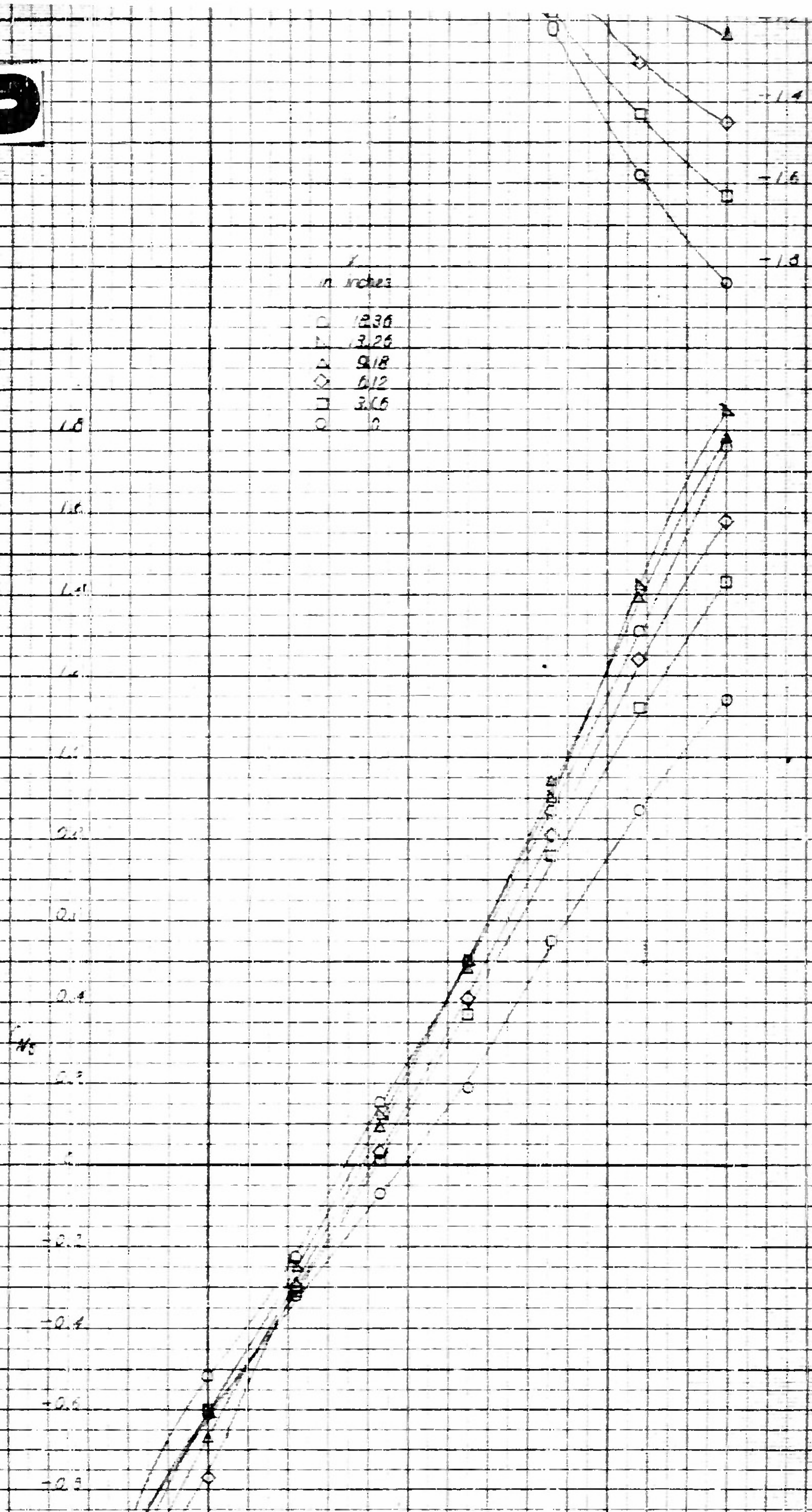

Figure 15 (Continued)

(n) z = 1.02 Inches, $\theta_E = 0°$, $\psi_S = 0°$, $\psi = 0°$, Pylon On

FIGURE 15n

CONFIDENTIAL

-101-

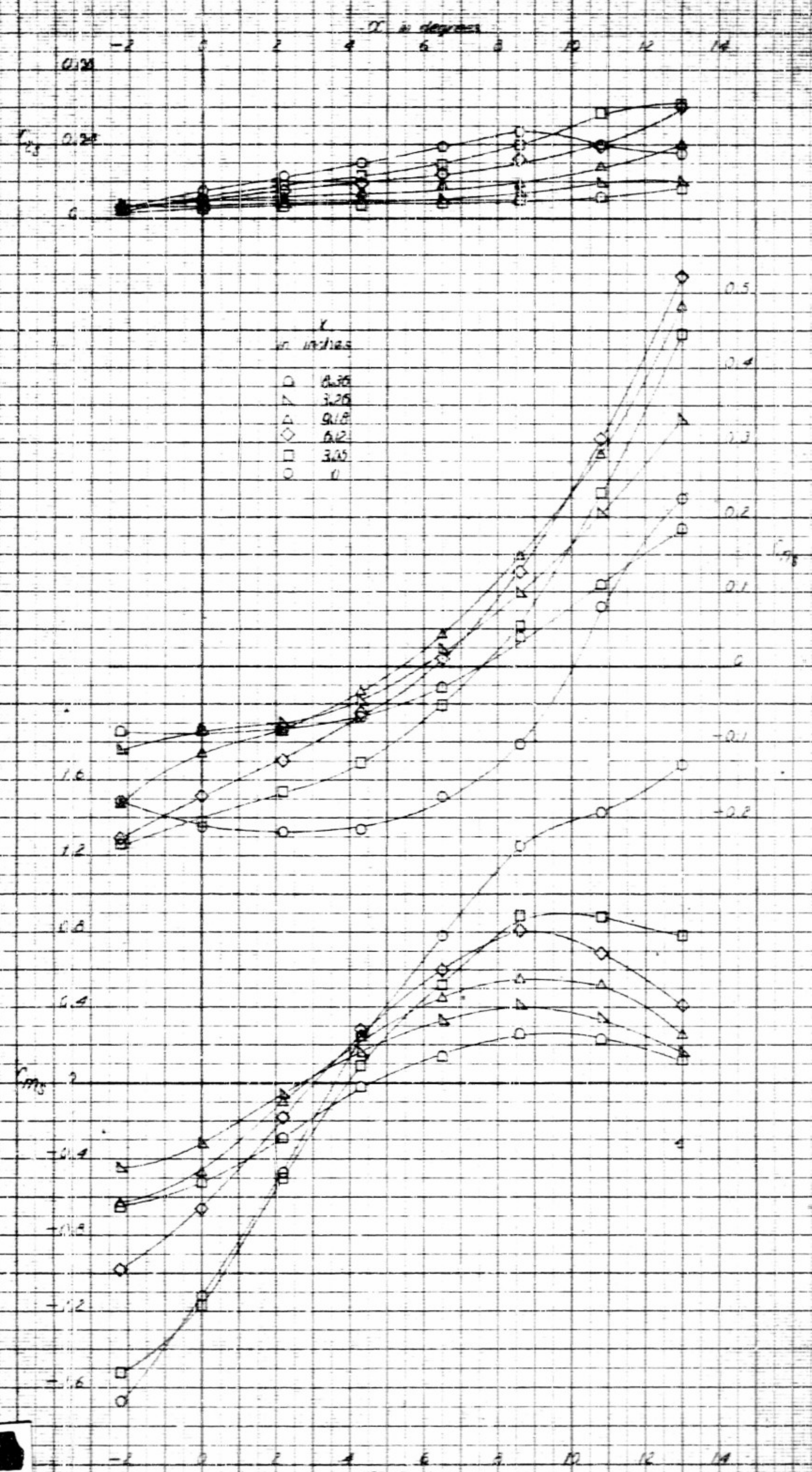

CONFIDENTIAL

[redacted]

Figure 15 (Continued)

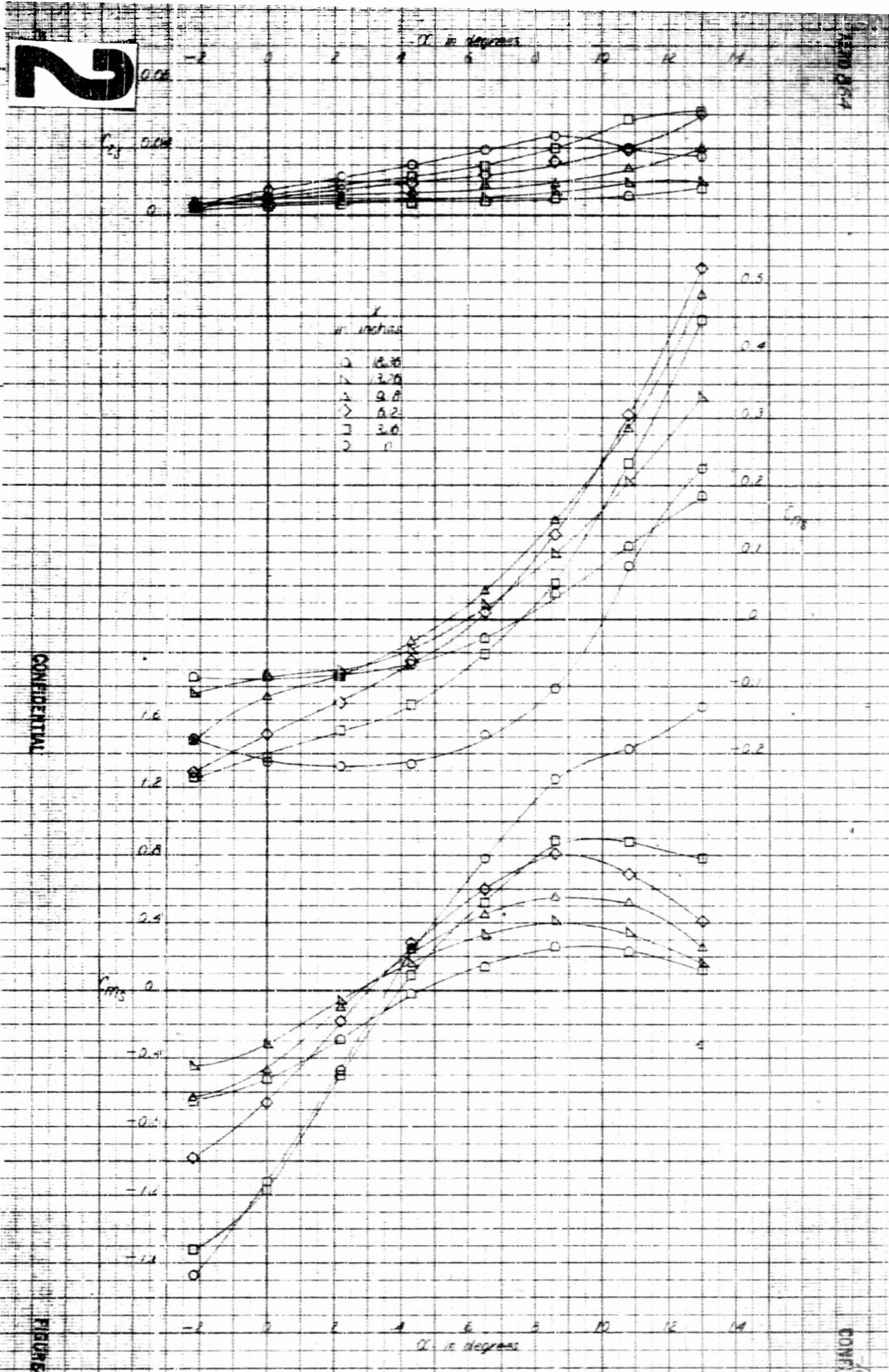

Figure 15 (Continued)

(b) Concluded

CONFIDENTIAL

FIGURE 15(b) (Concl.)

CONFIDENTIAL

Figure 34

AERO 869

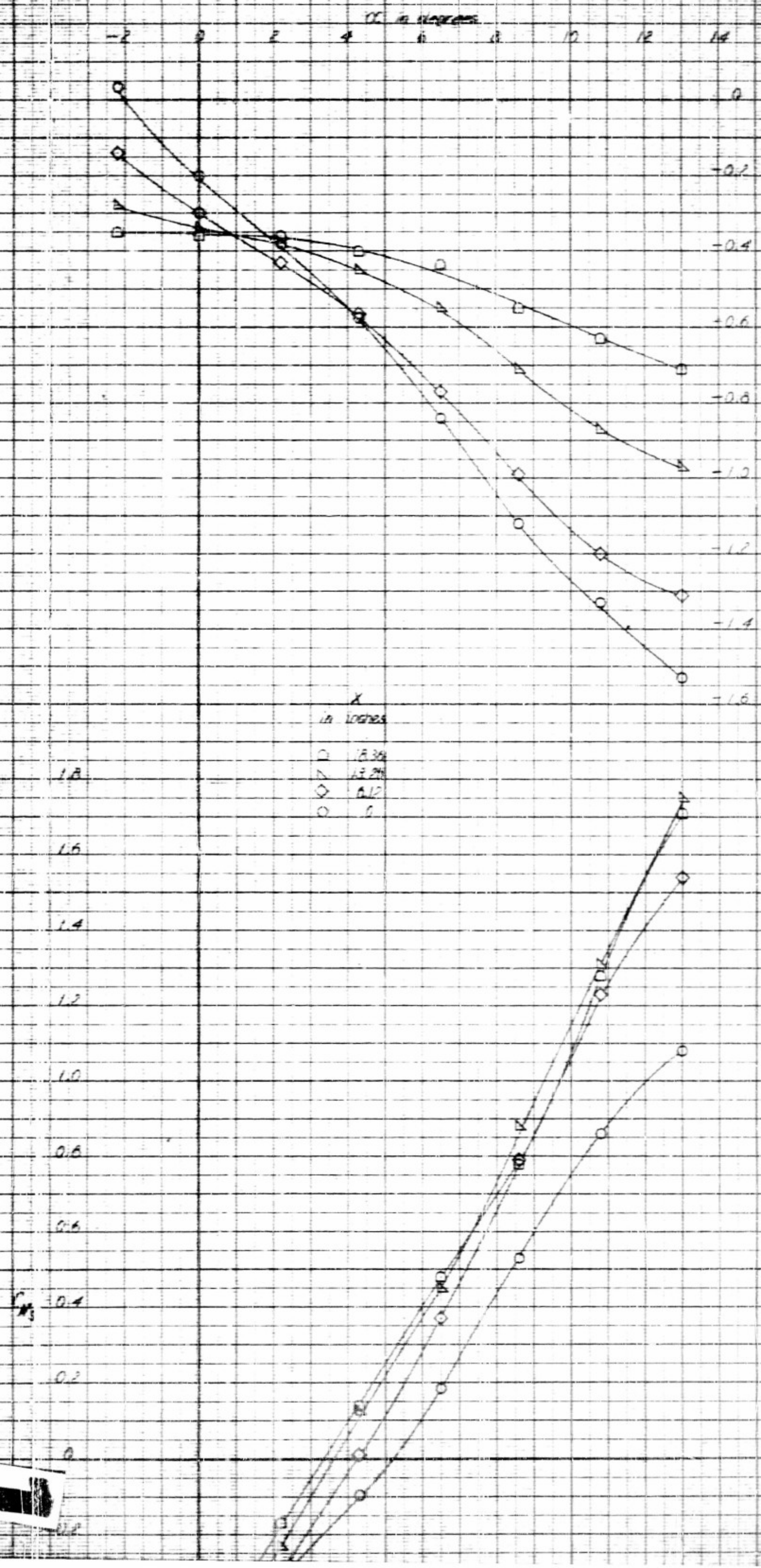

CONFIDENTIAL

[redacted]

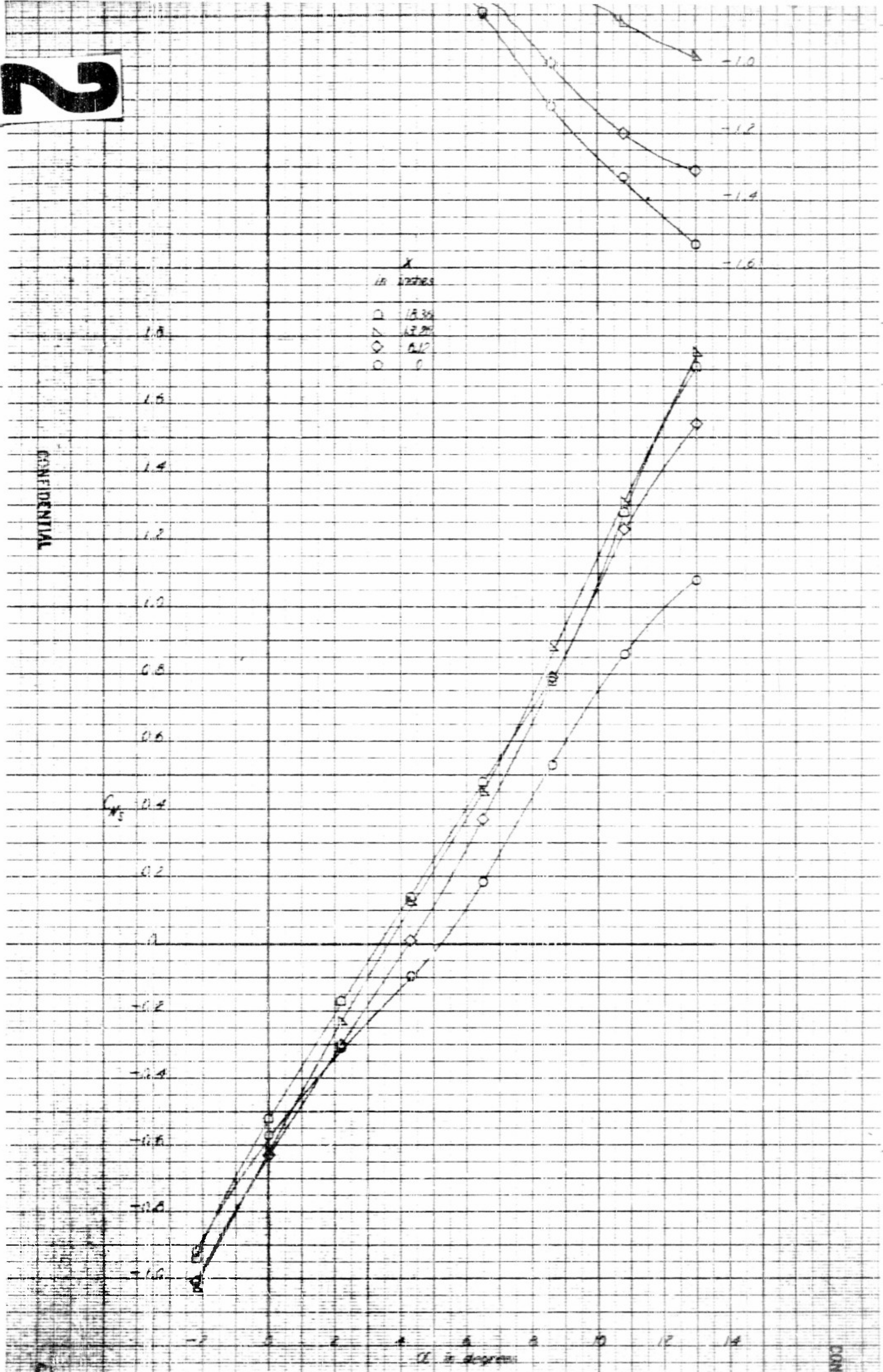

Figure 15 (Continued)

(c) z = 2.04 inches, [illegible] = 0°, [illegible] = 0°, 15° 0°, Pylon On

CONFIDENTIAL

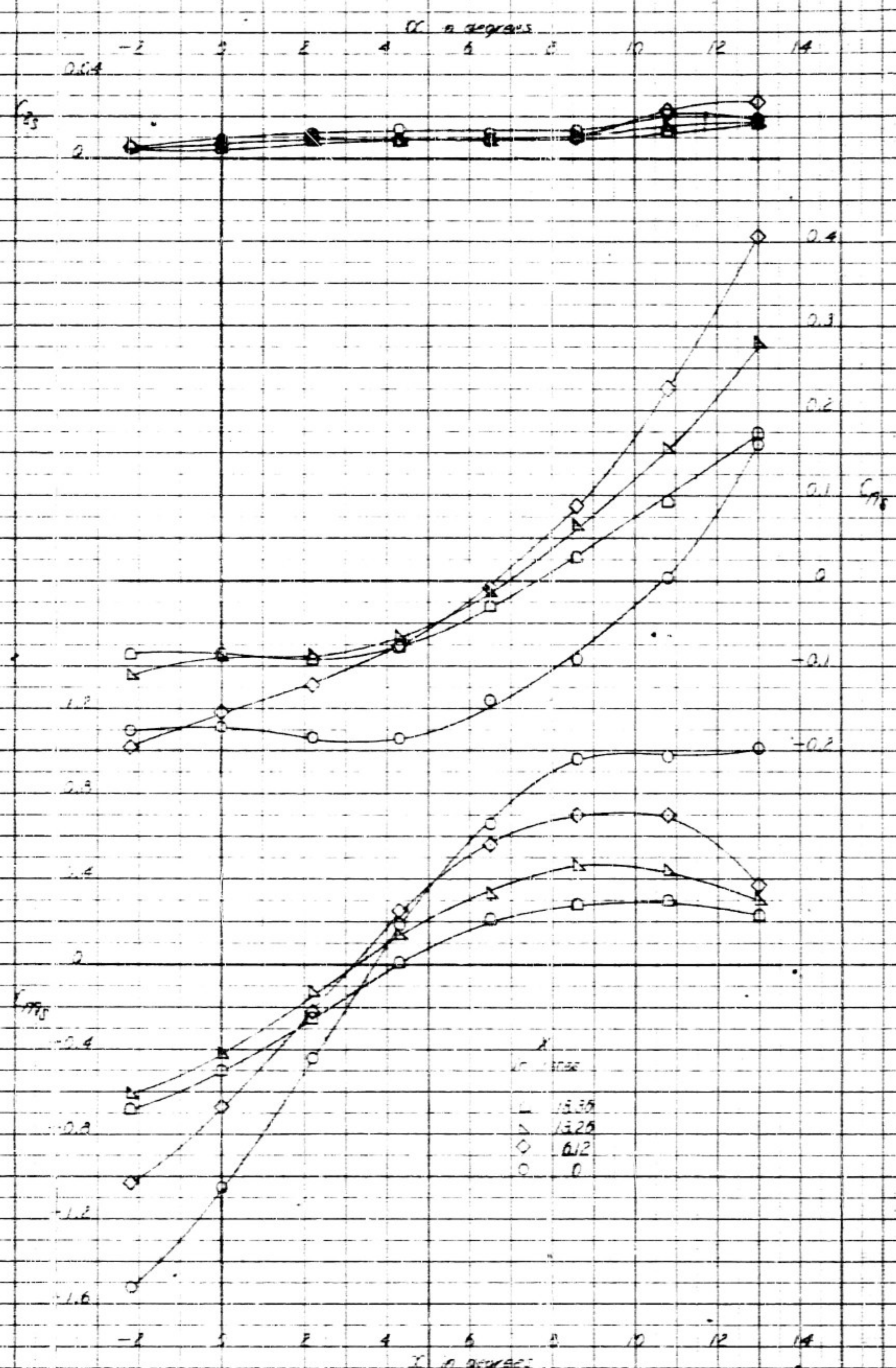

Figure 15 (Concluded)
(c) Concluded

FIGURE 15c (concl)

CONFIDENTIAL

Fig. 31

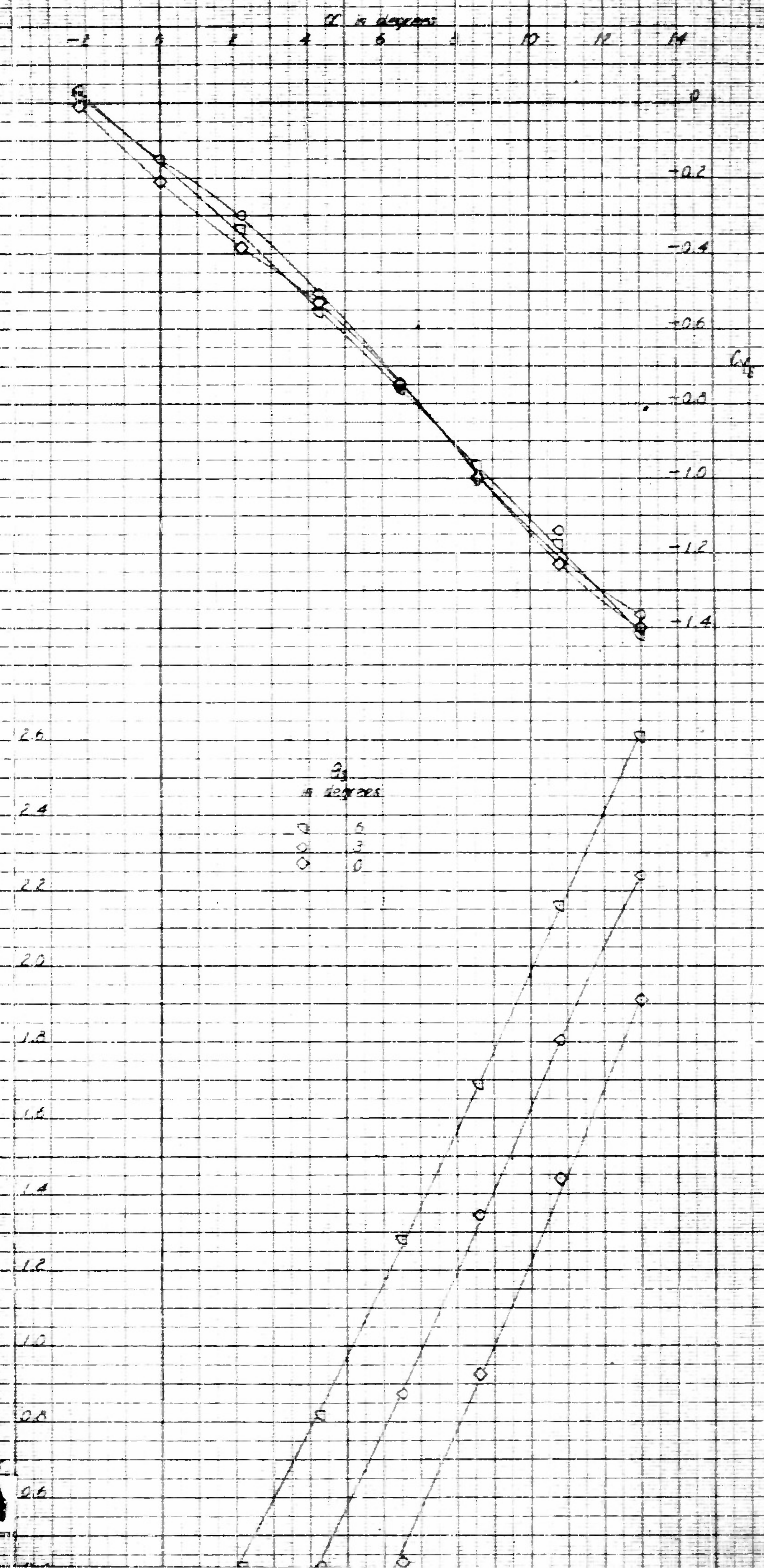

CONFIDENTIAL

[redacted]

CONFIDENTIAL

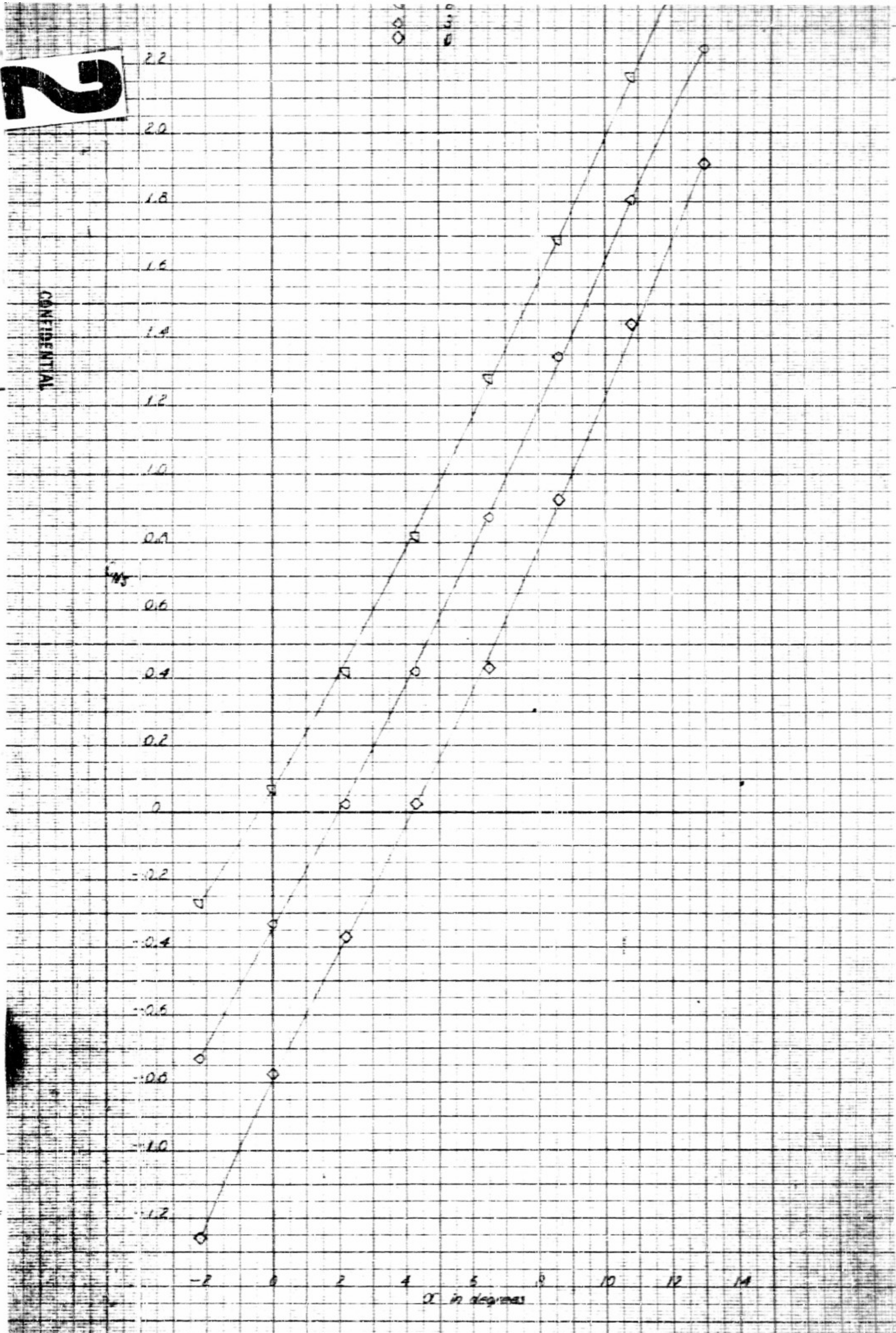

Figure 15 - Aerodynamic Characteristics of a 0.17-Scale Model XAAM-N-4 [illegible] Missile Due to Missile Pitch in the Proximity of a 0.179-Scale Model F4D-1 Airplane at the Outboard Station

(a) z = 0 Inch, y = 6.12 Inches, [illegible], Pylon Off

AERO 864

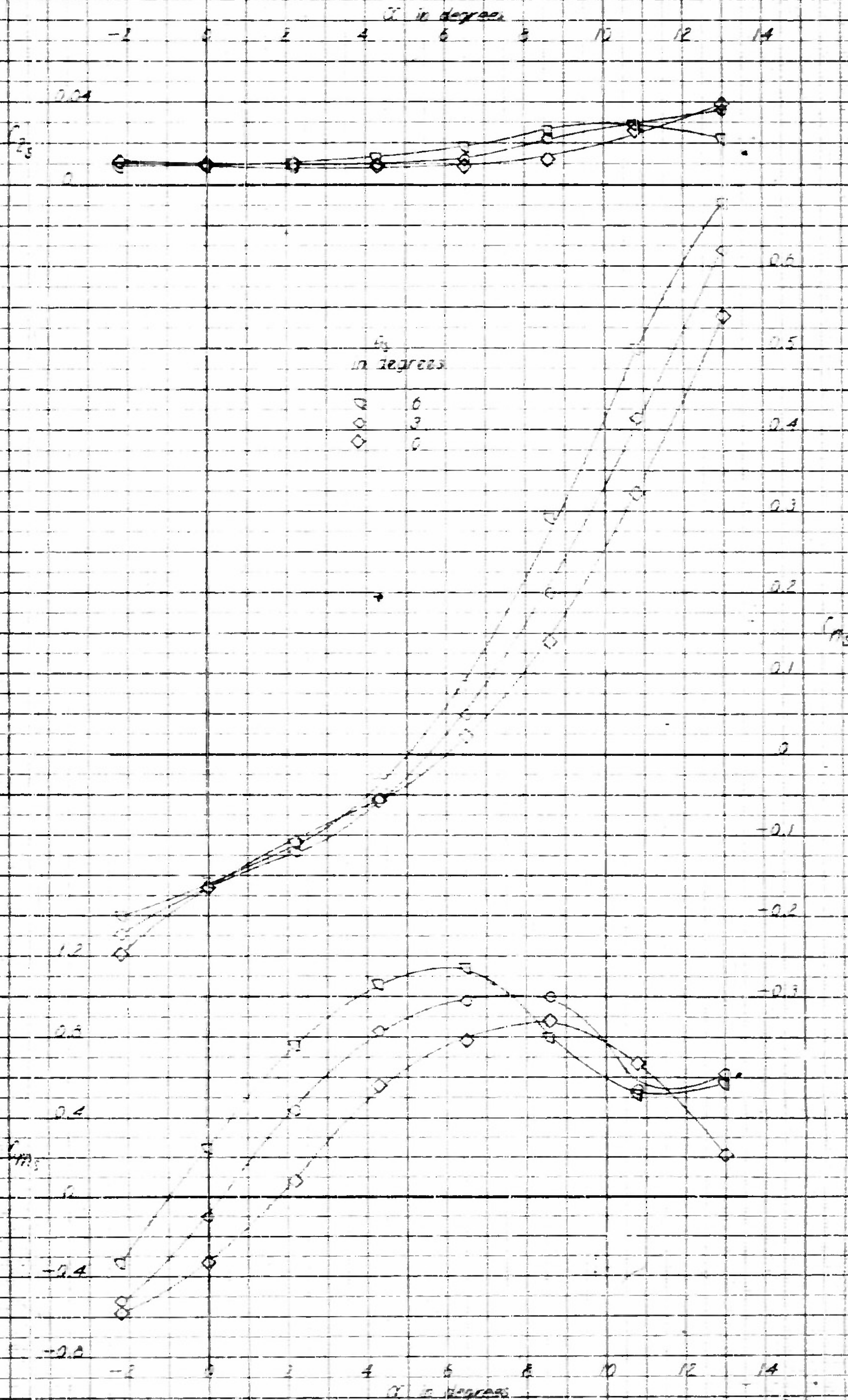

Figure 15 (Continued)

(a) Concluded

CONFIDENTIAL

FIGURE 15(a)(concl)

CONFIDENTIAL

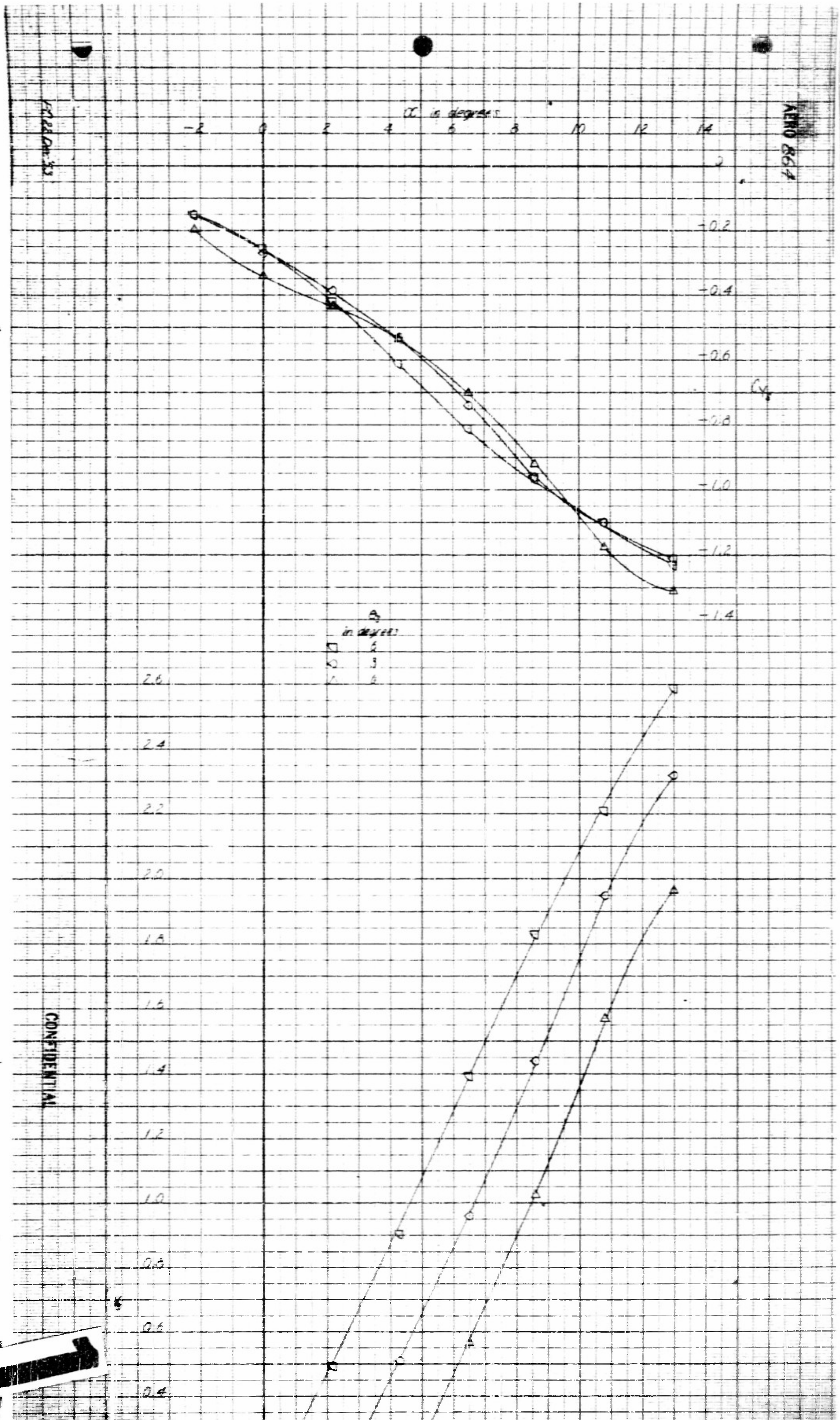

AERO 864

CONFIDENTIAL

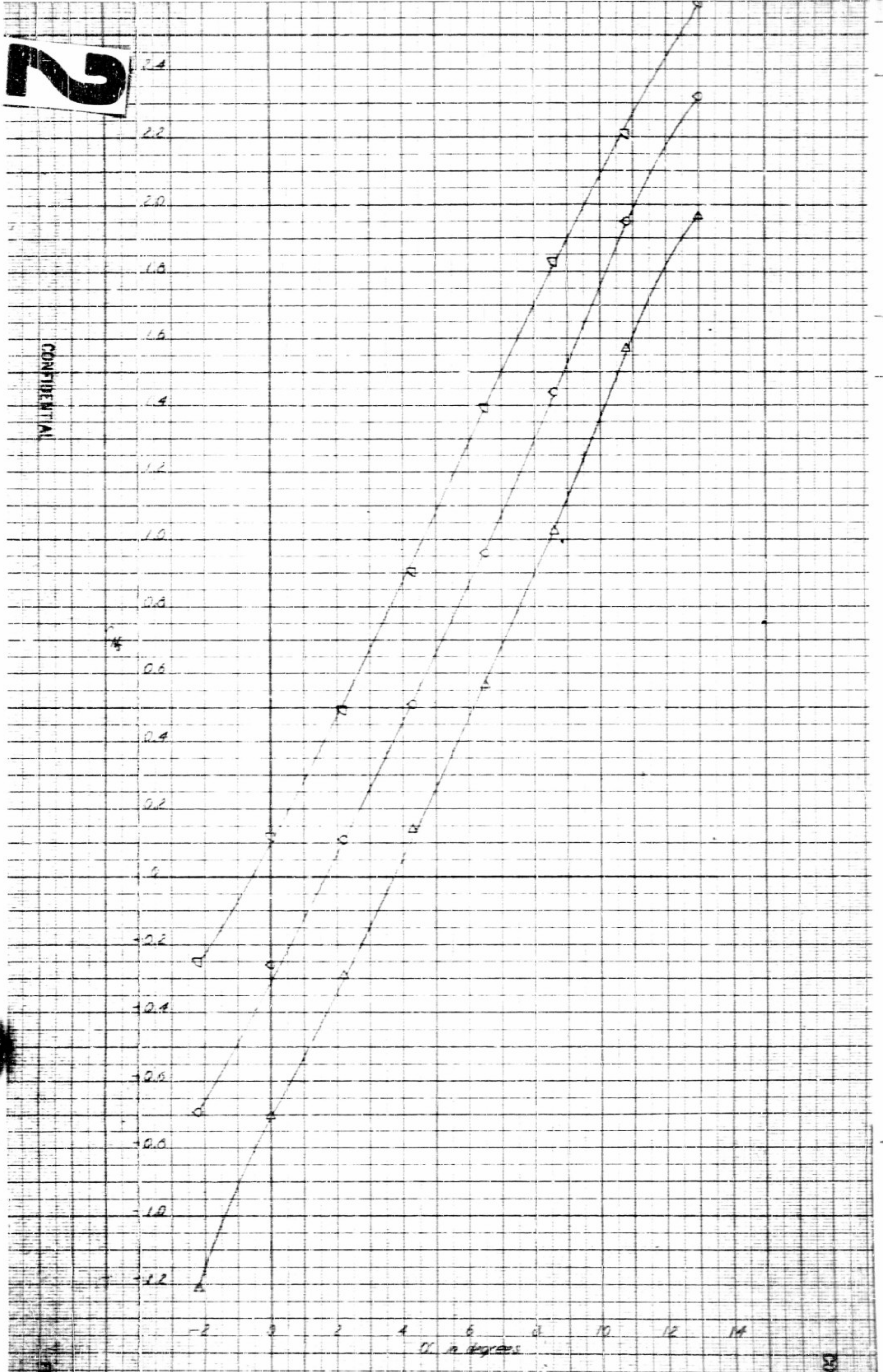

Figure 16 (Continued)

(b) r=0 Inch, x=3.16 Inches, ψ_0=0°, ψ=0°, Pylon On

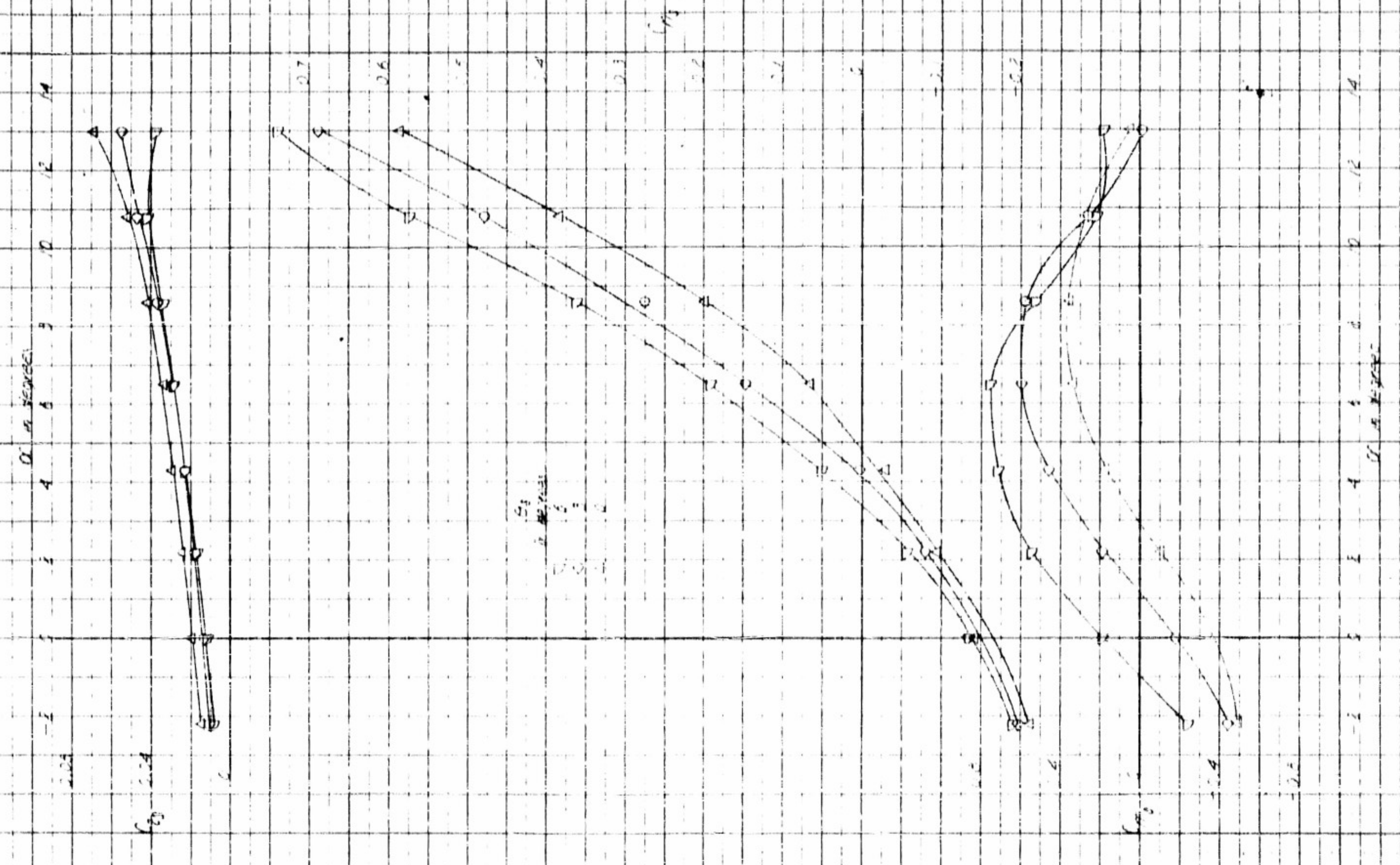

Figure 16 (Continued)
(b) Concluded

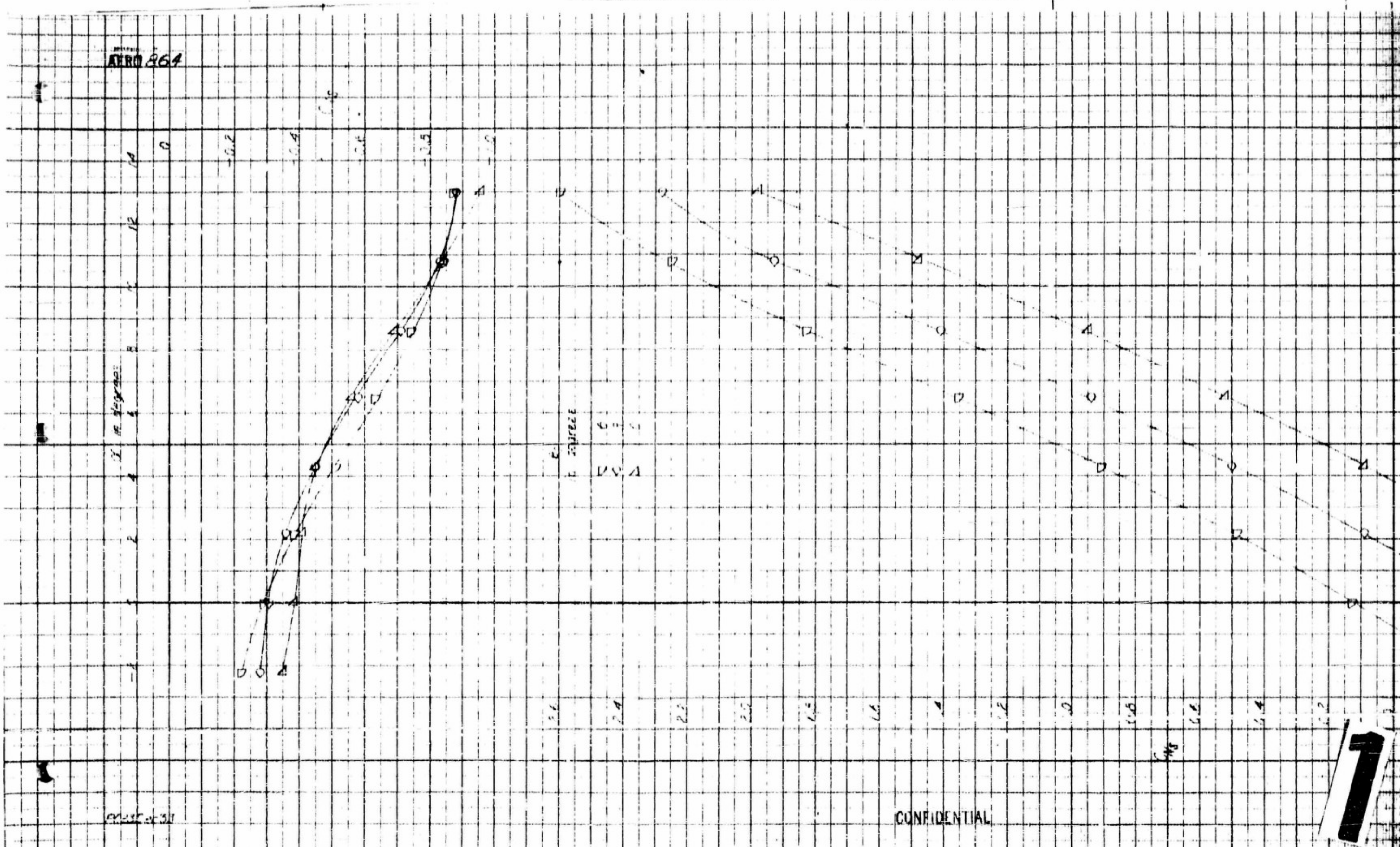

CONFIDENTIAL

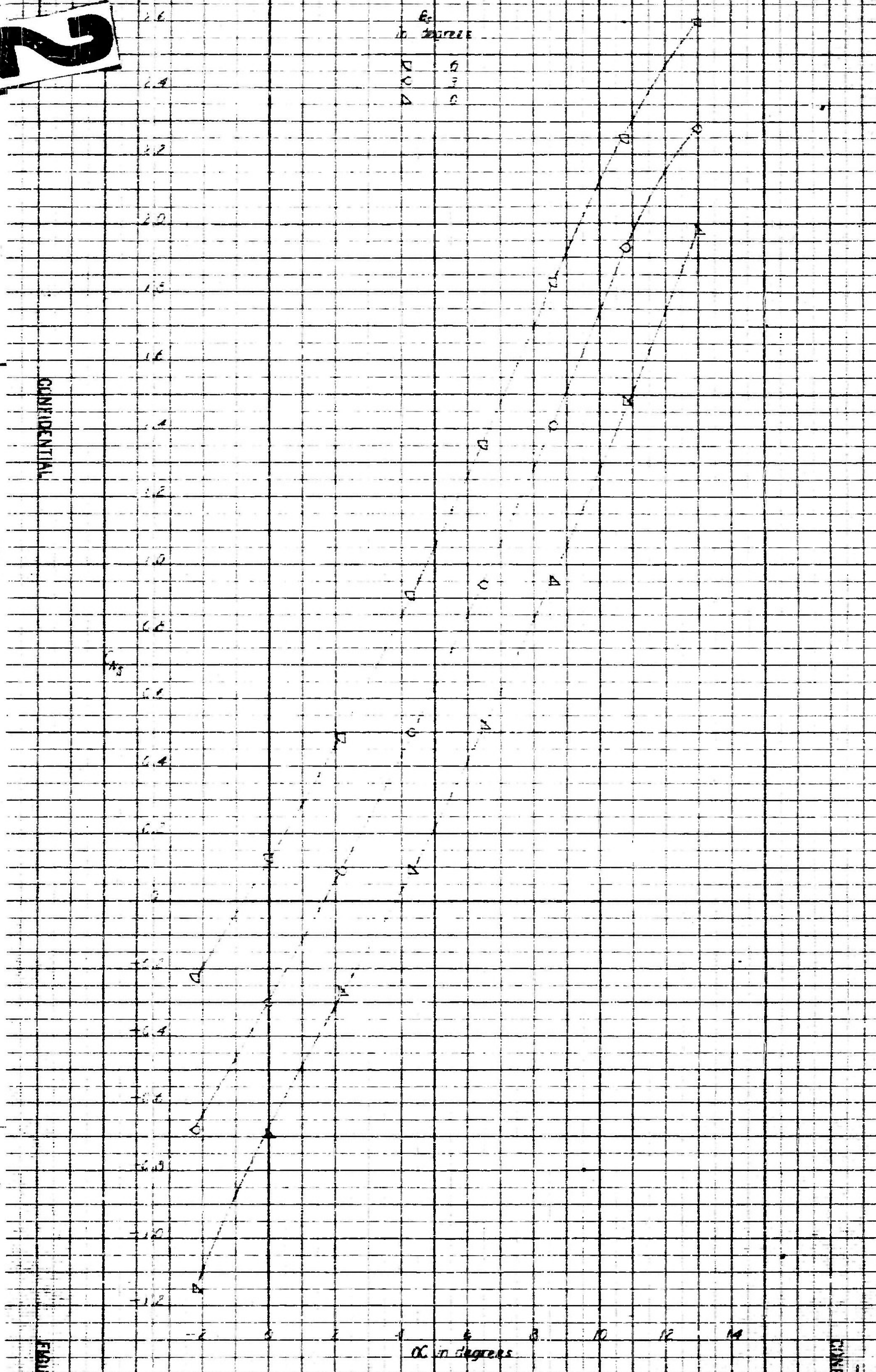

Figure 16 (Continued)

(c) Z = 0 Inch, x = 13.26 Inches, ... = 0°, ... = 0°, Pylon On

CONFIDENTIAL

FIGURE 16 C

CONFIDENTIAL

CONFIDENTIAL

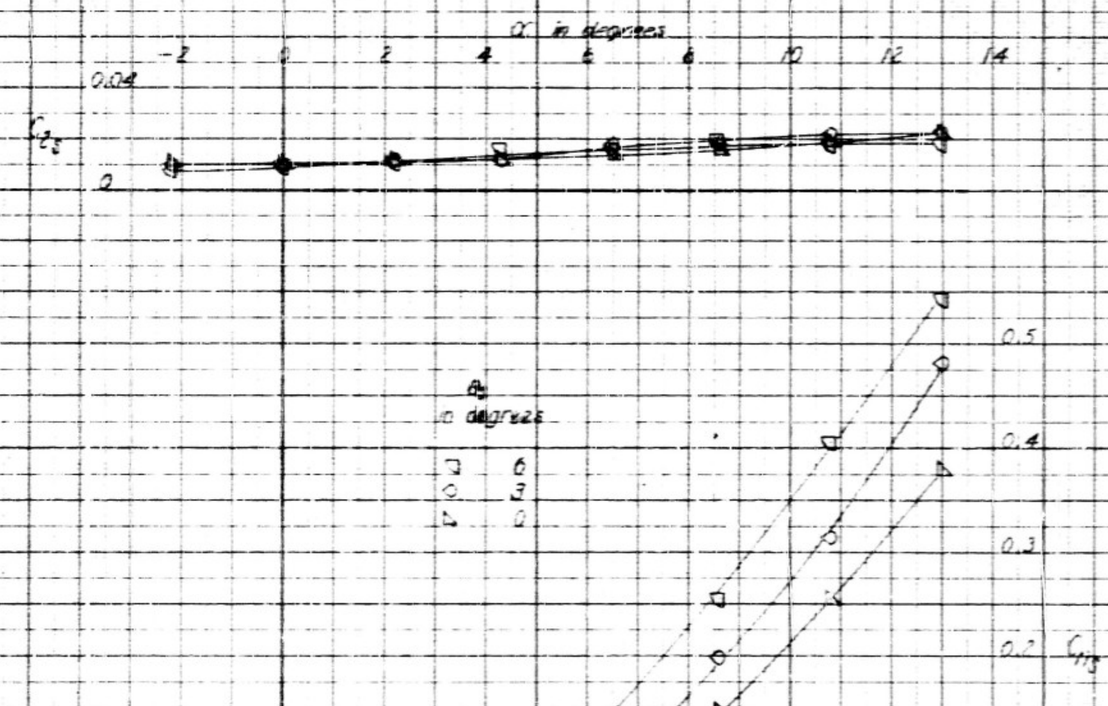

Figure 16 (Continued)

(c) Concluded

FIGURE 16c (concl)

CONFIDENTIAL

AERO 864

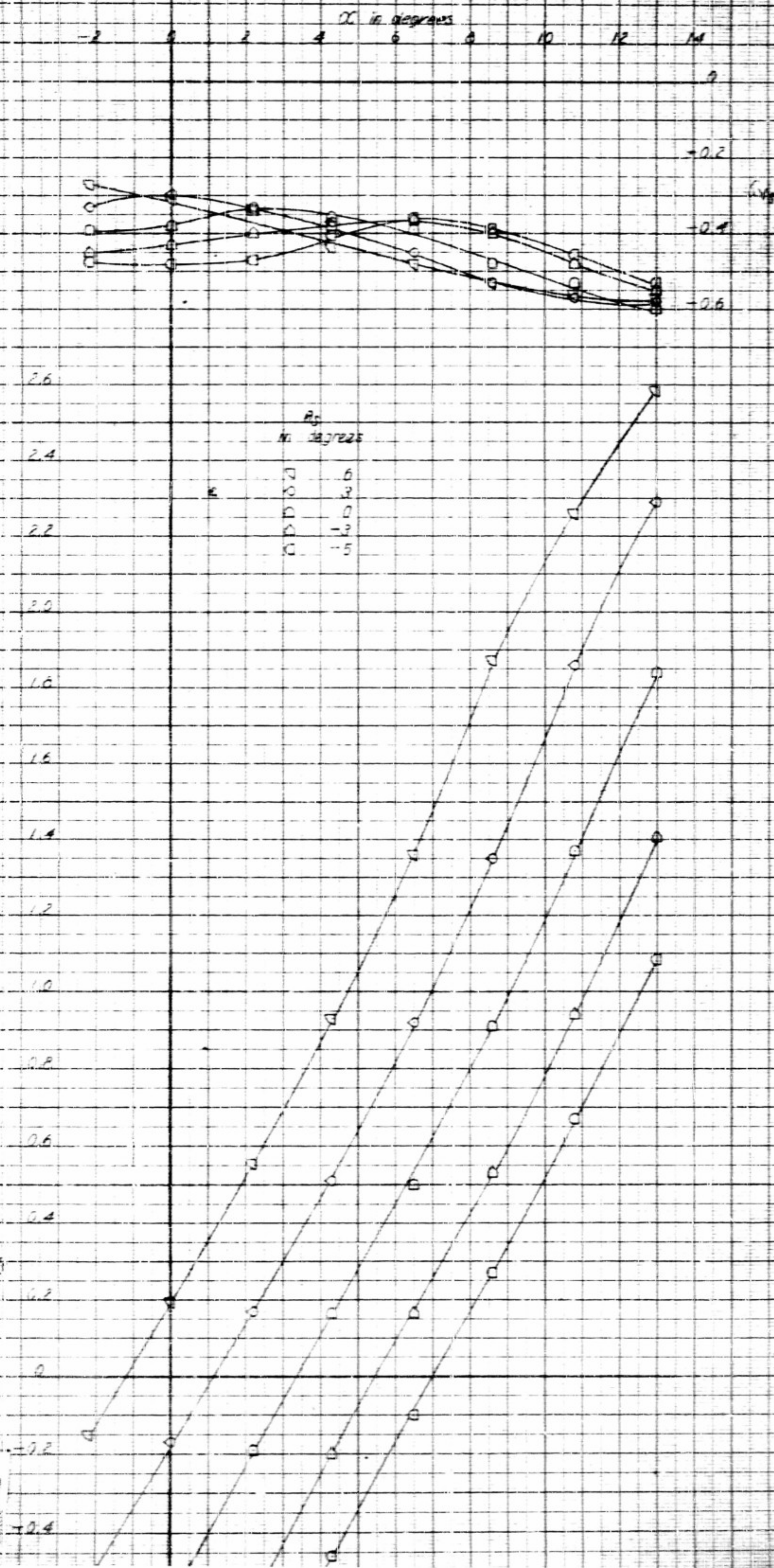

CONFIDENTIAL

[redacted]

CONFIDENTIAL

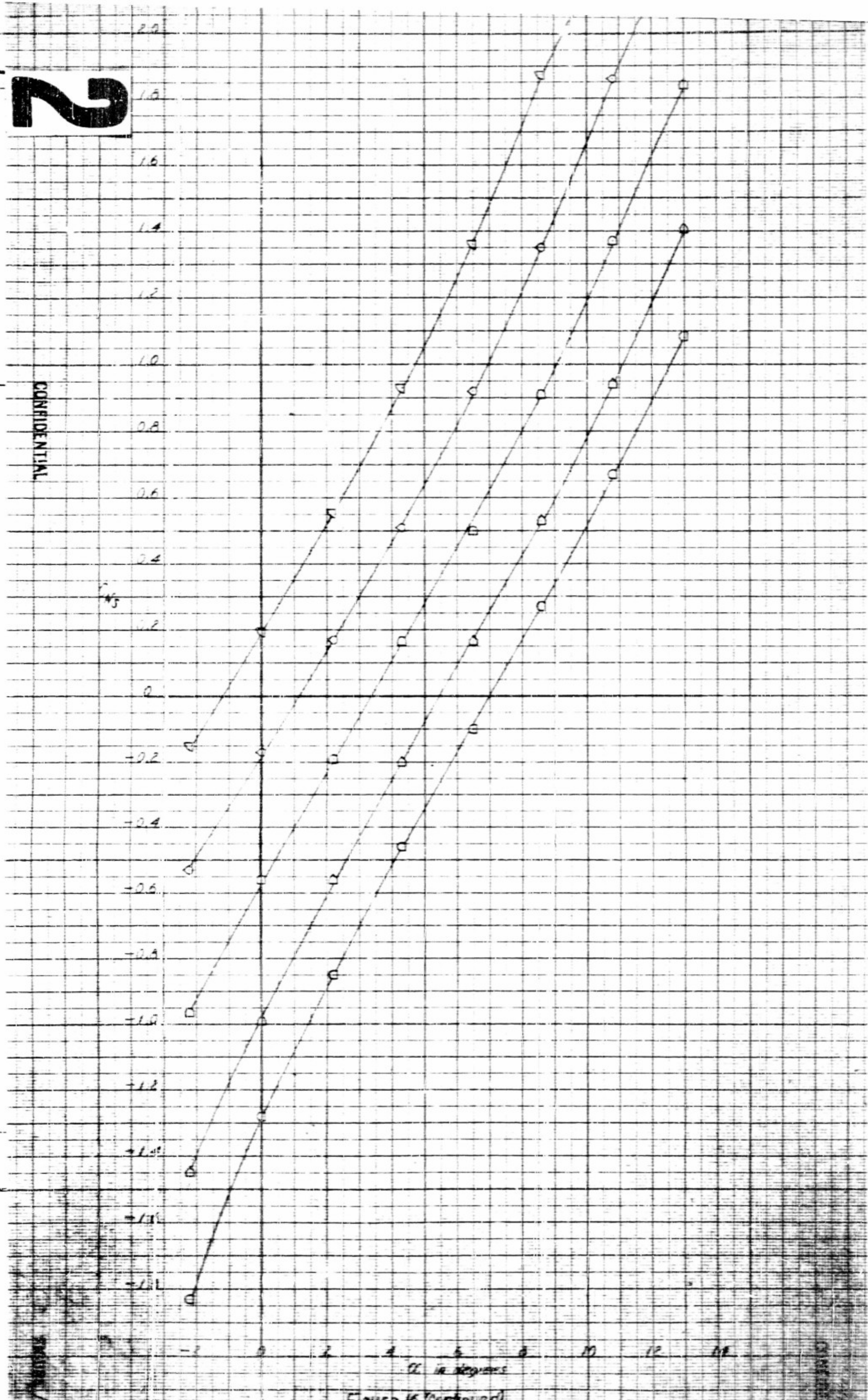

Figure 16 (Continued)

(l) $x = 0$ Inch, $y = 11.36$ Inches, $\delta_f = 0°$, $\psi = 0°$, Power On

CONFIDENTIAL

CONFIDENTIAL

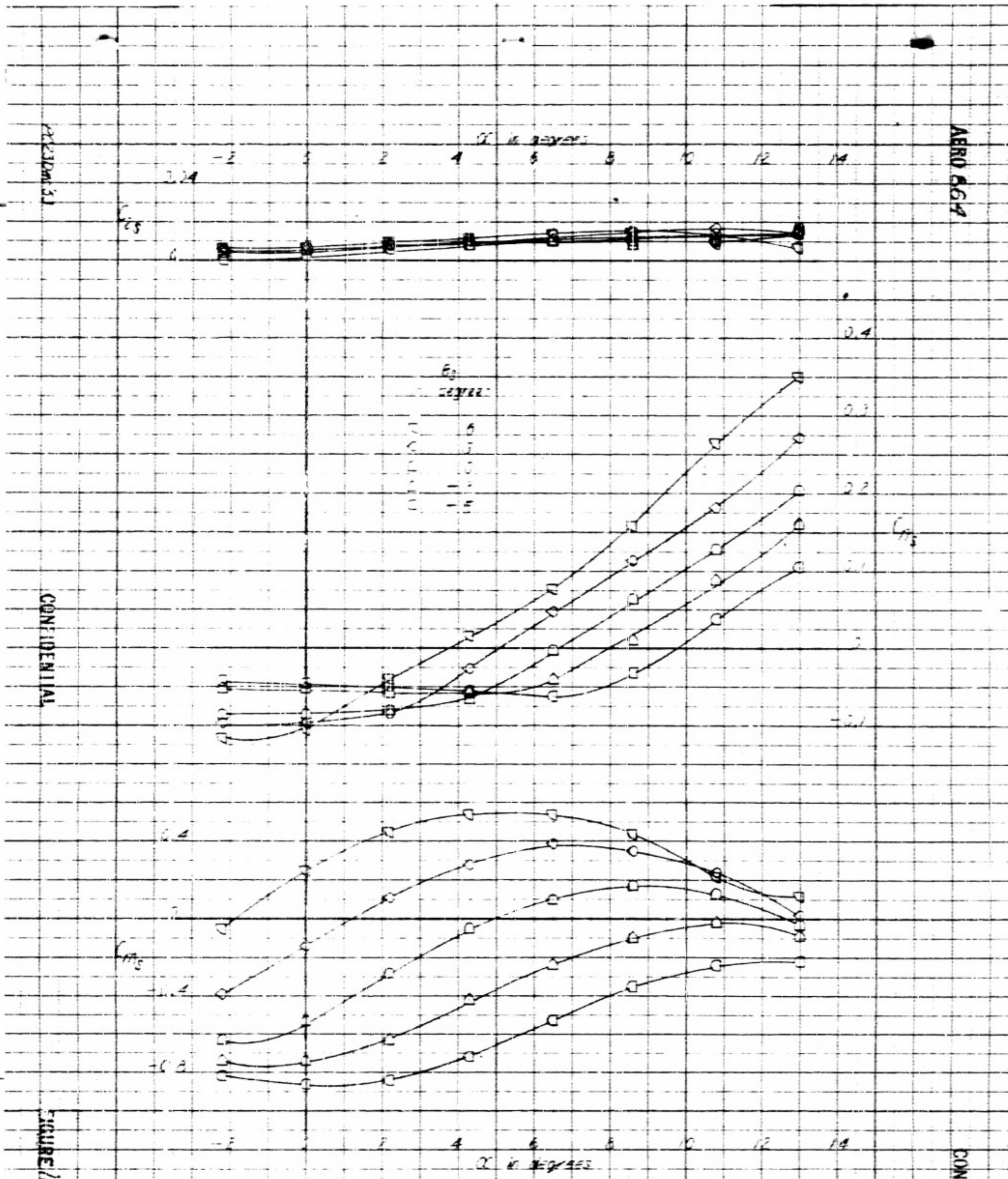

Figure 16 (Continued)

(d) Concluded

FIGURE 16(d) (concl)

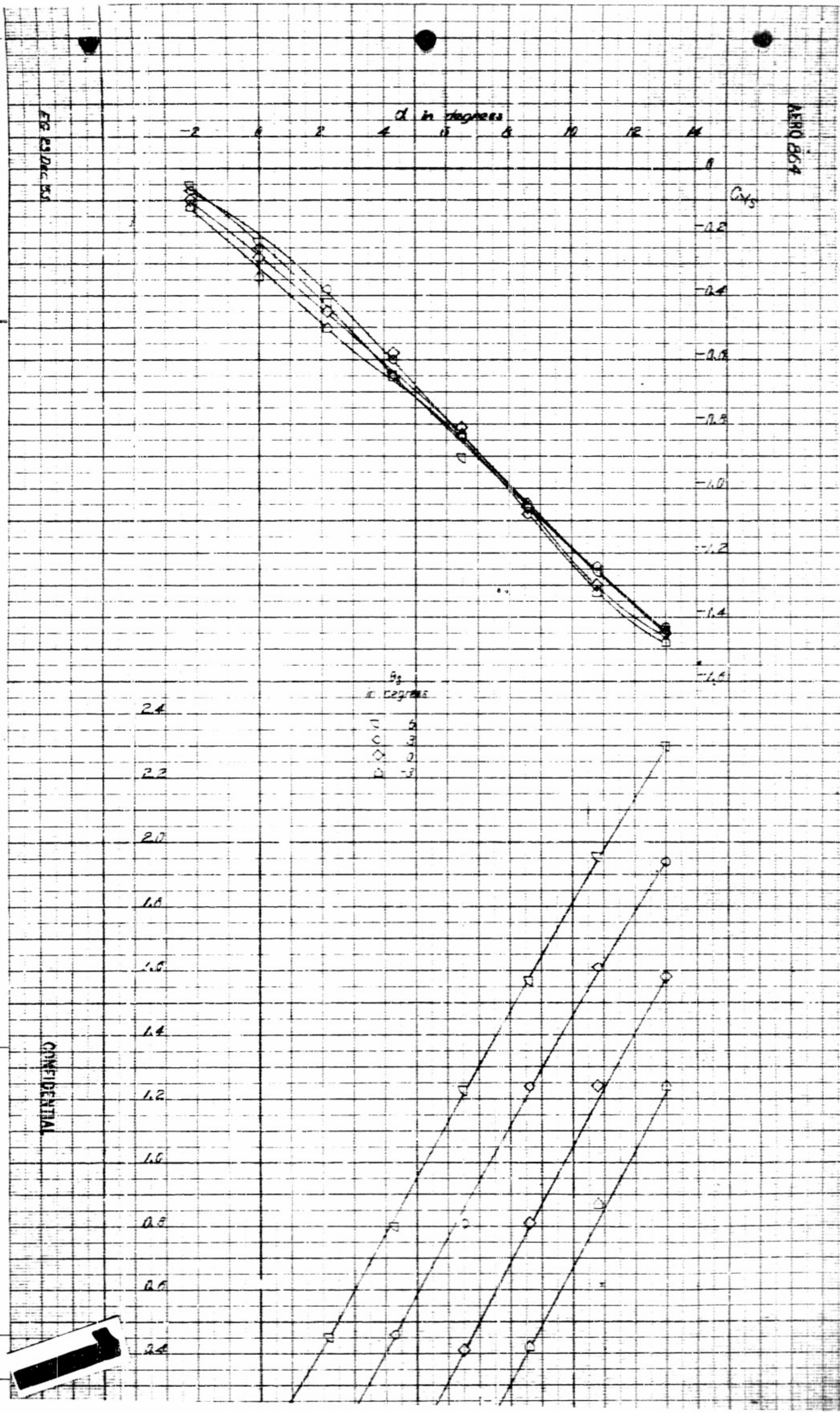
AERO 864
CONFIDENTIAL
α in degrees
-2
0
2
4
6
8
10
12
14
C_{Y_S}
-0.2
-0.4
-0.6
-0.8
-1.0
-1.2
-1.4
-1.6
θ_s in degrees
5
3
0
-3
2.4
2.2
2.0
1.8
1.6
1.4
1.2
1.0
0.8
0.6
0.4

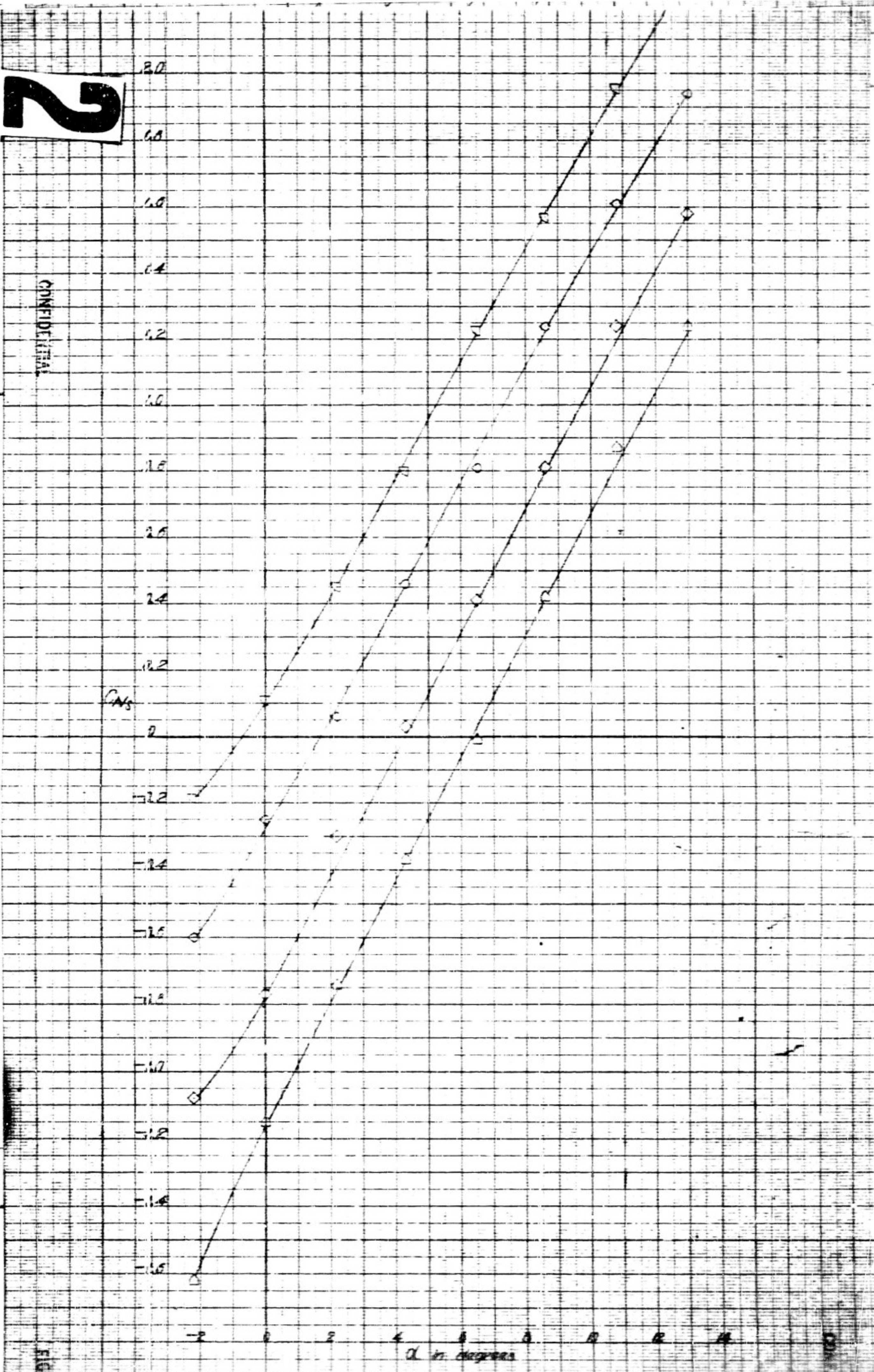

Figure 16.(Continued)

(e) $z = 1.02$ Inches, $x = 6.12$ Inches, $\psi_S = 0$, $\theta = 0$, Pylon On

CONFIDENTIAL

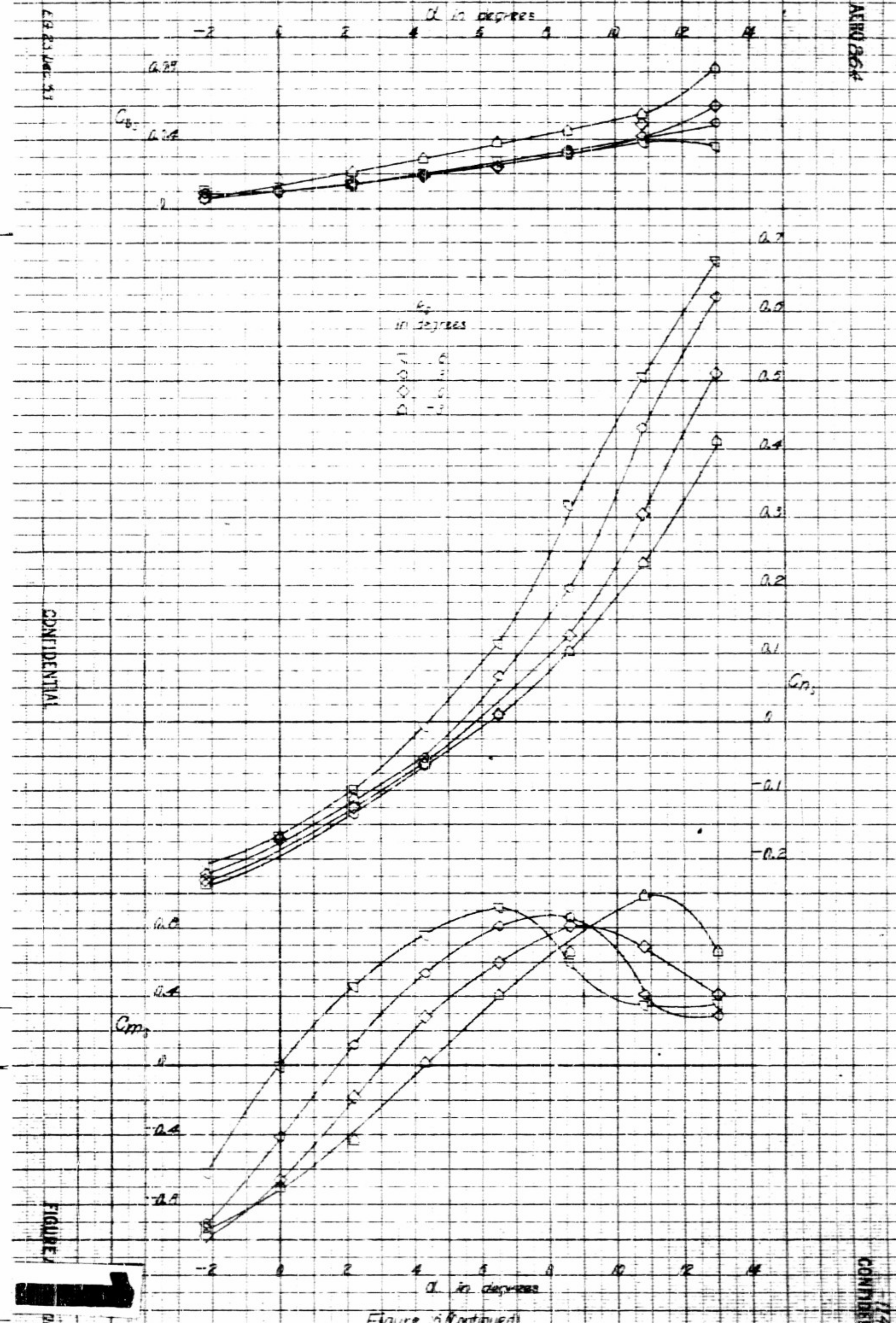

Figure 5 (Continued)

(e) Concluded

FIGURE [redacted]

AERO 5644

CONFIDENTIAL

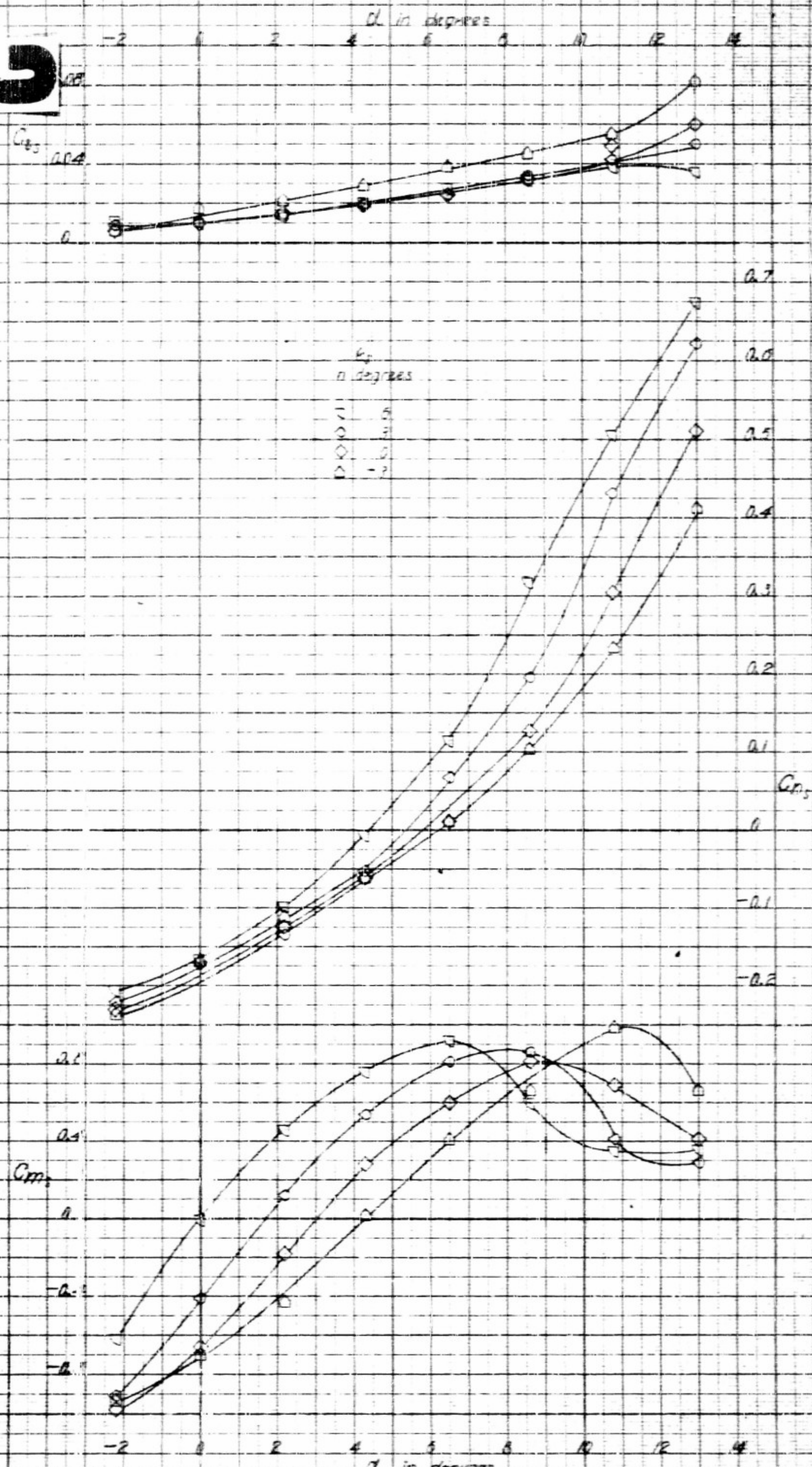

Figure 16 (Continued)

(e) Concluded

FIGURE 16e (concl.)

CONFIDENTIAL

E9 21 Dec 53

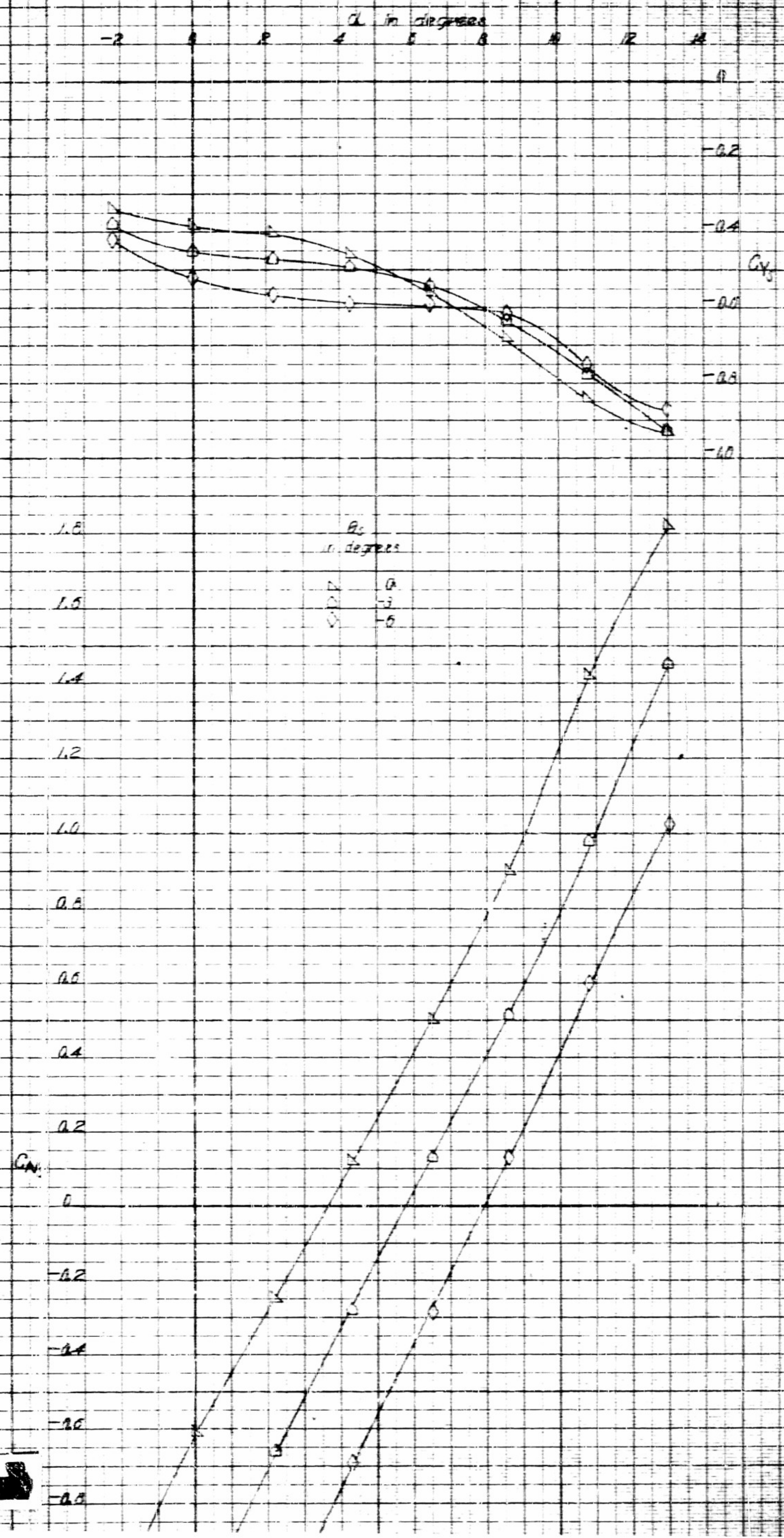

CONFIDENTIAL

AERO 864

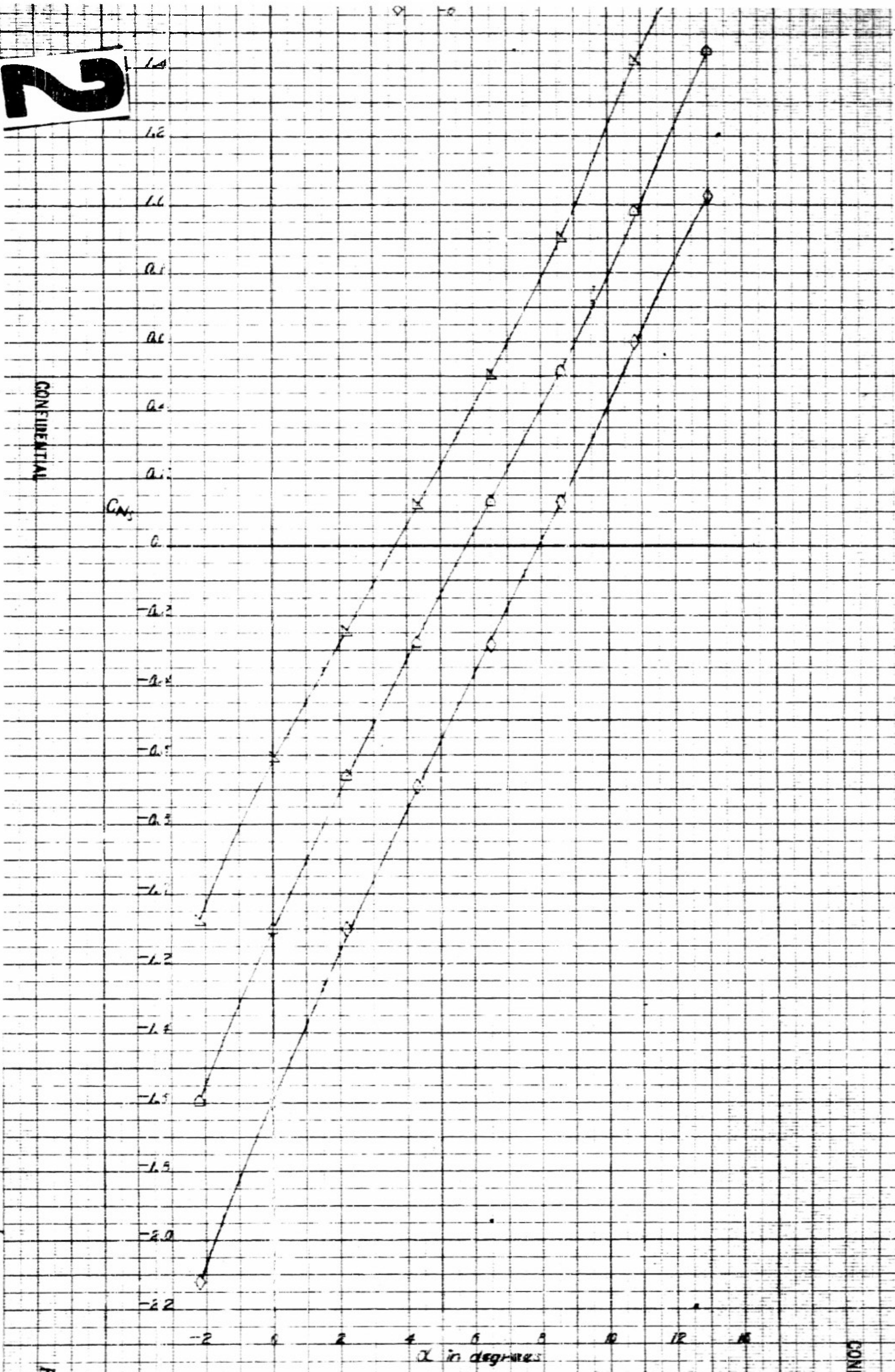

Figure 16 (Continued)

(f) $z = 1.02$ Inches, $x = 13.86$ Inches, $\Psi_s = 0°$, $\Psi = 0°$, Pylon On

FIGURE 16f

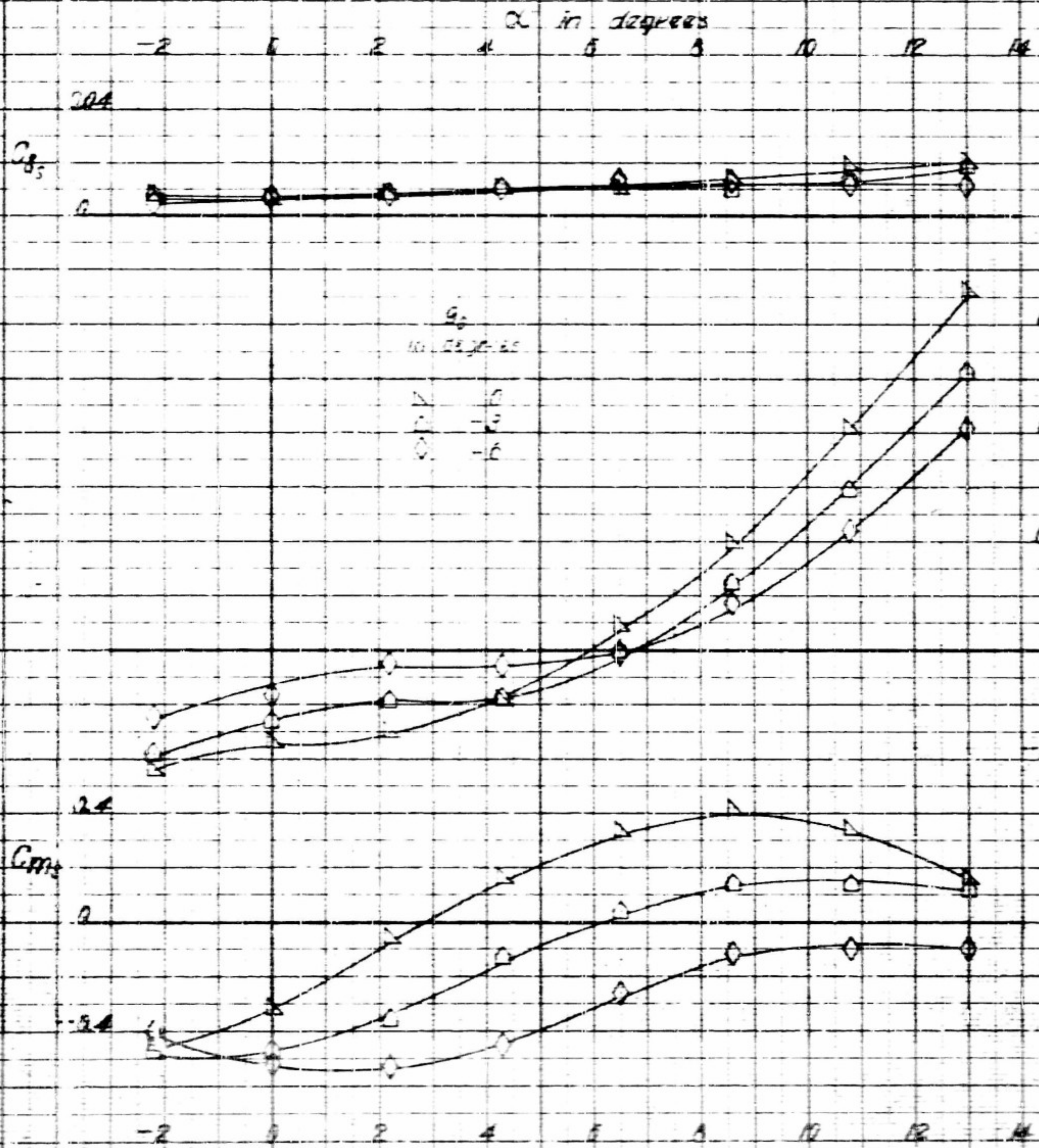

Figure 16 (Continued)

(f) Concluded

CONFIDENTIAL

FIGURE 16(f) Concl.

CONFIDENTIAL

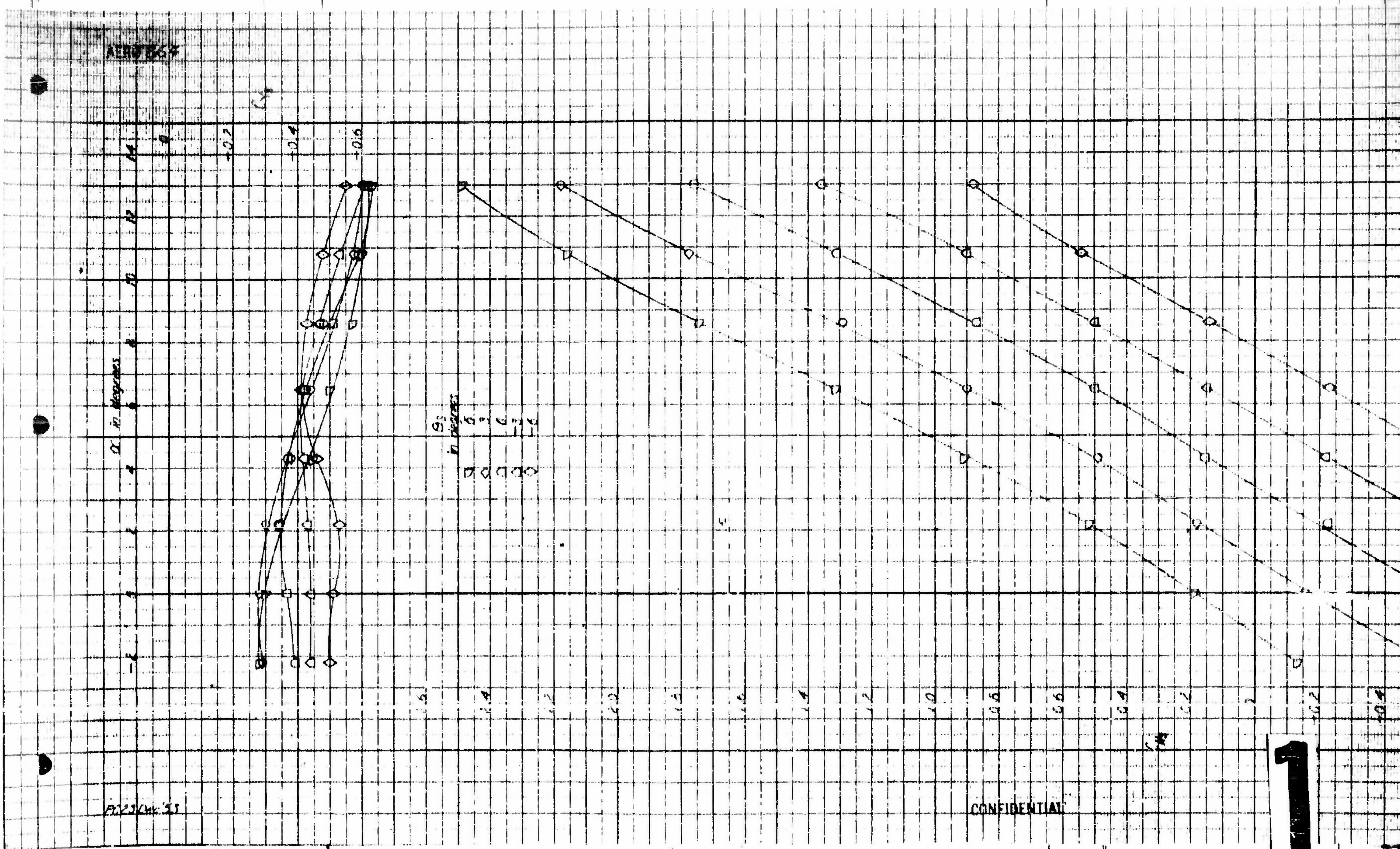
α in degrees
C_Y
in degrees
CONFIDENTIAL

CONFIDENTIAL

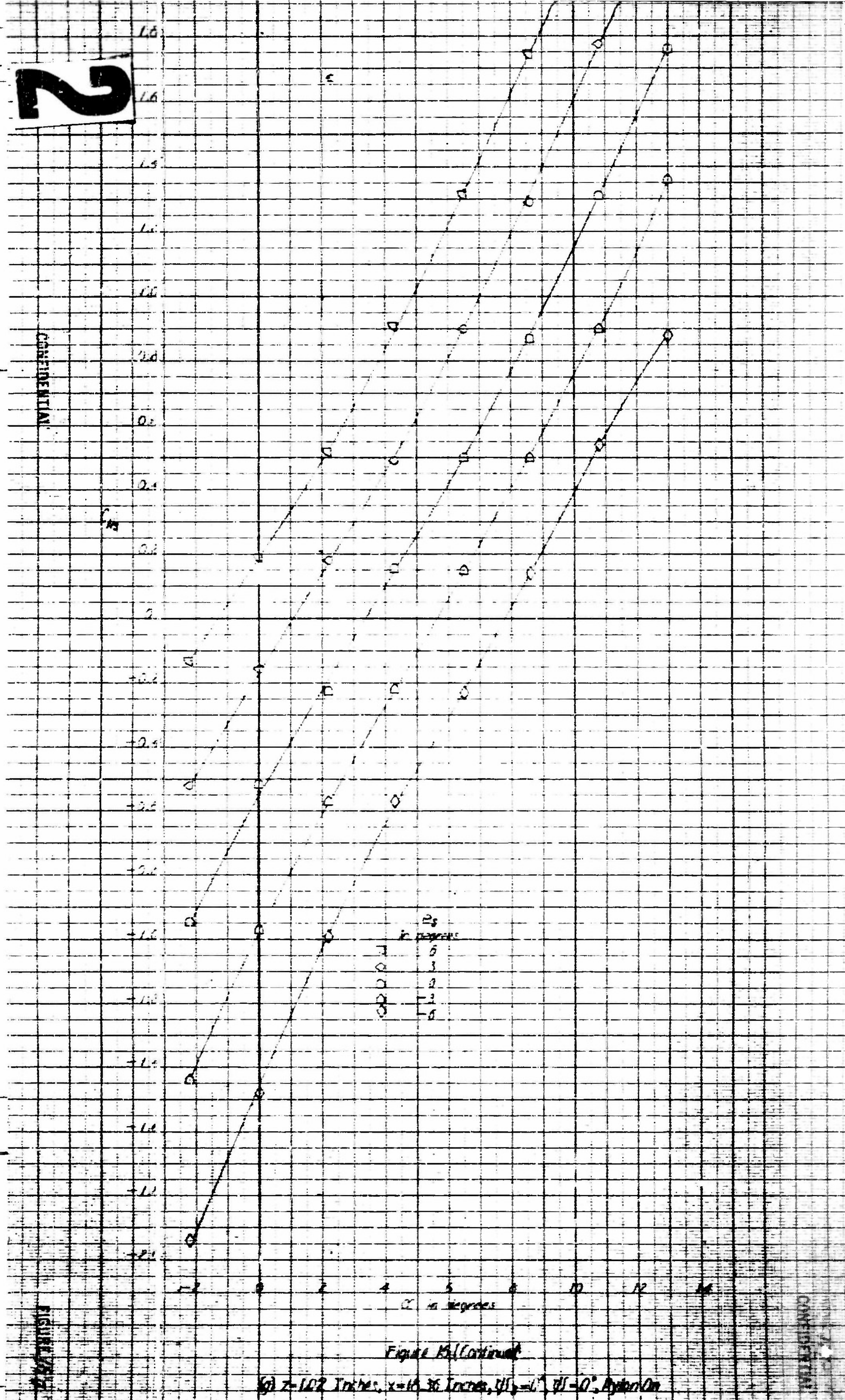

Figure 15 (Continued)

(g) z=1.02 Inches, x=18.36 Inches, ψ_s=0°, ψ=0°, Pylon On

FIGURE 15g

CONFIDENTIAL

CONFIDENTIAL

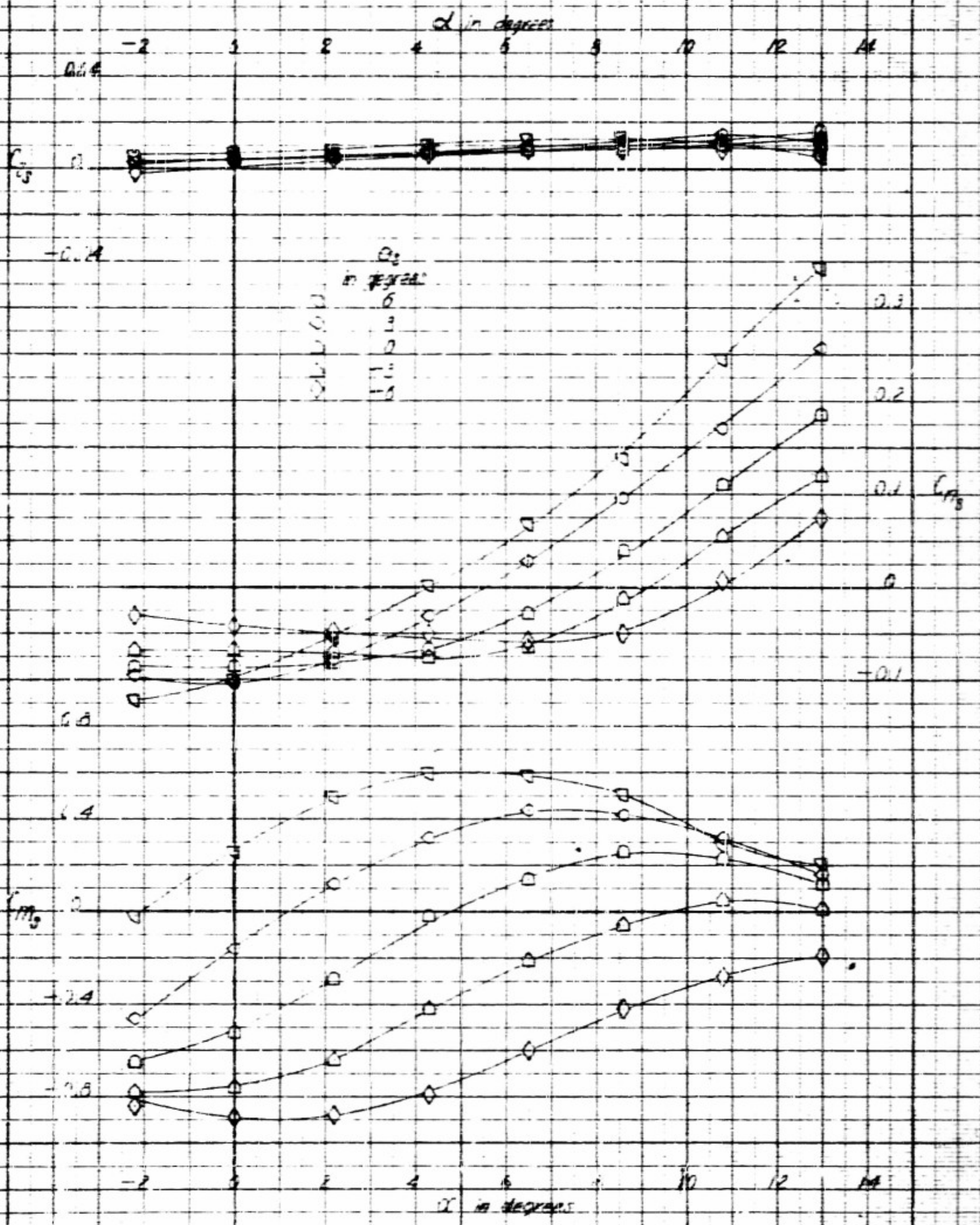

Figure 16 (Continued)

(g) Concluded

FIGURE 16 g (concl)

CONFIDENTIAL

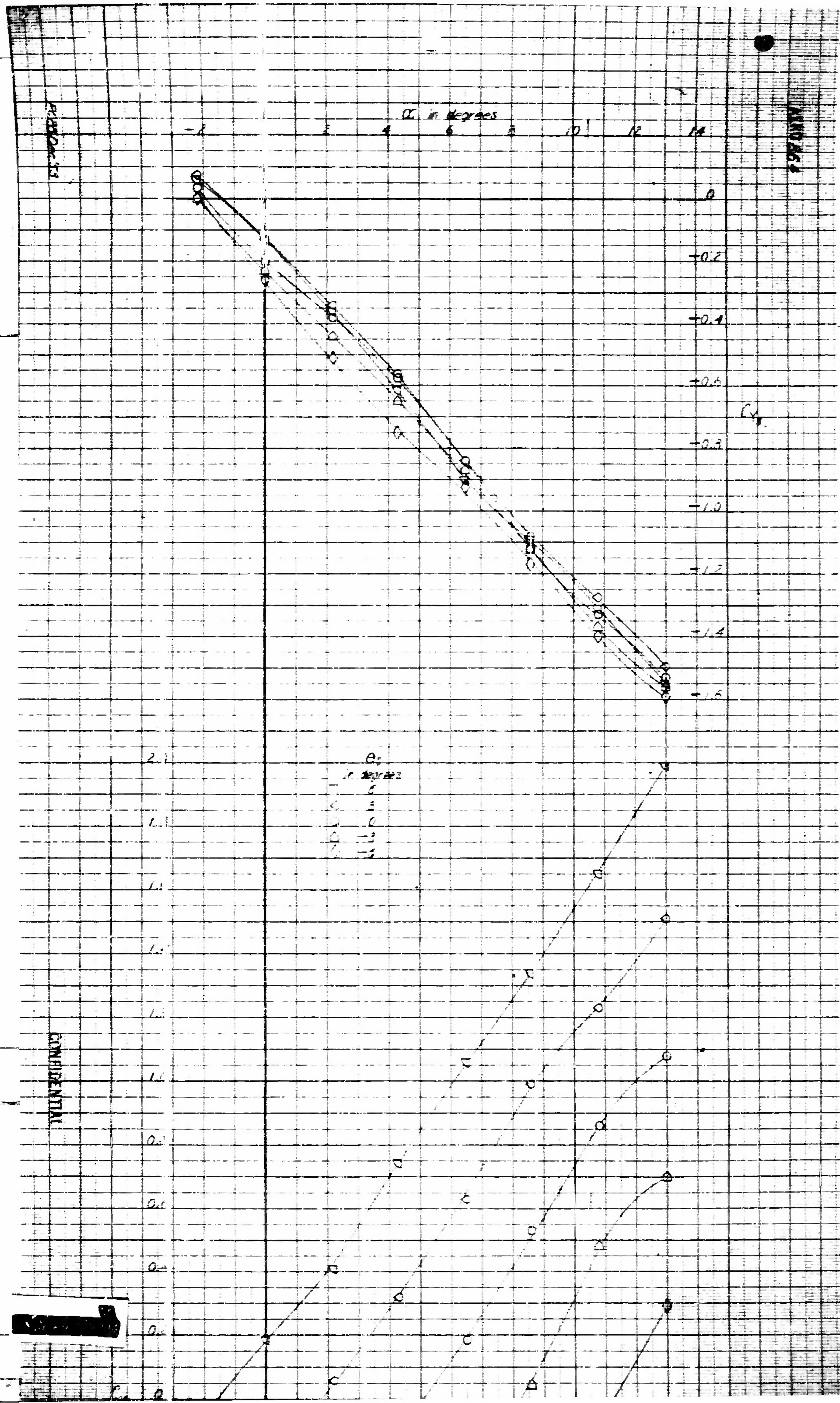

CONFIDENTIAL

[redacted]

CONFIDENTIAL

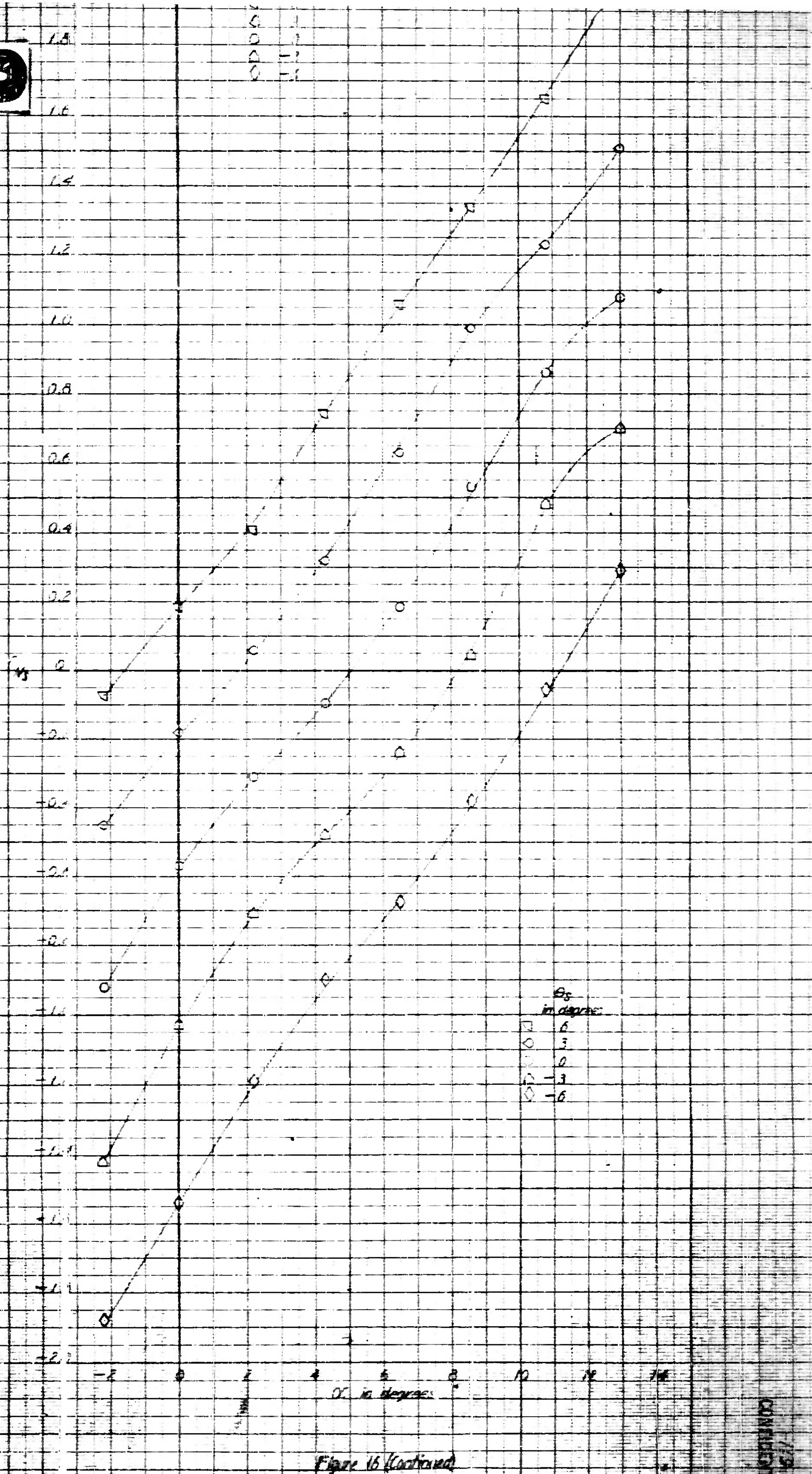

Figure 16 (Continued)

(h) z = 2.04 Inches, x = 0 Inch, ψ_S = 0°, ψ = 0°, Pylon On

FIGURE 16.h

CONFIDENTIAL

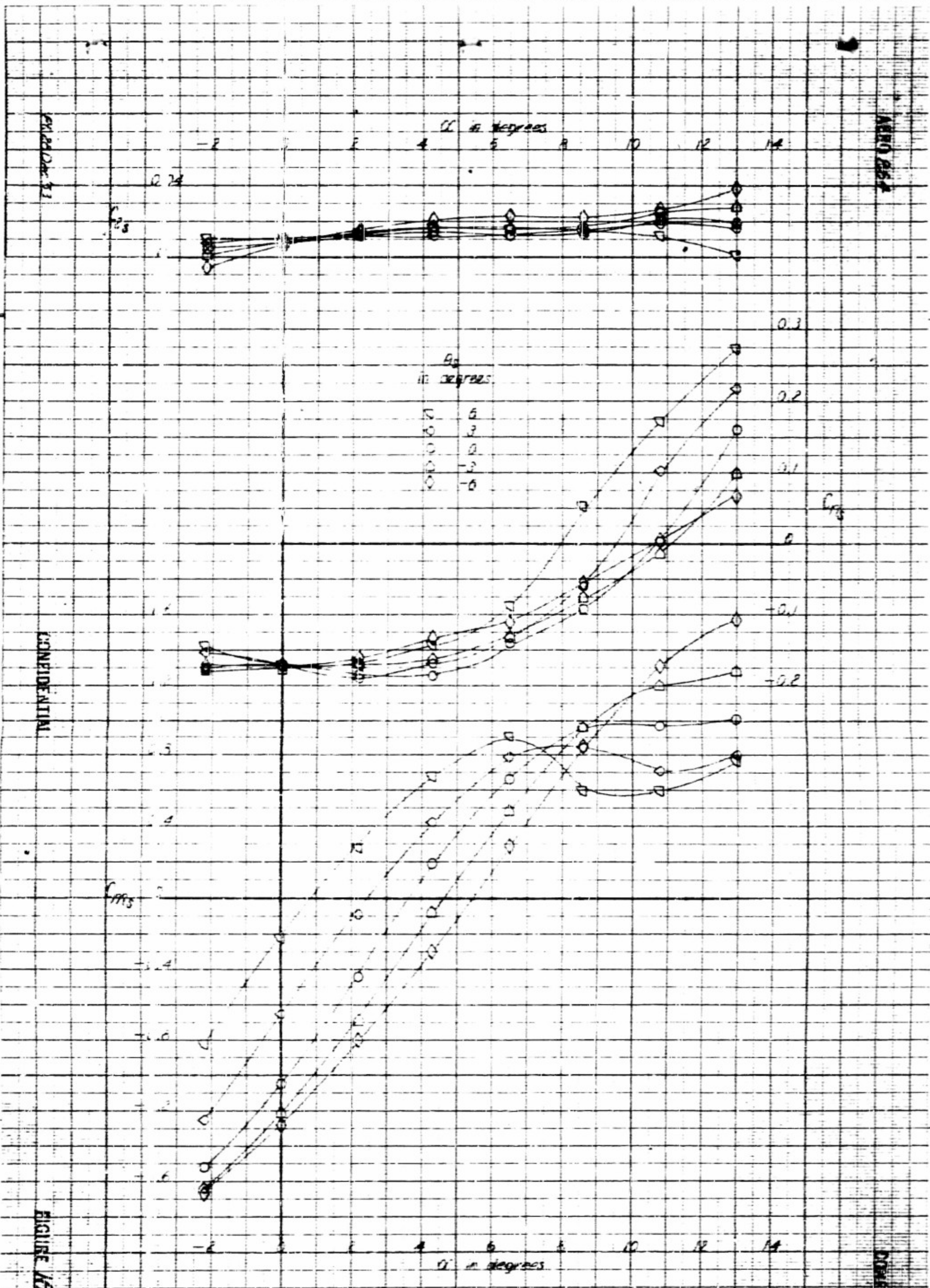

Figure 16 (Continued)

(h) Concluded

CONFIDENTIAL

FIGURE 16(h) (cont)

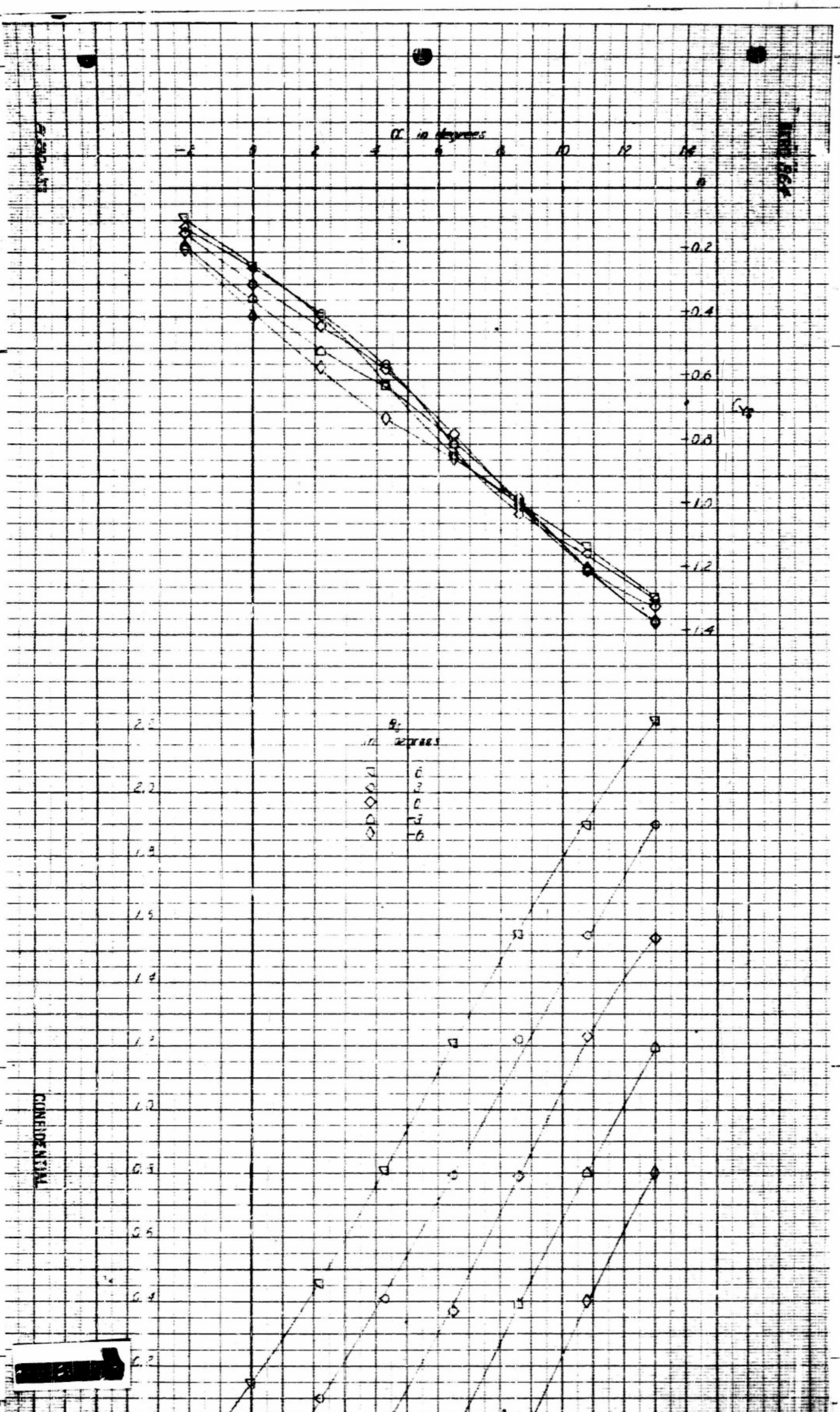
α in degrees
C_{Y_β}
δ_t in degrees
6
3
0
-3
-6
CONFIDENTIAL

CONFIDENTIAL

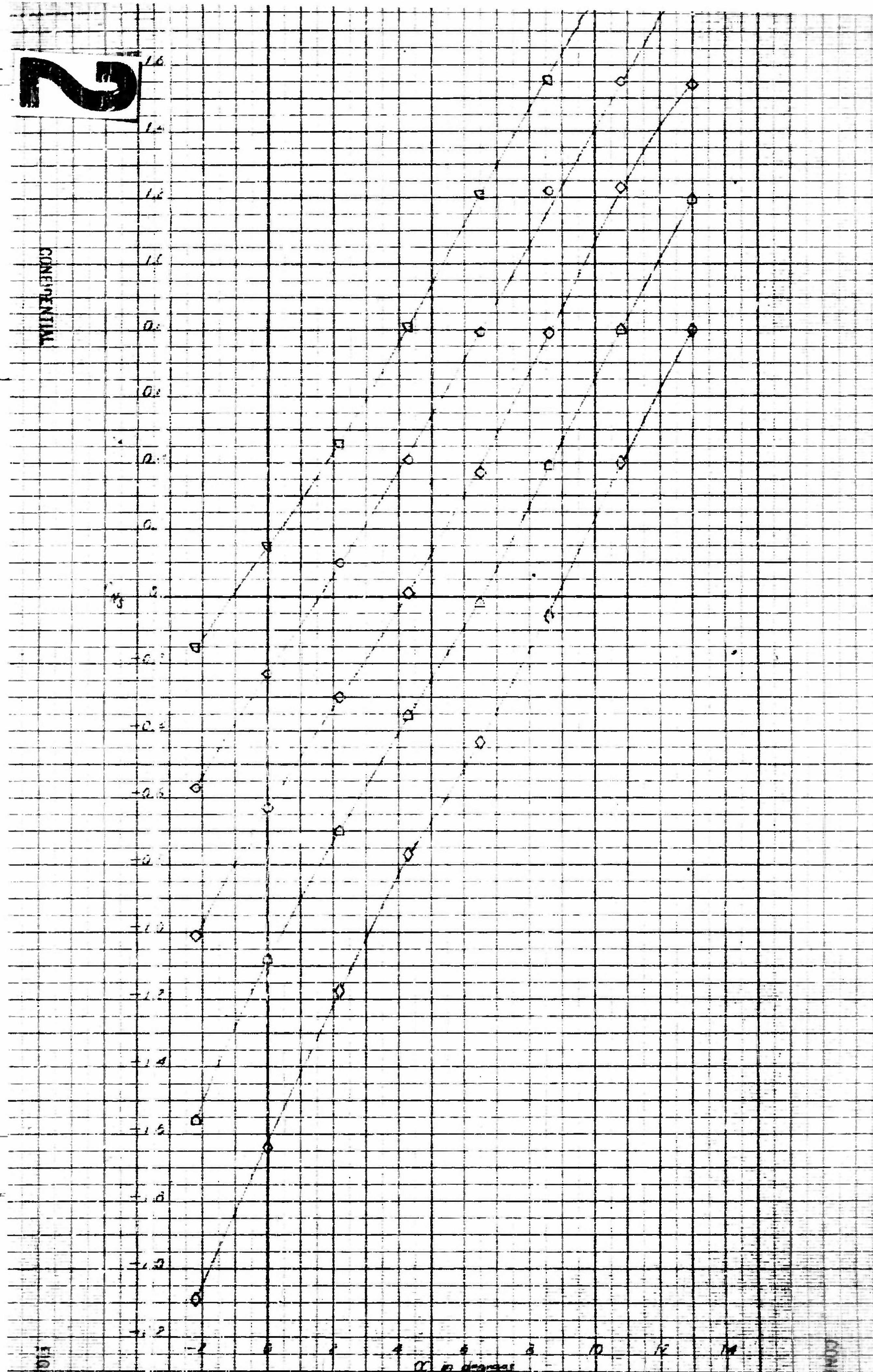

Figure 16 (Continued)

(i) z = 2.04 Inches, y = 6.12 Inches, $\psi_j = 0$, $\psi = 0$, Pylon On

FIGURE 127

CONFIDENTIAL

CONFIDENTIAL

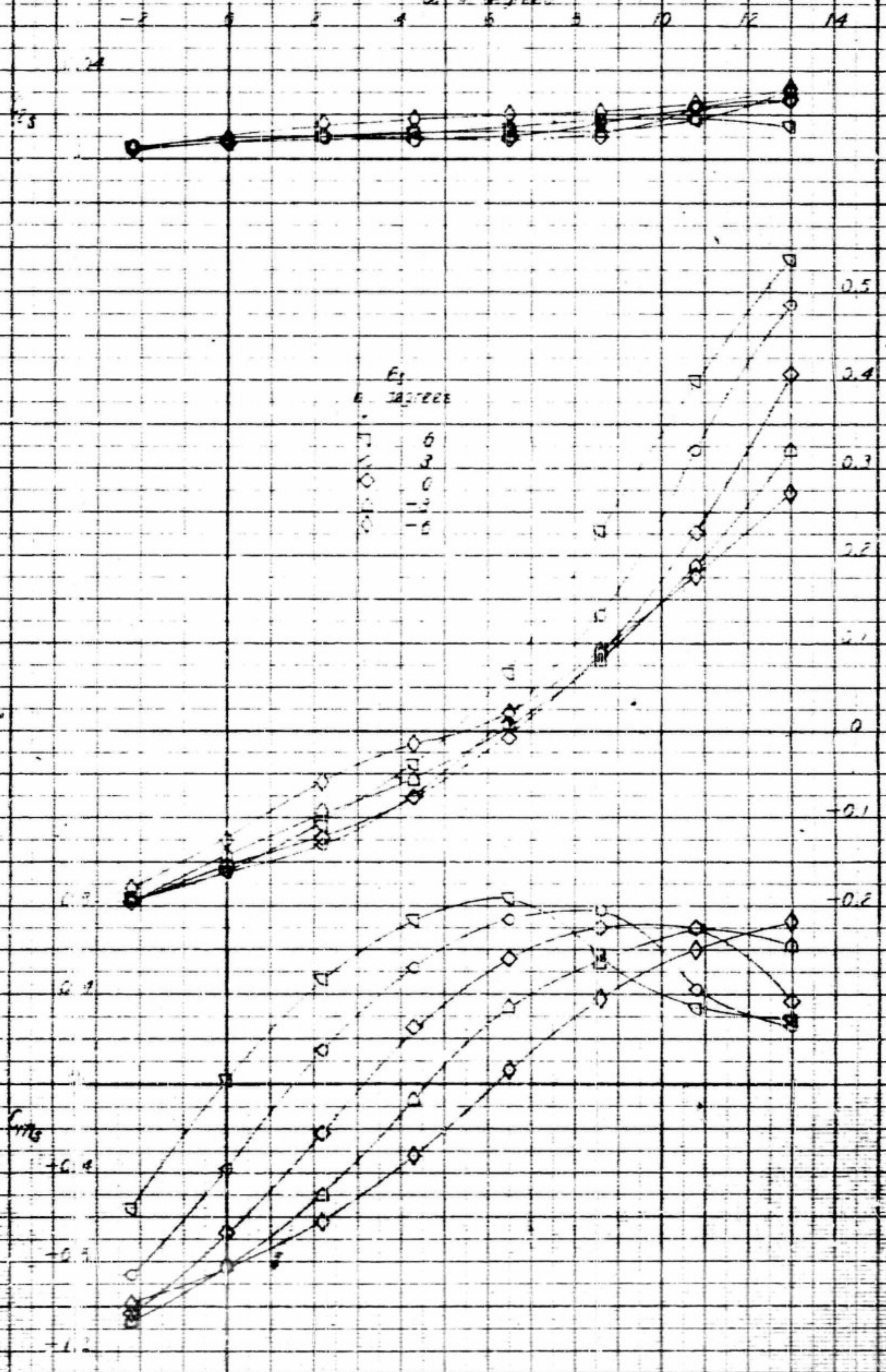

Figure 16 (Continued)

(i) Concluded

FIGURE 16 (cont'd)

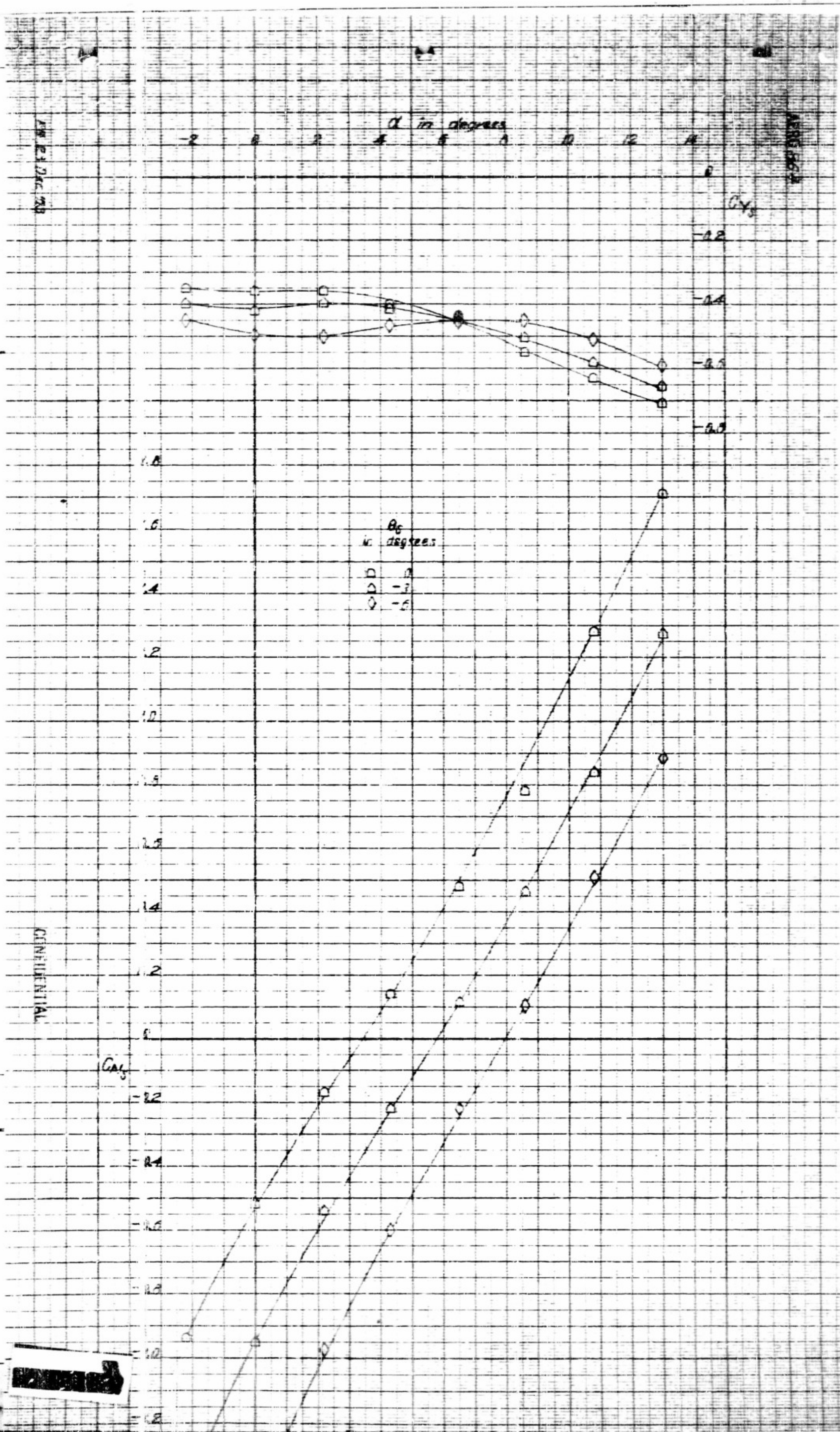
α in degrees
C_{Y_δ}
C_{n_δ}
θ_δ in degrees
0
-3
-6
CONFIDENTIAL

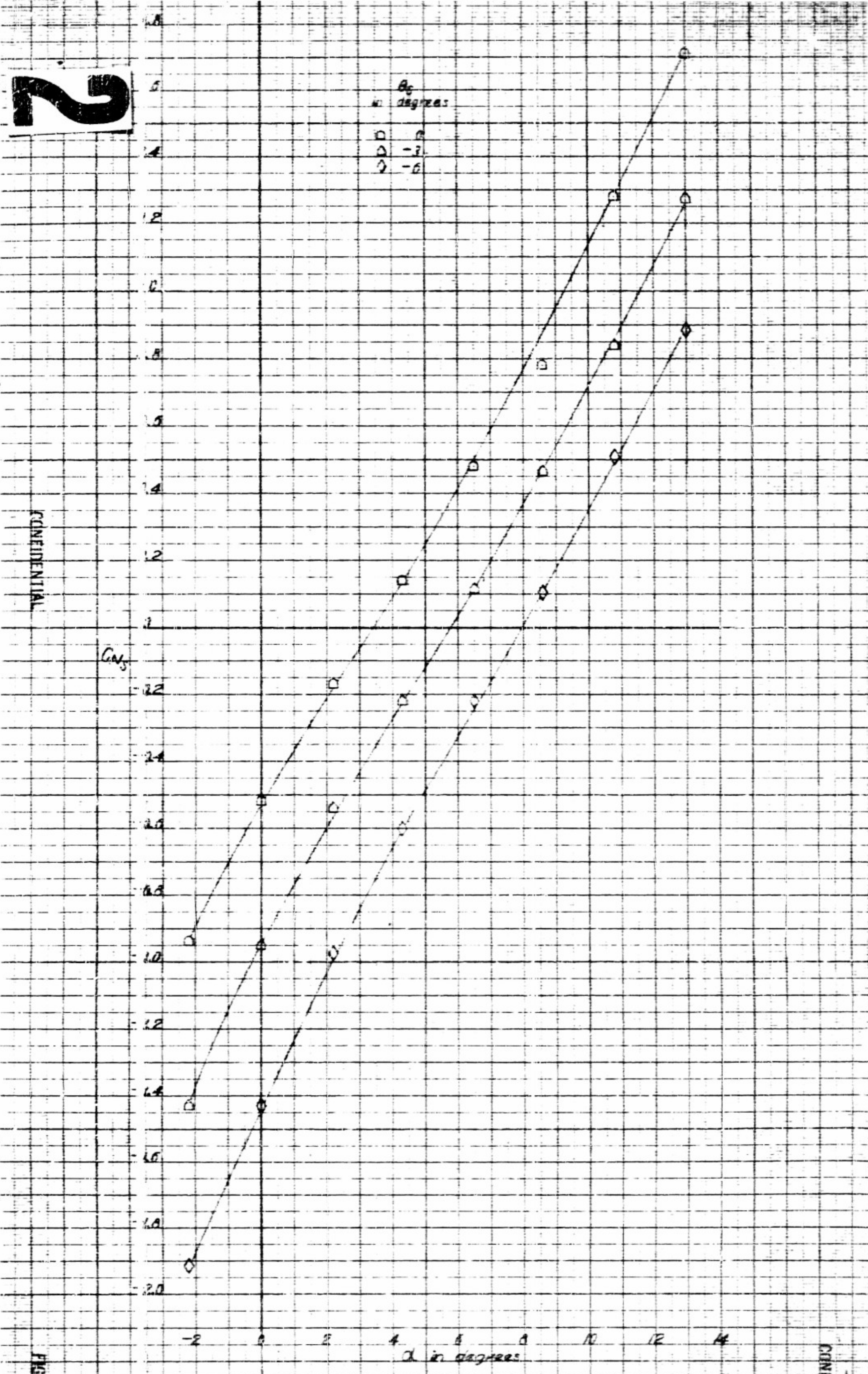

Figure 16 (Continued)

(j) $z = 2.14$ Inches, $x = 19.36$ Inches, $\psi = 0$, Pylon On

CONFIDENTIAL

FIGURE 16j

CONFIDENTIAL

CONFIDENTIAL

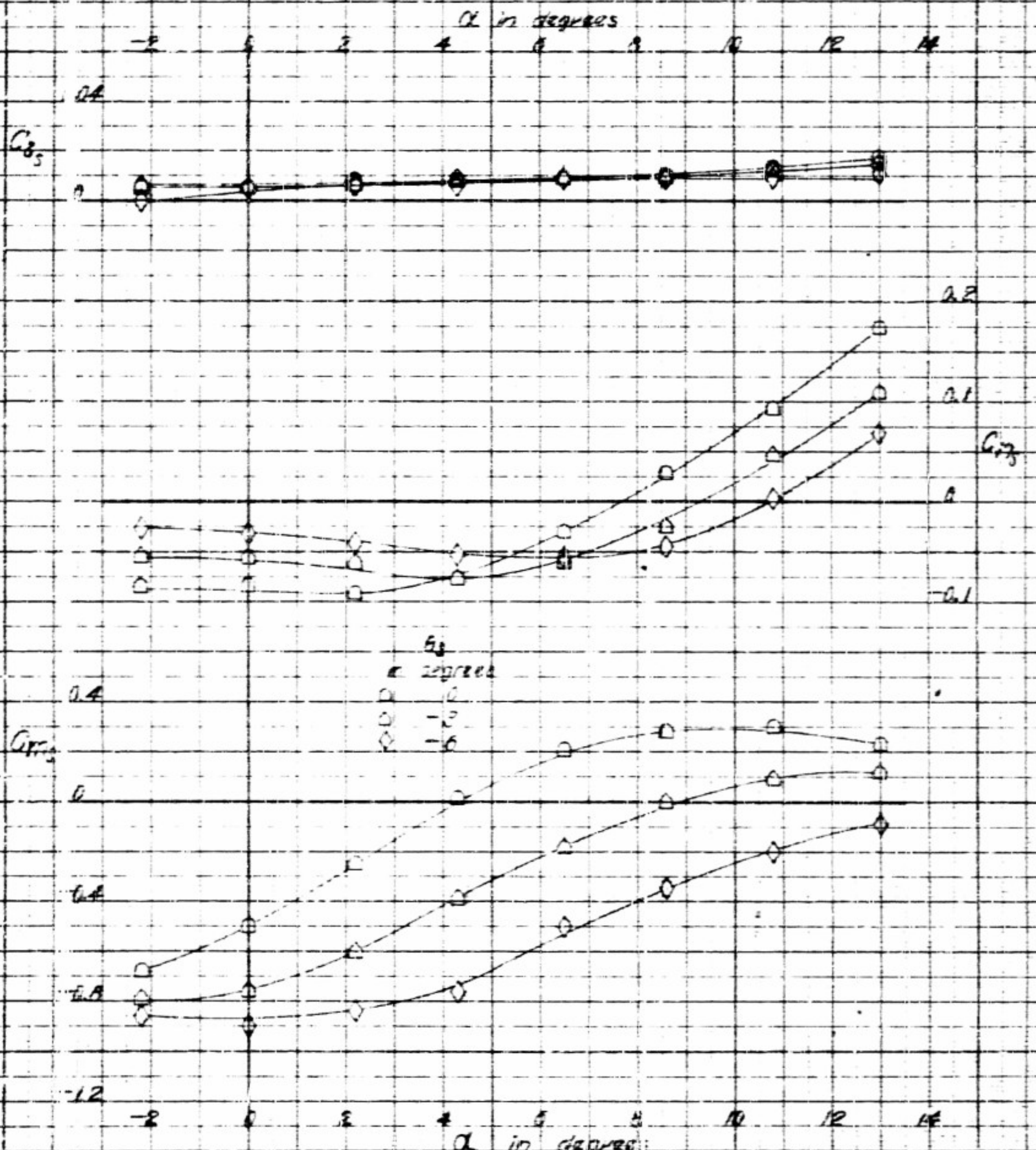

Figure 16 (Continued)
(j) Concluded

FIGURE 16(j) (Concl)

CONFIDENTIAL

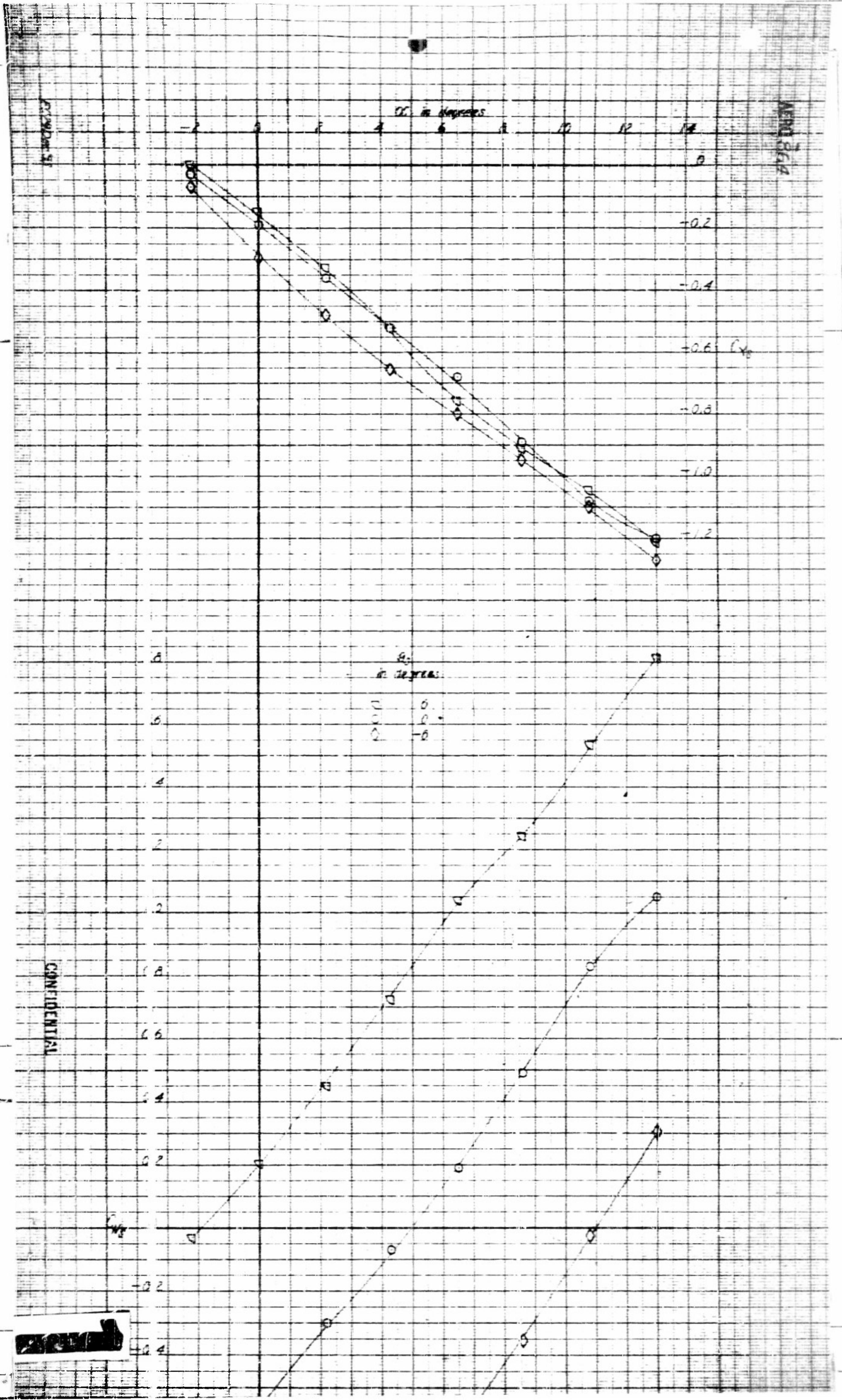

AERO 864

CONFIDENTIAL

CONFIDENTIAL

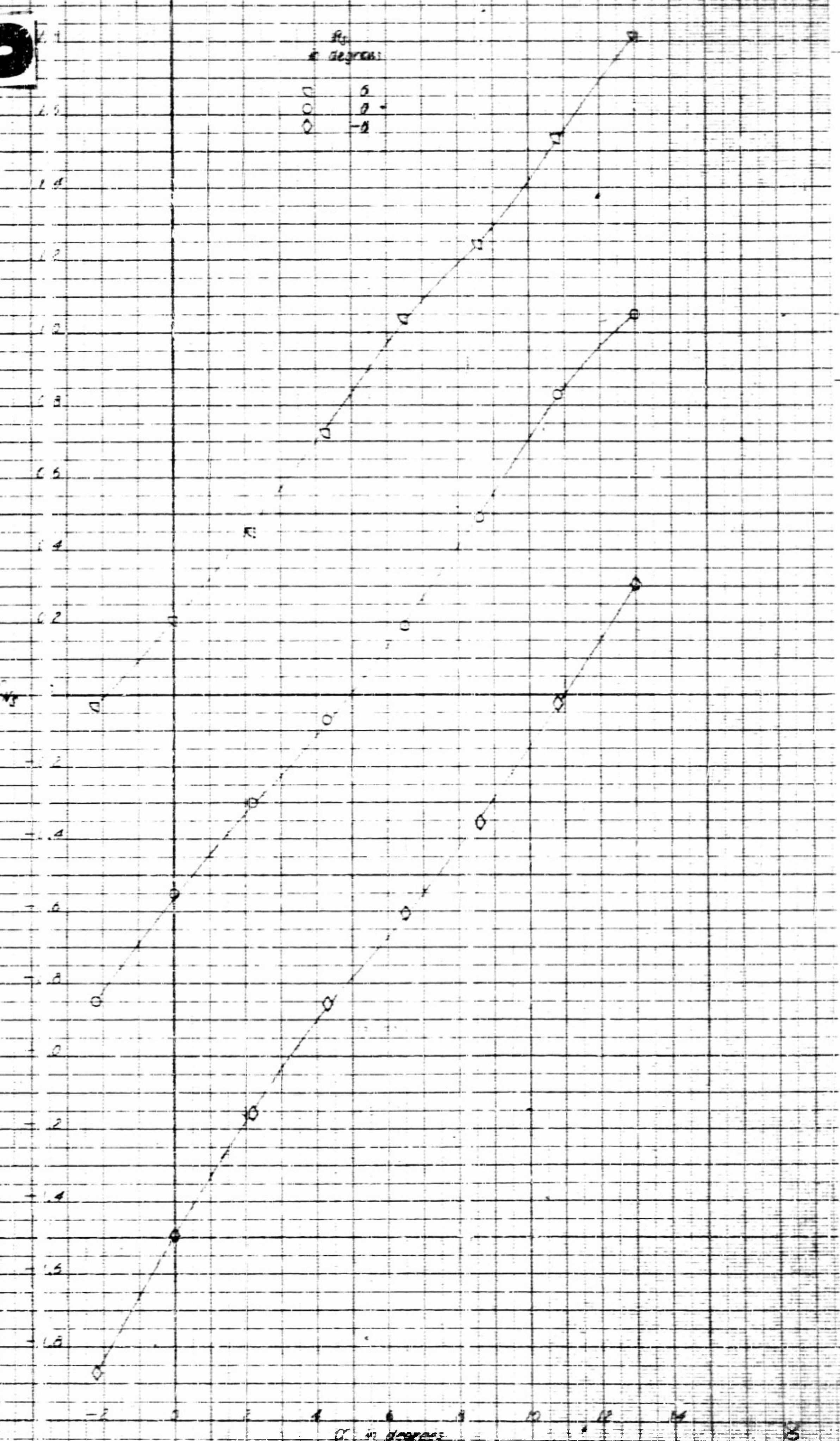

Figure [illegible] Continued

(k) z = 4.25 inches, x = 0 inch, $\psi_s = 0°$, $\psi = 0°$, Pylon On

CONFIDENTIAL

AERO 864

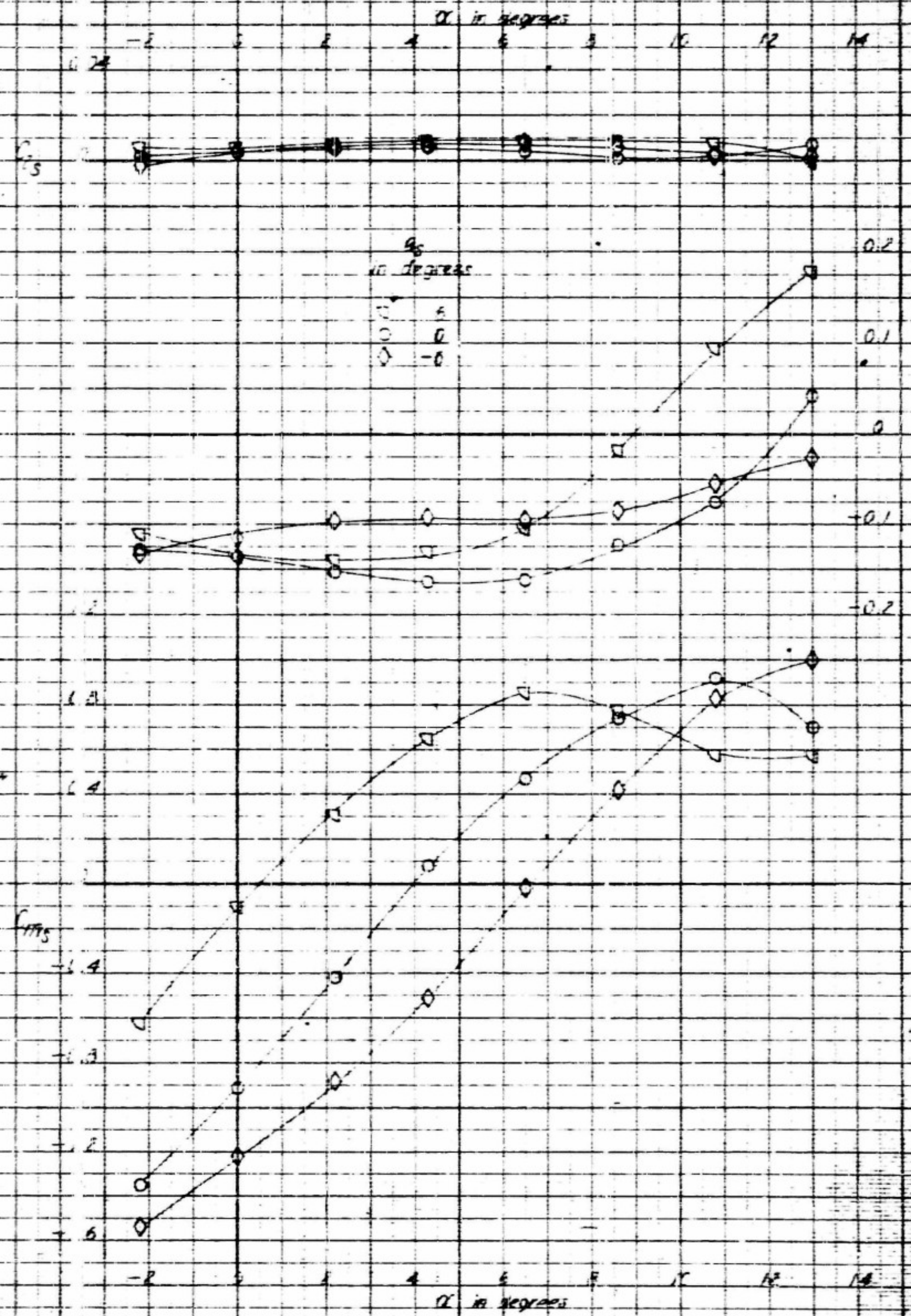

Figure 16 (Concluded)

(k) Concluded

CONFIDENTIAL

FIGURE 16K (concl.)

726

CONFIDENTIAL

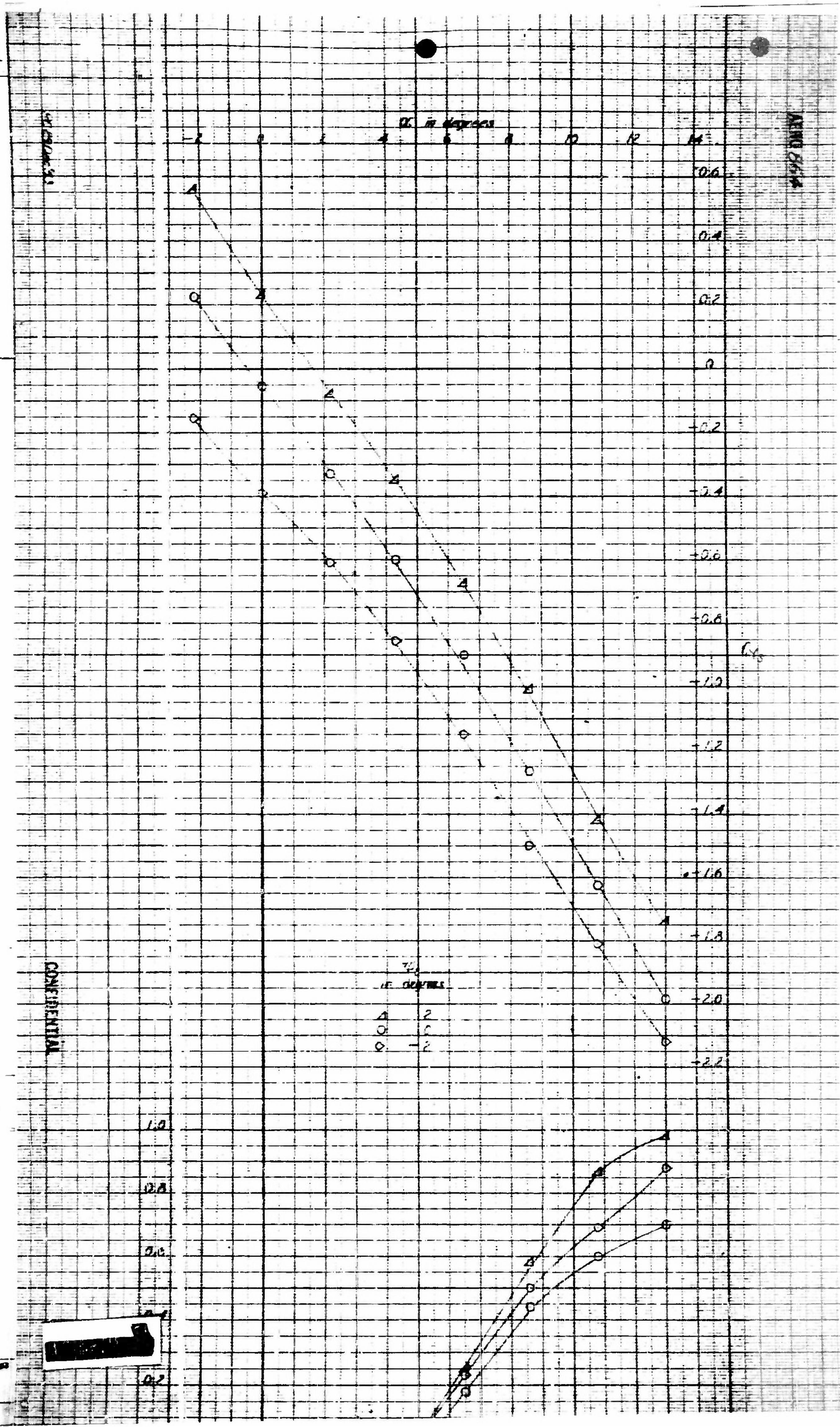

AERO 664
α in degrees
-2
0
2
4
6
8
10
12
14
0.6
0.4
0.2
0
-0.2
-0.4
-0.6
-0.8
-1.0
-1.2
-1.4
-1.6
-1.8
-2.0
-2.2
1.0
0.8
0.6
0.4
0.2
in degrees
2
0
-2
CONFIDENTIAL

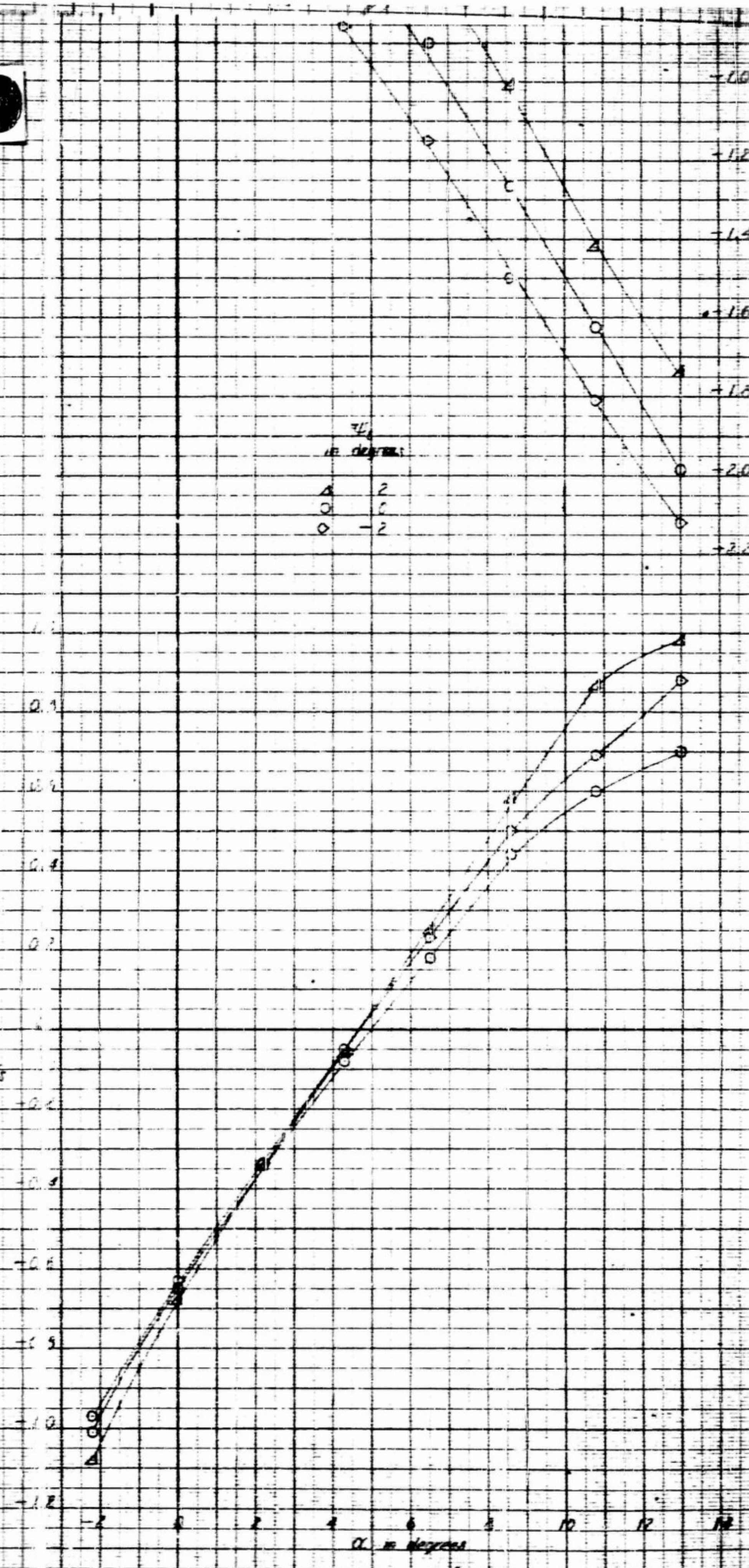

Figure 17 – Aerodynamic Characteristics of a 0.17-Scale Model XAAM-N-4 Oriole Missile Due to Missile Yaw in the Proximity of a 0.179-Scale Model F4D-1 Airplane at the Outboard Station

(a) z = 0 Inch, x = 0 Inch, $\theta_S = 0°$, $\psi = 0°$, Pylon On

CONFIDENTIAL

FIGURE 17a

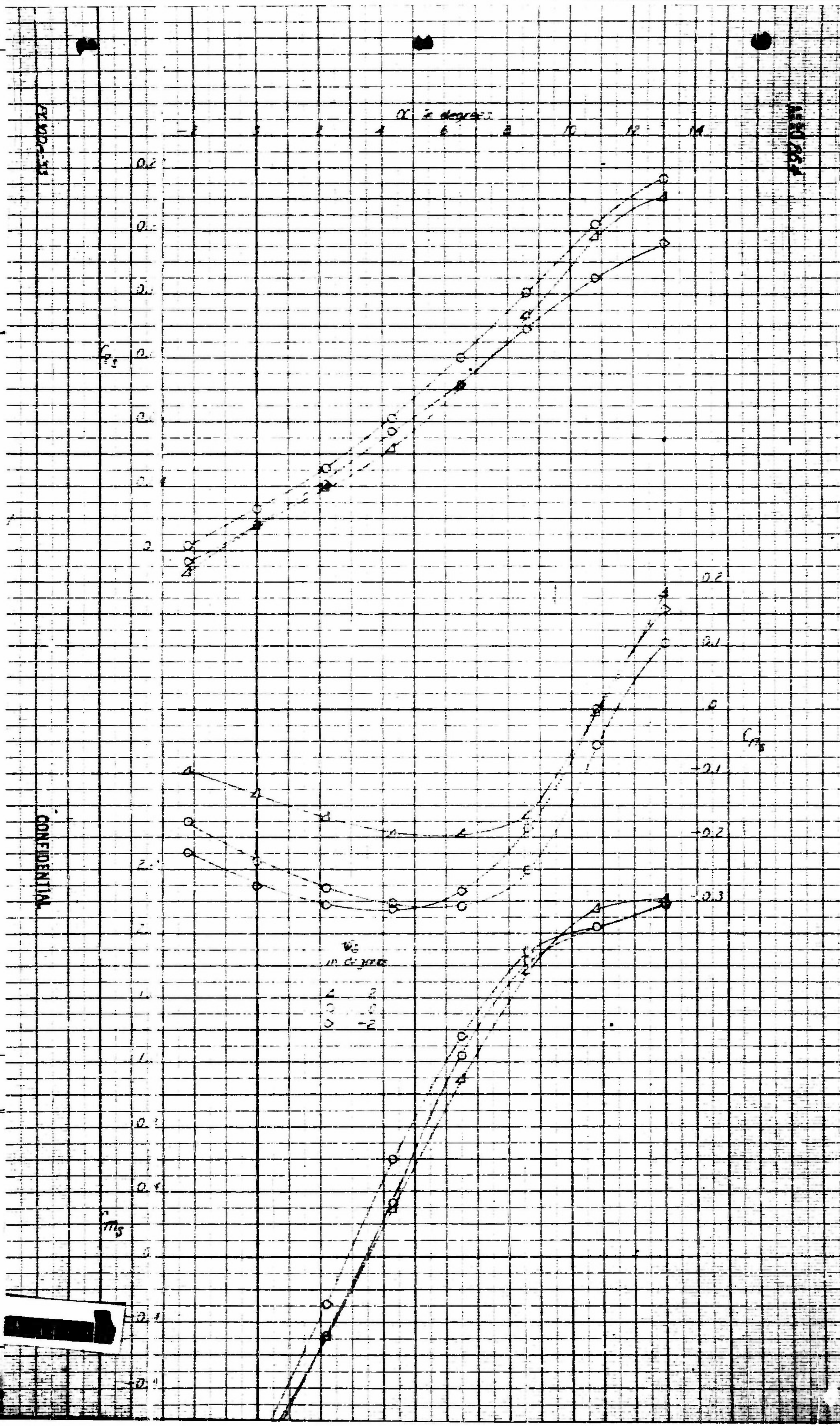

[redacted]

CONFIDENTIAL

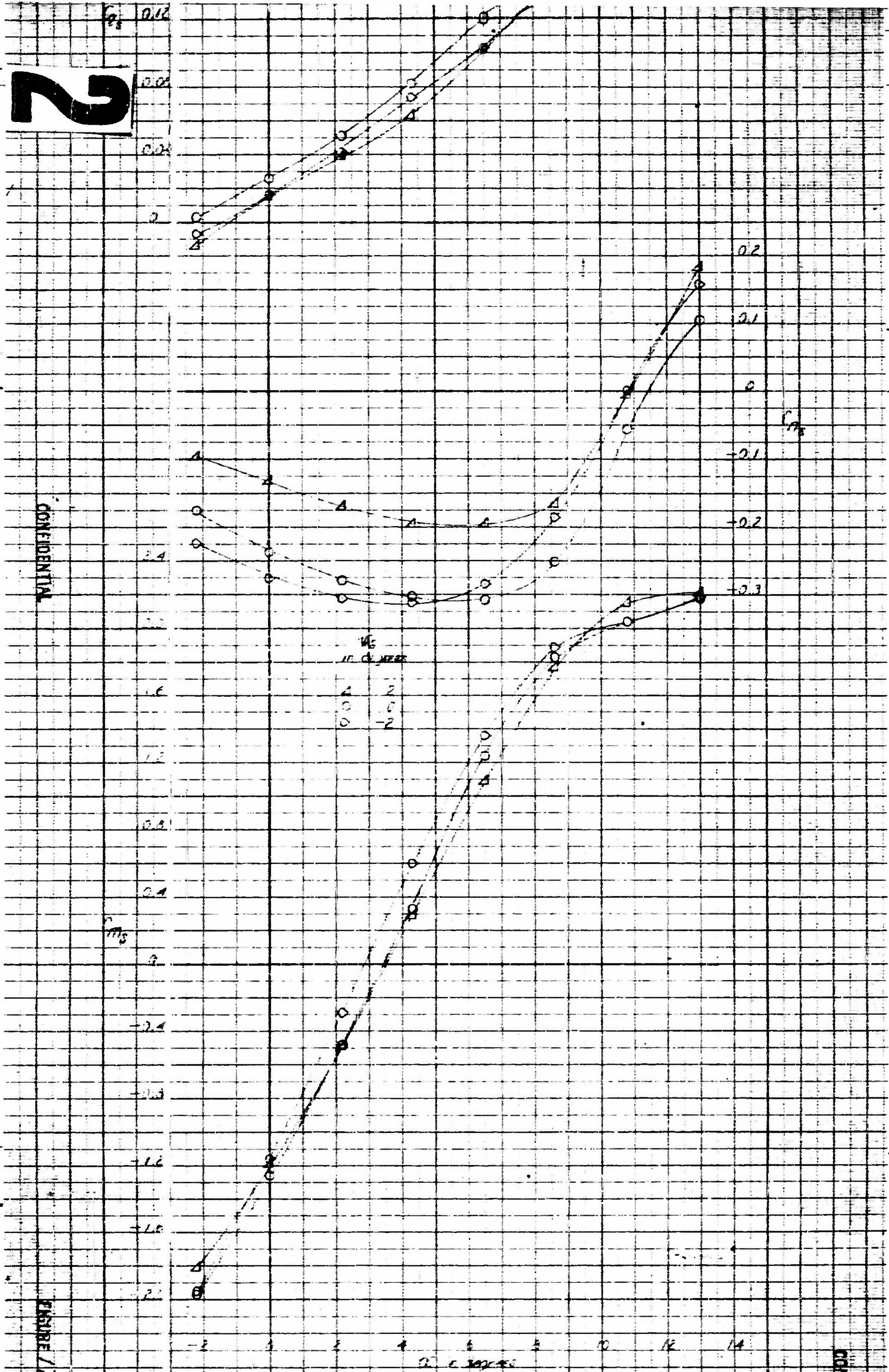

Figure 17 (Continued)

(b) Concluded

FIGURE 17a (cont'd)

CONFIDENTIAL

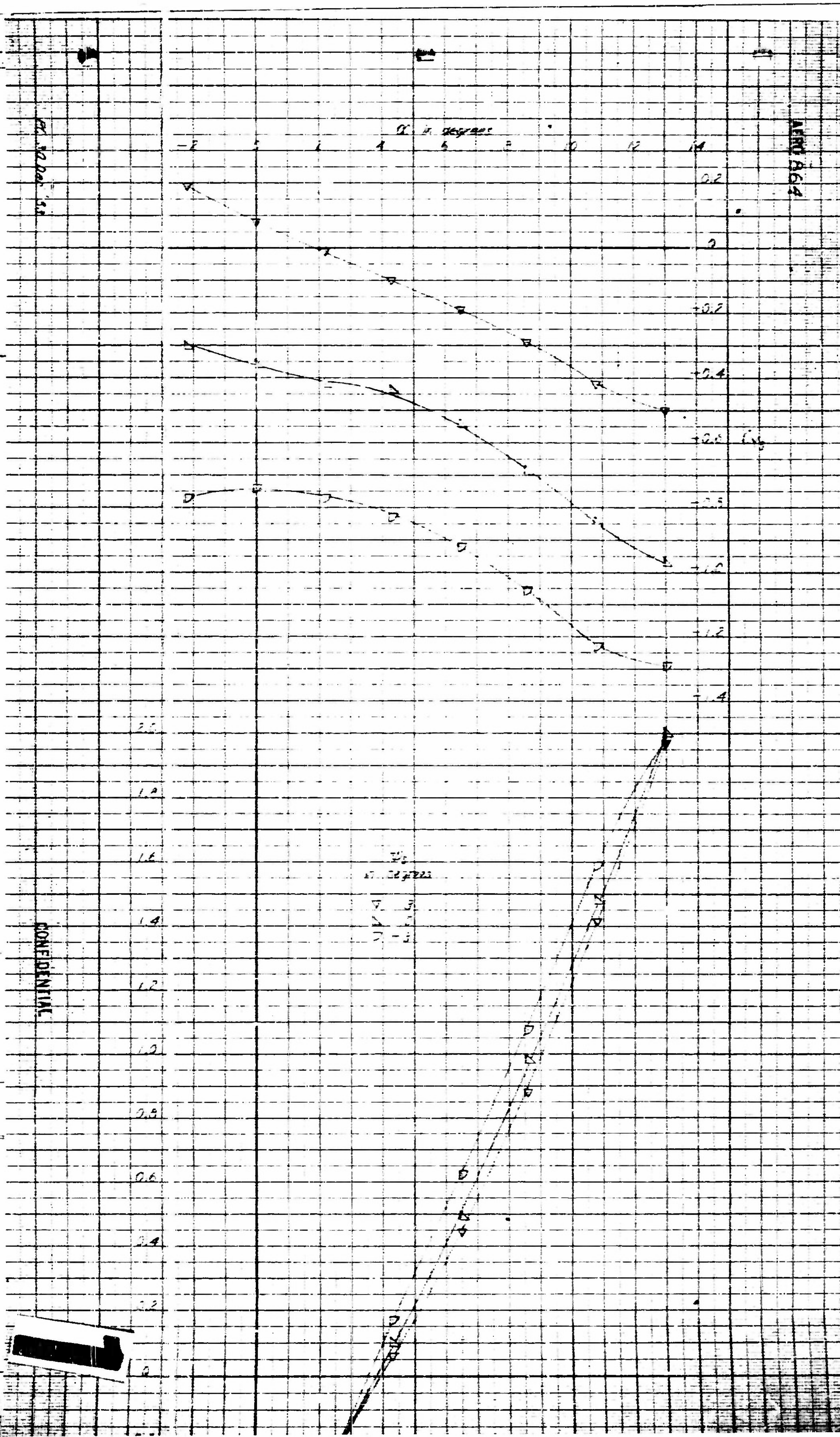
α in degrees
-2
0
2
4
6
8
10
12
14
AERO 864
CONFIDENTIAL

CONFIDENTIAL

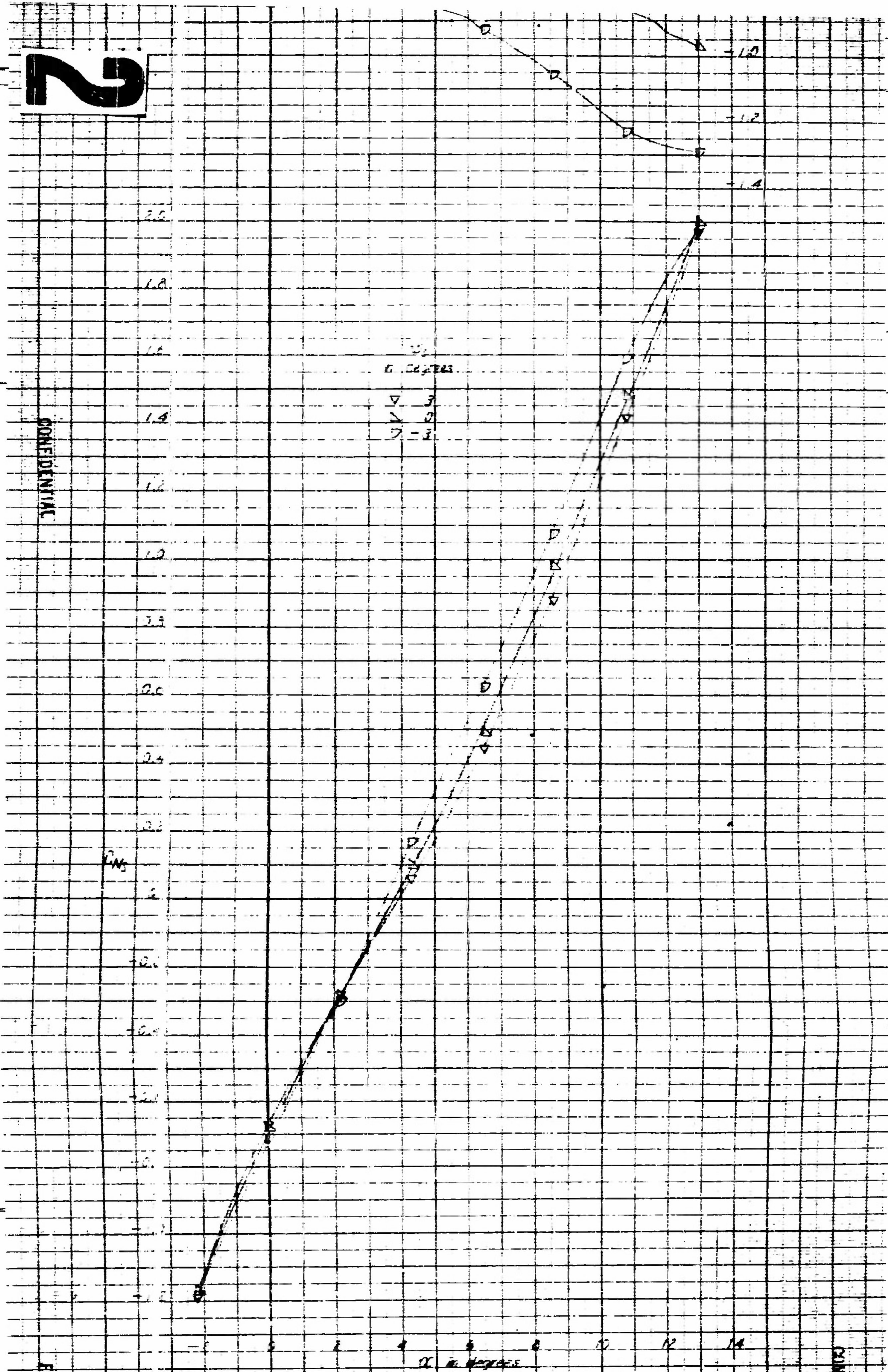

Figure 17 (Continued)

(h) z = 0 Inch, x = 13.26 Inches, $\theta_z = 0°$, $\psi = 0°$, Pylon On

FIGURE 17 A

CONFIDENTIAL

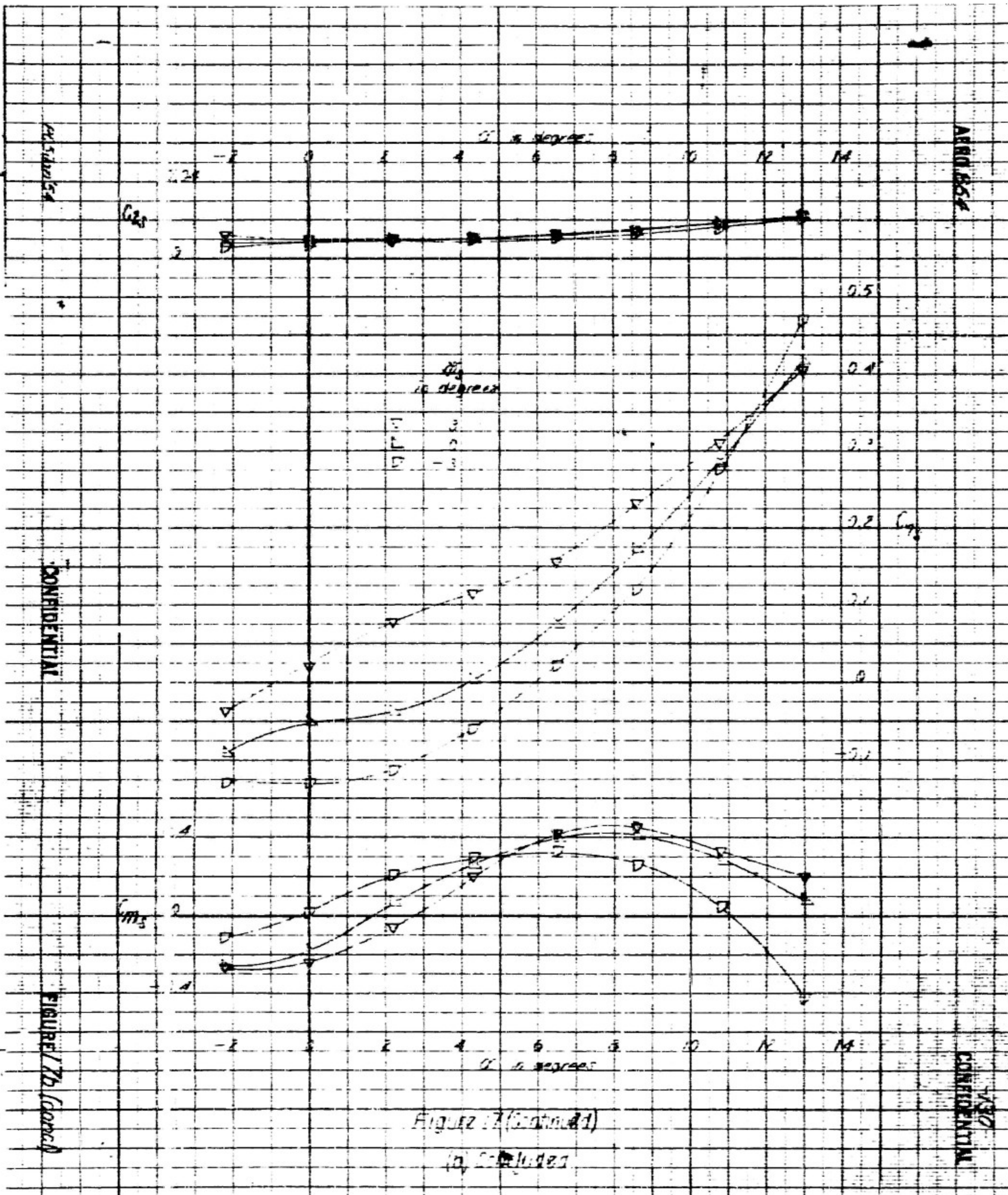

Figure 17 (Continued)

(b) Concluded

FIGURE 17b (concl)

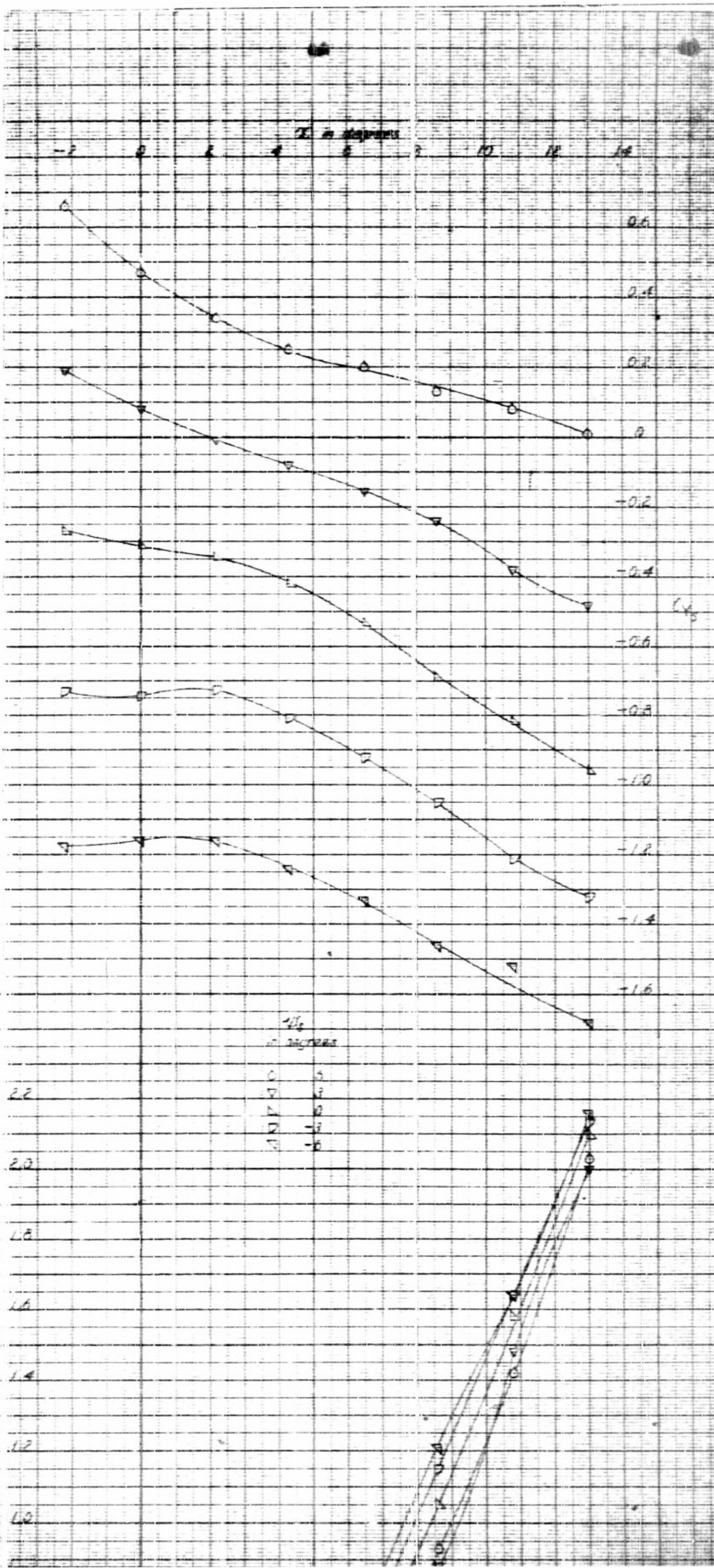

CONFIDENTIAL

[redacted]

CONFIDENTIAL

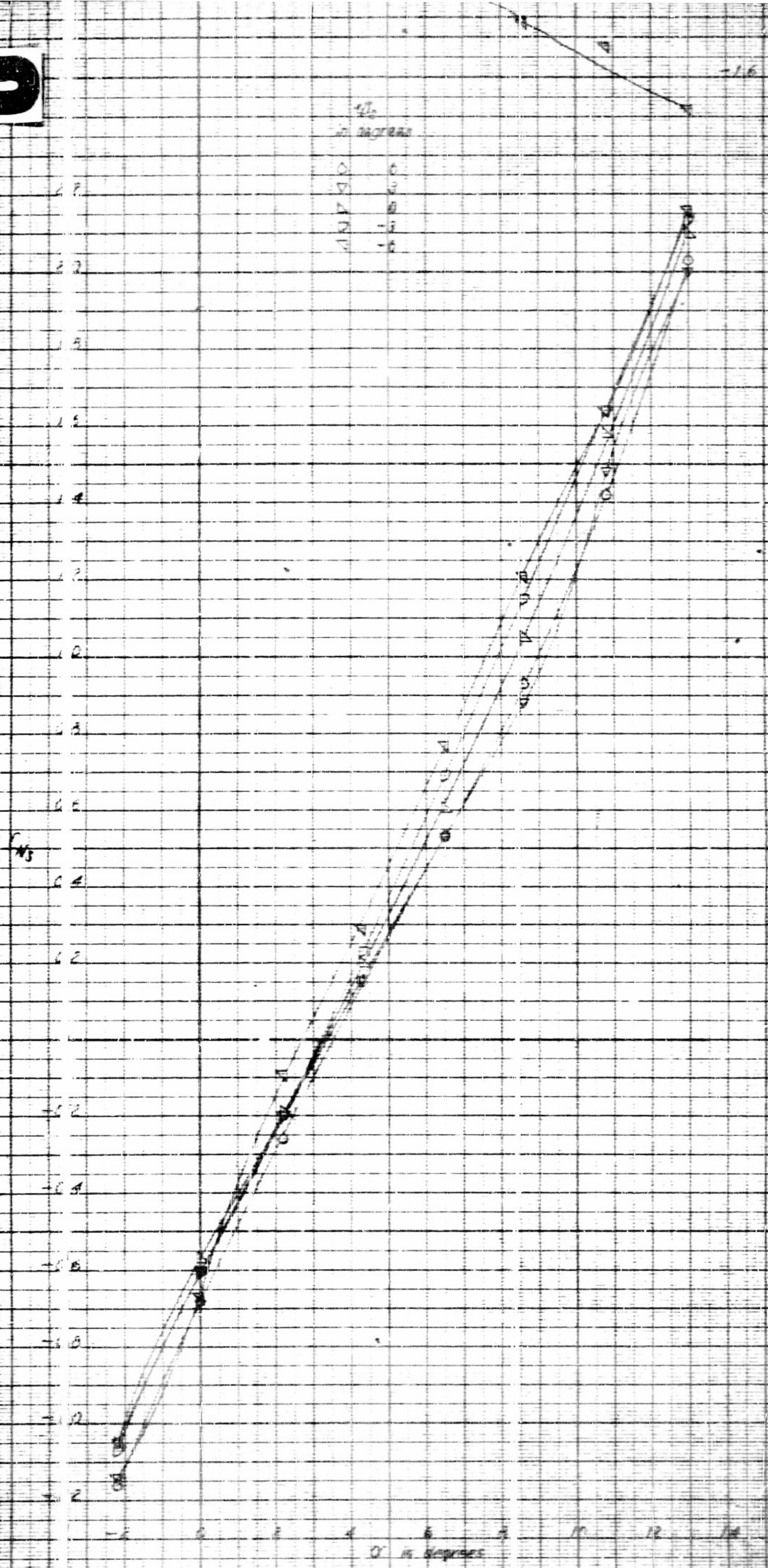

Figure 17 (Continued)

(k) z = 0 Inch, x = 13.26 Inches, $A_T = 0°$, $\psi = 0°$, Pylon 0?

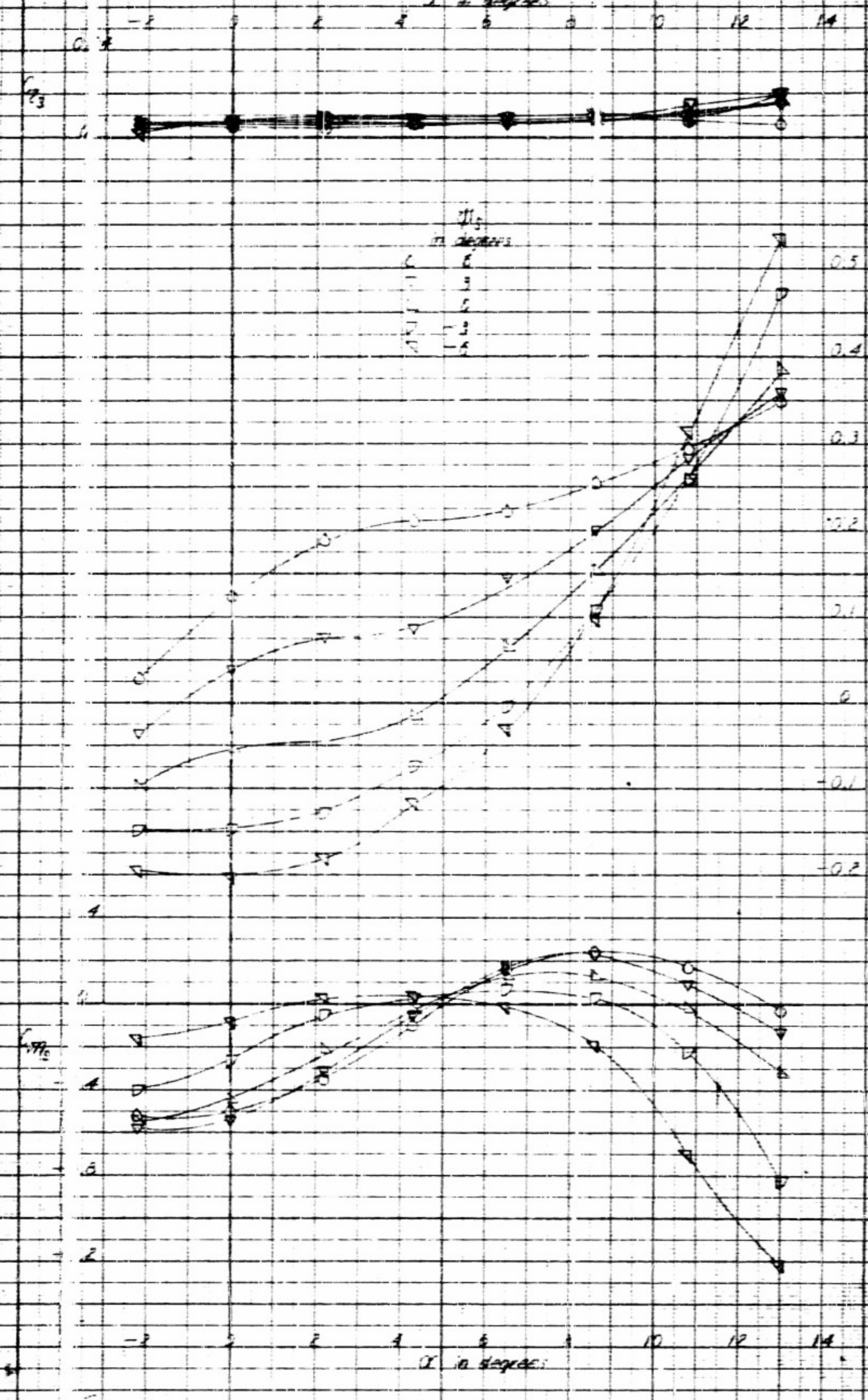

Figure 17 (Continued)

(c) Concluded

FIGURE 17c

CONFIDENTIAL

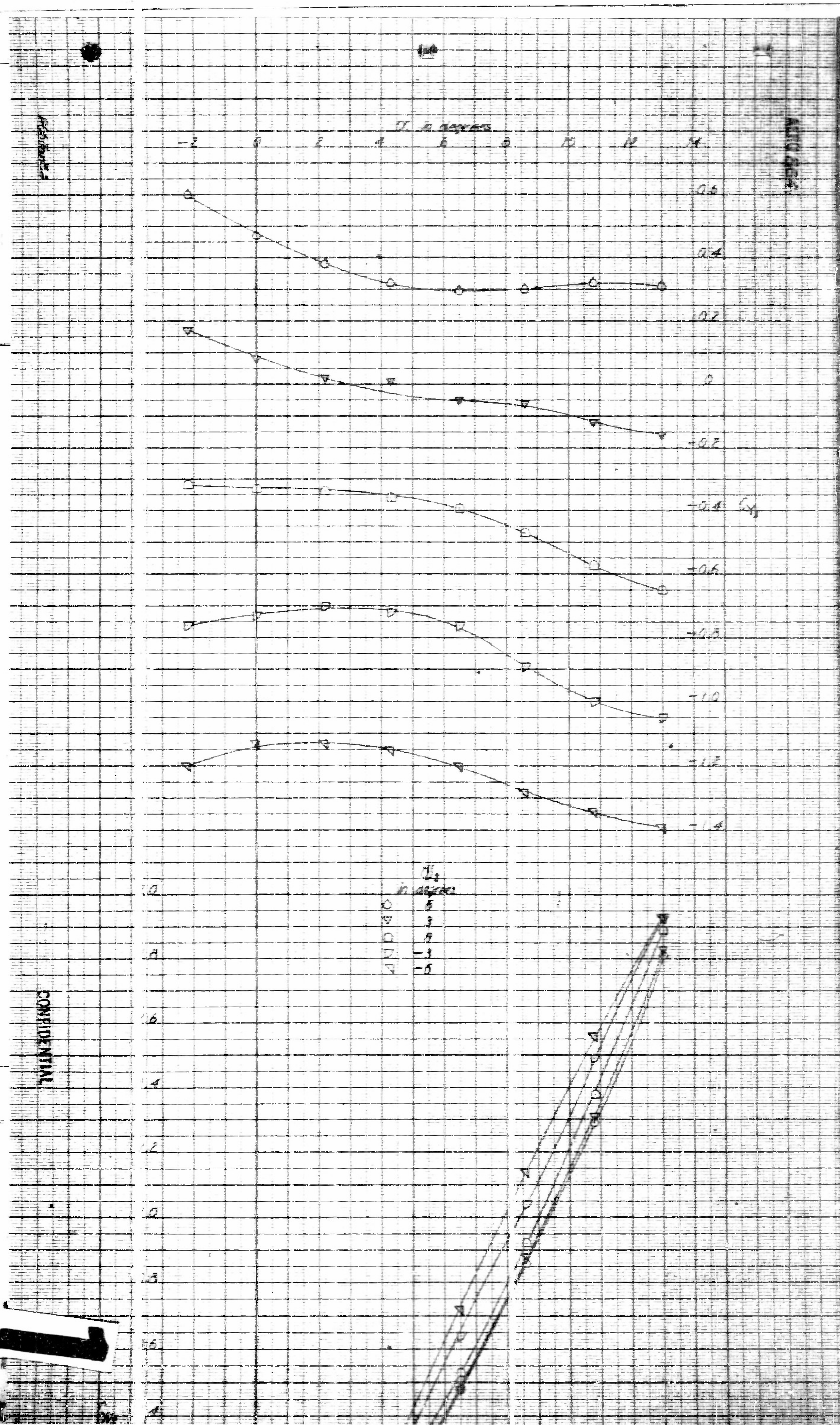

α in degrees
-2
0
2
4
6
8
10
12
14
0.6
0.4
0.2
0
-0.2
-0.4
-0.6
-0.8
-1.0
-1.2
-1.4
C_{Y_1}
CONFIDENTIAL

CONFIDENTIAL

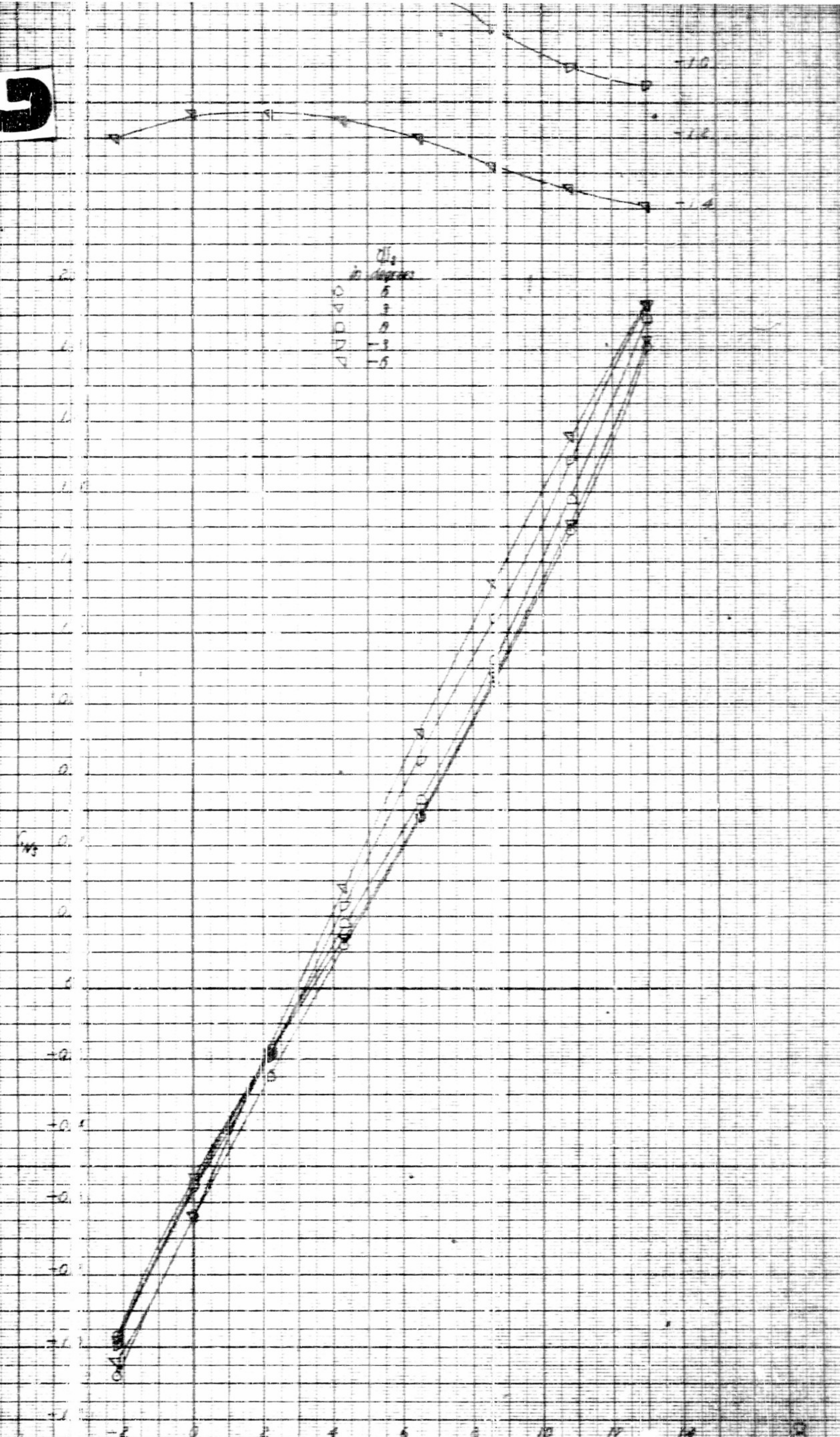

Figure 17 (Continued)

(i) z = 0 Inch; x = 18.36 Inches; $\delta_0 = 0°$; $\beta = 0°$; Pylon fin

CONFIDENTIAL

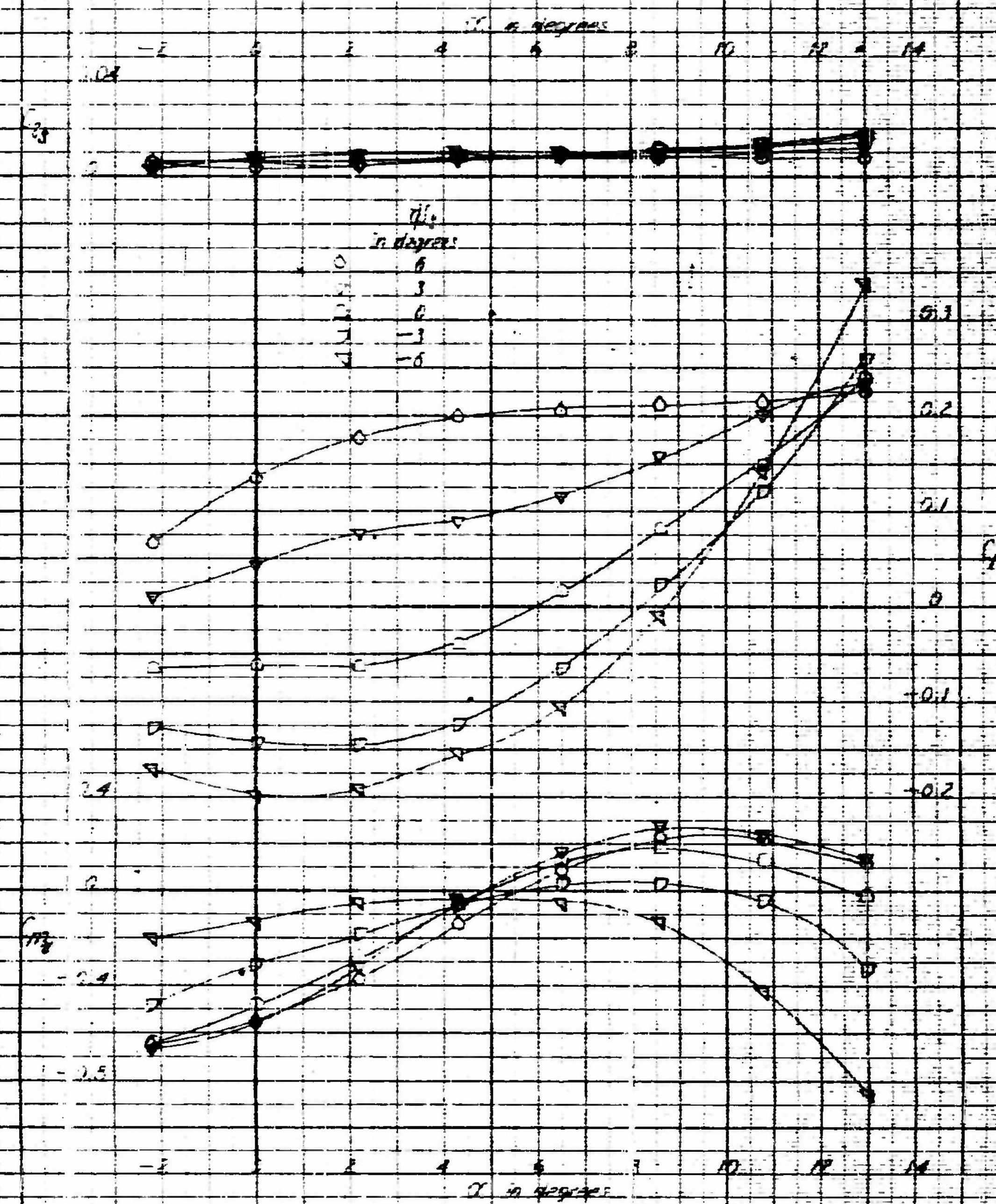

Figure 17 (Concluded)
(d) Concluded

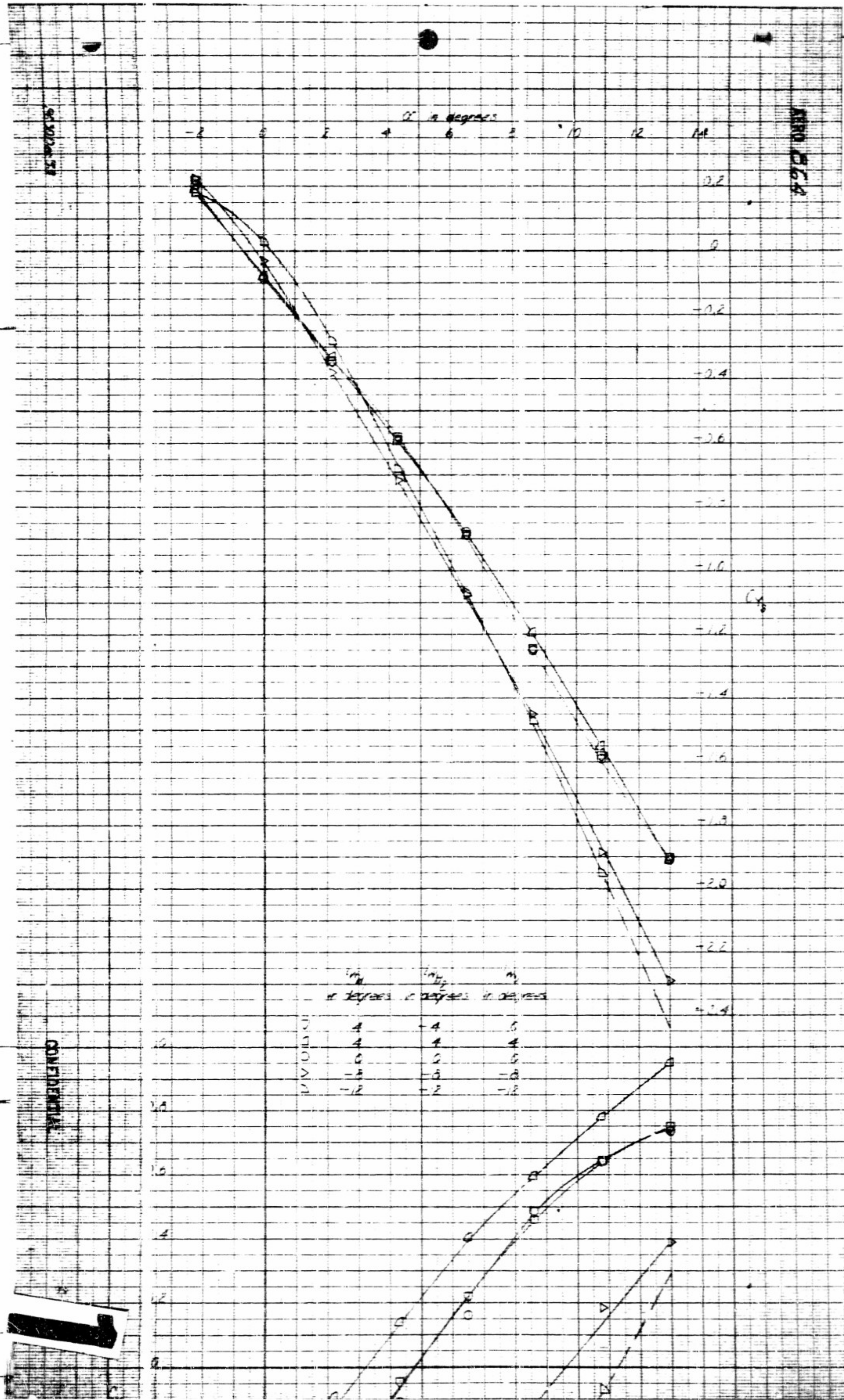

AERO 864
CONFIDENTIAL
α in degrees
-2
0
2
4
6
8
10
12
14
0.2
0
-0.2
-0.4
-0.6
-1.0
-1.2
-1.4
-1.6
-2.0
-2.2
-2.4
in degrees
○ 4 -4 6
□ 4 4 4
◇ 0 0 0
△ -8 -8 -8
▽ -12 -12 -12

CONFIDENTIAL

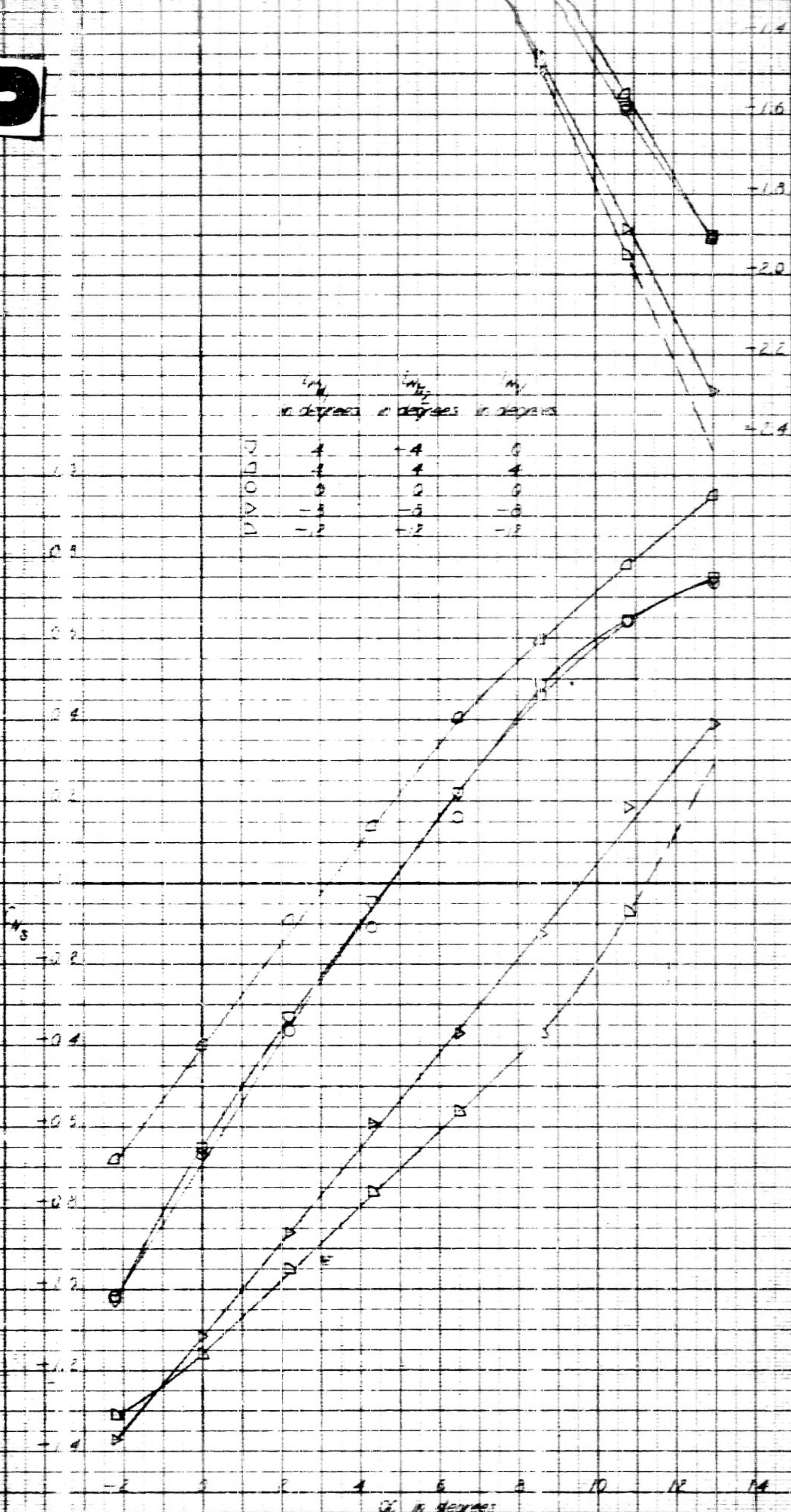

Figure 18 – Aerodynamic Characteristics of a 0.17-Scale Model XAAM-N-4 Oriole Missile Due to Missile Wing Incidence in the Proximity of a 0.179-Scale Model F4D-1 Airplane at the Outboard Station

(e) Z = 0 inch, X = 0 inch, $\theta_s = 0°$, $\psi_s = 0°$, $\psi = 0°$, Pylon On.

FIGURE 18e

CONFIDENTIAL

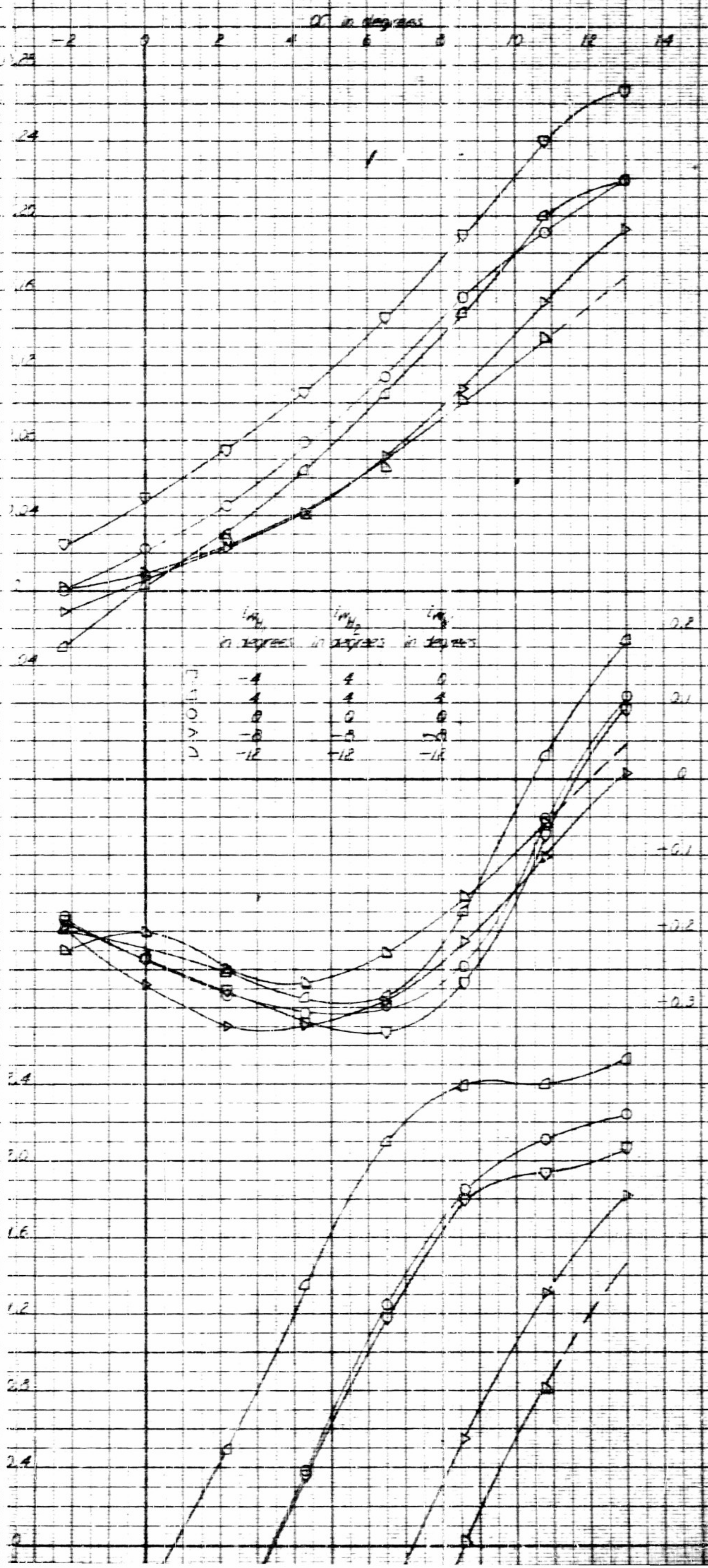

CONFIDENTIAL

CONFIDENTIAL

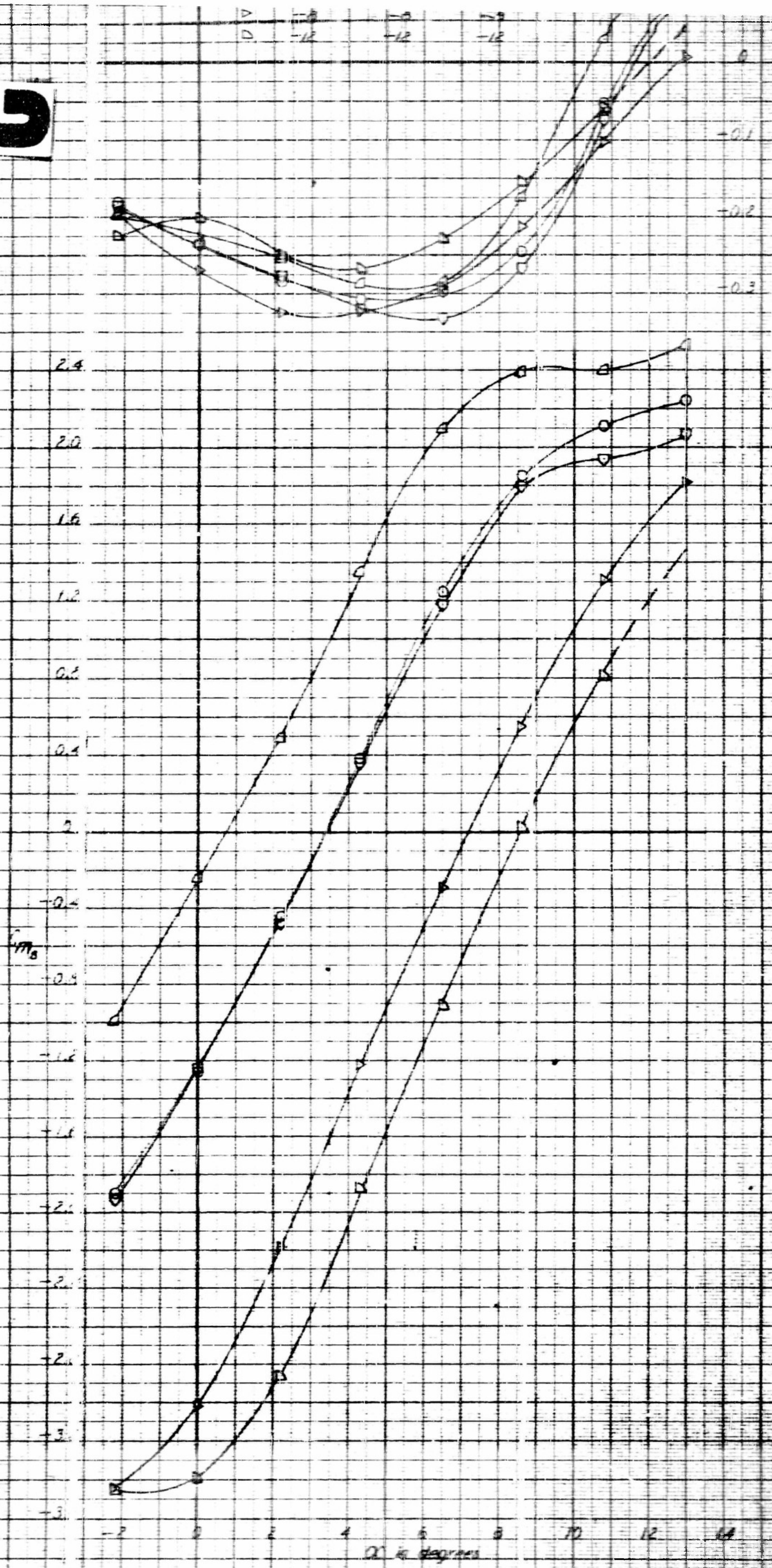

Figure 18 (Continued).
(a) Concluded

FIGURE 18(a) concl.

CONFIDENTIAL

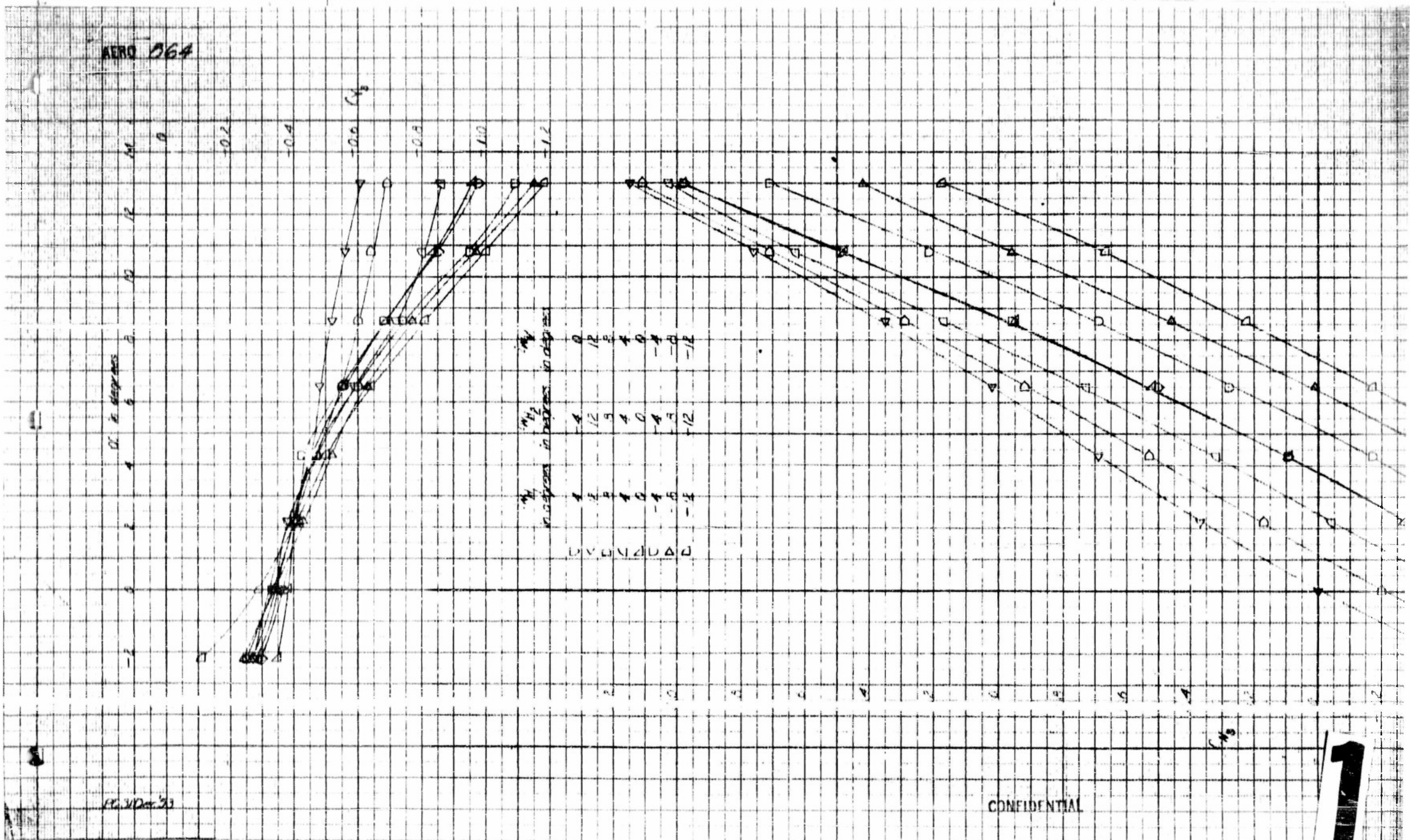

AERO 964
α in degrees
C_{Y_3}
C_{N_3}
in degrees
in degrees
in degrees
PC 3/Dec'53
CONFIDENTIAL

CONFIDENTIAL

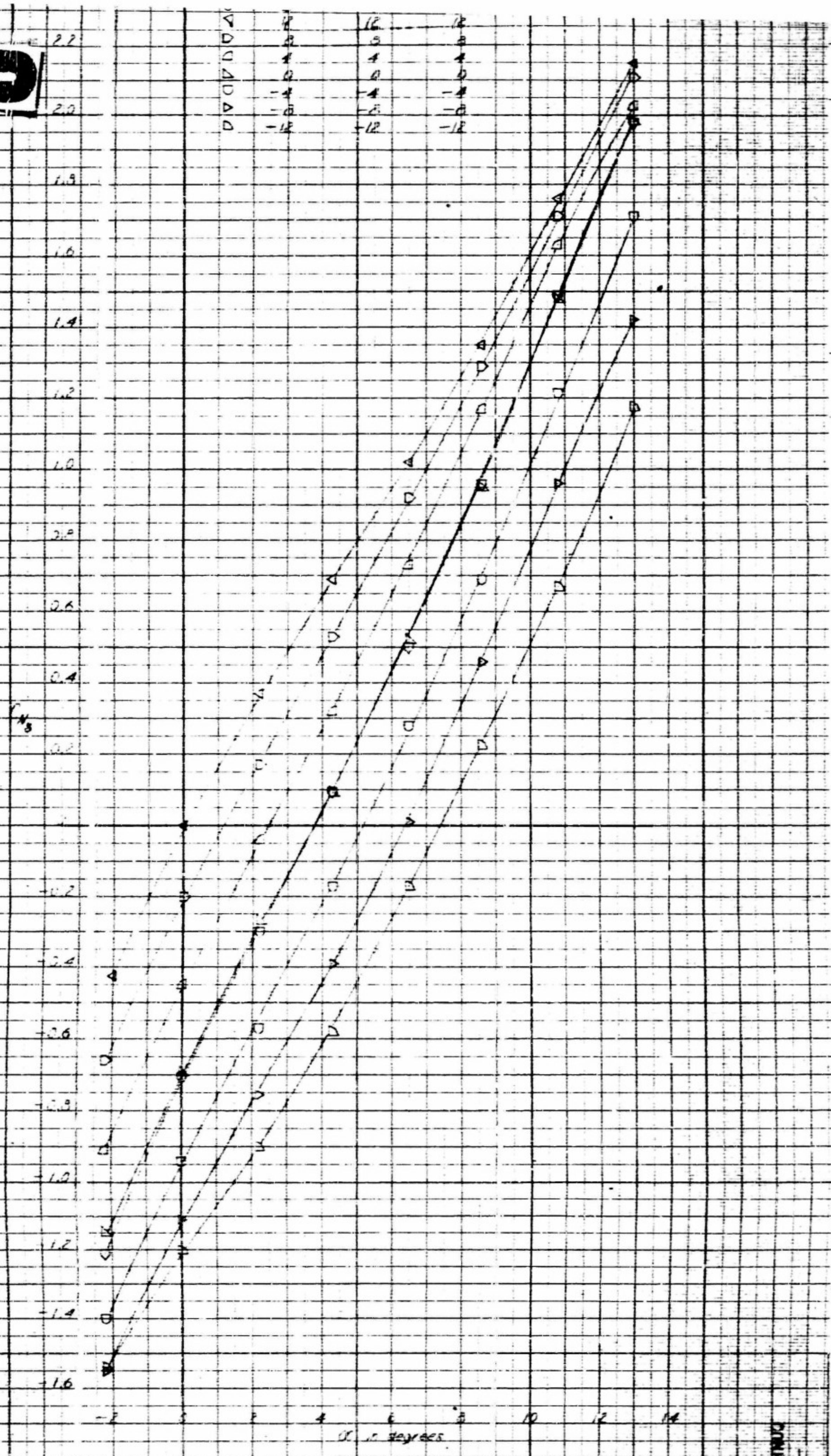

Figure 18 (Continued)

(h) Z = 0 inch, X = 13.76 inches, $\theta_S = 0°$, $\psi_S = 0°$, $\psi = 0°$, Pylon On

FIGURE 18h

CONFIDENTIAL

AERO 764

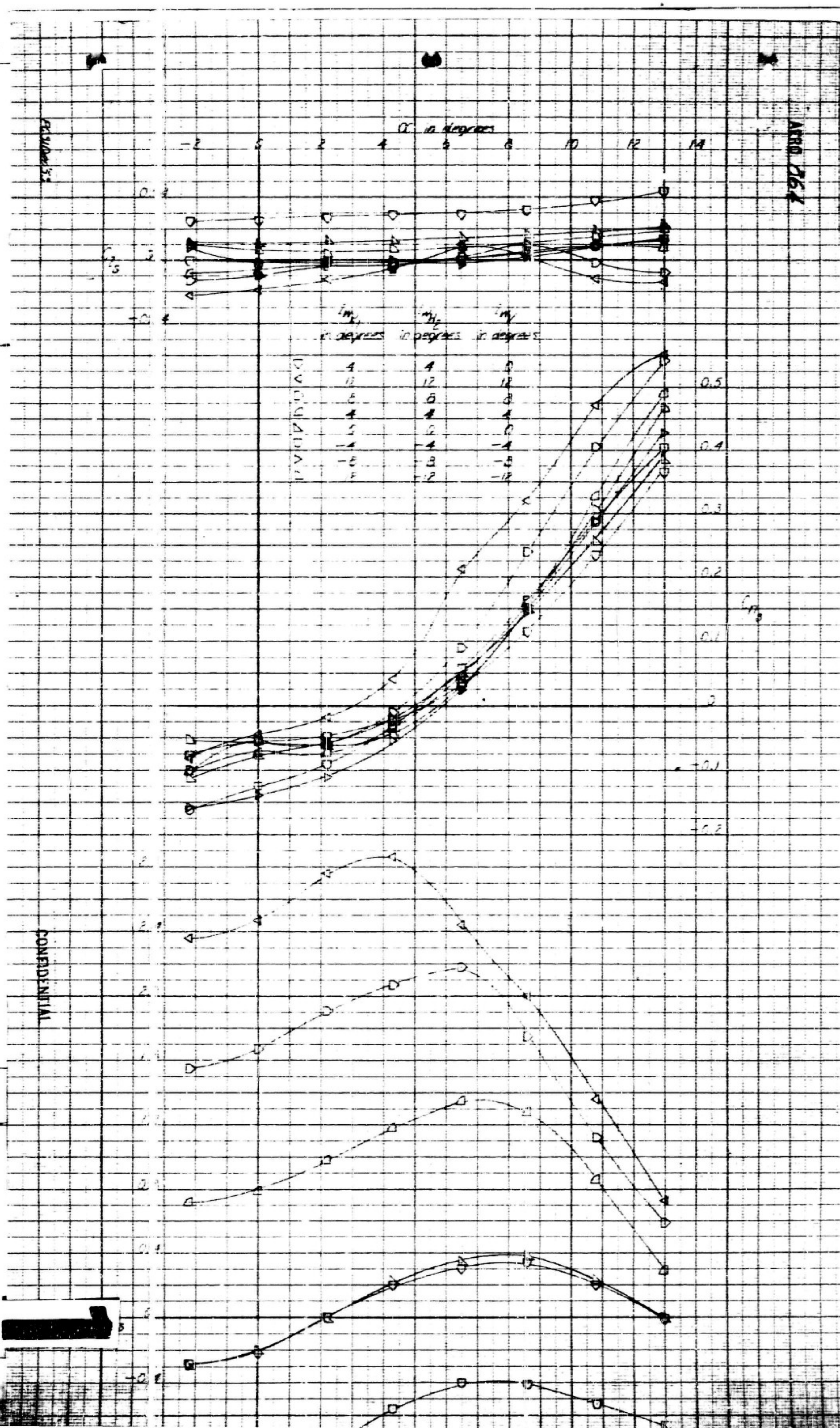

CONFIDENTIAL

[redacted]

CONFIDENTIAL

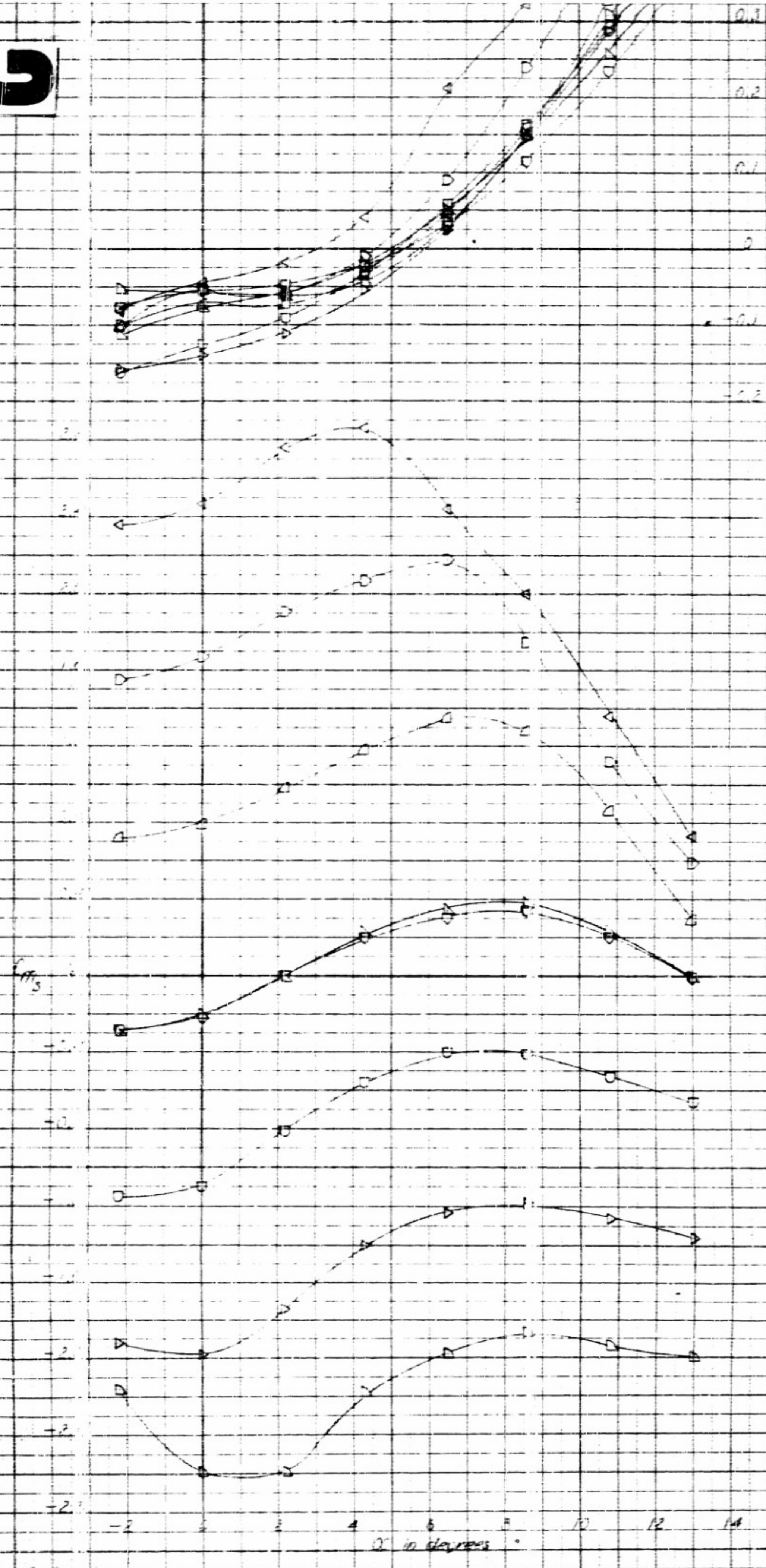

Figure 18 Continued

(b) Concluded

FIGURE 18 Concl.

CONFIDENTIAL

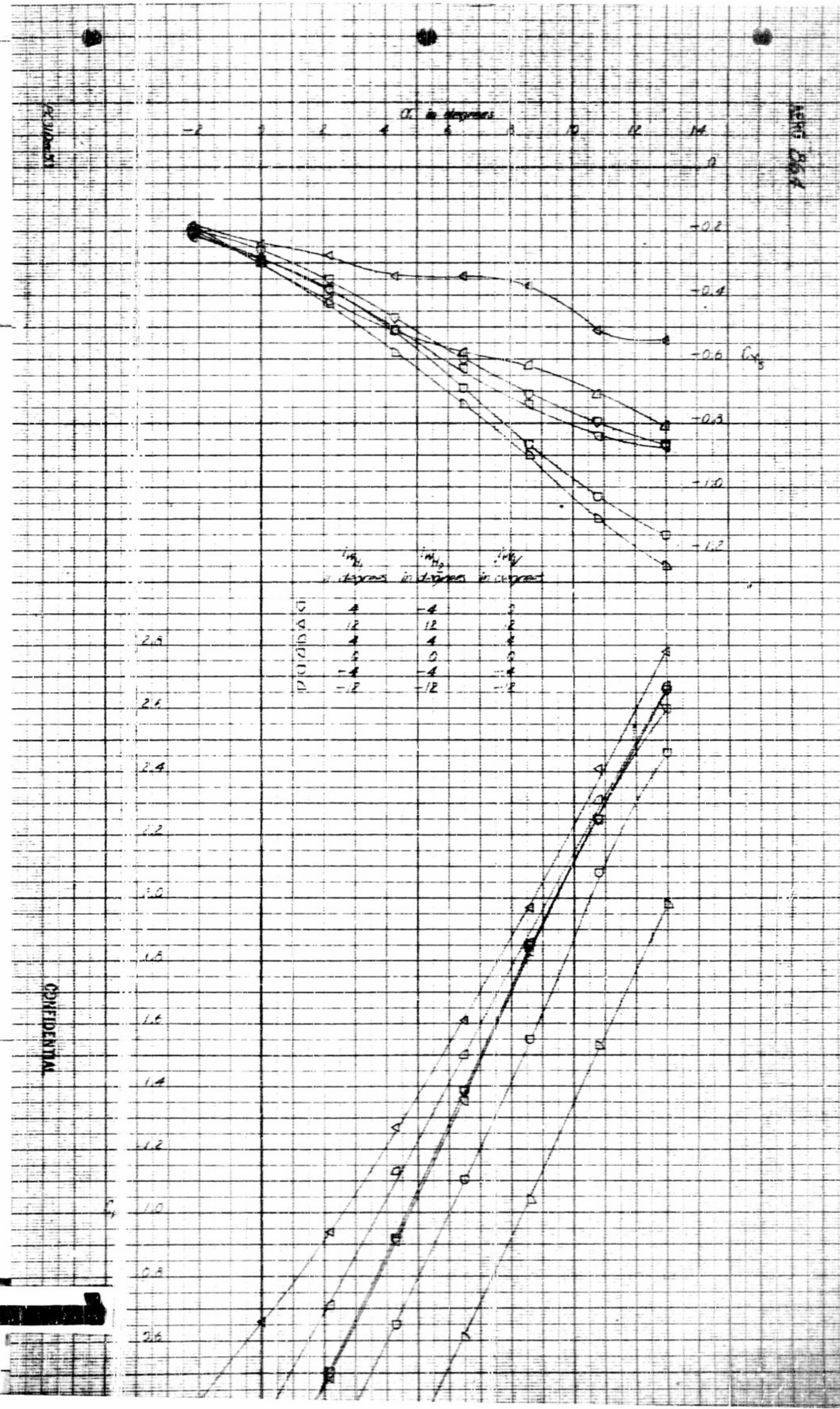

CONFIDENTIAL

[redacted]

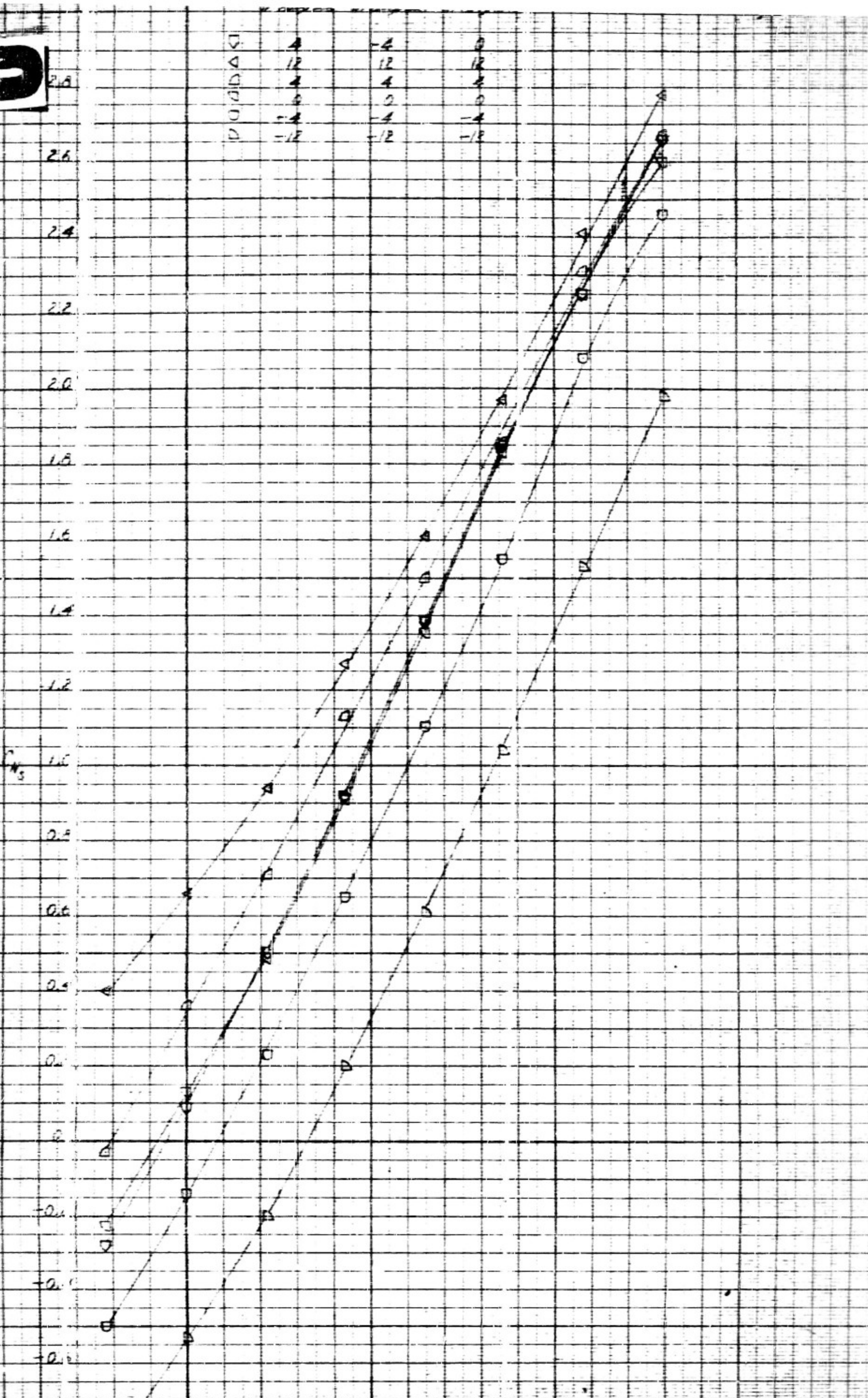

CONFIDENTIAL

Figure 18 (Continued)

(c) Z = 0 inch, X = 13.26 inches, θ_s = 6°, ψ_s = 0°, ψ = 0°, Pylon On

FIGURE 102

CONFIDENTIAL

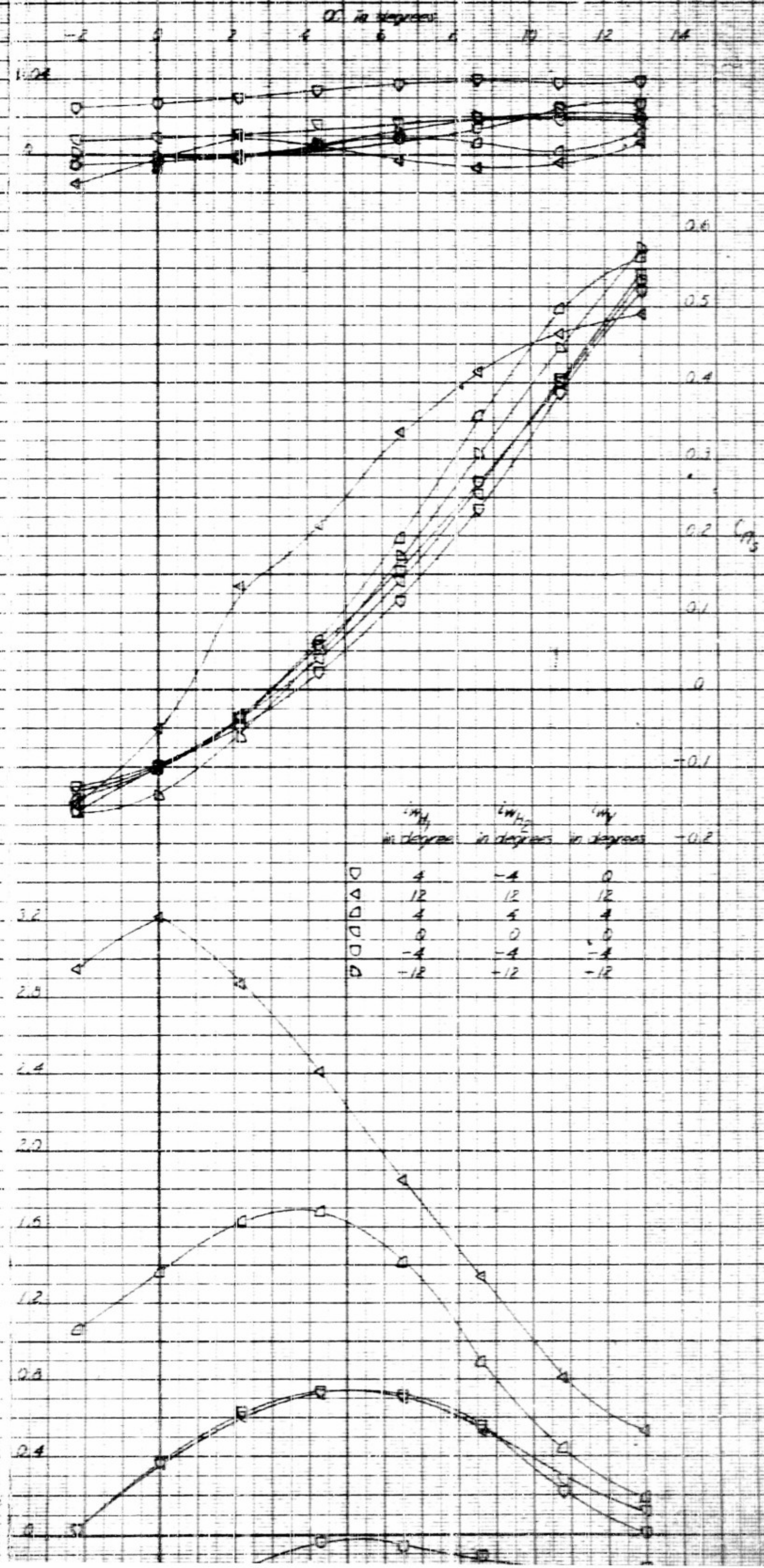

AERO 364

CONFIDENTIAL

[redacted]

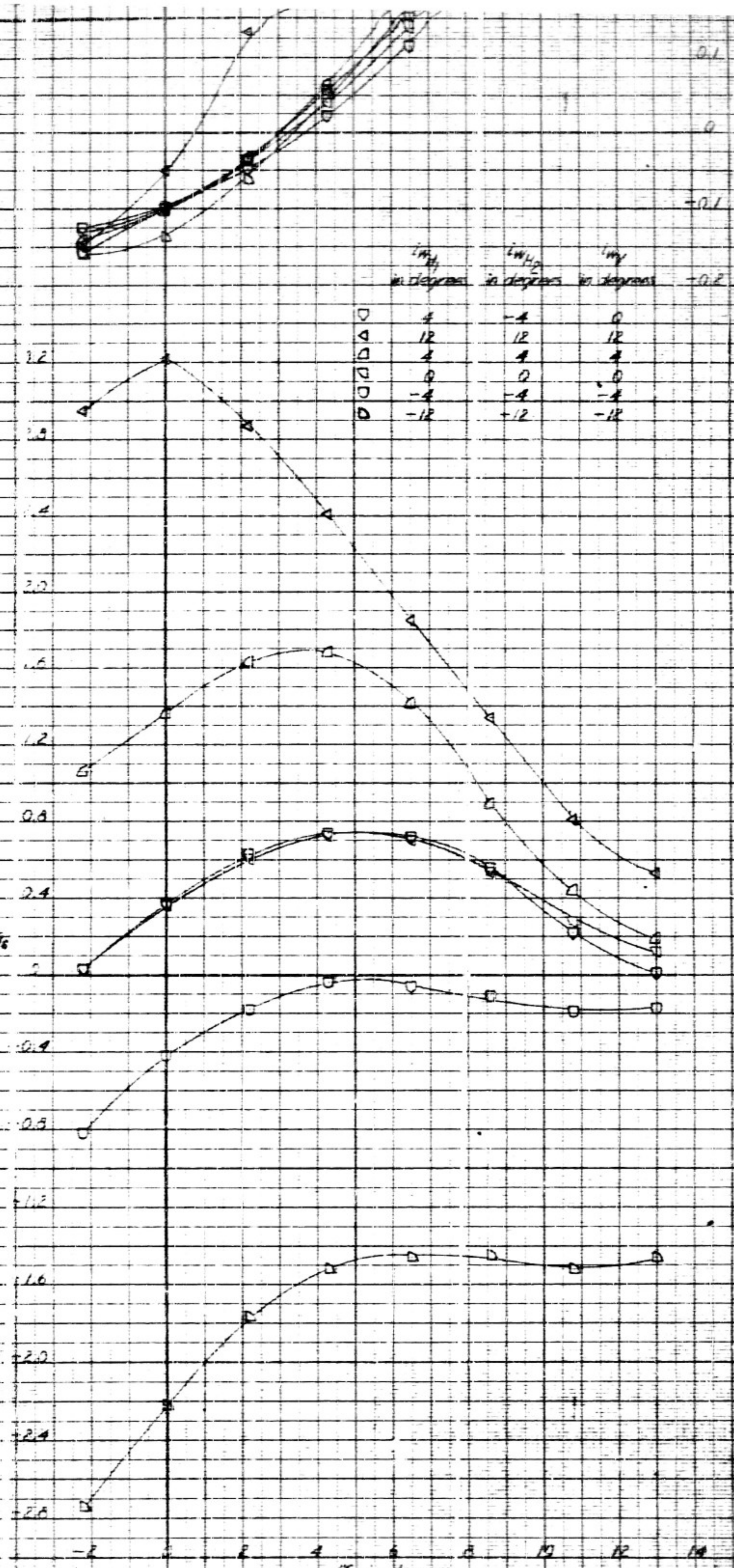

CONFIDENTIAL

Figure 18 (Continued)

(c) Concluded

FIGURE 18(c) (concl)

CONFIDENTIAL

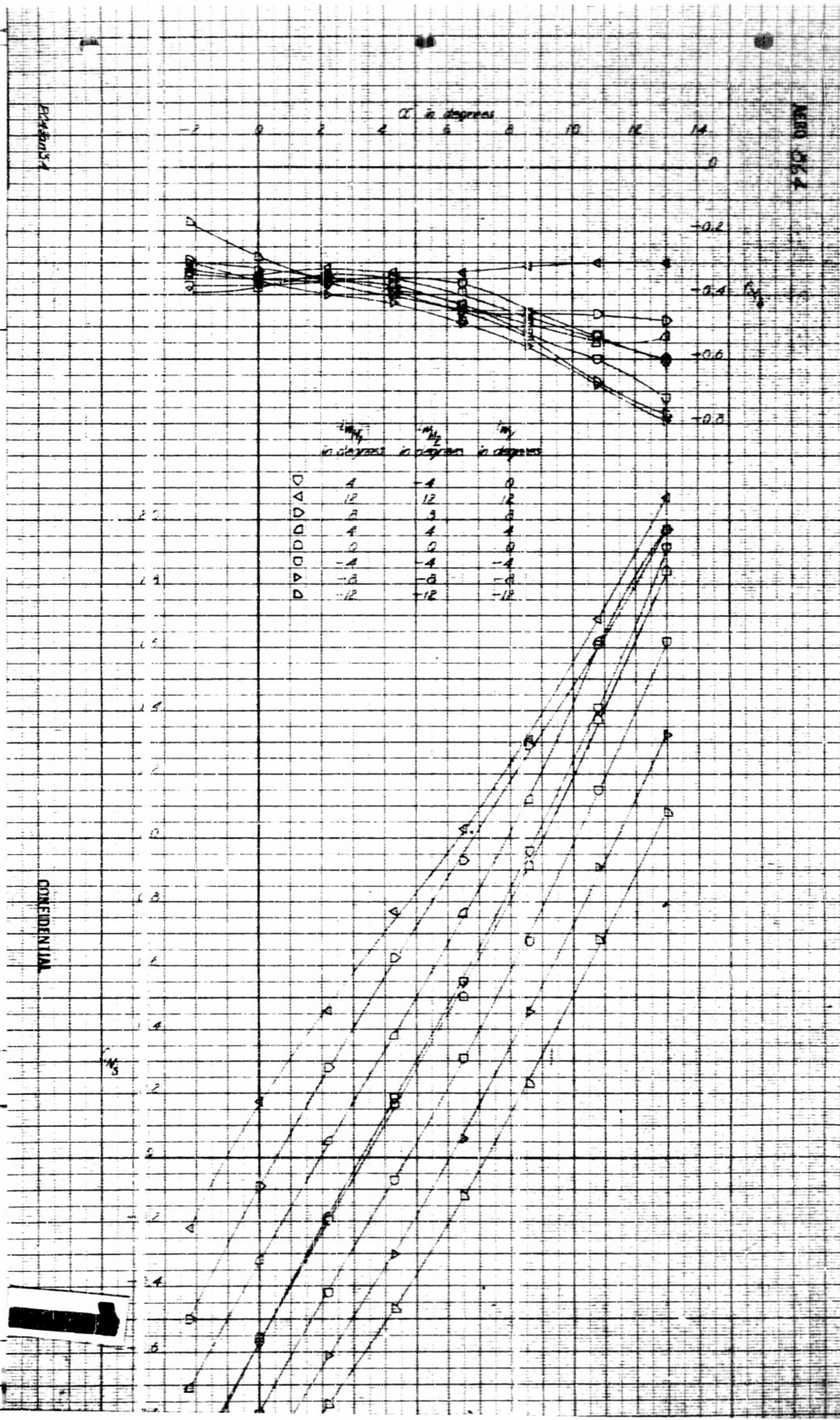

α in degrees
-2 0 2 4 6 8 10 12 14
0
+0.2
+0.4
+0.6
+0.8
$i_{m_{H_1}}$ in degrees
$i_{m_{H_2}}$ in degrees
i_{m_V} in degrees
4 -4 0
12 12 12
8 8 8
4 4 4
0 0 0
-4 -4 -4
-8 -8 -8
-12 -12 -12
CONFIDENTIAL

[redacted]

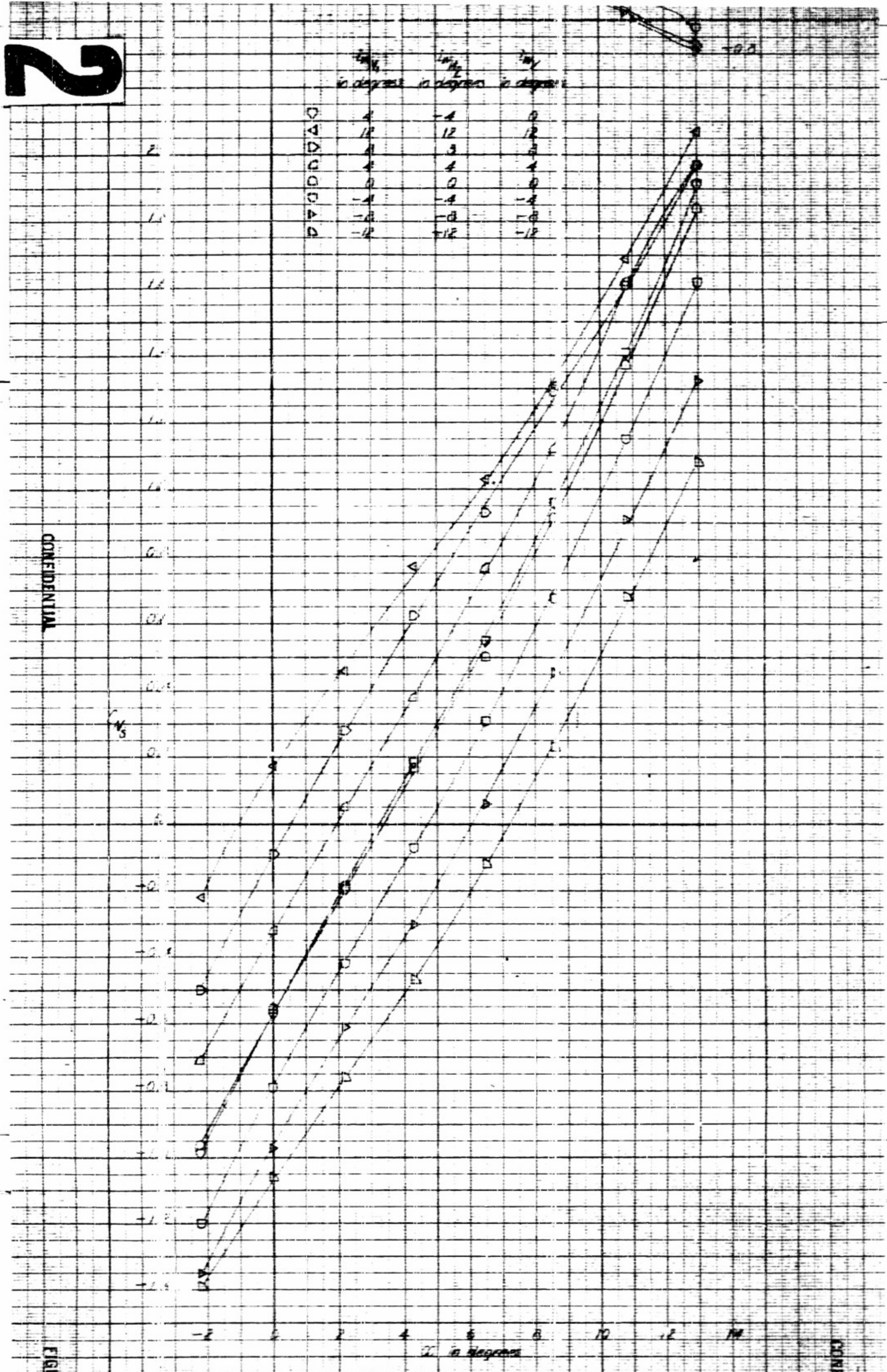

Figure 18 (Continued)

(d) Z = 5 inch, X = 13.36 inches, $\epsilon_s = 0°$, $\psi_s = 0°$, $\psi = 0°$, Pylon On

FIGURE 18d

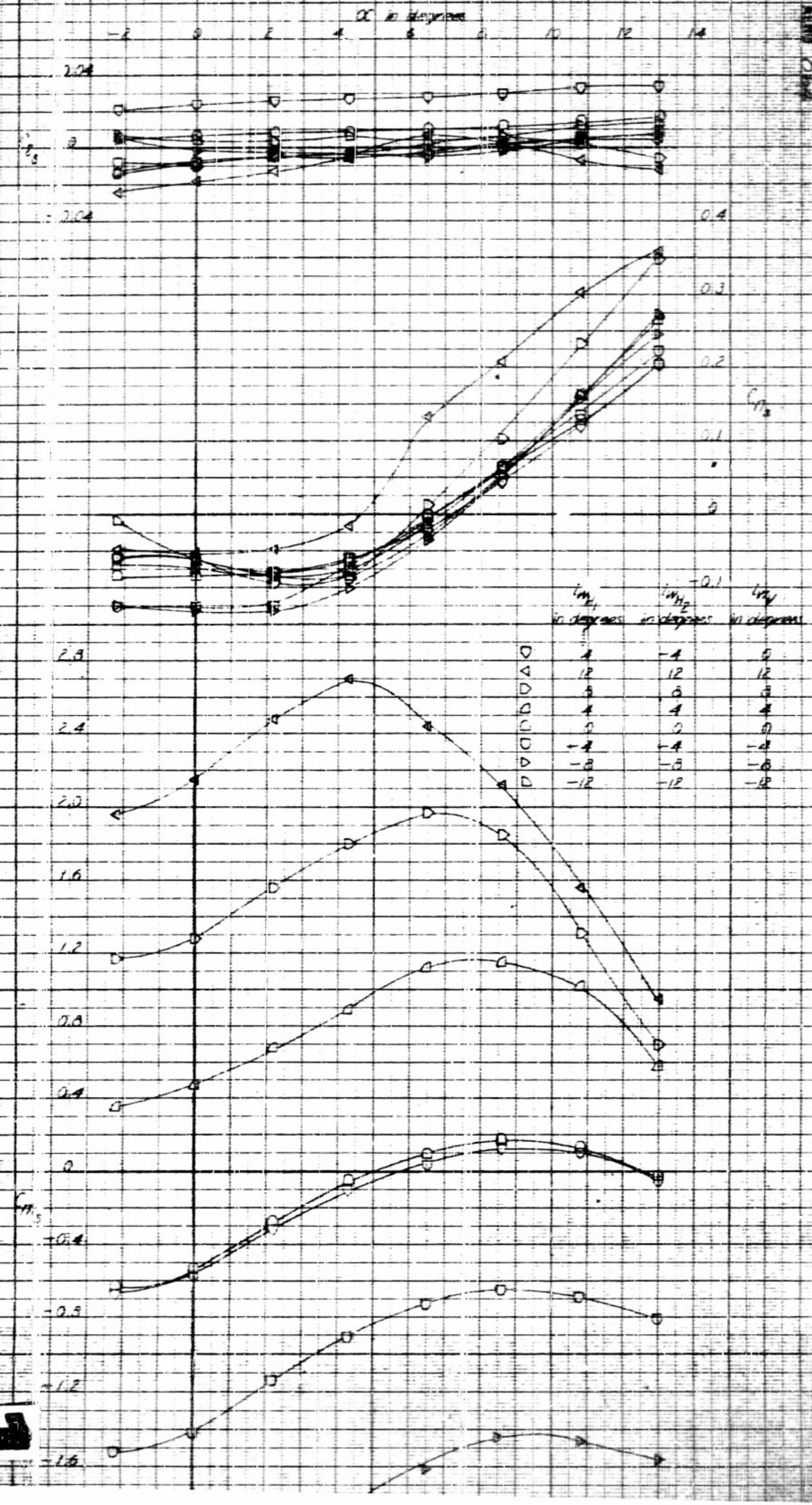

CONFIDENTIAL

[redacted]

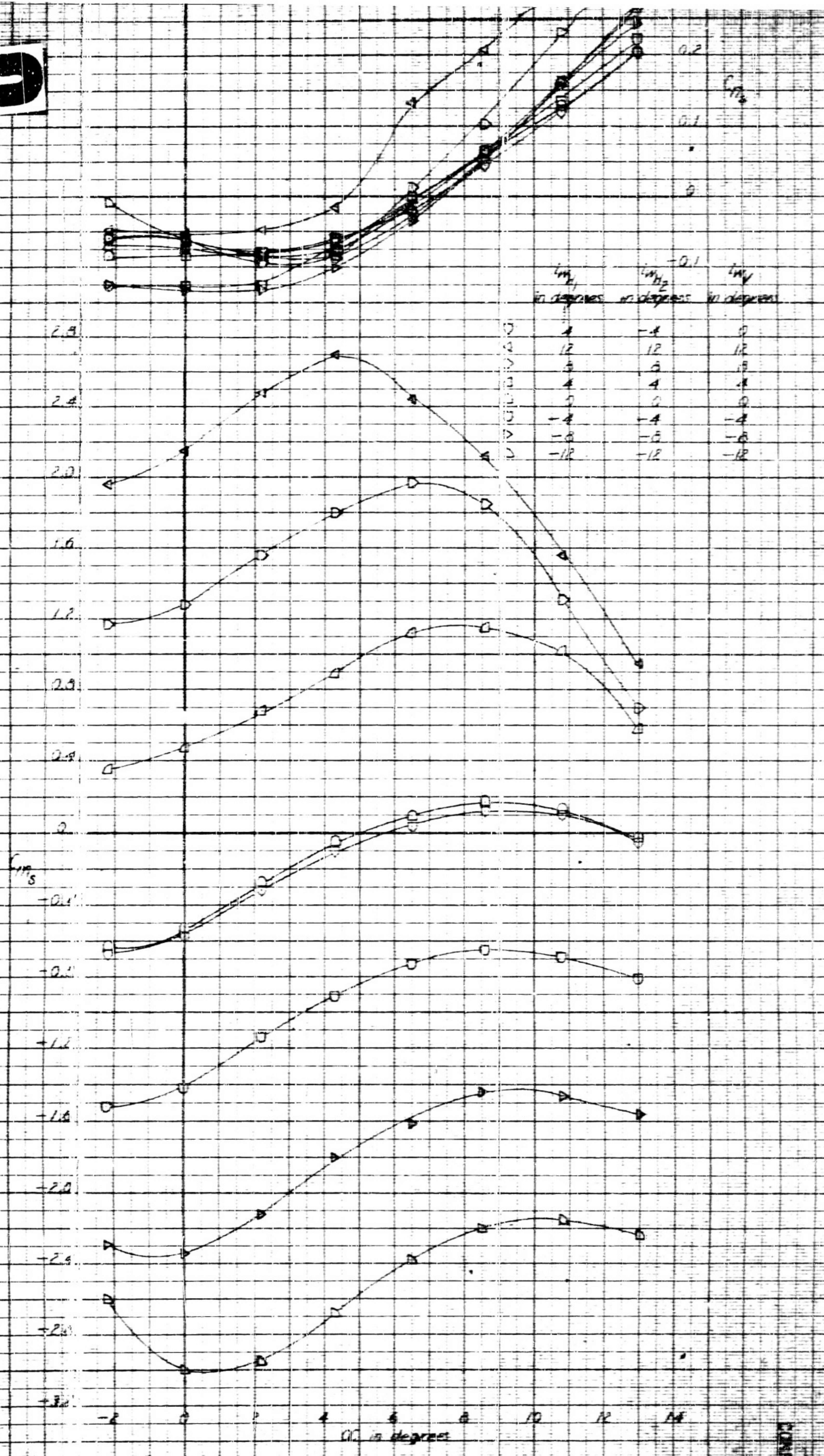

Figure 18 (Continued)

(b) Concluded

FIGURE 18 (Continued)

AERO 964

Figure 34

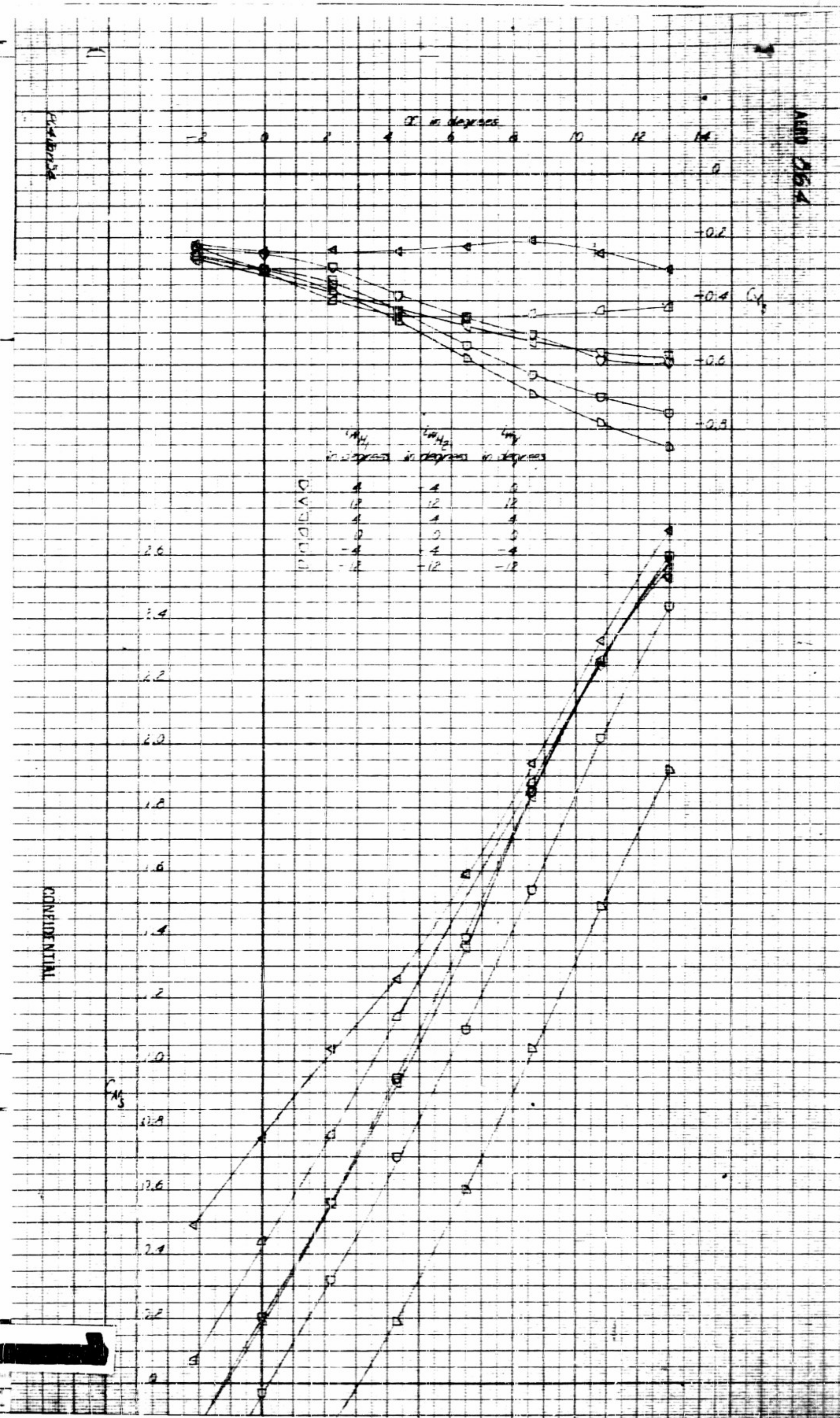

CONFIDENTIAL

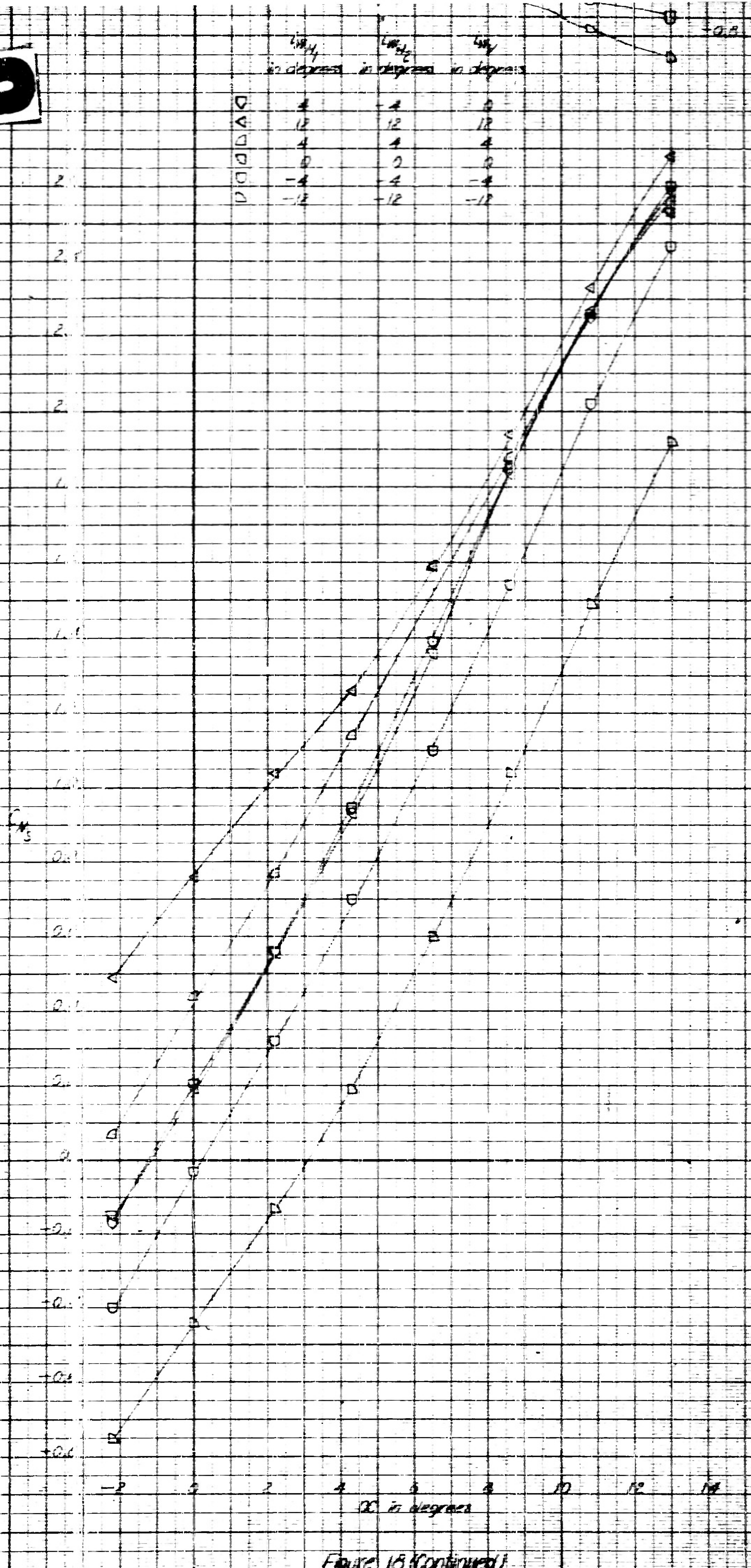

Figure 18 (Continued)

(e) Z = 0 inch, X = 16.36 inches, $\theta_s = 6^\circ$, $\psi_s = 0^\circ$, $\psi = 0^\circ$, Pylon On

FIGURE 18e

CONFIDENTIAL

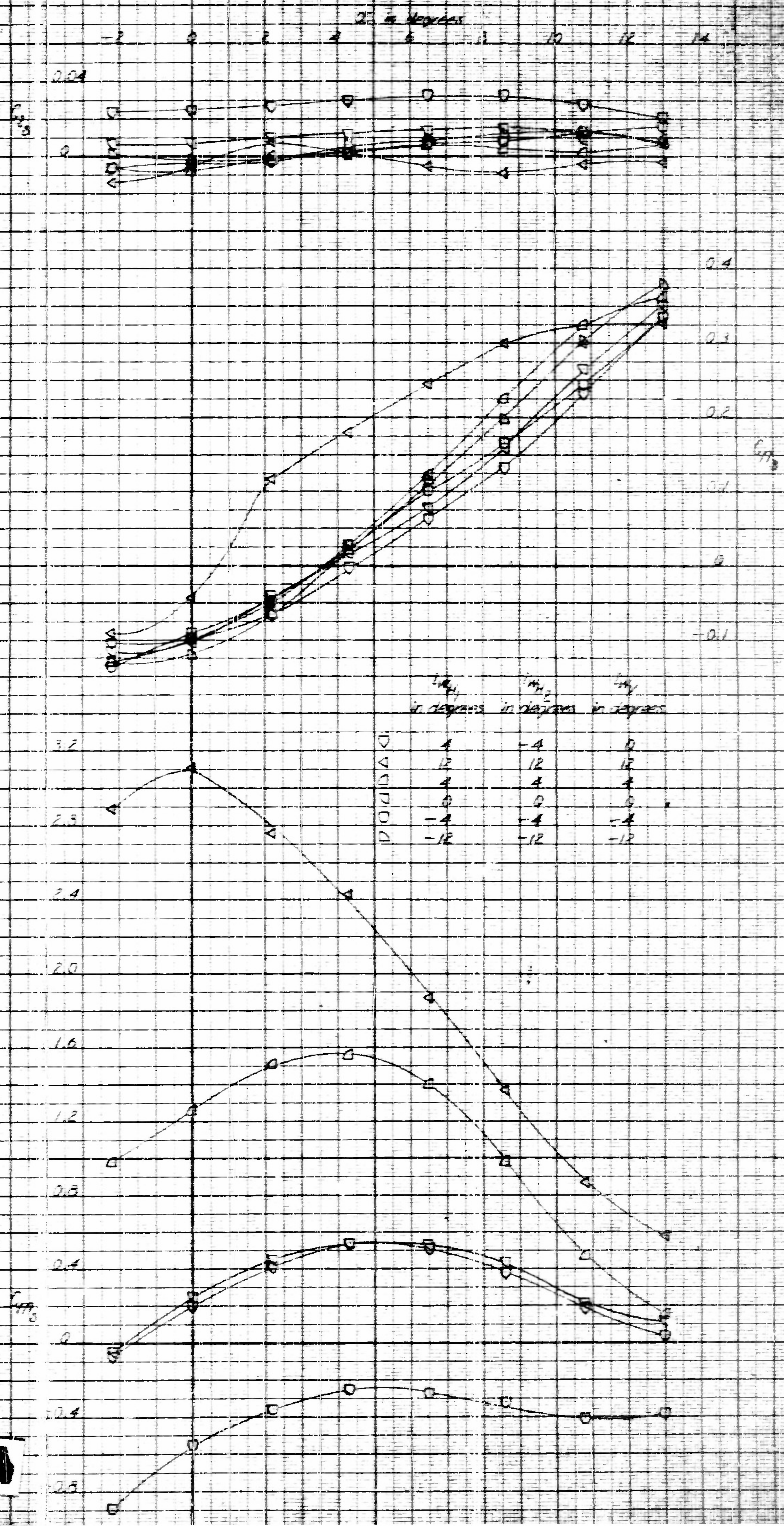

Figure 34.

CONFIDENTIAL

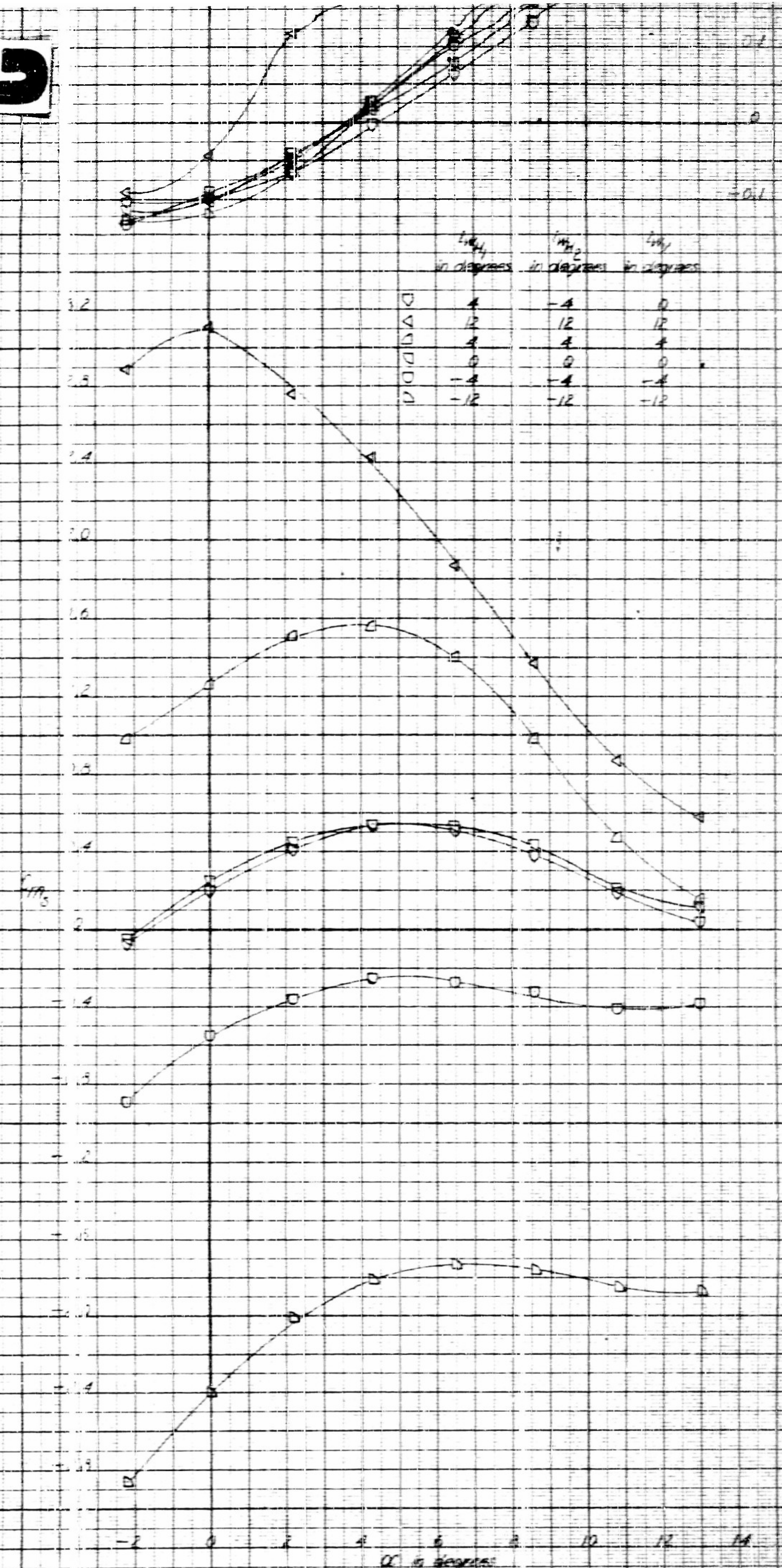

Figure 18 (Concluded.)

(e) Concluded

FIGURE 18 (Concluded)

CONFIDENTIAL

AERO 864

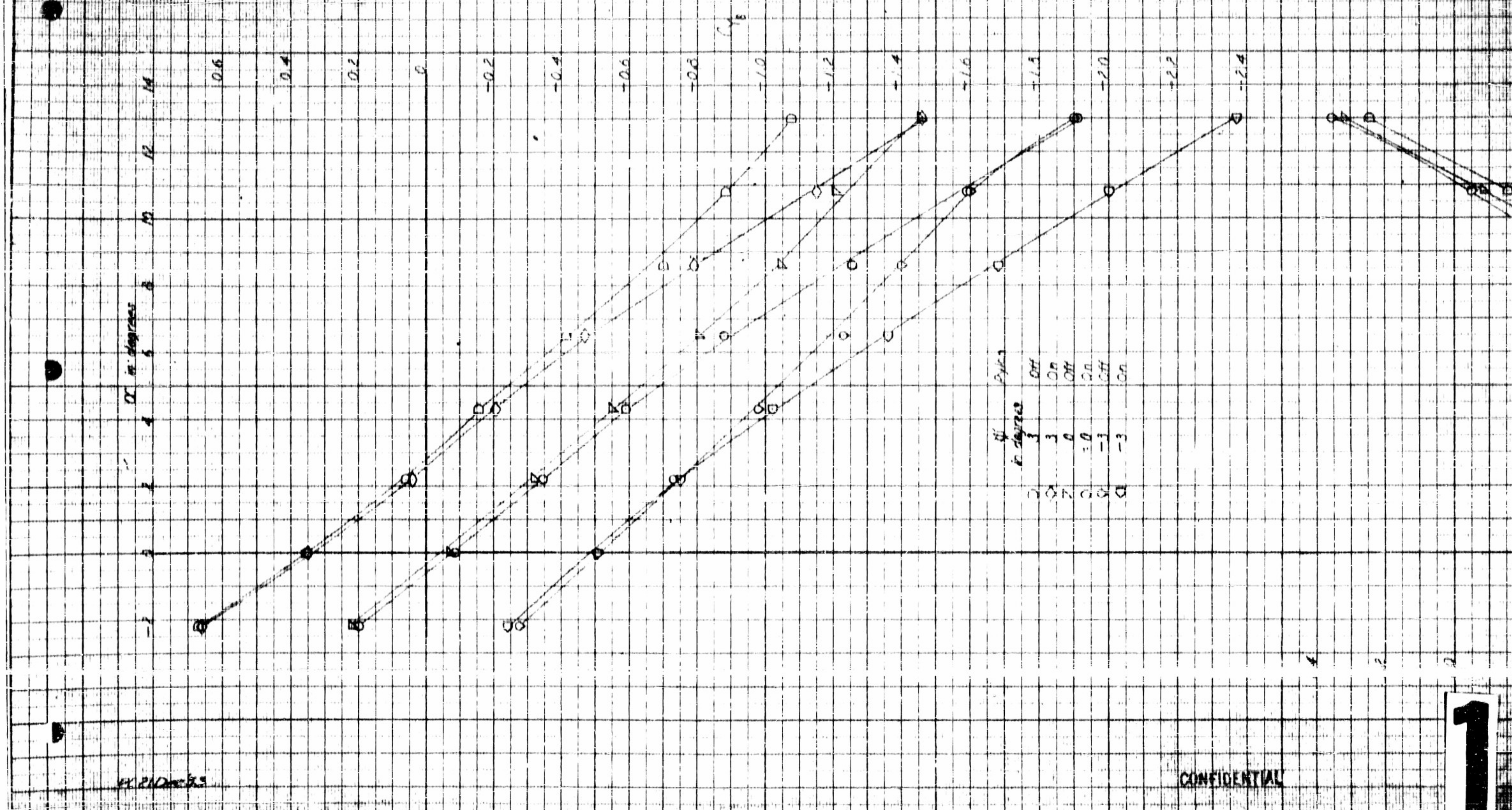

FL 21Dec53

CONFIDENTIAL

CONFIDENTIAL

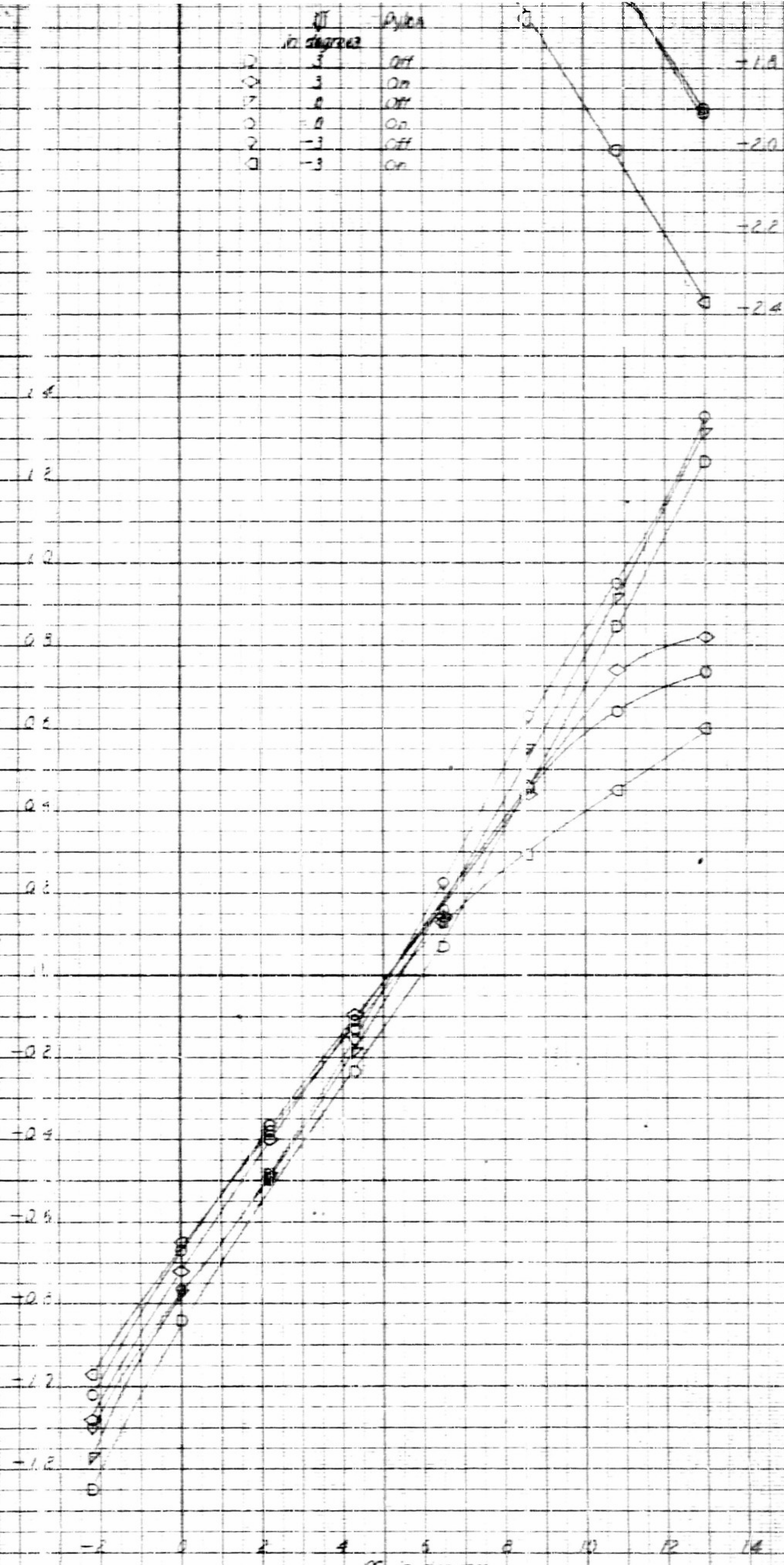

Figure 19-Effects of the Pylon and Airplane Yaw on the Aerodynamic Characteristics of a 0.17-Scale Model X44M-N-4 Cruise Missile in the Proximity of a 0.170-Scale Model F4D-1 Airplane at the Outboard Station

(1) z=4 Inch, x=0 Inch, $\theta_p=0°$; $\Psi_i=0°$

FIGURE 19 a

CONFIDENTIAL

145

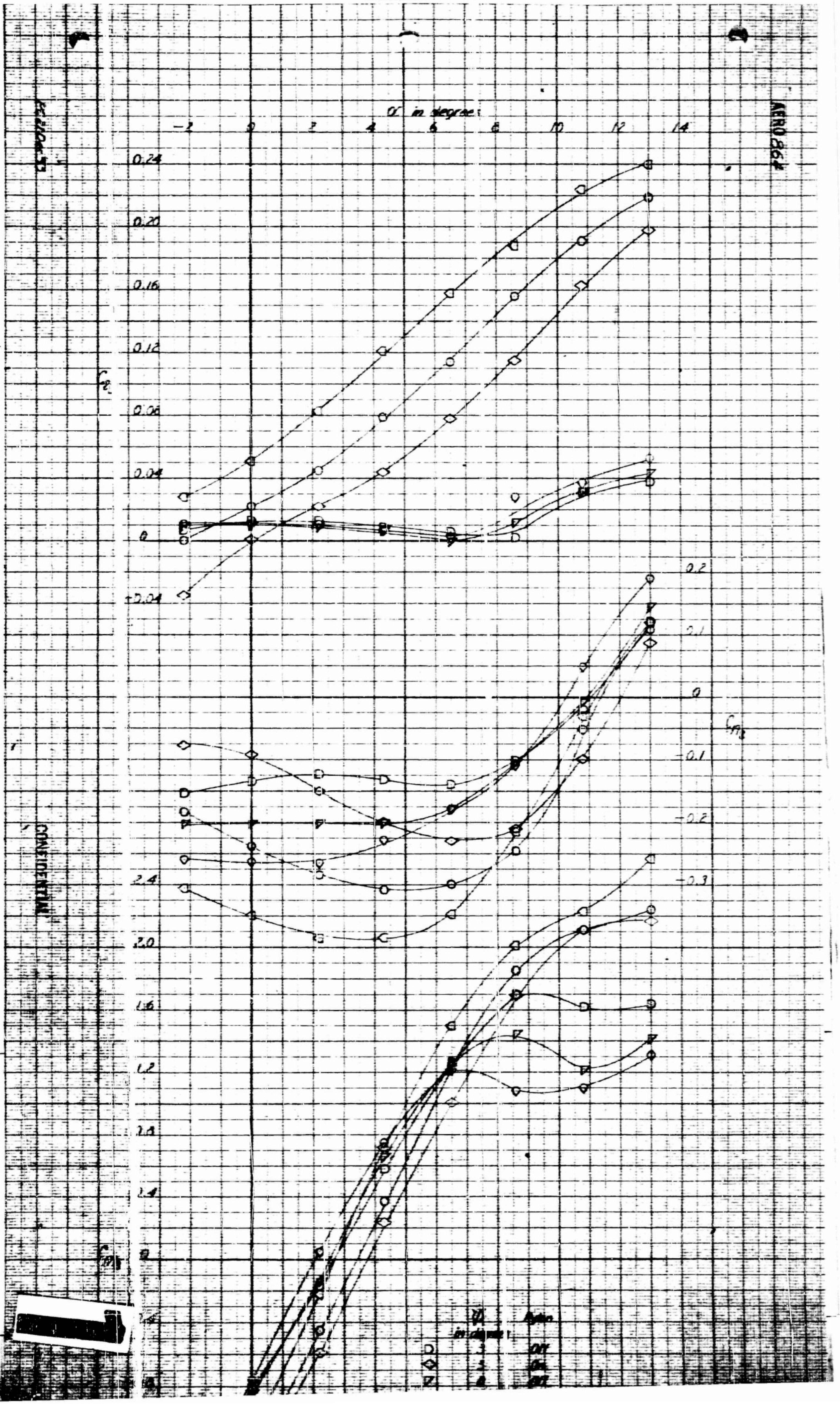
AERO 864
α in degrees
-2
0
2
4
6
8
10
12
14
0.24
0.20
0.16
0.12
0.08
0.04
0
-0.04
C_{l_3}
0.2
0.1
0
-0.1
-0.2
-0.3
C_{n_3}
2.4
2.0
1.6
1.2
0.8
0.4
0
C_{m_3}
CONFIDENTIAL
in degrees
Rudder
Off
On
Off

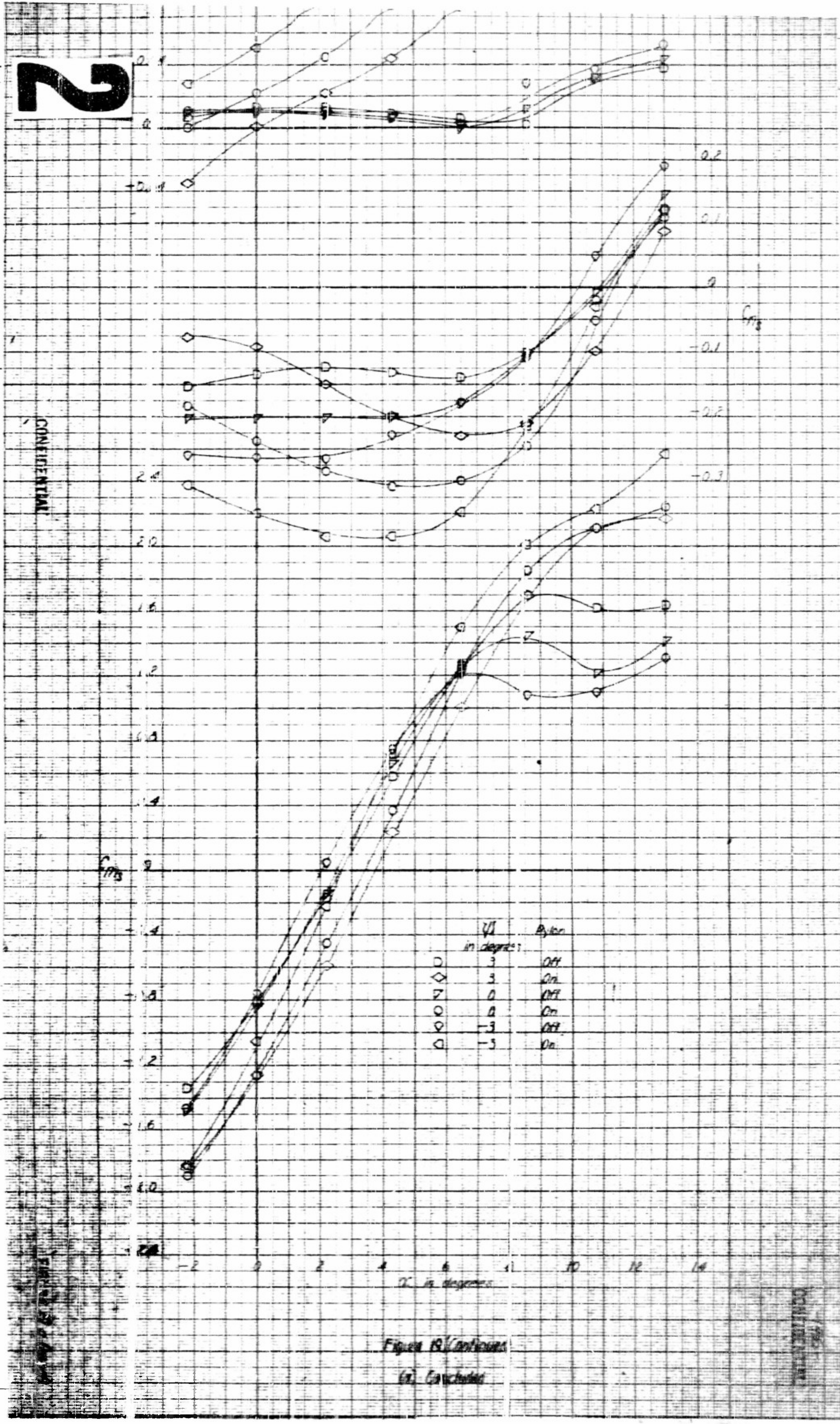

CONFIDENTIAL

Figure 19.- Continued.
(a) Concluded.

CONFIDENTIAL

AERO 864

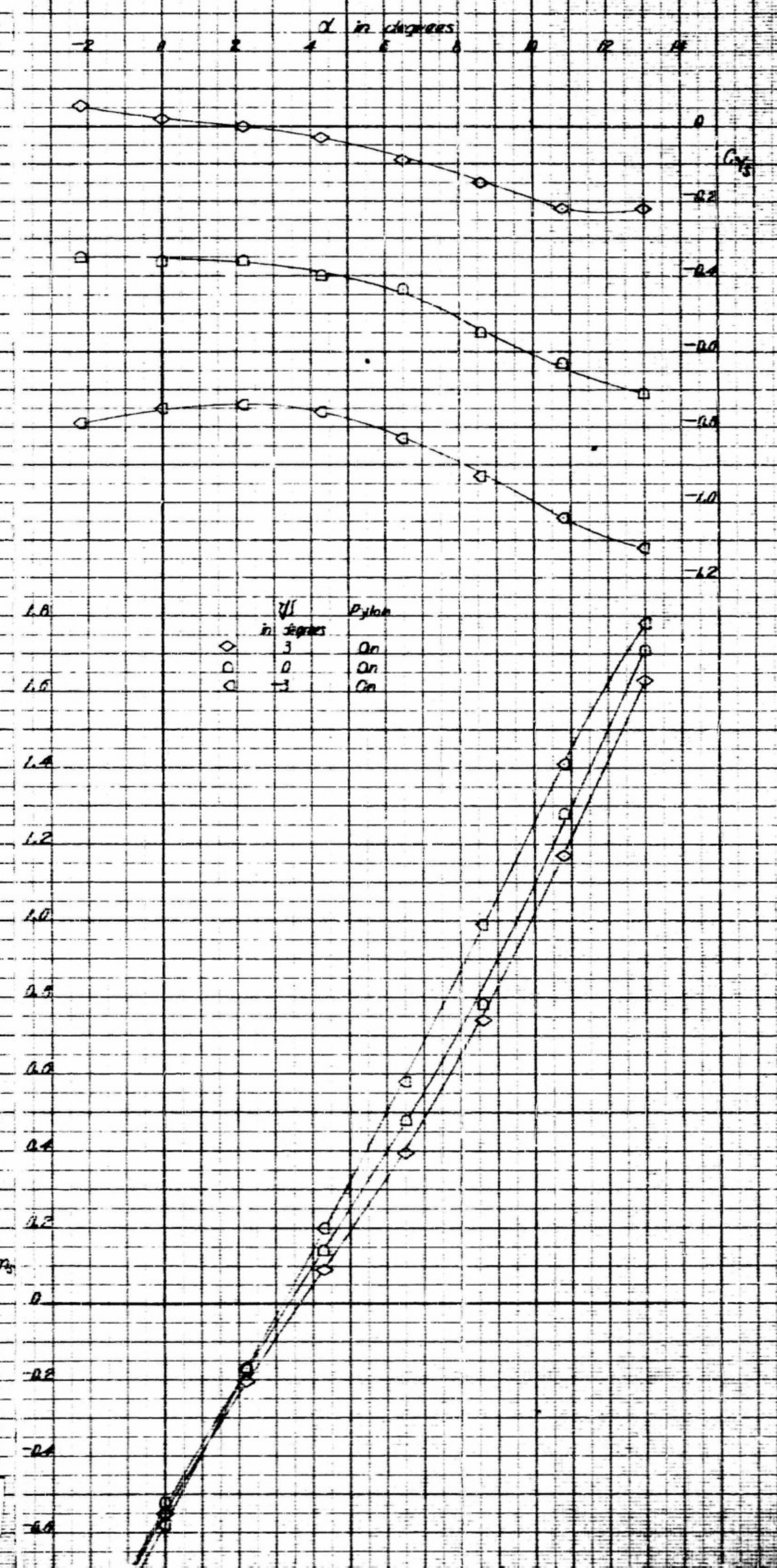

CONFIDENTIAL

CONFIDENTIAL

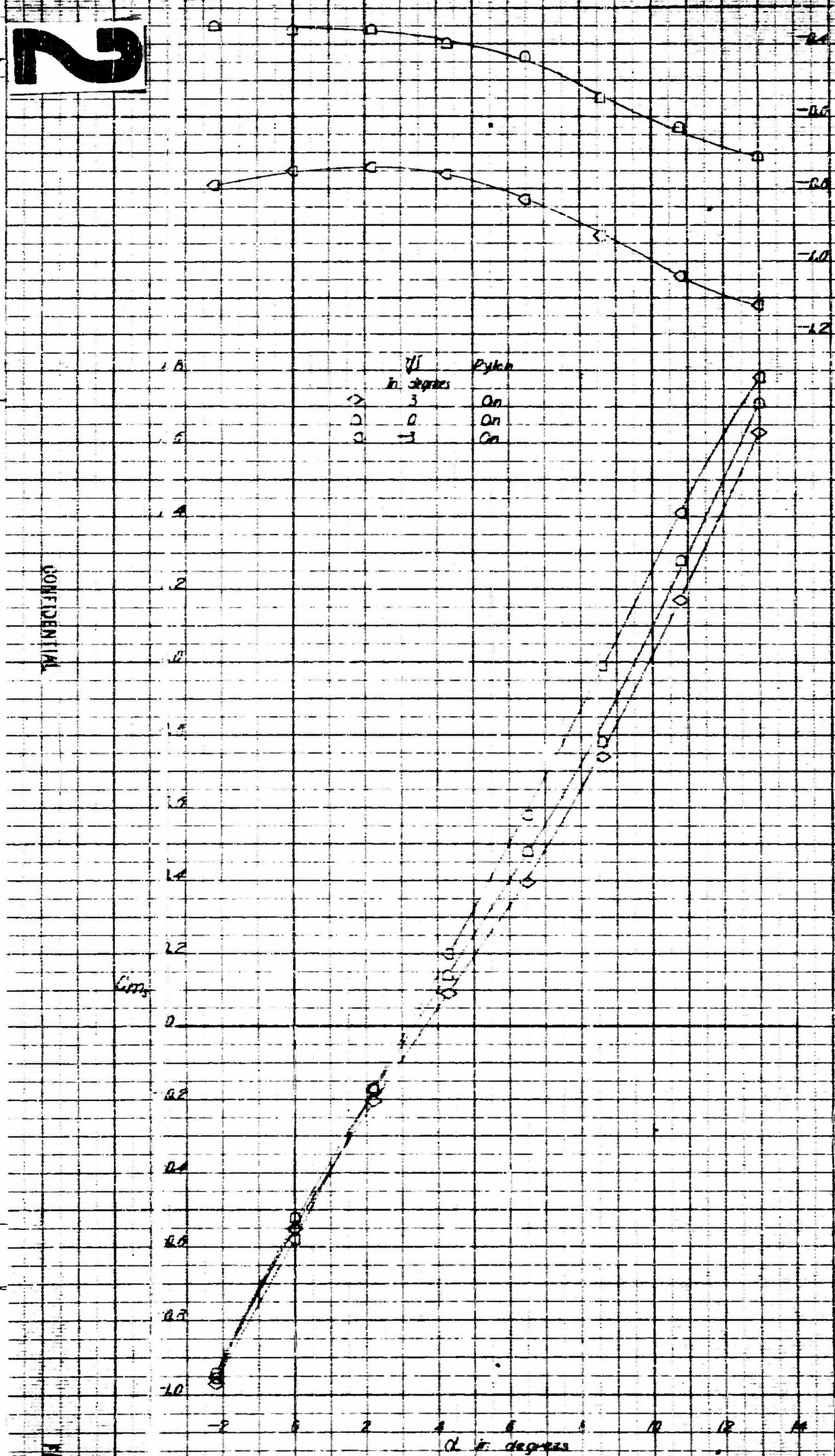

Figure 19 (Continued)

(b) $z = 2.04$ Inches, $x = 18.36$ Inches, $\theta_s = 7°$, $\psi_s = 0°$

FIGURE 19 b

CONFIDENTIAL

AERO 864

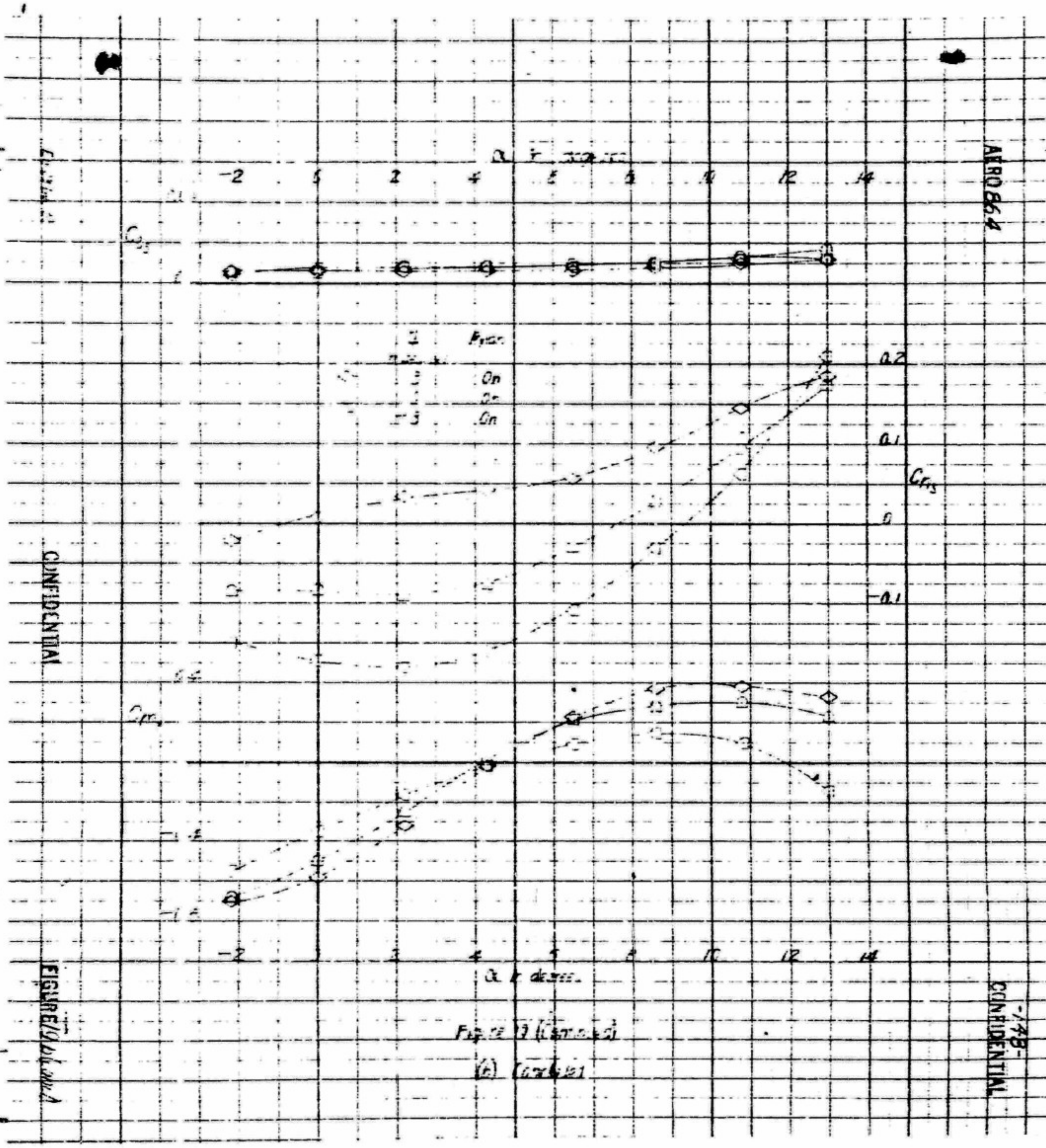

CONFIDENTIAL

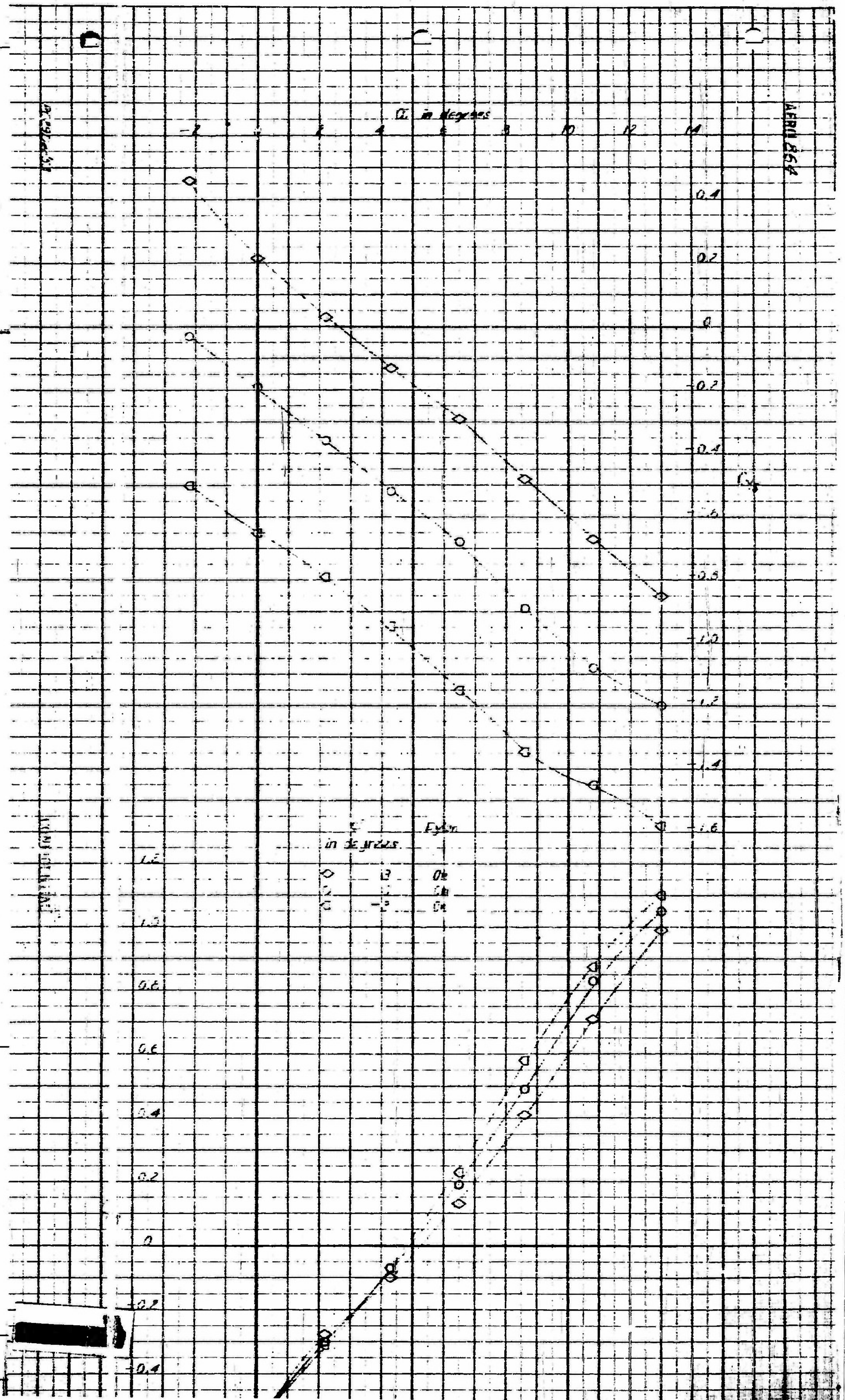

α in degrees
-2
2
4
6
8
10
12
14
0.4
0.2
0
-0.2
-0.4
-0.8
-1.0
-1.2
-1.4
-1.6
in degrees
1.2
1.0
0.8
0.6
0.4
0.2
0
-0.2
-0.4
AERIL 864

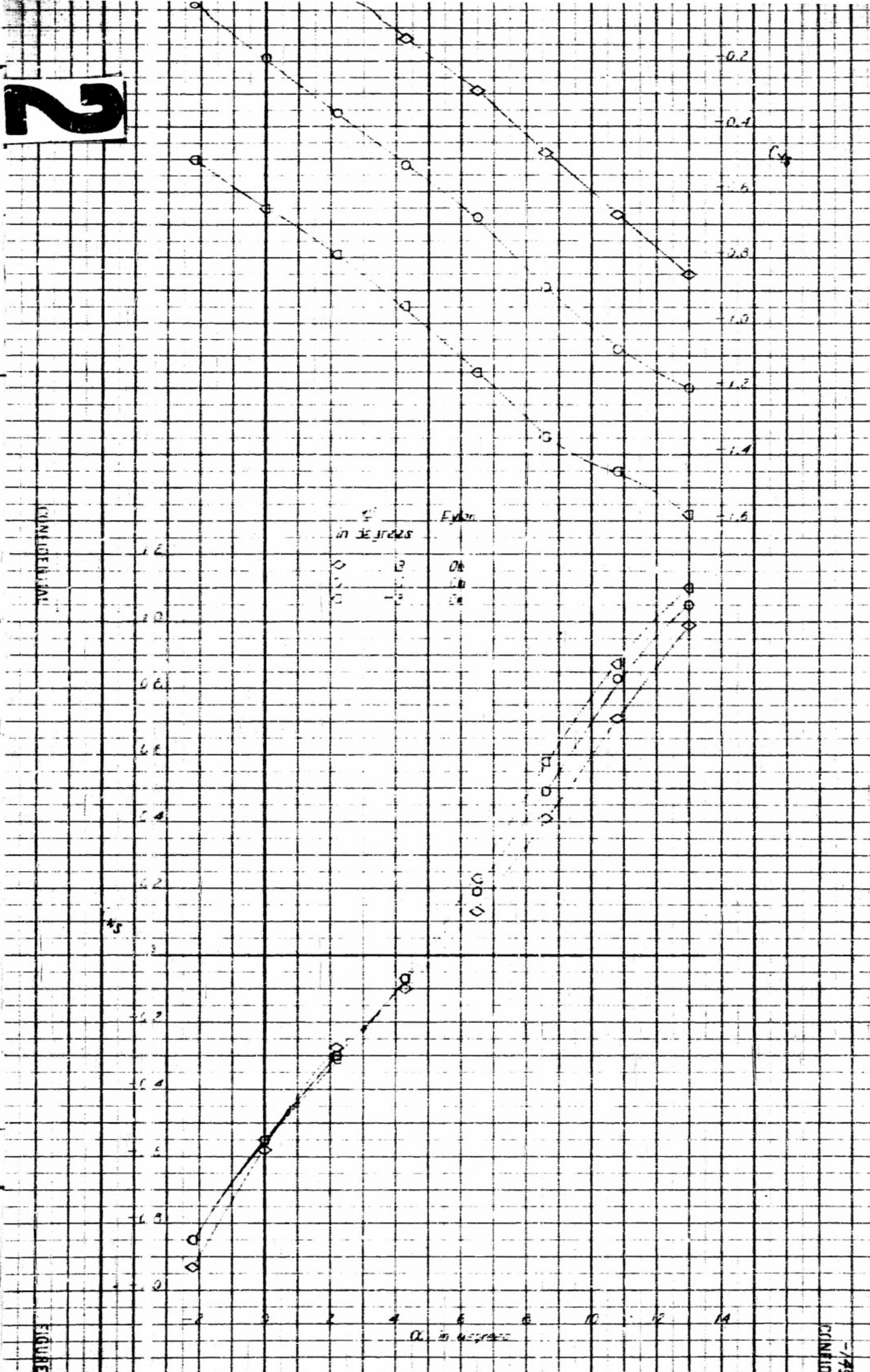

Figure 19(Continued)

(c) $z = 4.06$ inches, $x = 0$ inch, $\theta_s = 0°$, $\psi_s = 0°$

CONFIDENTIAL

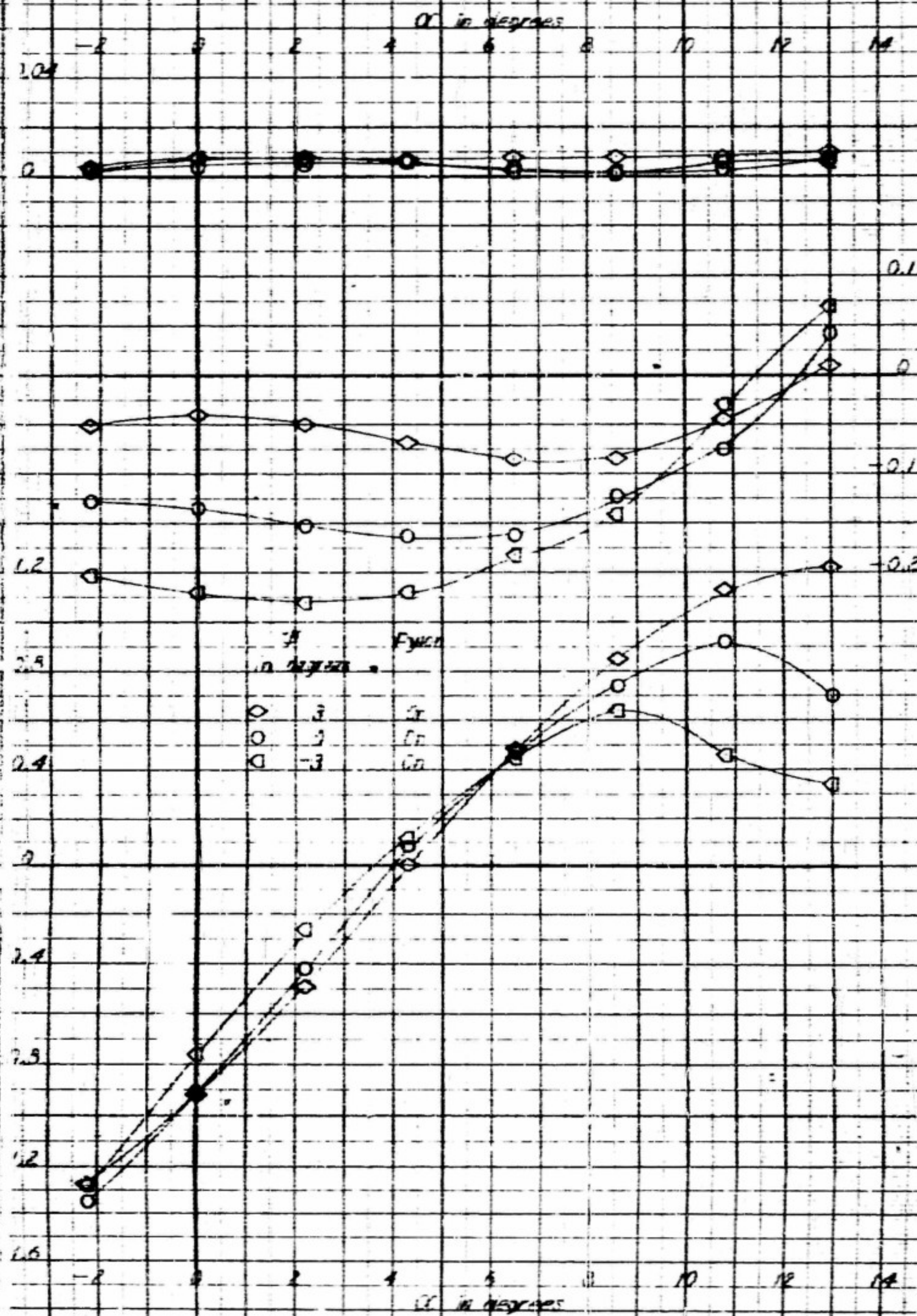

Figure 19 (Concluded)

(c) Concluded

FIGURE 19c (Concl)

CONFIDENTIAL

CONFIDENTIAL

AERO 664

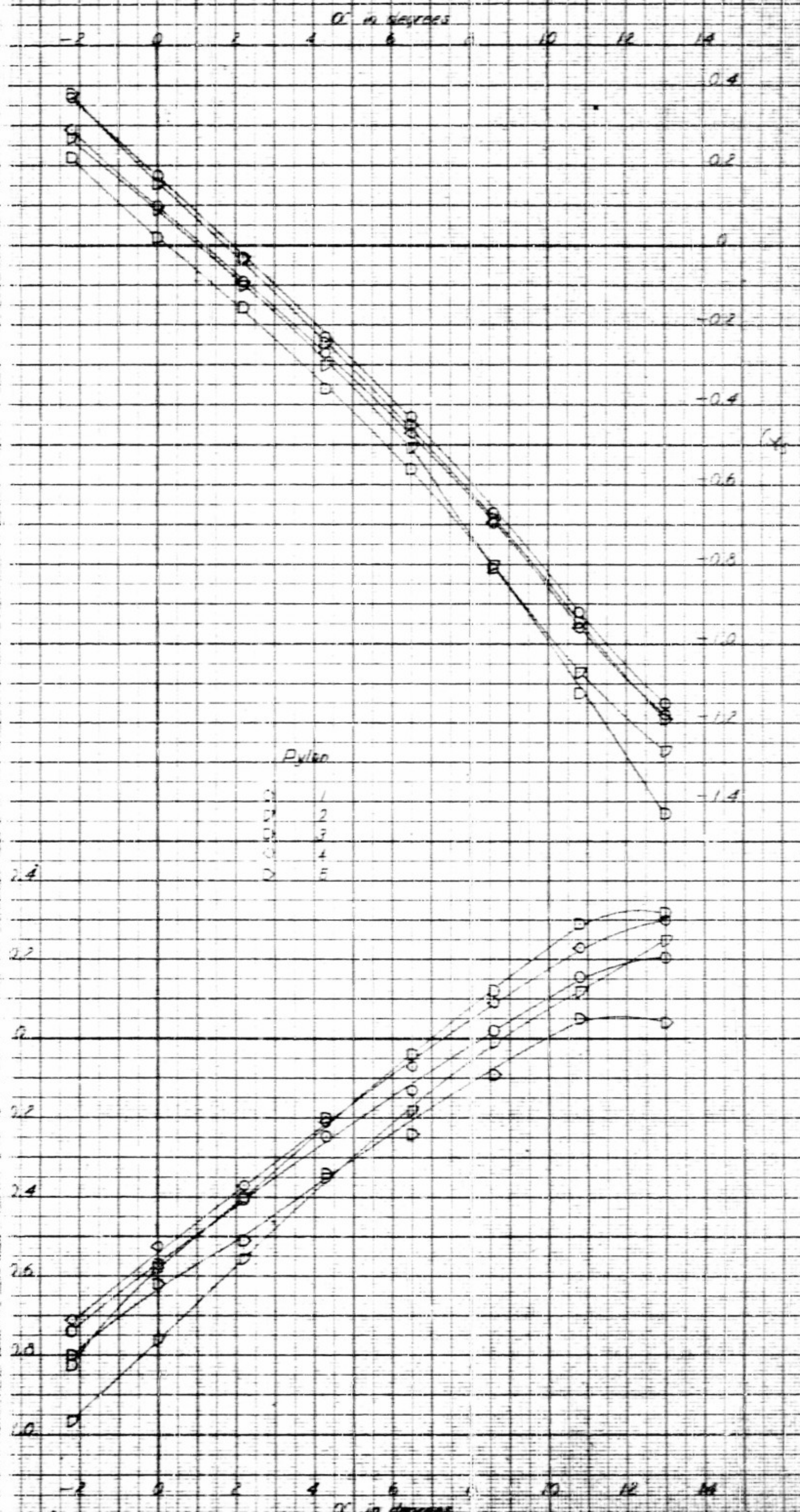

[redacted]

Figure 80 – Effect of Several Pylon Configurations on the Aerodynamic Characteristics of [illegible] Scale Model XAAM-N-2 Missile [illegible] on α

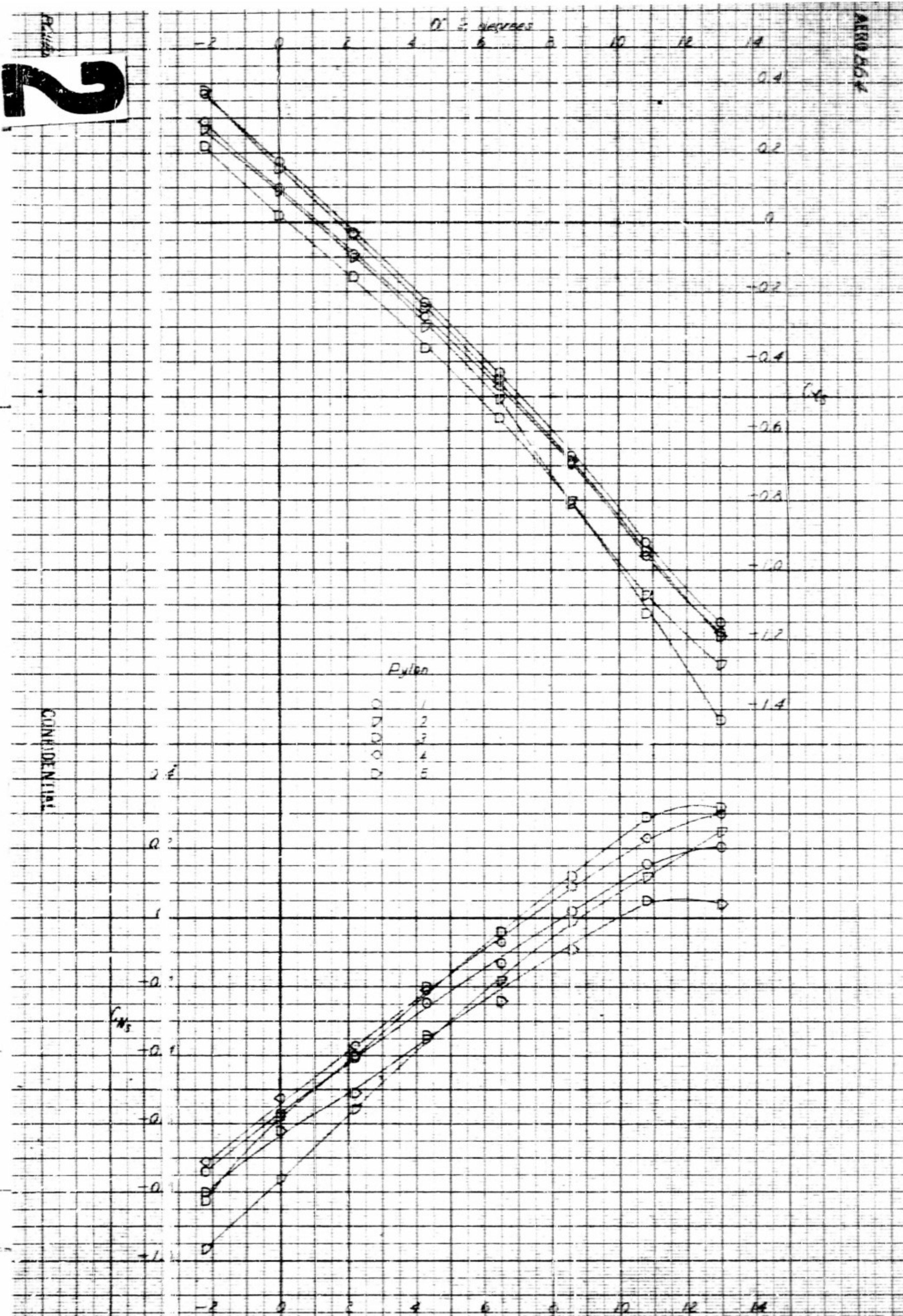

Figure 20 - Effect of Several Pylon Configurations on the Aerodynamic Characteristics of a 0.1?-Scale Model XAAM-N-4 Guide Missile Mounted on a 0.??-Scale Model F4D-1 Airplane

(a) Inboard Station, ψ = 0°

Figure 34

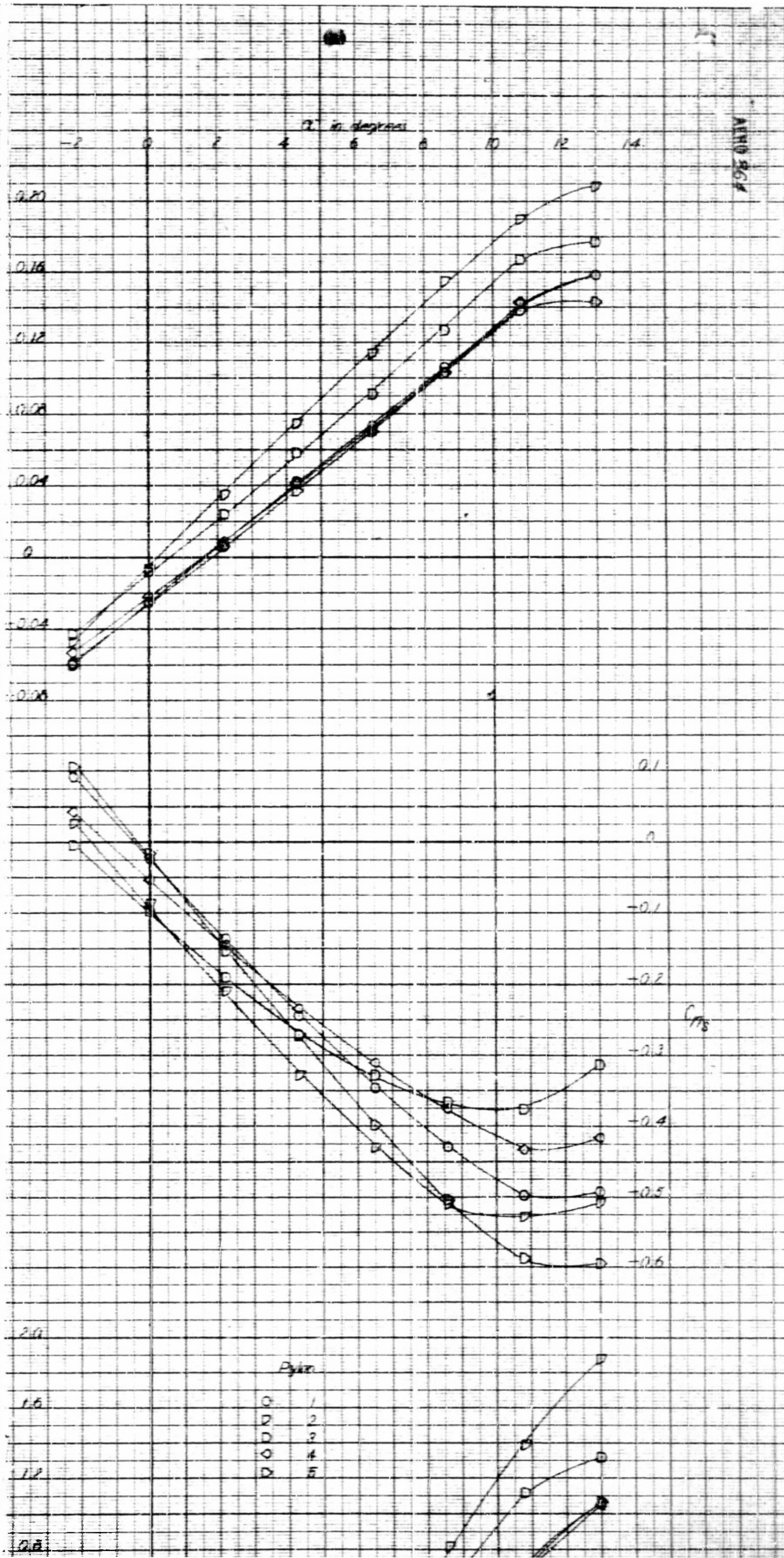

AERO 864

CONFIDENTIAL

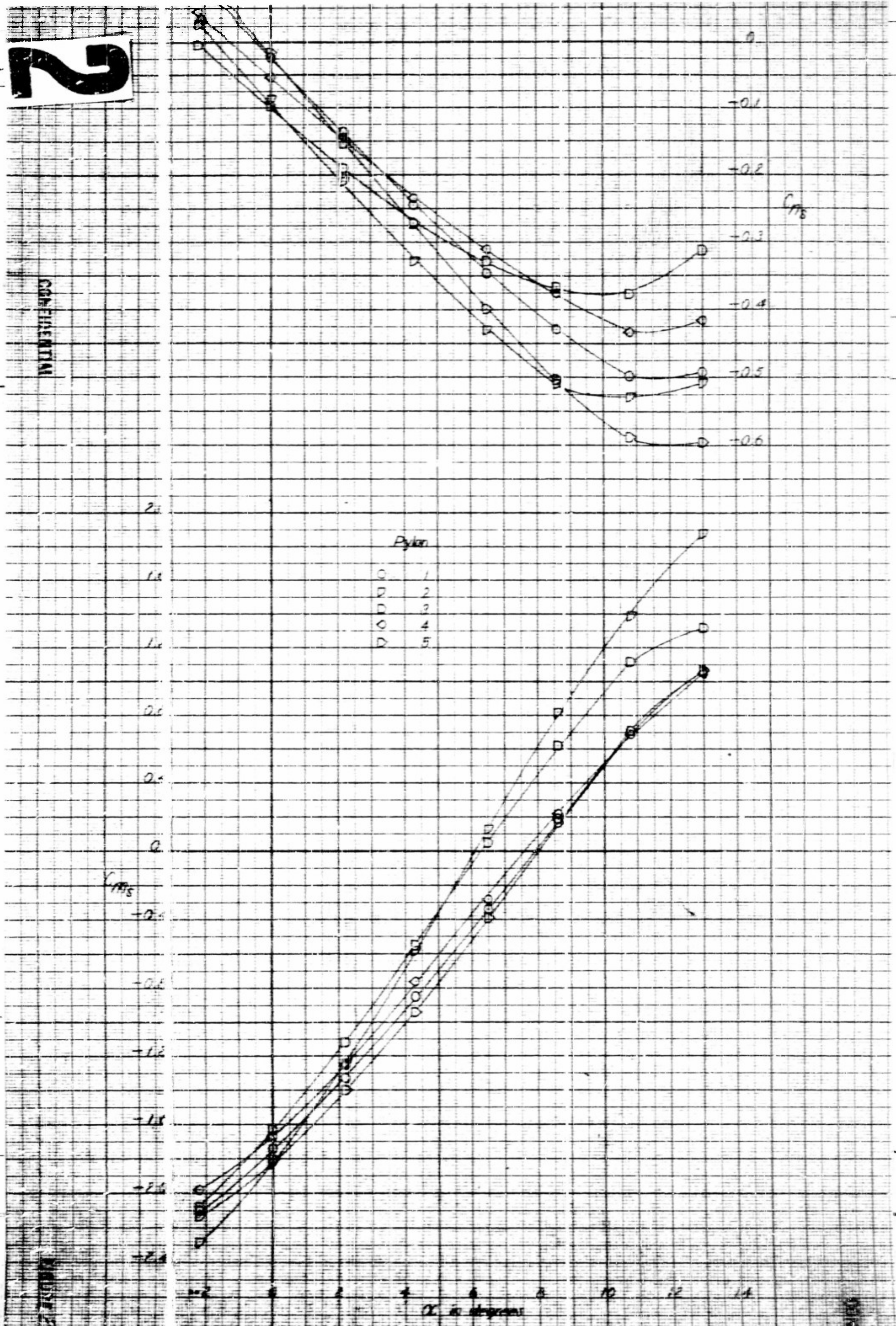

Figure 20(continued)

(i) Concluded

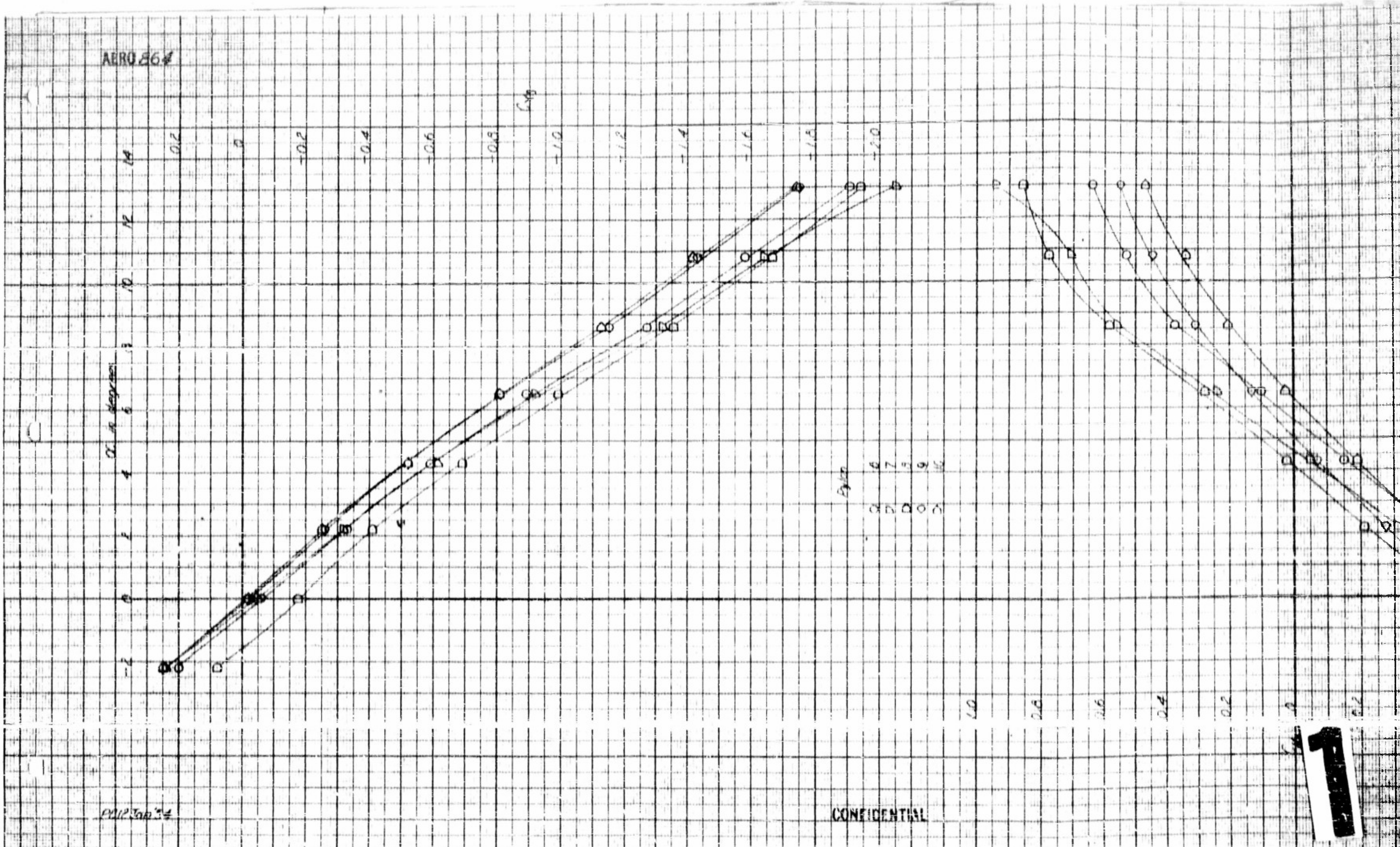

AERO 864
α in degrees
Pylon
6
7
8
9
10
CONFIDENTIAL

CONFIDENTIAL

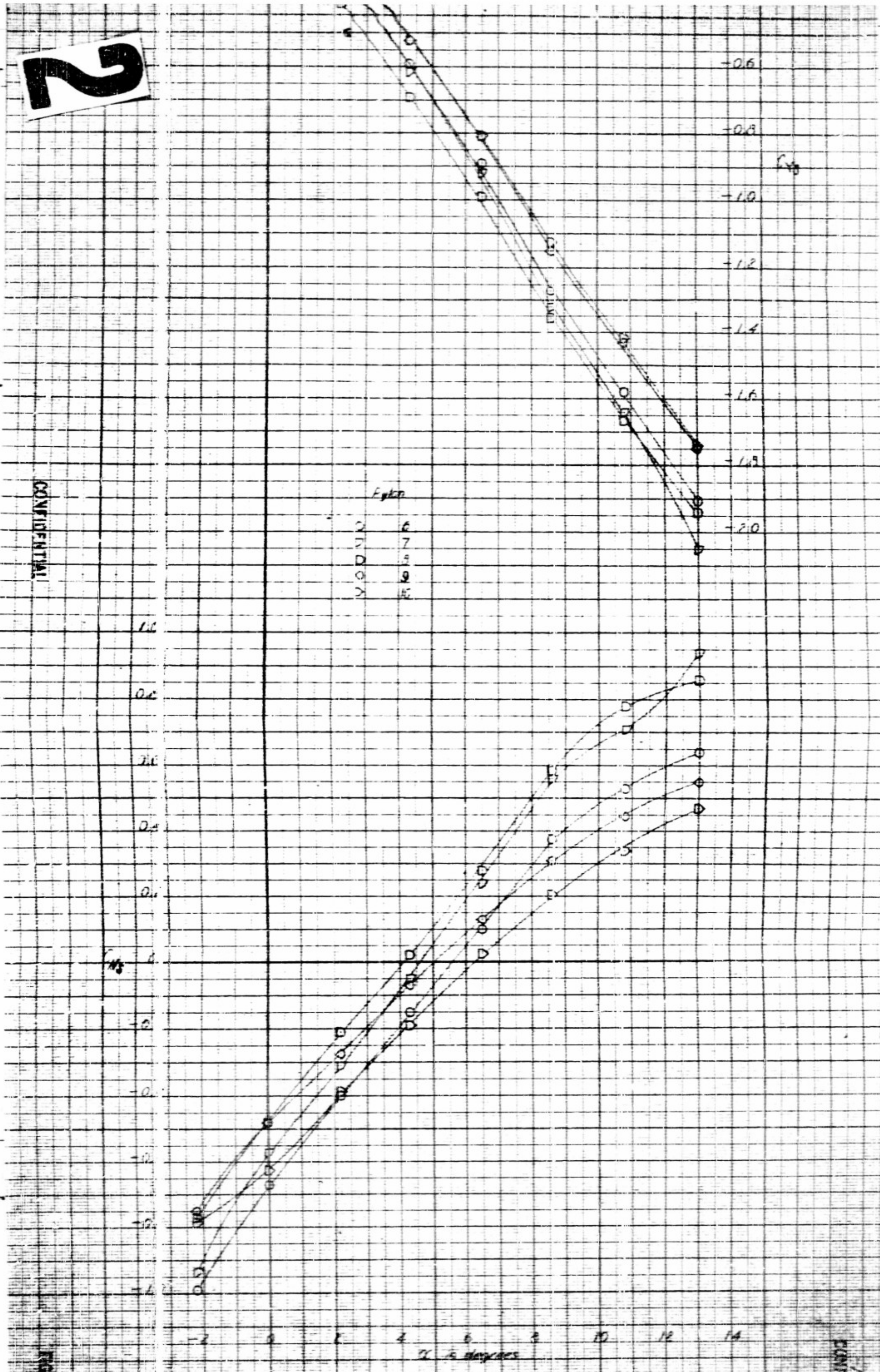

Figure 20 (Continued)

(b) Outboard Station, $\Psi = 0°$

CONFIDENTIAL

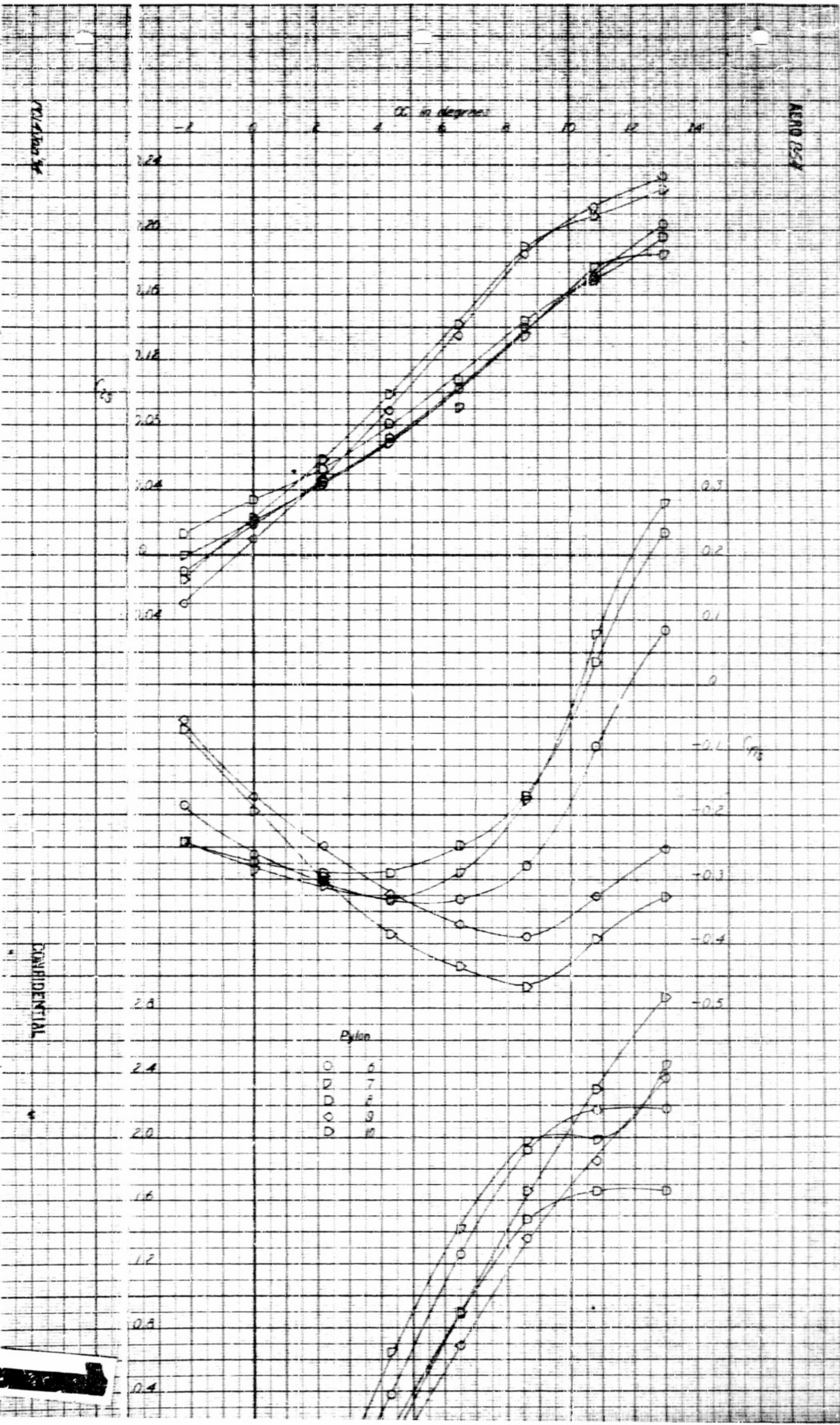

Jan '47
AERO 2554
α in degrees
-2 0 2 4 6 8 10 12 14
0.24 0.20 0.16 0.12 0.08 0.04 0 -0.04
0.3 0.2 0.1 0 -0.1 -0.2 -0.3 -0.4 -0.5
2.8 2.4 2.0 1.6 1.2 0.8 0.4
Pylon
6
7
8
9
10
CONFIDENTIAL

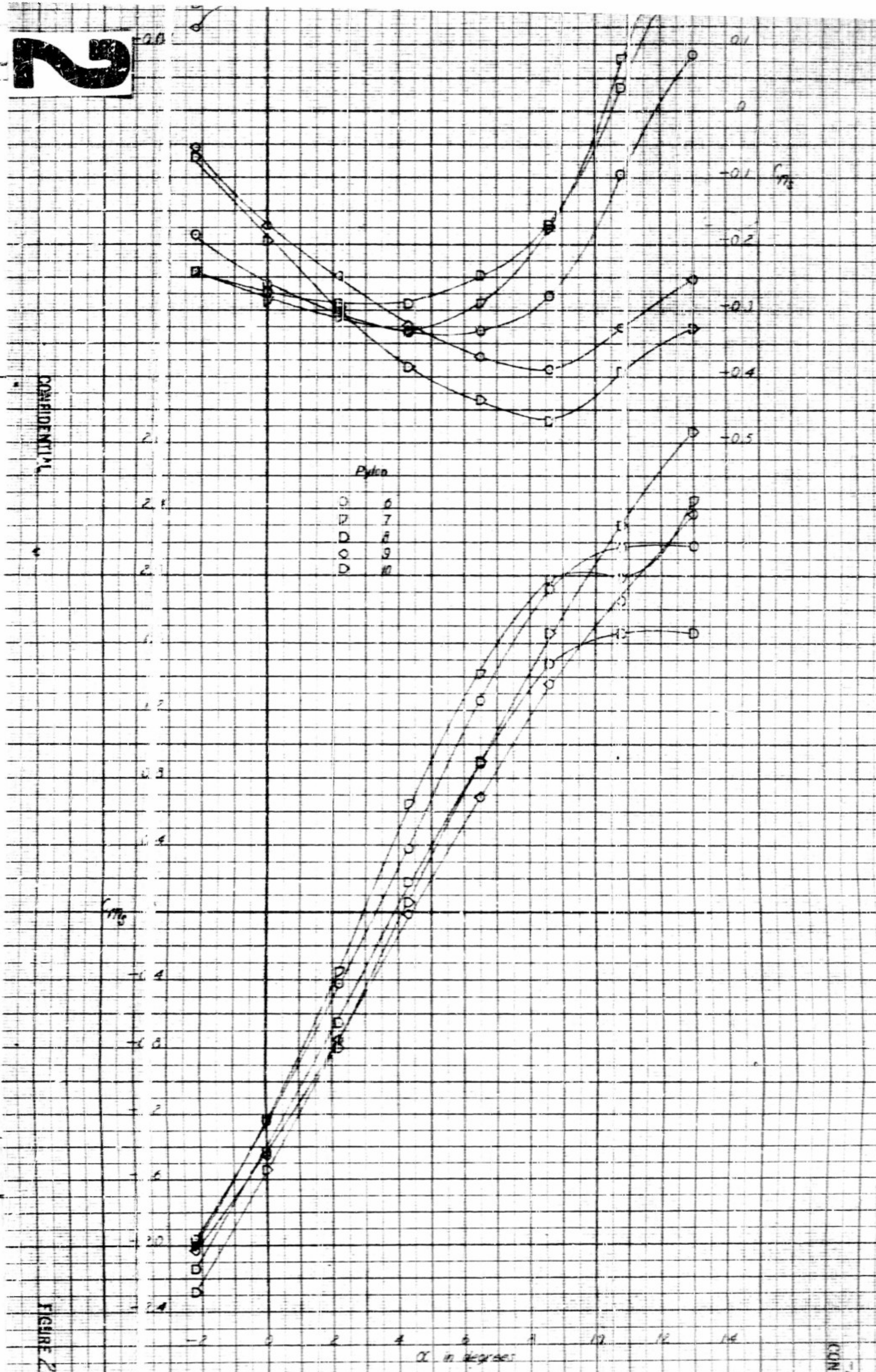

Figure 20 (Concluded)

(n) Concluded

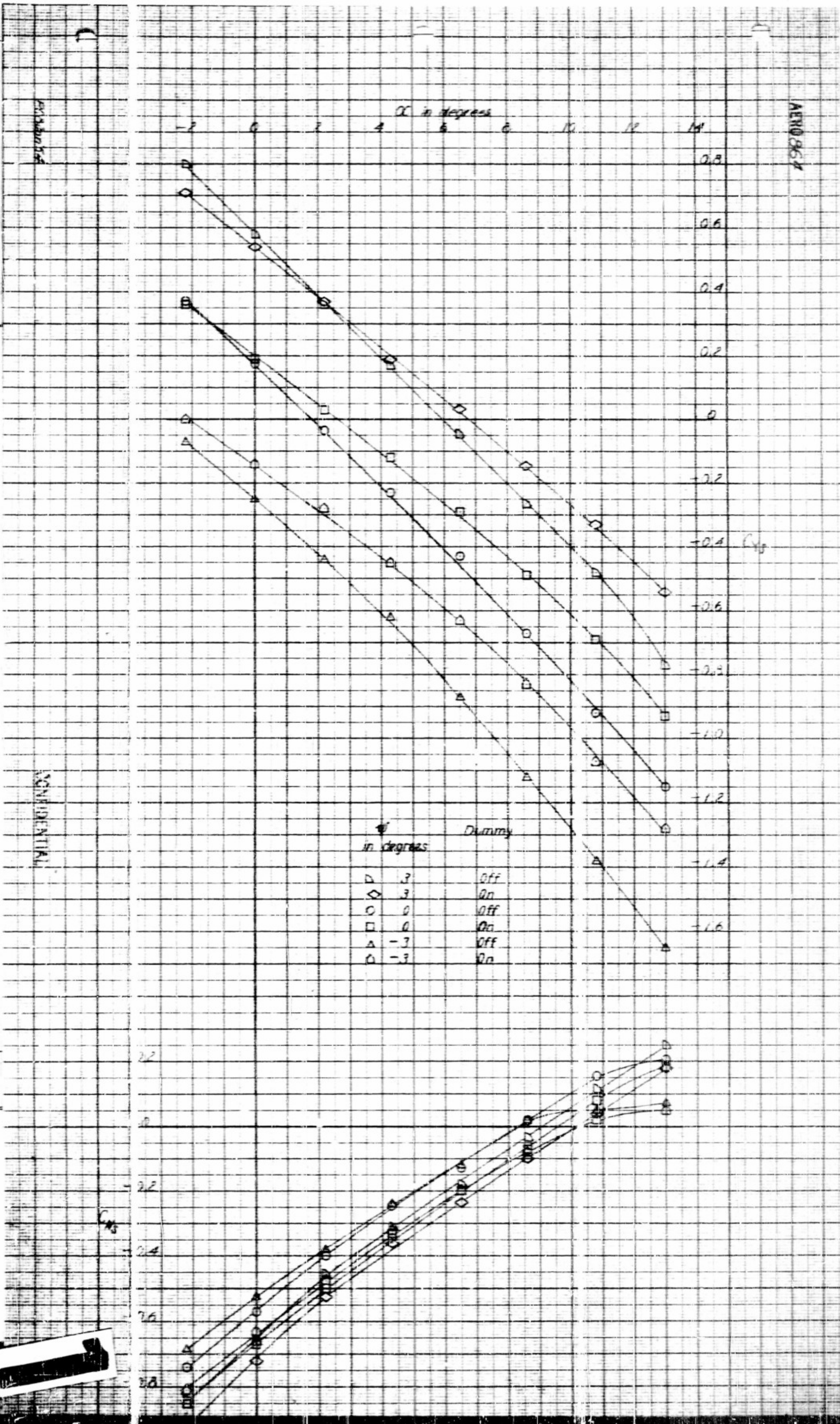

CONFIDENTIAL

AERO 864

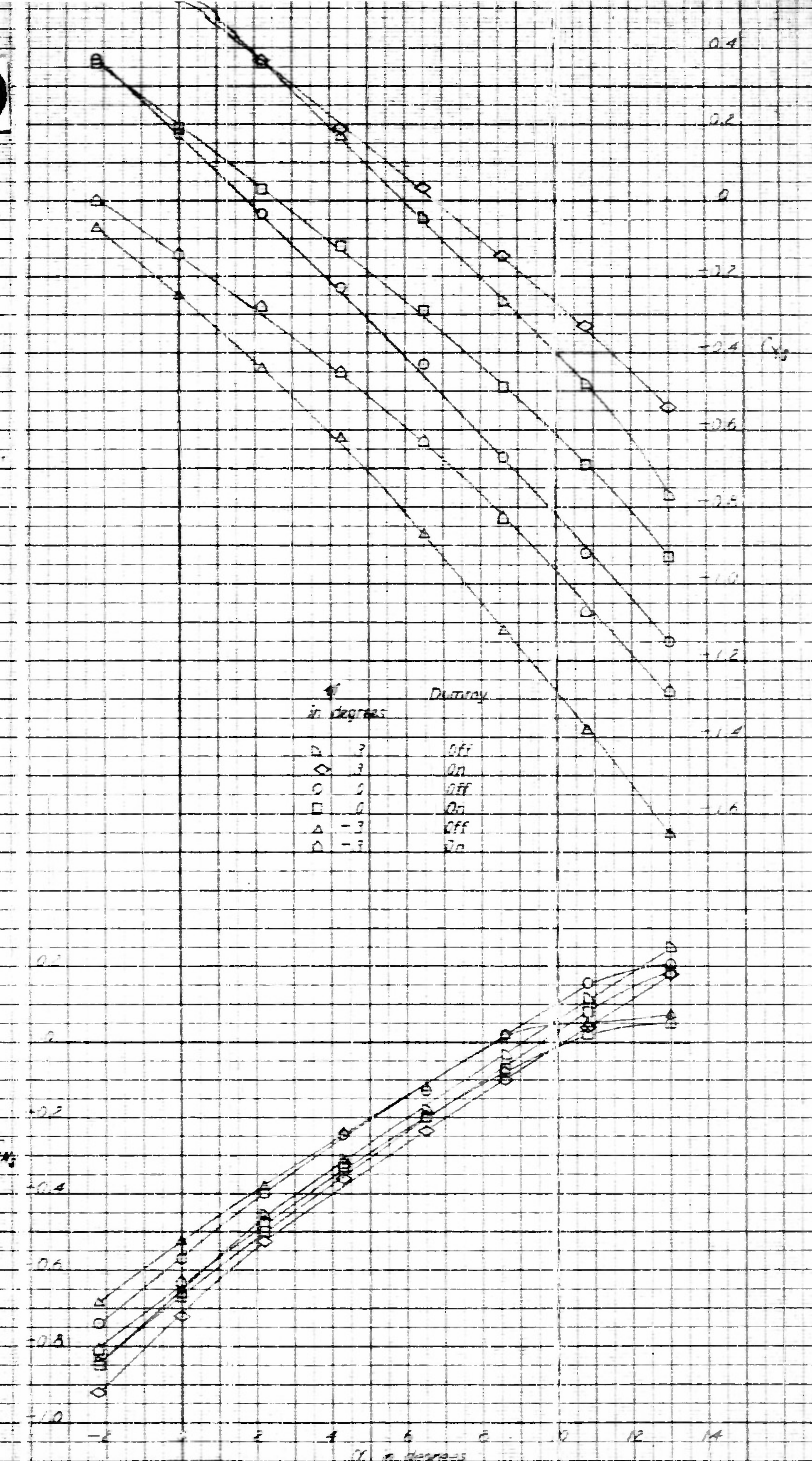

Figure 21 – Effect of Airplane Yaw and Dummy Missile on the Aerodynamic Characteristics of a 0.17-Scale Model XAAM-N-4 Dummy Missile Mounted on a 0.079-Scale Model F4D-1 Airplane.

(a) Inboard Station, Pylon 1.

FIGURE 21a

CONFIDENTIAL

CONFIDENTIAL

Figure 34

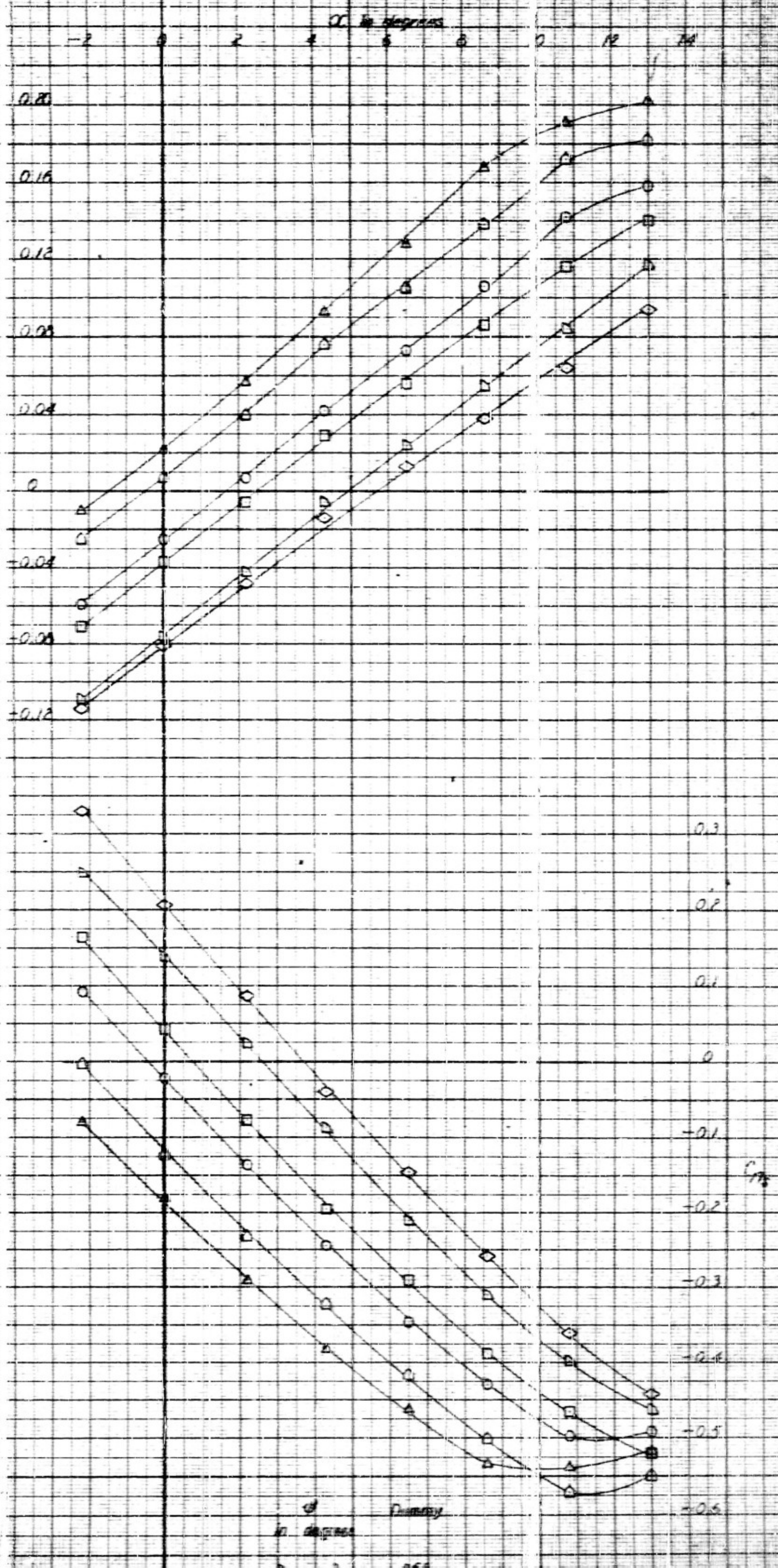

CONFIDENTIAL

AERO 2662

CONFIDENTIAL

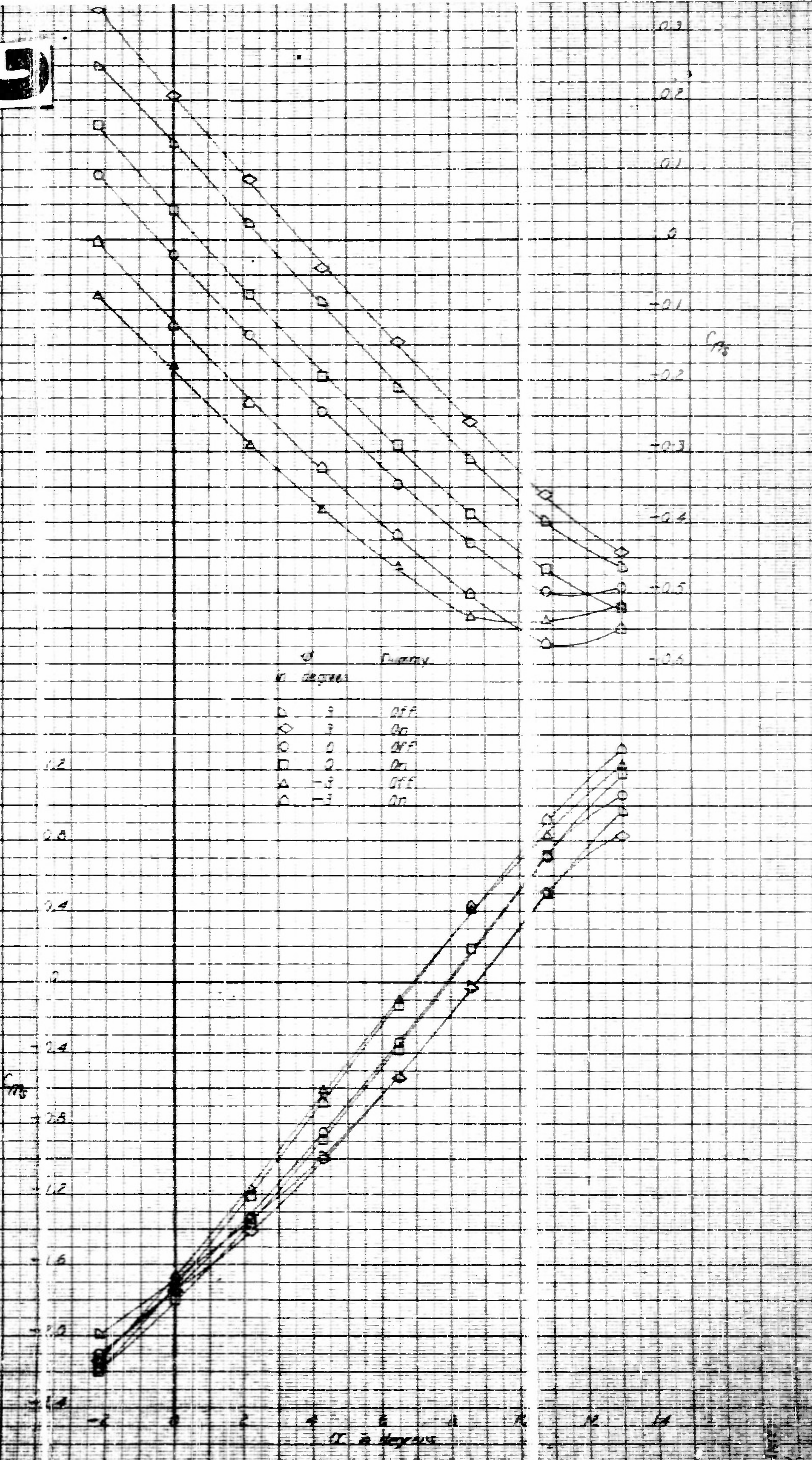

Figure 21(Continued)

(a) Concluded

CONFIDENTIAL

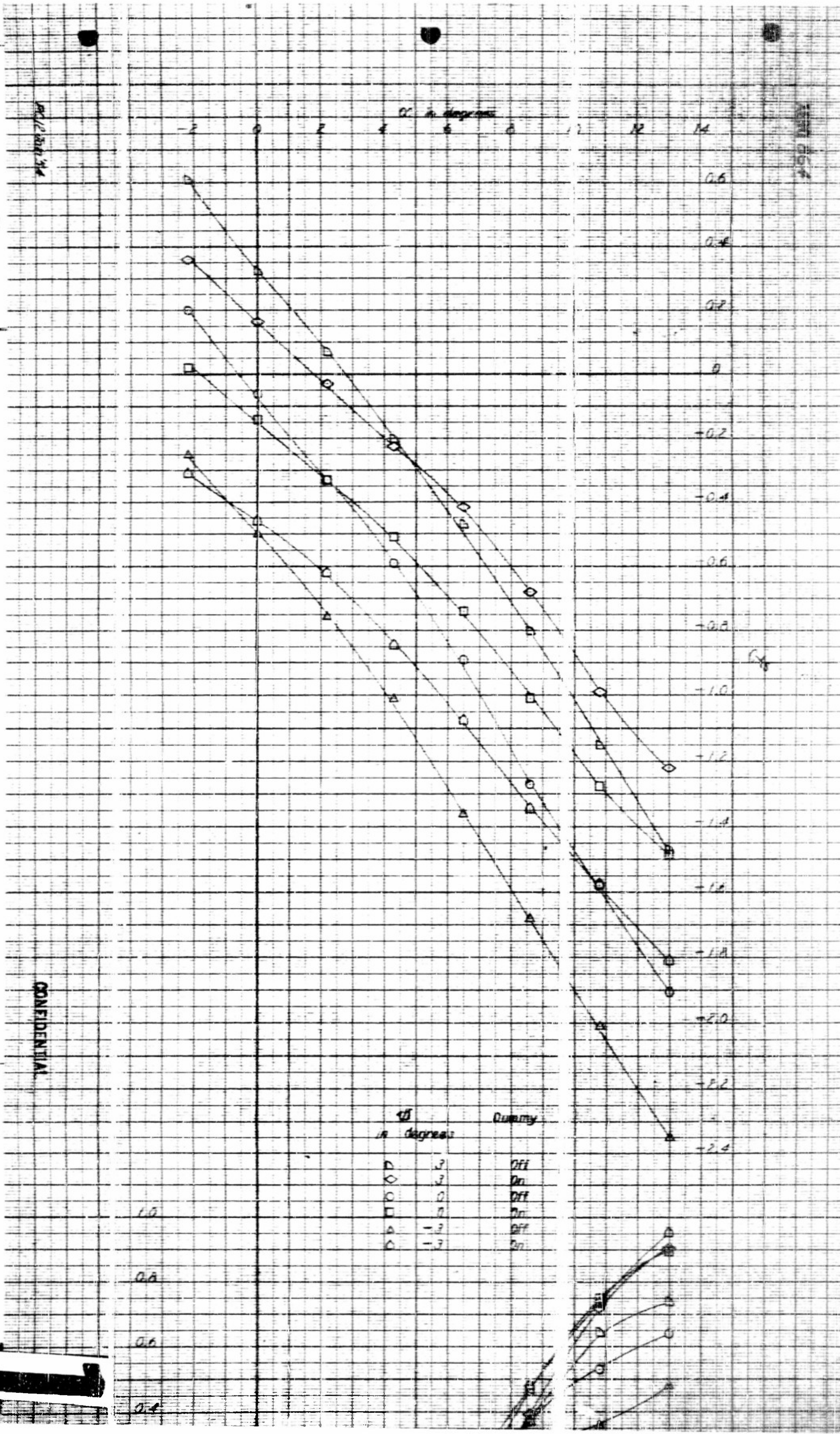

CONFIDENTIAL

CONFIDENTIAL

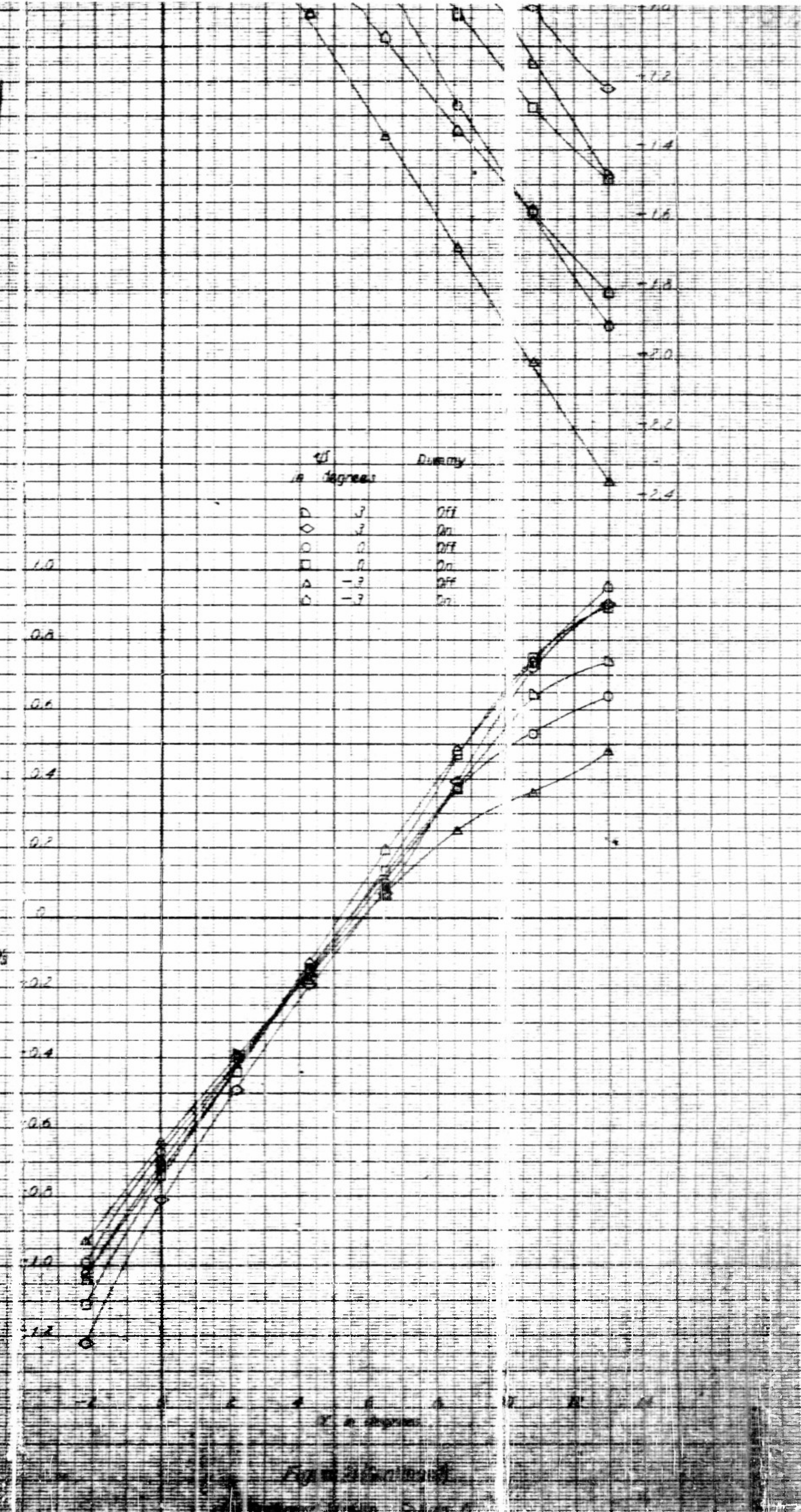

(Continued)

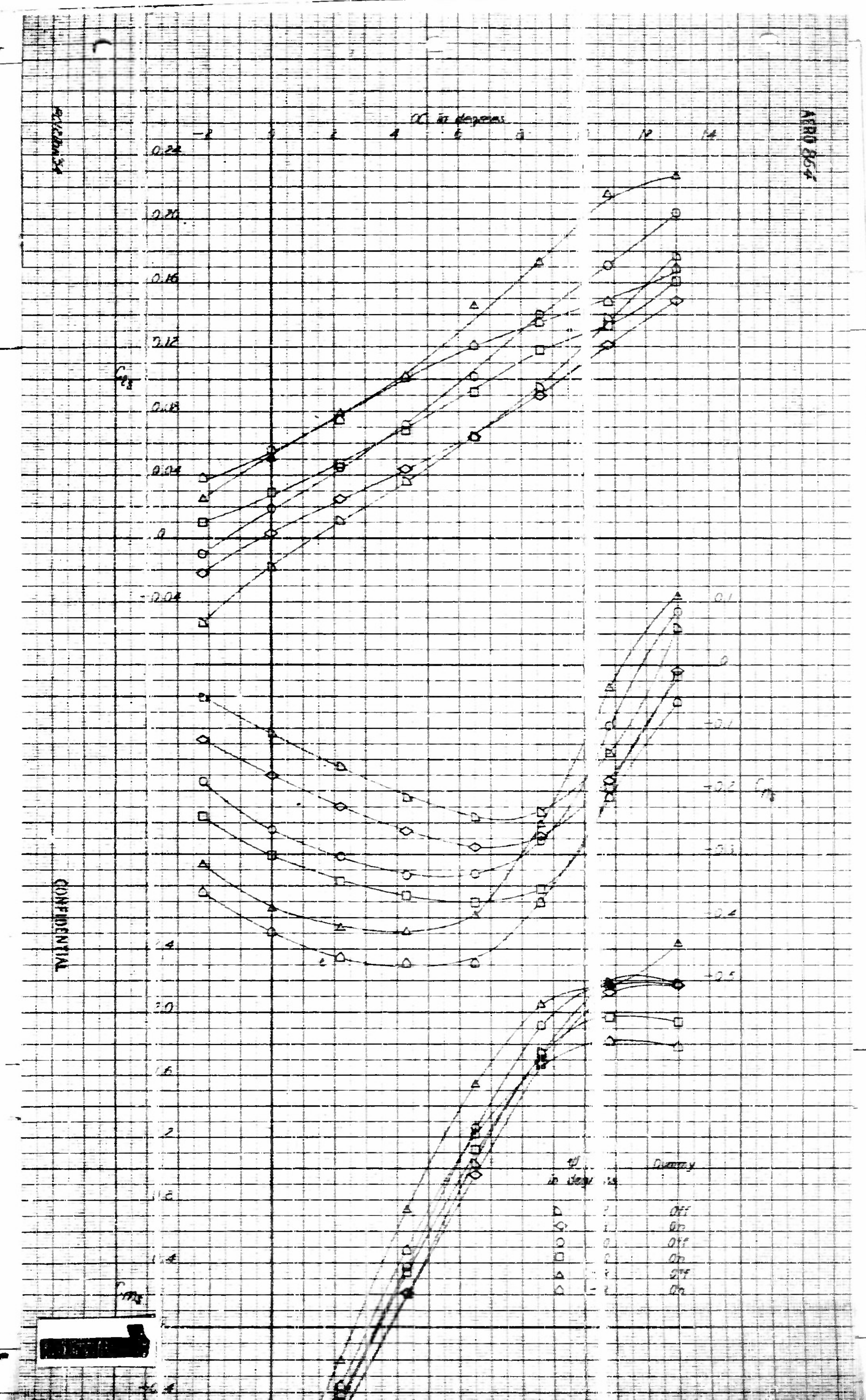

AERO 864
α in degrees
-2
0
2
4
6
8
10
12
14
0.24
0.20
0.16
0.12
0.08
0.04
0
-0.04
0.1
0
-0.1
-0.2
-0.3
-0.4
-0.5
Dummy
Off
On
Off
On
Off
On
CONFIDENTIAL

CONFIDENTIAL

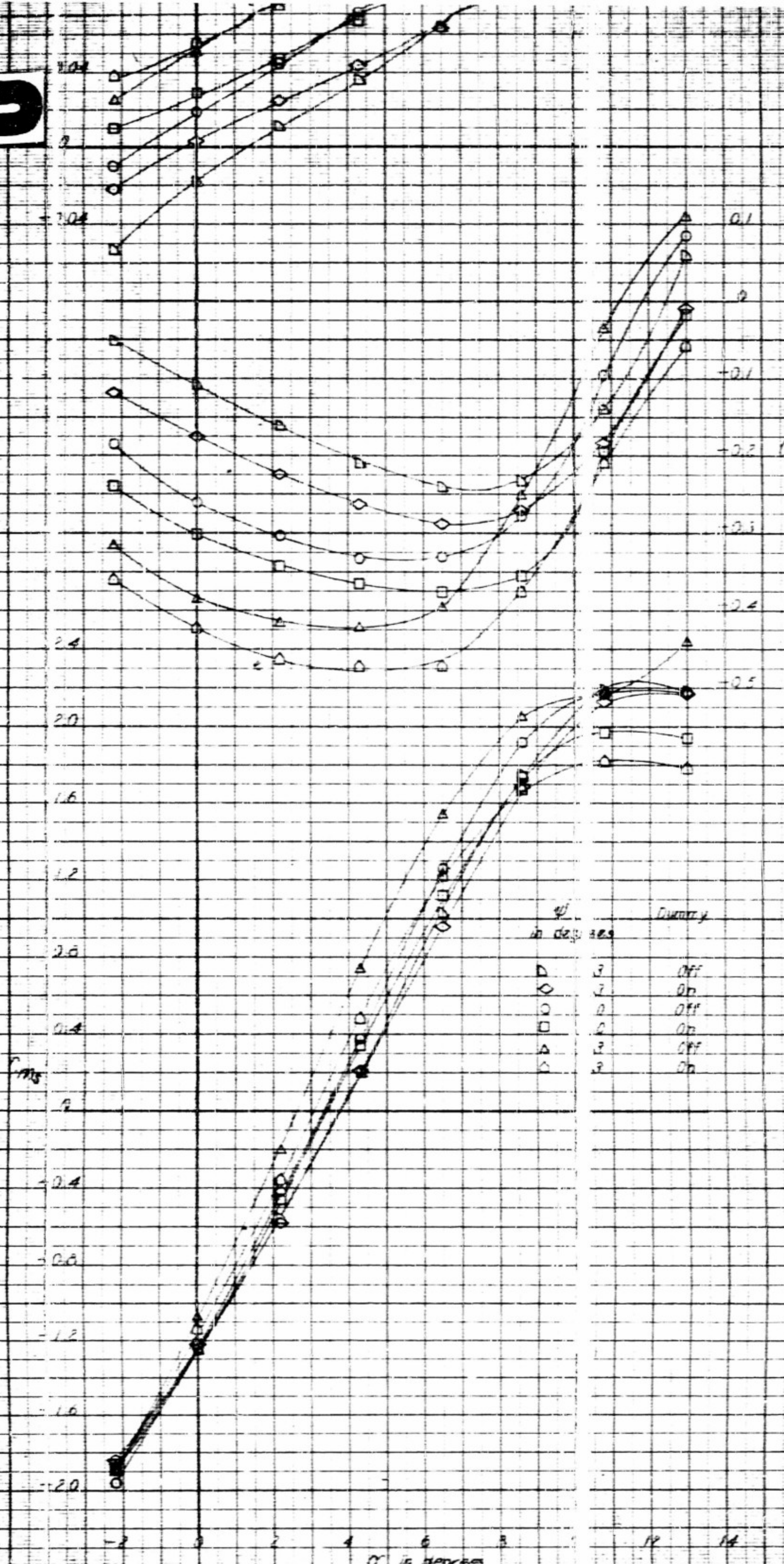

Figure 21(Concluded)

(b) Concluded

FIGURE 21b (cont.)

CONFIDENTIAL

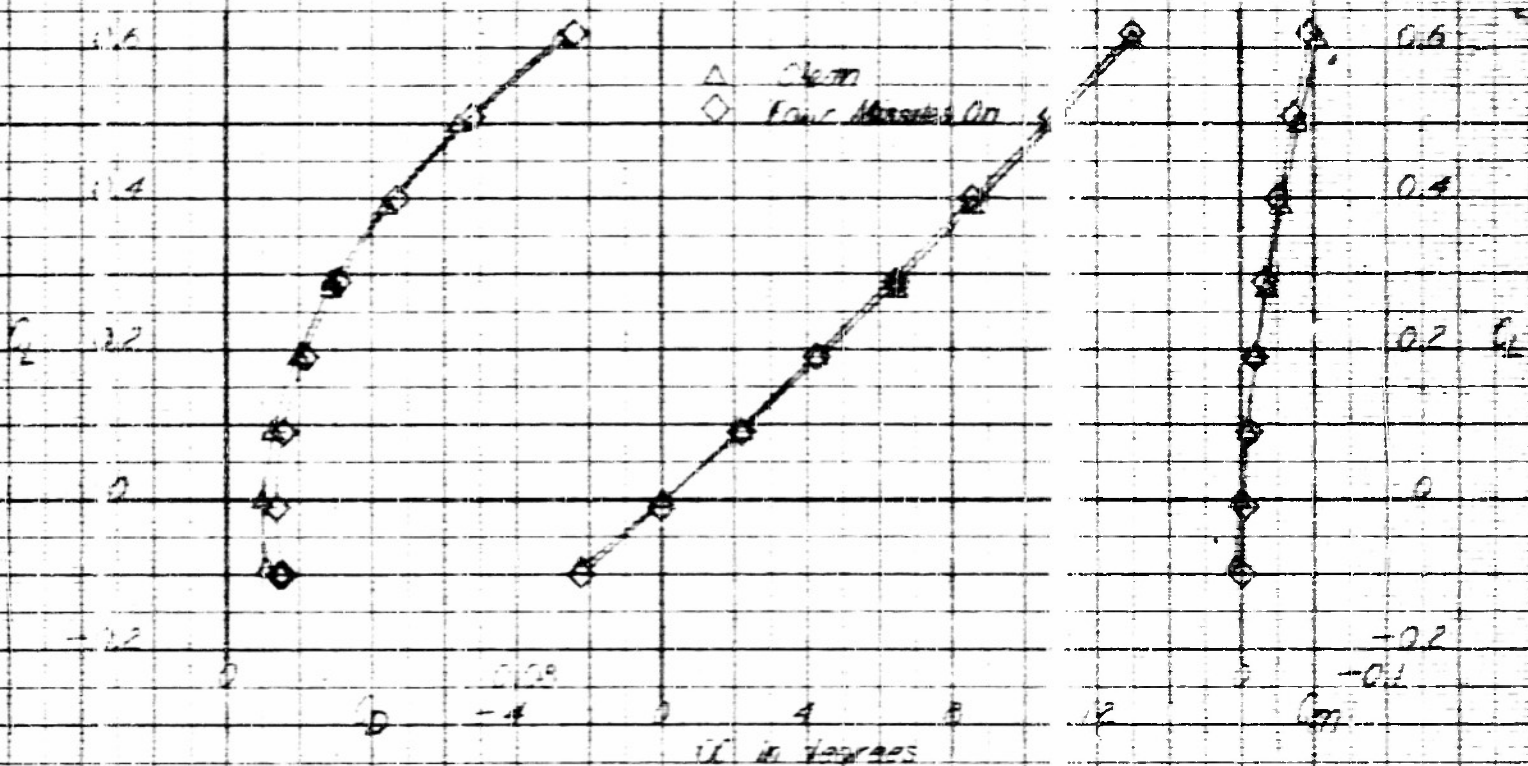

Figure 22—Longitudinal Characteristics of a 0.175-Scale Model F4D-1 Airplane Showing the Effect of Four 0.07-Scale Model XAAM-N-4 Circle Missiles Mounted on the Airplane

(a) Model Inverted, Tail Off

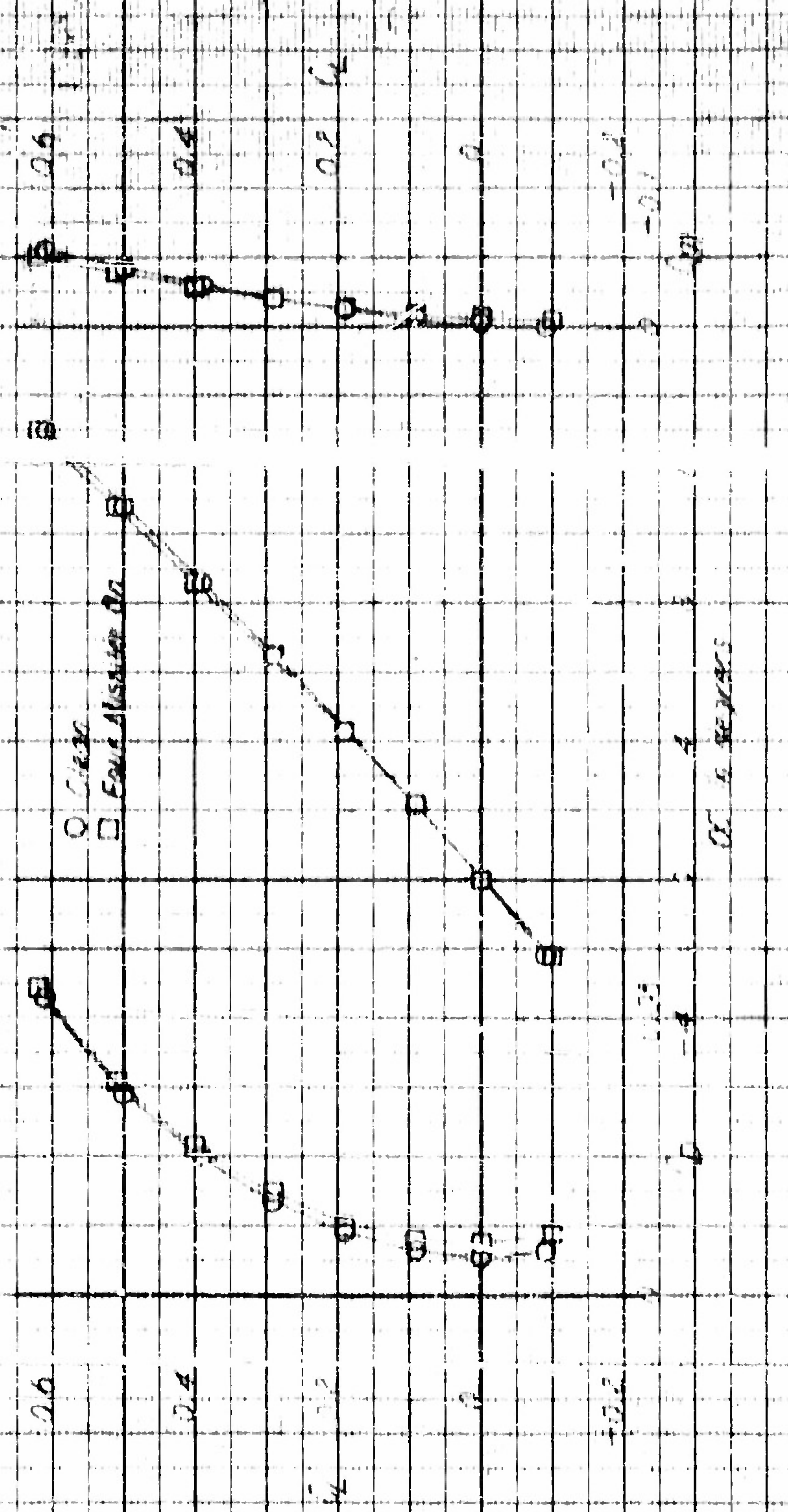

Figure 22 (Concluded)

1/4 Model Exit, Tail On

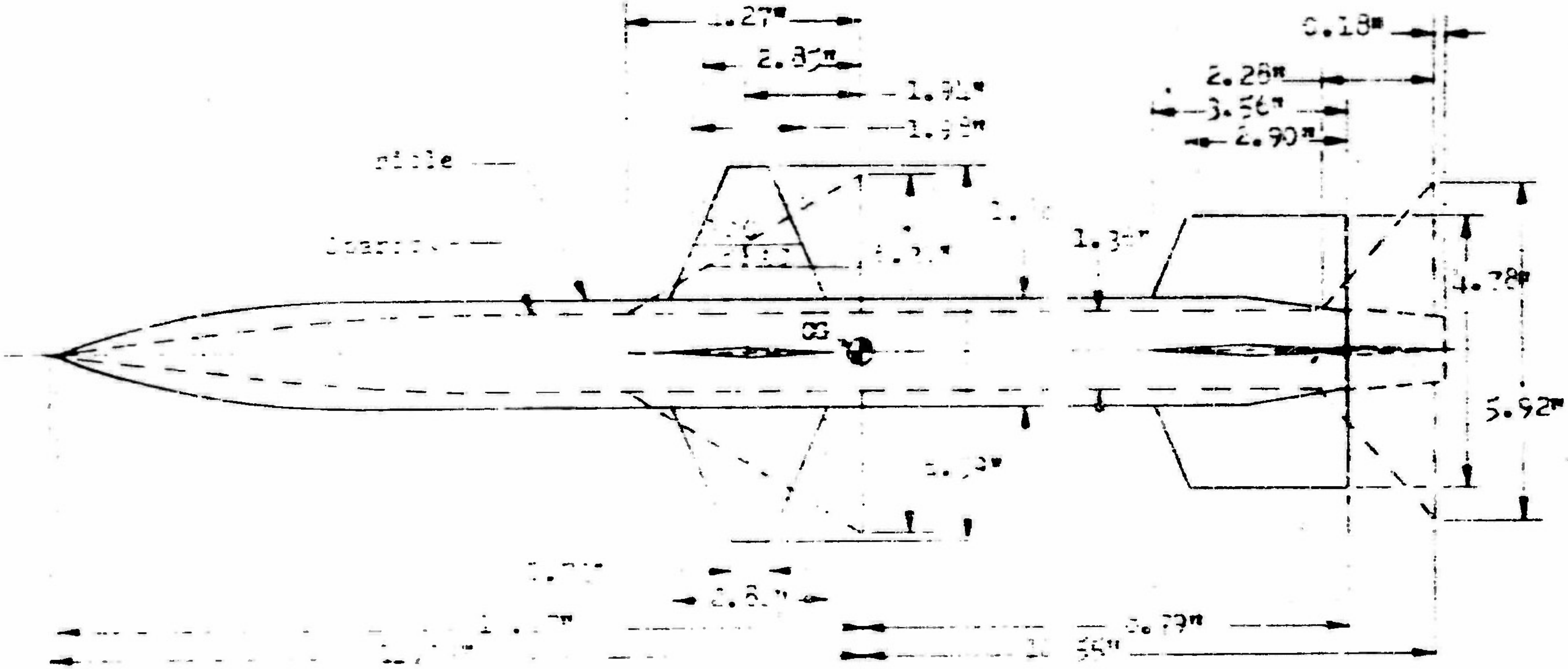

	Oriole	Sparrow
Exposed horizontal or vertical wing area in square feet	[illegible]	0.0731
Exposed horizontal or vertical tail area in square feet	[illegible]	0.0362

Figure 23 - Sketch Showing Comparative Design of Model of an XAAM-N-4 Oriole Missile and an XAAM-N-2 Sparrow I Missile

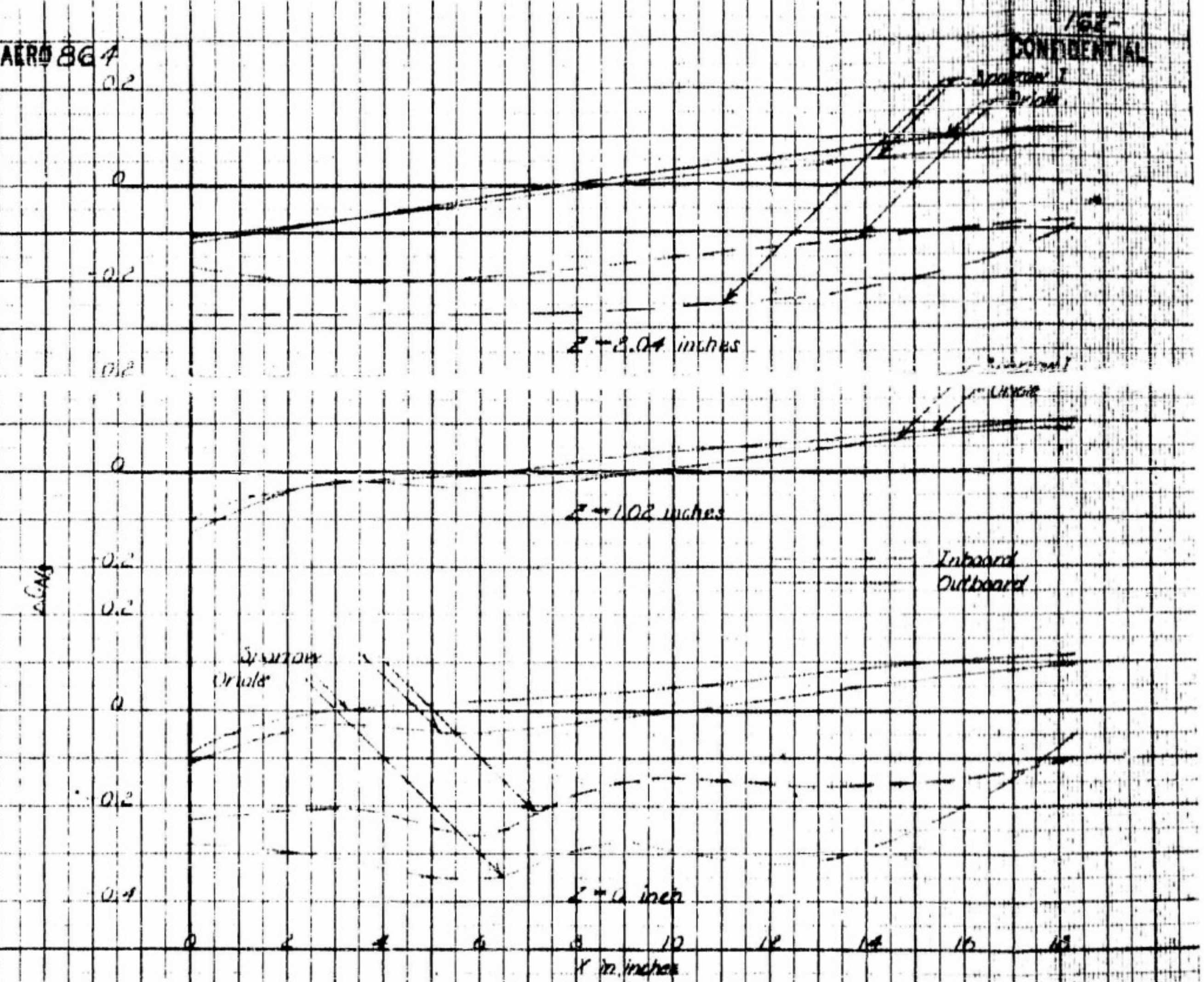

Figure 24 Variation of Airplane Interference on the Normal-Force Coefficient of the Oriole and Sparrow I Missiles With Distance Forward of the Carry Position

(a) $\theta_S = 0°$, $\alpha_o = 0°$, $\alpha = 4°$

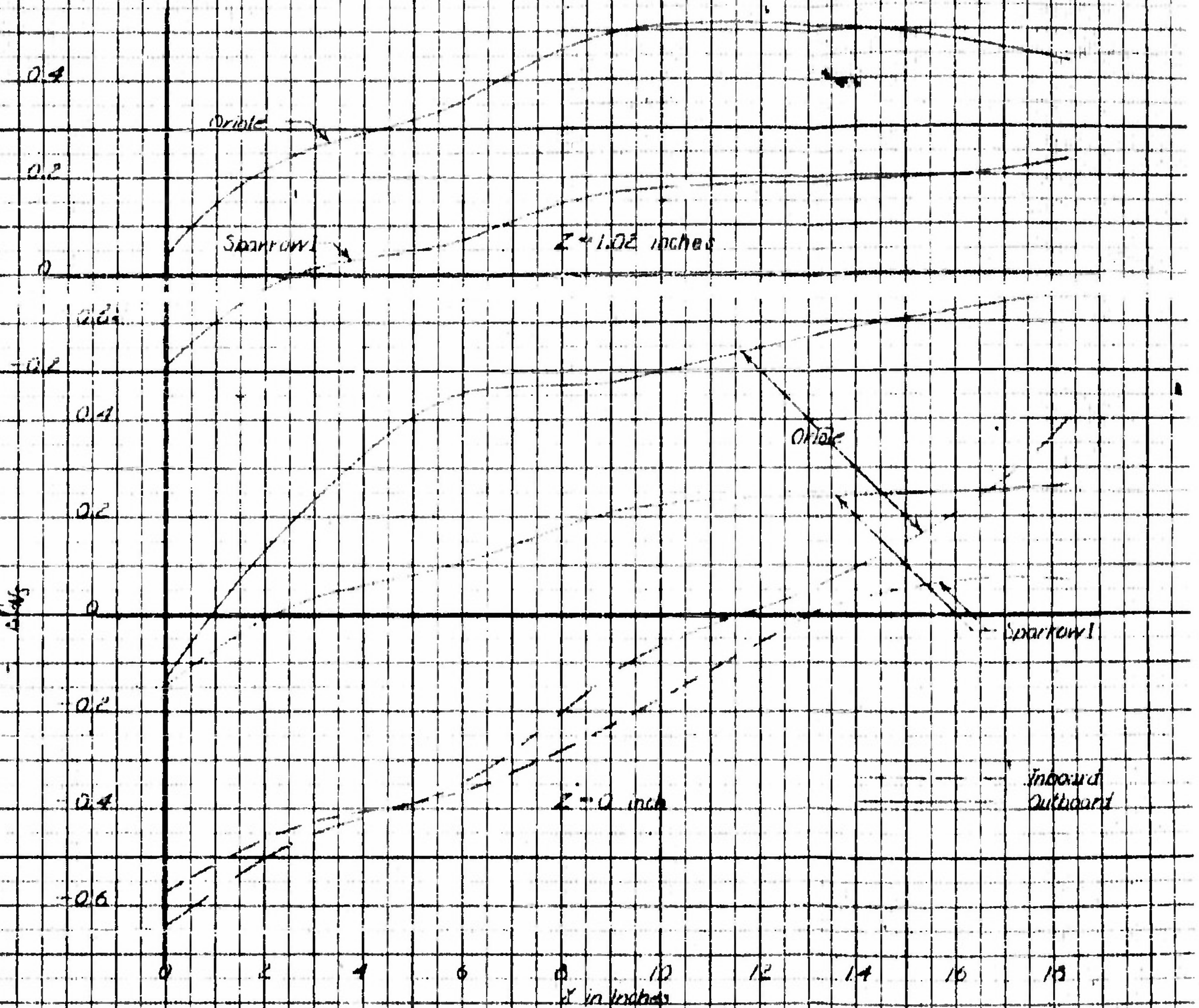

Figure 24 (Continued)

(b) $\theta_s = 0°$, $\alpha_s = 0°$, $\alpha = 10°$

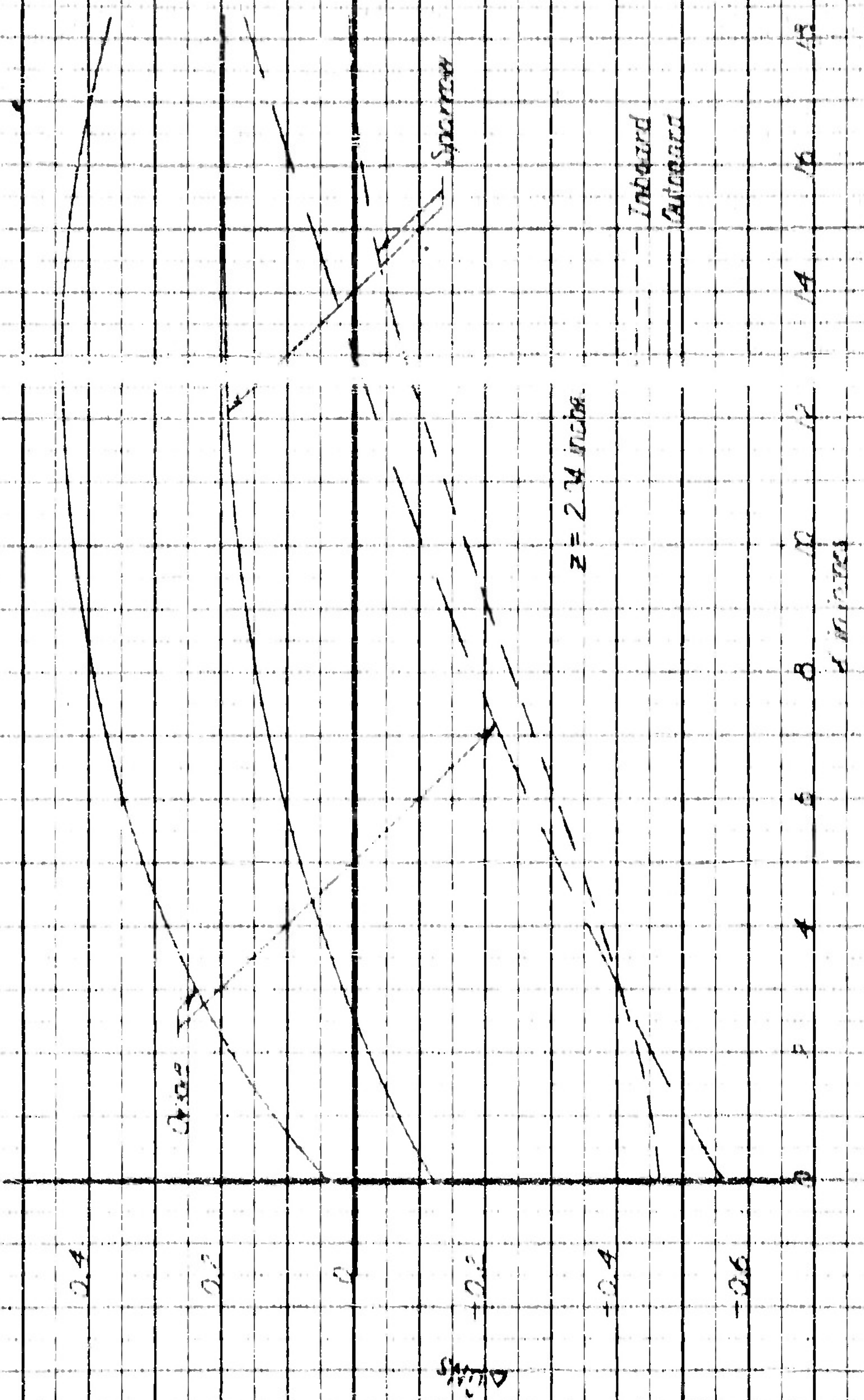

Figure 24 (Concluded)
(h) Concluded

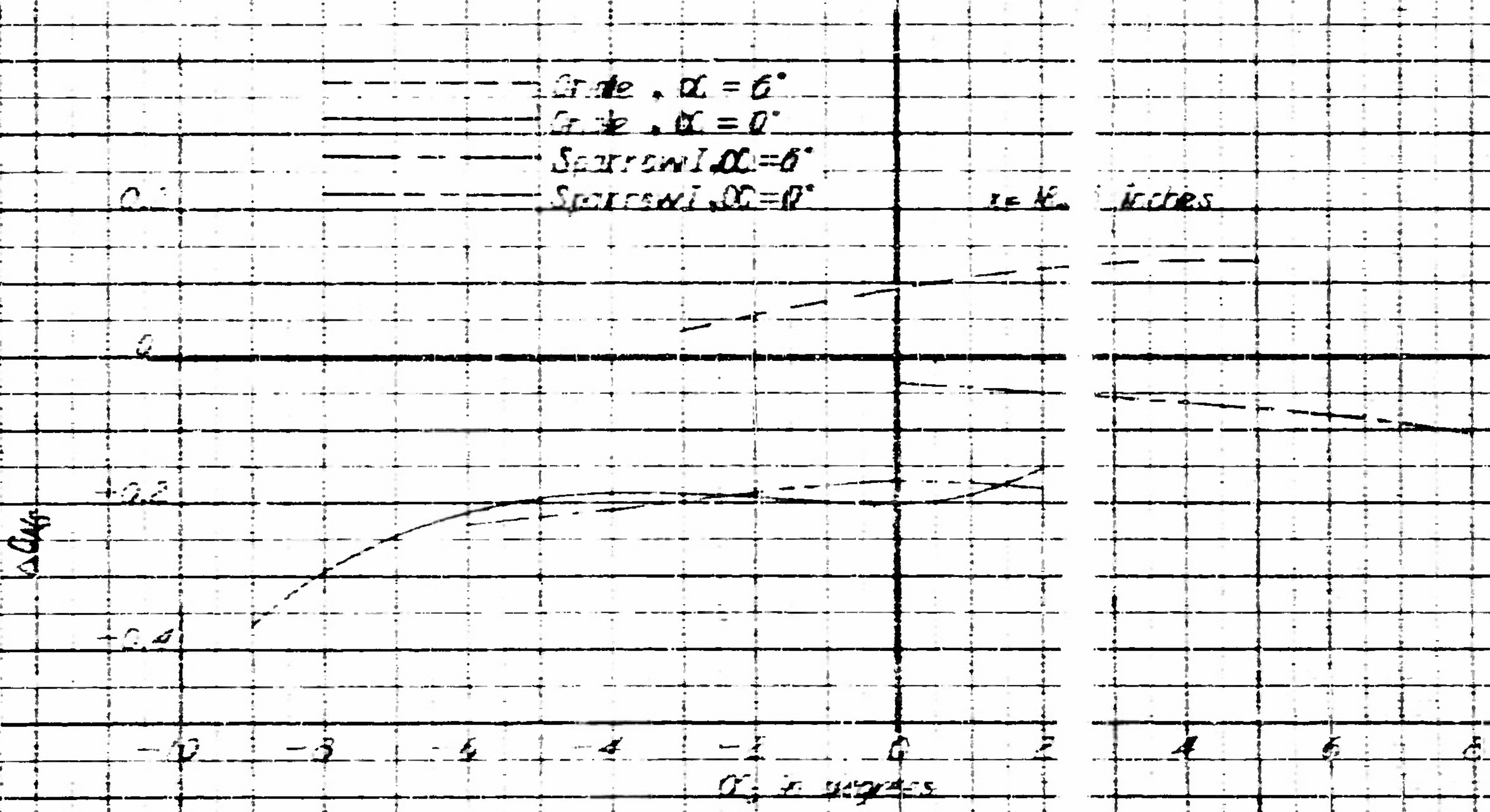

Figure 25 – Variation of Airplane Interference [illegible] the Normal-Force Coefficient of the [illegible] and Sparrow I Missiles With Missile Angle of Attack

(a) Inboard, Z = 0 Inch

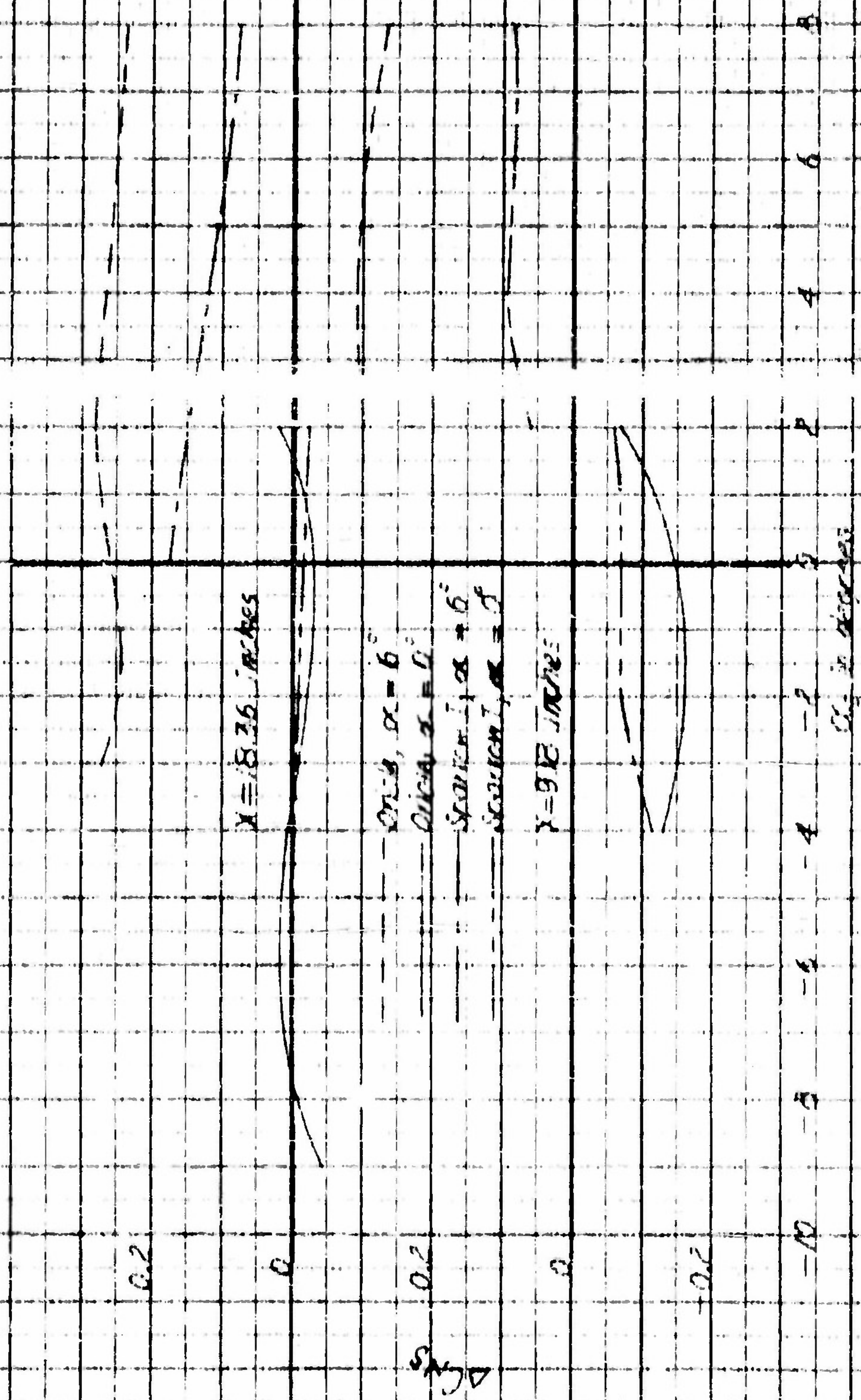

Figure 25 (Continued)

(b) Buttock, z = 0 Inch

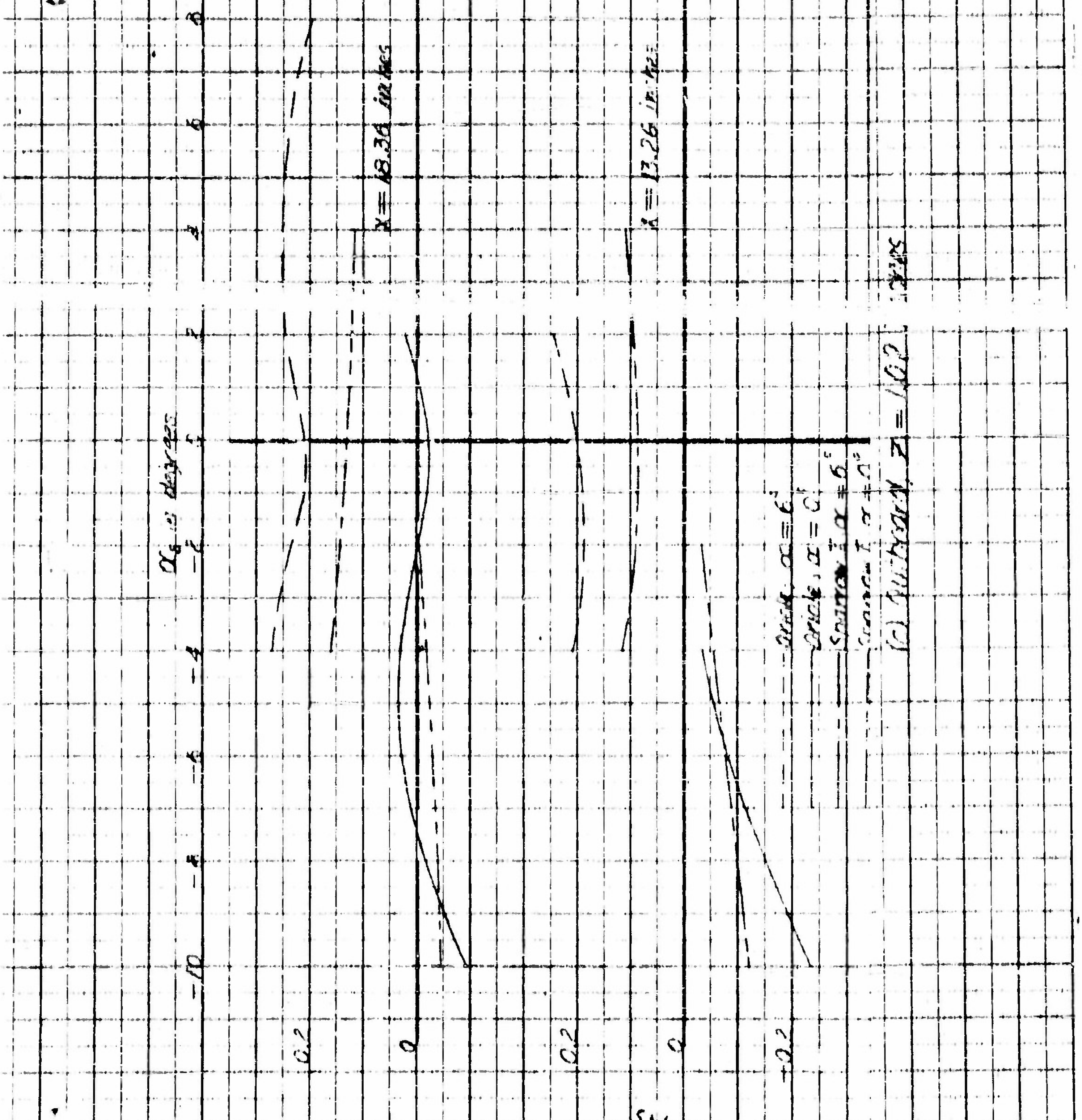
x = 18.36 inches
x = 13.26 inches

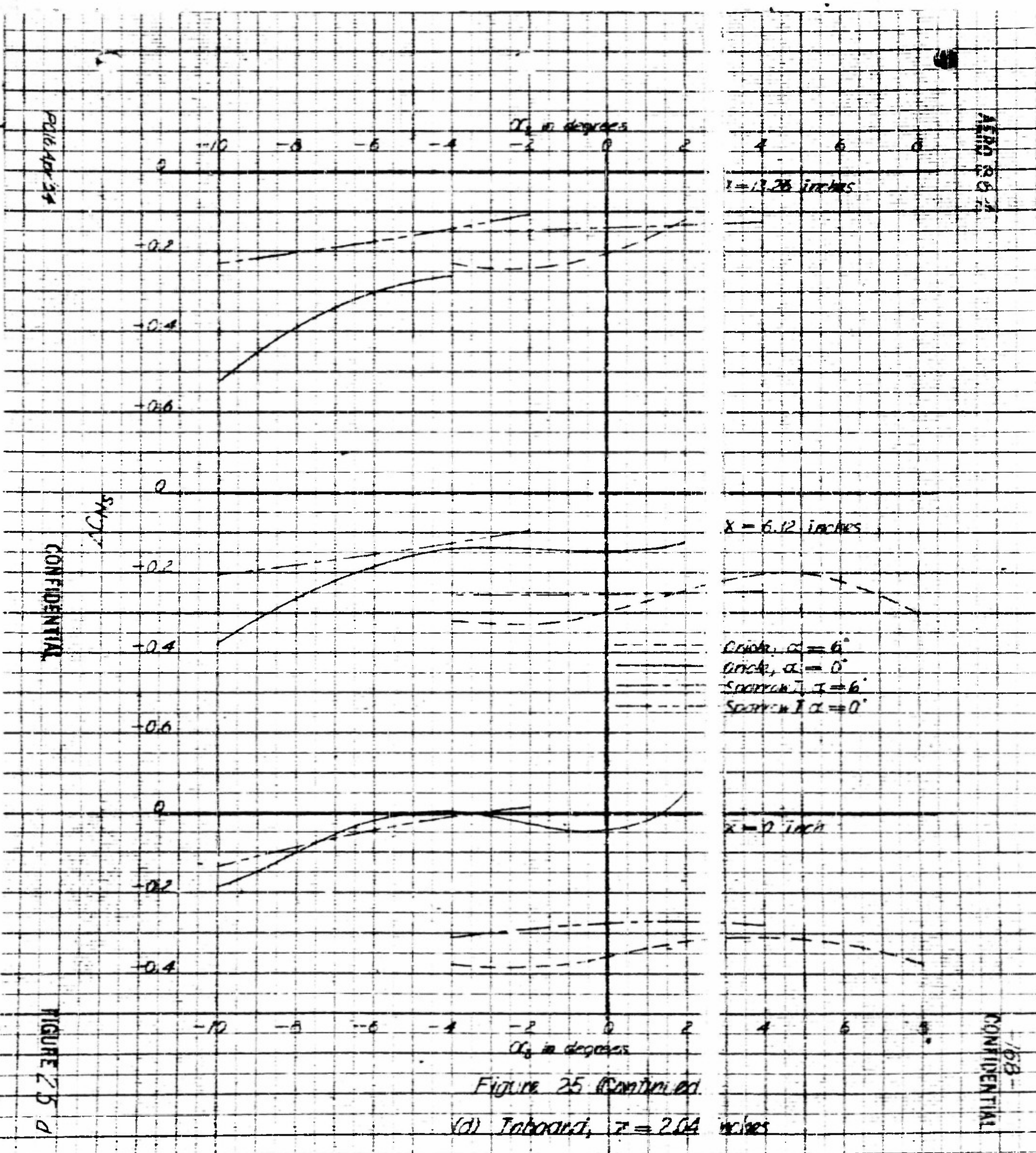

Figure 25 (Continued)

(d) Inboard, z = 2.04 inches

CONFIDENTIAL

FIGURE 25 d

CONFIDENTIAL

PC 20 Apr '54

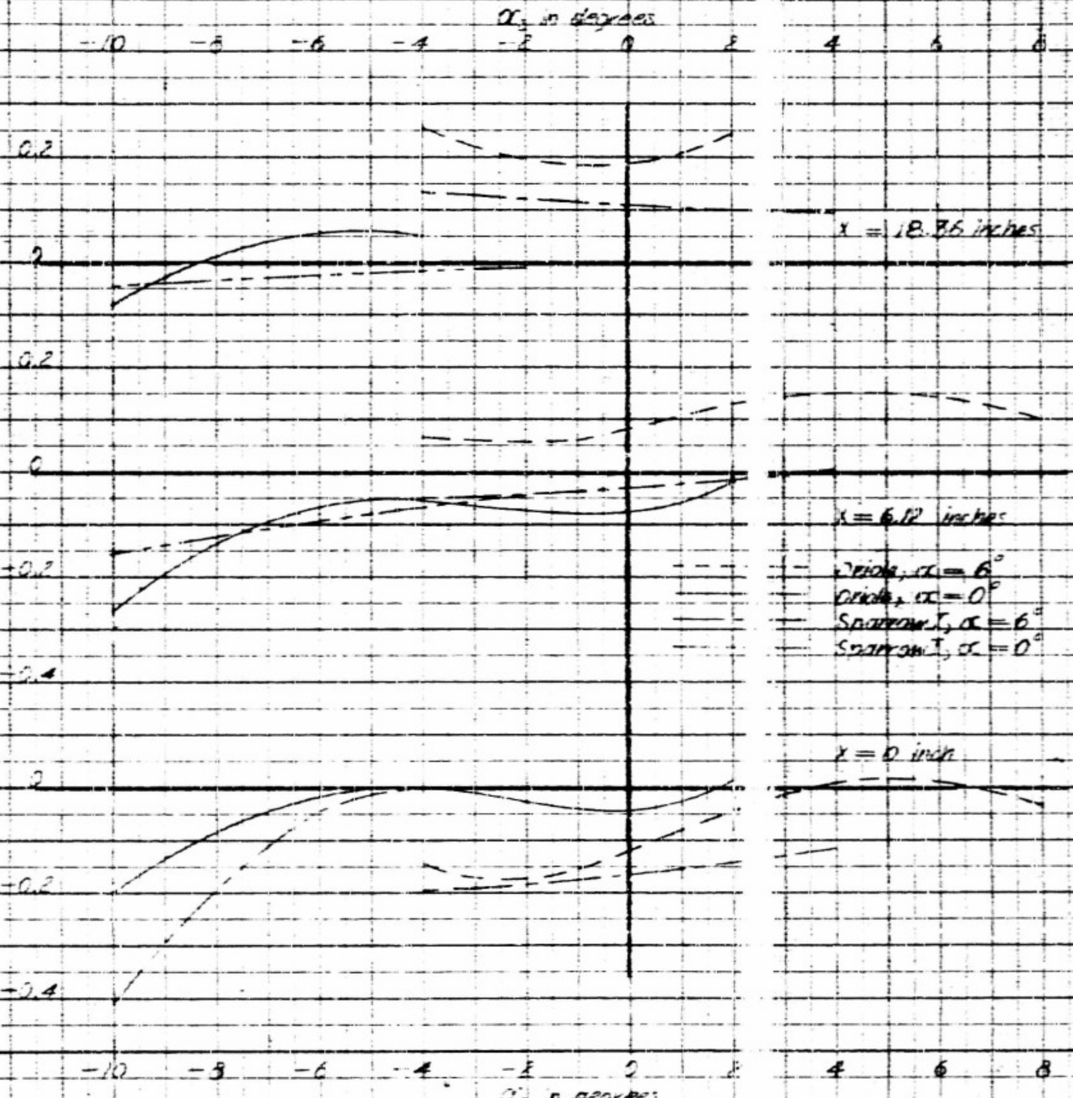

Figure 25 (Continued)

(e) Outboard, $z = 2.04$ inches

CONFIDENTIAL

FIGURE 25 e

CONFIDENTIAL

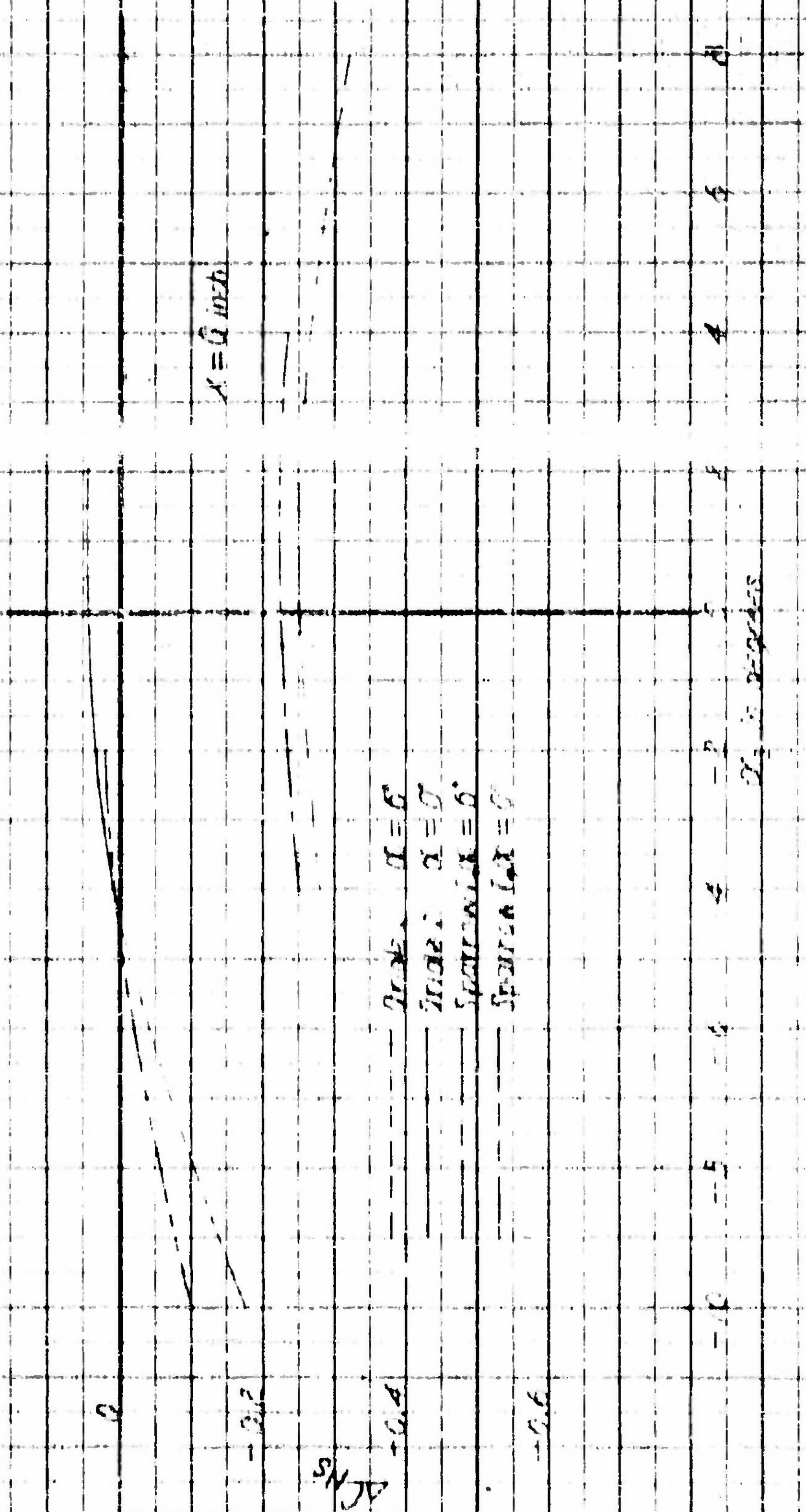

Figure 25 (Continued)

Outboard, z = 4.03 Inches

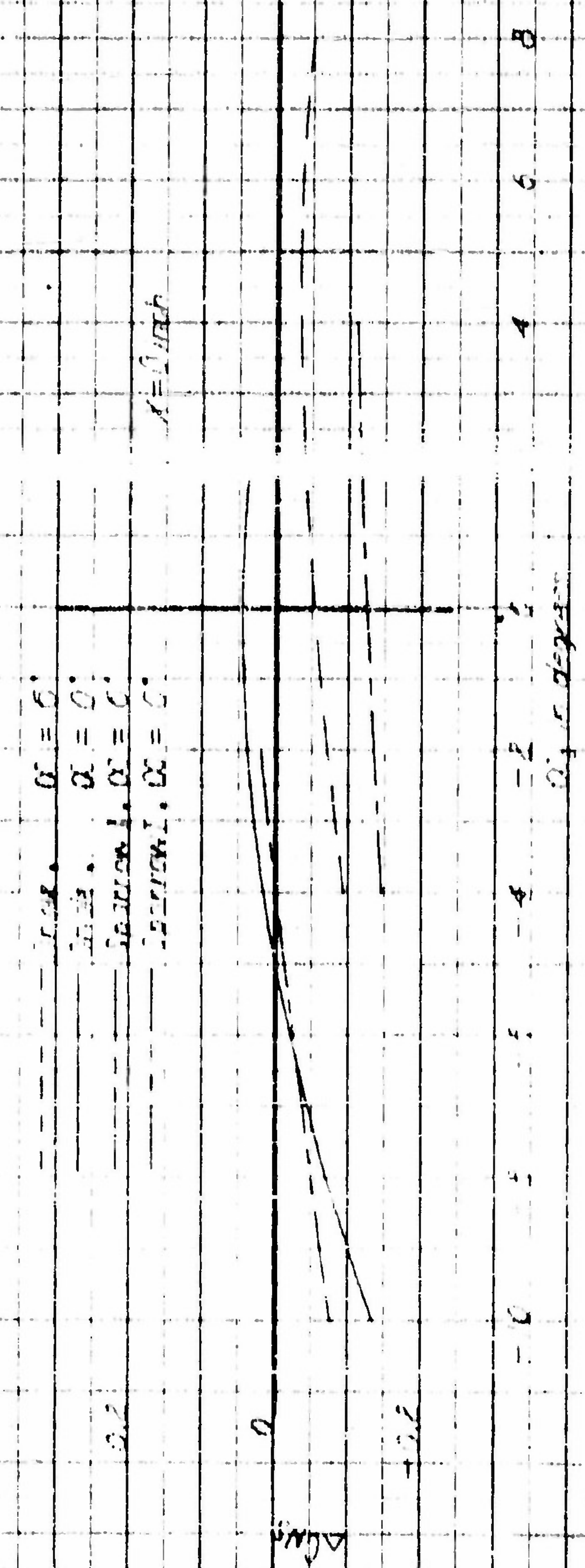

Figure 25 (concluded)

PC 7 Apr 54

CONFIDENTIAL

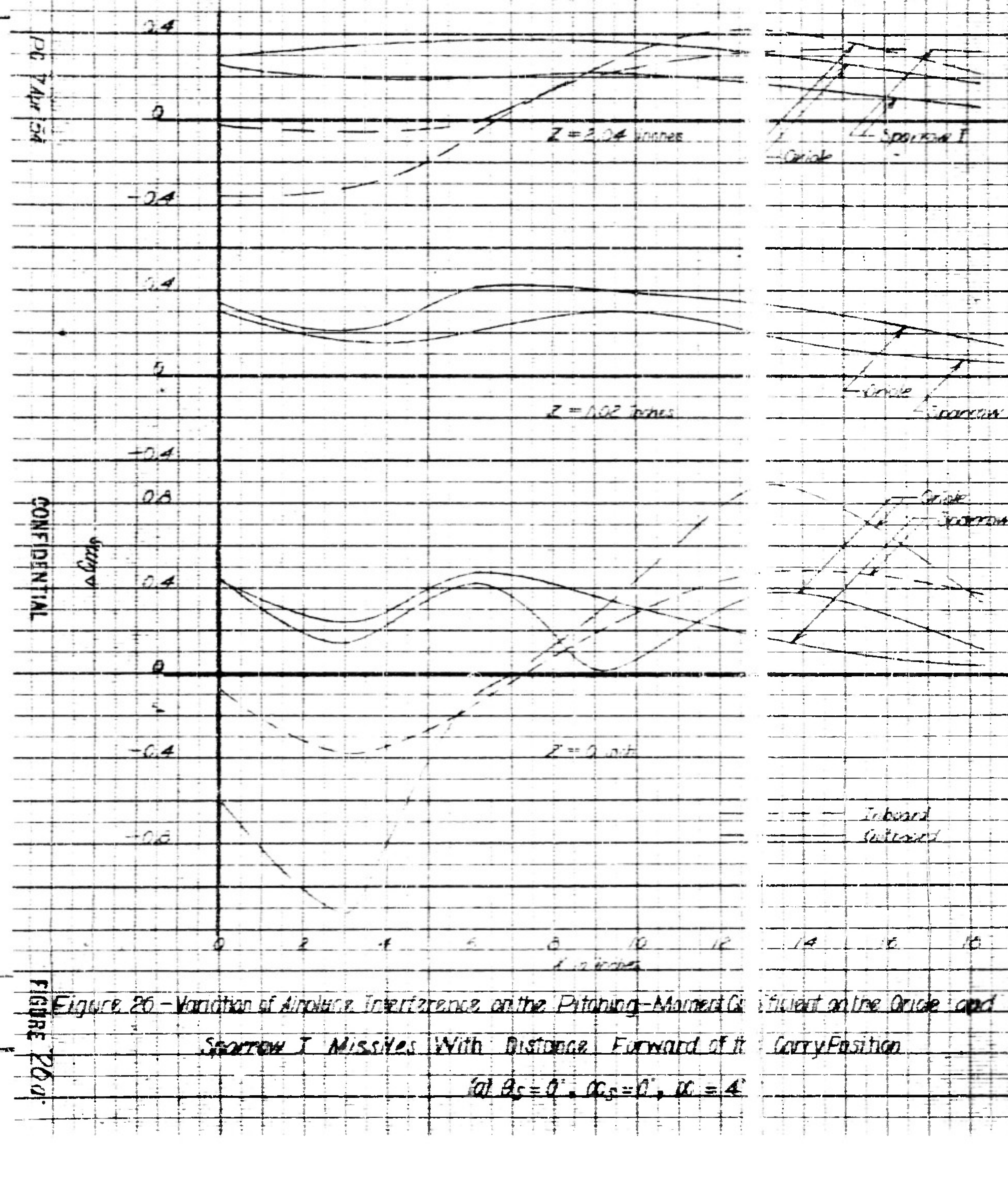

Figure 26 – Variation of Airplane Interference on the Pitching-Moment Coefficient on the Oriole and Sparrow I Missiles With Distance Forward of the Carry Position

(a) $\theta_s = 0°$, $\alpha_s = 0°$, $\alpha = 4°$

FIGURE 26a

CONFIDENTIAL

Figure 20 (Continued)

(b) $\theta_s = 0°$, $\alpha_s = 0°$, $\alpha = 10°$

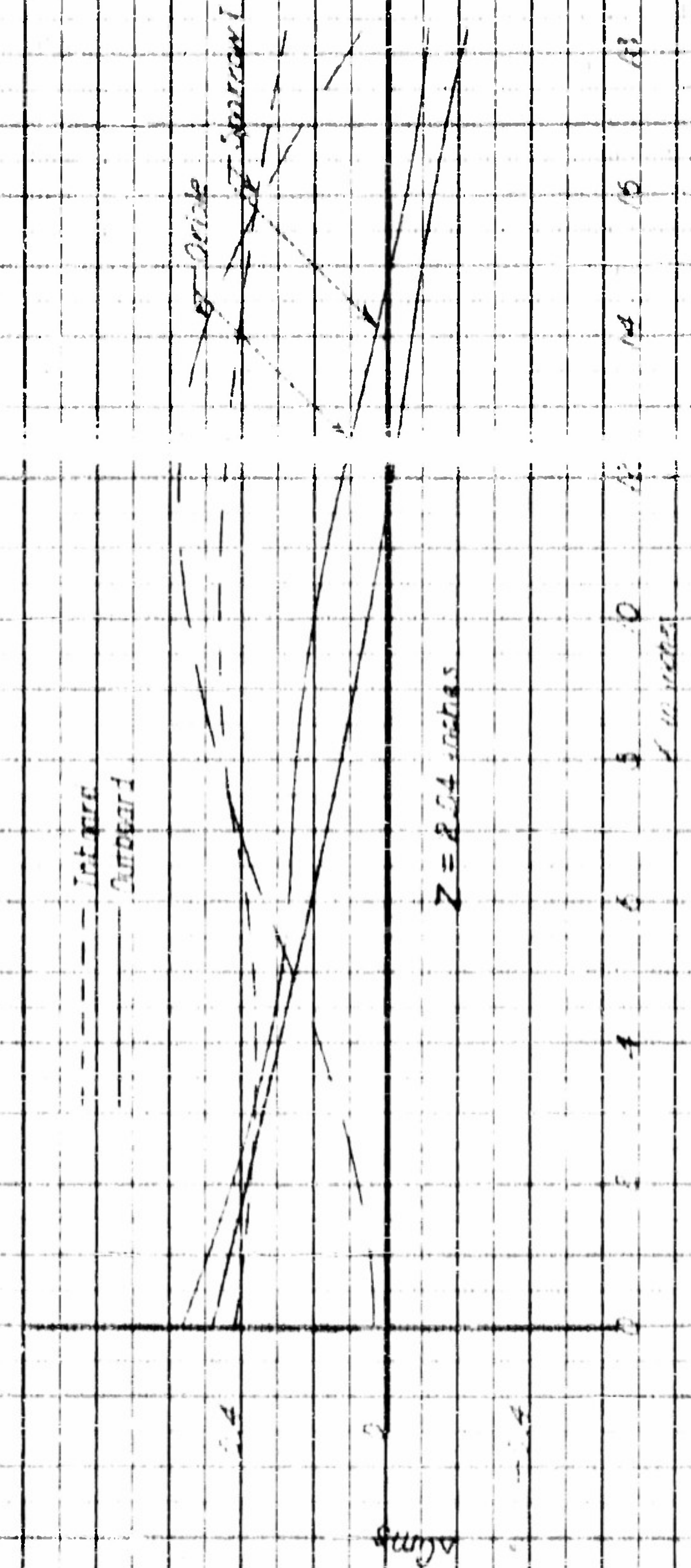

Figure 26 (Concluded)

(b) Concluded

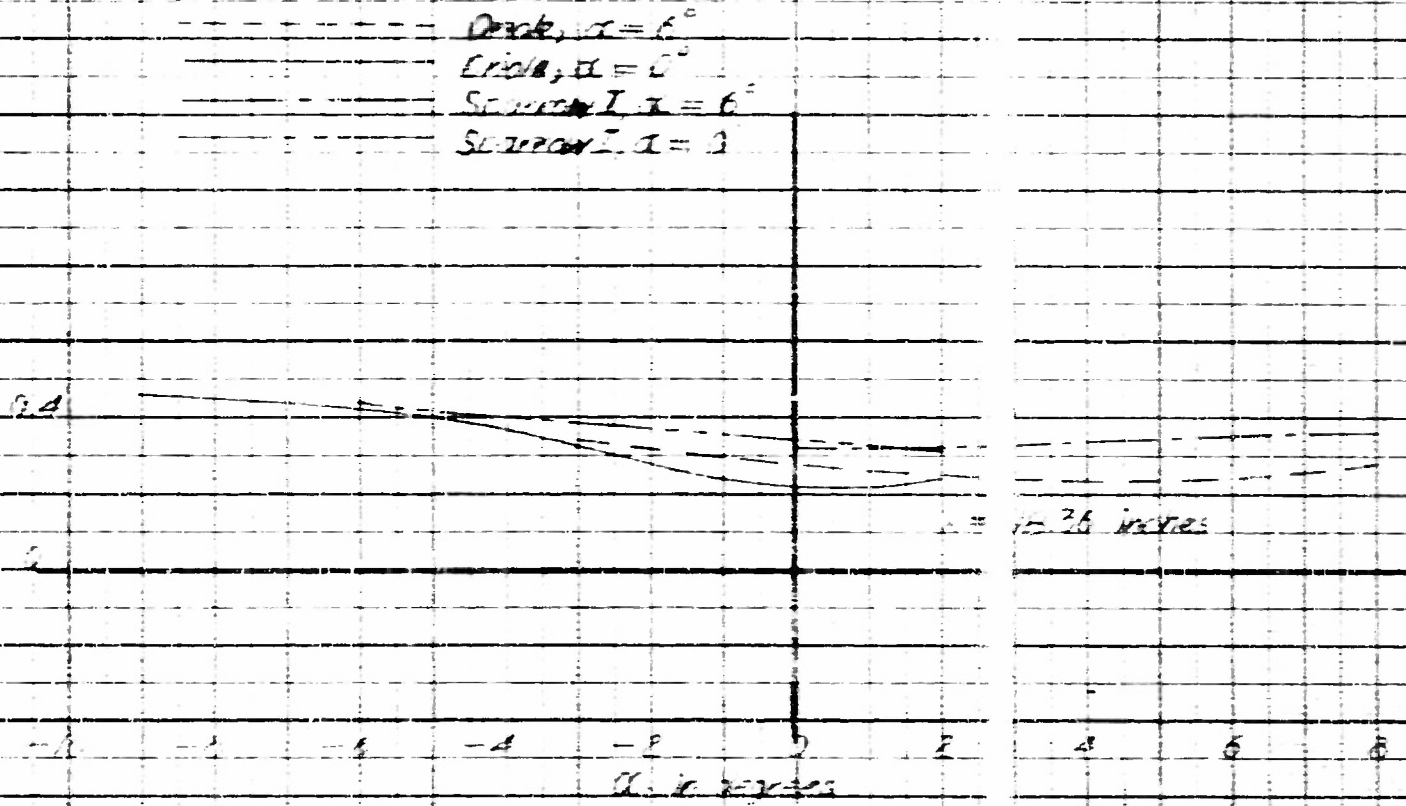

Figure 27—Variation of Airplane Interference on the Pitching-Moment Coefficient of the Oriole and Sparrow I Missiles With Missile Angle of Attack

(a) Inboard, z = 0 Inch

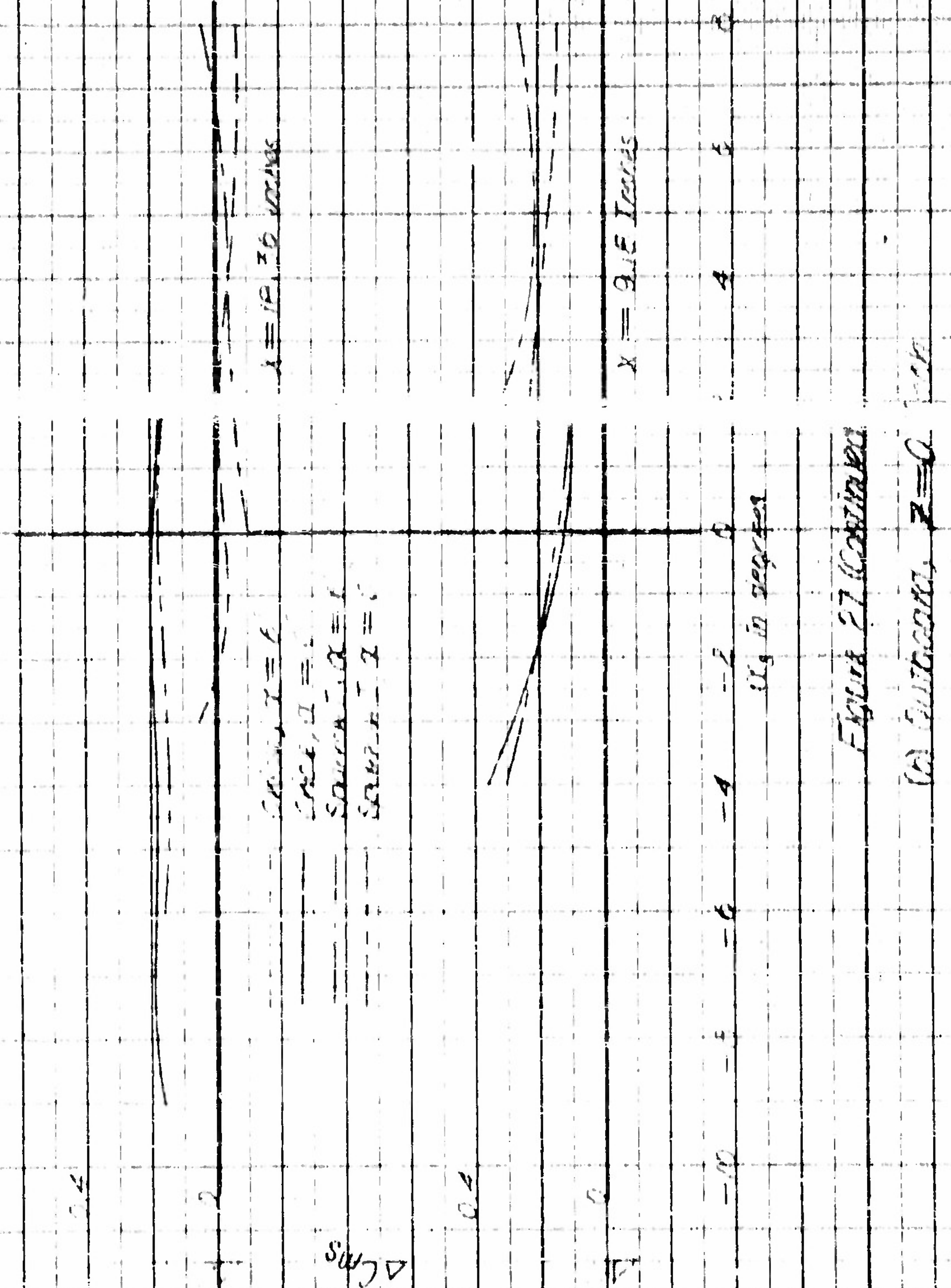

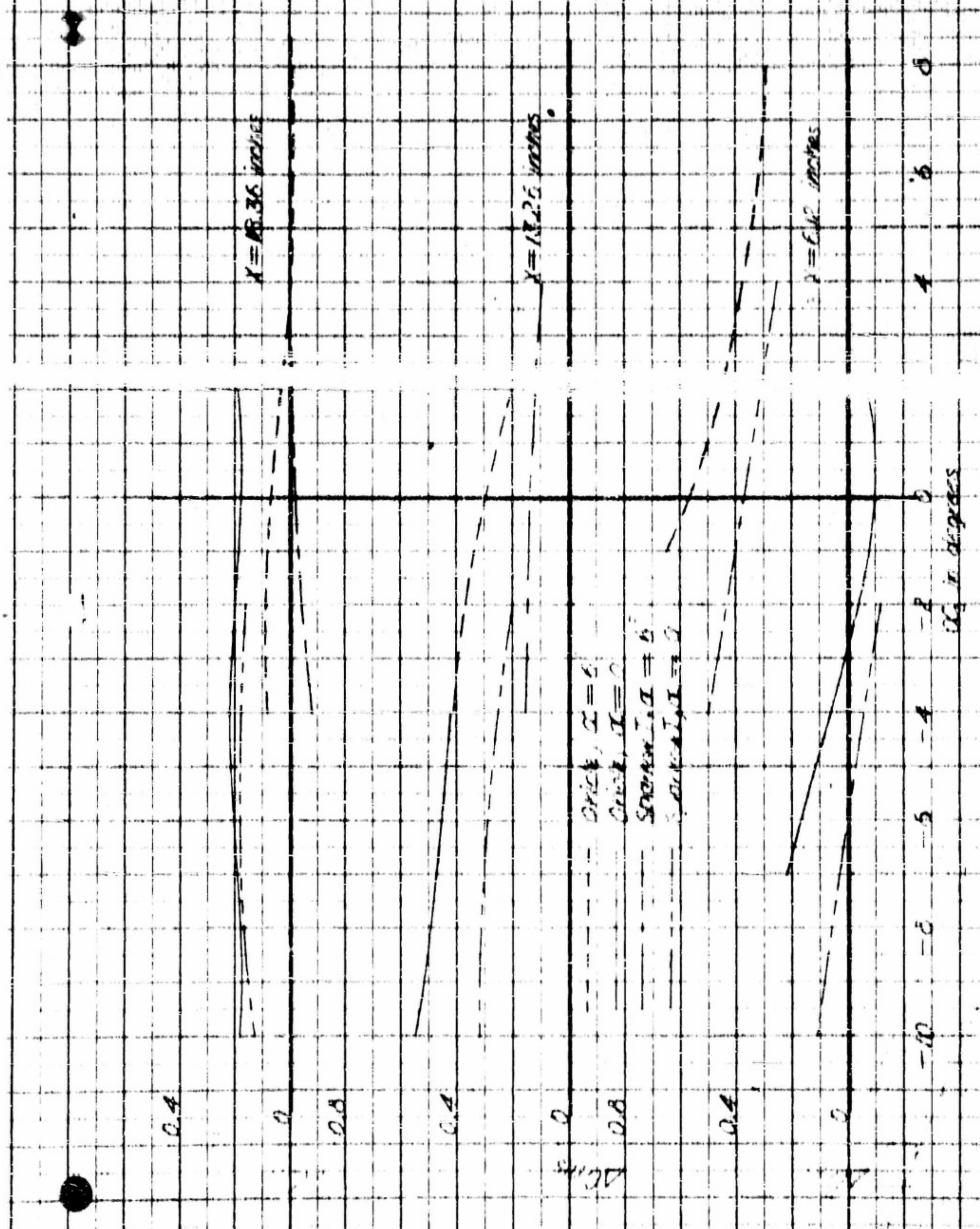

Figure 27 (Continued)

(c) Outboard, ... = 1.52 inches

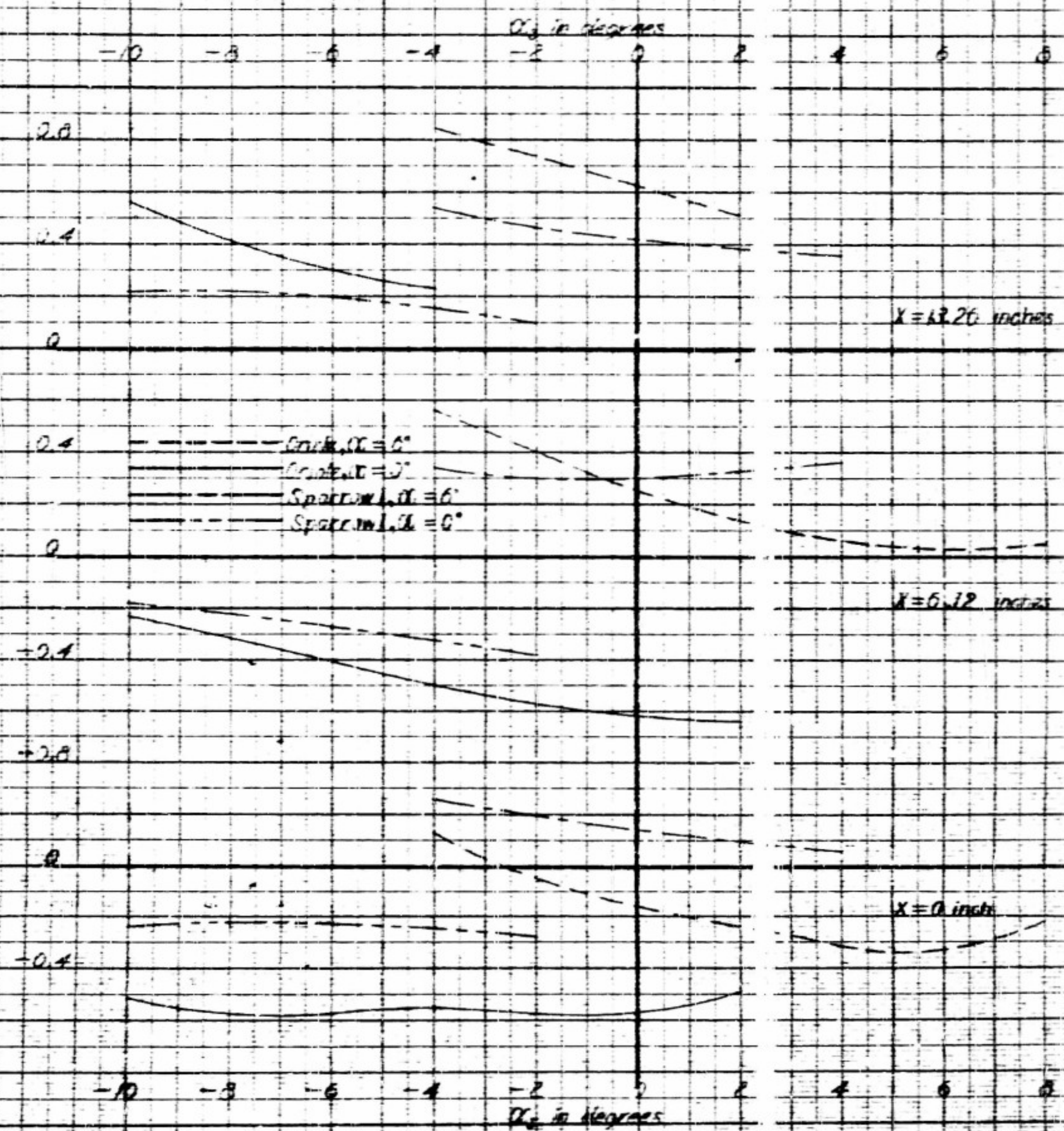

Figure 27 (Continued)

(d) Inboard, z = 2.04 in.

FIGURE 27 d

CONFIDENTIAL

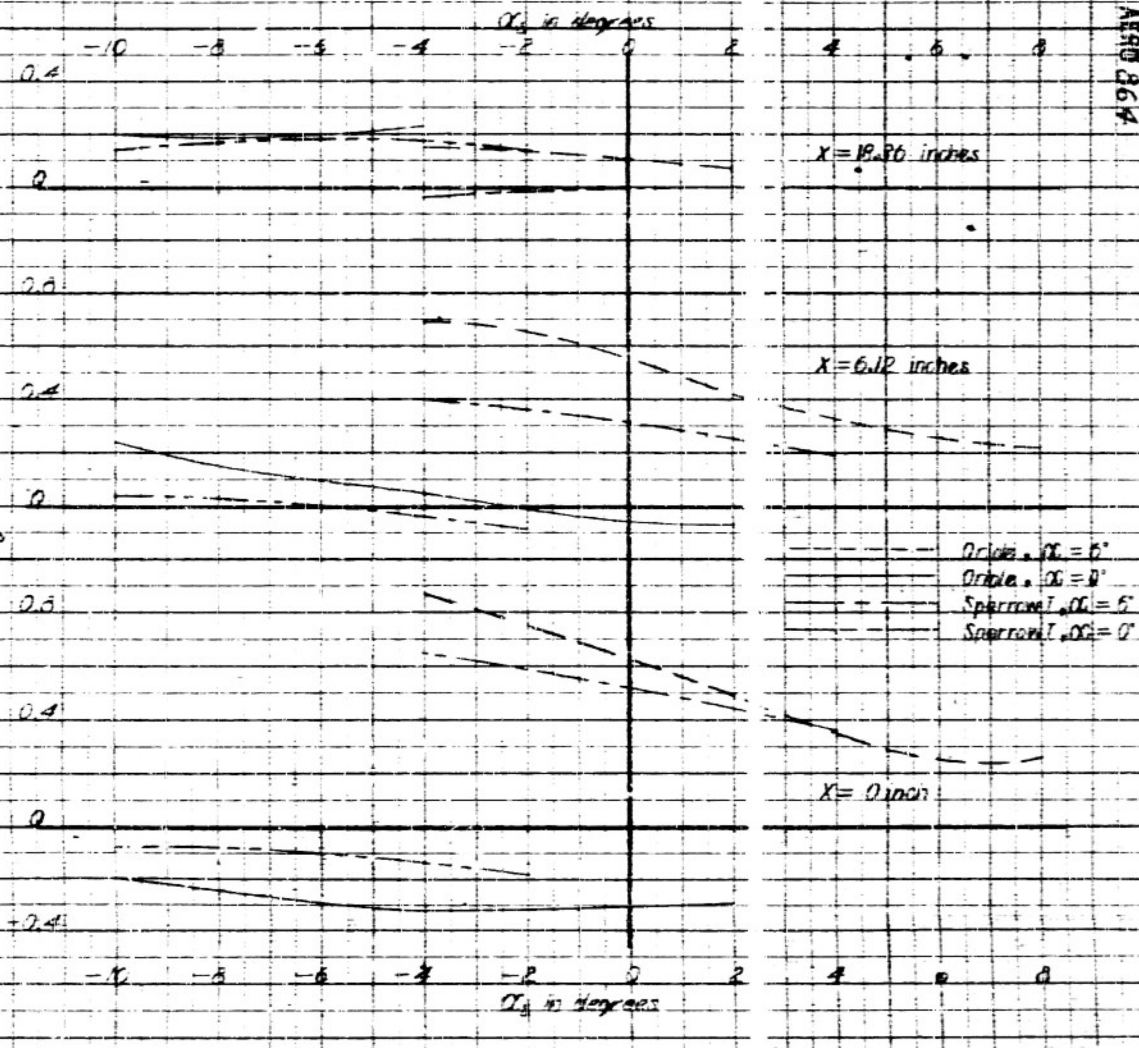

Figure 27 (Continued)

(e) Outboard, z = 20.41 inches

FIGURE 27e

CONFIDENTIAL

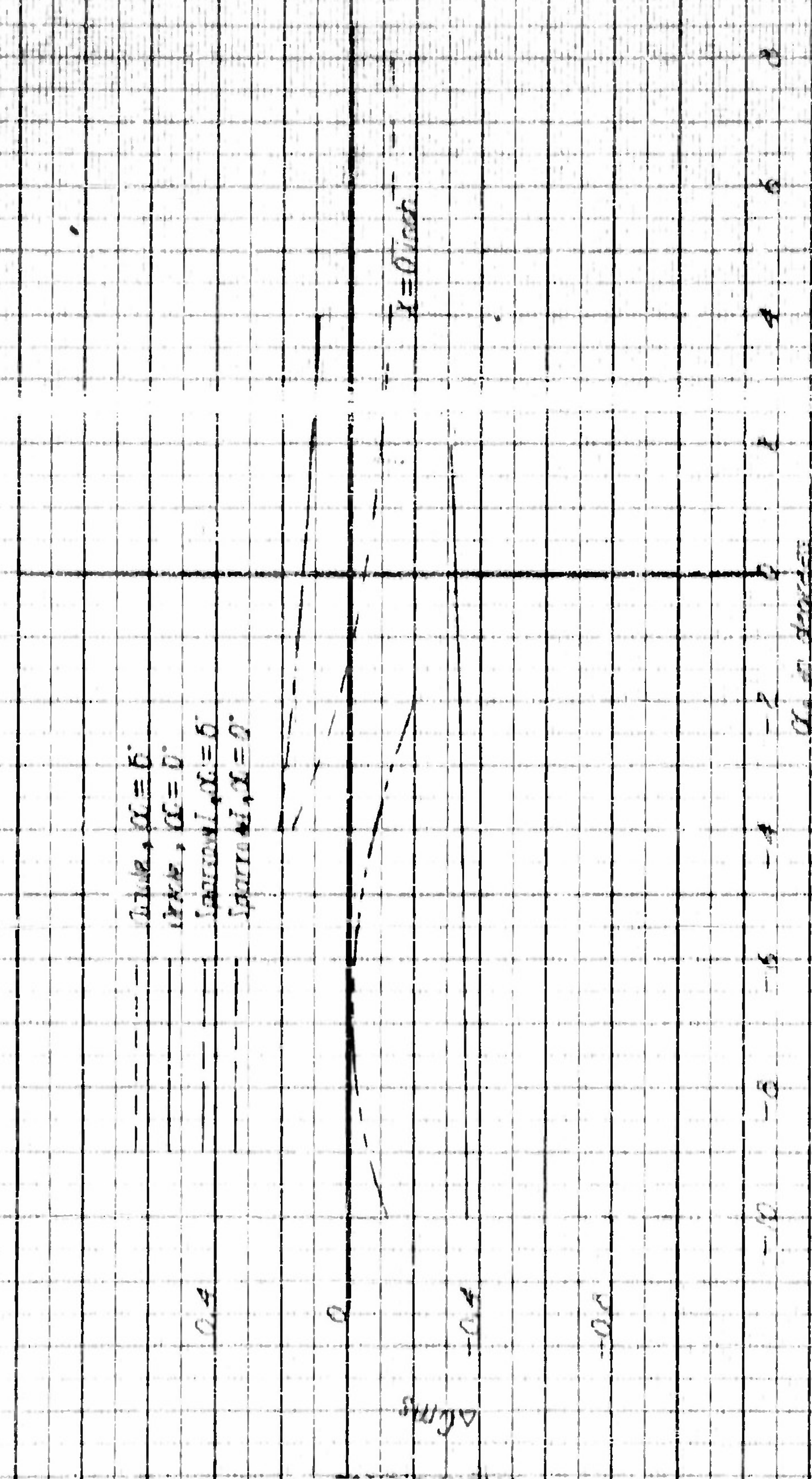

Figure 27 (Continued)

(f) Inboard, x = 4.08 Inches

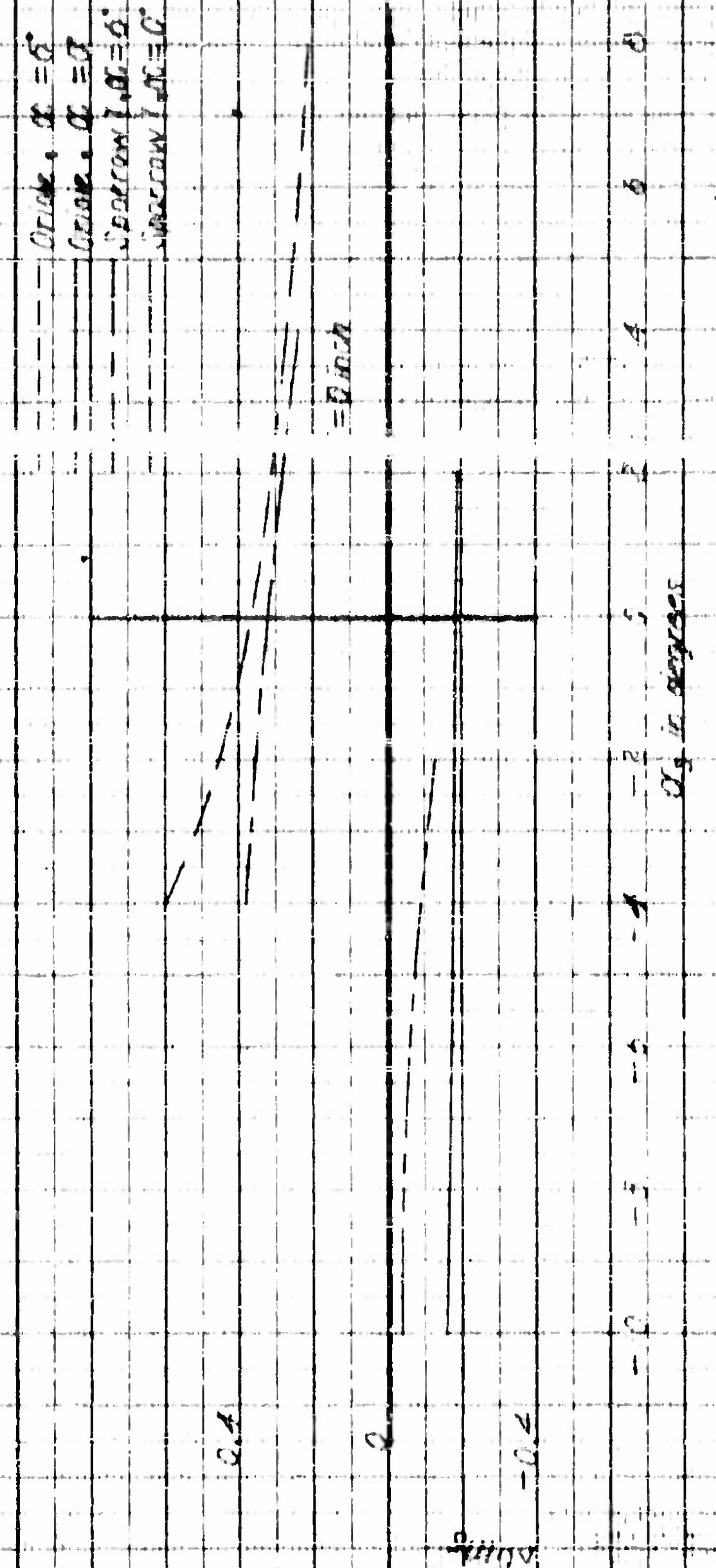

Figure 27 (Concluded)

(g) Outboard, $\bar{x}$ = 4.06 Inches

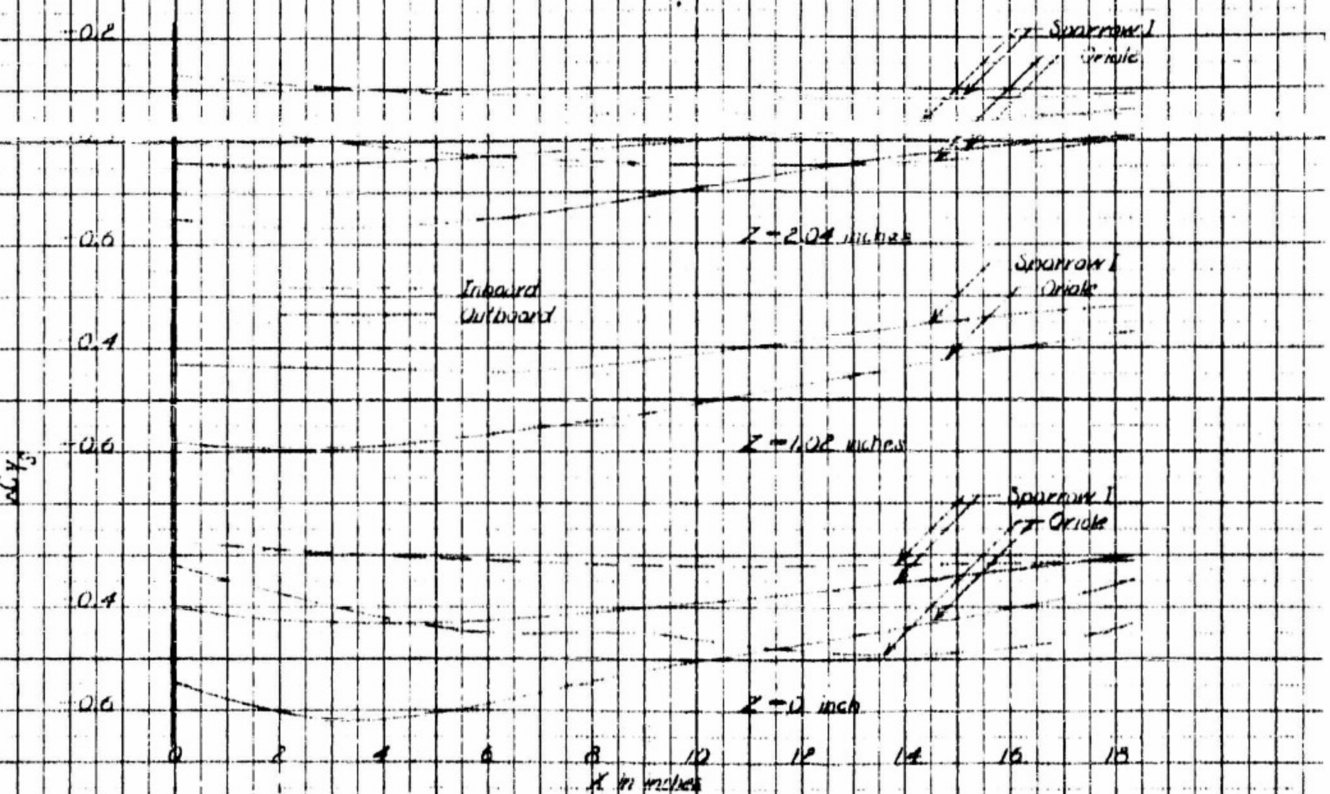

Figure 28 - Variation of Airplane Interference on the Lateral-Force Coefficient of the Oriole and Sparrow I Missiles With Distance Forward at the Carry Position

(a) $\theta_s = 0^\circ$, $\alpha_s = 0^\circ$, $\alpha = 4^\circ$

AERO 864

CONFIDENTIAL

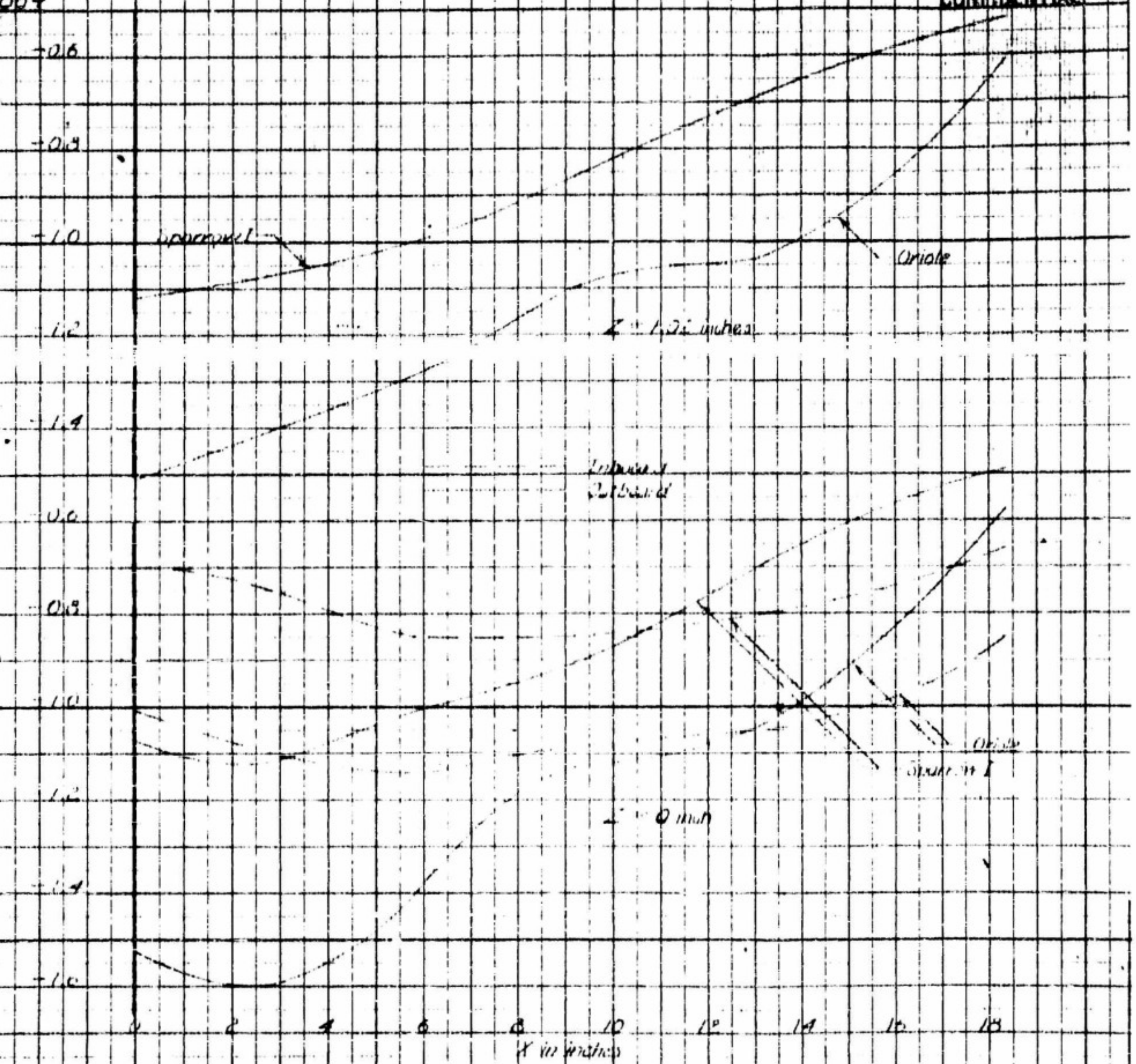

Figure 28 (Continued)

(b) $\theta_S = 0°$, $\alpha_S = 6°$, $\alpha = 10°$

CONFIDENTIAL

PCO Apr '54

FIGURE 28b

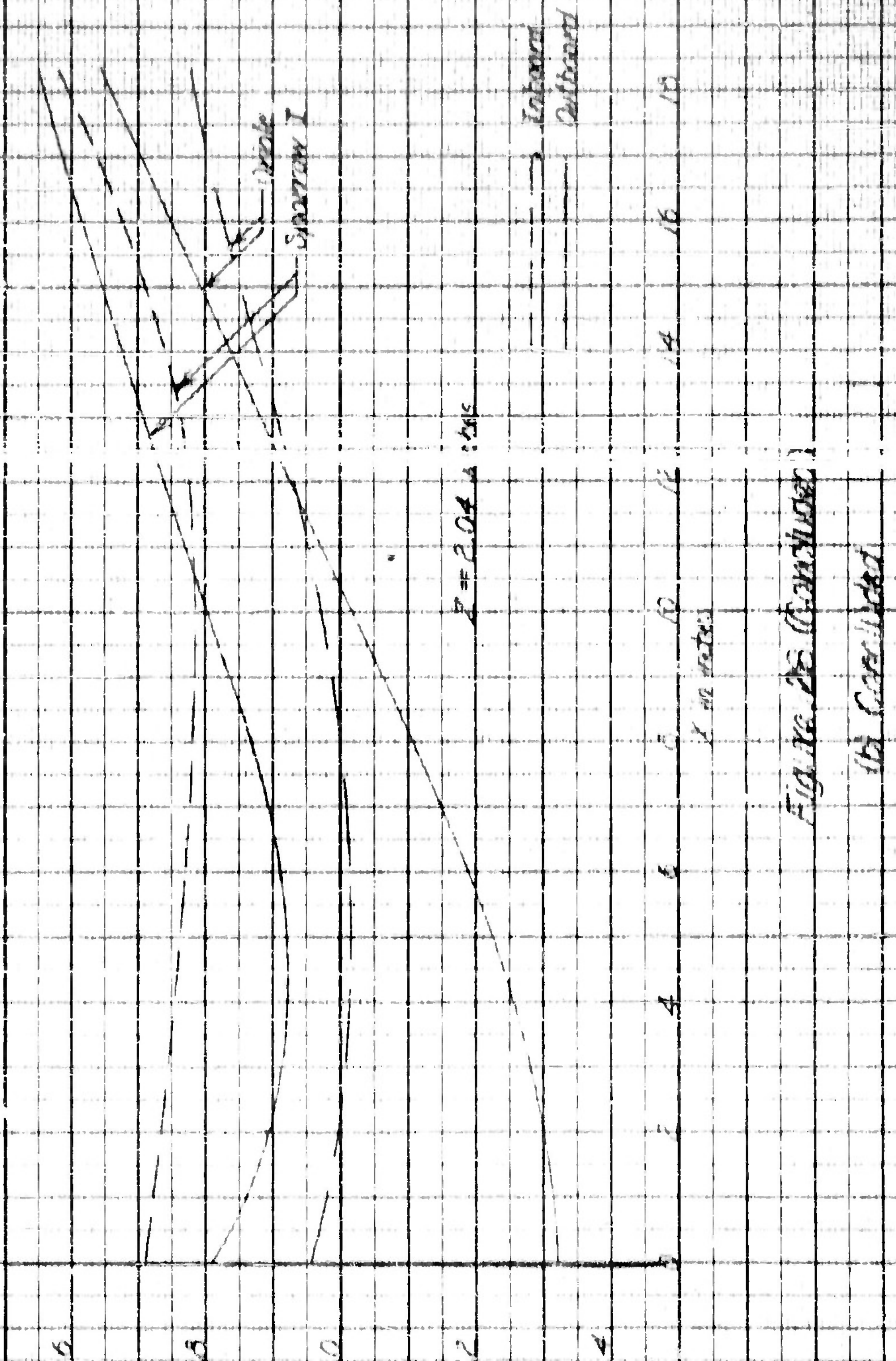

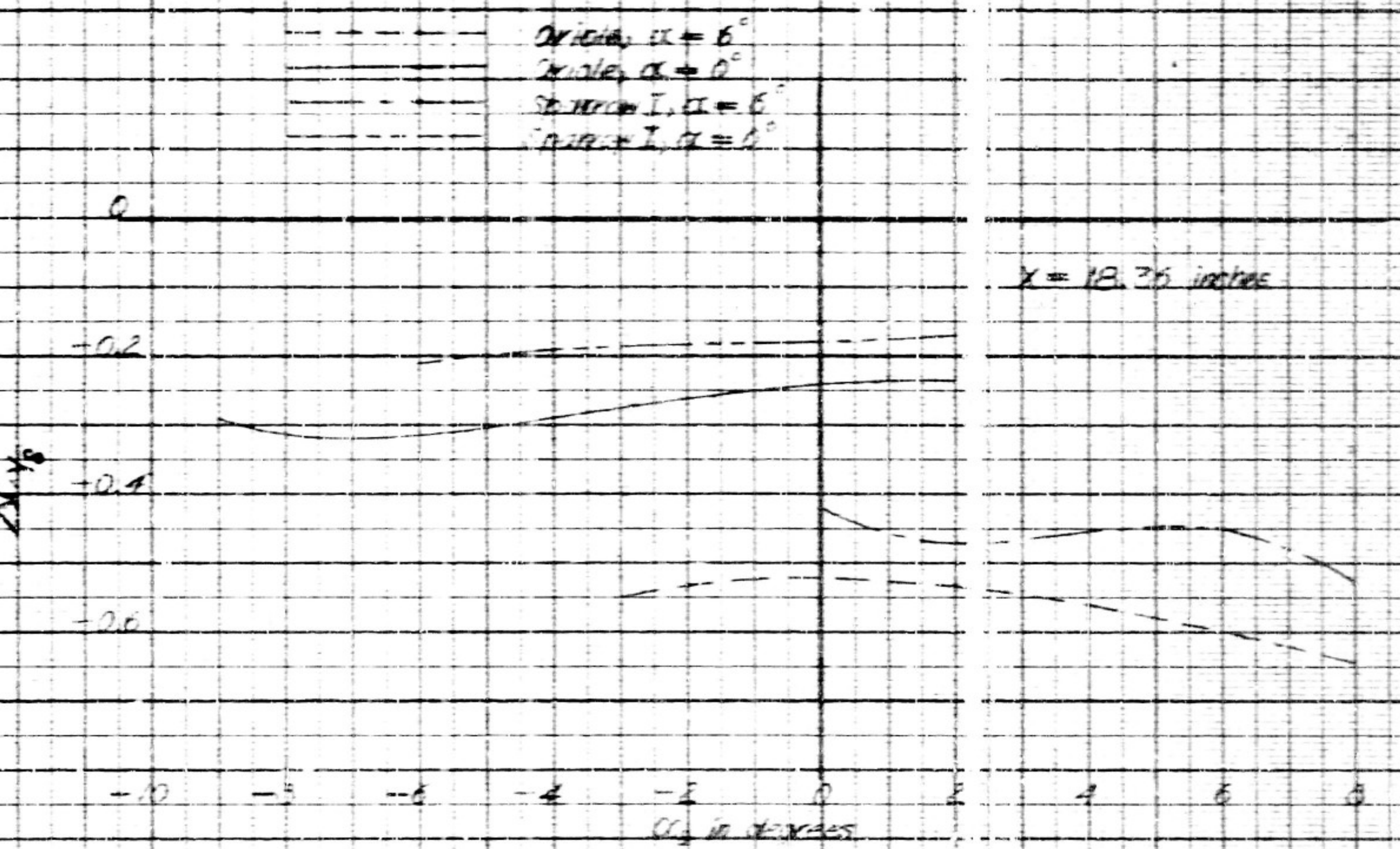

Figure 29—Variation of Airplane Interference on the Lateral-Force Coefficient of the Oriole and Sparrow I Missiles With Missile Angle of Attack

(a) Inboard, Z = 0 Ins.

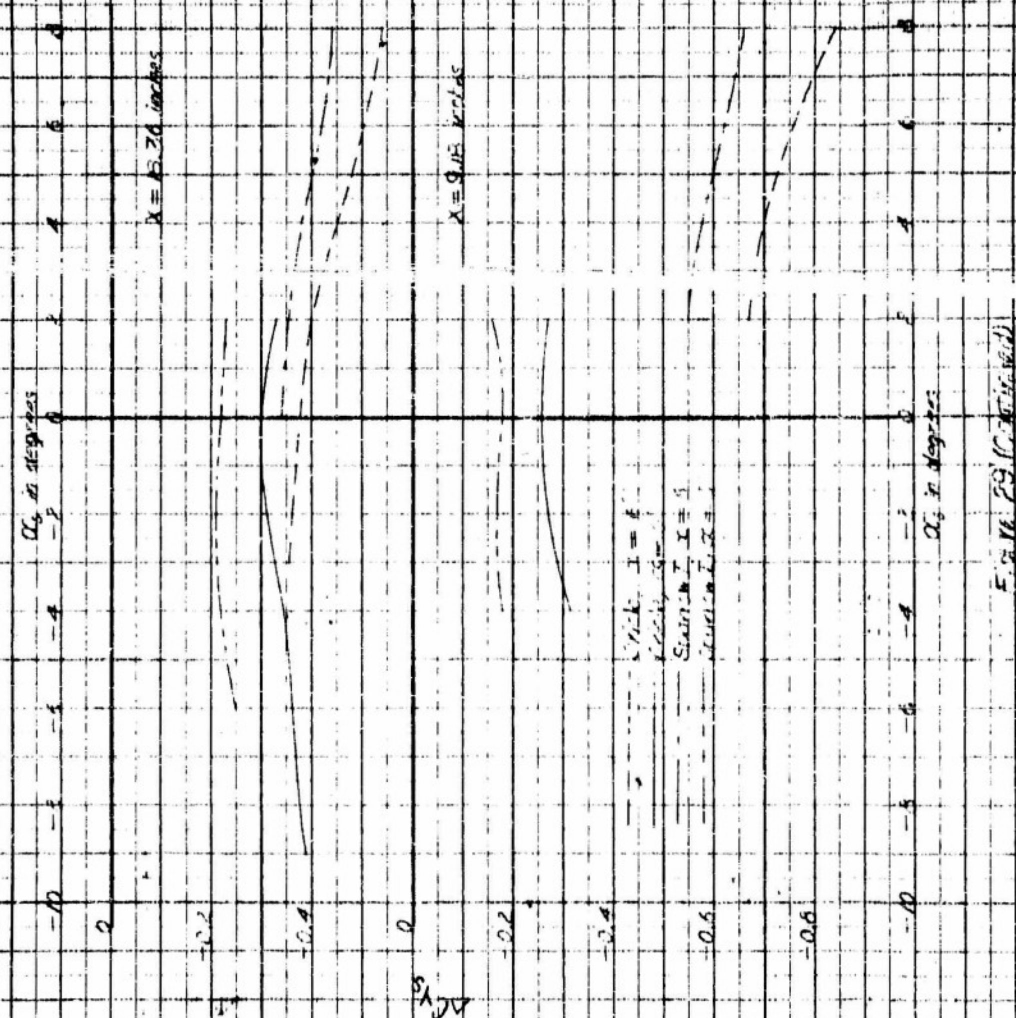

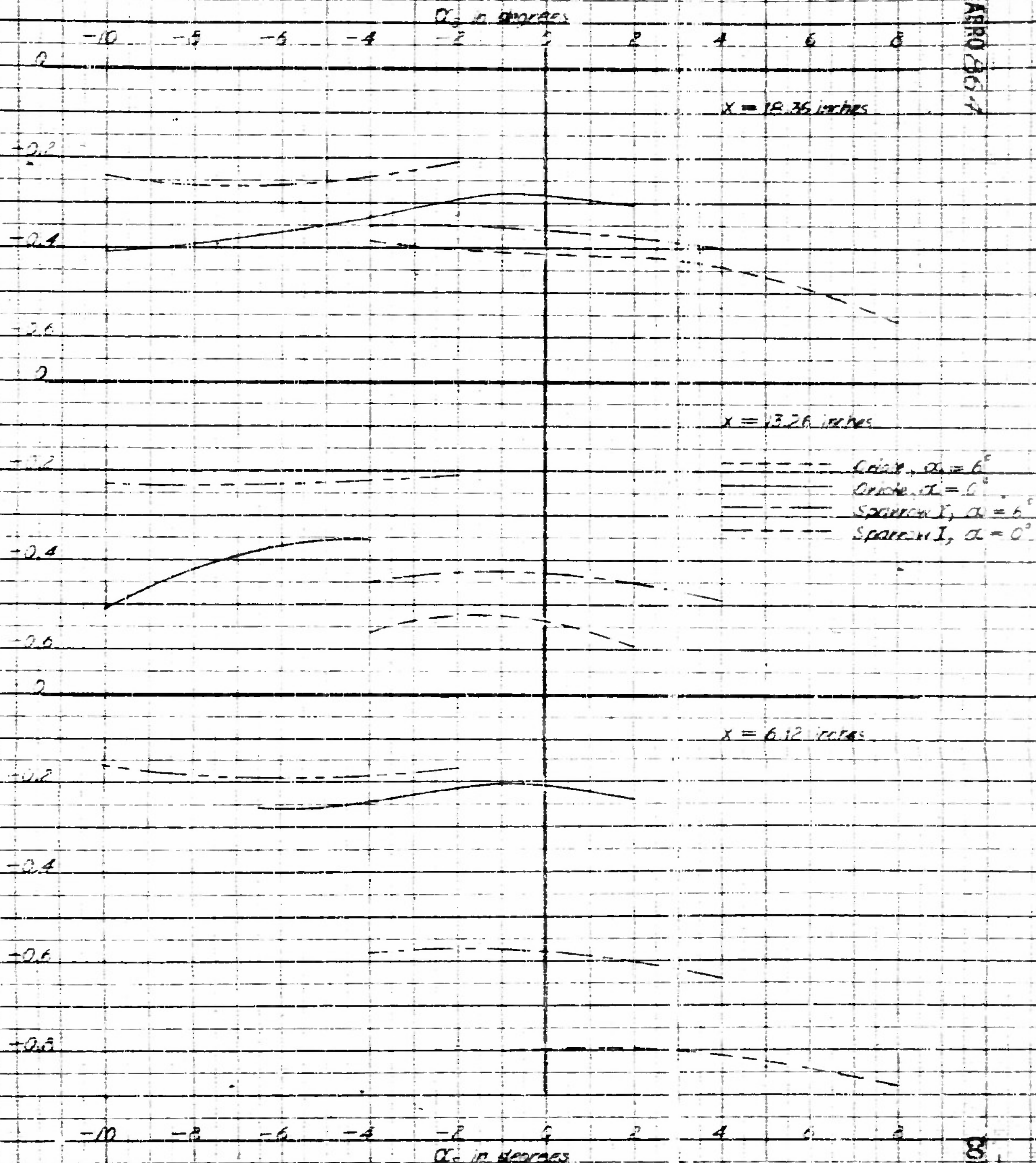

Figure 29 (Continued)

(c) Outboard, $z = 1.02$ Inches

FIGURE 29

CONFIDENTIAL

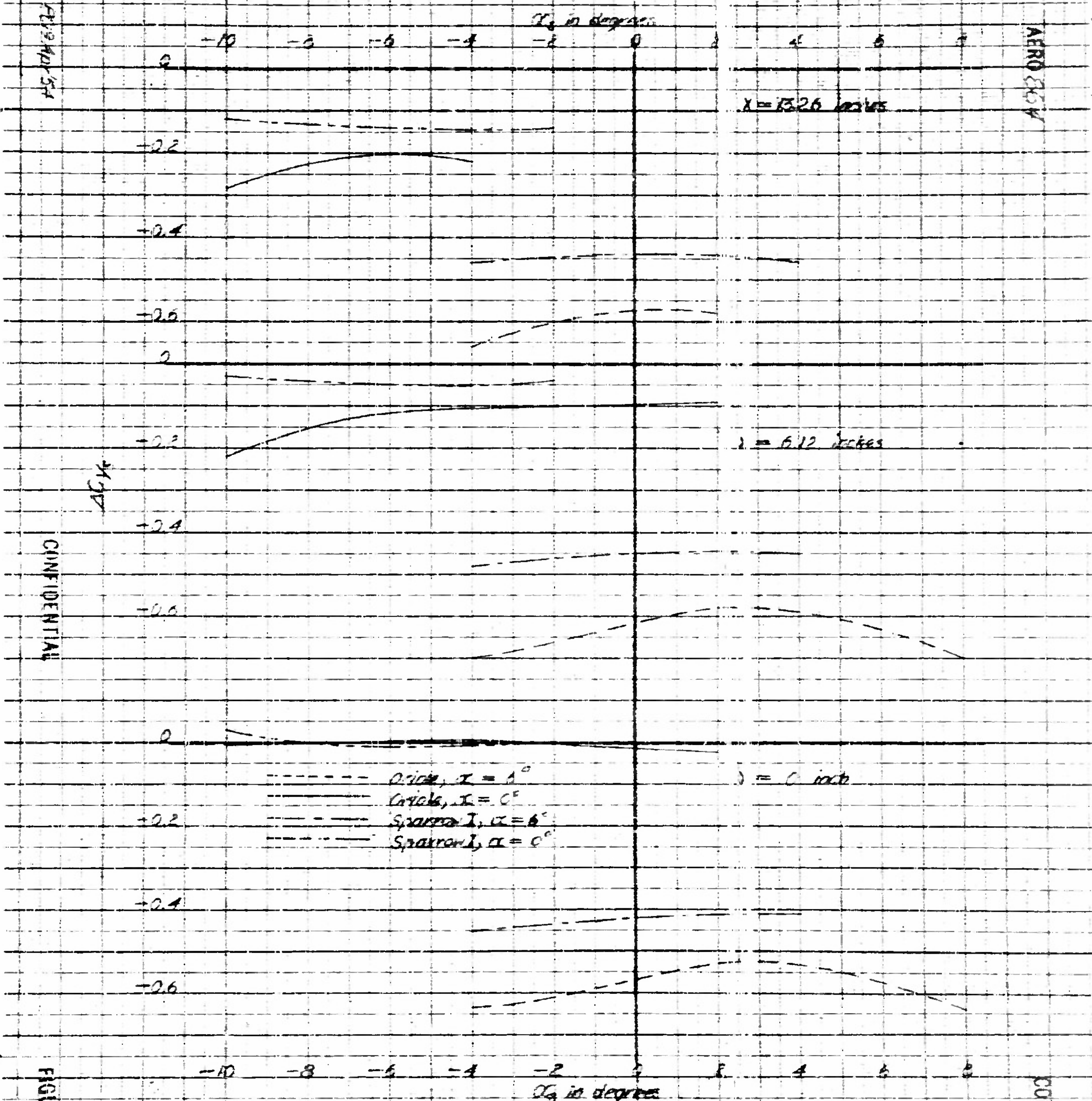

Figure 29 (Continued)

(d) Inboard, z = 2.04 Inches

FIGURE 29d

CONFIDENTIAL

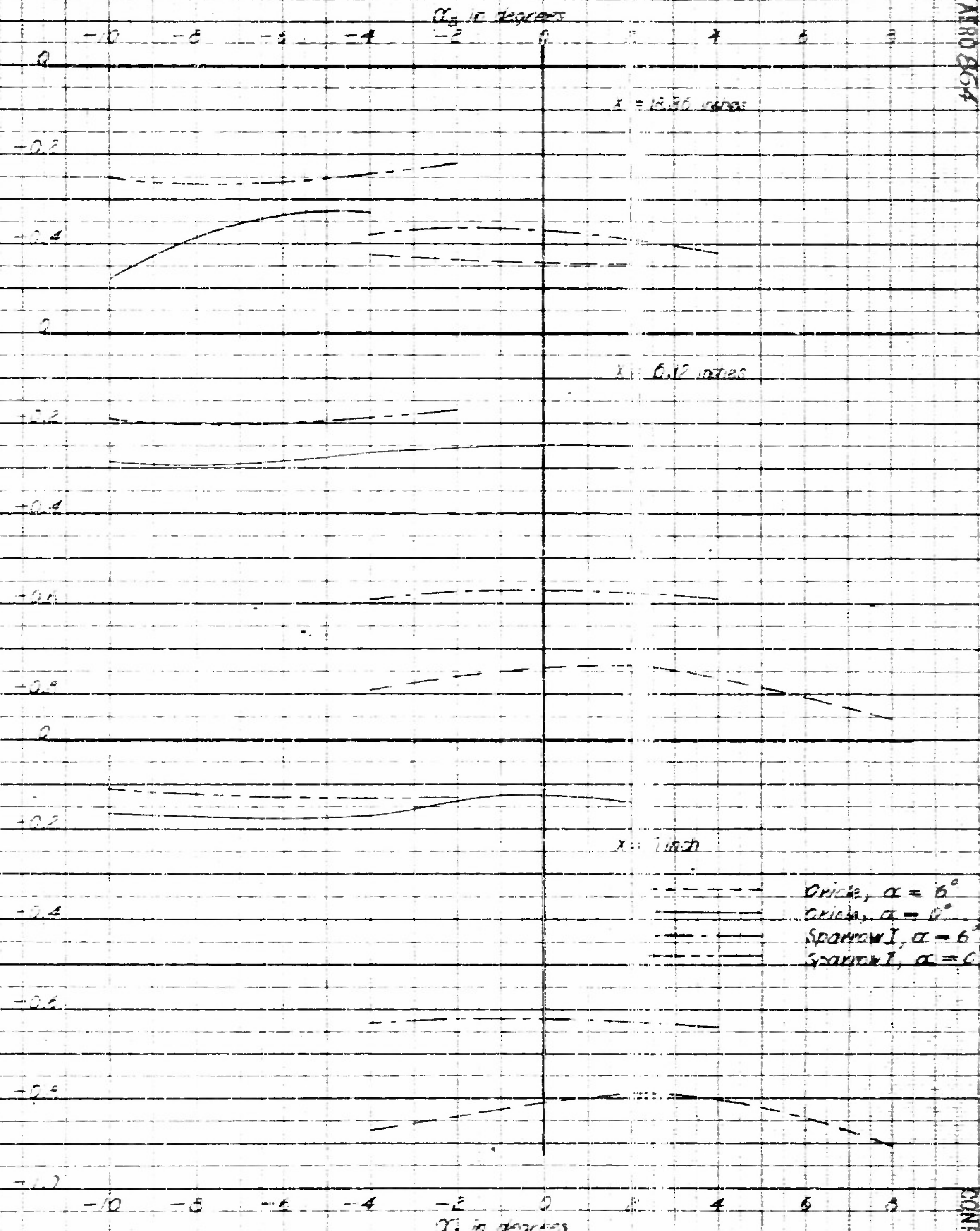

Figure 29 (Continued)

(e) Outboard, z = 2.04 Inches

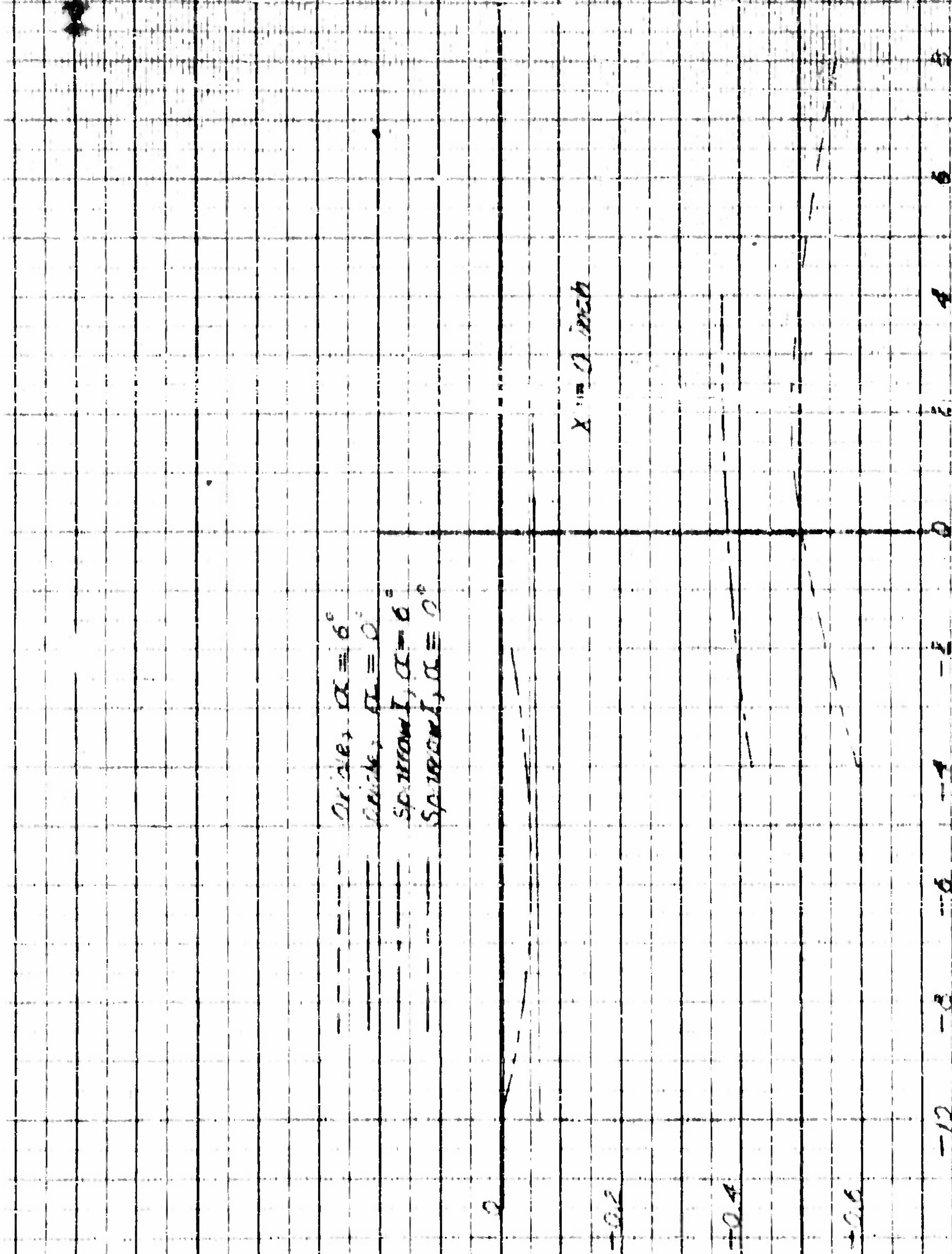

Figure 29 (continued).

(f) Inboard, $z = 4.08$ inches.

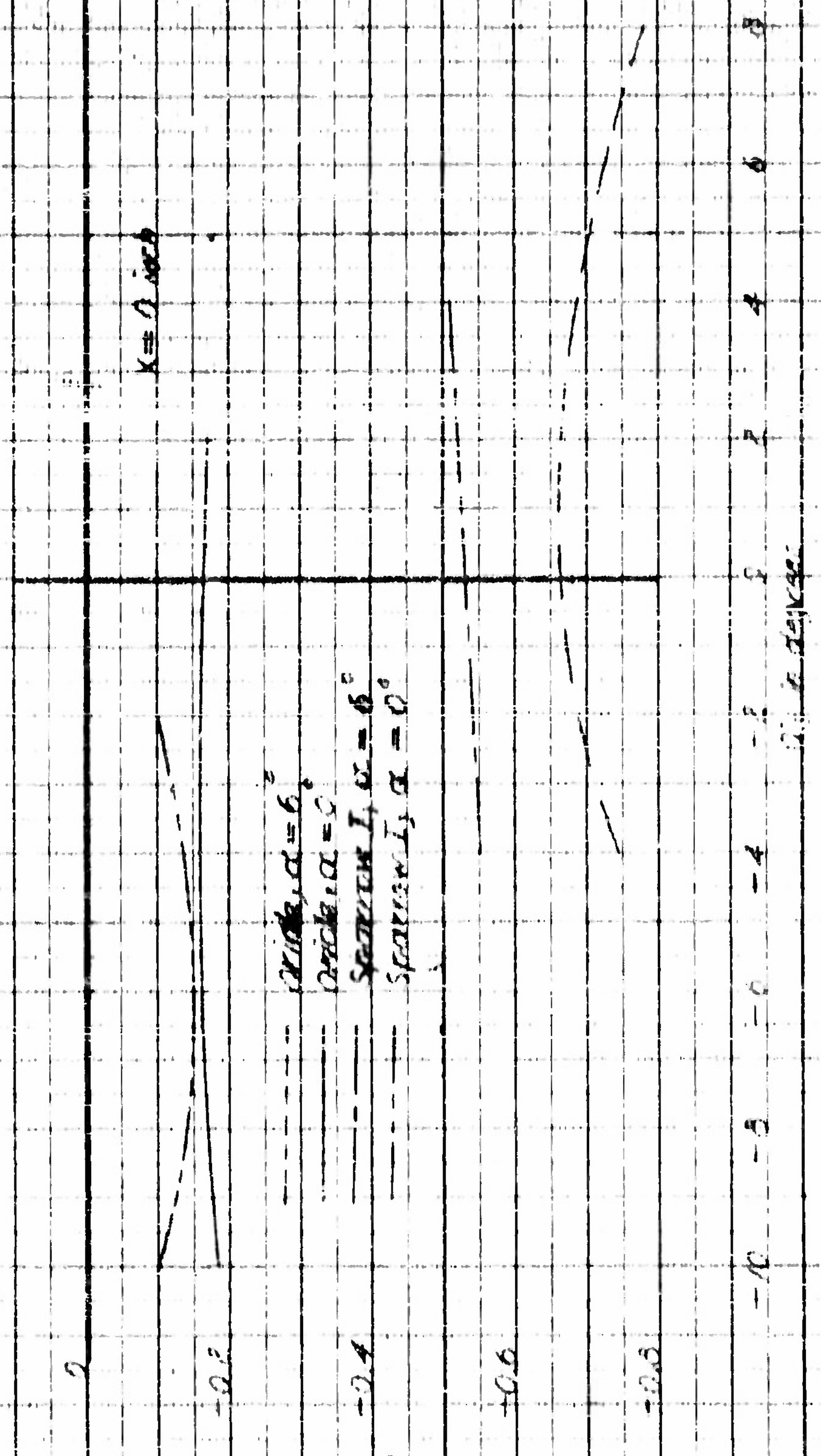

Figure 29 (Concluded)

(g) Outboard, z = 4.98 inches

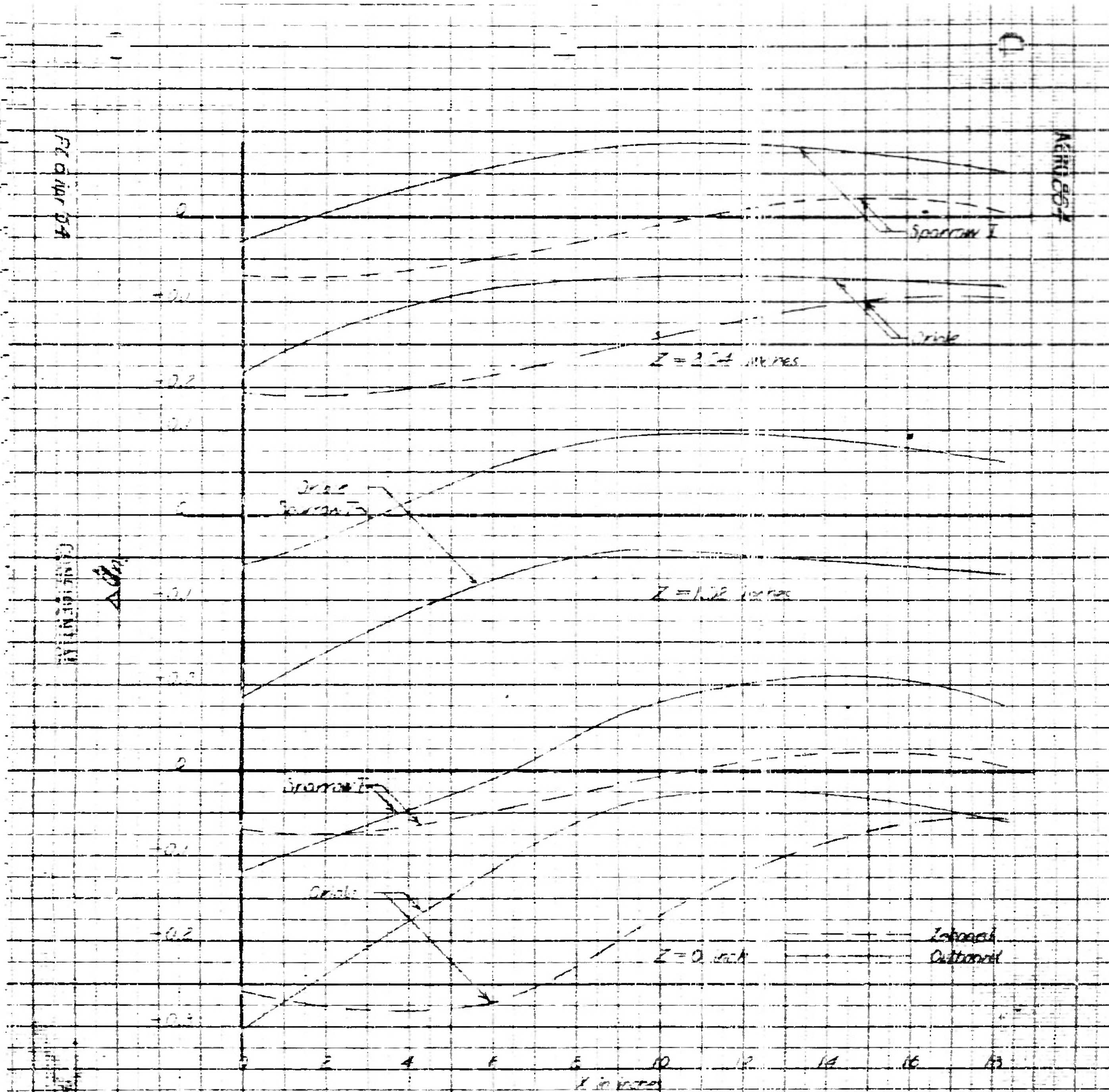

Figure 30—Variation of Airplane Interference on the Yawing Moment Coefficient of the Oriole and Sparrow I Missile With Distance Forward of the Carry Position

(a) $\delta_s = 0°$; $\alpha_s = 0°$; $\alpha = 4°$

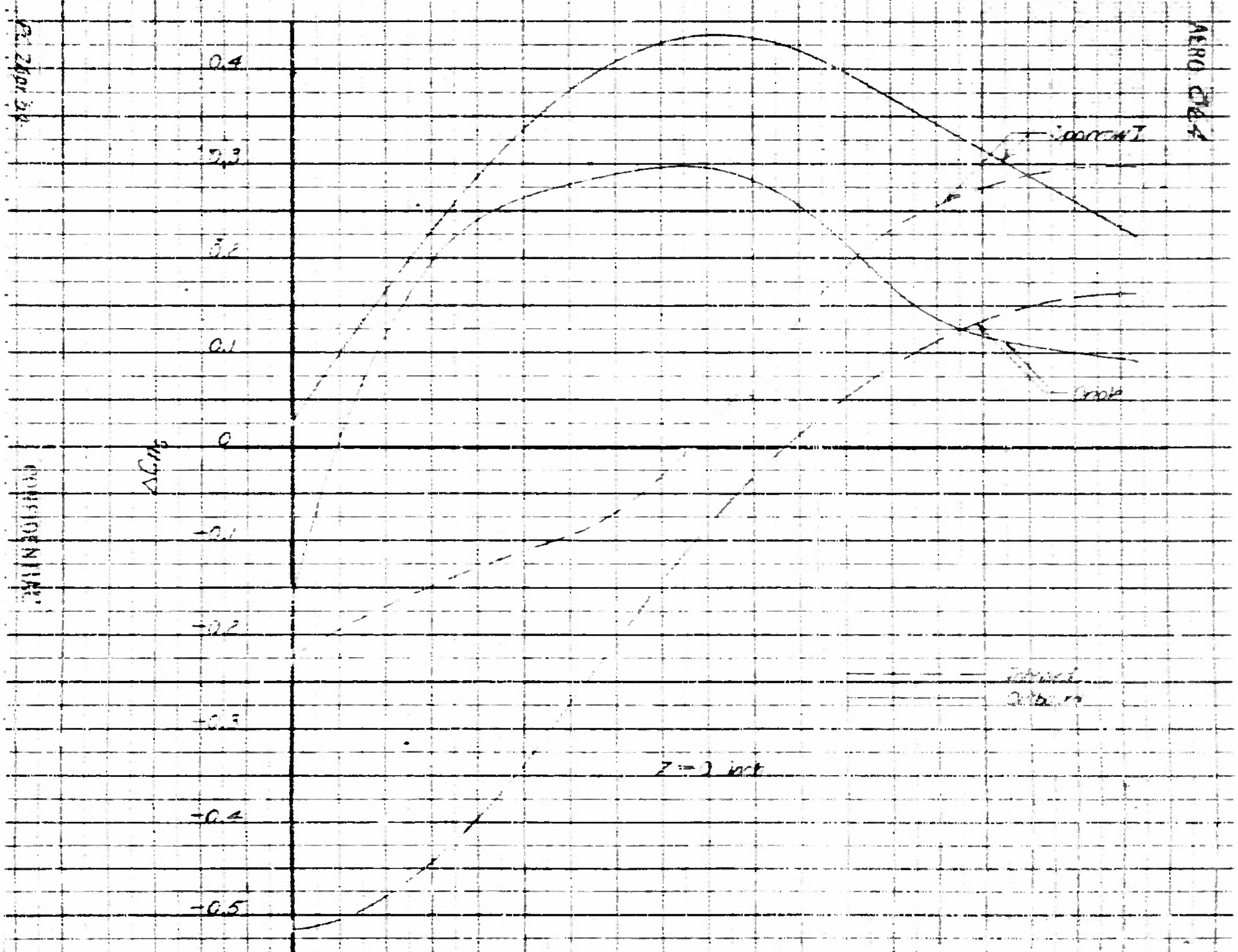

Figure 30(Continued)

(f) $\varepsilon_s = 0°$, $\alpha_s = 6°$, $\alpha = 10°$

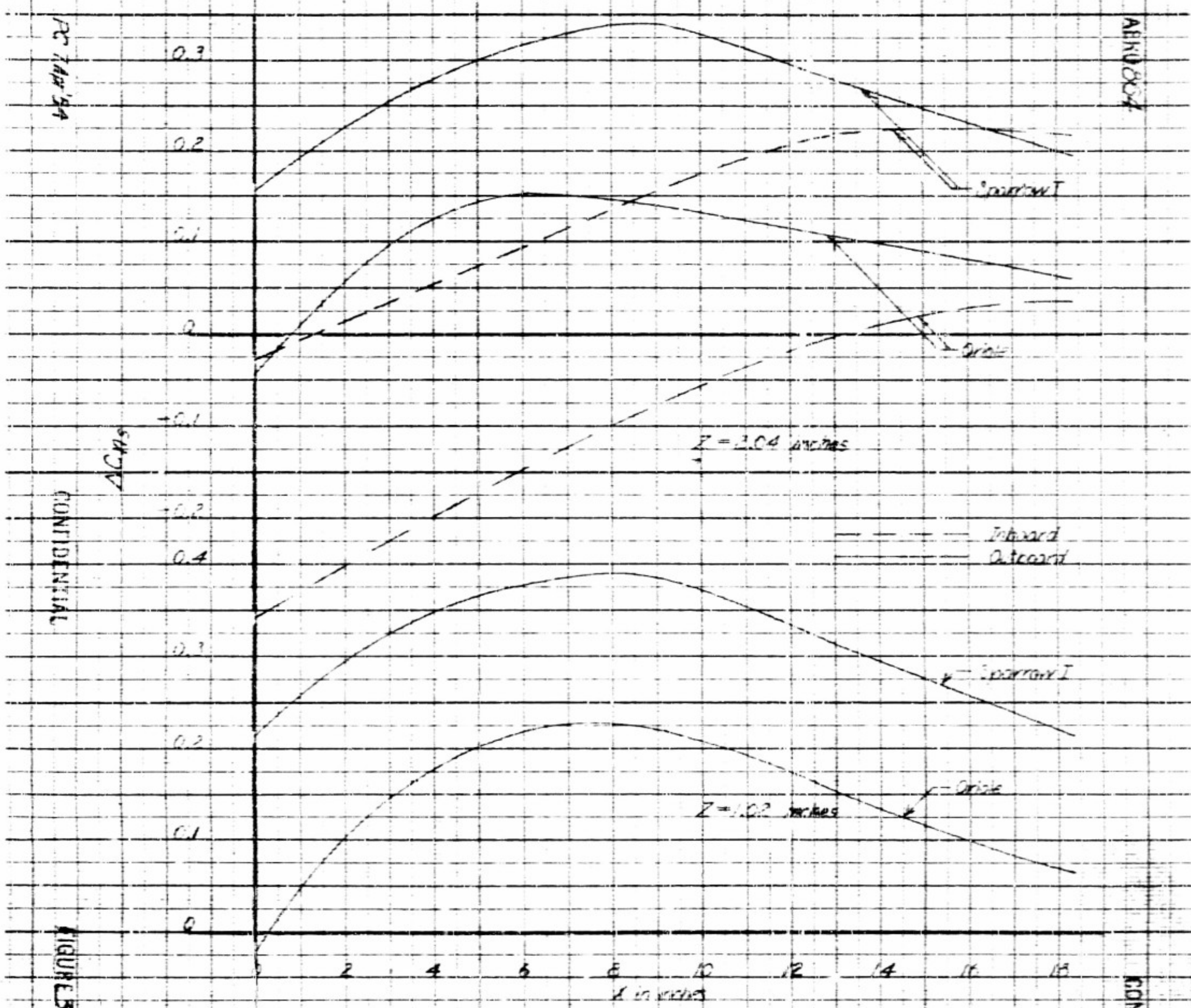

Figure 30 (Concluded)

(b) Concluded

CONFIDENTIAL

FIGURE 30(b) conc'd

CONFIDENTIAL

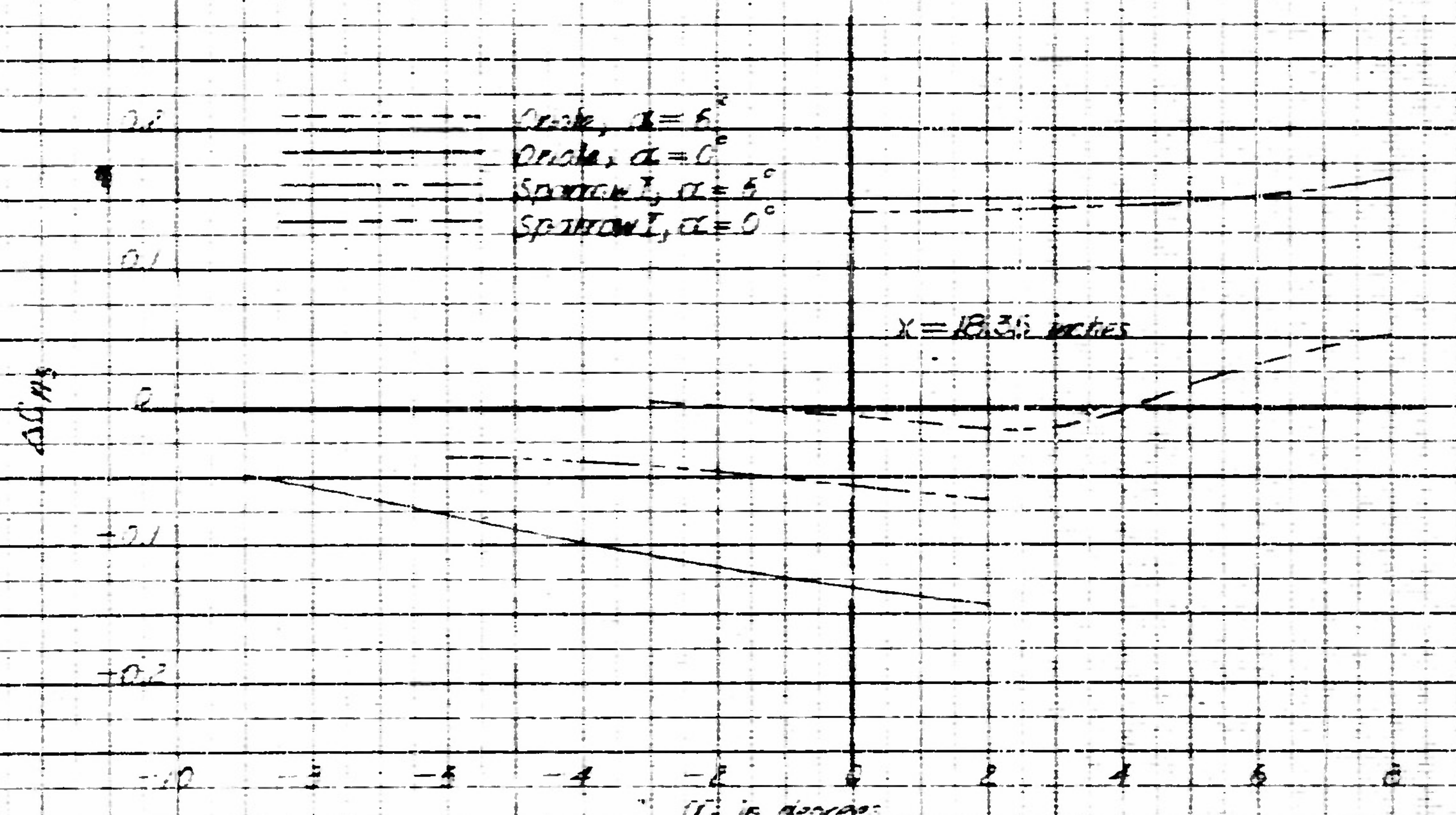

Figure 31—Variation of Airplane Interference on the Yawing-Moment Coefficient of the Oriole and Sparrow I Missiles with Missile Angle of Attack

(a) Inboard, $z = 0$ Inch

PC 19 Apr '54

CONFIDENTIAL

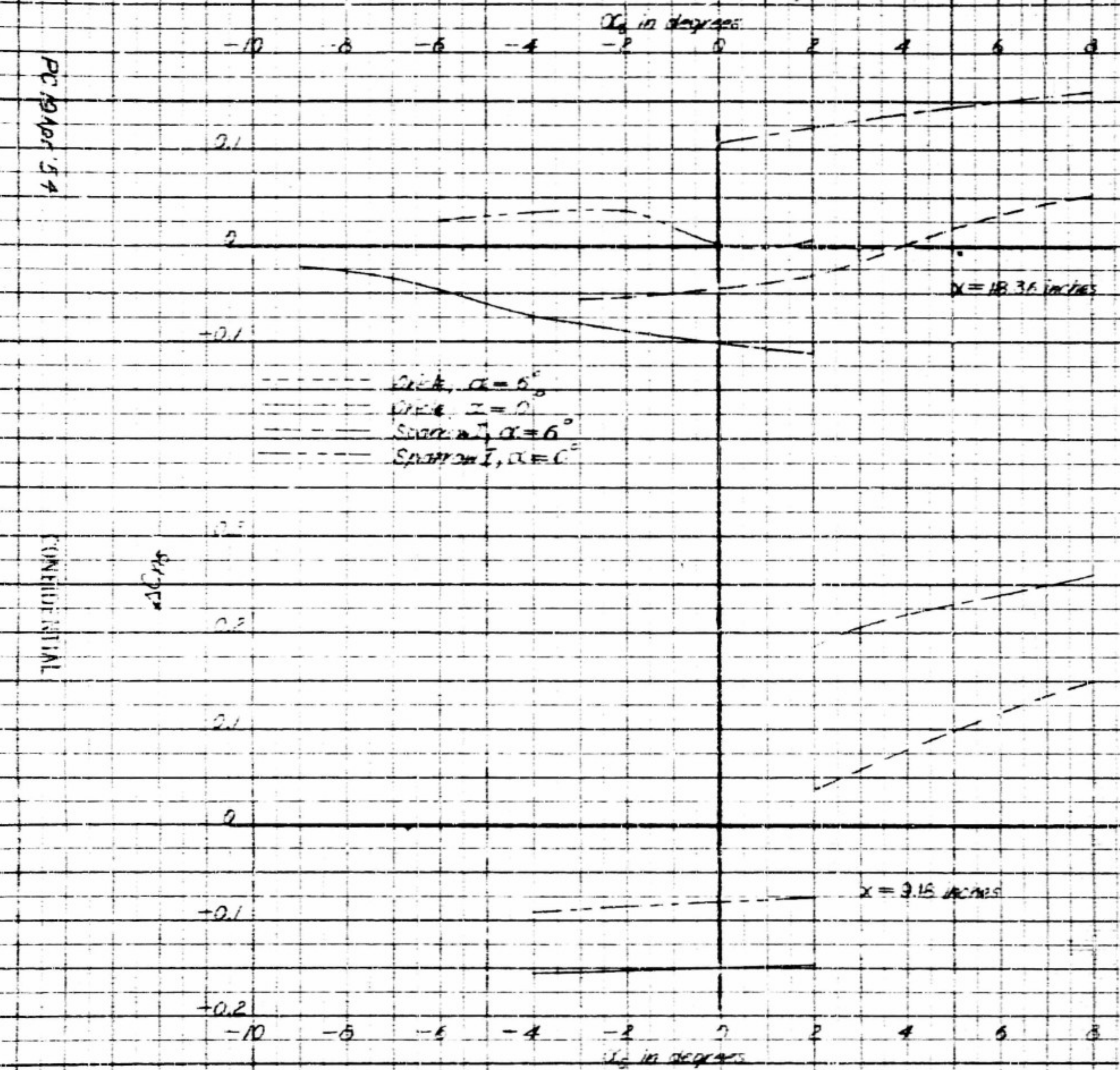

Figure 31 (Continued)

(b) Outboard, z = 0 inch

CONFIDENTIAL

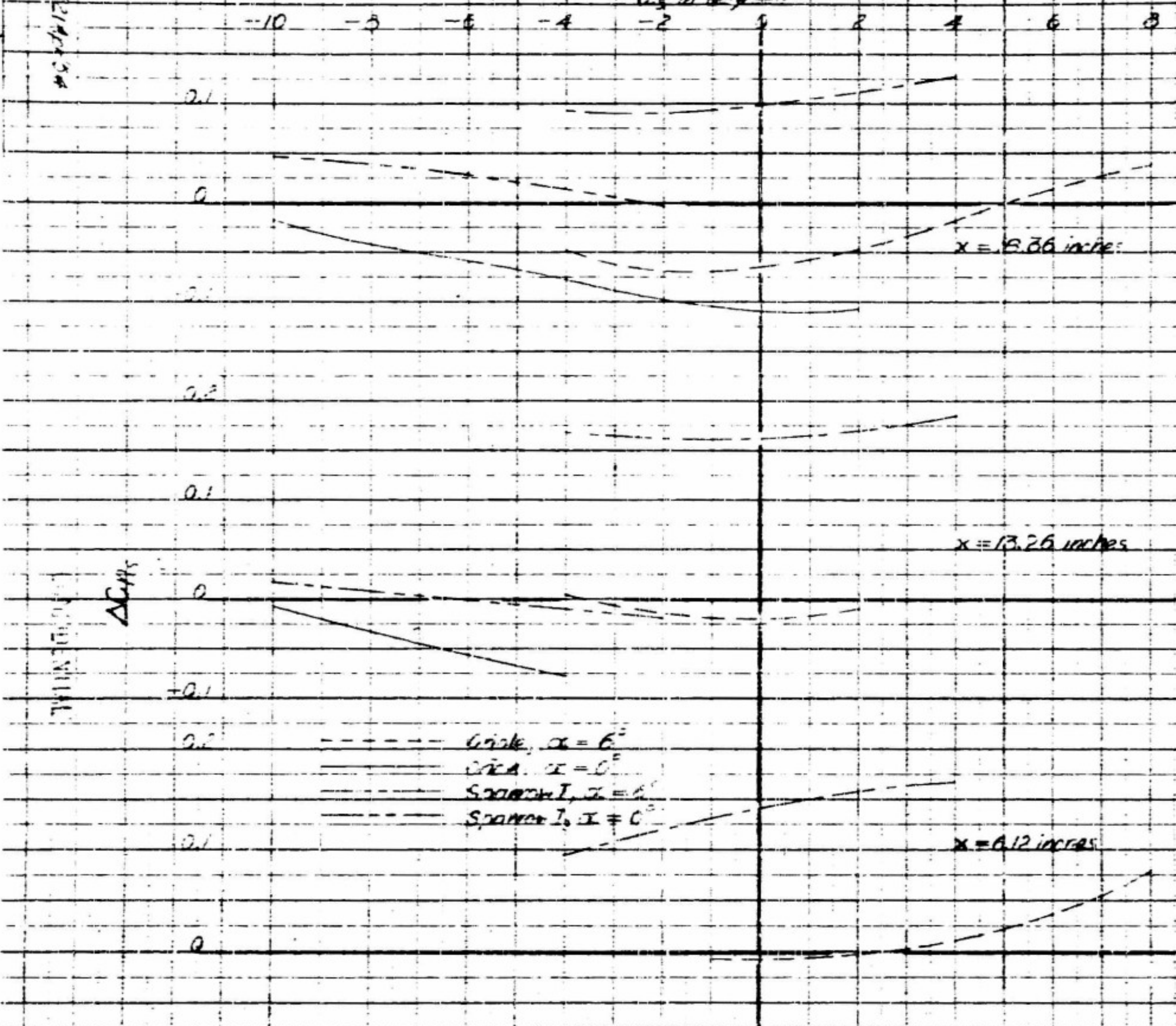

Figure 31 (Continued)

(c) Outboard; z = 1.02 Inches

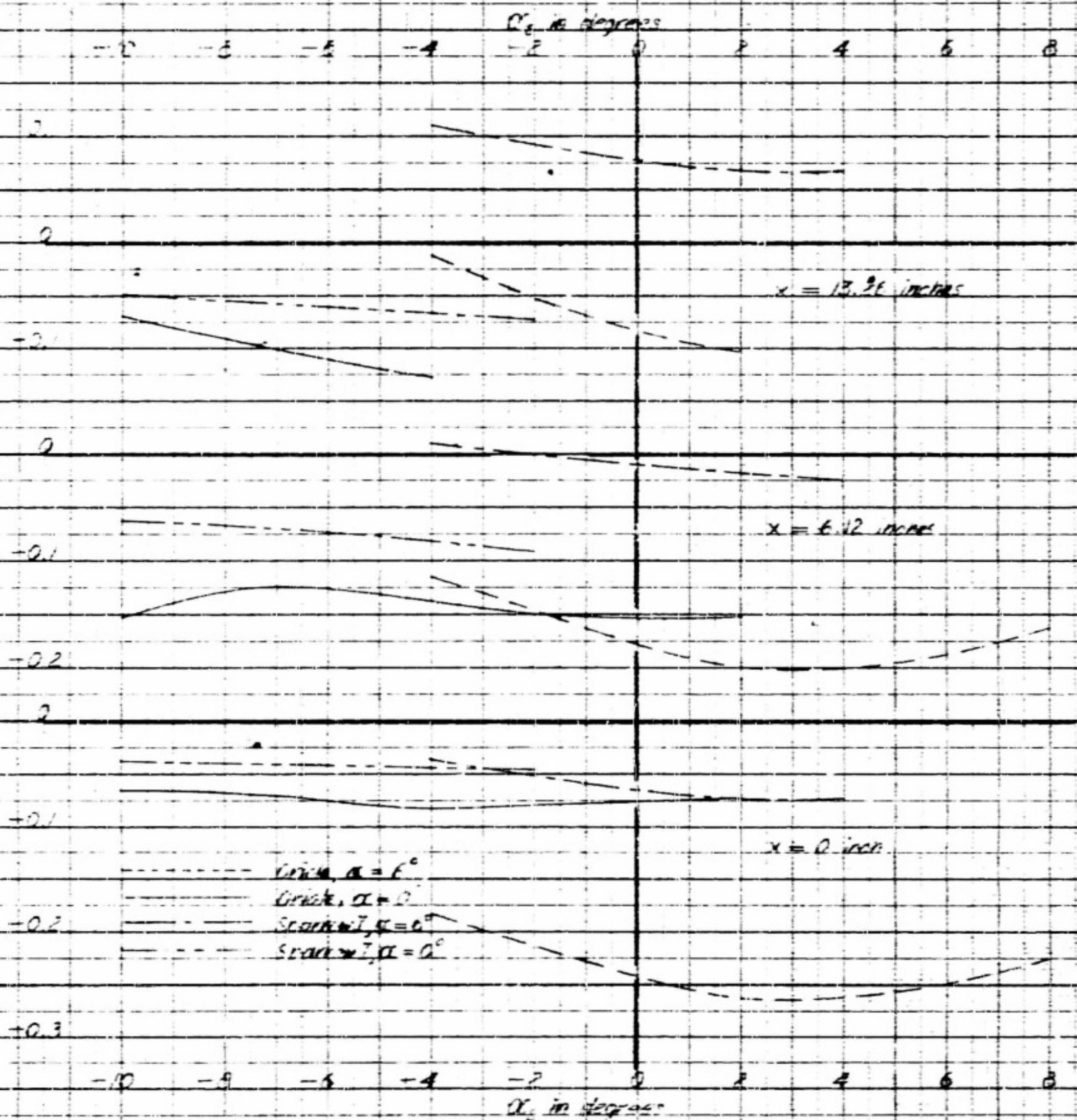

Figure 31 (Continued)

(d) Inboard, z = 2.04 Inches

FIGURE 31 d

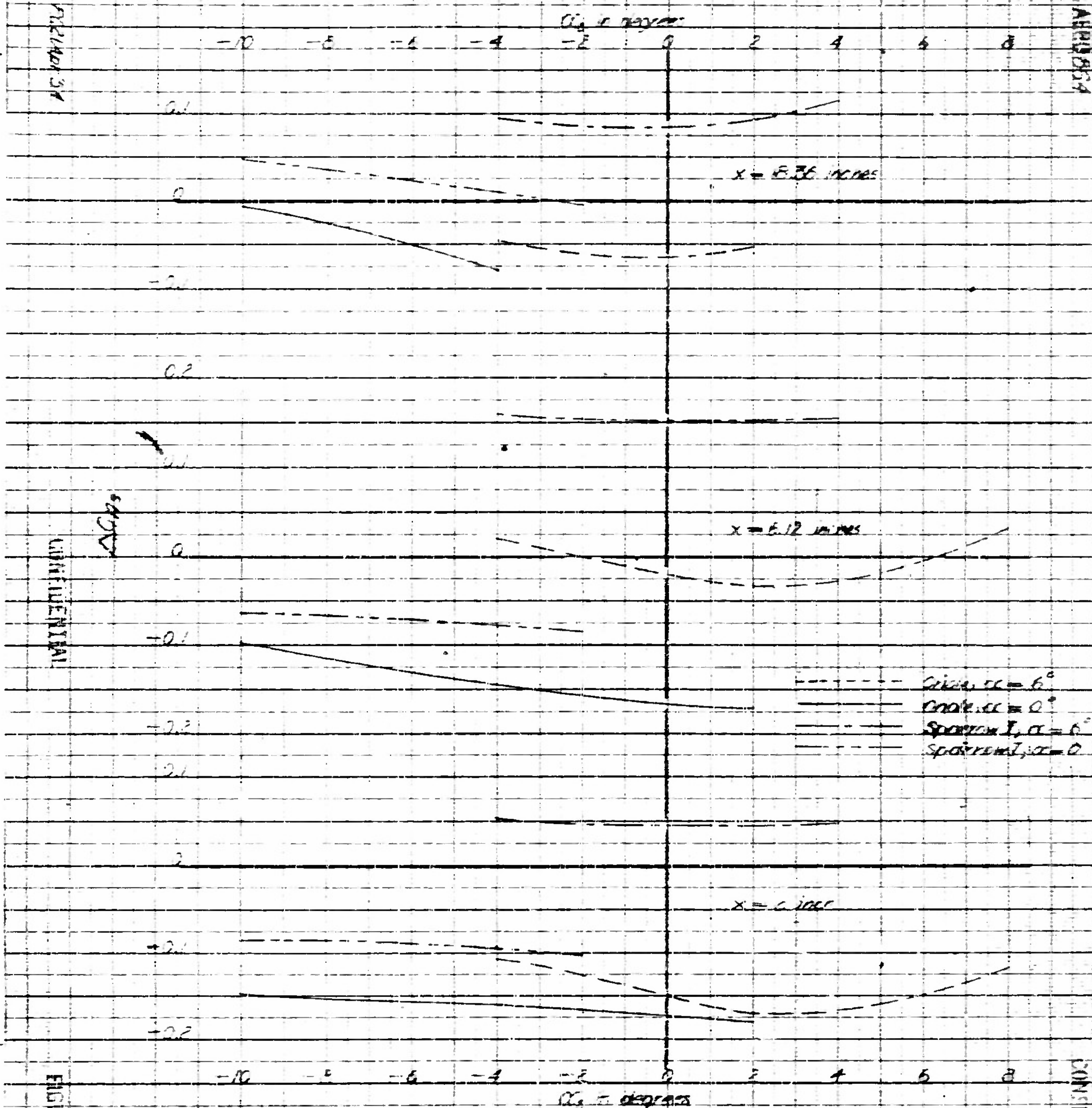

Figure 31 (Continued)

(e) Outboard, z = 2.04 Inches

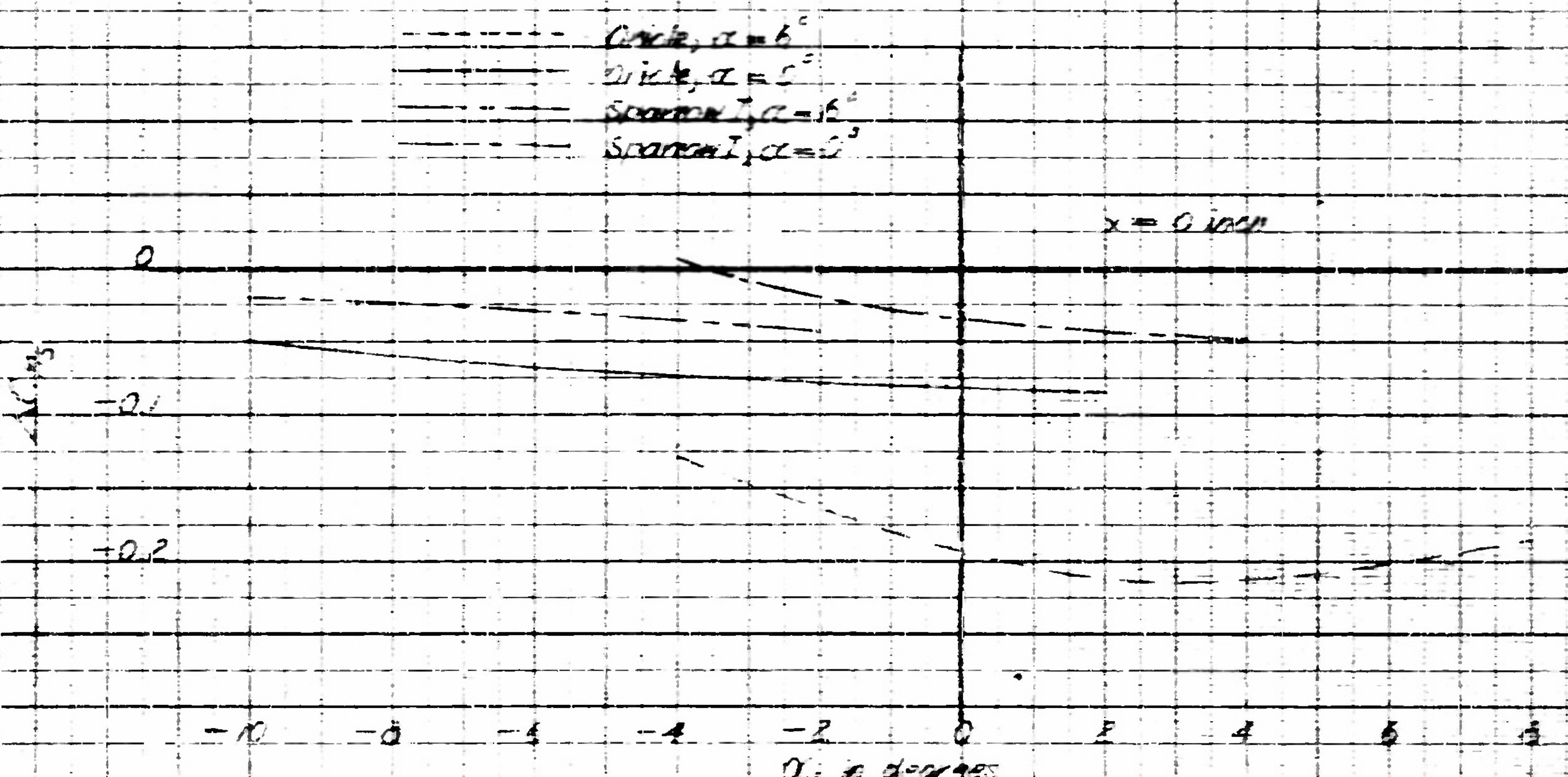

Figure 31 (Continued)

(f) Inboard, z = 4.08 Inches

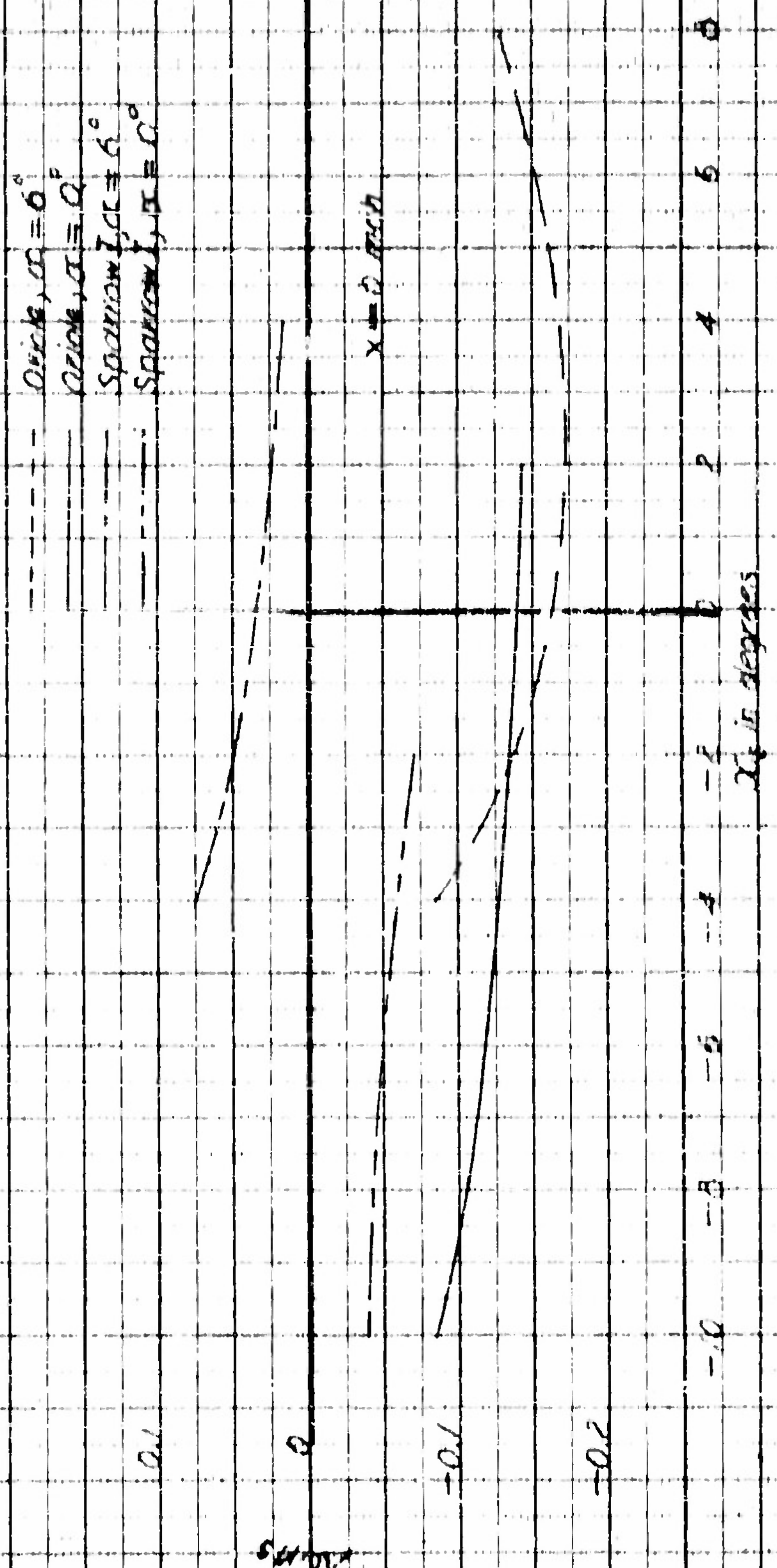

Figure 31 (concluded)

(g) Outboard, z = 4.05 Inches

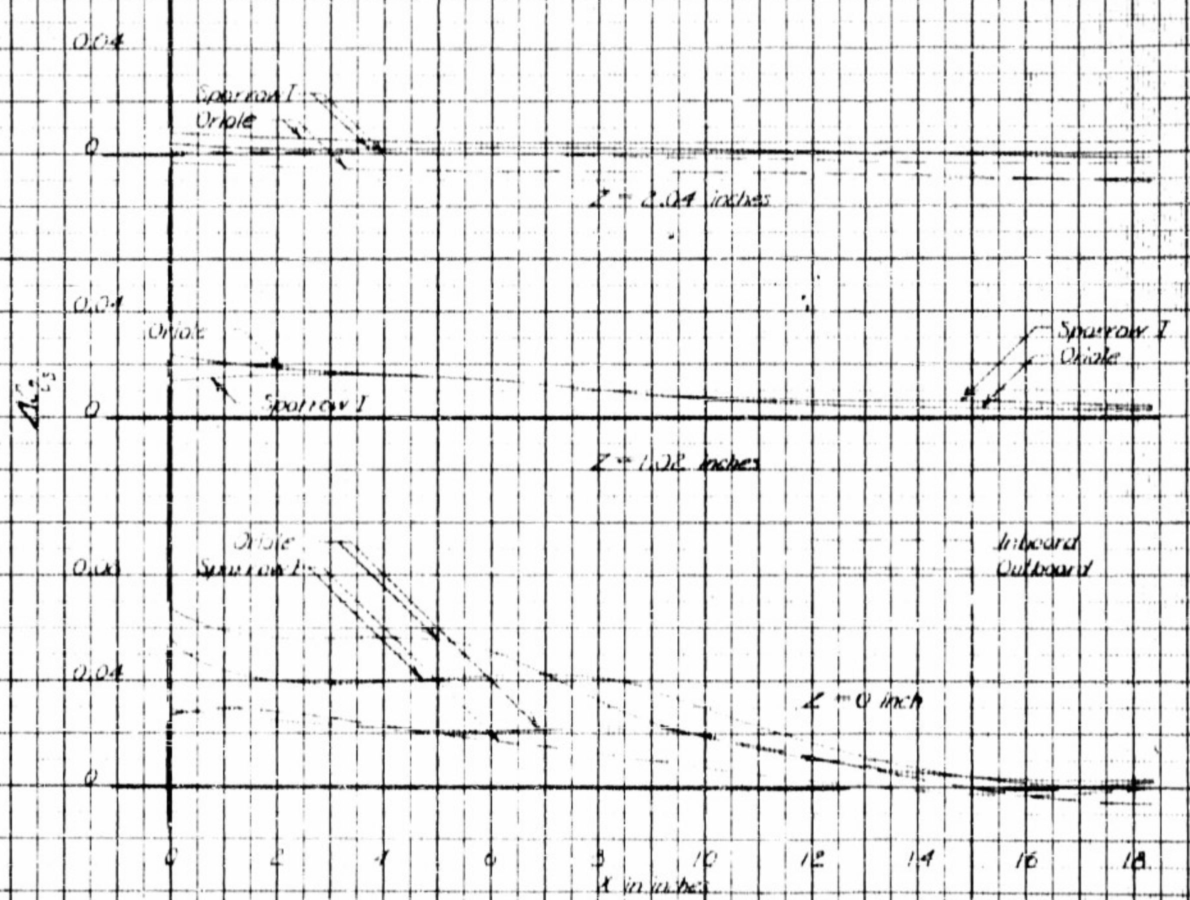

Figure 32 - Variation of Airplane Interference on the Rolling-Moment Coefficient of the Oriole and Sparrow I Missiles With Distance Forward of the Carry Position

(a) $\theta_s = 0°$, $\alpha_s = 0°$, $\alpha = 4°$

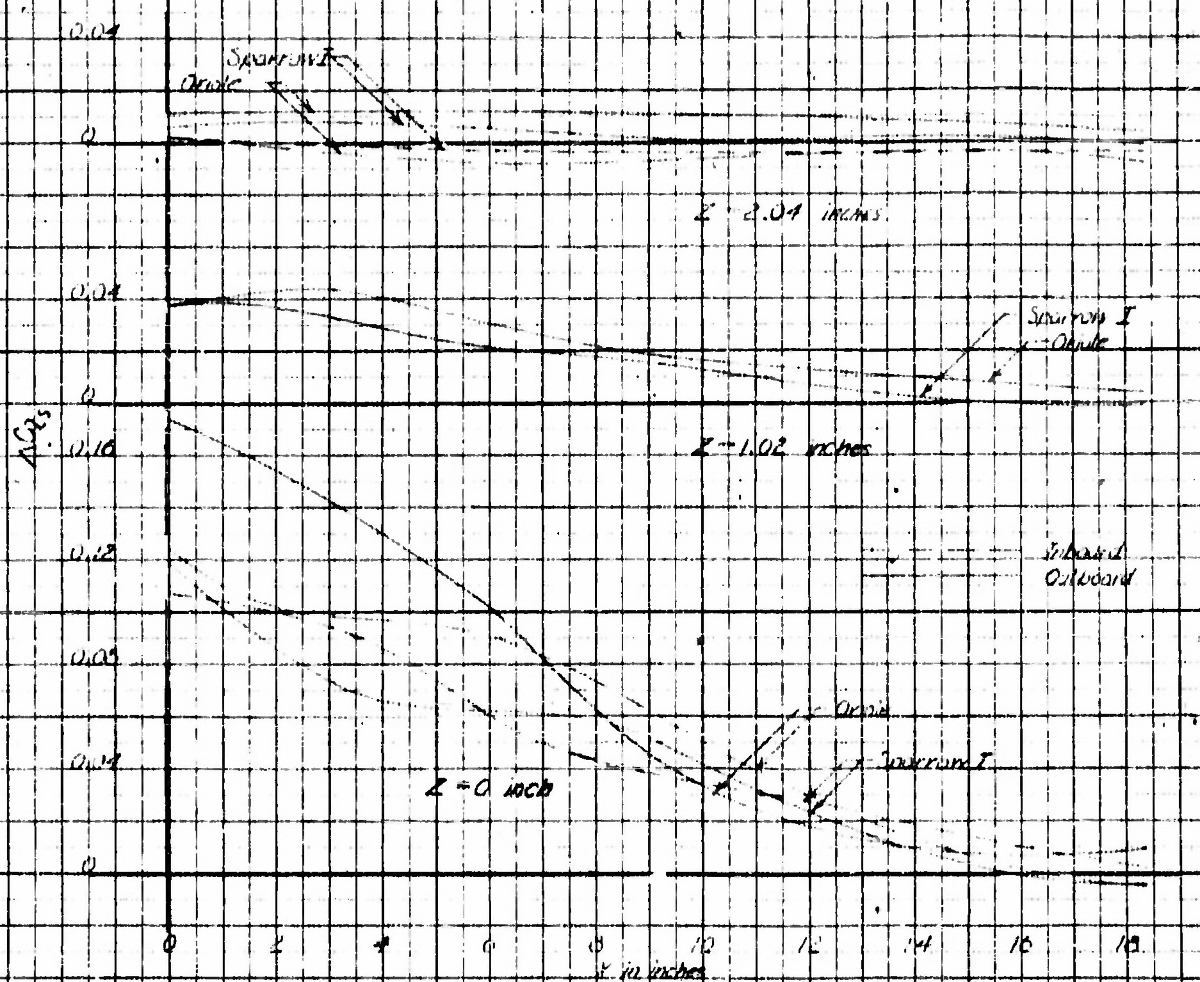

Figure 32 (Concluded)

(b) $\beta_s = 0°, \alpha_s = 6°, \alpha = 10°$

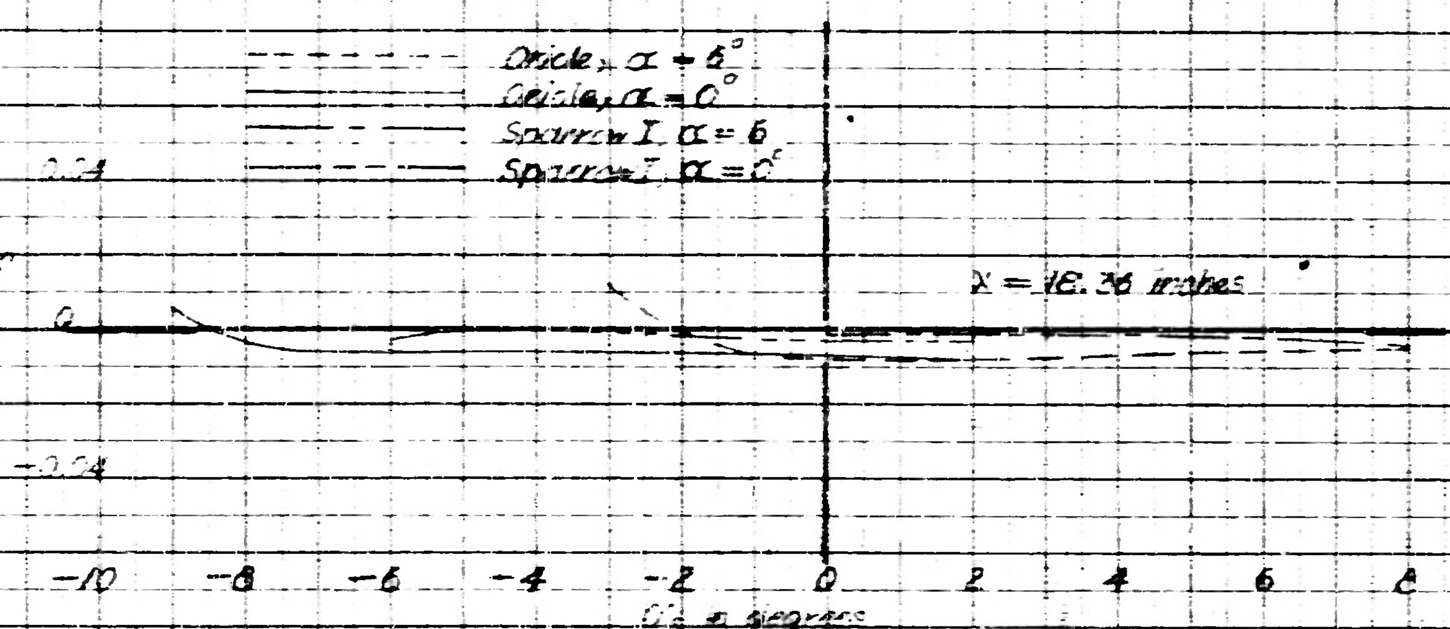

Figure 33– Variation of Airplane Interference on the Rolling-Moment Coefficient of the Oriole and Sparrow I Missiles with Missile Angle of Attack

(a) Inboard, z = 0 Inch

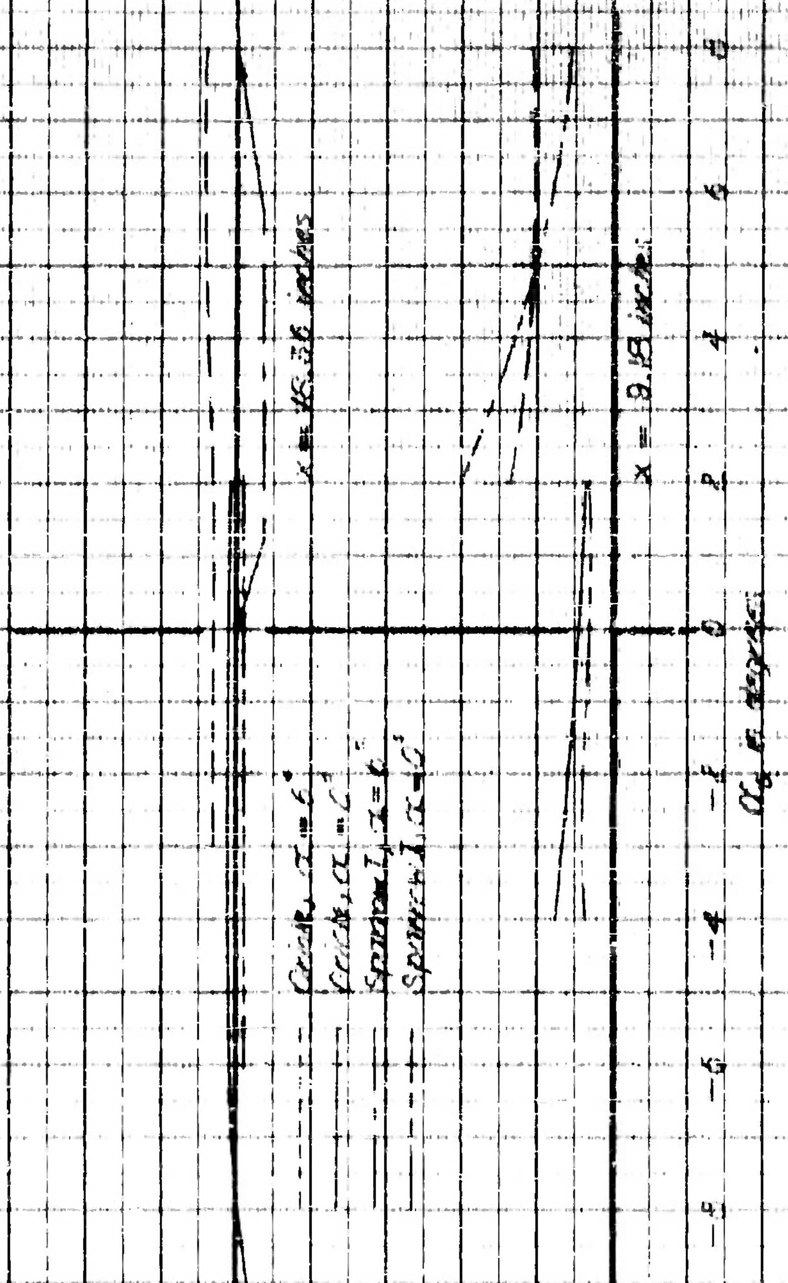

Figure 33 (Continued)

(b) Caliber, z = 0 Inch

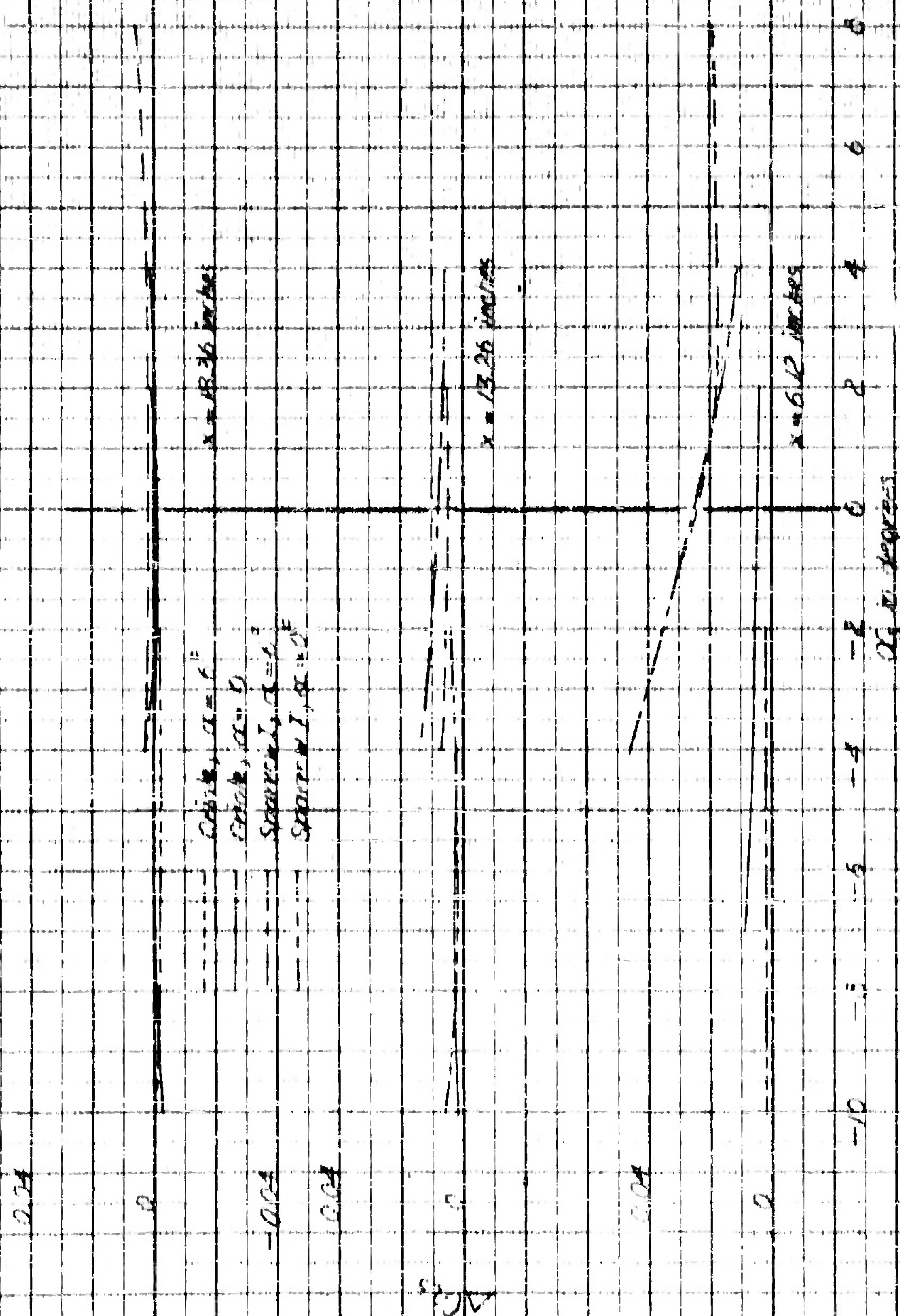

Figure 33 (Continued)

(c) Outboard, z = 1.02 Inches

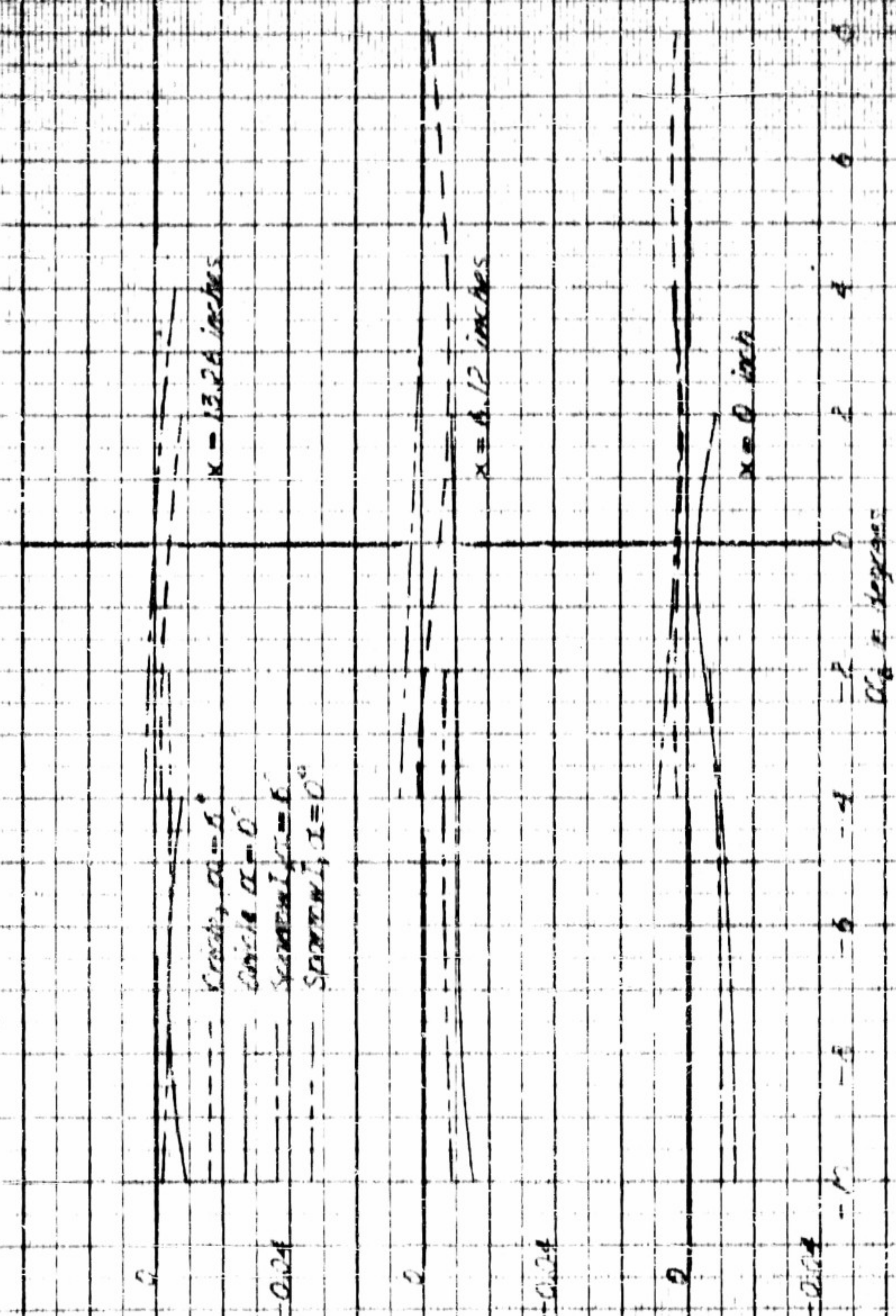

Figure 33 (Continued)

(d) Inboard, z = 2.04 inches

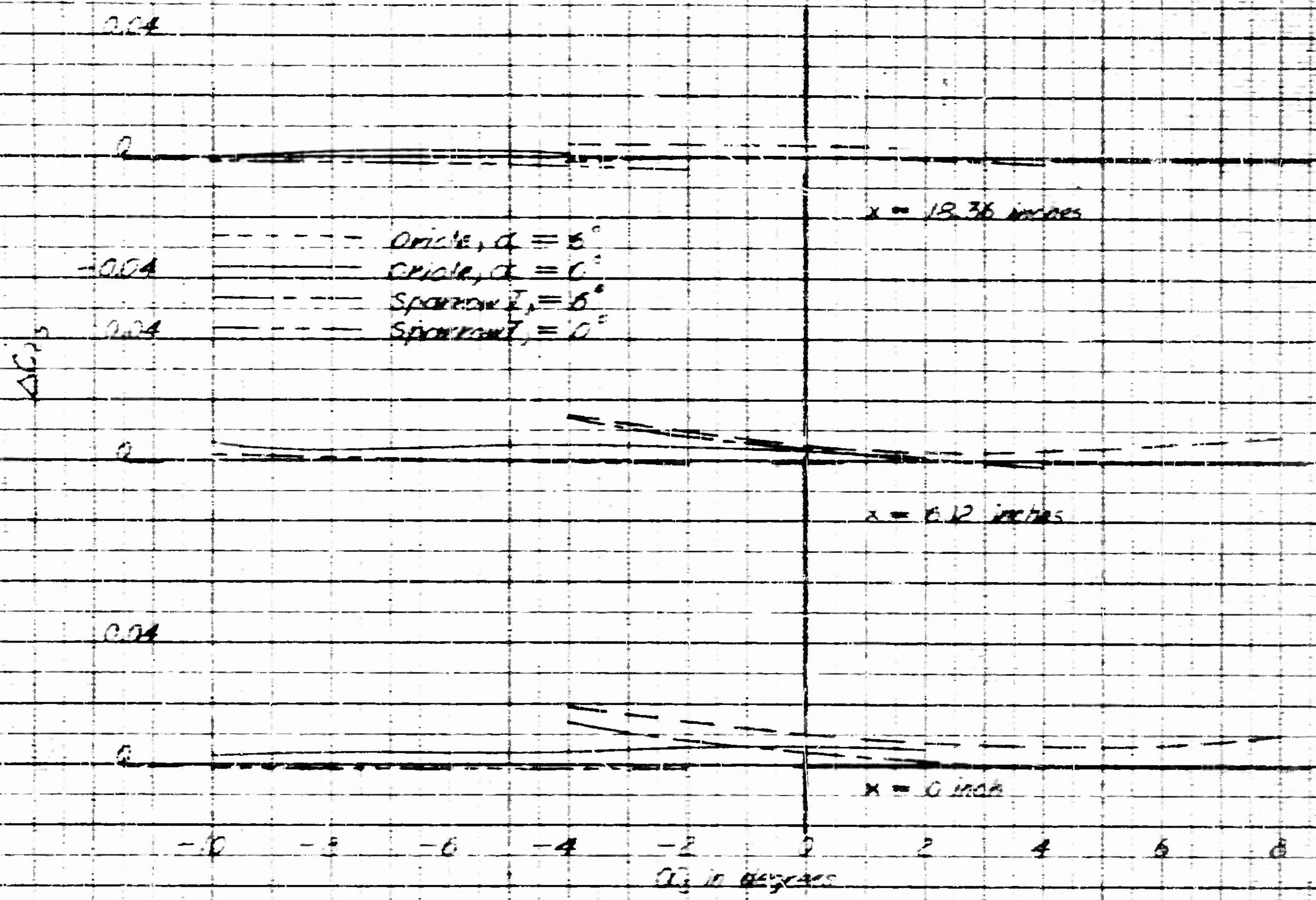

Figure 33 (Continued)

(e) Outboard, z = 2.04 Inches

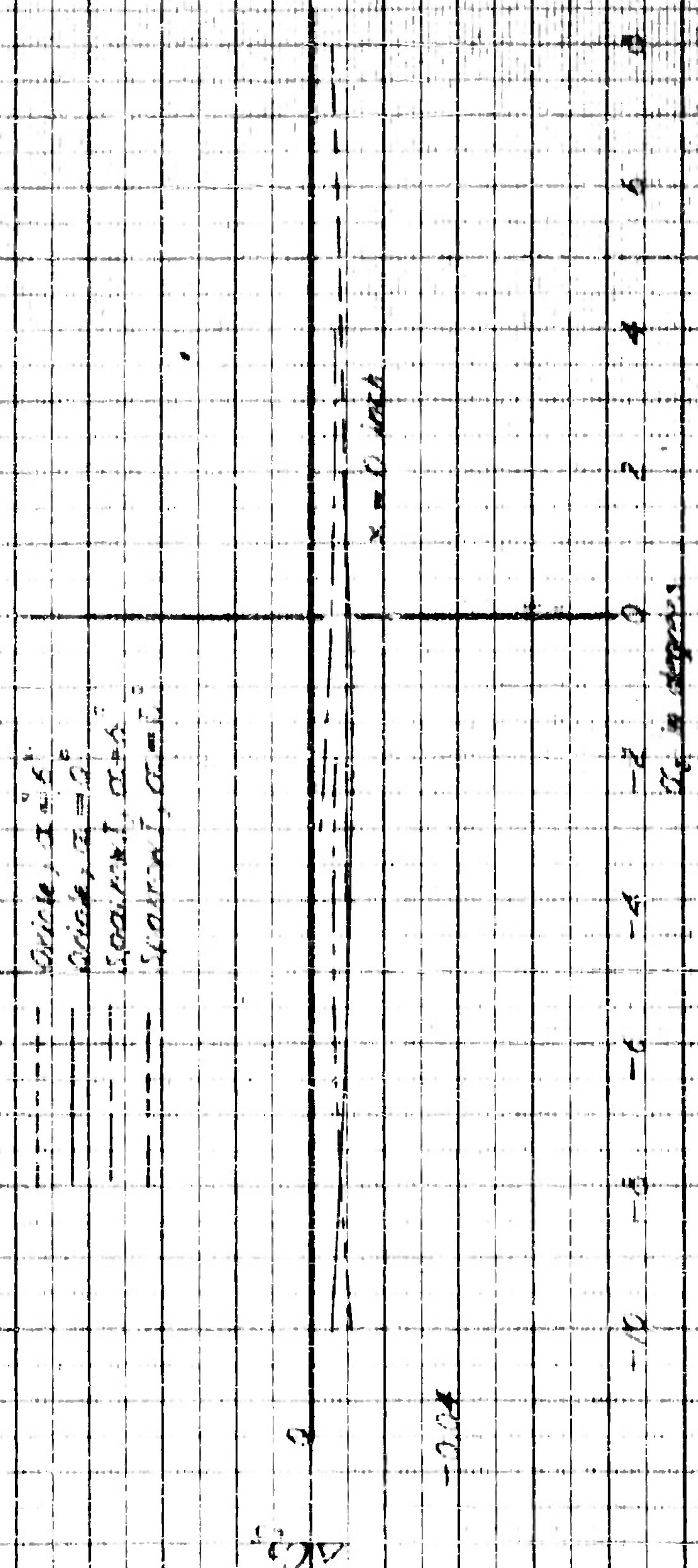

Figure 33 Continued

(f) Inboard, z = 4.08 Inches

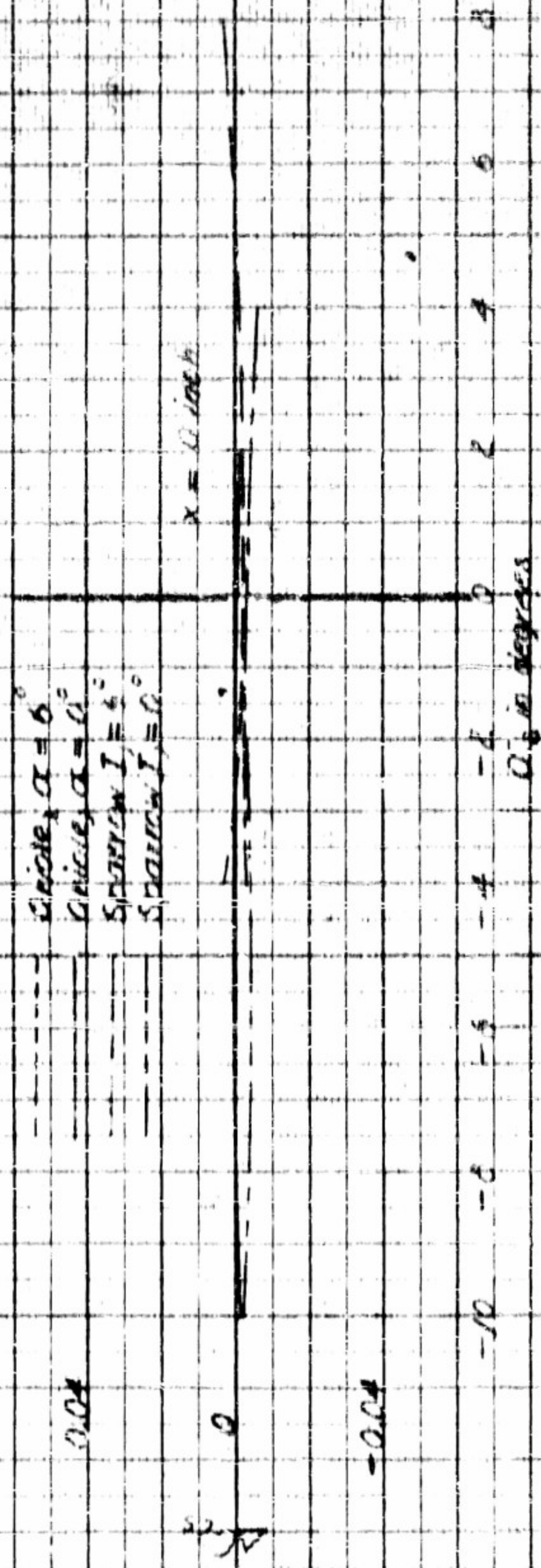

Figure 33 (Concluded)

(g) Outboard, z = 4.0 Inches

DTMB Aero Rpt 864 Pt.2.
David W. Taylor Model Basin
WIND-TUNNEL TESTS OF THE AIRPLANE INTERFERENCE ON A 0.17-SCALE MODEL OF THE XAAM-N-4 ORIOLE MISSILE AND COMPARISON WITH THE AIRPLANE INTERFERENCE ON A 0.17-SCALE MODEL OF THE XAAM-N-2 SPARROW I MISSILE. PT. 2: MISSILES IN THE PROXIMITY OF A 0.179-SCALE MODEL OF THE F4D-1 AIRPLANE, by E.M. Brower. Wash., Aug 1954. 210p. incl. illus. 5 refs. (Aerodynamics Lab. Aero Rpt 864 Pt. 2. Aero Test A-355. TED TMB AD 3158) CONFIDENTIAL

5-component strain-gage balance measured all missile forces & moments except axial force. Missile tested at 2 spanwise locations. 3 non-instrumented dummy missile models used to obtain interference effects due to proximity of missiles & effect of 4 missiles on plane.

CONFIDENTIAL

1. AIRPLANES (DOUGLAS F4D-1)
2. GUIDED MISSILES (SPERRY AAM-N-2)
3. GUIDED MISSILES (MARTIN AAM-N-4)
4. INTERFERENCE
5. EXTERNAL STORES
6. PYLONS

I. Brower, Elayne M.

DTMB Aero Rpt 864 Pt.2
David W. Taylor Model Basin
WIND-TUNNEL TESTS OF THE AIRPLANE INTERFERENCE ON A 0.17-SCALE MODEL OF THE XAAM-N-4 ORIOLE MISSILE AND COMPARISON WITH THE AIRPLANE INTERFERENCE ON A 0.17-SCALE MODEL OF THE XAAM-N-2 SPARROW I MISSILE. PT. 2: MISSILES IN THE PROXIMITY OF A 0.179-SCALE MODEL OF THE F4D-1 AIRPLANE, by E.M. Brower. Wash., Aug 1954. 210p. incl. illus. 5 refs. (Aerodynamics Lab. Aero Rpt 864 Pt. 2. Aero Test A-355. TED TMB AD 3158) CONFIDENTIAL

5-component strain-gage balance measured all missile forces & moments except axial force. Missile tested at 2 spanwise locations. 3 non-instrumented dummy missile models used to obtain interference effects due to proximity of missiles & effect of 4 missiles on plane.

CONFIDENTIAL

1. AIRPLANES (DOUGLAS F4D-1)
2. GUIDED MISSILES (SPERRY AAM-N-2)
3. GUIDED MISSILES (MARTIN AAM-N-4)
4. INTERFERENCE
5. EXTERNAL STORES
6. PYLONS

I. Brower, Elayne M.

DTMB Aero Rpt 864 Pt. 2
David W. Taylor Model Basin
WIND-TUNNEL TESTS OF THE AIRPLANE INTERFERENCE ON A 0.17-SCALE MODEL OF THE XAAM-N-4 ORIOLE MISSILE AND COMPARISON WITH THE AIRPLANE INTERFERENCE ON A 0.17-SCALE MODEL OF THE XAAM-N-2 SPARROW I MISSILE. PT. 2: MISSILES IN THE PROXIMITY OF A 0.179-SCALE MODEL OF THE F4D-1 AIRPLANE, by E.M. Brower. Wash., Aug 1954. 210p. incl. illus. 5 refs. (Aerodynamics Lab. Aero Rpt 864 Pt. 2 Aero Test A-355. TED TMB AD 3158) CONFIDENTIAL

5-component strain-gage balance measured all missile forces & moments except axial force. Missile tested at 2 spanwise locations. 3 non-instrumented dummy missile models used to obtain interference effects due to proximity of missiles & effect of 4 missiles on plane.

CONFIDENTIAL

1. AIRPLANES (DOUGLAS F4D-1)
2. GUIDED MISSILES (SPERRY AAM-N-2)
3. GUIDED MISSILES (MARTIN AAM-N-4)
4. INTERFERENCE
5. EXTERNAL STORES
6. PYLONS

I. Brower, Elayne M.

DTMB Aero Rpt 864 Pt.2
David W. Taylor Model Basin
WIND-TUNNEL TESTS OF THE AIRPLANE INTERFERENCE ON A 0.17-SCALE MODEL OF THE XAAM-N-4 ORIOLE MISSILE AND COMPARISON WITH THE AIRPLANE INTERFERENCE ON A 0.17-SCALE MODEL OF THE XAAM-N-2 SPARROW I MISSILE. PT. 2: MISSILES IN THE PROXIMITY OF A 0.179-SCALE MODEL OF THE F4D-1 AIRPLANE, by E.M. Brower. Wash., Aug, 1954. 210p. incl. illus. 5 refs. (Aerodynamics Lab. Aero Rpt 864 Pt. 2. Aero Test A-355. TED TMB AD 3158) CONFIDENTIAL

5-component strain-gage balance measured all missile forces & moments except axial force. Missile tested at 2 spanwise locations. 3 non-instrumented dummy missile models used to obtain interference effects due to proximity of missiles & effect of 4 missiles on plane.

CONFIDENTIAL

1. AIRPLANES (DOUGLAS F4D-1)
2. GUIDED MISSILES (SPERRY AAM-N-2)
3. GUIDED MISSILES (MARTIN AAM-N-4)
4. INTERFERENCE
5. EXTERNAL STORES
6. PYLONS

I. Brower, Elayne M.

UNCLASSIFIED

UNCLASSIFIED